GEOTECHNICAL EXTREME EVENTS RECONNAISSANCE (GEER) ASSOCIATION

Turning Disaster into Knowledge

Geotechnical Engineering Reconnaissance of the August 24, 2014 M6 South Napa Earthquake

Report of the NSF Sponsored GEER Association Team, California Geological Survey, Pacific Earthquake Engineering Research Center, and U.S. Geological Survey

Editors:
Jonathan Bray, Julien Cohen-Waeber, Tim Dawson, Tadahiro Kishida, and Nicholas Sitar

Lead Authors:
Christine Beyzaei, UC Berkeley; Jonathan Bray, UC Berkeley; Julien Cohen-Waeber, UC Berkeley; Tim Dawson, CGS; Les Harder, HDR; Ken Hudnut, USGS; Keith Kelson, U.S. Army Corps of Engineers; Tadahiro Kishida, PEER; Robert Lanzafame, UC Berkeley; Roberto Luque, UC Berkeley; Dan Ponti, USGS; Michelle Shriro, GEI Consultants; Nicholas Sitar, UC Berkeley; Nathaniel Wagner, UC Berkeley; John Wesling, State of California, Office of Mine Reclamation

Contributing Authors:
N. Abrahamson, PG&E; N. Avdievitch, USGS; T. Bayham, ENGEO; M. Bennett, USGS; Y. Bozorgnia, UC Berkeley; D. Branum, CGS; B. Brooks, USGS; C. Brossy, Fugro; B. Bryant, CGS; M. Buga, Fugro; H. Carlosama, UC Berkeley; B. Chiou, Caltrans; B. Collins, USGS; R. Darragh, Pacific Engineering and Analysis; C. Davenport, CGS; M. Delattre, CGS; S. DeLong, USGS; A. Donnellan, NASA – JPL; D. Dreger, UC Berkeley; U. Eliahu, ENGEO; Y-Nhi Enzler, California Division of Safety of Dams; T. Ericksen, Univ. of Hawaii; E. Fielding, NASA – JPL; S. Foti, Politecnico di Torino; M. Gardner, UC Berkeley; M. Glasscoe, NASA – JPL; C. Glennie, Univ. of Houston; C. Gutierrez, CGS; G. Harris, HDR; W. Haydon, CGS; S. Hecker, USGS; C. Hitchcock, InfraTerra; D. Hiteshew, City of Vallejo; J. Hollenback, PEER/UC Berkeley; T. Holzer, USGS; M. Jewett, Miller Pacific; P. Johnson, CSA; J. Lancaster, CGS; J. Lienkaemper, USGS; Y. Lu, UC Berkeley; A. Lutz, InfraTerra; J. Macedo, UC Berkeley; S. Mahin, UC Berkeley; M. Mareschal, CGS; C. Markham, UC Berkeley; S. Mazzoni, UC Berkeley; M. McAuley, California Highway Patrol; A. Morelan, UC Davis; S. Muin, UC Berkeley; M. Oskin, UC Davis; S. Owen, NASA – JPL; M. Panagiotou, UC Berkeley; J. Parker, NASA – JPL; A. Perez, CGS; M. Perlea, U.S. Army Corps of Engineers; V. Perlea, U.S. Army Corps of Engineers; A. Pickering, USGS; J. Pratt, RGH Consultants; C. Prentice, USGS; C. Pridmore, CGS; C. Rosa, USGS; R. Rubin, CGS; B. Schmidt, California Highway Patrol; D. Schwartz, USGS; G. Seitz, CGS; P. Shires, CSA; R. Sickler, USGS; M. Silva, CGS; M. Stanley, HDR; J. Stewart, UCLA; J. Thornburg, CGS; J. Tinsley, USGS; J. Treiman, CGS; D. Trench, Fugro; C. Trexler, UC Davis; B. Vanciel, City of Vallejo; S. Wang, UC Berkeley; J. Weber, HDR; D. Wells, AMEC; M. Wiegers, CGS; S. Yun, NASA – JPL; D. Zaccone, GeoVit

GEER Association Report No. GEER-037

Version 1: September 15, 2014

Geotechnical Engineering Reconnaissance of the August 24, 2014 M6 South Napa Earthquake

Table of Contents

Acknowledgments and Collaborations

The response to the August 24, 2014 M6 South Napa, California earthquake was a highly collaborative effort with significant collaboration amongst members of the following organizations:

California Geological Survey (CGS)
National Science Foundation (NSF)-Sponsored Geotechnical Extreme Events Reconnaissance (GEER) Association
Pacific Earthquake Engineering Research Center (PEER)
University of California, Berkeley (UCB)
U.S. Geological Survey (USGS)

This specific reconnaissance effort benefitted further from collegial interactions and collaborations with members of a variety of organizations. The collaborations and cooperation with the following organizations are most gratefully recognized:

California Earthquake Clearinghouse
California Department of Transportation (Caltrans)
California Division of Safety of Dams (DSOD)
California Highway Patrol (CHP)
California Office of Emergency Services
California Seismic Safety Commission
California Strong Motion Instrumentation Program (CSMIP)
City of Napa, Public Works
Cotton, Shires & Associates, Inc. (CSA)
County of Napa, Public Works
Department of Water Resources (DWR)
Earthquake Engineering Research Institute (EERI)
ENGEO, Inc.
Fugro, Inc.
GEI Consultants
HDR Engineering, Inc. (HDR)
NASA Jet Propulsion Laboratory
Pacific Gas and Electric Company (PG&E)
Univ. of California, Davis
Univ. of California, Los Angeles
U.S. Army Corps of Engineers (USACE)

The work of the GEER Association is based upon work supported in part by the National Science Foundation through the Geotechnical Engineering Program under Grant No. CMMI-0825734. Any opinions, findings, and conclusions or recommendations expressed in this material are those of the authors and do not necessarily reflect the views of the NSF. The GEER Association is made possible by the vision and support of the NSF Geotechnical Engineering Program Directors: Dr. Richard Fragaszy and the late Dr. Cliff Astill. GEER members also donate their time, talent, and resources to collect time-sensitive field observations of the effects of extreme events.

The sections of this report were prepared by topic leaders who worked collaboratively with dozens of researchers who contributed their observations and data. Their efforts are acknowledged as follows:

Section 1 was prepared by Julien Cohen-Waeber and Nicholas Sitar of the Univ. of California, Berkeley with contributions from Nathaniel Wagner, Univ. of California, Berkeley.

Section 2 was prepared by Tadahiro Kishida of the Pacific Earthquake Engineering Research Center, with Shanshan Wang, Univ. of California, Berkeley, Silvia Mazzoni, Univ. of California, Berkeley, Christopher Markham, Univ. of California, Berkeley, Yuan Lu, Univ. of California, Berkeley, Yousef Bozorgnia, Univ. of California, Berkeley, Stephen Mahin, Univ. of California, Berkeley, Jonathan Bray, Univ. of California, Berkeley, Marios Panagiotou, Univ. of California, Berkeley, Jonathan Stewart, Univ. of California, Los Angeles, Robert Darragh, Pacific Engineering and Analysis, Norman Abrahamson, Pacific Gas and Electric Company, Justin Hollenback, Pacific Earthquake Engineering Research Center, Carlos Gutierrez, California Geological Survey, Brian Chiou, California Department of Transportation, Sifat Muin, Univ. of California, Berkeley, and Douglas S. Dreger, Univ. of California, Berkeley. Much of this effort was financially supported by the Pacific Earthquake Engineering Research Center. The authors of this section would also like to thank Grace Kang, Stephen LaBounty for managing the timeline of the report and Claire Johnson for organizing and editing of this section of the report. Authors acknowledge California Geological Survey, California Strong Motion Instrumentation Program, and USGS for the access of the strong motion records for the event.

Section 3 was prepared by Tim Dawson, California Geological Survey, Keith Kelson, U.S. Army Corps of Engineers, John Wesling, State of California, Office of Mine Reclamation, Ken Hudnut, U.S. Geological Survey, and Dan Ponti, U.S. Geological Survey, with contributions from Nikita Avdievitch (USGS), Mike Bennett (USGS), Dave Branum (CGS), Jonathan Bray (UCB), Ben Brooks (USGS), Cooper Brossy (Fugro), Bill Bryant (CGS), Mike Buga (Fugro), Julien Cohen-Waeber (UCB), Brian Collins (USGS), Clif Davenport (CGS),Marc Delattre (CGS), Steve DeLong (USGS), Andrea Donnellan (NASA – JPL),Todd Ericksen (Univ. of Hawaii), Eric Fielding (NASA – JPL), Margaret Glasscoe (NASA – JPL), Craig Glennie (Univ. of Houston), Les Harder (HDR), Wayne Haydon (CGS), Suzanne Hecker (USGS), Chris Hitchcock (InfraTerra), Tom Holzer (USGS), Michael Jewett (Miller Pacific),, Jeremy Lancaster (CGS), Jim Lienkaemper (USGS), Andy Lutz (InfraTerra), Max Mareschal (CGS), Alexander Morelan (UC Davis), Mike Oskin (UC Davis), Susan Owen (NASA – JPL), Jay Parker (NASA – JPL), Ante Perez (CGS), Alexandra Pickering (USGS), Carol Prentice (USGS), Jared Pratt (RGH Consultants), Cindy Pridmore (CGS), Ron Rubin (CGS), Carla Rosa (USGS), David Schwartz (USGS), Gordon Seitz (CGS), Robert Sickler (USGS), Mike Silva (CGS), Nicholas Sitar (UCB), Jenny Thornburg (CGS), Jerry Treiman (CGS), John Tinsley (USGS), David Trench (Fugro), Chad Trexler (UC Davis), Donald Wells (AMEC), Mark Wiegers (CGS), Sang-Ho Yun (NASA – JPL), Dana Zaccone (GeoVit)

Section 4 was prepared by Julien Cohen-Waeber, Univ. of California, Berkeley, Robert Lanzafame, Univ. of California, Berkeley, and Jonathan Bray, Univ. of California, Berkeley, with contributions from Heyder Carlosama, Univ. of California, Berkeley, Sebastiano Foti, Politecnico di Torino, Michael Gardner, Univ. of California, Berkeley, Garrett Harris, HDR Engineering Inc., Justin Hollenback, Univ. of California, Berkeley, Philip Johnson, Cotton Shires & Associates Inc., Roberto Luque, Univ. of California, Berkeley, Christopher Markham, Univ. of California, Berkeley, Nicholas Sitar, Univ. of California, Berkeley, Nathaniel Wagner, Univ. of California, Berkeley, and Joseph Weber, HDR Engineering Inc. This section was also made possible by the consent of the 27 property owners whose homes were investigated, we are grateful for their cooperation.

Section 5 was prepared by Nathaniel Wagner, Univ. of California, Berkeley, Roberto Luque, Univ. of California, Berkeley, and Nicholas Sitar, Univ. of California, Berkeley, with contributions from Jonathan Bray (UCB), Heyder Carlosama (UCB), Julien Cohen-Waeber, Univ. of California, Berkeley, Michael Gardner (UCB), and Robert Lanzafame, Univ. of California, Berkeley.

Section 6 was prepared by Christine Beyzaei, Univ. of California, Berkeley, Michelle Shriro, GEI Consultants, and Jonathan Bray, Univ. of California, Berkeley, with contributions from Julien Cohen-Waeber, Univ. of California, Berkeley, Roberto Luque, Univ. of California, Berkeley, Christopher Markham, Univ. of California, Berkeley, Michael Gardner, Univ. of California, Berkeley, Philip Johnson, Cotton, Shires and Associates, Inc., Patrick O. Shires, Cotton, Shires and Associates, Inc., Ted Bayham, ENGEO, Uri Eliahu, ENGEO, and representatives of Lennar Mare Island, LLC.

Section 7 was prepared by Les Harder, HDR Engineering, Inc. with contributions from Jorge Macedo, Univ. of California, Berkeley with additional information or assistance contributed from Y-Nhi Enzler, California Division of Safety of Dams; Keith Kelson, United States Army Corps of Engineers; Mary Perlea, United States Army Corps of Engineers; Vlad Perlea, United States Army Corps of Engineers; Mark Stanley, HDR Engineering, Inc.; Brian Vanciel, City of Vallejo; Dan Hiteshew, City of Vallejo; Mike McAuley, California Highway Patrol; and Ben Schmidt, California Highway Patrol.

Section 8 was prepared by Jonathan Bray, Univ. of California, Berkeley, and Nicholas Sitar, Univ. of California, Berkeley.

We thank Anne Rosinski of the California Earthquake Clearinghouse whose coordination efforts empowered the authors of this report to complete effectively their documentation of this earthquake. We thank the staff at EERI, and in particular Heidi Tremayne, for their collaborative interactions and event coordination activities. We also thank the California Highway Patrol, Golden Gate Division, whose Napa Airport helicopter pilots donated their time and resources to provide overflight coverage of the affected area, including: Mike McAuley, Pilot, Ben Schmidt, Flight Officer, Bruce Hooley, Lieutenant, and James Libby, Captain. Lastly, we thank all of the contributors to this report, lead authors and contributing authors, who unselfishly volunteered their time and talent to complete this effort.

Extreme Event Reconnaissance requires careful planning and implementation. In many cases, the hazards are not just the result of already existing collapses but are just as likely to be the result of additional extreme events such as earthquake aftershocks or delayed collapse of already weakened infrastructure systems due to ongoing rescue and recovery activities. To ensure that individuals participating in such reconnaissance activities due so with the utmost attention to safety, GEER has developed a culture of safety and collaboration as it plans and implements its activities and considers these two factors to be critical components of their work.

1 INTRODUCTION AND GEOLOGIC SETTING

1.1 Introduction

On August 24, 2014 10:20:44 (UTC), a magnitude M_w 6.0 earthquake occurred on the West Napa Fault zone, a system of faults striking NNW from American Canyon and along the western edge of Napa Valley in Northern California. The epicenter was located at N 38.220 W 122.313, approximately 8 km SSW of Napa, California, 14 km ESE of Sonoma, California, and 81 km WSW of Sacramento, California, with a focus depth of 10 km. The West Napa Fault zone is located within the greater San Francisco Bay regional fault system in association with the western tectonic boundary of the North American plate, which accommodates approximately 40 mm/year of dextral shear. Effects of the earthquake were widely observed across the Napa Valley region from Vallejo and Mare Island in the South to the North end of Napa Valley. Clear expressions of surface fault rupture extended approximately 12 - 15 km northward from Cuttings Wharf to Alston Park and approximately 1-2 km southeast in American Canyon (Figure 1.1). The South Napa Earthquake is the first to produce significant surface rupture in Northern California since the 1906 San Andreas fault event, and the first to rupture through a densely populated area in Northern California.

In response to this event, the National Science Foundation (NSF) funded Geotechnical Extreme Events Reconnaissance association (GEER) deployed teams throughout the region to investigate the effects of the earthquake. The preliminary objective of the reconnaissance was to record the effects of strong shaking and ground failure on infrastructure, such as the prevalence of liquefaction, landsliding and surface fault rupture. Within 24 hours of the event, the initial observations showed a remarkable absence of liquefaction or landslide induced ground deformations. However, there was well defined surface rupture that produced various types of damage to structures and there was a pattern of damage to sidewalks and curbs suggesting sympathetic ground deformations within the vicinity of the fault zone.. As a result the subsequent investigative effort was focused on documenting the following:

- Seismology and ground motions of the event,
- Detailed mapping of surface fault rupture and the affected fault traces,
- Recording infrastructural damage due to ground surface rupture,
- Measuring ground deformation in the very near fault region,
- Assessing the performance of ground and buried utilities,
- And, assessing the performance of dams and levees.

The results of these efforts are presented in this report.

The characteristics of the strong-motion recordings from the earthquake, in the vicinity of American Canyon, CA, are summarized in Section 2 and Appendix A. The data are compared to the latest ground motion prediction equations (GMPEs) and current design spectra.

Section 3 and Appendix B document the key observations of surface fault rupture in the weeks following the South Napa event. Given the rare opportunity to study the effects of surface rupture, a significant effort was made to document the rupture both in the field and using various remote sensing methods as Interferometric Synthetic Aperature RADAR (InSAR), Light Detection And Ranging (LiDAR), and Global Positioning Systems (GPS).

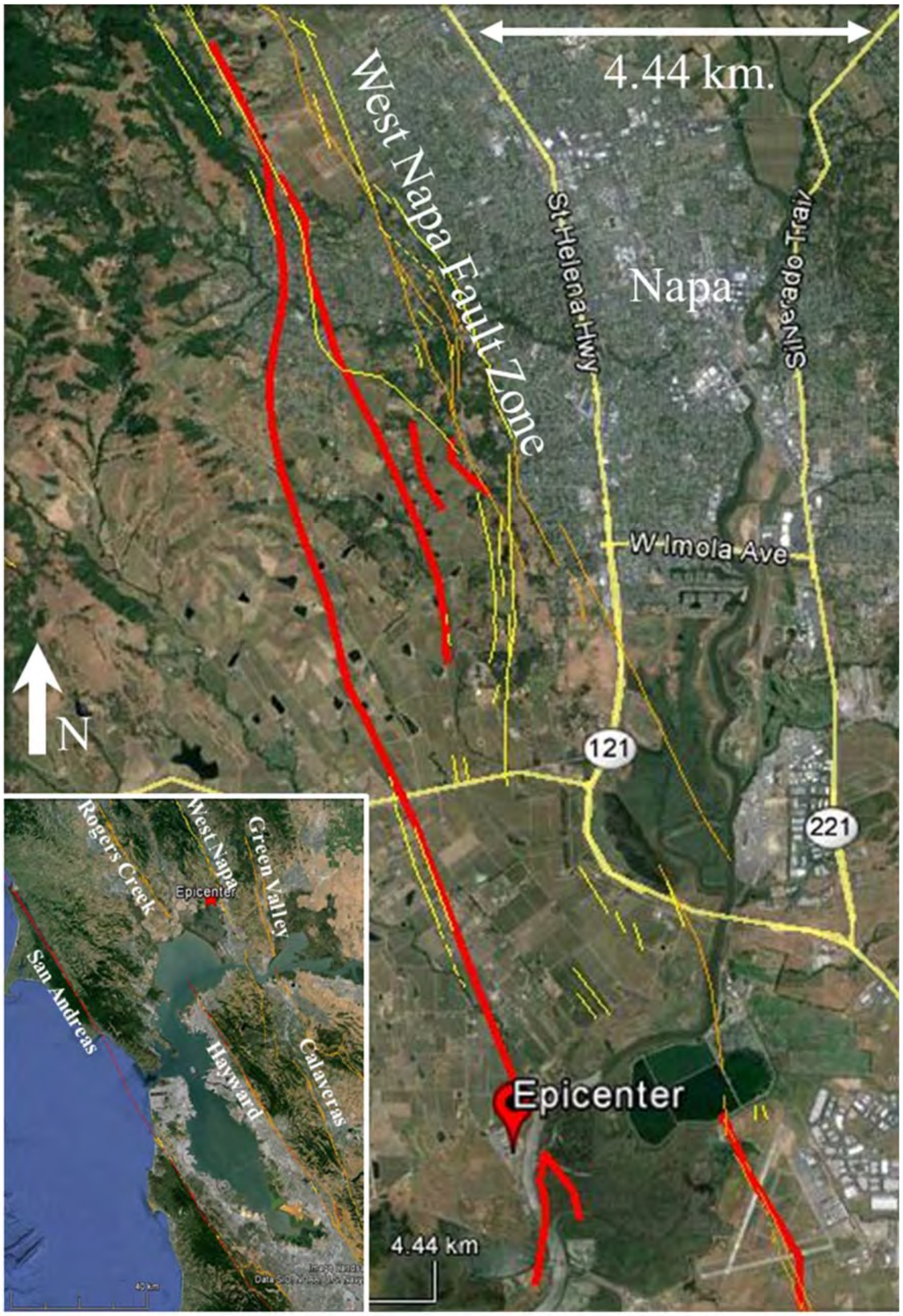

Figure 1.1 Map of the approximate tectonic rupture trace for the August 24, 2014 $M_w = 6$ South Napa Earthquake with Regional Fault Map of the San Francisco Bay Area. [NSF-GEER; J. Cohen-Waeber; 09/14/2014]

Section 4 and Appendix C address the effects of surface fault rupture on infrastructure. This effort consisted of an extensive investigation of damaged property along densely populated lengths of the rupture trace. Permanent deformation of and damage to different types of residential structures were carefully recorded and are summarized here.

Section 5 and Appendix D address ground deformation in the very near fault region. The focus of activities for this section was to record deformation near areas with prominent surface fault rupture, primarily in sidewalk pavement. Local and global (on the order of street lengths) strain measurements were computed to provide insight into the distribution of strains in the fault parallel and the fault normal directions. Additional observations concerning deformation of long, linear infrastructure were noted and addressed as necessary.

Section 6 and Appendix E address the performance of ground and buried utilities. This section describes the investigations of damage outside the zone of surface fault rupture and associated very near fault ground deformation. Notably, the low occurrence of liquefaction and landslide induced ground deformation is discussed, as well as several isolated instances of broken underground pipelines and masonry building damage.

Section 7 and Appendix F address the performance of dams and levees. 34 dams are located within 20 kilometers of the South Napa Earthquake energy source, all of which experienced little to no significant damage. Observations of their performance from aerial and field reconnaissance are summarized.

1.2 **Geologic Setting**

The August 24, 2014 M_w = 6 South Napa Earthquake occurred near the North shore of San Pablo Bay, and the South end of the Napa Valley, at the North end of the greater San Francisco Bay, California. The local geology is the product of an approximately 360 million year old accretionary process during which the North American Plate margin transitioned from subduction of the Farallon Plate to a transform boundary against the Pacific Plate. Geomorphically the region is within the California Coast Range province and is characterized by northwest trending valleys and low lying mountain ranges.

The Napa Valley is underlain by marine Cretaceous and Jurassic sedimentary rock which are overlain by Early Tertiary marine sedimentary rocks and Late Tertiary volcanics which outcrop primarily at higher elevations within the Valley. The Valley itself is filled with up to 160 m of older Pleistocene alluvial deposits overlain by up to 10 m of recent Holocene alluvial deposits, generally composed of moderately to poorly sorted sands, gravels, silts and clays. Where the South end of the Napa valley meets San Pablo Bay, recent Holocene Bay Mud deposits reach up to 40 m in thickness. Groundwater tables range in depth from 1.5 – 24 m with seasonal fluctuations of 1.5 – 3 m.

The West Napa Fault zone is generally considered as a relatively minor but active system of faults within the greater and seismically active San Francisco Bay Region which accommodates approximately 40 mm/yr of dextral shear. It is located East of the Hayward-Rogers Creek Fault zone, and West of the Concord-Green Valley Fault zone. The South Napa Earthquake occurred along the West Napa Fault, near the Carneros-Franklin fault and is known to be a right lateral fault with a slight westerly dip-slip component. Though this is the largest seismic event to have occurred in the San Francisco Bay Area since the M_w = 6.9 1989 Loma-Prieta Earthquake, an unmapped fault West of the West Napa fault produced the $M_w = 5$ Yountville/Napa Earthquake in September of 2000, within 30 km of the South Napa Earthquake epicenter. Hence this area is clearly seismically active.

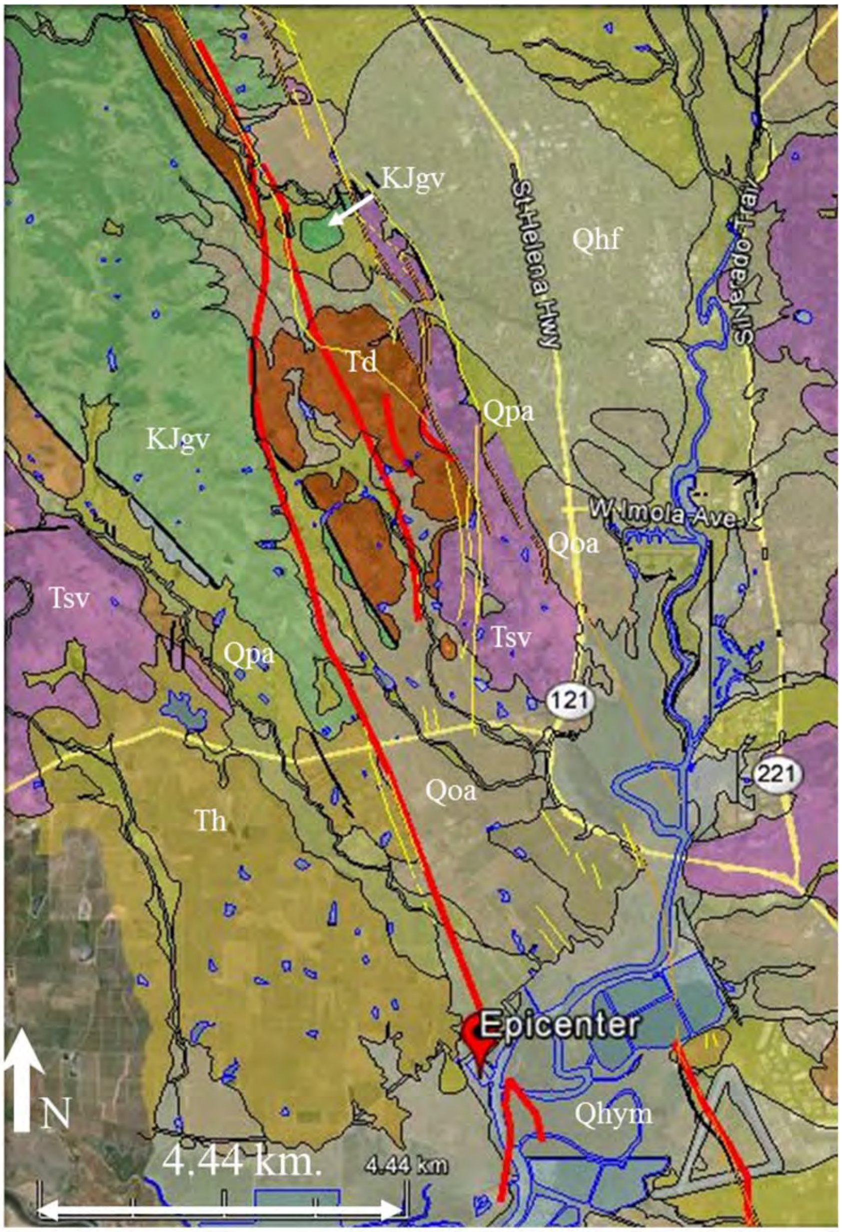

Figure 1.2 Geologic map and approximate trace of tectonic rupture (red) for the August 24, 2014 $M_w = 6$ South Napa Earthquake. Qhym - Holocene Bay Mud Deposits, Qhf - Holocene Alluvial Fan Deposits, Qpa/Qoa - Pleistocene Alluvium, Th - Pliocene/Pleistocene Huichica Fm. Sedimentary, Tsv - Miocene/Pliocene Sonoma Volcanics (Mafic flows and Tuffs), Td - Eocene/Miocene Domengine Sandstone, KJgv - Cretaceous/Jurassic Great Valley Sequence Sedimentary. [NSF-GEER; J. Cohen-Waeber; 09/14/2014]

2 SEISMOLOGY AND EARTHQUAKE GROUND MOTIONS

This report summarizes a preliminary study on the characteristics of the strong-motion recordings from the **M** 6.0 South Napa, California, Earthquake of August 24, 2014. The effort includes strong-motion data collection, data processing, metadata computation such as source-to-site distances, and estimates of site parameters such as V_{s30}. Strong motion recordings (PGA $\geq$0.30g) are reviewed at near-fault stations. Pseudo-Spectral Acceleration (PSA) values (5% damped) are compared to those estimated with the latest ground motion prediction equations (GMPEs) and current design spectra.

1.1 INTENSITY DISTRIBUTIONS

The South Napa Earthquake occurred on August 24, 2014 at 10:20:44 (UTC) in the West Napa fault zones. Figure 1 shows the ShakeMap from USGS website for this event (http://earthquake.usgs.gov/earthquakes/eventpage/nc72282711#shakemap, last accessed 09/10/2014). The hypocenter is located at the south end of Napa Valley of a depth of 10 km. Instrumental intensity measurements from ShakeMap were distributed along the Napa Valley with a maximum of IX at Napa Fire Station No. 3. The figure also shows the stations for which strong-motion data were processed for inclusion of the PEER strong motion database.

1.2 STRONG MOTION RECORDS

1.2.1 Acceleration Time Series Observations

Strong ground motions were downloaded from the Center for Engineering Strong Motion Data (CESMD) at the web site (http://strongmotioncenter.org/, last accessed 09/13/2014). A total of 214 three-component uncorrected digital accelerograms were downloaded. These records were processed following the PEER standard procedure (Ancheta et al. 2014), which includes inspection of record quality, selection of time windows, such as P-waves, S-waves, and coda waves, and component specific filter corner frequencies to optimize the usable frequency range.

Table 1 shows seven stations that recorded a median horizontal peak ground acceleration (PGA) (RotD50; Boore. 2010) greater than 0.3 g. Three stations in Table 1 are in the City of Napa, for which the arithmetic average of PGA was 0.40 g. The average PGA decreased to 0.07 g in the cities of Petaluma and Pinole, and less than 0.03 g in Berkeley and San Francisco.

Figure 2 shows the acceleration time series recorded at the stations listed in Table 1. Figure 2a, 2b, and 2c show the time series for Up-Down (UD), North-South (NS), and East-West (EW) components, respectively. The records from the Carquinez Bridge Geotechnical Array #1 shows high-frequency spikes and recorded the largest PGA of nearly 1.0 g in NS direction (Figure 2b). Napa, Fire station No. 3 shows a long-period pulse in EW direction (Figure 2c), and recorded the largest instrumental intensity of IX (Figure 1). Figure 2 also shows that all the records have a significant duration of less than 10 seconds

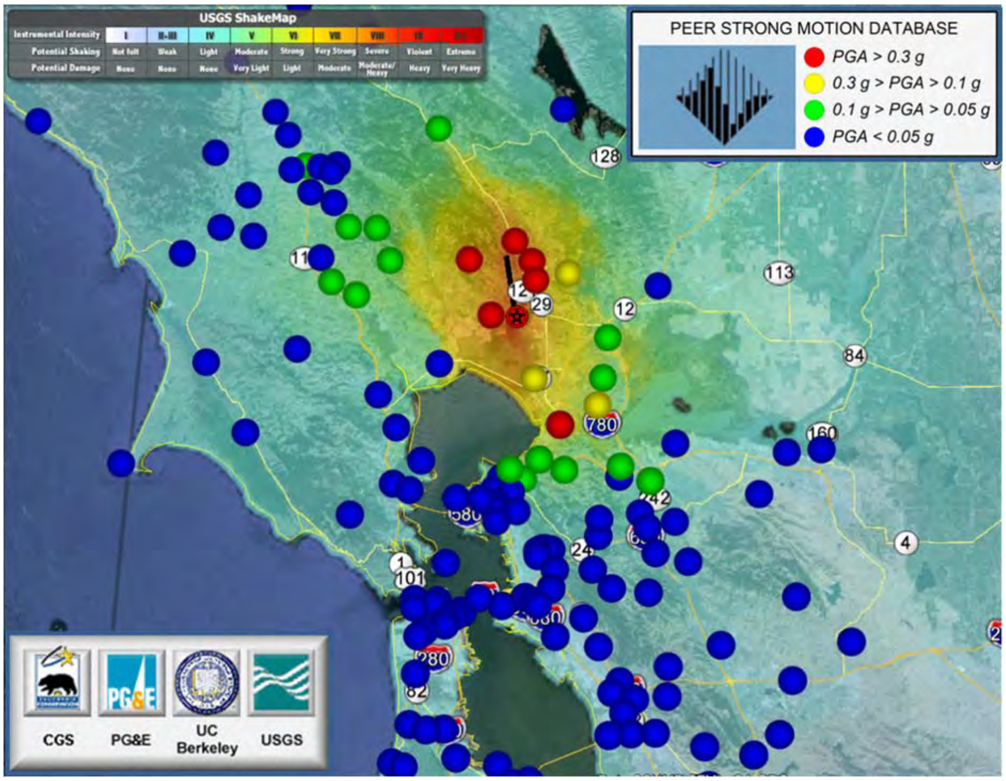

Figure 1 ShakeMap for South Napa Earthquake from the USGS overlaid with S strong motion stations processed by PEER

Table 1. Stations that recorded median PGA (RotD50) greater than 0.3 g

Station Name	Network [a)]	Station ID	Latitude (deg)	Longitude (deg)	R_{rup} [b)] (km)	V_{s30} [c)] (m/s)	PGA (g)
Napa; Fire Station No. 3	USGS	1765	38.330	-122.318	2.6	332	0.42
Huichica Creek	NCSN	NHC	38.217	-122.358	3.9	217	0.31
Main St, Napa	NCSN	N016	38.299	-122.285	3.9	285	0.45
Napa – Napa College	CGS	68150	38.270	-122.277	4.1	339	0.34
Lovall Valley Loop Rd	NCSN	N019B	38.301	-122.402	6.1	710	0.35
Crockett – Carquinez Bridge Geotechnical Array #2	CGS	68259	38.055	-122.226	19.9	342	0.34
Crockett – Carquinez Bridge Geotechnical Array #1	CGS	68206	38.054	-122.225	20.0	342	0.70

a) CGS = California Geological Survey \ California Strong Motion Instrumentation Program, NCSN = USGS Northern California Seismic Network

b) Source-to-site distance based on Boatwright (2014) preliminary finite fault plane model

c) Estimated V_{s30}

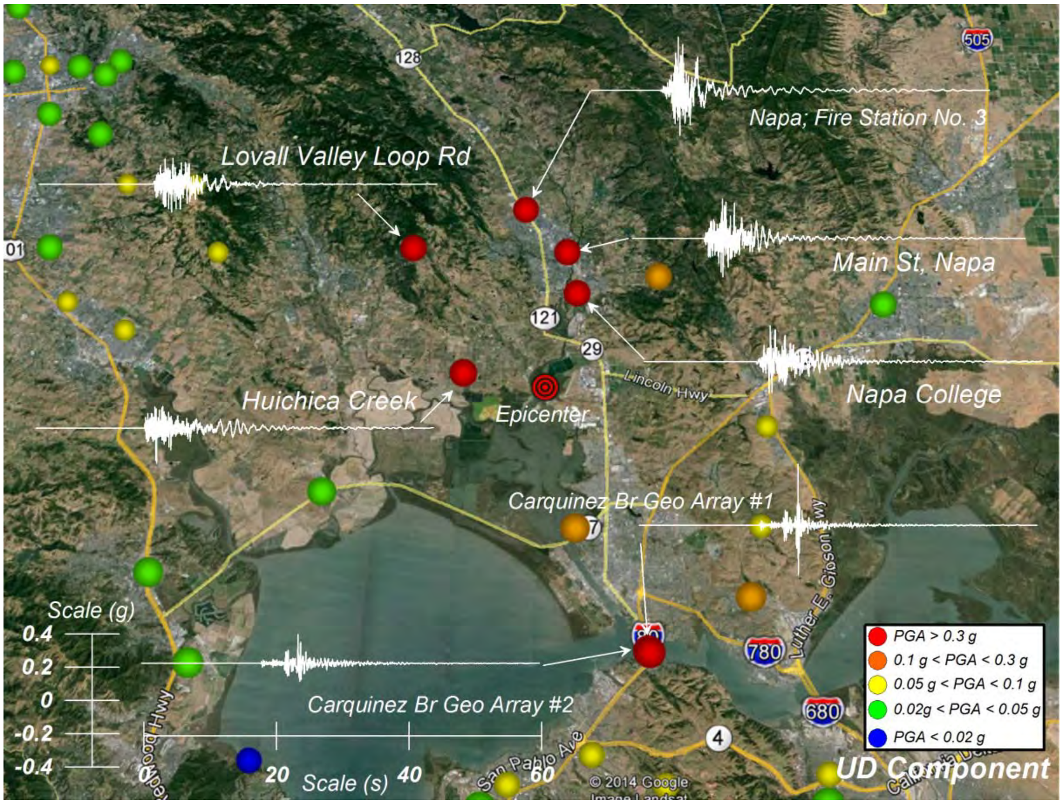

Figure 2a. Acceleration Time Series, UD Component

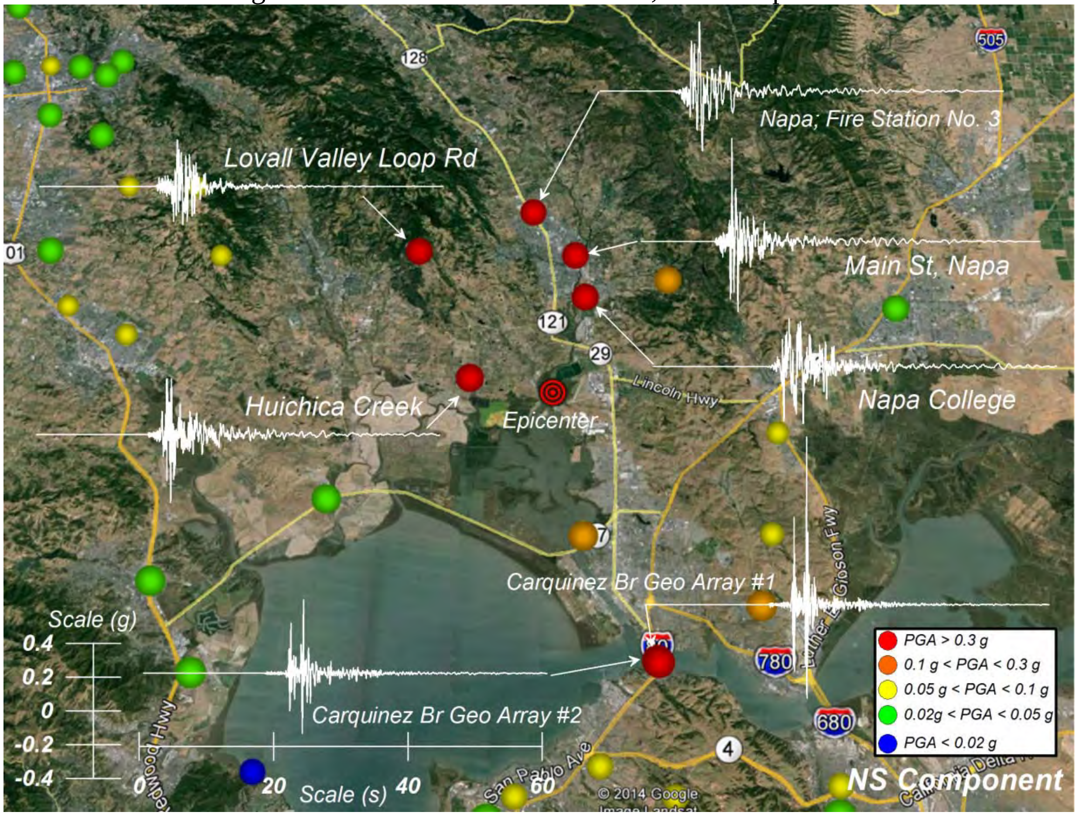

Figure 2b. Acceleration Time Series, NS Component

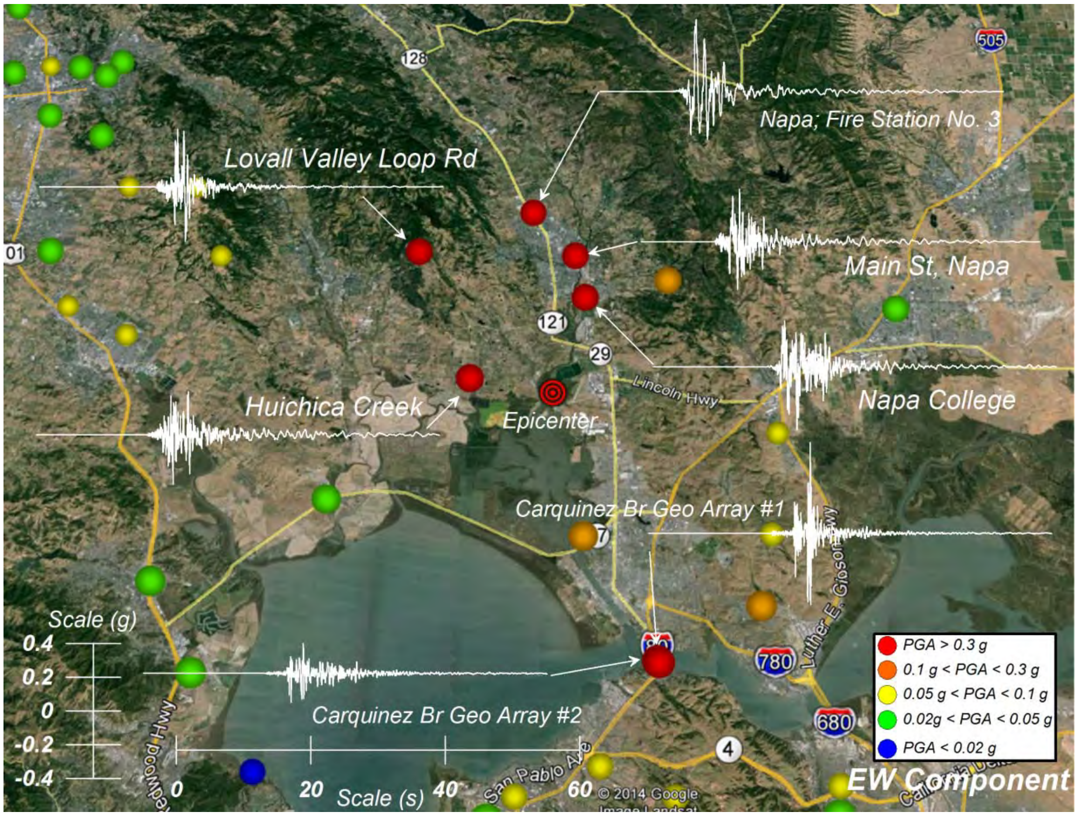

Figure 2c. Acceleration Time Series, EW Component

1.2.2 Near-Fault Pulse Observations

Pulse-like waveforms were observed in several of the velocity time series at the near-fault stations shown in Figure 2. On the basis of this observation, the horizontal components of near-fault velocity time series were rotated into fault-normal (FN) and fault-parallel (FP) orientations where the fault strike was taken as 155 degree (Figure 3). Maximum Peak Ground Velocity (PGV) was recorded as 84 cm/s in FP direction at Napa Fire Station No. 3. Based on visual inspection of Figure 3, Napa Fire Station No. 3 (FN, FP components), Lovall Valley Loop Rood (FN, FP components), Main St. (FN component), Huichica Creek (FP component), and Napa College (FN, FP components) show pulse-like waveforms in the velocity time series.

Appendix A Table 1 shows the recorded PGV (RotD50), expected PGVs and the periods by Bray et al. (2009) for these five stations. The Bray et al. (2009) relationship estimates a median PGV of about 50 to 60 cm/s for the fault-normal component of the five near-fault strong motion stations with a 16% to 84% range of about 35 to 85 cm/s. This captures the recorded near fault normal component PGVs fairly well. The period of the near-fault fault-normal velocity pulse was estimated to be within the range of 0.7 s to 2.0 s (16% to 84% values, respectively). The recorded velocity time series of the five near-fault records for the M6 South Napa earthquake contained shorter period velocity pulses within this estimated range, but they also contained longer period pulses significantly higher than this range. It is not clear if the longer period pulses were due to fault mechanism or site effects (e.g., deep basin response).

The following sections describe the characteristics of the velocity pulse near the fault evaluated by several different approaches.

1.2.2.1 Examination of Velocity Pulse by Hayden (2014) and Shahi (2013) Approaches

The presence of pulse-like motions in the near-fault region was studied through the examination of velocity records at five recording stations. Two methods were used to classify motions as pulse-like or non-pulse-like. The first scheme was proposed by Hayden et al. (2014), while the second classification scheme was proposed in Shahi (2013). Table 2 lists the recording stations examined and summarizes the results of the classification process. Plots of the resulting velocity records for the components with the highest “pulse-like tendencies” for each recording station for both the Hayden et al. (2014) and Shahi (2013) methods are provided in Appendix A.

For three of the five stations examined (Fire Station No. 3, Lovall Valley Loop Rd., and Huichica Creek) the two methods agree with regards to pulse classification. For the two remaining stations (Napa College and Main St. Napa) the two methods disagree with regards to the identification of a pulse-like motion. For the Napa College station, the Shahi (2013) scheme identifies a pulse, while the Hayden et al. (2014) method yields a pulse score of 25%, which is below the proposed pulse score threshold of 60%. The discrepancy between the two classifications for this station could be due to the presence of two significant cycles in the velocity time history, which downgrades the significant cycle sub-score that contributes to the overall pulse score in the Hayden et al. (2014) procedure. The discrepancy between the classification results for the Main St. Napa station is not as easily explained through the salient features of the velocity time series.

Importantly, the Huichica Creek station was in a backward directivity location and its maximum velocity and pulse component was roughly in the fault-parallel orientation. Three of the four remaining sites were in forward directivity locations and their maximum velocity and pulse components were within 30 degrees of the fault normal orientation.

Table 2: Results of Pulse Classification Methods

	Hayden et al. (2014)				Shahi (2013)		
Station Name	Pulse Score (%)	PPV[1] (cm/s)	Pulse Period (s)	Azimuth of Max PPV (°)	Pulse Identified	Azimuth of Max Pulse (°)	Pulse Period (s)
Fire Station No. 3	100	111	3.8	62	Yes	61.5	4.4
Huichica Creek	100	58.5	5.5	351	Yes	283.6	2.8
Lovall Valley Loop Rd.	100	64.3	3.9	61	Yes	20.7	3.6
Main St. Napa	92	62.3	3.4	56	No	29.7	3.9
Napa College	25	104	1.6	340	Yes	296.0	2.0

1) PPV = Peak-to-Peak Velocity (see Hayden et al. 2014)

1.2.2.2 Characterization of Near-fault Ground Motion Records by Lu and Panagiotou (2014)

This section presents a wavelet analysis of the ground motions recorded at two stations during the **M** 6 South Napa earthquake: Napa Fire Station No. 3 and Main St. recording stations. The originally recorded ground motion records were rotated (by Lu and Panagiotou) to the fault-normal (FN) and fault-parallel (FP) directions. The rotated ground acceleration and ground velocity histories, as well as the acceleration and displacement response spectra, for both components are shown in Appendix D Figure 1 and 2 for the Napa Fire Statiomn #3 and in Appendix D Figures 3 and 4 for the Main St. records. Both stations were expected to have been significantly affected by forward directivity.

The wavelet analysis was conducted using the cumulative pulse extraction (CPE) method described in Lu and Panagiotou (2014). The analysis was conducted in the velocity time domain and the order of the extracted pulses was determined based on the energy of the pulses ($CPE_{V,EN}$ method). For each motion, three pulses were extracted. The sum of the pulses in the time domain results in a representation of the ground motion. Appendix D Figures 1 to 4 show the extracted pulses in both the acceleration and the velocity time domain.

The Napa Fire Station No. 3 recordings include multiple strong pulses of significantly different predominant period T_P. The FP component (Appendix D Figure 1) exhibits the largest PGV which is the result of two pulses, one with $T_{P,1}$ = 1.1 s and another with $T_{P,2}$ = 3.9 s. The peaks of these two pulses are well correlated in the time domain. The FN component (Appendix D Figure 2) of the ground motion at Napa Fire Station No. 3 includes a strong pulse of $T_{P,1}$ = 1.9 s which determines the PGV of this motion. After that pulse a pulse with $T_{P,3}$ = 1.1 s follows in the time domain. The spectral demands for T larger than 3 s are dominated from the combination of the two pulses with $T_{P,1}$ =1.9 s and $T_{P,3}$ = 3.3 s. The FP component of the Main St. record (Appendix D Figure 3) exhibits a larger PGA than that of the FN component while the latter exhibits a larger PGV. The ground velocity waveform of the FN component is quite complex with the three pulses (T_{P1} = 3.1 s, $T_{P,2}$ = 1.2 s and $T_{P,3}$ = 0.6 s) to be highly correlated in the time domain.

1.2.1 Carquinez Bridge Records

This section discusses the time series recorded at the two Crockett – Carquinez Bridge Geotechnical Arrays by comparing the records along the source-to-site path and those from the three downhole arrays. The Geotechnical Arrays are a cooperative project of California Department of Transportation (Caltrans) and CSMIP.

The Crockett – Carquinez Bridge Geotechnical Array #1 recorded the largest PGA during the **M** 6 South Napa earthquake where the NS component reached approximately 1.0 g as shown in Figure 2a. Figure 4 shows the acceleration time series along strike direction from the epipocenter to the Carquinez Bridge. The recording at Carquinez Bridge Geotechnical Array #1 shows two high frequency spikes (approximately 10 Hz) after the S-wave arrival that have peak amplitudes of approximately 1.0 g in the North direction. Similar spikes were observed in the recordings at Carquinez Bridge Geotechnical Array #2, the Vallejo – Hwy 37/Napa River East Geotechnical Array, and at Napa College in Figure 4, although these amplitudes are smaller than those measured at the Carquinez Bridge Geotechnical Array #1. The record at Pinole Ridge did not show these spikes in the records. This observation may indicate that these spikes were amplified from the source to the Carquinez Bridge Geotechnical Array #1 site by path effects.

Figure 5 shows the downhole records for acceleration time series, 5%-damped Pseudo-Spectral Acceleration (PSA) and Fourier Amplitude Spectra (FAS) at Carquinez Bridge Geotechnical Array #1, #2, and Vallejo – Hwy. 37/Napa River East Geotechnical Array. Figures 5a and 5c show that the frequency content near 10 Hz were amplified through subsurface soil deposits of less than 20 m where Figure 5b shows that the frequency content near 3 Hz were amplified through subsurface soil deposit of less than 60 m. At all three arrays most of the amplification occurs between the middle sensor and the surface with less amplification between the deepest recording and the middle recording. The two high frequency spikes are observed after the direct S-wave arrival at all downhole arrays, these arrivals may be from S-waves radiated from other portions of the fault rupture to the north (e.g. http://earthquake.usgs.gov/earthquakes/eventpage/nc72282711#scientific_finite-fault).This observation may indicate that the large PGA observed at Carquinez Bridge could be a site effect caused by the soft soil deposits. These observations do not exclude the possibility of soil-structure interaction effects on the measured recordings, because these time series were recorded near bridge abutments and structures. Additional study is needed to understand the effects of source, path, site, and nearby structures on these recordings.

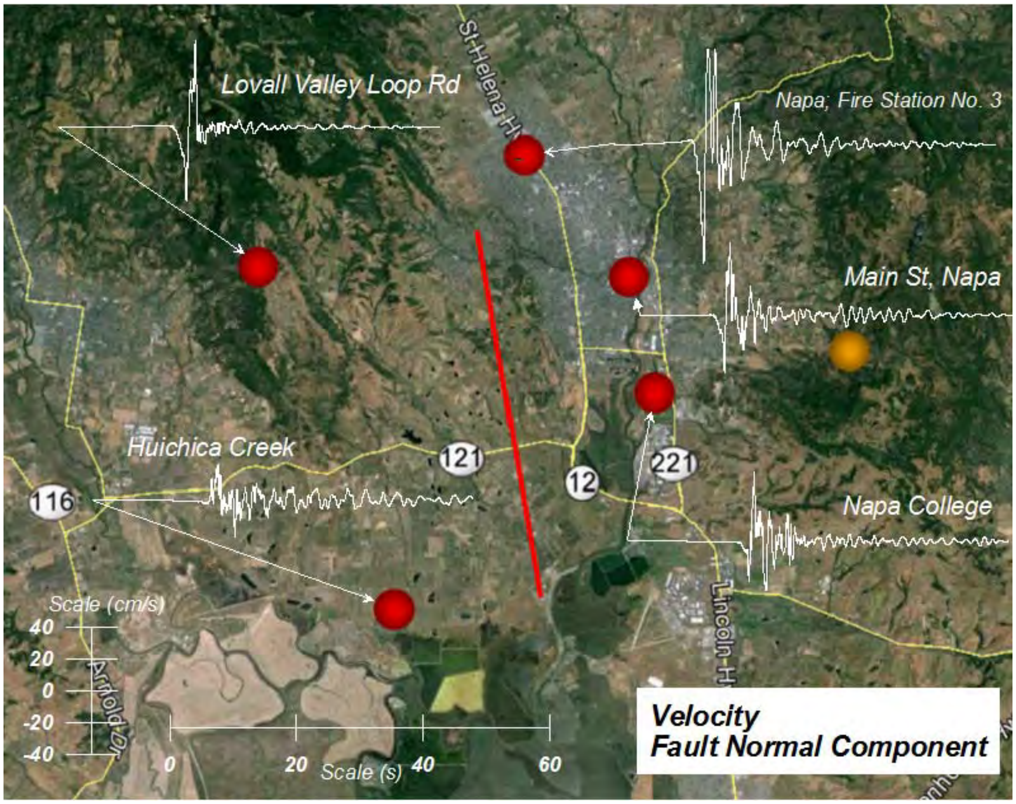

Figure 3a. Fault Normal Velocity Time Series

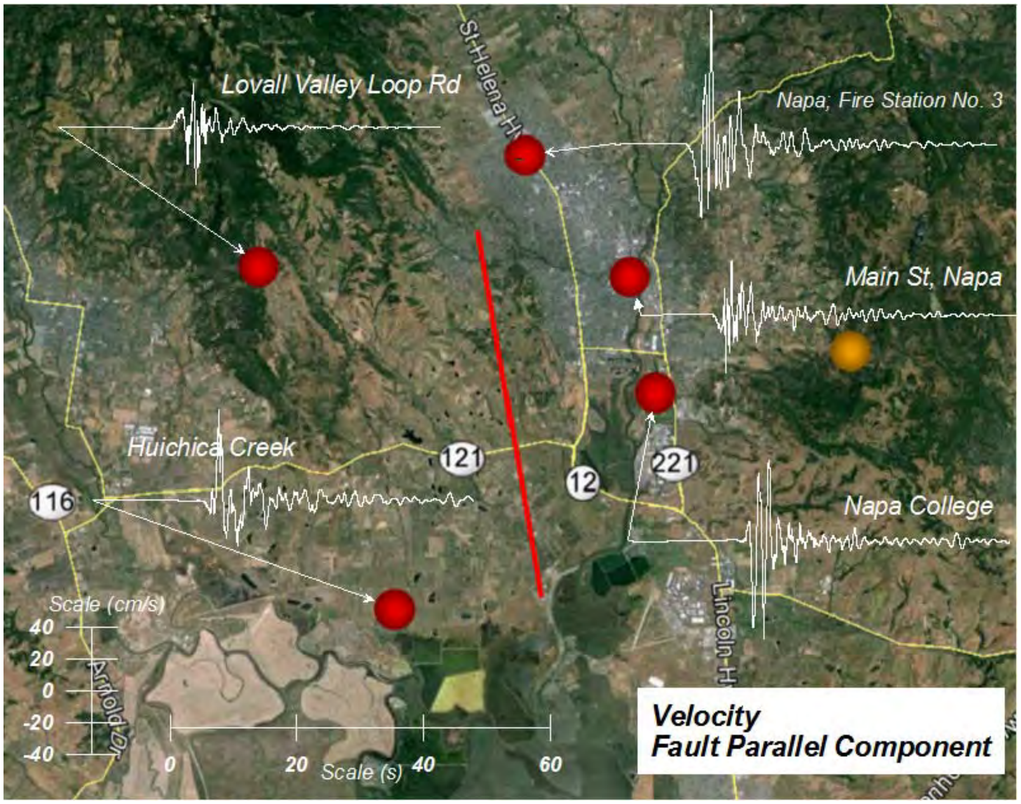

Figure 3b. Fault Parallel Velocity Time Series

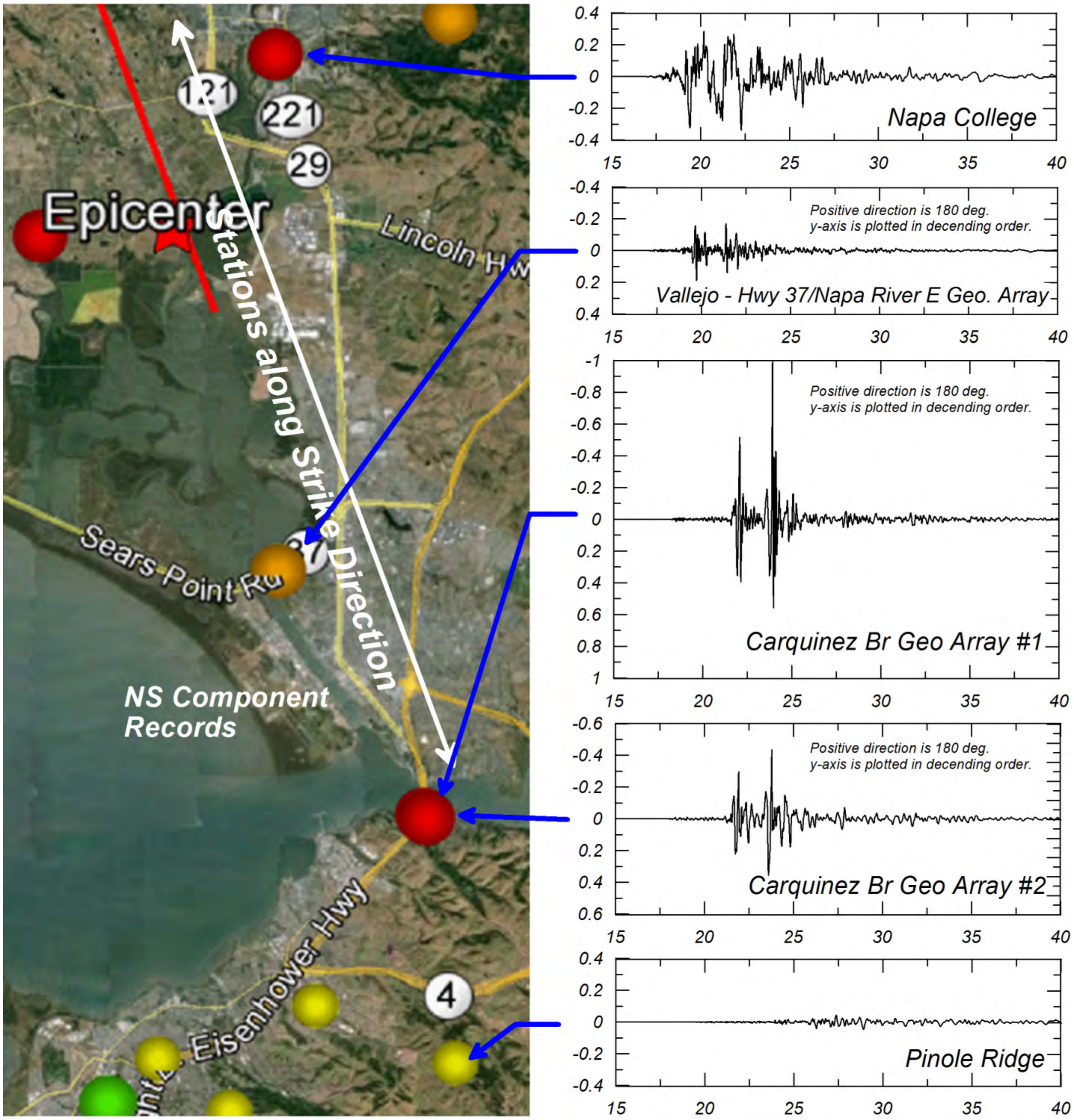

Figure 4. Acceleration time series along strike direction from source to Carquinez Bridge

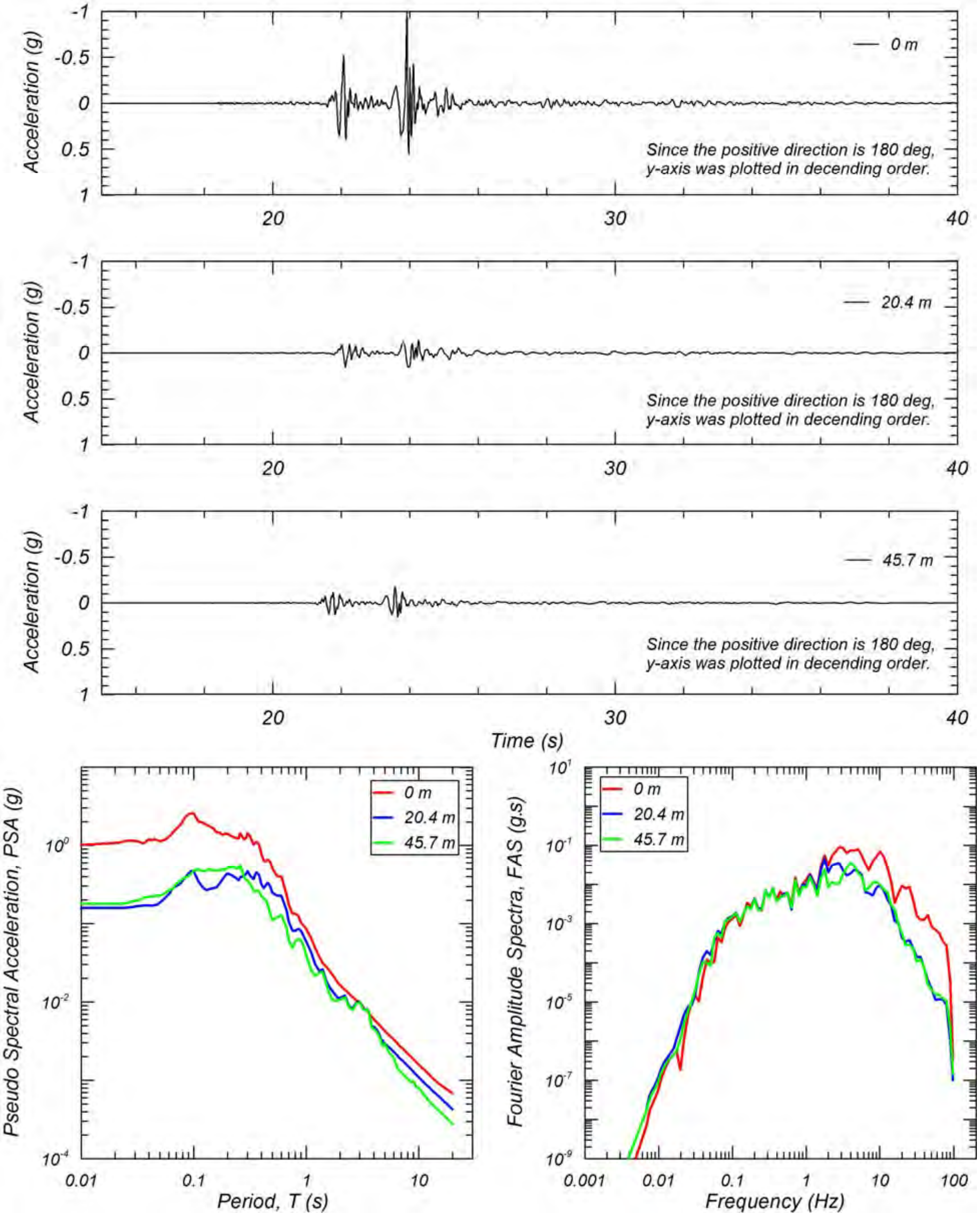

Figure 5a. Acceleration time series, 5% damped PSA, and FAS for Carquinez Bridge Geotechnical Array #1, NS Component

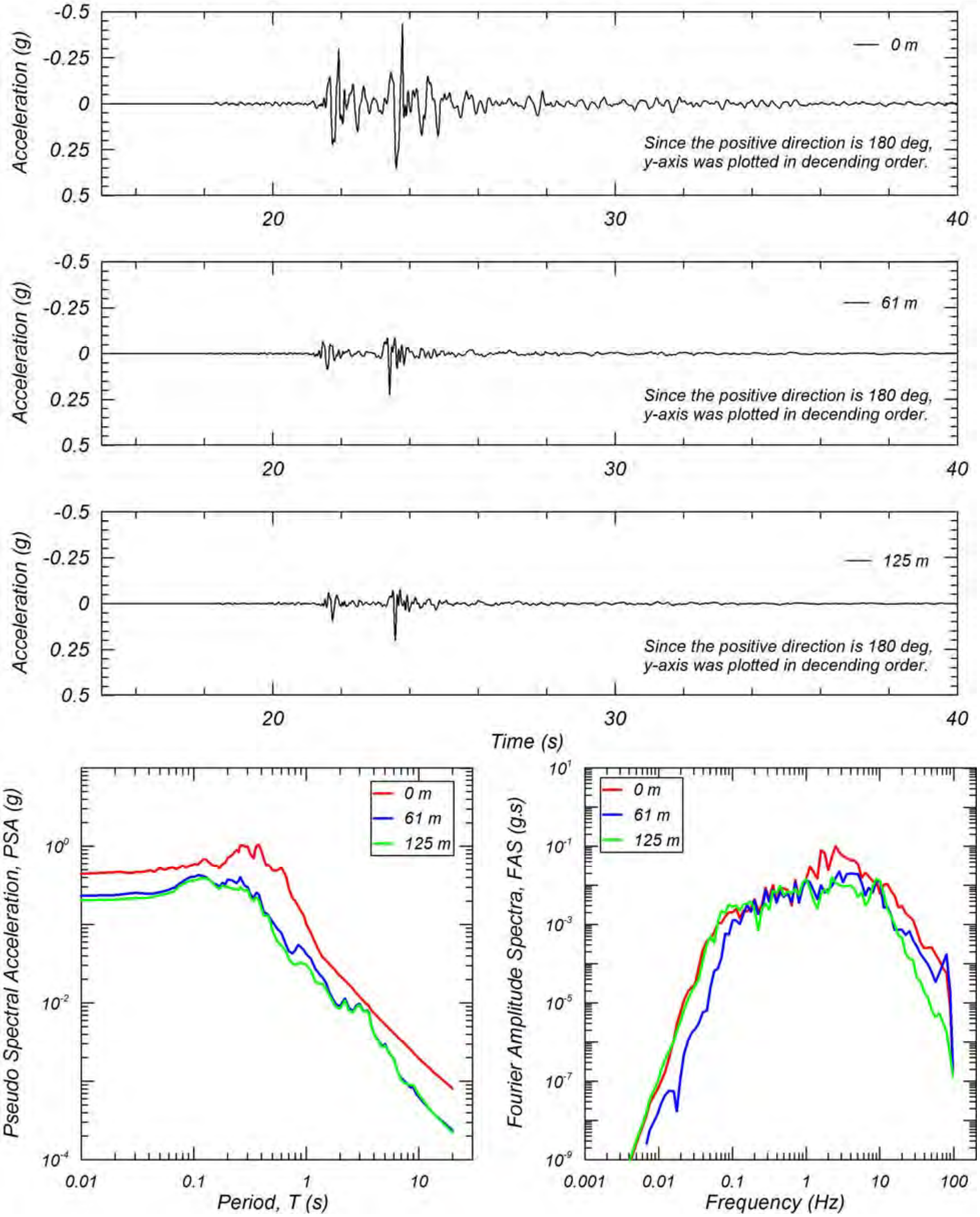

Figure 5b. Acceleration time series, 5% damped PSA, and FAS for Carquinez Bridge Geotechnical Array #2, NS Component

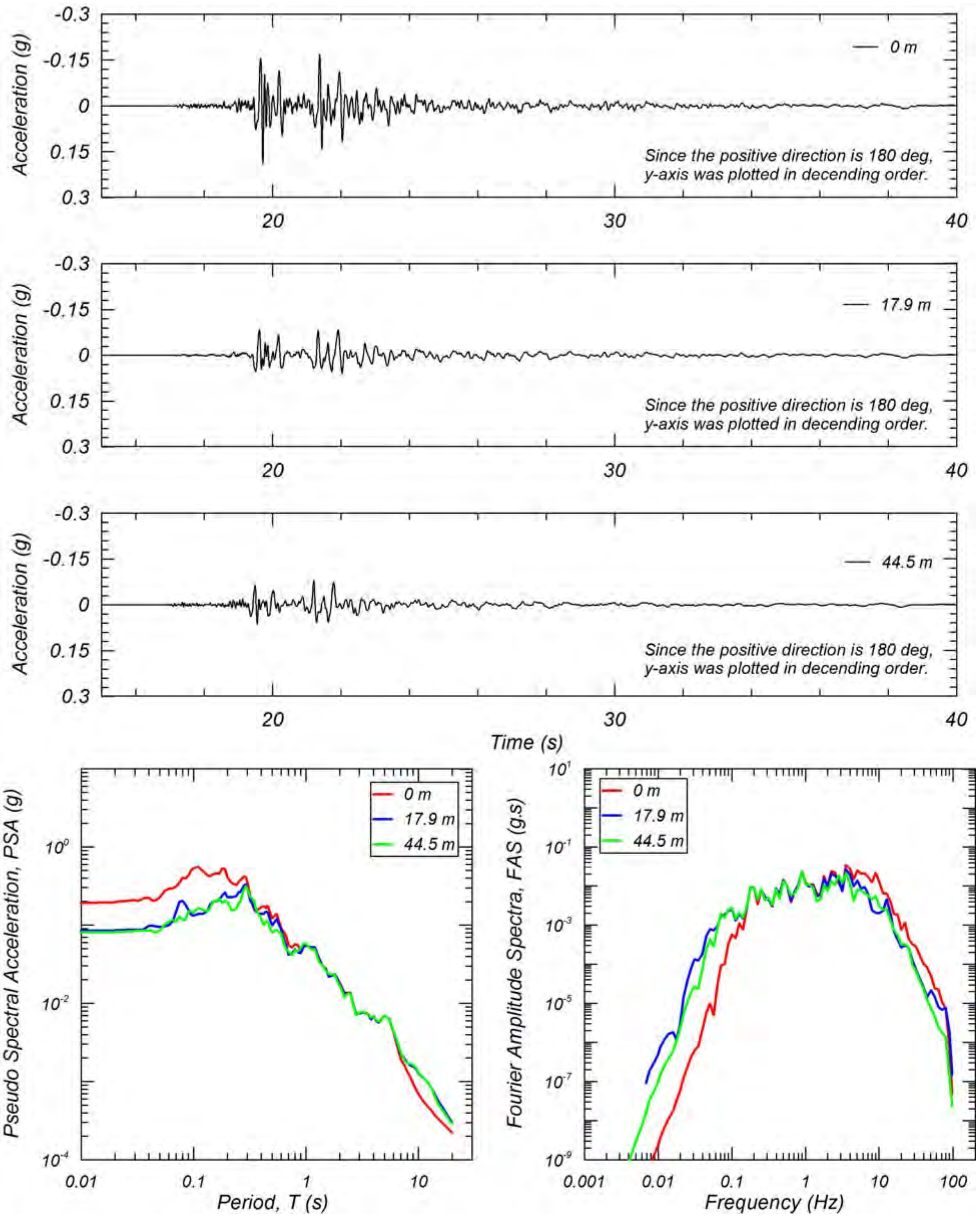

Figure 5c. Acceleration time series, 5% damped PSA, and FAS for Vallejo – Hwy 37/Napa River East Geotechnical Array, NS Component

1.3 ACCELERATION, VELOCITY AND DISPLACEMENT TIME SERIES

The acceleration, velocity, and displacement time series are plotted in Figure 6 for the NS component of Napa College Station. The figure also shows the Arias Intensity (AI), 5%-damped PSA, and FAS.

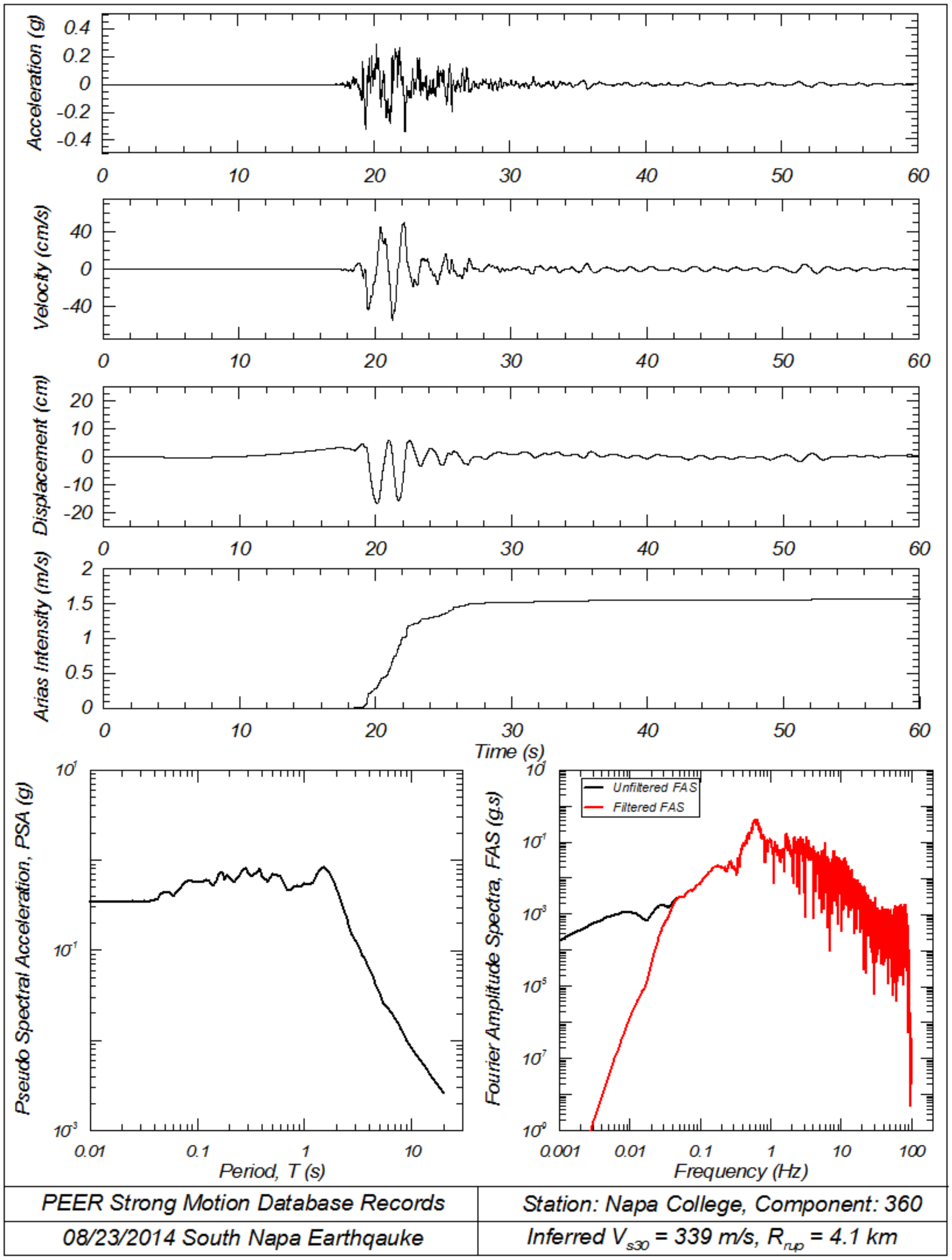

.

Figure 6. Summary of time series and spectra at Napa College Station (NS Component)

The PGA, PGV and AI recorded at this station were 0.339 g, 54.8 cm/s, and 1.56 m/s, respectively. The figure also shows the clear velocity pulse in the S-wave arrivals which was discussed in the previous section. The period of this waveform is approximately 1.5 s which is also seen in the pseudo-spectral acceleration (PSA) values (5% damped) in the figure. Similarly, the FAS has a peak amplitude near 0.7 Hz. Similar plots are presented in Appendix B for the other stations listed in Table 1.

1.4 COMPARISON TO GROUND-MOTION PREDICTION EQUATIONS

1.4.1 Fault Location and Recording Site Conditions

We reviewed the available surface slip and fault slip inversions and selected a preliminary preferred fault model for distance calculations. Fault mechanism and hypocenter location were obtained from the Northern California Earthquake Data Center (NCEDC) (http://www.ncedc.org/, last accessed 09/07/2014) (Table 3). The table shows that the earthquake fault mechanism is cstrike-slip based on the rake angle. Two preliminary finite fault models were available at the USGS website (http://earthquake.usgs.gov/earthquakes/eventpage/nc72282711#scientific_finite-fault, last accessed at 09/07/2014). One model inverts regional seismic waveforms for slip amplitude on the fault (Dreger, 2014). The second inverts regional GPS and InSAR data obtained by the USGS NEIC (Barnhart, 2014). Field observation of surface rupture are also available from the University of California, Davis (http://blogs.agu.org/tremblingearth/2014/08/30/earthquake-rupture-u-s-suburb/, last accessed at 09/07/2014) (Elliot 2014) The model using regional GPS and InSAR agree closely to the inversion model using regional seismic data regarding the depth and amount of peak slip. On the basis of these observations, we selected the finite fault model based on the inversion model using regional seismic data in Table 4 where rupture was extended to the ground surface based on the study (Boatwright 2014, http://earthquake.usgs.gov/product/shakemap/nc72282711/nc/1409779655706/download/boat_fault.txt, last accessed at 09/10/2014) that was based on observation of surface rupture. By using this preliminary fault model, the distance measures (R_{epi}, R_{hyp}, R_{rup}, R_{jb}, R_{sei}, and R_x) were computed for all 214 records. The strike and dip of the selected finite fault model in Table 4 are 170 and 90, respectively. These values are different from those by NCEDC in Table 3. However, we preferred the preliminary fault model in Table 4, because it will potentially provide distances with smaller errors taking into account the uncertainties in dip direction and the number of rectangular fault segments

Table 3. Fault mechanism and hypocenter location (NCEDC, 2014)

Moment Magnitude (**M**)	6.02
Fault strike (deg)	155
Fault dip (deg)	82
Fault rake (deg)	172
Hypocenter Latitude (deg)	38.20837
Hypocenter Longitude (deg)	-122.29894
Hypocenter Depth (km)	10.117

Table 4. Rectangular Finite fault models used in this study (Boatwright 2014)

Corner	Latitude (deg)	Longitude (deg)	Depth (km)
1	38.2200	-122.3130	0.0000
2	38.3100	-122.3331	0.0000
3	38.3100	-122.3330	11.0000
4	38.2200	-122.3131	11.0000

For site conditions, the site database developed by PEER during NGA-West2 study was used (Seyhan et al. 2014). From the NGA-West2 site database, site parameters such as V_{s30}, $Z_{1.0}$ and $Z_{2.5}$ were obtained for 98 stations out of the 214. For 116 stations, for which we did not have V_{s30} values, the estimated values were computed (Gutierrez 2014, personal communication) according to the methodology described by Seyhan et al. (2014). V_{s30} for the selected stations were also estimated from Geomatrix 3rd letter and by the method by Wald and Allen (2007). $Z_{1.0}$ and $Z_{2.5}$ are estimated from V_{s30} as described in Chiou and Young (2014) and Campbell and Bozorgnia (2014), respectively. Based on this approach, these site condition metadata were estimated for all 214 stations. As a result, the number of stations belonging to site class A, B, C, D, and E (ASCE 2010) are 0, 8, 126, 75, and 5, respectively. The median V_{s30} of all sites is 490 m/s, which will be used in the following section as reference V_{s30} to compare the recorded PSA to GMPE predictions.

1.4.2 Comparison of Pseudo-Spectral Acceleration (PSA) to Ground-Motion Prediction Equations (GMPEs)

The 5%-damped PSA for the motions recorded at the stations listed in Table 1 were compared to the 2014 NGA-West2 GMPEs (Abrahamson et al. 2014 [ASK14], Boore et al. 2014 [BSSA14], Campbell and Bozorgnia 2014 [CB14], and Chiou and Youngs 2014 [CY14]) by using the appropriate distance metrics and site conditions described in the previous sections. Figure 7 shows the horizontal PSA based on RotD50 compared with the weighted geometric mean of the GMPEs (ASK14, BSSA14, CB14, and CY14 with equal weight). The results show that the PGA predicted by the GMPEs match well with the recorded values except Carquinez Bridge Geotechechnical Array #1 and #2 shown in Figure 7(c) and (d). This observation indicates that the amplification of high frequency content described in the previous section is larger than the site effects expected from GMPEs by V_{s30}. It is also observed that the GMPEs tend to underestimate the PSA at periods greater than 0.5 s at Lovall Valley Loop Rd and Napa Fire Station No. 3 in Figure 7(e) and (f). These stations are located at northern edge of the fault model as shown in Figure 3. It is also observed that GMPEs do not capture the pulse observed at a period of 1.5 seconds for the Napa College records in Figure 7(a).

Figure 8 shows the vertical PSA compared with the GMPE by Bozorgnia and Campbell (, 2014**)**. The comparisons show a general satisfactory agreement between recorded and estimated values, especially at the short vertical periods that are important for the vertical component, with the following exceptions. Figure 8 shows that PGA are underestimated for Carquinez Br Geotech Array #1 and #2 in Figure 8(c) and (d). Similarly, PSA greater than 1 s are underestimated at Lovall Valley Loop Rd and Napa Fire Station No. 3 in Figure 8(e) and (f). These trends observed in vertical PSA are similar to those observed in horizontal PSA.

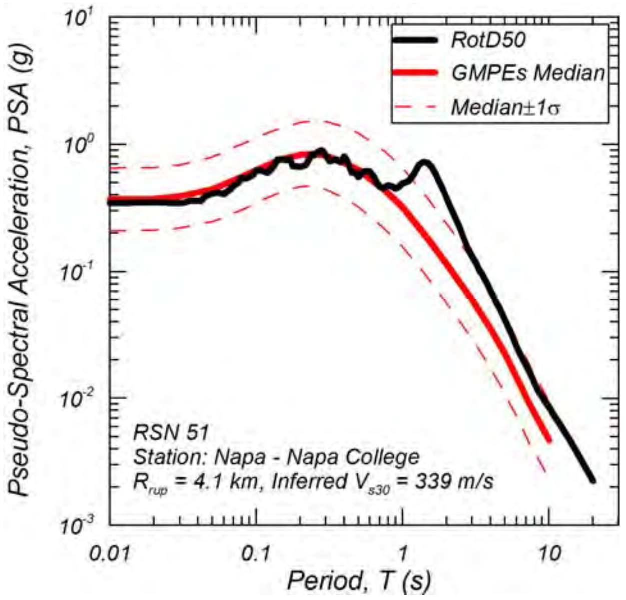

(a) Napa College

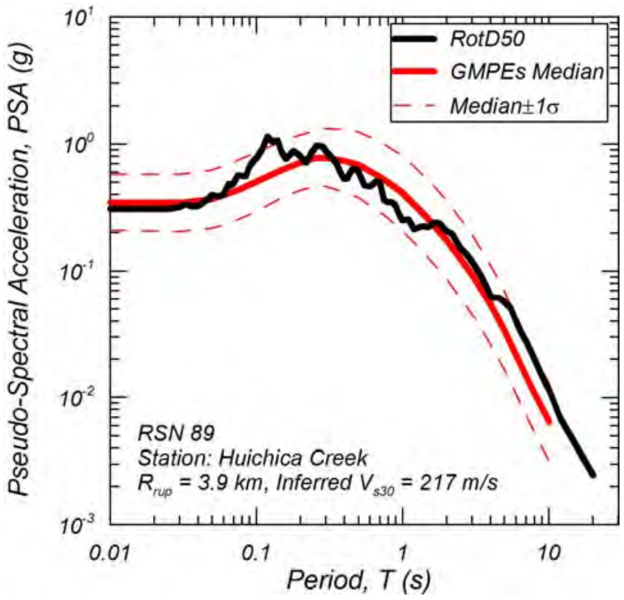

(b) Huichica Creek

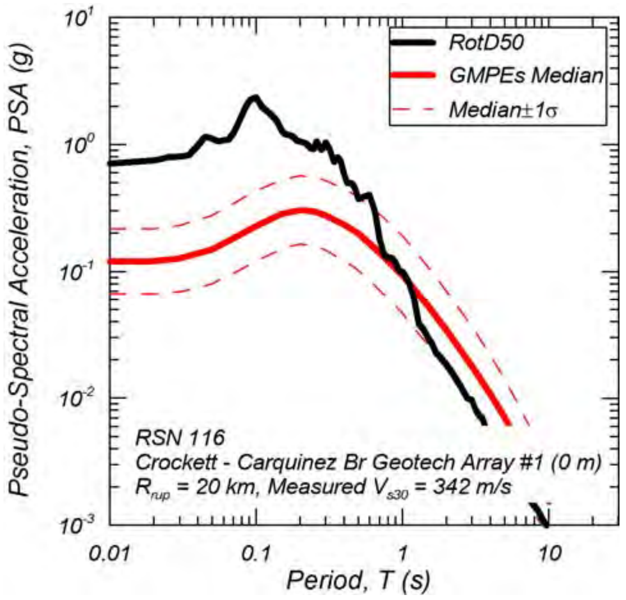

(c) Carquinez Br Geotech Array #1

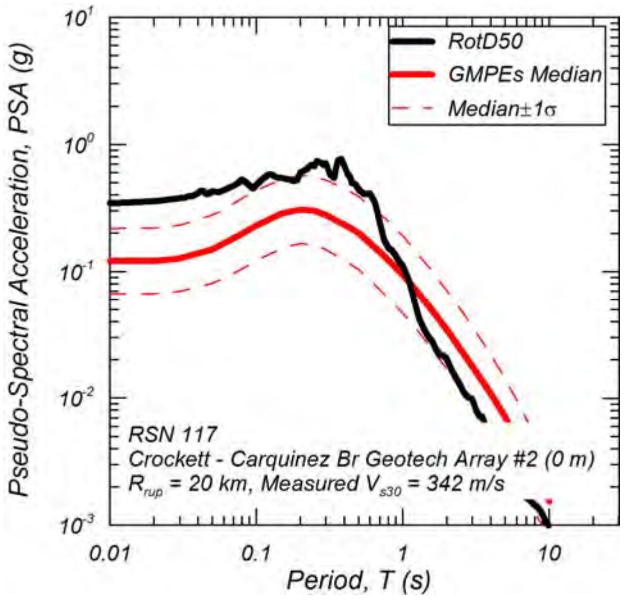

(d) Carquinez Br Geotech Array #2

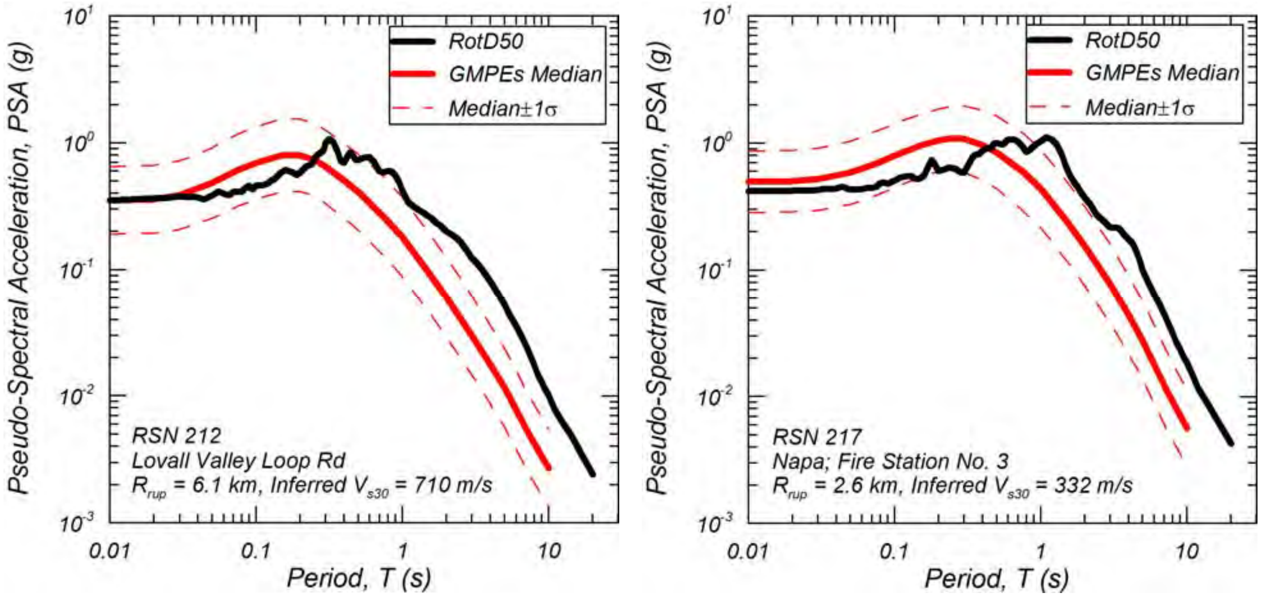

(e) Lovall Valley Loop Rd

(f) Napa Fire Station No. 3

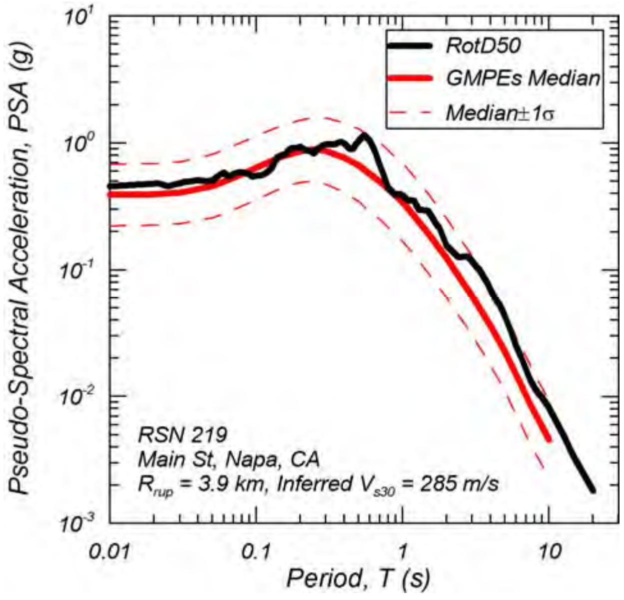

(g) Main St. Napa

Figure 7 Horizontal PSA (RotD50) compared to mean NGA-West2 GMPEs (2014)

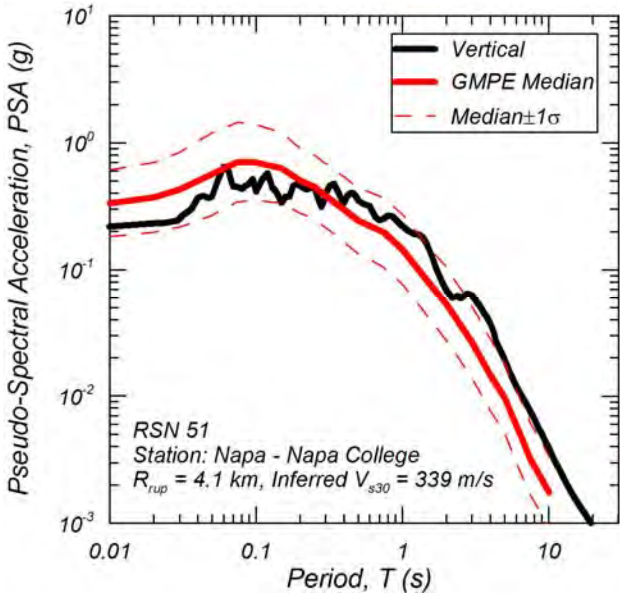

(a) Napa College

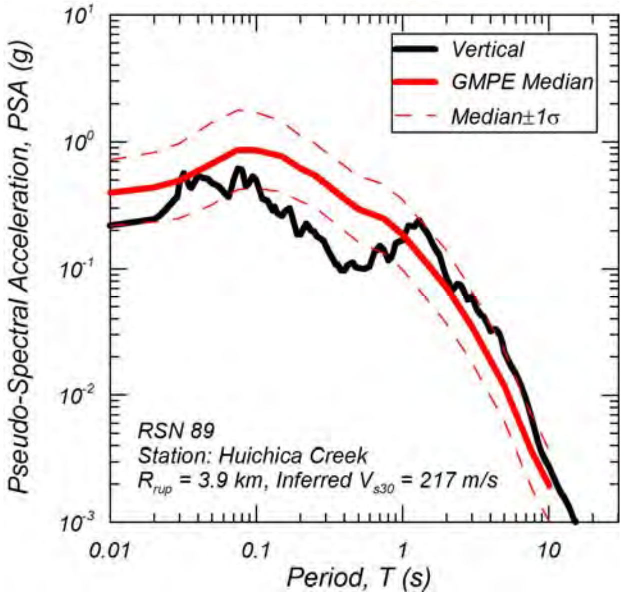

(b) Huichica Creek

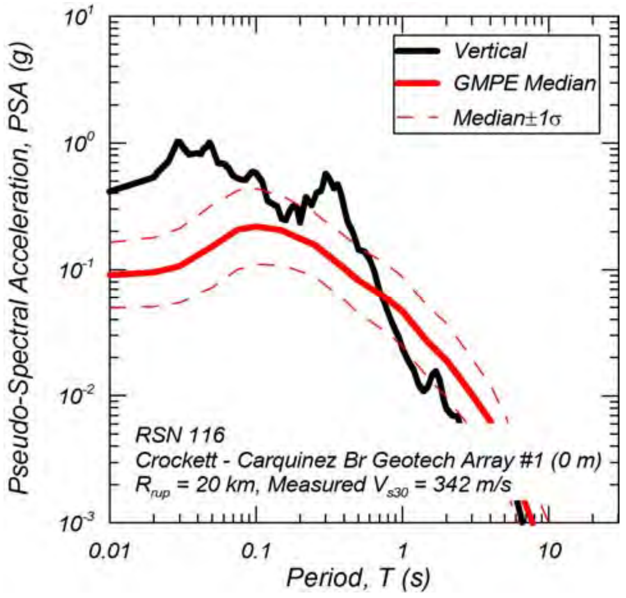

(c) Carquinez Bridge Geotechnical Array #1

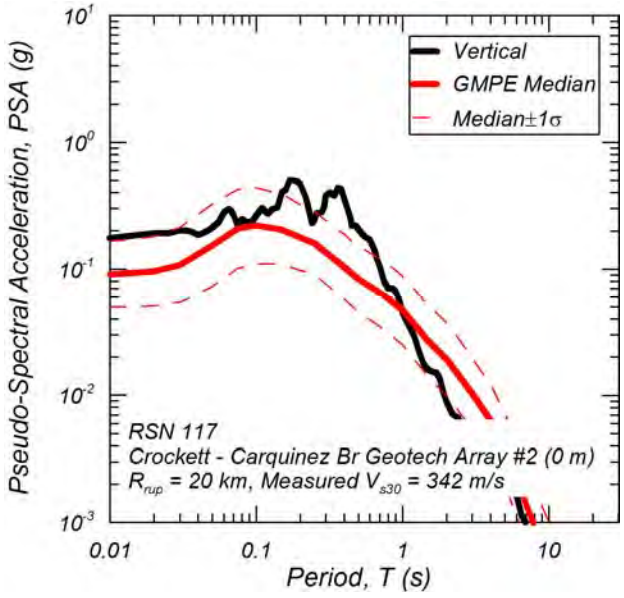

(d) Carquinez Bridge Geotechnical Array #2

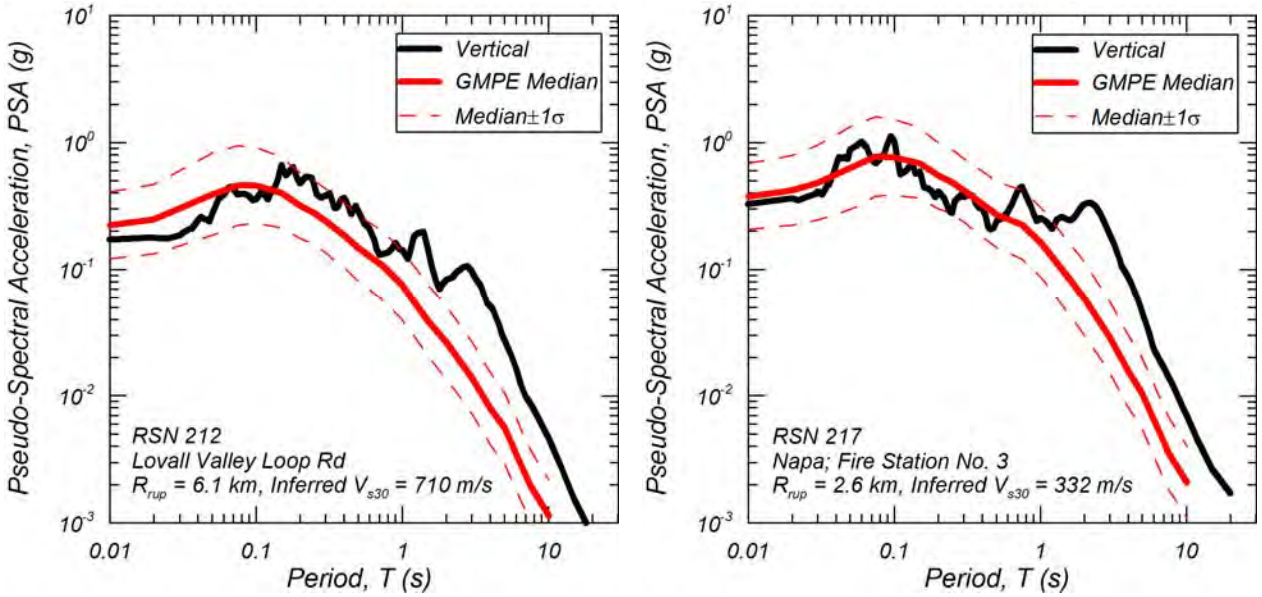

(e) Lovall Valley Loop Rd

(f) Napa Fire Station No. 3

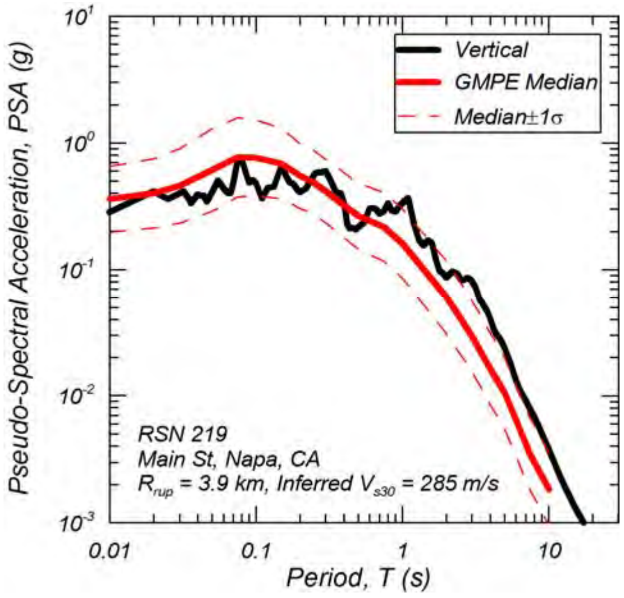

(g) Main St. Napa

Figure 8 Vertical Acceleration Resposne Spectra compared to Bozorgnia and Campbell (2014)

Horizontal PSA for all the stations were compared to the predicted median values obtained by taking the geometric mean of ASK14, BSSA14, CB14, and CY14. Figure 9 shows the comparison of PGA, PSA at T=0.2 s (PSA(0.2)), PSA at T=1.0 s (PSA(1.0)), and PSA at T=3.0 s (PSA(3.0)) against R_{rup} where the V_{s30} of 490 m/s is used in the GMPEs. The PSA of the records were adjusted to a reference V_{s30} of 490 m/s by V_{s30} scaling to these records. The figures show that PGA and PSA(0.2) are reasonably predicted within R_{rup} of 10 km whereas PSA(1.0) is underpredicted for this range. At distances greater than about 10 km the median GMPE tends to overpredict PGA and spectral values at 0.2 and 1.0 sec.

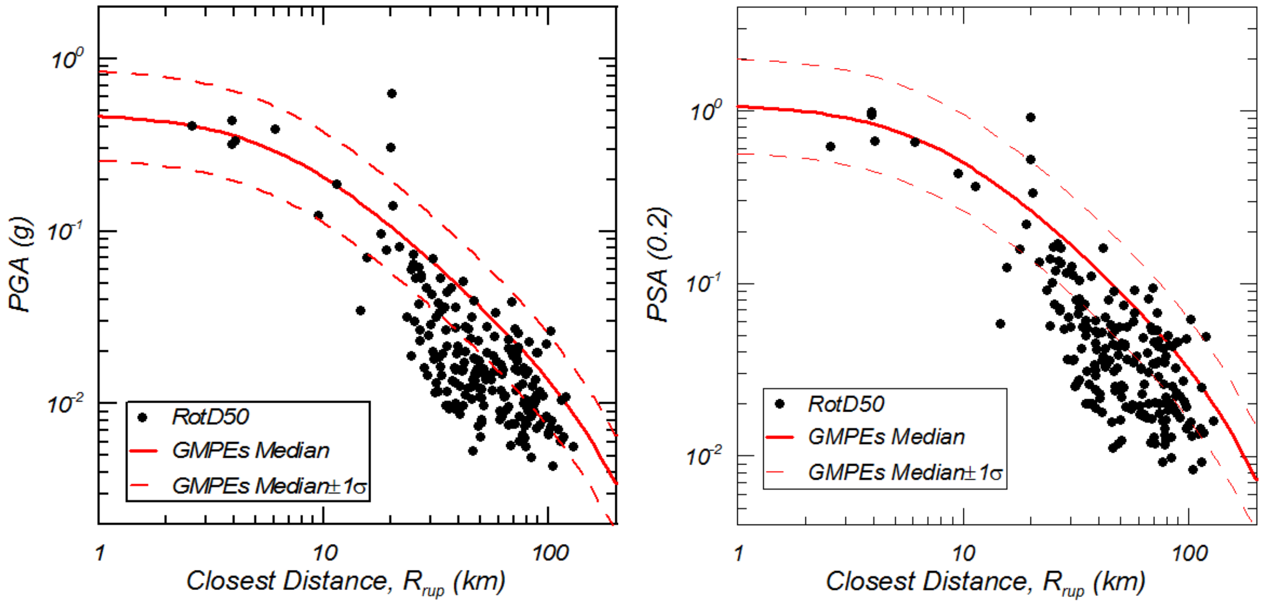

(a) PGA

(b) PSA (0.2)

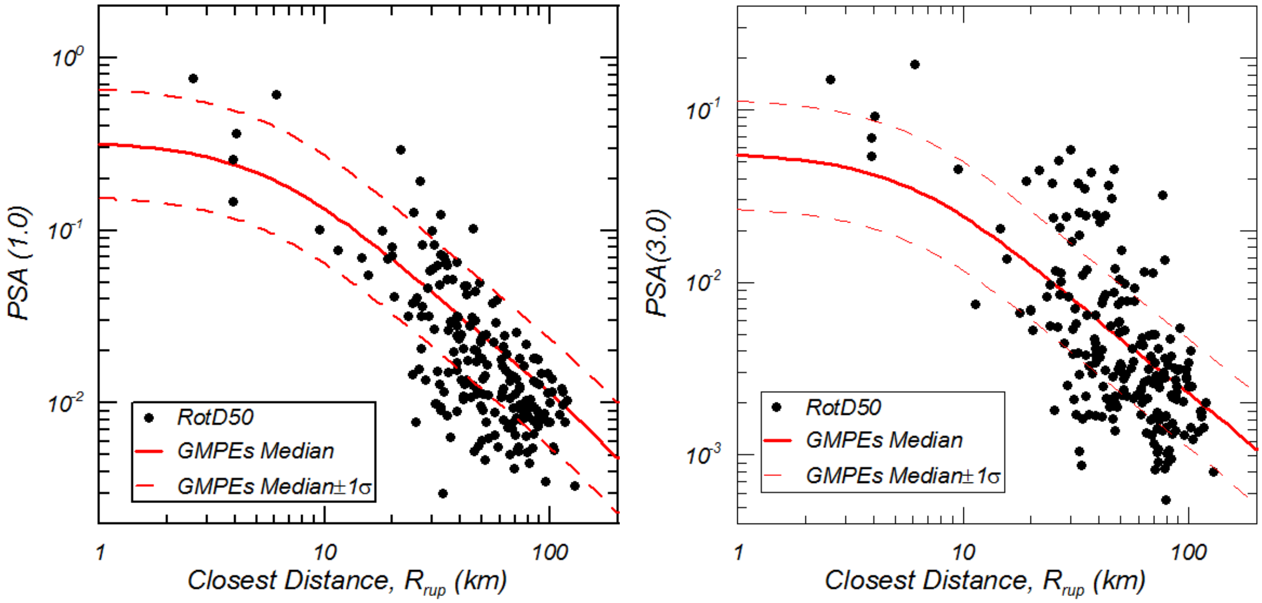

(c) PSA(1.0)

(d) PSA(3.0)

Figure 9 Comparison of horizontal PSA (RotD50) with GMPEs against R_{rup}

Figure 10 shows the within-event residuals of PGA, PSA(0.2), PSA(1.0) and PSA(3.0) against R_{rup} after subtracting the event terms from the residuals. Event terms were computed for R_{rup} less than 50 km. The figures show that the event terms are negative for all parameters indicating that the ground shaking was lower than the median predicted by the GMPEs.

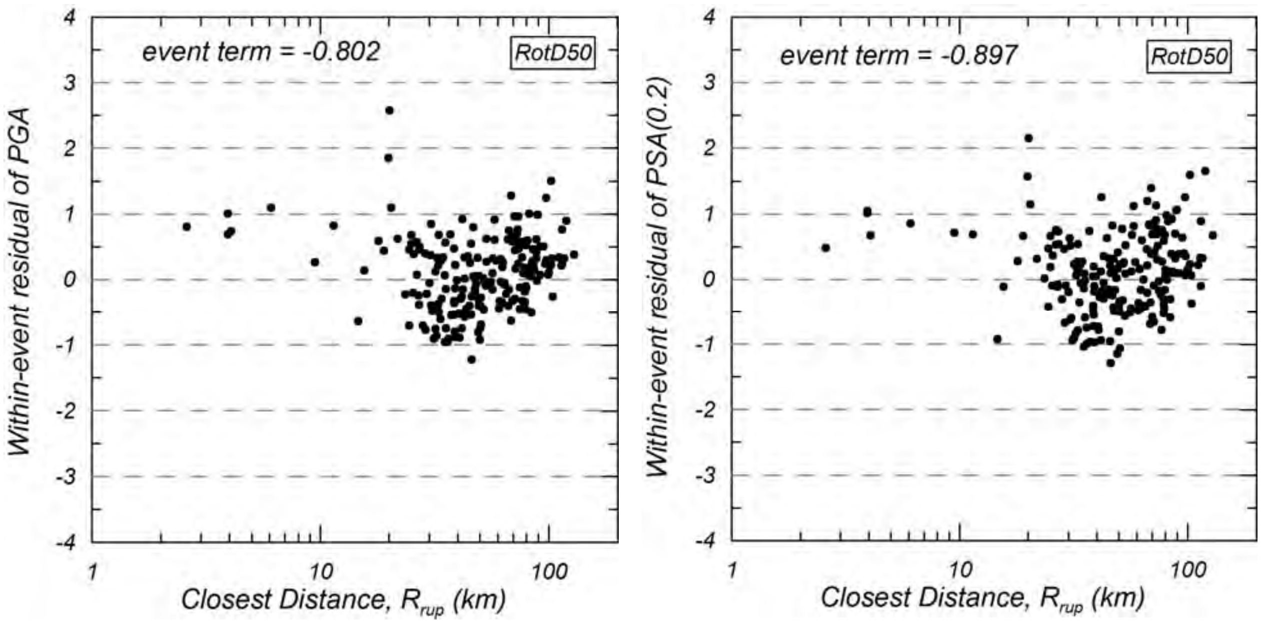

(a) PGA (b) PSA(0.2)

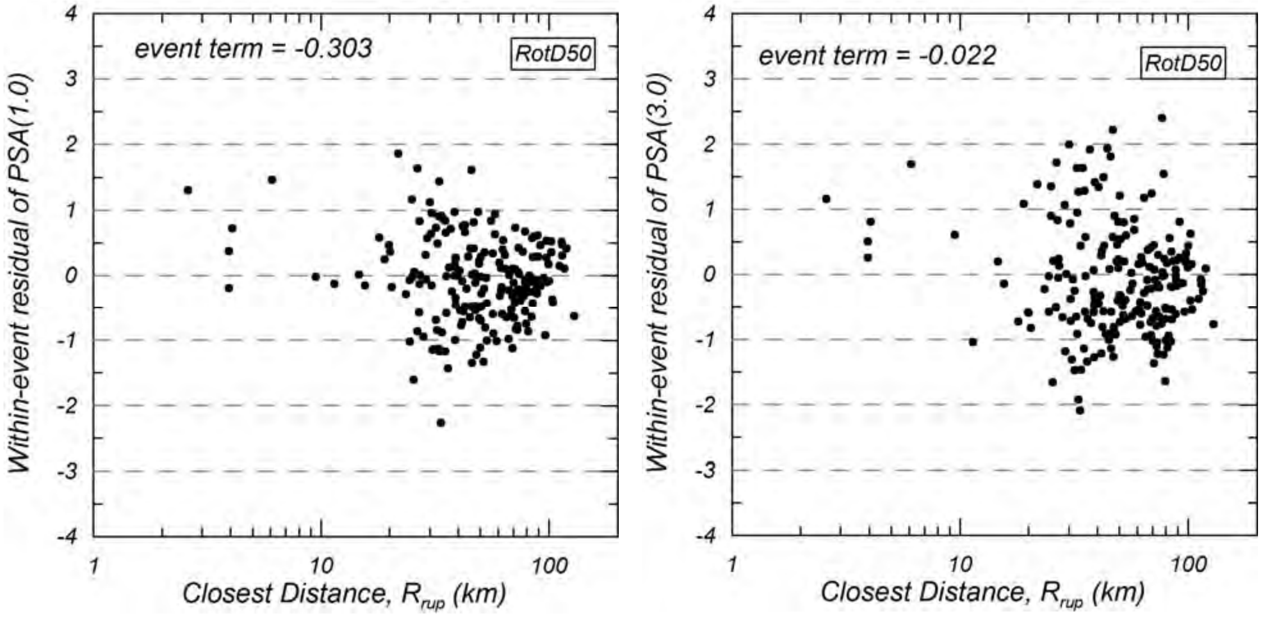

(c) PSA(1.0) (d) PSA(3.0)

Figure 10 Within-event residuals of horizontal PSA (RotD50) with GMPEs against R_{rup} (event term was computed within R_{rup} of 50 km.)

Vertical PSA were compared to the predicted values obtained by Bozorgnia and Campbell (2014). Figure 11 shows the comparison of PGA, PSA(0.2), PSA(1.0) and PSA(3.0) against R_{rup} where V_{s30} of 490 m/s is used in the GMPE. The PSA of the records were also adjusted to a V_{s30} of 490 m/s, as was done for the horizontal records. The comparison shows that PSA are reasonably estimated within R_{rup} of 10 km, although it shows an underestimation for PSA(1.0) and PSA(3.0).

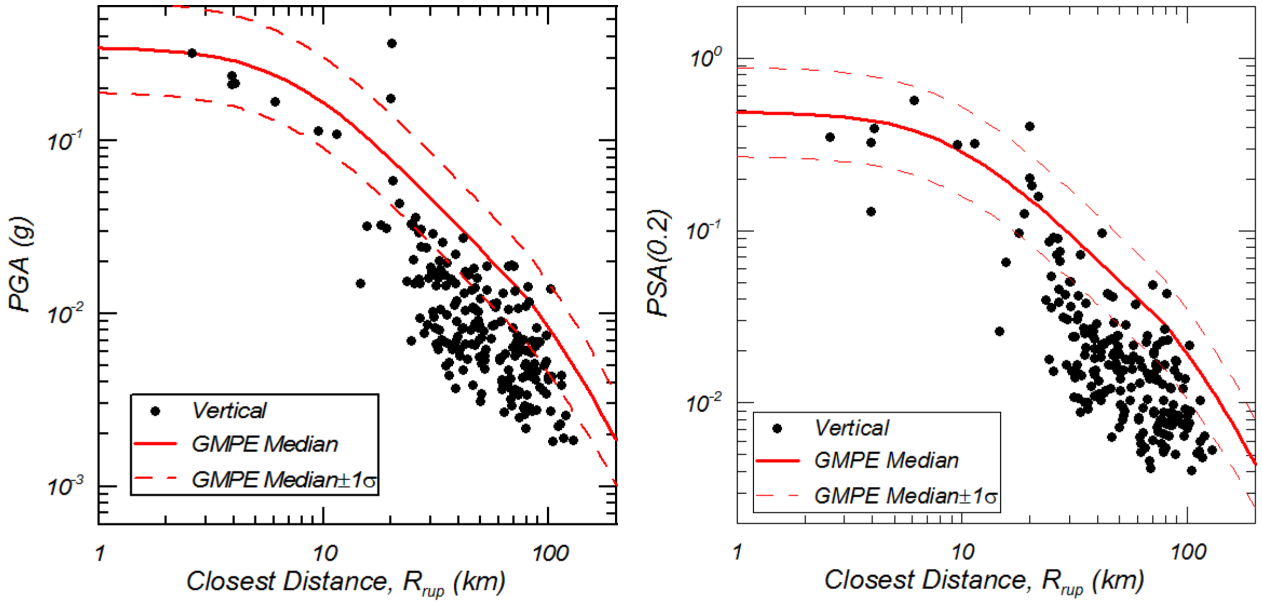

(a) PGA (b) PSA(0.2)

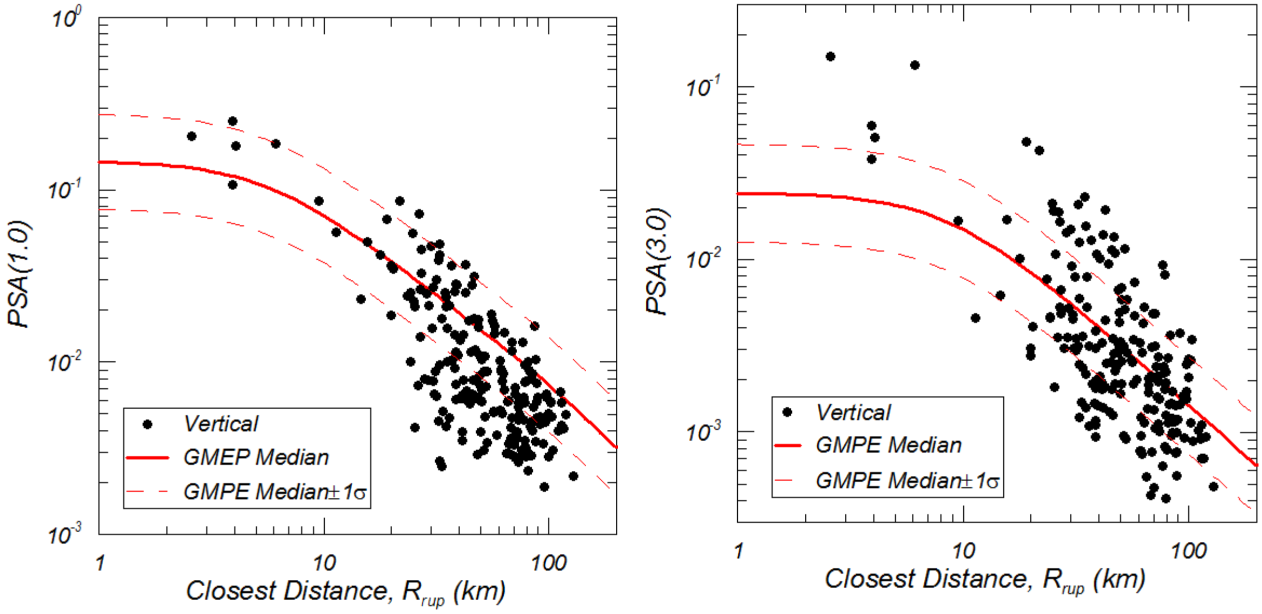

(c) PSA(1.0) (d) PSA(3.0)

Figure 11 Comparison of vertical PSA with GMPE against R_{rup}

Figure 12 shows the within-event residuals of PGA, PSA(0.2), PSA(1.0), and PSA(3.0) against R_{rup} after subtracting the event term from the residuals. Event terms were computed for R_{rup} less than 50 km. The figures show that the event terms are negative for all PSA indicating that the ground shaking was lower than the median values predicted by the GMPE.

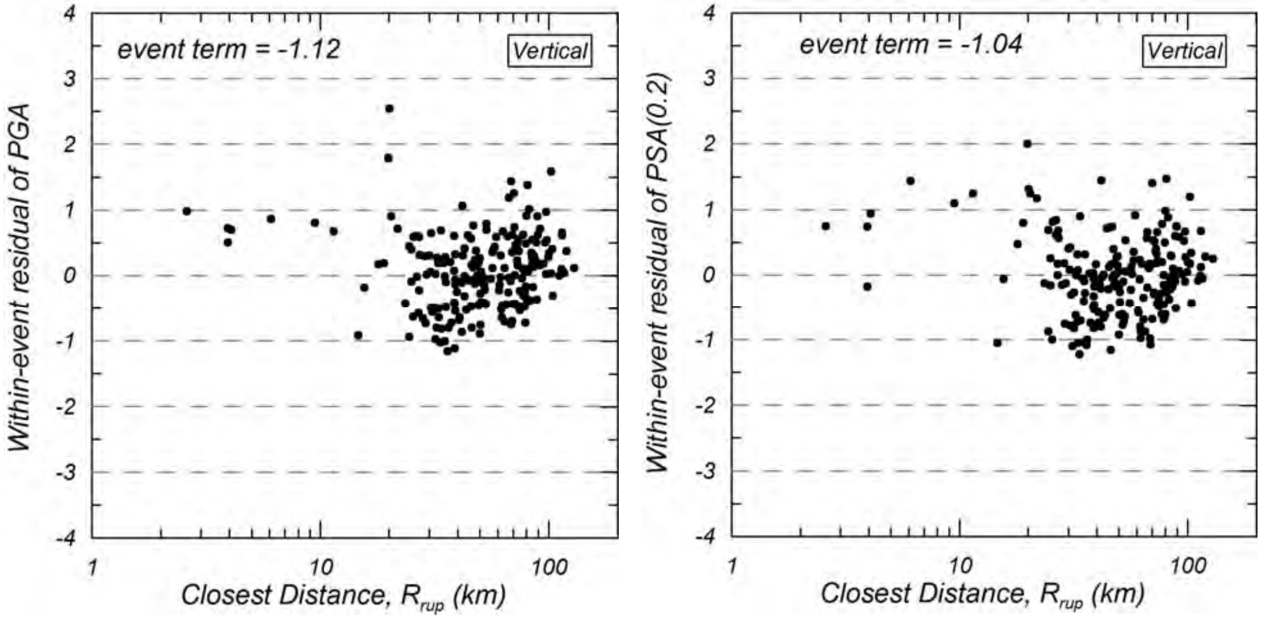

(a) PGA

(b) PSA(0.2)

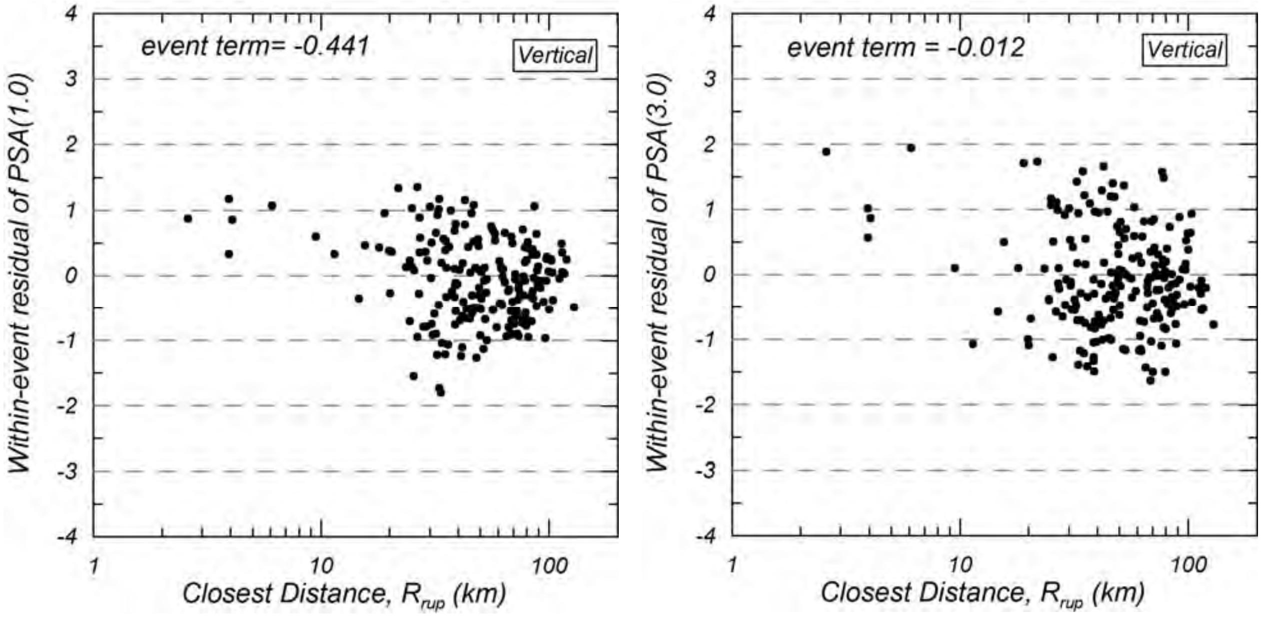

(c) PSA(1.0)

(d) PSA(3.0)

Figure 12 Within-event residuals of vertical PSA with GMPE against R_{rup} (event term was computed within R_{rup} of 50 km.)

1.5 COMPARISON OF RECORD RESPONSE SPECTRA TO CODE-BASED DESIGN SPECTRA

In this section, the 5% damped acceleration response spectra of the recorded ground motions are compared to the various code-based design spectra. Two sets of plots are presented. The first set directly compares the three recorded components with the code spectra. The second set compares the processed spectra with the code-based spectra; this comparison is for design purposes with respect to certain ground motion selection requirements documented in ASCE 7-10. In addition, the pseudo-spectral acceleration, Uniform Hazard Response Spectra (UHRS), and displacement spectra for different return periods are presented for Napa College, Napa Main Street, Napa Fire Station No. 3, and the surface recording from the Vallejo-Hwy 37 Geotechnical Array. Similar plots for the other stations listed in Table 1 are presented in Appendix C. All the spectra presented in this section correspond to a 5% damping ratio.

1.5.1 Design Spectra

The design spectra for buildings were constructed based on ASCE 7-10, Chapter 11, while the Caltrans Seismic Design Criteria, Appendix B (version 1.7, 2013), was used to construct the design spectra for bridges, such as Highway 37/Napa Valley Bridge.

1.5.1.1 ASCE 7-10 Design Spectra for Buildings

The site class for each station is determined based on the site's estimated V_{s30} value, as discussed in section 1.4.1. The risk-targeted mapped acceleration parameters such as S_{d1}, S_{ds}, S_{m1}, S_{ms} were obtained using the USGS Seismic Design Maps online tool: http://earthquake.usgs.gov/designmaps/us/application.php. With those values, the design spectra for Design Based Earthquake (DBE) and Maximum Considered Earthquake (MCE) were constructed for different period ranges. The period range is 0 to 3.0 second for all spectra plotted in this chapter, because this range covers nearly all of the fundamental periods for structures in built-up areas in Napa.

1.5.1.2 Caltrans Design Spectra for Bridges

The Caltrans design spectrum was based on the envelope of a deterministic and probabilistic spectrum for each location. The deterministic spectrum was calculated as the arithmetic average of the median response spectra calculated using CB08, CY08, and the probabilistic spectrum was obtained from the USGS Seismic Hazard Map (Petersen et al, 2008) for the 5% in 50 year probability of exceedance (975 year return period) taking into account of the spectrum adjustment factors due to near-fault effects, basin effects, etc. Site specific analyses are also required if the soil profile includes soft clay deposits.

1.5.2 Resultant Spectra

The Square Root Sum of Squares (SRSS) of the two horizontal components was calculated for each recording station. Additional resultants, such as the RotD50 (median rotated component) and RotD100 (maximum rotated direction component), were also calculated (Boore et al. 2010).

1.5.3 UHRS

Another set of plots comparing the median-rotated component and UHRS for different hazard levels are also included. The UHRS for selected station were calculated using the USGS online tool: http://geohazards.usgs.gov/hazardtool/application.php.

Station Name: Napa College

V_{s30}(m/sec): 339

Soil Type: D

PGA: 0.344 g

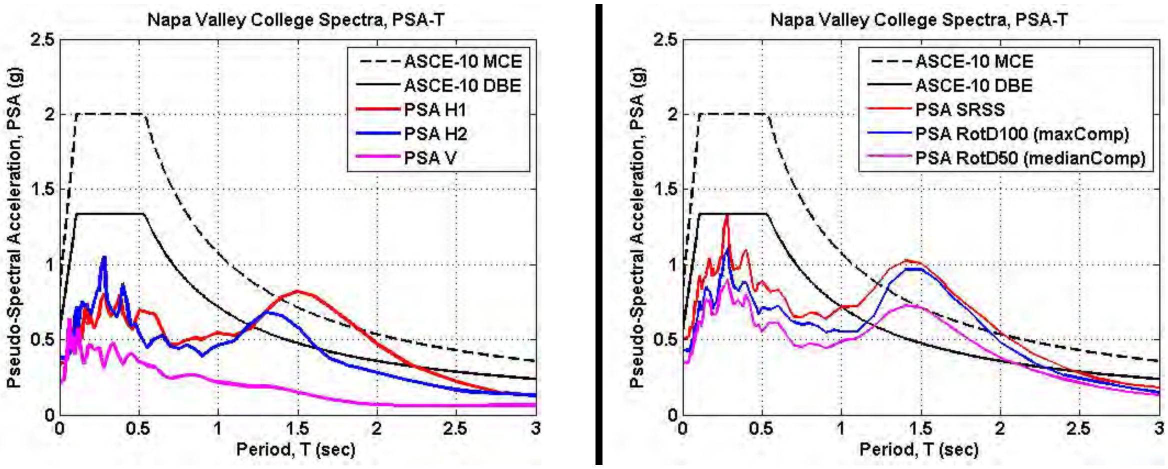

(a). Code-based vs. as-recorded PSA

(b). Code-based vs. resultant PSA

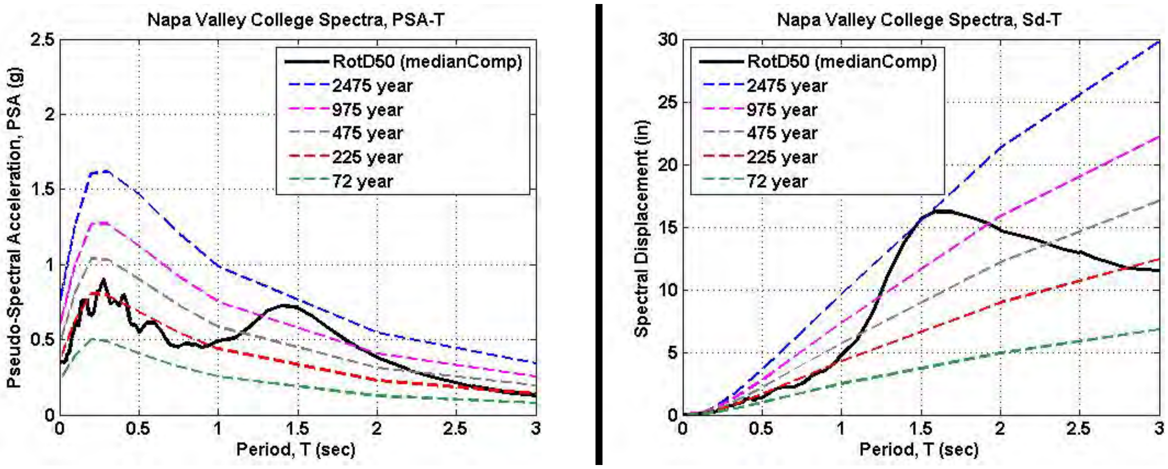

(c). UHRS vs. median component PSA

(d). UHRS vs. median component Sd

Figure 13 Spectra comparison for Napa Valley College

Station Name: Napa Main Street

V_{s30} (m/sec): 285

Soil Type: D

PGA: 0.445 g

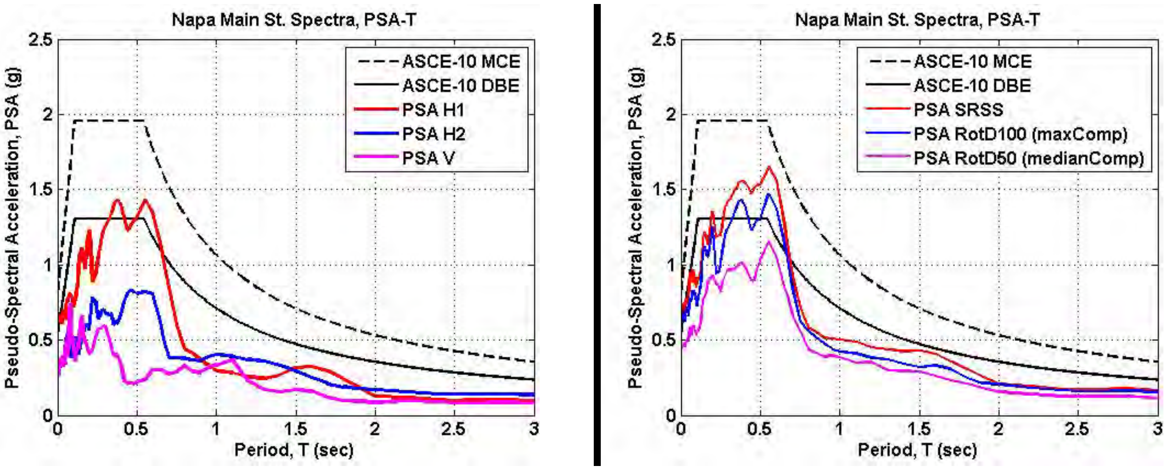

(a). Code-based vs. as-recorded PSA

(b). Code-based vs. resultant PSA

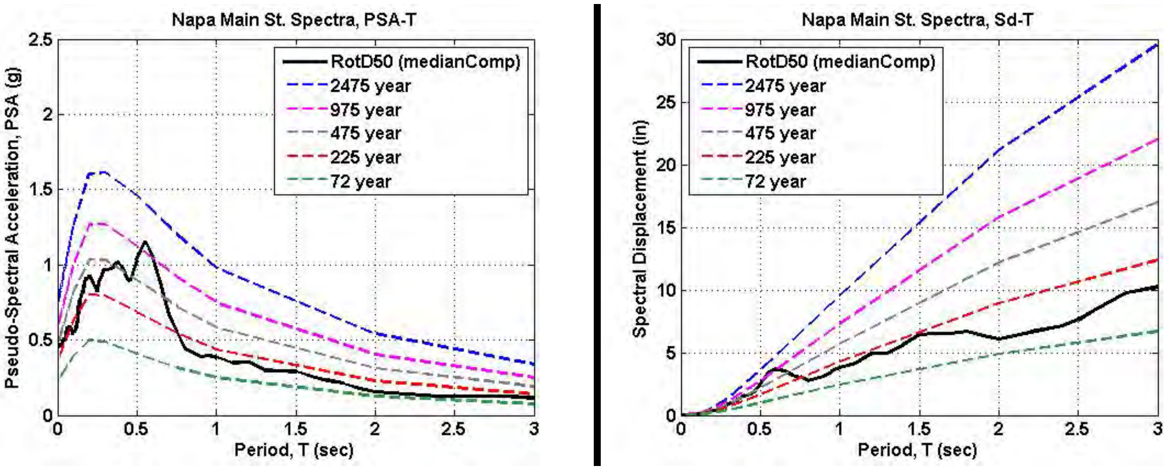

(c). UHRS vs. median component PSA

(d). UHRS vs. median component Sd

Figure 14 Spectra comparison for Napa Main Street

Station Name: Napa; Fire Station No. 3

V_{s30} (m/sec): 332

Soil Type: D

PGA: 0.346 g

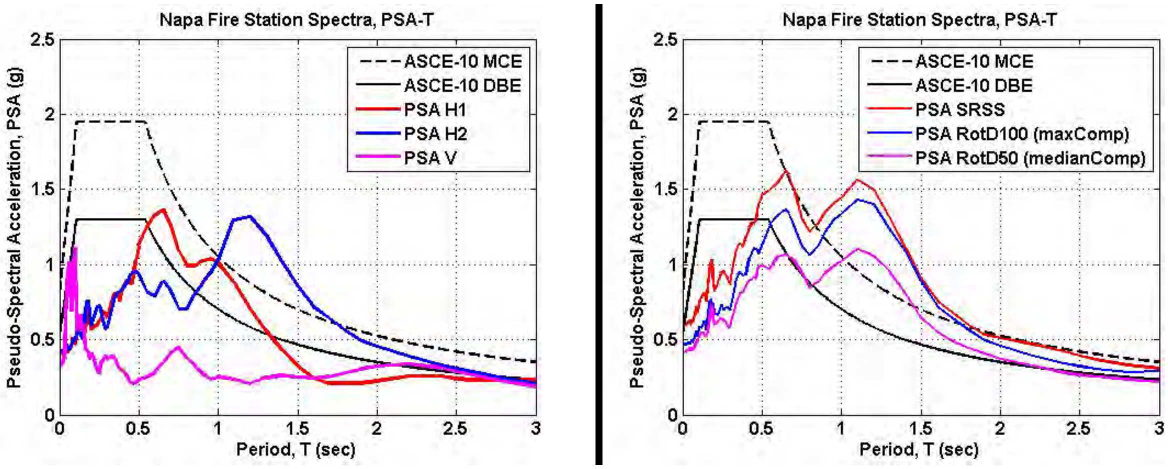

(a). Code-based vs. as-recorded PSA

(b). Code-based vs. resultant PSA

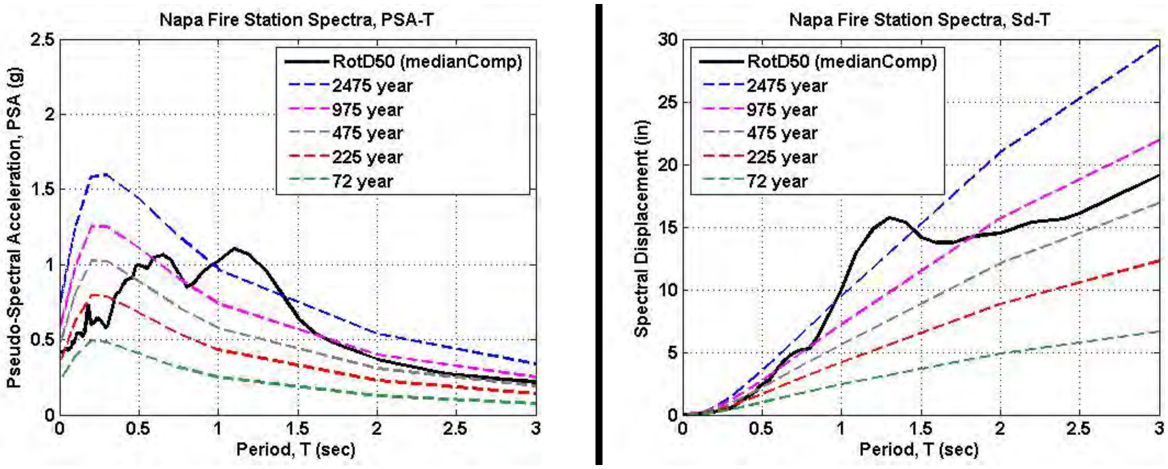

(c). UHRS vs. median component PSA

(d). UHRS vs. median component Sd

Figure 15 Spectra comparison for Napa; Fire Station No. 3

Station Name: Vallejo - Hwy 37/Napa River E Geotech Array (0m)

V_{s30} (m/sec): 509

Soil Type: C

PGA: 0.198 g

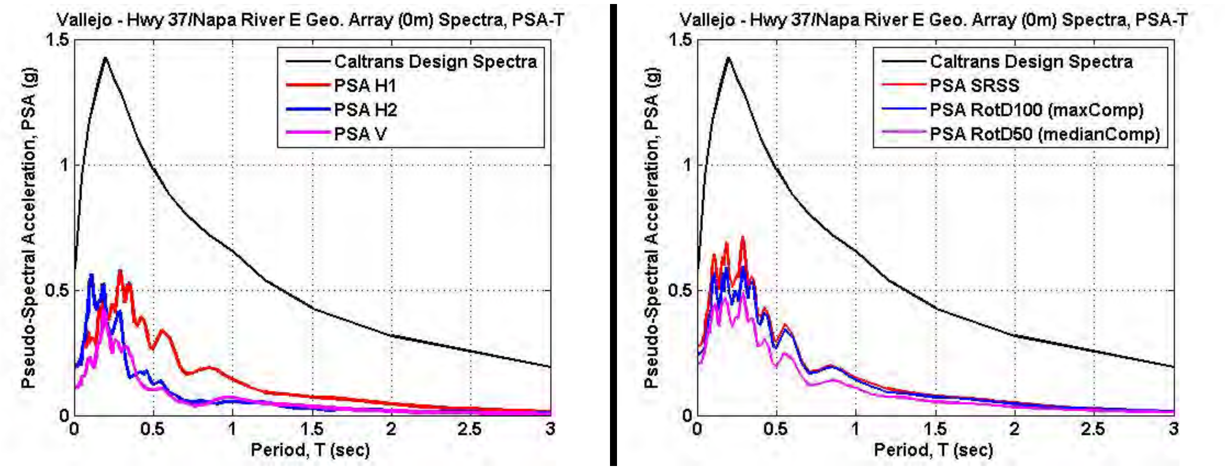

(a). Code-based vs. as-recorded PSA spectra

(b). Code-based vs. resultant PSA spectra

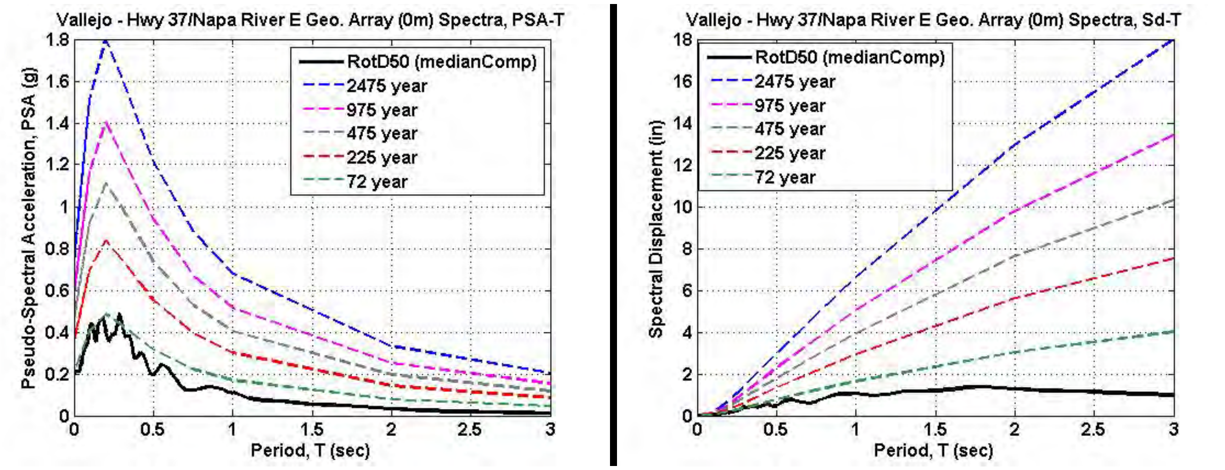

(c). UHRS vs. median component PSA

(d). UHRS vs. median component Sd

Figure 16 Spectra comparison for Vallejo - Hwy 37/Napa River E Geotech Array (0m)

1.6 SUMMARY OF GROUND MOTION OBSERVATIONS

This report summarizes a preliminary study on the characteristics of the strong-motion recordings from the South Napa Earthquake of August 24th, 2014. The strong-motion data were downloaded from CESMD website and processed following the PEER standard data processing methodology. Associated metadata such as source-to-site distances and estimated site parameters such as V_{s30} were estimated following the approached developed in the PEER NGA-West2 study. Strong ground motions were observed within Napa Valley where PGA values greater than 0.3 g were recorded.

Velocity pulses were observed near the fault for which five time series were examined by using the approaches by Hayden et al. (2014) and Shahi (2013). The results show that these records were classified as pulse-type motions in the near-fault region even though a discrepancy between these approaches exists for the Main St. Napa and Napa College stations.

Four near fault ground motions were similarly characterized using the proposed method by Lu and Panagiotou (2014) (Napa Fire Station No. 3, Napa Main St., Fault Normal and Fault Parallel directions). Analyses showed that each of the records includes more than one strong long-period pulse with the predominant period (T_P) of the multiple pulses to differ significantly. The T_P of the long-period pulses ranged between 0.8 and 3.9 s. All four ground motions, included two strong long-period pulses of significantly different T_P that were well correlated in the time domain. All motions also included strong short-period pulses ($T_P < 0.6$ s).

High-frequency spikes were observed in the records at Carquinez Bridge Geotechnical Array #1 which reached approximately 1.0 g for the NS component. These spikes were investigated by comparing the acceleration time series at several stations along the path from the epicntert to the sites and the downhole array records. These spikes were observed in the S-wave portion of the records based on visual inspection. Acceleration time series along the source to site travel path shows the similar spikes at the recordings at Napa College, Vallejo – Hwy 37/Napa River East Geotechnical Array, and Carquinez Bridge Geotechnical Arrays #1 and #2. This suggests that the spikes could be a result of path effects. The spikes increase in amplitude from Vallejo – Hwy 37/Napa River East Geotechnical Array to Carquinez Bridge Geotechnical Array #1. Downhole records show that two high frequency spikes are observed in the S-wave portion of the waveform from a depth below 100 m to the surface. This observation may indicate that the large PGA observed at Carquinez Bridge Geotechnical Array #1 could also be the result of site amplification through the soft soil deposits. However, these observations do not exclude the possibility of soil-structure interaction effects on the measured recordings. Further investigation is recommended to study the observed high-frequency content near the Carquinez Bridge.

The pseudo-spectral accelerations (5% damped) from the recorded ground motions were compared to the recent NGA-West2 GMPEs for PGA, 0.2, 1.0 and 3.0 seconds. The comparison shows generally a good agreement for both of horizontal and vertical components near the fault with the exception of the large high frequency motions observed near the Carquinez Bridge.

Recorded ground motions were also compared to the code-based design spectra. The comparison shows that the pseudo-spectral accelerations recorded at Napa College and Napa Fire Station No. 3 exceeded the MCE design spectra at a period around 1.5 s near the fault. This observation is related to the near-fault velocity pulses discussed in the report. The comparison also shows that the pseudo-spectral acceleration recorded at Carquinez Bridge exceeded the Caltrans design spectra for short periods. This observation is related to the amplification of high frequency spikes discussed in the report. Further investigation is recommended to study the damage observations related to the recorded ground motions and design spectra. There needs to be more researchinto which pulse featuresmay have damaging effects on elastic and inelastic systems.

1.7 REFERENCES

Abrahamson, N. A., Silva W. J., and Kamai, R., 2014. Summary of the Abrahamson, Silva, and Kamai NGA-West2 ground-motion relations for active crustal regions, Earthquake Spectra, EERI, Pre-Print.

Abrahamson, N., Atkinson, G., Boore, D., Bozorgnia, Y., Campbell, K., Chiou, B, Idriss, I.M., Silva, W. and Youngs, R., 2008. Comparisons of NGA Ground-Motion Relations, Earthquake Spectra, EERI, Vol. 24, No. 1, Feb., pp. 45-66.

Ancheta, T. D., Darragh, R. B., Stewart, J. P., Seyhan, E., Silva, W. J., Chiou, B. S. J., Wooddell, K. E., Graves, R. W., Kottke, A. R., Boore, D. M., Kishida, T., Donohue, J. L., 2014, PEER NGA-West2 Database. Earthquake Spectra, EERI, Pre-Print.

Boore, D. M, 2010. Orientation-independent, nongeometric-mean measures of seismic intensity from two horizontal components of motion, Bull. Seismol. Soc. Am., 100, 1830 – 1835.

Boore, D. M., Stewart, J. P., Seyhan, E., and Atkinson, G. A., 2014. NGA-West2 equations for predicting response spectral accelerations for shallow crustal earthquakes, Earthquake Spectra, EERI, Pre-Print.

Bozorgnia, Y., and Campbell, K.W., 2014. Vertical ground motion model using NGA-West2 database, Earthquake Spectra, EERI, submitted.

Bray, J.D., Rodriguez-Marek, A., and Gillie, J. L., “Design Ground Motions Near Active Faults,” Bulletin of the New Zealand Society for Earthquake Engineering, 42 (1), March, 2009, 8 pp.

Campbell, K. W. and Y. Bozorgnia (2008), “NGA ground motion model for the geometric mean horizontal component of PGA, PGV, PGD and 5% damped linear elastic response spectra for periods ranging from 0.01 to 10s”, Earthquake Spectra, 24(1), 139-171.

Campbell, K. W., and Bozorgnia, Y., 2014. Campbell-Bozorgnia NGA-West2 ground motion model for the average horizontal components of PGA, PGV, and 5%-damped linear Response Spectra, Earthquake Spectra, EERI, Pre-Print.

Chiou, B. S. J., and Youngs, R. R., 2014. Update of the Chiou and Youngs NGA ground motion model for average horizontal component of peak ground motion and response spectra, Earthquake Spectra, EERI, Pre-Print.

Chiou, B. S.-J. and Youngs R. R. (2008), An NGA model for the average horizontal component of peak ground motion and response spectra, Earthquake Spectra, 24(1), 173-215.

Hayden, C.P., Bray, J.D., and Abrahamson, N.A. (2014). ”Selection of Near-Fault Pulse Motions.” J. Geotech. Geoenviron. Eng., 140(7), 04014030.

Lu, Y., and Panagiotou, M. (2014). “Characterization and Representation of Near-fault Ground Motions Using Cumulative Pulse Extraction with Wavelet Analysis,” *Bulletin of the Seismological Society of America,* 104:410-426.

Petersen, M.D., Frankel, A. D., Harmsen, S. C., Mueller, C. S., Haller, K. M., Wheeler, R. L., R. L. Wesson, Zeng, Y., Boyd, O. S., Perkins, D. M., Luco, N., Field, E. H., Wills, C. J. and Rukstales, K. S. “Documentation for the 2008 Update of the United States National Seismic Hazard Maps”, USGS, Open-File Report 2008–1128.

Shahi, S. (2013). “A probabilistic framework to include the effects of near-fault directivity in seismic hazard assessment.” Ph.D. Thesis, Stanford University, Stanford, CA.

3 SURFACE FAULT RUPTURE ASSOCIATED WITH THE M6.0 SOUTH NAPA EARTHQUAKE OF AUGUST 24, 2014

Tim Dawson (CGS), Keith Kelson (USACE), John Wesling (OMR), Ken Hudnut (USGS), and Dan Ponti (USGS)[1]

3.1 **Introduction**

The M6.0 South Napa earthquake of August 24, 2014 was the first earthquake in the San Francisco Bay Region (SFBR) to produce significant, through-going surface rupture since the 1906 San Andreas Fault earthquake and the first earthquake in northern California to rupture through a densely populated area. The South Napa earthquake rupture affected residential structures, roads, and lifelines, and provides information on the possible effects of future surface-rupturing earthquakes on other faults in the region. The occurrence of surface rupture within the densely populated SFBR prompted a large number of earth scientists representing government, academia, and the private sector to document the rupture in the hours and days immediately after the main shock. This summary report documents some of the key observations made by these workers following the earthquake.

Surface rupture associated with the South Napa earthquake occurred on parts of the West Napa fault, a zone of discontinuous faults that extends from American Canyon to the north along the west edge of Napa Valley, and is thought to be a relatively minor strike-slip fault within the system of northwest-trending dextral faults in the SFBR (Figure 3-1). The surface rupture extends approximately 12 to 15 km from the town of Cuttings Wharf in the south to beyond the northern boundary of Alston Park in the city of Napa, in the north (Figure 3-2). The surface rupture is expressed largely to the west of most mapped Quaternary traces of the West Napa fault, and is only coincident with the western-most previously mapped trace of the West Napa fault zone, which is depicted in the U.S. Geological Survey (USGS) Quaternary Fault and Fold Database (Bryant, 2000) as a 4 km long, northwest trending fault and assigned a Late Quaternary age.

Field reconnaissance began almost immediately following the earthquake; some observations of surface deformation were made within 2.5 hours of the main shock. As of September 12, 2014, field teams were still evaluating the extent of rupture in the north, so the total rupture length is not yet known precisely. Most ruptures were located by the field teams driving roads across the area, looking for disrupted or offset cultural features and then following those features into areas on either side of the road. Also, several aerial overflights were completed along the rupture and adjacent areas; the overflights were accomplished via helicopter as part of the California Highway Patrol (CHP) earthquake response. Field teams were later aided in their search for surface rupture by the acquisition of Synthetic Aperture Radar (SAR) data, initially by satellite-based COSMO-SkyMed (X-band) interferograms using data provided especially by the Agencia Spaziale Italiana and prepared by scientists of NASA's Jet Propulsion Laboratory (JPL) and the Advanced Rapid Imaging and Analysis (ARIA) Center for Natural Hazards, and a week later by L-band interferograms from NASA/JPL's airborne uninhabited aerial vehicle system acquisition system, UAVSAR and the European Space Agency's C-band satellite, Sentinel-1A. These images revealed additional lineaments, formed by discrete line-of-sight changes between pre- and post-earthquake missions. Many of these lineaments have been verified in the field (Figure 3-3).

---

[1] Agency Abbreviations: California Geological Survey (CGS), United States Army Corps of Engineers (USACE), California Office of Mine Reclamation (OMR), United States Geological Survey (USGS)

Other lineaments observed from the UAVSAR imagery most recently still need to be field checked, and those lineaments initially field checked and/or thought to be connected to mapped tectonic ruptures are shown on Figure 3-2.

Displacements along the surface rupture are predominantly right-lateral and amounts are variable along strike, both in the near-field (on the order of tens of meters perpendicular to strike), as well as along the entire length of the rupture, as shown on Figure 3-4. The rupture is highly variable in terms of expression at the surface, but is typically expressed as a zone of *en echelon* left-stepping fractures (Figure 3-5) varying from less than a meter in width to tens of meters, or more, wide. The expression of surface rupture varies where the fault crosses paved roads, in some cases being complex, with some fractures oriented nearly orthogonal to the orientation of the fault trace (Figures 3-6a-b) and others oriented along strike.

The following sections summarize the key observations of surface rupture related to this earthquake collected by the field teams, although we note that this is still largely a work in progress, as field teams are still in the area mapping the details of the rupture and filling in gaps.

3.3 **Cuttings Wharf to Congress Valley Road**

The epicenter of the M6.0 main shock is located near Cuttings Wharf and nearly continuous surface rupture was mapped for about 7 km from the west bank of the Napa River, at Cuttings Wharf, to Congress Valley Road. In the area north of Cuttings Wharf, the fault trends about 340°, crossing numerous vineyards that provide abundant opportunities to collect offset data along the rows of grapes. Measureable lateral displacements along this stretch of the rupture are typically in the 20-25 cm range (Figure 3-7), but there are right-lateral displacements as high as 40-45 cm measured between Henry and Congress Valley Roads. The surface rupture through alluvium, colluvial deposits and agricultural fields is notably wider than that observed across asphalt roads, and the amount of surface offset recorded by vineyard rows appears greater than that recorded by roadway asphalt.

3.4 **Congress Valley Road to Browns Valley**

Near the intersection between Buhman and Congress Valley Roads, surface rupture has not been completely mapped, although surface rupture in the area has been inferred based on a lineament interpreted from the UAVSAR. To the north the rupture is strongly expressed on the Buhman Ranch Property, west of Buhman Road (Figure 3-8), with right-lateral offsets in the range of 40-45 cm.

3.5 **Browns Valley to Alston Park**

Within Browns Valley, fault offset is in the range of 10 – 20 cm (Figure 3-3), as the fault steps to the east. The Browns Valley area is developed, consisting largely of residential units, and the fault cuts numerous cultural features including roads, sidewalks and residential structures (Figures 3-9). At the latitude of Browns Valley Road, a subparallel, northwest trending fault (herein referred to as the Eastern Strand) is approximately 500 meters east of the principal rupture (labeled Western Strand on Figure 3-2), and has a subordinate amount of right-lateral displacement, typically 2-8 cm (Figure 3-10). North of Browns Valley, the eastern and western strands merge in the vicinity of the Hendry Winery, located south of Alston Park. The northern end of the field-verified rupture has been traced as far as the northern boundary of Alston Park (Figure 3-11), and likely continues for a least several kilometers more, which will be confirmed as field teams continue to map the rupture.

On the eastern strand, rupture was verified as far south as Browns Valley Road. South of Browns Valley Road, limited access has hindered field teams in verifying the rupture trace, although a lineament interpreted from the UAVSAR, appears to connect surface deformation on the eastern strand to rupture observed in the vicinity of Thompson Road. Near Thompson Road, the rupture is mapped through a residential neighborhood crossing Thompson and Congress Valley Roads, before going into areas that are predominantly vineyard. In the vicinity of Thompson Road, the rupture is weakly expressed in soil, but shatters asphalt driveways (Figure 3-12), illustrating the variation in response to surface rupture of different materials even at apparently very small total offsets (these were not easily measureable, but likely < 5 cm).

3.6 **Southeast of Napa River: Napa County Airport**

South of Cuttings Wharf, previously mapped traces of the West Napa fault step about 2 km to the east, and trend from the Napa County Airport to the southeast through American Canyon. Minor surface rupture and offset was observed on Taxiways “C” and “E” at the Napa County Airport, expressed as warping and left-stepping, *en echelon* cracking in the asphalt, suggestive of right-lateral movement (Figure 3-13). The surface rupture is coincident with the mapped trace of the West Napa fault (Bryant, 2000; Wesling and Hanson, 2008), which is expressed at the airport as a low scarp and is visible in aerial imagery as a vegetation lineament adjacent to the taxiway (Figure 3-13). At the time of this writing, the origin of the airport deformation is not known, and could be related to either surface rupture or triggered slip. On August 27, 2014, evidence of surface rupture or triggered slip was not present across Green Island Road, or across features south of Green Island Road. An aerial overflight on August 27 showed an absence of perceptible ground cracking along the eastern banks of the Napa River, south of Green Island Road. Subsequent analysis of the UAVSAR data suggested the presence of possible surface deformation in this area, but this has not yet been field checked.

3.7 **Afterslip Observations**

Afterslip was documented within the first 24 hours and was expressed as the continued development of the rupture on the ground and the growth through time of observed offsets on roads and other cultural features (Figure 3-14). The USGS was able to establish four alignment arrays across the fault in order to monitor afterslip. Although results are not yet available, based on episodic field observations, afterslip appears to be common in the primary, 7-km-long epicentral part of the rupture. Little to no offset was observed within a few hours of the main shock at some locations that exhibited as much as 20 cm of right-lateral slip 48 hours after the mainshock. From qualitative observations made by the field teams, the majority of afterslip occurred within about 36 to 48 hours of the main shock, and the amount of afterslip was probably in the range of about 30 - 60% of the total slip. Additional time-series analyses of imagery and digital topographic data, using repeat mobile LiDAR, campaign and continuous GPS data acquired by the USGS, may provide information to define the pattern, timing, and amount of afterslip along the various sections of the surface rupture.

3.8 **Discussion**

The 2014 South Napa earthquake was notable as M6.0 earthquake with complex pattern of surface faulting that involved multiple fault strands over a length of about 12 to 15 km. Further, the maximum net surface offset of about 45 cm, is somewhat atypical for this magnitude. The surface rupture pattern corresponds to seismological interpretations of a south-to-north rupture of a very steeply west-dipping fault, and the maximum surficial displacement measured north of Henry Road, ~45 cm, spatially correspond with a zone of high subsurface slip in the preliminary finite fault models (USGS, 2014). Fundamental questions regarding the causative fault for this earthquake relevant for basic seismic hazard parameters such as slip rate, recurrence, timing of past events, are unknown at this time. Investigations into this earthquake are ongoing and much work still needs to be done in order to fully document the extent, complexity, and surface offsets produced by this earthquake, as well as basic data that feeds into regulatory zone and seismic hazard maps.

This earthquake offers a rare opportunity to study the effects of surface rupture using modern techniques such as aerial and ground based LiDAR, Structure from Motion (SfM) imaging, and various SAR techniques, all of which were deployed by various groups following this earthquake. These techniques will likely offer an unprecedented look into the effects of surface rupture and near-field ground deformation across the fault. Given the dense array of cultural features and new technological advancements, this earthquake rupture will provide much insight into the effects of surface rupture on the built environment and inform engineers regarding mitigation of surface rupture hazard imposed by active faults.

References

Bryant, W.A., 1982, West Napa fault zone; Soda Creek fault (East Napa fault): California Division of Mines and Geology Fault Evaluation Report FER-129, 9 pp.

Bryant, W.A., compiler, 2000, Fault number 36a, West Napa fault, Browns Valley section, in Quaternary fault and fold database of the United States: U.S. Geological Survey website, http://earthquakes.usgs.gov/hazards/qfaults, accessed 09/13/2014 05:49 PM.

U.S. Geological Survey, 2014, Updated finite fault results for the Aug 24, 2014 Mw 6.0 earthquake 6 km NW of American Canyon, California (Version 2), http://earthquake.usgs.gov/product/finite-fault/nc72282711/us/1409669093313/72282711.html, accessed 09/13/2014.

Wesling, J.R., and Hanson, K.L., 2008, Digital compilation of West Napa fault data for the Northern California Quaternary Fault Map Database: Final Technical Report submitted to the U.S. Geological Survey NEHRP, Award no. 05HQAG0002.

Contributors

Nikita Avdievitch (USGS)
Mike Bennett (USGS)
Dave Branum (CGS)
Jonathan Bray (UCB)
Ben Brooks (USGS)
Cooper Brossy (Fugro)
Bill Bryant (CGS)
Mike Buga (Fugro)
Julien Cohen-Waeber (UCB)
Brian Collins (USGS)
Clif Davenport (CGS)
Tim Dawson (CGS)

Marc Delattre (CGS)
Steve DeLong (USGS)
Andrea Donnellan (NASA JPL)
Todd Ericksen (Univ. of Hawaii)
Eric Fielding (NASA JPL)
Margaret Glasscoe (NASA JPL)
Craig Glennie (Univ. of Houston)
Wayne Haydon (CGS)
Les Harder (HDR)
Suzanne Hecker (USGS)
Chris Hitchcock (InfraTerra)
Tom Holzer (USGS)
Ken Hudnut (USGS)
Michael Jewett (Miller Pacific)
Keith Kelson (USACE)
Jeremy Lancaster (CGS)
Jim Lienkaemper (USGS)
Andy Lutz (InfraTerra)
Max Mareschal (CGS)
Alexander Morelan (UC Davis)
Mike Oskin (UC Davis)
Susan Owen (NASA - JPL)
Jay Parker (NASA – JPL)
Ante Perez (CGS)
Alexandra Pickering (USGS)
Dan Ponti (USGS)
Carol Prentice (USGS)
Jared Pratt (RGH Consultants)
Cindy Pridmore (CGS)
Ron Rubin (CGS)
Carla Rosa (USGS)
David Schwartz (USGS)
Gordon Seitz (CGS)
Robert Sickler (USGS)
Mike Silva (CGS)
Nicholas Sitar (UCB)
Jenny Thornburg (CGS)
Jerry Treiman (CGS)
John Tinsley (USGS)
David Trench (Fugro)
Chad Trexler (UC Davis)
Donald Wells (AMEC)
John Wesling (State of California, Office of Mine Reclamation)
Mark Wiegers (CGS)
Sang-Ho Yun (NASA - JPL)
Dana Zaccone (GeoVit)

USGS Disclaimer: These data are preliminary and are subject to revision and they are being provided to meet the need for timely best science. The report content does not necessarily reflect the views and policies of the U.S. Geological Survey. Any use of trade, firm, or product names is for descriptive purposes only and does not imply endorsement by the U.S. Government.

Figures:

Fig. 3-1 Map showing historic and Holocene mapped traces of the various right-lateral branches of the San Andreas Fault system. Red lines are historic surface ruptures, orange lines are Holocene faults. Those traces recently activated in association with the M 6.0 South Napa earthquake have been added, and are included as an update to previously mapped faults for the region. Faults from USGS Quaternary Fault and Fold Database, base from U.S. Geological Survey.

Figure 3-2. Map showing location of observed and inferred South Napa Earthquake fault rupture. Note: Due to scale issues, not all roads and place names listed in text are labeled. Readers are encouraged to use published road maps and online map resources for locating place names not included on Figures 3-2 and 3-4. Image base from Google Earth.

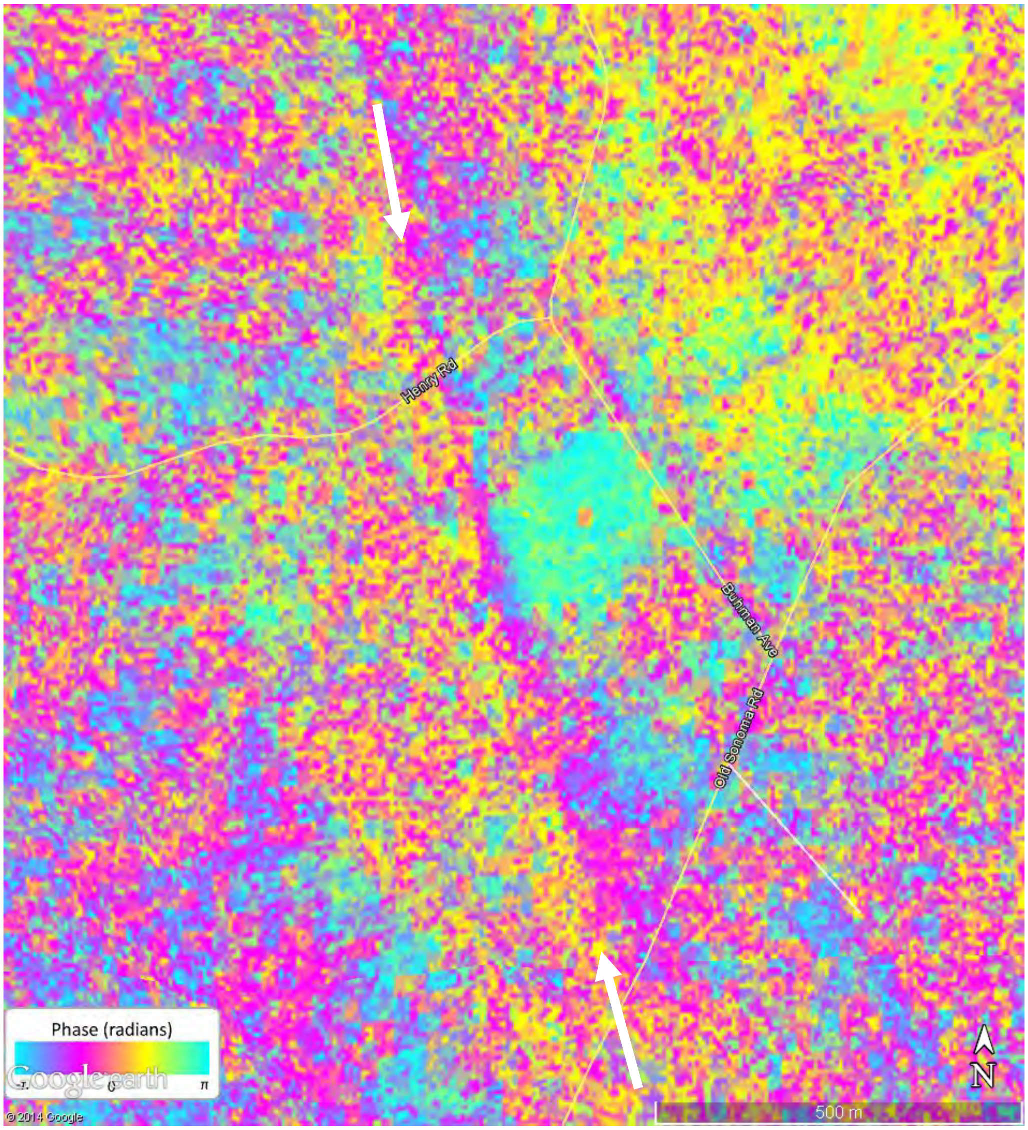

Figure 3-3. Image showing lineament observed on UAVSAR (denoted by white arrows) coincident with surface rupture in the vicinity of Old Sonoma and Henry Roads (UAVSAR image provided by NASA/Jet Propulsion Laboratory, California Institute of Technology).

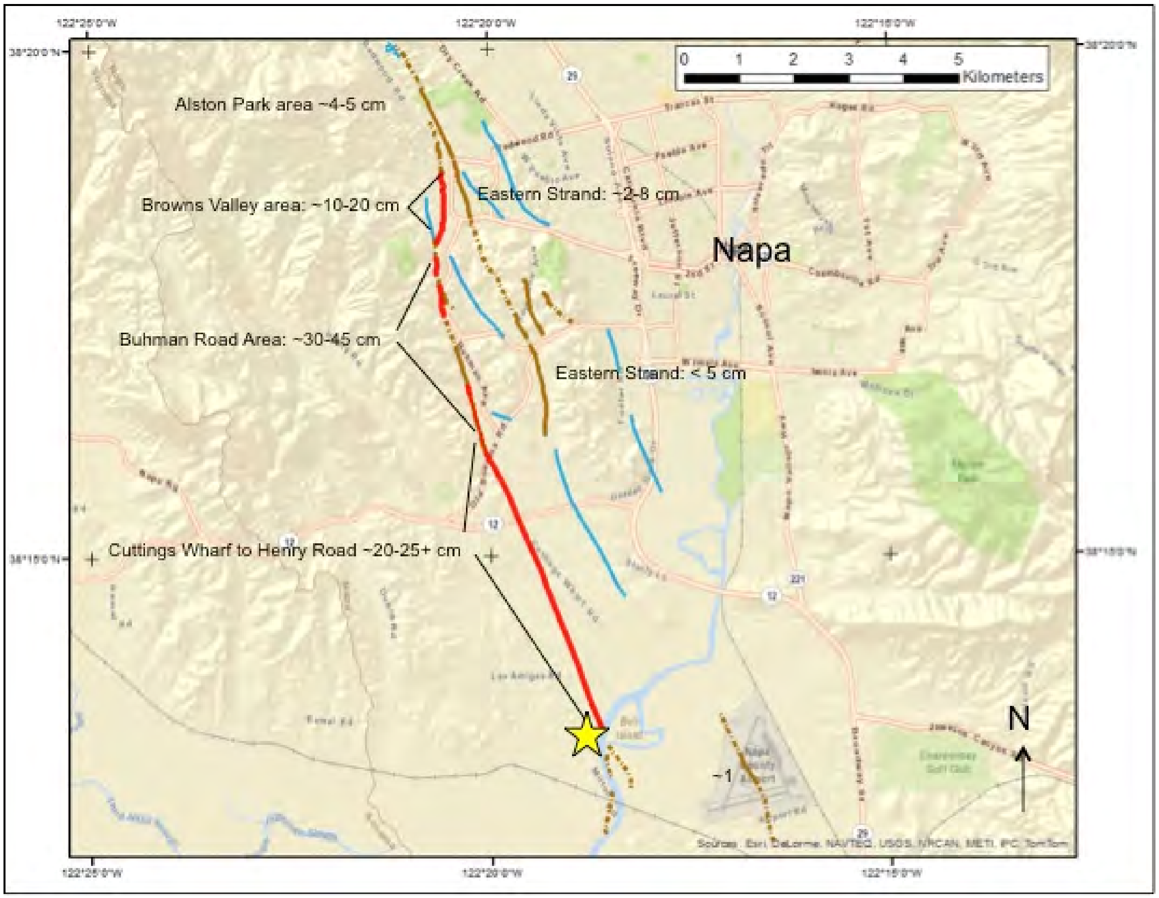

Figure 3-4. Map showing generalized right-lateral offsets along the surface rupture (in cm), measurements may include afterslip. Ruptures shown as red and brown lines, brown lines show areas of lesser, or distributed slip, or areas not yet field verified, but are likely areas of rupture, based on UAVSAR. Blue lines are lineaments identified from UAVSAR, and are still being field verified. Star shows approximate location of epicenter. Note how the surface rupture is located at, and north of the epicenter, and that the majority of the rupture involves about 20 to 25 cm of right-lateral offset at the surface, with slip decreasing in the vicinity of Browns Valley as the fault steps to the east.

Figure 3-5. Left-stepping pattern of surface fault rupture crossing horse corral near Cuttings Wharf Road. Note variation in width of zone. Offset at this location was initial on the order of ~10 - 20 cm, although offsets later grew due to afterslip. [NSF-GEER; GPS: 38.2555°, -122.3270°; 08/24/2014]

3-6a 3-6b

Figure 3-6a-b. Photos showing complexity of surface rupture as it crosses paved roads: 3-6a shows a broad zone, with fractures oriented nearly orthogonal to trend of fault at Middle Avenue [NSF-GEER; GPS: 38.2517°, -122.3251°; 08/24/2014]. The expression in 3-6b is narrower and fault-parallel, located where fault crosses Los Carneros Ave [NSF-GEER; GPS: 38.2431°, -122.3207°; 08/24/2014].

Figure 3-7. Surface fault rupture at northern part of Clos du Val Vineyard near 2121 Buhman Avenue (6.7 km NW of epicenter), showing measurement alignment along azimuth 090. Yellow engineer's scale shows measurement of 40 to 45 cm from base of thick wooden post; tape placed along southern edge of wooden posts aligned on east side of fault zone. [NSF-GEER; GPS 38.2776, -122.3377; 08/25/14: kik027]

Figure 3-8. Rupture west of Buhman Avenue. Right-lateral displacement was on the order of 40 cm, with a small amount (~12 cm) of up-on-the-west vertical displacement. [NSF-GEER; GPS: 38.2924°, -122.3432°; 08/25/2014]

Figure 3-9. Surface rupture disrupting sidewalks and curb on Twin Oaks Drive in Napa. Right-lateral displacement was on the order of 10 – 20 cm at this location [NSF-GEER; GPS 38.3024°, -122.3438°; 08/26/2014]

Figure 3-10. Surface rupture forming moletrack on asphalt road, tented concrete curb and displaced sidewalk in right-lateral sense on Partrick Road along eastern strand of the surface rupture. Right-lateral offset is on the order of between 5 - 10 cm. [NSF-GEER; GPS 38.3069°, -122.3374°; 08/24/2014]

Figure 3-11. Surface rupture near northern boundary of Alston Park. Note left-stepping pattern of extensional cracking, suggestive of right-lateral displacement, which was about 4-5 cm at this location. [NSF-GEER; GPS 38.3263°, -122.3459°; 09/01/2014]

Figure 3-12. Shattering of asphalt along southern part of eastern strand on driveway near Thompson Road. Rupture was difficult to see in soil on either side of driveway, but obvious on asphalt. Right-lateral offsets were around 5 cm in this area, although difficult to measure at this location [GEER-NSF; GPS: 38.2866°, -122.3259°; 8/25/2014].

Figure 3-13. Left-stepping en-echelon fractures without measurable displacement but of likely tectonic origin observed crossing only one of several runways at the Napa County Airport and located on the previously mapped section of the West Napa fault. Note vegetation lineament in grass, on trend with cracks on taxiway. [NSF-GEER; GPS: 38.2127°, -122.2814°; 8/27/2014].

Figure 3-14. Offset painted stripe on the side of Highway 12 is shown by these two photos taken approximately 24 hours apart on Aug. 24, 2014 and Aug. 25, 2014. The fracture opening is narrower and the paint stripe offset by a lesser amount on the day of the earthquake. During the ensuing day, the fracture grew and the offset of the paint stripe increased. The increase of offset along the surface rupture of an earthquake has been observed in previous earthquakes. What is different in the case of the South Napa earthquake is that in this case, afterslip in the first day after the earthquake was rapid, but then afterslip appeared to stop in the following days. In the southern half of the surface rupture zone, the initial evidence for rapid afterslip was pronounced, whereas in the northern portion there was little to no afterslip [NSF-GEER; GPS: 38.2559°, -122.3272°; 08/24/2014 and 08/24/2014.

Appendix B

The intent of this appendix is to provide a forum for the contributors to this report a place for additional figures, observations, and interpretations collected in the field not included in Section 3. The appendix sections are organized by field team and include additional figures and downloadable files. For further information regarding the individual subsections, please contact the field team lead.

Appendix B-1: Kelson and Wesling Detailed Observations
Appendix B-2: Fugro observations
Appendix B-3: U.C. Davis observations, made available on SCEC Earthquake Response site via Dropbox: https://ucdavis.app.box.com/s/9zsz84638fp90grhikzx

4 EFFECTS OF SURFACE FAULT RUPTURE ON INFRASTRUCTURE

4.1 Introduction

The preliminary reconnaissance efforts performed by GEER on August 24, 2014 (the day of the M6 South Napa earthquake) noted significant damage to infrastructure due to ground rupture in the areas northwest of the earthquake epicenter. While infrastructural damage in lightly populated areas was limited to roadways, boundary barriers or isolated structures, damage in heavily populated areas was extensive. The West Napa residential neighborhoods in the vicinity of Browns Valley Road and Buhman Avenue, herein referred to as the Browns Valley area (BVA), were observed to have been particularly affected by ground rupturing and intense seismic shaking. Located approximately 10 km north of the epicenter, the BVA experienced what was suspected to be surface fault rupture from Oak Rock Ln (southern end of this segment) to Redwood Rd (northern end), and west of Browns Valley Rd. and Buhman Rd. Although many residents in close proximity of the fault experienced significant damage to personal property from intense ground shaking, most of the structural damage was observed in conjunction with surface fault rupture. This section summarizes the GEER effort to document the effects of surface fault rupture on infrastructure in the BVA. Appendix C of this report contains all supporting documents upon which our observations have been drawn.

4.2 Reconnaissance and Data Collection

4.2.1 Investigation area

From August 25 through August 28, 2014, several teams collected measurements and observations throughout the Browns Valley area in the form of detailed maps of damage to individual properties. A total of 39 structures were summarily observed, of which 27 were carefully mapped with the consent of each owner. In each case, damaged properties coincided with the north trending trace of the surface rupture. Figure 4.1 illustrates the locations of mapped properties and surface fault rupture. For reference, each property has been numbered according to decreasing latitude and preceded by “H” (i.e., H39), as shown in the table of contents of Appendix C.

A second area, also exhibited significant infrastructure damage due to surface fault rupture. Herein referred to as BVA 2, this area is bounded approximately by Browns Valley Rd. to the west and south, Redwood Rd. to the north and Westview Dr. to the east. Due to time constraints, BVA 2 was visited during the afternoon of August 28 though not mapped to the same extent as the afore mentioned properties. A simplified map of the damage observed in BVA 2 is presented in the upper right corner of Figure 4.1.

4.2.2 Structures

Structures in the Browns Valley area consist of primarily single-family residences and associated structures such as swimming pools, detached garages, guest houses, tool sheds, and various forms of hardscape. Due to the extensive and persistent damage in this area, the BVA residential properties were made the primary focus for evaluating the effects of surface fault rupture on infrastructure after the M6 South Napa earthquake.

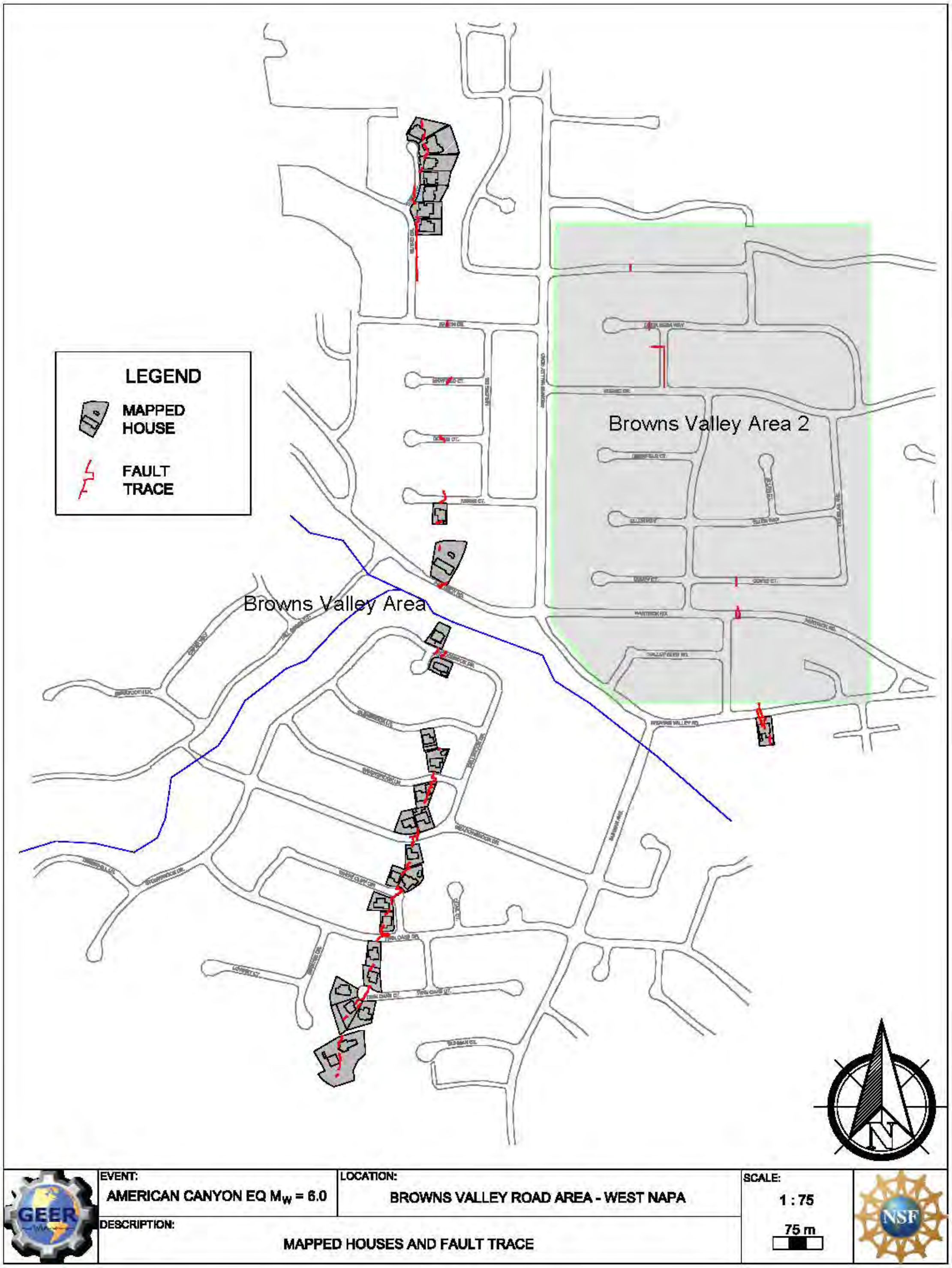

Figure 4.1 Location of mapped properties and surface fault rupture in the Browns Valley area. [NSF-GEER; J. Cohen-Waeber, R. Luque, R. Lanzafame, N. Wagner; 09/12/2014]

Residences typically consisted of single-story wood-frame structures with attached garages. A majority of the inspected structures south of Karen Dr. were founded on reinforced concrete perimeter strip footings with spread footing-supported wooden floor beams or reinforced concrete slab-on-grade. The inspected structures north of Karen Dr. were founded on reinforced concrete grade beams and 2-m to 4-m-deep reinforced concrete piers.

In addition to the physical residence, measurements were made on associated structures, including:

- Detached garages,
- Asphalt pavement,
- Concrete driveway slabs (reinforced and unreinforced),
- Concrete patios, curbs, gutters, sidewalks and driveway bibs (reinforced and unreinforced),
- Retaining walls and fences,
- Light structures (i.e., aluminum sheds with block foundations, wood trellis).

When possible, the property owners were interviewed to confirm if the damage observed was in fact associated with the August 24, 2014 M6 South Napa earthquake.

4.2.3 Methodology

Upon identifying a residence for mapping and obtaining permission from the property owner, a walk-through was conducted to observe seismic damage, after which a detailed map was developed. Only damage of clear seismic origin was mapped, including concrete and ground surface cracking, horizontal and vertical displacement of structures, and rotation of structures. Each damage feature was measured and photographed while an approximately scaled schematic representation of each feature was prepared. Specific measurements as reported in this section regularly included:

- Horizontal and vertical offset of new cracks
- Vertical depth of ground surface and structural cracks
- Displacement of structures away from adjacent ground
- Lengths of sidewalk sections before and after buckling
- Horizontal and vertical displacement of residence walls relative to foundations

In some cases structures showed apparent compression, either through buckling of stiff materials or by apparent strain relative to the adjacent ground surface (e.g., bulging of grass over concrete). Whereas pre-buckling dimensions of stiff structures such as sidewalks are typically possible to measure, some compressional features were not measurable.

Architectural damage was generally noted though not carefully measured or mapped. While drywall, stucco and paint cracks were prevalent as a result of minor structural deformation, these were recorded only to describe a specific structural failure mechanism or lack thereof. For example, radial floor cracks at H37 illustrate settlement of the foundation or door and window frame cracks at H31 illustrate the sense of movement within the structure. In the case of H13 however, the minor architectural damage observed was evidence of a successful seismic retrofit. Detailed maps for H13 and H37 are presented in Appendix C.

Residences in the BVA 2 (Figure 4.2) were not mapped individually. Due to time constraints, mapping

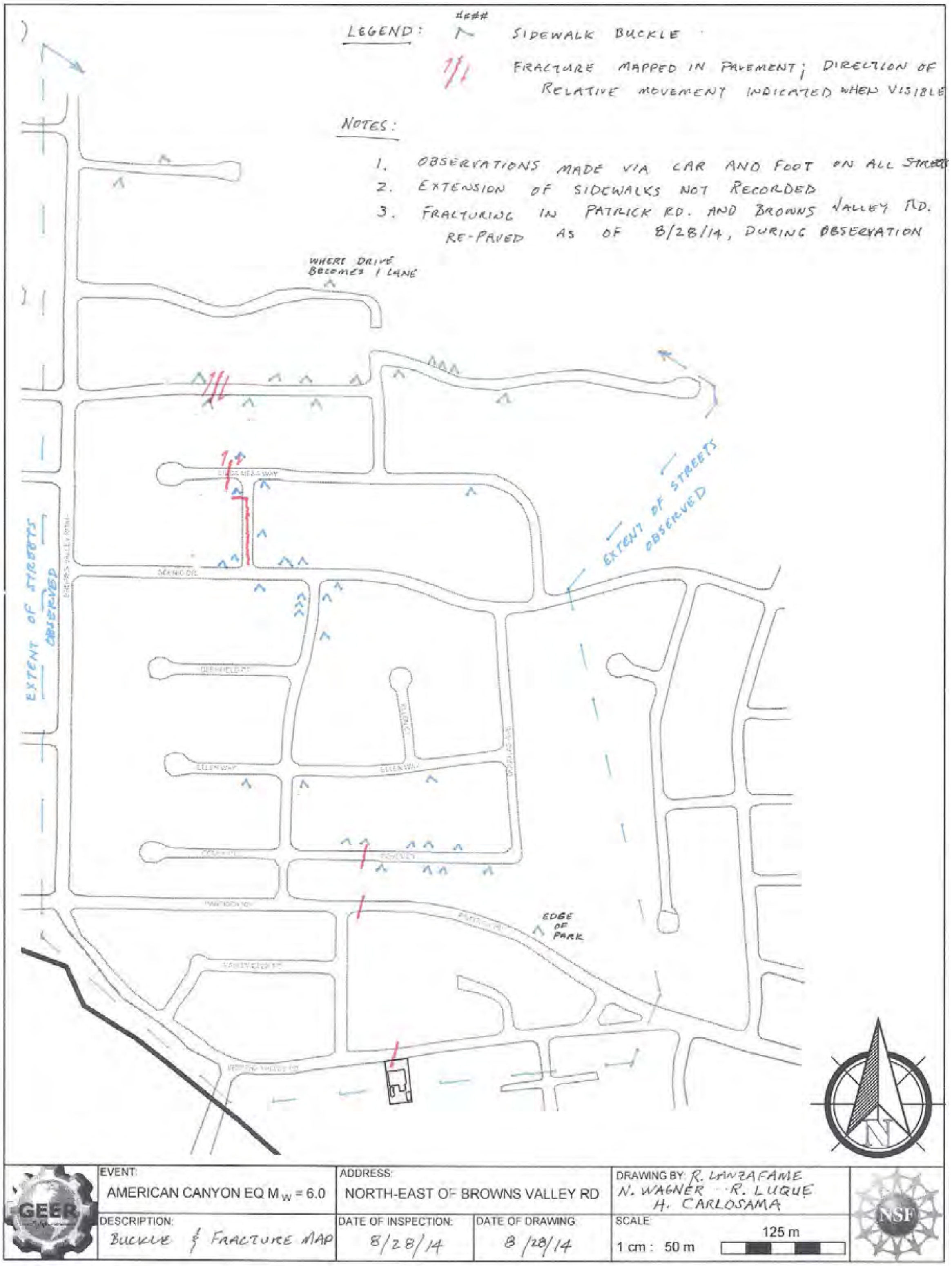

NOTES:

1. OBSERVATIONS MADE VIA CAR AND FOOT ON ALL STREETS
2. EXTENSION OF SIDEWALKS NOT RECORDED
3. FRACTURING IN PATRICK RD. AND BROWNS VALLEY RD. RE-PAVED AS OF 8/28/14, DURING OBSERVATION

EVENT: AMERICAN CANYON EQ $M_W = 6.0$

ADDRESS: NORTH-EAST OF BROWNS VALLEY RD

DRAWING BY: R. LANZAFAME N. WAGNER R. LUQUE H. CARLOSAMA

DESCRIPTION: BUCKLE & FRACTURE MAP

DATE OF INSPECTION: 8/28/14

DATE OF DRAWING: 8/28/14

SCALE: 1 cm : 50 m

125 m

Figure 4.2 Map of surficial damage in the Browns Valley Area 2, Northeast of Browns Valley. [NSF-GEER; H. Carlosama, R. Luque, R. Lanzafame, N. Wagner; 09/12/2014] was conducted on foot along roads and sidewalks and consisted of locating the general characteristics of ruptured asphalt pavement and buckled sidewalks. Asphalt cracking was drawn at approximate scale and the residential properties that were entered were identified. In some cases the asphalt pavement had already been repaired by the date of the reconnaissance.

4.3 Types of Damage

The damage typically observed during our field reconnaissance can generally be divided into the following three categories:

- Cracking of reinforced concrete and concrete masonry components within structures.
- Displacement between structures and adjacent ground or structures.
- Cracking of paved and unpaved areas at the ground level.

Though secondary to the scope of this investigation, additional recorded damage included: rupture of asphalt pavement, architectural damage, and failed chimneys.

Cracking of reinforced concrete and concrete masonry structures ranged from cosmetic cracking of swimming pool patios to cracking of building foundations. Table 4.1 summarizes and describes the different modes of concrete and masonry damage observed.

Where damage due to the displacement of structures with respect to adjacent ground or structures occurred, architectural damage was also prevalent. Generally, the most significant structural damage observed from displacement was horizontal and vertical offset of residence walls from the underlying foundations. Table 4.2 summarizes and describes the different modes of damage observed in relation to displacement across or between structural elements.

Damage due to ground cracking in paved and unpaved areas serves as a clear indication of the fault trace. Thus fracturing of asphalt pavement and unpaved ground surfaces were mapped in streets and residential properties where observed. These observations will be important for a better understanding of infrastructural behavior in the surface fault rupture area. Ruptures occurred with various degrees of severity from thin fissures to deep open cracks to buckled asphalt and soil mounds. While ruptures in unpaved surfaces (i.e., grass or dirt surfaces) did not exhibit as dramatic an appearance as those in asphalt, all fractures typically had distinct geometries which describe the sense of movement along the fault. Table 4.3 summarizes and describes the different modes of ground cracking observed during our reconnaissance.

Cracking of window and door frames in residences was common and generally consisted of hairline cracking in the wall façade, extending diagonally from the corners. Several toppled chimneys were also observed in the reconnaissance area. These failures typically occurred where unreinforced and unbraced brick chimneys extended above a structure roof more than approximately 0.5 m to 1 m. Although window and door frame cracking and chimney toppling were widely observed, their occurrence is typically not directly due to surface fault rupture; therefore, these observations are generally not uniformly included in the residential house mapping results.

Table 4.1 Observed types of reinforced concrete and concrete masonry structural cracking.

Cracking of concrete and masonry structures	
Foundations Primarily consisted of cracking of reinforced concrete strip footings or grade beams; visible from outside residence or within crawlspace. Photo reference: [NSF-GEER; N 38.3040 W 122.3430; 08/25/14 13:47]	
Concrete (non-foundation) Typically consisted of new fractures within garage concrete slabs, driveways, patio slabs, planter edges and other concrete structures, which were sometimes reinforced. Photo reference: [NSF-GEER; N 38.3024 W 122.3436; 08/27/14 11:33]	
Sidewalk/curb buckling Buckling of sidewalks, curbs or other linear concrete structures due to compressive forces during fault rupture displacement or seismic shaking. Photo reference: [NSF-GEER; N 38.3018 W 122.3439; 08/25/14 10:38]	

Table 4.2 Observed types of displacement between structures and adjacent ground or other structures.

Displacement between structures and adjacent ground or other structures	
Structure / Ground Displacement of structure relative to ground that had been immediately adjacent prior to the seismic event. Photo reference: [NSF-GEER; N 38.3042 W 122.3429; 08/25/14 13:56]	
Structure / Structure Displacement of structure relative to another structure that had been immediately adjacent prior to the seismic event. Photo reference: [NSF-GEER; N 38.3041 W 122.3429; 08/25/14 13:18]	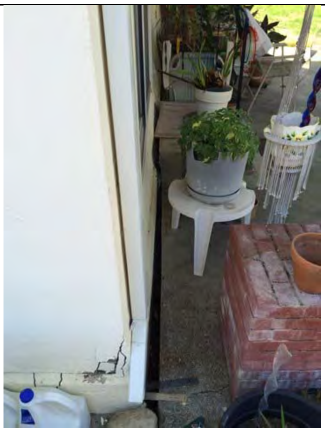
House frame on foundation Displacement of superstructure relative to its foundation in the horizontal or vertical direction. Photo reference: [NSF-GEER; N 38.3027 W 122.3436; 08/25/14 10:11]	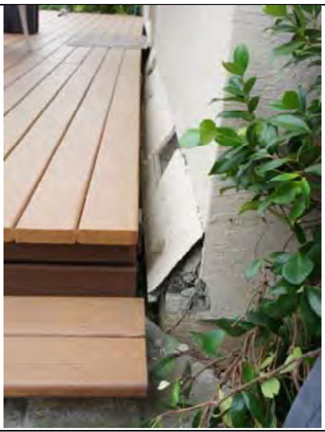

Displacement between structures and adjacent ground or other structures (Continued)	
Settlement Detached garage on strip footings and slab-on-grade. Structure settled west (i.e., right) approximately 5 cm due to surface fault rupture along edge of footing. Photo reference: [NSF-GEER; N 38.3052 W 122.3369; 08/28/14 10:00]	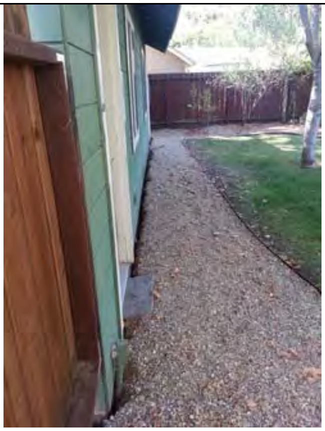
Light structures Displacement of light structures was measured where evidence of movement provided confirmation of displacement length. Photo reference: [NSF-GEER; N 38.3042 W 122.3429; 08/25/14 14:18]	
Retaining walls Separation of masonry blocks due to surface displacement in 1.5 - m tall landscape retaining wall. Photo reference: [NSF-GEER; N 38.3128 W 122.3429; 08/28/14 16:32]	
Compression of fences Fences were compressed in several cases; in one case a local strain measurement was obtained by measuring before and after length. Photo reference: [NSF-GEER; N 38.3015 W 122.3440; 08/25/14 10:55]	

Table 4.3 Observed types of ground rupture.

Ground Rupture	
Compression in paved areas Asphalt buckling from end [NSF-GEER; N 38.3038 W 122.3430; 08/25/14 10:24]	
Extension in paved areas Asphalt fracture away from compressed area shown above [NSF-GEER; N 38.3017 W 122.3440; 08/25/14 13:20]	
Compression in unpaved areas Soil mound from ground cracking [NSF-GEER; N 38.2980 W 122.3446; 08/26/14 12:25]	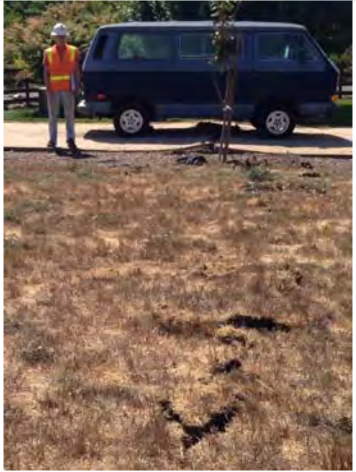
Extension in unpaved areas Ground surface rupture in side-yard [NSF-GEER; N 38.3045 W 122.3427; 08/25/14 15:24]	

4.4 Structural Performance Mapping

Illustrated in Figures 4.3 and 4.4 are the detailed structural performance maps for properties H01 and H21 (respectively). These cases demonstrate the performance of properties on pier and grade beam foundations (H01) and strip footings (H21), when directly affected by surface fault rupture.

In the case of H01, the site's geotechnical consultant allowed access to the property where surface rupture was observed to cross through the NE corner of the residence. Surface rupture was observed from a buckle in the wooden fence along the property's southern boundary, northward through displaced hardscape and under the structure. The rupture surface re-appeared along the north end of the residence from beneath the structure as a 3 cm open soil fissure with approximately 1 cm of right lateral displacement. Up to 5 cm of displacement was observed in the NE corner of the structure from gaps between the perimeter foundation and surrounding landscape. Damage to the northern external façade of the structure included approximately 0.5 cm cracks extending from the corners of the door frame, a roof beam apparently detached from the structure's wall, and a cracked foundation (approximately 0.5 cm). The consultant also reported damage to the floor boards within the structure which could be seen from the exterior though access to the structure was not possible to determine the cause.

In a similar fashion to H01, the residence at H21 experienced significant damage due to the surface rupture progressing directly through the structure. Along the southeast end of the property, an open fissure 8 cm wide and up to 70 cm deep cut adjacent to the West wall of a detached garage, causing the slab-on-grade building to tilt slightly to the West. The rupture was further pronounced to the North in the building crawl space by large open soil fissures. A 3 cm wide crack and several small gaps within the northern most perimeter strip footing were clearly a result of the ground rupture, also causing the structure's cripple wall to rack approximately 7 degrees to the East. North of the residence, the surface rupture was further pronounced through the paved driveway. Additionally, both wooden fences along the southern and northern property boundaries were buckled, with displaced fence posts up to 16 and 21 cm, respectively.

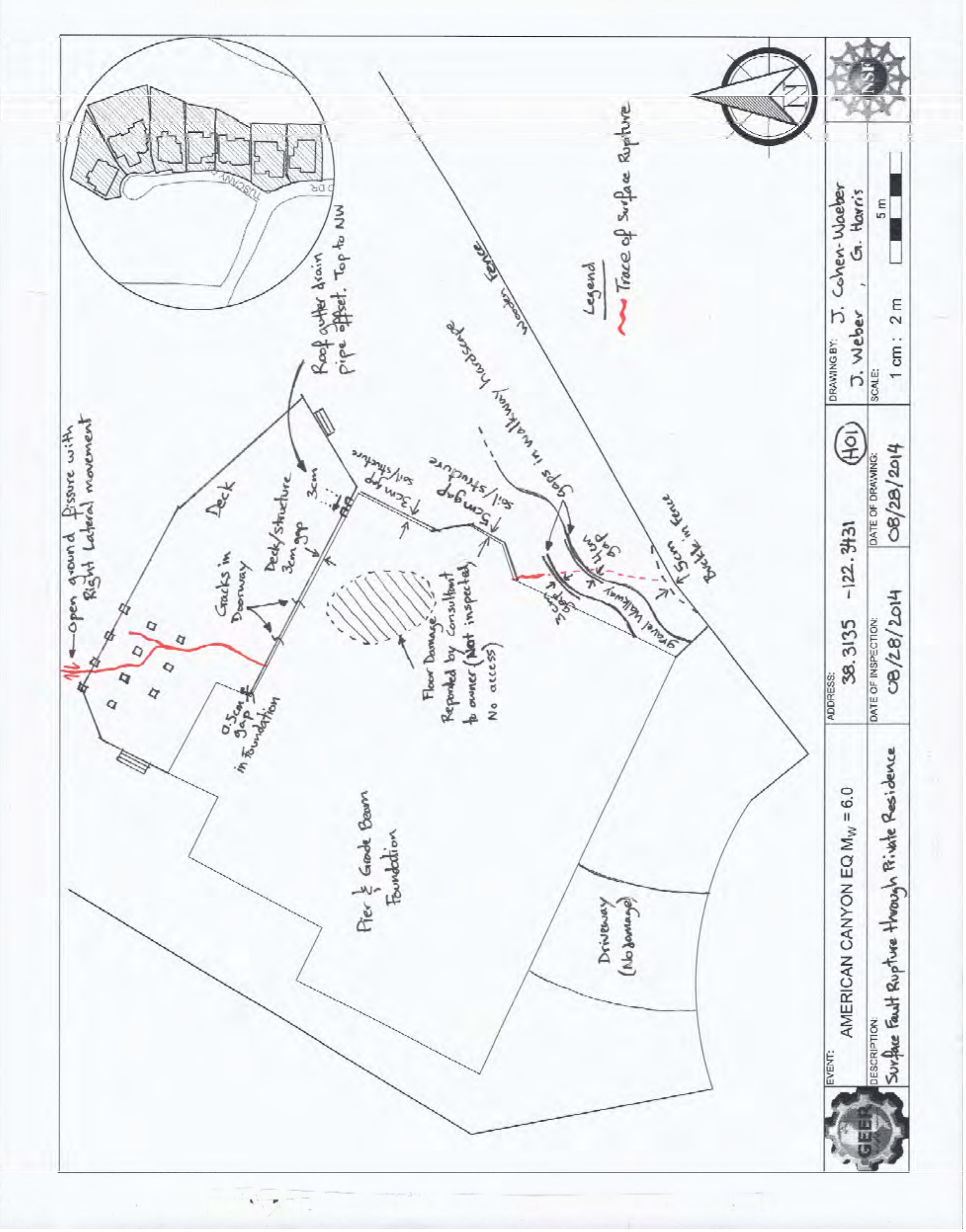

Figure 4.3 Map of Structural Performance, Northwest Browns Valley.
[NSF-GEER; J.Cohen-Waeber, J. Weber, G. Harris; 08/28/2014]

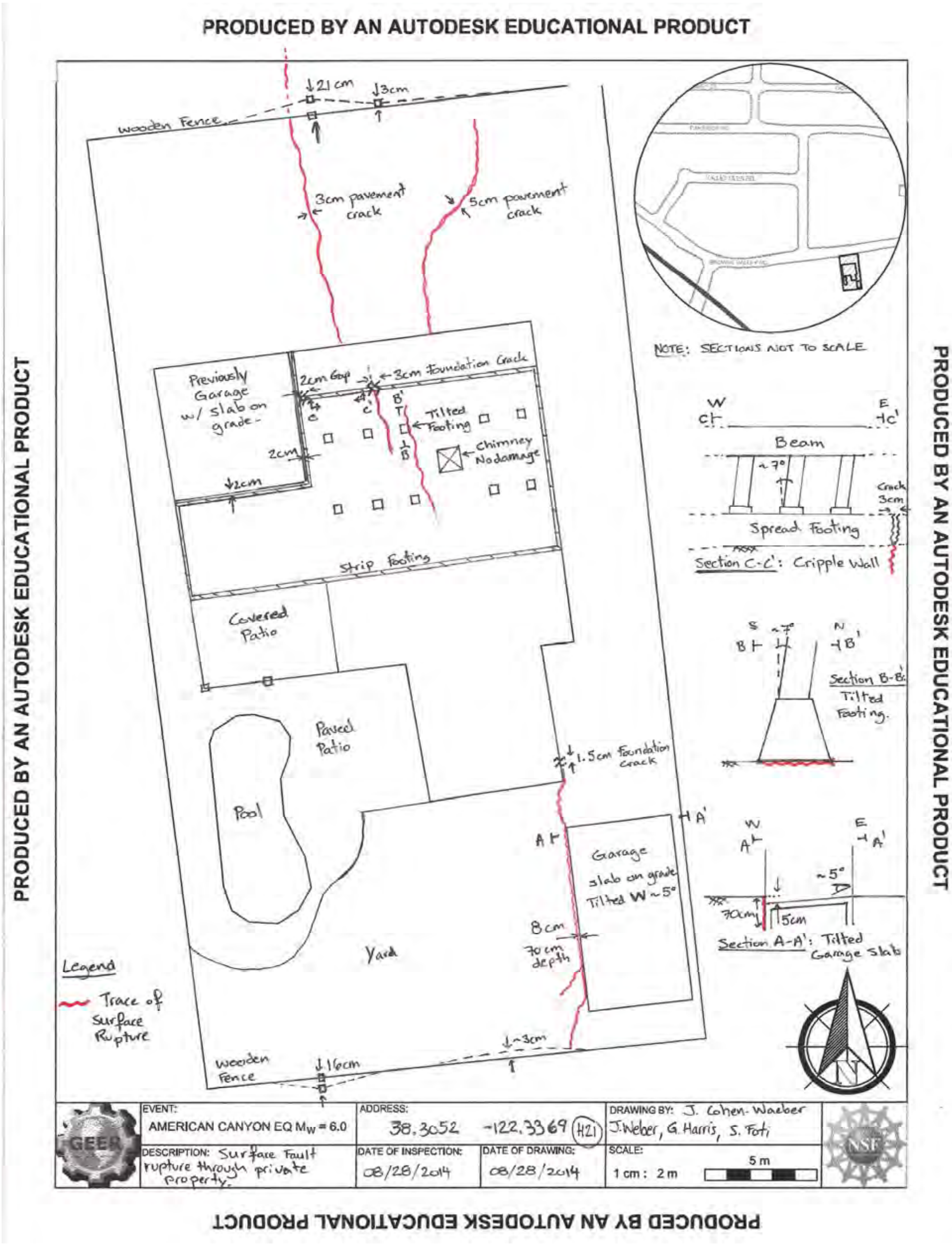

EVENT: AMERICAN CANYON EQ $M_W = 6.0$

ADDRESS: 38.3052 -122.3369 (H21)

DRAWING BY: J. Cohen-Waeber J. Weber, G. Harris, S. Foti

DESCRIPTION: Surface Fault rupture through private property.

DATE OF INSPECTION: 08/28/2014

DATE OF DRAWING: 08/28/2014

SCALE: 1 cm : 2 m

5 m

Figure 4.3 Map of Structural Performance, Northwest Browns Valley. [NSF-GEER; J.Cohen-Waeber, J. Weber, G. Harris; 08/28/2014]

4.5 Summary of Structural Damage

Tables 4.4 through 4.6 summarize our observations on damage to infrastructure due to surface fault rupture. Table 4.4 describes the location for each of the observed structures in the Browns Valley area, as well as the foundation type for mapped properties. Tables 4.5 and 4.6 summarize the various types and damage observed at each site, including quantitative measurements when available. The complete observations have been included as Appendix C of this report, in the form of detailed maps and selected photos. For reference, each property has been numbered according to decreasing latitude.

Table 4.4 Summary of mapped and observed properties in the Browns Valley area.

House No.	Lat. (°N)	Long. (°W)	Foundation Type (if mapped)	House No.	Lat. (°N)	Long. (°W)	Foundation Type (if mapped)
1	38.3135	122.3431	Piers and Grade Beams	21	38.3052	122.3369	Strip Footing / Slab
2	38.3133	122.3431	Piers and Grade Beams	22	38.3048	122.3427	Strip Footing
3	38.3131	122.3431	Piers and Grade Beams	23	38.3045	122.3429	Strip Footing
4	38.3128	122.3431	Piers and Grade Beams	24	38.3041	122.3429	Strip Footing
5	38.3126	122.3431	Piers and Grade Beams	25	38.304	122.3432	Strip Footing
6	38.3124	122.3432	Piers and Grade Beams	26	38.3037	122.3434	Not Mapped
7	38.3122	122.3432	Piers and Grade Beams	27	38.3036	122.3432	Strip Footing
8	38.3102	122.3426	Not Mapped	28	38.3033	122.3434	Strip Footing
9	38.3098	122.3426	Not Mapped	29	38.3032	122.3432	Strip Footing
10	38.3075	122.3426	Not Mapped	30	38.3029	122.3435	Strip Footing
11	38.3095	122.3428	Not Mapped	31	38.3027	122.3436	Strip Footing
12	38.309	122.3426	Not Mapped	32	38.3022	122.3438	Piers and Grade Beams
13	38.3087	122.3427	Not Mapped	33	38.3019	122.3439	Strip Footing
14	38.3082	122.3427	Strip Footing / Slab	34	38.3017	122.3443	Strip Footing
15	38.3076	122.3425	Strip Footing	35	38.3015	122.3442	Strip Footing
16	38.3066	122.3427	Strip Footing	36	38.3015	122.344	Strip Footing
17	38.3061	122.3427	Strip Footing	37	38.3011	122.3442	Strip Footing / Slab
18	38.3056	122.3423	Not Mapped	38	38.2981	122.3442	Not Mapped
19	38.3055	122.3432	Not Mapped	39	38.2967	122.3439	Not Mapped
20	38.3052	122.3429	Not Mapped				

Table 4-5 (Page 1 of 2) – Summary of Damage of Mapped Residences

		Cracking of concrete and masonry structures			Displacement between structures and adjacent ground or other structures								
House No.	Overall Level of Damage	Foundations	Concrete (non-foundation)	Sidewalk/gutter buckling	Structure / Ground	Structure / Structure	House frame on foundation	Settlement	Light structures	Retaining walls	Compression of fences	Ground rupture	Notes/Other
1	H	X			5				3			X	Patio detached from house, cracks in house floor, structural damage from shearing of building.
2	H	X	2	3	1	11					X	X	
3	H	X		X	5	5	11		60			X	Reinforced concrete driveway and garage slabs shifted N. Entry stair case shifted N. Front of house frame shifted N on foundation. Car in garage moved E-W.
4	H	3			2	2				3	X	3	Dry masonry wall damage
5	M	1.5				3							Damage to garage and front façade of home only.
6	M		3			2		8				5	Damage to entrance stair cases and retaining walls. Settlement of fill behind small wall.
7	M		5									X	Driveway and entry way stairs affected only.
14	L		X	X							X	X	Recently remodeled home with large moment frame parallel to fault trace
15	M	X		X	2					X		X	Principal door is not functional. Not cracks observed in the ground within the crawl space
16	M		X		5								General ground movement down-slope tilting light structures.
17	L		X		3								
20	L			X	4								
21	H	3			8 H 70 D	2	X	5	X		X	X	Garage slab tilted 5^{o} W, House shifted E on tilted cripple wall and footing (7^{o} N and E).
22	L			X		11						X	1.5 cm cracks in garage N-S walls
23	L			X	4				5	1			Extensive rupturing in gravel side-yard; shed displaced vertically due to rupture beneath.

1. Numbers represent maximum measurements in cm of the particular type of damage found for each house; H = horizontal, V = vertical, D = depth.
2. Overall Level of Damage types are: H = high, M = medium, L = low, X = observed but not measured as discussed in the text.

Table 4-5 (Page 2 of 2) – Summary of Damage of Mapped Residences

		Cracking of concrete and masonry structures			Displacement between structures and adjacent ground or other structures								
House No.	Overall Level of Damage	Foundations	Concrete (non-foundation)	Sidewalk/gutter buckling	Structure / Ground	Structure / Structure	House frame on foundation	Settlement	Light structures	Retaining walls	Compression of fences	Ground rupture	Notes/Other
24	H	0.5	5	X	10		6 H 3 V		20			X	Shed displaced horizontally on concrete slab. Significant movement of house frame on foundation and displacement between structures and ground/foundation.
25	L			X	4								Breaking/deformation of rebar in driveway/sidewalk joint; house structure undamaged.
27	H	X	X			11	13			3		X	Rupture between two retaining walls at SW property corner with no apparent damage to retaining walls. S end of house shifted W on foundation.
28 / 29	L			150 H 32 V							X		Rupture between two apparently undamaged homes.
30	L		5	X	8								Damage primarily to driveway and sidewalk.
31	H	5	8				5		5		X	X	Garage: slab apparently unreinforced, door shifted. House shifted on spread footing at NW corner.
32	H	X	2.5 H 1 D		14	10						X	Split redwood tree. Right-lateral deformations apparent throughout survey. Significant cacking in garage slab and of adjacent wall strip foundation.
33	L				5.5				27			8 H 20 D	Displaced wood trellis structure on concrete slab and rupture along backyard slope.
34	L					1.5							Cracking of concrete at edge of pool and displacements between side-drive slab.
35	M		X	X	2					1	0.0033	5-6 V 70 D	Multiple cracks in retaining wall up to 0.8 cm. Strain due to compression along wood fence measured as ε = 0.33%.
36	M			X	3					X		13 H 76 D	Fallen statues and 23 cm diameter tree; localized comp. of wall bulged 20 cm H over 1.47 m
37	M	X	5	10 H 8 V	5 H 64 D			3			X	5	Radial cracks in bathroom due to settlement of cracked foundation

1. Numbers represent maximum measurements in cm of the particular type of damage found for each house; H = horizontal, V = vertical, D = depth.
2. Overall Level of Damage types are: H = high, M = medium, L = low, X = observed but not measured as discussed in the text.

Table 4-6 Summary of Pavement Damage.

Street	Latitude (degrees N)	Longitutde (degrees W)	Asphaltic Pavement Cracking	Asphaltic Pavement Buckling
Buhman Ct	38.3007	122.3443	5 H	8 V
Twin Oaks Dr	38.3025	122.3438	10 H	20 V
Twin Oaks Ct	38.3017	122.344	12 V 20 H 50 D	20 V
White Cliff Cir	38.3031	122.3434	5 H 16-50 V	8 V
Meadowbrook Dr	38.3038	122.3441	5 H	24 V
Sandybrook Dr	38.3046	122.3428	5 H	20 V
Browns Valley Rd	38.3055	122.3370	5 H	
Kerns Ct	38.3085	122.3427	X	
Sutro Dr	38.3123	122.3432	X	
Tuscany	38.3129	122.3432	3 H	
Westminster Way	38.3117	122.3395	X	
Linda Mesa Way	38.3109	122.3391	X	
Mason St	38.3104	122.3388	X	
Covey Ct	38.3074	122.3375	X	
Partick Rd	38.3069	122.3375	X	

1. Numbers represent maximum measurements in cm of the particular type of damage found for each house; H = horizontal, V = vertical, D = depth.
2. Overall Level of Damage types are: H = high, M = medium, L = low, X = observed but not measured, as discussed in the text.

4.6 Discussion

4.6.1 Generalized Damage Assessment

A preliminary assessment of the quantitative descriptions of damage summarized above shows certain characteristic interactions between surface fault rupture and the mapped damage of the overlying infrastructure. Based on these general observations, 13 of the 27 investigated properties showed concrete slabs cracked up to 8 cm wide. Similarly, 12 of the 27 observed cases, experienced cracking of their foundation by up to 3 cm, and 5 of these structures were shifted up to 11 cm off of their foundation.

The performance of different foundation types under similar circumstances is also a significant observation. Of the 8 investigated properties that were founded on pier and grade beam foundations, 6 had foundation damage, 4 exhibited cracks in concrete, 6 experienced displacement between the structure and ground as well as between structures and 1 experienced displacement of the structural frame from the foundation. Of the 19 investigated properties that were founded on strip footings, 6 had foundation damage, 9 exhibited cracks in concrete, 16 experienced displacement between the structure and ground as well as between structures and 4 experienced displacement of the structural frame from the foundation.

However, with the gathered information, it is not yet possible to draw conclusions on the differences in behavior between different foundation types.

4.6.2 Special Cases

There were several special cases in which atypical occurrences may warrant further investigation.

Though located several km south of the Browns Valley study area, a right-lateral offset of approximately 10 cm was observed through Los Carneros Ave. This offset occurred at the Stone Bridge School where windows were observed to have broken. Although detailed measurements of the Stone Bridge School were not collected as a part of this effort, data may have been collected by others and should be compiled. In comparison, no significant damage was observed at the Browns Valley School.

The properties located at investigation points H27-H29 are connected by two retaining walls. The retaining walls stand end to end and are approximately 2.5 m to 3 m in height and separate the properties at H28 and H29 from H27. As the fault rupture propagated north, it passed between the properties at H28 and H29 and between the retaining walls through a 16 cm gap. While the property at location H27 sustained significant damage due to concrete cracking and structural deformation, the retaining walls showed no clear signs of deformation. The foundation elements of the retaining walls are not known.

The performance of pier foundations under surface fault rupture conditions is an important question. Of the 8 investigated properties constructed on pier and grade beam foundations, the property at location H01 experienced the most damage. The surface rupture trace appears to have sheared the NE corner of the structure by passing between piers. Though it was not possible to enter the home, significant foundation and structural damage was visible from the exterior.

5 GROUND DEFORMATION IN THE VERY NEAR FAULT REGION

5.1 Introduction

Initial reconnaissance of the residential neighborhoods in West Napa immediately following the earthquake on 8/24 and 8/25 noted extensive zones of surface deformations consisting of buckled sidewalks, curbs, and pavement. While some of this deformation was clearly associated with surface faulting, much of the observed deformation consisted of compressional features which could not be immediately attributed to any particular faulting mechanism. These features were particularly well expressed in the neighborhood of West Napa, CA bounded by Partrick Road and Browns Valley Road to the north and Buhman Avenue to the east (Figure 5-1) and, therefore, this area was mapped in detail over a period of three days, 8/26 to 8/28, 2014. Specifically, detailed measurements were made of compression and extension along streets and sidewalk parallel to the fault trace and along the cross streets, roughly orthogonal to the fault trace. A summary of these observations and recordings are provided in this section.

Figure 5.1: Observation and measurement sections of ground strain (red lines) and approximate observed fault trace (yellow line); produced in Google Earth; [NSF-GEER; Napa, CA; N 38.3040 W 122.3443; 8/26/14 - 8/28/14]

5.2 Overview of Ground Strain Observations

The compression features were predominantly concentrated in concrete sidewalks and were quite readily apparent while extension cracks were typically quite innocuous and required a careful inspection. A typical buckled compression zone and extension crack is shown in Figure 5.2. It should be noted that frequently there was no evidence of similar deformation in the adjacent bituminous pavement in the street.

Figure 5.2: Typical buckled compression zone (left) and extension crack (right) [NSF-GEER; N 38.3037 W 122.3433; 8/26/2014 15:41 (left); N 38.3055 W 122.3455; 8/26/2014 18:34 (right)]

5.2.1 Measurement Methodology

A consistent measurement procedure was developed in the field to standardize the observations of compression zones and extension cracks. First, a 100 meter tape measure with 1 millimeter increments was stretched in the road parallel to the sidewalk approximately 2 meters from the edge of the curb in 25 meter segments. This configuration was chosen since the road was essentially free of topographic expressions (primarily tree root uplift and buckled sidewalk pavement, etc.) that would cause the 25 meter segment to be shorter than it should actually have been. The ends of the 25 meter segment were marked with spray paint and numbered, and then the bearing along the segment was estimated with a compass. At intersections, the segment measurement was continued until the concrete curb contacted the asphalt and the reduced (or augmented) segment length was recorded.

Next, the sidewalk in the segment was carefully inspected and the compression zones and extension cracks were measured relative to the start of the segment. Extension cracks were measured to the nearest 1/16 inch with a ruler or tape measure spanning perpendicular to the crack at various locations, and then a representative value was reported. When possible, area residents were consulted as to which cracks existed prior to the earthquake. Small cracks filled with debris (<1/16 inch) were not considered since debris-filled cracks were observed with a modest (up to 1/8 inch) gaps on at least one side. This suggests that the debris-filled cracks with no gaps were not due to the earthquake. Additionally, cracks in sidewalk pavement that had been previously ground down were not considered. These cracks were often in expansion joints and had been shaved to offer a smoother transition between uplifted sections of pavement.

Deformation in the buckled compression zones was assessed by first measuring the lengths of the uplifted sidewalk section along the top surface on the same edge to obtain the original length of the section. Then, the distance between the new outer edges of the sidewalk was measured to obtain the new length of the section. The difference between the measurements was recorded as the compression in the zone. Measurements for a typical buckled section are shown in Figure 5.3 below.

Figure 5.3: Measuring a typical buckled compression zone in sidewalk pavement [NSF-GEER; N 38.3039 W 122.3430; 8/26/2014 15:24]

In some locations, compression in the sidewalk pavement manifested as an overlap instead of a buckled section. In such cases the overlap was measured and recorded as the compression in the zone. The measurement for an overlapping compression zone is shown in Figure 5.4 below. In cases where both gaps and overlaps were observed, the gaps were subtracted from the overlap measurement and this value was recorded as the compression in the zone. The measurement for an overlapping compression zone with a gap is shown in Figure 5.5 below.

Figure 5.4: Measuring an overlapped compression zone in sidewalk pavement [NSF-GEER; N 38.3065 W 122.3454; 8/28/2014 14:00]

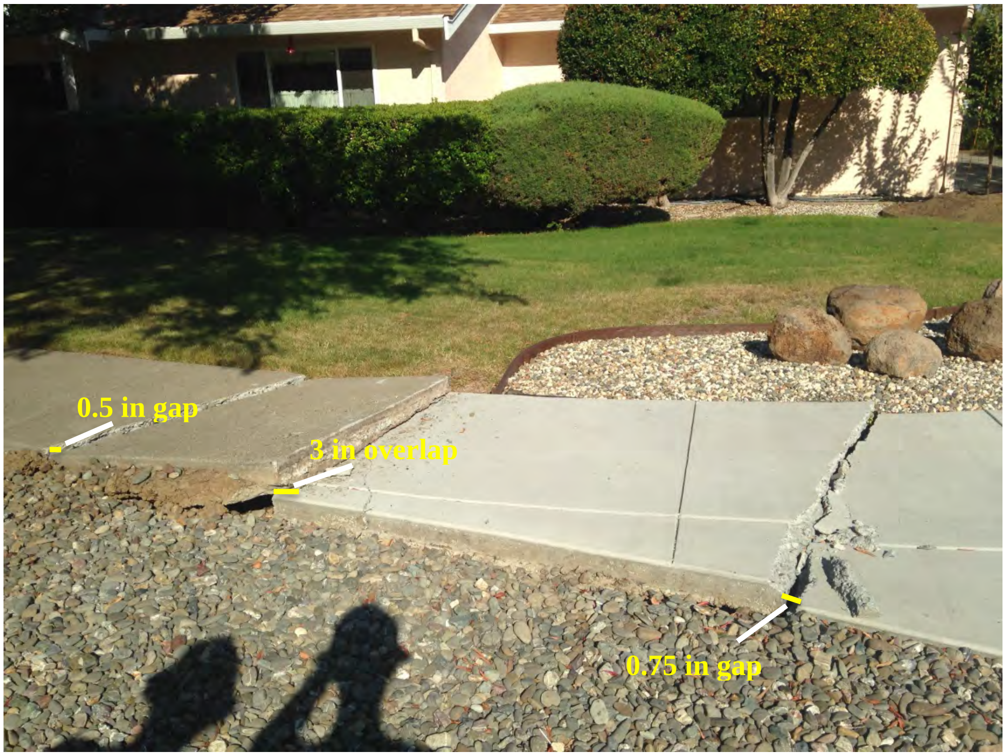

Figure 5.5: Measuring an overlapped compression zone with a gap in sidewalk pavement [NSF-GEER; N 38.3047 W 122.3459; 8/26/2014 16:52]

5.2.2 Ground Strain Computations and Map

Ground strain was computed over each 25 meter segment by adding the measured extension cracks (positive) and compression zones (negative) to the measured segment length to obtain the original segment length. This became the “gage length” of the strain measurement. Then, the difference between the measured and the estimated original length was divided by the estimated original length to obtain the decimal strain, which was converted to a percent strain. Additionally, the average strain for each sidewalk section as a whole was computed in a similar manner by considering all measured extension cracks and compression zones added to the total length of the segments of a single sidewalk. The results of the average strain over each total sidewalk are shown in Table 5.1 and Table 5.2 below for sidewalks parallel and perpendicular to the fault, respectively. The measurements and computations for individual segments are shown in Appendix D. A schematic showing the approximate location of each extension crack and compression zone is shown in Figure 5.6 below.

Figure 5.6: Observed and measured tension (orange) and compression (green) locations; produced in AutoCAD; [NSF-GEER; Luque, R.; Wagner, N.; processed 9/5/14]

Table 5.1: Summary of strain measurements in parallel trending roads [NSF-GEER; Wagner, N.; processed 9/3/2014]

N-S (PARALLEL) TRENDING ROADS				
	East Side		West Side	
	Total Length (m)	Average Strain (%)	Total Length (m)	Average Strain (%)
West of Fault				
Estates Dr	90.0	-0.01	77.5	-0.07
White Cliff Cir (West)	71.4	0.05	71	-0.02
Stonybrook Dr	459.2	-0.04	508.0	-0.03
Tall Grass Dr	N/A	N/A	199.0	-0.05
Casper Way	203.9	0.01	220.2	-0.01
Weighted Average Strain		**-0.01**		**-0.03**
East of Fault				
Twin Oaks Ct	69.8	0.00	69.8	0.00
Dellbrook Dr	75	0.00	44.15	0.00
Weighted Average Strain		**0.00**		**0.00**
Crossing Fault				
White Cliff Cir (East)	50.7	**0.01**	50.7	**0.36**

Table 5.2: Summary of strain measurements in perpendicular trending roads [NSF-GEER; Wagner, N.; processed 9/3/2014]

E-W (PERPENDICULAR) TRENDING ROADS				
	North Side		South Side	
	Total Length (m)	Average Strain (%)	Total Length (m)	Average Strain (%)
West of Fault				
Twin Oaks Dr	297.3	-0.02	274.1	0.01
White Cliff Cir	163.0	-0.05	164.5	0.04
Meadowbrook Dr	221.7	0.00	221.7	0.00
Weighted Average Strain		**-0.02**		**0.01**
East of Fault				
Twin Oaks Dr	212.1	0.00	208.9	0.00
Meadowbrook Dr	209.4	0.00	N/A	N/A
Weighted Average Strain		**0.00**		**0.00**
Crossing Fault				
Meadowbrook Dr	40	**-0.24**	30	**-0.17**

5.3 Additional Observations

In addition to the deformations in the concrete sidewalks compression features in the curb strip adjacent to the sidewalk, cracking in asphalt, damaged curbs and a fence adjacent to the fault trace were measured and documented.

5.3.1 Compression Features in Curb Strip

Compression features in the curb strip were observed at various locations adjacent and perpendicular to the sidewalk pavement. Two of the compression features (Figure 5.7 and Figure 5.8) are located across from the creek running parallel to the fault trace through the neighborhood. In these cases the sidewalk pavement moved laterally toward the free face of the creek. Additionally, it was noted that the compression feature in Figure 5.7 occurred at the end of the bend at a corner.

One of the compression features was located near the fault trace adjacent to a buckled compression zone in a sidewalk perpendicular to the fault trace (Figure 5.9). The compression feature is parallel to the fault trace. It was noted that there was separation between the asphalt and the curb in line with the compression feature in the curb strip.

Figure 5.7: Crushed section in pavement parallel to fault with compression features in curb strip perpendicular to fault, across from creek [NSF-GEER; N 38.3055 W 122.3467; 8/28/2014 14:30]

Figure 5.8: Compression feature in curb strip perpendicular to fault, across from creek [NSF-GEER; N 38.3065 W 122.3455; 8/28/2014 13:52]

Figure 5.9: Buckled section in pavement perpendicular to fault with compression features in curb strip and lawn parallel to fault, near observed fault trace [NSF-GEER; N 38.3018 W 122.3439; 8/25/2014 10:38]

5.3.2 Cracking in Asphalt

One of the more enigmatic observations was that bituminous pavement was largely devoid of compression features except immediately along the fault trace. Most of the cracks in bituminous pavement were transverse to the direction of the street and appeared to be extensional. In addition, most manholes and other penetrations in the pavement were ringed by apparently fresh cracks. (Figure 5.10).

Figure 5.10: Cracks in asphalt perpendicular to fault trace near manhole covers [NSF-GEER; N 38.3063 W 122.3458; 8/28/2014 14:15 (left); N 38.3068 W 122.3465; 8/28/2014 15:19 (right)]

5.3.3 Damaged Curbs

Damaged curbs were observed throughout the neighborhood along roads both parallel and perpendicular to the fault trace. The damage included crushing (Figure 5.11), extension cracks (Figure 5.12) and buckling failures (Figure 5.13). In general, the damaged curbs were not directly adjacent to the buckled compression zones in the sidewalk pavement. However, the curbs were not included in the detailed surveying because in most cases the broken pieces were missing or could not be reconstructed into the original configuration.

Figure 5.11: Crushed curb perpendicular to fault trace [NSF-GEER; N 38.3035 W 122.3411; 8/25/2014 14:47]

Figure 5.12: Extension crack in curb parallel to fault trace [NSF-GEER; N 38.3066 W 122.3475; 8/28/2014 15:08]

Figure 5.13: Buckled curb parallel to fault trace [NSF-GEER; N 38.3073 W 122.3443; 8/28/2014 13:41]

5.3.4 Strain Measurements in Fence

In addition to calculating strains in sidewalk pavement, strain was computed for a section of fence running parallel and adjacent to the fault trace (Figure 5.14). To compute the strain, the horizontal boards at the top of the fence were measured in segments to obtain an estimate of the original length of the fence. Then, the ground along the base of the fence was measured to obtain an estimate of the new length of the fence. The data and computations are shown in Table 5.3 below. Note that the average strain in the fence is the same order of magnitude as the average strain in the sidewalk pavement for roads crossing the fault trace (Table 5.1 and Table 5.2).

Figure 5.14: Buckled section of fence of the surveyed fence [NSF-GEER; N 38.3015 W 122.3442; 8/25/2014 09:57]

Table 5.3: Summary of strain measurements in parallel trending fence [NSF-GEER; Wagner, N.; processed 9/3/2014]

Section Number (Top)	Length (m)	Section Number (Bottom)	Length (m)
1	1.5	1	11.9
2	4.8		
3	2.4		
4	2.4		
5	4.9	2	9.8
6	4.9		
7	2.4		
8	2.4		
9	2.4	3	11.2
10	2.4		
11	2.4		
Total	33.0		32.9
		Average Strain	**-0.36**
		Average Disp. (m)	**-0.12**

6 PERFORMANCE OF GROUND AND BURIED UTILITIES

6.1 Introduction

Preliminary reconnaissance efforts were made outside the zone of surface fault rupture and associated very near fault ground deformation on August 24, 2014 by GEER team members in the cities of Napa, Vallejo, including Mare Island, American Canyon, and surrounding areas (Figure 6.1). Most notable in this reconnaissance was the absence of ground failure, including that due to liquefaction, relative to what has been observed after previous earthquakes of this size or larger in the San Francisco Bay area. Several isolated instances of broken underground pipelines and masonry building damage were observed, but overall ground performance was good. Several GEER teams focused on trying to find locations with evidence of soil liquefaction (e.g., sand boils). However, instances of liquefaction or lateral spreading were observed in only two locations with no significant effects on the supporting system or adjacent structures. Detailed observations and select photographs of ground performance during the M6 South Napa earthquake are provided in Appendix E of this report.

The American Society of Civil Engineers Technical Council on Lifeline Earthquake Engineering (ASCE-TCLEE) published a quick report on September 1, 2014 (*South Napa M 6.0 Earthquake of August 24, 2014*, ASCE TCLEE Quick Reconnaissance Report, Revision A) detailing the performance of power systems, water and wastewater systems, highway bridges and roads, and communication systems during and after the earthquake. Their report also includes information on regional geology, seismic hazard, recorded ground motions, and surface fault rupture. The ASCE-TCLEE report can be downloaded at: http://www.asce.org/Technical-Groups-and-Institutes/TCLEE/ASCE-TCLEE-Preliminary-Reconnaissance-Report-of-the-August-2014-South-Napa-Earthquake/. There are additional quick reports being prepared by lifeline organizations, such as Caltrans and PEER, which should be referred to for additional information. This section focuses on information collected by GEER team members.

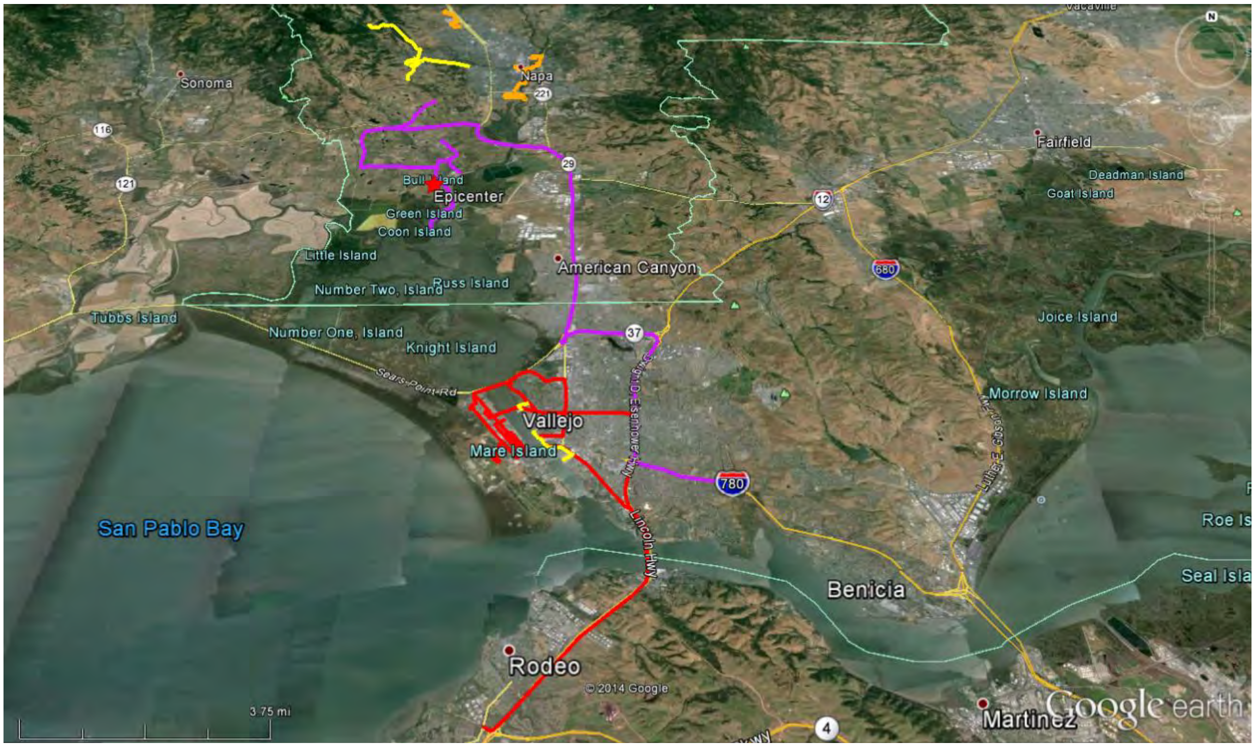

Figure 6.1: GPS tracks for GEER reconnaissance teams that focused on ground failure observations; produced in Google Earth; [NSF-GEER; Vallejo, CA and Napa, CA; 8/24/14]

6.2 City of Vallejo

6.2.1 Vallejo Waterfront (east side of Mare Island Straight)

Along Mare Island Way and at the Vallejo Marina up to the Ferry Terminal, no damage was noted except for two broken water pipes along the road. Observations for the Vallejo waterfront are summarized in Table E.3 in Appendix E. Based on telephone discussions with the City of Vallejo, no fires were reported within the city limits.

6.2.2 Highway 37 Bridge

No significant damage was observed along the Highway 37 Bridge alignment. The bridge was observed from vantage points at the east and west abutments and from a vehicle while crossing. The eastern abutment was observed in greater detail (Figure 6.2). There was an absence of ground cracking and ground deformation, indicating good performance of the ground at the site.

Figure 6.2: Highway 37 Bridge pier with no significant ground damage; [NSF-GEER; Mare Island, Vallejo, CA; GPS N38.122 W122.276; 08/24/14; 18:24]

6.2.3 Water, power, and fire

A total of 13 water main breaks were reported by the City of Vallejo on August 24, 2014, the day of the earthquake, and 8 additional breaks were reported on August 25, based on conversations with city representatives and press releases. A total of 6 water main breaks were observed during GEER reconnaissance. Four of the water main breaks were observed on Mare Island, and two breaks were observed along Mare Island Way on the Vallejo waterfront. Locations of the additional breaks will be reported upon receipt of a report from the City of Vallejo. Of the four water main breaks on Mare Island, two breaks were located along Pintado Road in the vicinity of Railroad Avenue, and one break was visible on Railroad Avenue, just north of G Street. Repairs were underway on these three water main breaks. The fourth water main break was observed on the north end of the island adjacent to Earthquake Protection Systems, just west of Azuar Drive and L Street. A second water main break may have occurred in this vicinity; however, repairs were not yet underway at these locations and were not confirmed.

No fires were reported in the City of Vallejo. Several power outages occurred, based on discussions with City representatives, but the locations were unavailable. Power was observed to be out at a number of intersections across the Mare Island base, however conversations with Lennar Mare Island (LMI) indicated that power had been intentionally turned off in those locations due to safety concerns during inspections and repairs, and there were no unplanned outages on the base. LMI representatives indicated that some buildings, particularly those in the historic core, experienced water leaks within the sprinkler systems or water delivery systems inside several structures. Examples of this were observed on during GEER reconnaissance on August 24, 2014.

6.2.4 Mare Island

6.2.4.1 Officers' Quarters on Walnut Avenue

While investigating the occurrence of ground deformation, the GEER team members observed the performance of some structures. Brick chimneys were observed to have fallen from a number of the historic structures on Walnut Avenue (Figure 6.3), many formerly used as Officer's Quarters by the Navy. Of the 19 structures along Walnut Avenue, 5 had metal chimneys with no visible damage, 11 had brick chimneys with some degree of damage, 2 had brick chimneys with no visible damage, and 1 had no visible chimney or damage. Observations of external structural damage are summarized in Table E.1 in Appendix E.

Figure 6.3: Brick chimney damage; [NSF-GEER; Mare Island, Vallejo, CA; GPS N38.099 W122.273; 08/24/14; 14:19]

6.2.4.2 Mare Island Waterfront and Historic Core

Several buildings along the historic Mare Island waterfront, opposite the dry docks on the west side of Nimitz Avenue were observed to have brick façade or corrugated siding damage (Figure 6.4). The buildings consist of mix of industrial and commercial buildings and warehouses, formerly associated with the Mare Island Naval Base and now under civilian use, owned and leased by LMI. Cracks were observed along corner columns and around windows of some brick structures. No signs of collapse were evident, though some buildings were blocked off and red-tagged pending structural inspection. Several buildings also had broken glass windows although it was unclear by observation which instances were due to earthquake damage. Deformation of rollup doors was evident on one of the waterfront structures. Ground deformation was not widespread, but was observed in localized pockets near one of the larger, more modern structures. Observations of external structural damage are summarized in Table E.2 in Appendix E.

Figure 6.4: Brick facade damage; [NSF-GEER; Mare Island, Vallejo, CA; N38.095 W122.268; 08/24/14; 15:38]

6.2.4.3 Ground Cracking

Deformed pavement was visible in localized areas around structures of the historic core (e.g., Figure 6.5). Paving stones along sidewalks and walkways along Walnut Avenue appeared to be slightly out of place. Evidence of persistent ground rupture in the vicinity of Mare Island was not observed by GEER team members, nor was evidence of significant ground rupture reported by representatives of LMI, who inspected much of the island with representatives of the City of Vallejo and ENGEO Incorporated, their engineering consultant. Linear east west running berms associated with the Navy's former firing range were viewed from a nearby vantage point and ground rupture was not apparent.

Figure 6.5: Pavement damage at hydrant; [NSF-GEER; Mare Island, Vallejo, CA; GPS N38.098 W122.269; 08/24/14; 14:37]

6.2.4.4 Mare Island Causeway Bridge

The Mare Island Causeway Bridge, a historic drawbridge providing access to Mare Island from Highway 80 via Tennessee Street, was observed to be intact and under unrestricted access during a visit on August 24, 2014. No damage was visible that could be attributed to the earthquake. A railing appeared to be down for repair near the west abutment; however, the railing was under repair for reasons unrelated to the August 24 earthquake, according to LMI representatives.

6.2.4.5 Residences along Flagship Drive

Perimeter slopes of residential communities, which were mapped by the USGS as having a high likelihood of liquefaction (i.e., USGS OFR-06-1037, Sheet 2 of 2, Liquefaction Susceptibility), were inspected where access was possible. A sound-wall along Flagship Drive at Klein Avenue was inspected for signs of cracking. A single crack on the order of 6 mm or smaller was observed in the stucco of the wall. This small, isolated crack and the general absence of ground cracking was considered to be evidence of good performance of the slope. Surcharge slopes located south of Kirkland Avenue were inspected for geotechnical damage, and no damage was observed in this area.

6.2.4.6 Saint Peter's Chapel

Saint Peter's Chapel, located on Walnut Avenue at Azuar Drive, appeared to be undamaged. Paving stones along the access pathways may have been displaced as some stones were unstable, but the pre-earthquake condition of the stones is unknown. A perimeter walkover revealed no visible damage to the structure of the chapel. The chapel's rare Tiffany stained glass windows appeared to be intact, though close inspection from inside the chapel was not made to observe whether hairline cracks had damaged the windows.

6.3 Napa River, Downtown Napa and Mobile Home Park Observations

6.3.1 Napa River Observations

GEER team members walked along the Napa River from North (Lincoln Bridge) to South (Napa Marina) looking for any ground related damage. The observations are described below for locations with similar damage. Some additional observations of the downtown Napa levees and floodwalls are presented in Section 7 of this report.

6.3.1.1 Lincoln Bridge and 1st St. Bridge

The Lincoln and 1st St. Bridges cross over the Napa River in an EW direction. No ground or structural damage was observed at these two locations.

6.3.1.2 Railroad and Soscol Bridge

These two bridges cross the Napa River in a NS direction. They showed similar cracking at the interface between the foundation of the abutments and the adjacent soil. The cracks were primarily oriented parallel to the sloped free face. At the south abutment of Soscol Bridge an old masonry retaining wall failed, as shown in Figure 6.6. The Soscol Ave. pavement also settled with respect to the South end of the bridge deck.

Figure 6.6: Failure of masonry retaining wall below the south abutment of Soscol Bridge [NSF-GEER; N 38.2997 W -122.2834; 08/24/14 13:09]

6.3.1.3 **Excavation Site near 1st St. Bridge**

A sheet pile wall installed south of the 1st St. Bridge serves as the supporting structure for an excavation associated with the construction of a new bypass around an ox-bow section of the Napa River, allowing for improved flow of flood waters. The day of the earthquake the dewatered area was flooded and the water was being pumped into the Napa River. According to the superintendent for the contractor, the flooding was produced by water main breaks that flowed into an upstream channel and then to the dewatered area. The sheet pile wall did not show any evident damage.

6.3.1.4 **3rd Street Bridge**

The 3rd St. Bridge crosses the Napa River in an EW direction. The bridge has 2 intermediate piers, which consist of two large reinforced concrete columns. A detailed account of observations in the 3rd Street bridge area is provided in Section 7.5.1 as part of a discussion of levee performance along the Napa River. Site visits revealed overall good performance of embankments and structures with evidence of localized lateral spreading, sand boils, and liquefaction settlements and ground cracking in the vicinity of the 3rd Street Bridge. Specifically:

- Between the eastern pier of the bridge and the East abutment a natural sand deposit has formed (Point Bar). Minor liquefaction-induced ground deformation was observed in this area. Ground cracking and sand boils observed on the east bank of the river, south of the 3rd Street Bridge. On August 24th, the area photographed was under 15 to 30 cm of water. Dry conditions at these locations allowed for closer inspection, revealing signs of liquefaction and sand boils as discussed in Section 7.5.1.
- Ground cracking parallel to the shore to the south and north of the bridge
- Around 5 cm of horizontal displacement of the deck at each abutment
- Separation of approximately 2 cm between concrete walkway and adjacent floodwalls below the west abutment

- Settlement of soils around the western column on the order of 5 cm and 25 cm. Around the columns of the pier, cracks spaced every 25 cm to 30 cm were observed in a radial pattern

Figure 6.7, Figure 6.8, and Figure 6.9 show the ground cracks in the 3rd St. Bridge area.

Figure 6.7: Ground cracking and submerged sand boils due to liquefaction in Napa River point bar, east bank, south of 3rd St. Bridge [NSF-GEER; N 38.2980 W -122.2830; 08/24/14 14:44]

Figure 6.8: Ground cracking due to liquefaction in Napa River point bar below 3rd St. Bridge, between the two columns of the eastern pier. [NSF-GEER; N 38.2980 W -122.2840; 08/24/14 14:44]

Figure 6.9: Ground cracking and settlement due to liquefaction in Napa River point bar below 3rd St. Bridge [NSF-GEER; N 38.2980 W -122.2840; 08/24/14 14:44]

6.3.1.5 Napa River West Bank from Riverside Park to Napa Marina

GEER members drove south along the western shore of the Napa River looking for liquefaction damage or slope stability failures. None were found. Stops were made at Riverside Park, the Napa Valley Yacht Club, a parking lot in the Tannery area, and the Napa Marina. The embankments and slopes in all these places did not reflect any damage.

6.3.2 Downtown Napa

6.3.2.1 Pedestrian Bridge at Coombs Street

A pedestrian bridge crosses the Napa Creek in a SW-NE direction, from Coombs St. (SW) to Clinton St. (NE). It consists of a single steel beam supported by 2 reinforced concrete abutments. Along the SW side of the bridge, on Coombs St., parallel to the creek (NW-SE direction), there is a retaining wall of approximately 3 m in height. This retaining wall supports the North end of Coombs Street, pedestrian bridge South abutment and a house. A large crack was observed parallel to the retaining wall and about three meters behind the wall face. The crack was observed at the interface between the soil and a sheet pile wall (Figure 6.10). At the north of Coombs St. a crack was observed indicating the deformation of the backfill, which was also confirmed by 30 cm of settlement of the pavement adjacent to the retaining wall. Figure 6.11 shows the pavement crack, and Figure 6.12 shows the settlement in the pavement. At the NW end of the bridge, the deck was observed to be 15 cm above the bridge access ramp. Also in the parking lot located N of the abutment, tension cracks were found parallel to the creek.

Figure 6.10: Crack along sheet pile wall behind the retaining wall in the Pedestrian Bridge [NSF-GEER; N 38.3003 W -122.2881; 08/24/14 17:58]

Figure 6.11: Crack in pavement behind the retaining wall in the pedestrian bridge [NSF-GEER; N 38.3003 W -122.2881; 08/24/14 17:58]

Figure 6.12: Settlement of backfill near the retaining wall in the pedestrian bridge [NSF-GEER; N 38.3003 W -122.2881; 08/24/14 17:58]

6.3.2.2 Water main breaks

Several water main breaks were reported on the day of the earthquake in Downtown Napa. The GEER members in Downtown Napa documented three of them, one on Arroyo Dr. and two on Brown St. Arroyo Dr. is located just north of the NW abutment of the Pedestrian Bridge and is oriented parallel to the Napa Creek. The water main break occurred where recent trench work was apparent. The pavement around the break is also uneven with a large depression towards the East. According to the residents this depression occurred during recent construction along the Napa Creek. The other two water main breaks were observed on Browns St., at its intersection with Napa St. and Caymus St. All of these water line breaks ejected trench sand to the ground surface. An example is shown on Figure 6.13.

Figure 6.13: Soil ejected from water main break in Arroyo Dr. [NSF-GEER; N 38.3008 W -122.2894; 08/24/14 16:34]

6.3.3 Napa Valley Mobile Home Park (NVMHP)

The NVMHP is located in NW Napa near HW 29 and is where a fire took place and the press focused much of its attention. It does not appear that the fire was produced due to breakage of a gas-line generated by ground movement. The ground conditions at this site were dry. A creek located west of the complex did not show flow of water, and no cracks were observed in the crest of the slope to suggest any ground deformation.

6.4 Napa Winery Landslide Stability

6.4.1 Background

In 1995, Cotton, Shires, & Associates (CSA) began an initial landslide investigation of the subject Napa winery site, following the failure of a slope that destroyed the primary access road and decorative entrance fountain located just east of the main winery building. Based upon this investigation, CSA identified three large, deep-seated landslides that impacted the winery building and access roads, labeled Landslides A, B, and C on the winery landslide map (Appendix E). These landslides likely failed in late Quaternary time and remained relatively dormant prior to site development, although they appear very obvious on aerial photographs. The active landslide that impacted the road and fountain was a reactivated portion of Landslide A that failed on sheared claystone beds within the Huichica Formation.

Following the investigation, CSA designed a tied-back shear pin wall and shear cleats to protect the upper access road, fountain area and large winery building that sits at the top of the hill from active and potentially expanded movement of Landslide A. A large grading repair, consisting of a mid-slope shear key, was constructed to buttress Landslide A and provide a stable fill platform for the primary access road to cross over/through that landslide. Later, additional tied-back shear pins were also installed at the top of the slope to protect the winery building from Landslides B and C. In addition to protecting facilities at the top of the slope, these shear pin walls also relieved some of the driving force from the landslide masses that remained downslope of the walls. No mitigation measures were installed in the lower portions of Landslides B and C, so they remain somewhat vulnerable to reactivation. Following completion of various phases of shear pin and tieback installation, as well as installation of the shear key, slope inclinometers were installed in the locations shown on the site map. These slope inclinometers have been monitored annually by CSA since installation (in the late 1990's) during the late spring of each year. The last inclinometer reading before the earthquake was recorded in June of 2014.

6.4.2 Post-Earthquake Response

The Napa winery site is located approximately 6.6 km from the epicenter of the M6.0 South Napa Earthquake and 1.7 km from the fault trace that experienced coseismic slip. Based upon peak ground acceleration (PGA) data provided by the USGS, the PGA at the winery site was approximately 0.5g during the main shock. During the afternoon of August 24, 2014, approximately 10 hours after the M6.0 earthquake, CSA performed a site reconnaissance. CSA observed no evidence of active landsliding such as scarps, ground cracks, bulging ground, or displacement of roads or rows of grape vines. On the following day, CSA monitored the site slope inclinometers and determined that most of them remained static (Appendix E). However, discrete deflections of 0.1 to 0.3 inch were recorded in slope inclinometers SI-1A, SI-14, SI-15, and SI-17 located downslope from the shear pin walls and slope inclinometers SI-10A and SI-3 located upslope of the shear pin walls. CSA interprets the small deflections that occurred in slope inclinometers located above the shear pins as limited seismic displacement that was absorbed by the shear pin and tieback system as they reached their reserve capacity. Of the slope inclinometers installed downslope of the shear pin walls, only SI-14 was within the formerly active portion of Landslide A. Displacement of over 0.3 inch at the depth of the existing landslide plane in SI-14 appears to represent loading of the shear key buttress by the landslide mass that was left in place upslope of the buttress. Deep deflections (in the range of 0.2 to 0.3 inch) in slope inclinometers SI-1A and SI-15 indicate reactivation of previously static portions of Landslides A and B below the shear pin walls. SI-17 is located outside of the mapped landslides in an area where Huichica Formation is exposed. Thus, CSA interprets the deep deflection in SI-17 (0.2 inch) as new landslide activity that was triggered by strong ground motion. CSA will continue to monitor this inclinometer to see if it will continue to deflect in the absence of strong ground motion.

Very little earthquake-related damage was sustained by the winery, other than items falling from shelves in the tasting room, a few cases of wine bottles breaking, and a few wine barrels that fell and broke open.

In conclusion, it appears that the shear pin and tieback walls successfully protected the winery building from significant seismic displacements resulting from intense ground shaking and high PGA values. The landslide debris that remained in place below the protection walls experienced small, localized displacements in response to strong ground motion. Below average rainfall over the preceding two years (with resulting low pore-water pressures) likely helped to minimize seismic slope displacements at the winery site during the South Napa Earthquake.

6.5 References

U.S. Geological Survey, *Maps of Quaternary Deposits and Liquefaction Susceptibility in the Central San Francisco Bay Region, California*, Open-File Report 2006-1037, Sheet 2 of 2, Liquefaction Susceptibility

ASCE-TCLEE, *South Napa M 6.0 Earthquake of August 24, 2014*, Quick Reconnaissance Report, http://www.asce.org/Technical-Groups-and-Institutes/TCLEE/ASCE-TCLEE-Preliminary-Reconnaissance-Report-of-the-August-2014-South-Napa-Earthquake/ (Accessed 09-15-2014)

7 PERFORMANCE OF DAMS AND LEVEES

7.1 Introduction

Preliminary reconnaissance efforts of dams and levees were made by GEER team members between August 24 and September 7, 2014 following the main shock. Reconnaissance efforts included several flights in a California Highway Patrol (CHP) helicopter over several dams and levee reaches to look for any major damage from the air. No significant damage was observed at any of the areas viewed from the air. These efforts were then followed up by ground investigations in areas where higher accelerations were thought to have been sustained, notably in the central Napa area and in Vallejo. Again, no major damage was observed at any of the dams or levee reaches visited by GEER team members. The majority of damage observed on either dams or levees consisted of relatively small longitudinal cracks either on the dam/levee crest, or in one location along the landside toe of a small dike on Green Island. New cracking associated with the earthquake, or any other damage, was often not observed at all. Where present, the cracking was commonly less than a few millimeters in width. The largest crack observed was on the crest of Lake Marie Dam and was only about 2½ centimeters in width. Overall, the performance of the small to medium-sized dams and the relatively small levees in the area was very good. The good performance of the dams was confirmed in discussions with several dam owners and with the California Division of Safety of Dams (DSOD).

7.2 Overview of Dams in Earthquake Area

The DSOD regulates non-federal dams in the State of California. According to DSOD's listings of jurisdictional dams (dams that are typically over 2 meters in height and with a minimum reservoir size) there were 34 dams within 20 kilometers of the energy source associated with the 2014 South Napa Earthquake. The locations of these dams are shown in the Google Earth plot presented in Figure 7-1. Tables 7-1 and 7-2 list the names, locations, and basic dimensions for each dam. Tables 7-1 and 7-2 also present estimated peak ground accelerations sustained by the dams during the main shock. The peak accelerations were estimated using two approaches. The first approach estimated peak ground accelerations at the dams by interpolating or extrapolating from the nearest peak accelerations recorded from any nearby strong motion instruments (from ShakeMap, United States Geological Survey). The second approach was to use the geometric mean of the four NGA-W2 GMPEs currently available (ASK14, BSSA14, CB14, and CY14). As shown in the two tables, the two different approaches result in generally similar estimates, although there are some differences in some locations. Table 7-3 presents the numbers of dams shaken to various levels of peak ground acceleration.

The majority of the dams are relatively small, older earth dams. Two of the dams are concrete dams: Milliken Dam is a concrete arch dam that appears to have sustained only about 0.1g peak ground acceleration, whereas the Old Waterworks Dam in Napa is a concrete gravity dam, but its reservoir has not been in use for some time and was empty at the time of the earthquake. As summarized in Table 7-4, the dam heights range from 6 to 50 meters in height, but 20 of the 34 dams are between only 6 and 15 meters in height. Only two dams with heights greater than 20 meters are believed to have sustained peak accelerations greater than about 0.1g: Summit Reservoir Dam (Height = 38 meters, PGA ~0.25g) and Swanzy Lake Dam (Height = 26 meters, PGA ~0.30g), both in the Vallejo area (see Table 7-5).

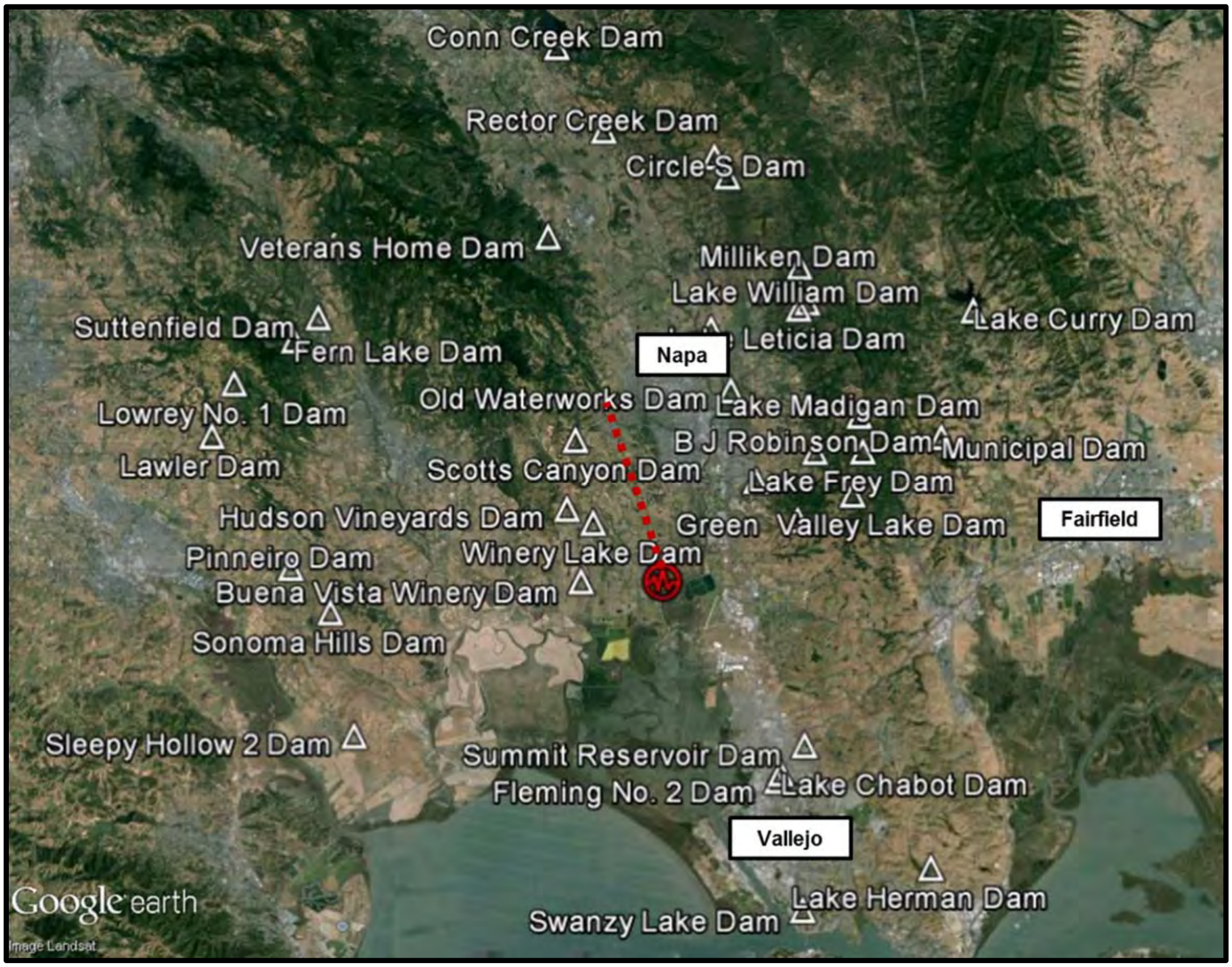

Figure 7-1: Locations of Jurisdictional Dams within 20 kilometers of the energy source associated with the 2014 South Napa Earthquake [NSF-GEER; Harder, L. F.; 09/11/14]

Table 6 shows that the majority of the dams within 20 kilometers of the energy source of the earthquake are also quite old, with several dams having been originally constructed back in the 19th century. Only six of the dams have been constructed since 1960. Of course, several of the dams have had dam safety modifications and improvements since their original construction.

In addition to the jurisdictional dams, there are dozens of small agricultural ponds in the area that are used principally to support the wine industry. These are small ponds with retaining embankments generally less than 3 to 6 meters in height. Many of these ponds were created by borrowing from the pond area for materials to construct the retaining embankments; thus, the upstream slopes are often higher than the downstream slopes. Some of the ponds also have synthetic geomembrane liners.

Due to the ongoing California Drought, many of the reservoirs and ponds were at less than their maximum operating level at the time of the earthquake, and some were very low.

Table 7-1: Summary of Dams in Napa County within 20 kilometer of the energy source of the 2014 South Napa Earthquake [NSF-GEER; Harder, L. F.; Escudero, J. L. M.; 09/11/14)]

Dam	Height (m)	Crest Length (m)	Crest Width (m)	Year Completed	Approx. Distance (km)	Latitude/ Longitude	Prel. PGA[1] (g)
B J Robinson	14	213	5	1957	9.1	N 38° 17.4’ W 122° 13.2’	0.11[a]/0.20[b]
Circle S	9	126	4	1979	13.7	N 38° 25.2’ W 122° 16.3’	0.10/0.15
Conn Creek	38	213	6	1946	18.7	N 38° 28.9’ W 122° 22.4’	0.10/0.10
Foss Valley	17	762	6	1988	14.2	N 38° 25.7’ W 122° 16.7’	0.10/0.15
Hudson Vineyards	8	122	4	1983	2.8	N 38° 15.9’ W 122° 22.0’	0.41/0.37
Lake Camille	9	183	7	1880	6.8	N 38° 16.6’ W 122° 15.3’	0.27/0.29
Lake Curry	33	174	5	1926	19.1	N 38° 21.4’ W 122° 7.5’	0.05/0.13
Lake Cynthia	7	229	3	1955	6.9	N 38° 20.9’ W 122° 16.9’	0.35/0.30
Lake Leticia	15	119	5	1960	11.2	N 38° 21.5’ W 122° 13.7’	0.11/0.20
Lake Marie	18	138	2	1908	8.0	N 38° 15.6’ W 122° 13.8’	0.19/0.22
Lake William	20	175	6	1960	11.8	N 38° 21.6’ W 122° 13.4’	0.11/0.18
Milliken Dam*	34	197	8	1924	12.3	N 38° 22.7’ W 122° 13.6’	0.10/0.17
Old Waterworks**	13	66	2	1883	6.1	N 38° 19.2’ W 122° 16.1’	0.35/0.31
Rector Creek	50	271	9	1946	14.3	N 38° 26.5’ W 122° 20.7’	0.10/0.13
Scotts Canyon	12	98	6	1948	1.6	N 38° 17.8’ W 122° 21.7’	0.45/0.47
Veterans Home	14	98	2	1908	13.6	N 38° 23.5’ W 122° 22.7’	0.10/0.18
Winery Lake	9	189	4	1953	2.1	N 38° 15.5’ W 122° 21.1’	0.41/0.41

Notes: [1] PGA estimates are based on: a) nearest recorded motions and b) NGA-W2 GMPEs

* Denotes concrete arch dam

** Denotes concrete gravity dam, reservoir empty and out of service

🟫 Denotes dam inspected or viewed by GEER team

Table 7-2: Summary of Dams in Solano and Sonoma Counties within 20 kilometers of the energy source of the 2014 South Napa Earthquake [NSF-GEER; Harder, L. F.; Escudero, J. L. M., 09/11/14)]

Dam	Height (meters)	Crest Length (meters)	Crest Width (meters)	Year Completed	Approx. Distance (km)	Latitude/ Longitude	Prel. PGA (g)
Buena Vista Winery	12	169	4	1971	3.6	N 38^{o} 13.8’ W 122^{o} 21.5’	0.41^{a}/0.38^{b}
Fern Lake	12	91	5	1921	14.7	N 38^{o} 20.6’ W 122^{o} 31.8’	0.09/0.11
Fleming Hill No. 2	12	174	12	1912	11.1	N 38^{o} 8.2’ W 122^{o} 14.5’	0.30/0.20
Green Valley	12	101	4	1956	11.2	N 38^{o} 16.3’ W 122^{o} 11.8’	0.10/0.19
Lake Chabot	13	113	5	1870	10.9	N 38^{o} 8.4’ W 122^{o} 14.4’	0.30/0.21
Lake Frey	25	175	5	1894	11.7	N 38^{o} 17.5’ W 122^{o} 11.5’	0.10/0.19
Lake Herman	16	213	4	1905	11.6	N 38^{o} 5.8’ W 122^{o} 9.0’	0.09/0.12
Lake Madigan	27	203	5	1908	11.6	N 38^{o} 18.5’ W 122^{o} 11.6’	0.10/0.19
Lawler	12	351	7	1910	19.1	N 38^{o} 17.9’ W 122^{o} 34.7’	0.08/0.09
Lowrey No. 1	6	64	3	1954	17.9	N 38^{o} 19.4’ W 122^{o} 33.8’	0.08/0.10
Municipal	17	131	5	1939	15.6	N 38^{o} 17.9’ W 122^{o} 8.6’	0.07/0.11
Pinneiro	8	220	4	1967	17.5	N 38^{o} 14.2’ W 122^{o} 34.7’	0.04/0.10
Sleepy Hollow 2	12	183	4	1949	17.7	N 38^{o} 9.5’ W 122^{o} 29.7’	0.03/0.10
Sonoma Hills	12	98	5	1991	17.1	N 38^{o} 12.9’ W 122^{o} 30.5’	0.04/0.13
Summit Reservoir	38	274	6	1968	10.4	N 38^{o} 9.2’ W 122^{o} 13.5’	0.25/0.19
Suttenfield	23	294	3	1938	13.6	N 38^{o} 21.3’ W 122^{o} 31.0’	0.10/0.14
Swanzy Lake	26	114	5	1931	17.4	N 38^{o} 4.6’ W 122^{o} 13.6’	0.30/0.13

Notes: [1] PGA estimates are based on: a) nearest recorded motions and b) NGA-W2 GMPEs

▨ Denotes dam inspected or viewed by GEER team

Table 7-3: Estimated Peak Ground Accelerations at dams within 20 kilometers of the energy source of the 2014 South Napa Earthquake [NSF-GEER; Harder, L. F.; processed 09/11/14)

Range in estimated Peak Ground Acceleration (g)	Number of Dams
< 0.10	9
0.10 – 0.19	14
0.20 – 0.29	2
0.30 – 0.39	5
> 0.40	4
Total	34

Table 7-4: Heights of dams within 20 kilometers of the energy source of the 2014 South Napa Earthquake [NSF-GEER; Harder, L. F.; processed 09/11/14)

Range in Dam Height (meters)	Number of Dams
0 – 5	0
6 – 10	7
10 – 15	13
16 – 20	5
21 – 25	2
26 – 30	2
31 – 35	2
36 – 40	2
> 40	1
Total	34

Table 7-5: Dams with the highest estimated peak ground accelerations associated with the 2014 South Napa Earthquake [NSF-GEER; Harder, L. F.; processed 09/11/14)

Dam	Height (meters)	Year Completed	Estimated PGA (g)
Scotts Canyon	12	1948	0.45
Winery Lake	9	1953	0.41
Buena Vista Winey	12	1971	0.41
Hudson Vineyards	8	1983	0.41
Lake Cynthia	7	1955	0.35
Old Waterworks*	13	1883	0.35
Lake Chabot	13	1870	0.30
Fleming Hill No. 2	12	1912	0.30
Swanzy Lake	26	1931	0.30
Lake Camille	9	1880	0.27
Summit Reservoir	38	1968	0.25

* Denotes concrete gravity dam, reservoir empty and out of service

Table 7-6: Original construction dates for dams within 20 kilometers of the energy source of the 2014 South Napa Earthquake [NSF-GEER; Harder, L. F.; processed 09/11/14)

Year of Original Dam Construction	Number of Dams
1870 - 1900	4
1901 - 1920	6
1921 - 1940	7
1941 - 1960	11
1961 - 1980	3
1980 -2014	3
Total	34

7.3 Performance of Dams

Immediately following the main shock of the 2014 South Napa Earthquake, personnel in DSOD received information from ShakeCast (USGS) regarding the level of shaking in the area and began putting together a list of dams that received different levels of shaking. For dams that were within areas having a Damage Intensity of V or more, DSOD staff contacted the owners within a day and asked them to inspect their dams. Dams in areas associated with a Damage Intensity of VII or greater were contacted within a few hours. The DSOD then put together a priority list of dams for their own inspections with priorities based on the estimated level of shaking and the history of the dam. Dams with the highest priorities were inspected later the same day as the earthquake. Dams with lower priorities were inspected within a few days after the earthquake. As a result of these inspections, DSOD found little to no damage to the dams and appurtenances. As mentioned previously, the main type of damage noted, where any damage at all was observed, reportedly consisted of relatively minor longitudinal cracks on the crest of the dam. The largest such cracking was found on Lake Marie Dam and was approximately 2½ centimeters wide at its widest location.

The GEER team inspected on the ground or viewed from the air 11 of the 34 dams within 20 kilometers of the energy source associated with the earthquake (see brown shaded areas in Tables 7-1 and 7-2). The GEER team inspections that were done supported the results from the dam owners and DSOD inspections in that little to no damage was observed at the dams in the area. The reasons for this low level of damage likely include:

- The level and duration of shaking for most of the dams was relatively small
- Many of the dams are relatively small
- Many of the dams and their foundations are made out of clayey materials and the depths in the foundation to bedrock are small
- Some of the reservoirs were relatively low either due to the ongoing California Drought or due to restrictions imposed for dam safety
- Some of the dams have had various retrofits made to increase their static and seismic stability

Details and photographs for three of the dams inspected by the GEER team are presented in the following sections:

- ➢ Lake Marie Dam
- ➢ Lake Chabot Dam
- ➢ Summit Reservoir Dam

7.3.1 Lake Marie Dam

Lake Marie Dam was originally constructed in 1908 and currently has a maximum height of approximately 18 meters. It is owned by the Napa State Hospital, but is operated as part of a recreation area. According to DSOD's files, Lake Marie Dam is reportedly a clayey earthfill dam (not hydraulic fill) with a concrete core wall. In 1931, the dam crest was reportedly raised 0.6 meters using vertical rock walls on both edges of the crest with soil fill placed in between to improve freeboard. While the records indicate that the dam crest is about 3 meters in width, the inspection by the GEER team on September 1st indicated that the crest width is only about 2 meters. The crest length of the dam is approximately 138 meters. The upstream slope is relatively steep with a slope of approximately 1.5:1, while the downstream slope is significantly flatter at about a 2.5:1 slope. A 1947 inspection report indicated that the freeboard at that time between the dam crest and the uncontrolled spillway was about 3.2 meters. However, following a seismic evaluation in the 1980's, a 30-centimeter diameter steel riser pipe was installed downstream of the upstream valve of the outlet pipeline. This riser pipe limits the maximum reservoir storage to about 7.5 meters below the dam crest. At the time of the September 1st GEER inspection, the reservoir was more than 10 meters below the crest of the dam, leaving less than 8 meters of water on the 18-meter-high dam itself.

Lake Marie Dam was approximately 8.0 kilometers away from the energy source associated with the South Napa Earthquake and is estimated to have sustained a peak ground acceleration of about 0.19g based on nearby strong motion instruments. DSOD personnel inspected the dam during the same day as the earthquake and noted only a longitudinal crack in the upstream portion of the dam crest. The crack ran approximately 17 meters in length along the left central portion of the dam (see Figure 7-2 for general location) and had a maximum width of about 2½ centimeters (see Figure 7-3). Figures 7-3 and 7-4 present photographs taken by DSOD and by the GEER team of the cracking. The cracking may be related to movement of the upstream rock wall reportedly placed on the upstream edge of the dam crest in 1931. The cracking is considered minor, but DSOD staff report that they may require the cracking to be remediated.

7.3.2 Lake Chabot Dam

Lake Chabot Dam was originally constructed in 1870 and currently has a maximum height of approximately 13 meters. It is owned by the City of Vallejo and retains the lake used by the Six Flags Discovery Kingdom in Vallejo. According to DSOD's files, Lake Chabot Dam is a clayey earthfill dam generally composed of stiff clay and clayey gravel. The depth to shale bedrock is less than 3 meters below the foundation. The crest of the dam is approximately 5 meters wide and approximately113 meters in length. Due to stability concerns, a wide berm was added to the downstream side of the dam several years ago. Figure 7-5 presents a cross section of the dam obtained from DSOD files illustrating the general geometry of the dam and downstream berm. Figure 7-6 presents a photograph of the dam taken by the GEER team also illustrating the dam and berm geometry.

Lake Chabot Dam was approximately 11 kilometers away from the energy source associated with the South Napa Earthquake and is estimated to have sustained a peak ground acceleration of about 0.30g based on nearby strong motion instruments. A member of the GEER team inspected the dam on August 27th and found only minor longitudinal cracking less than 2 centimeters in

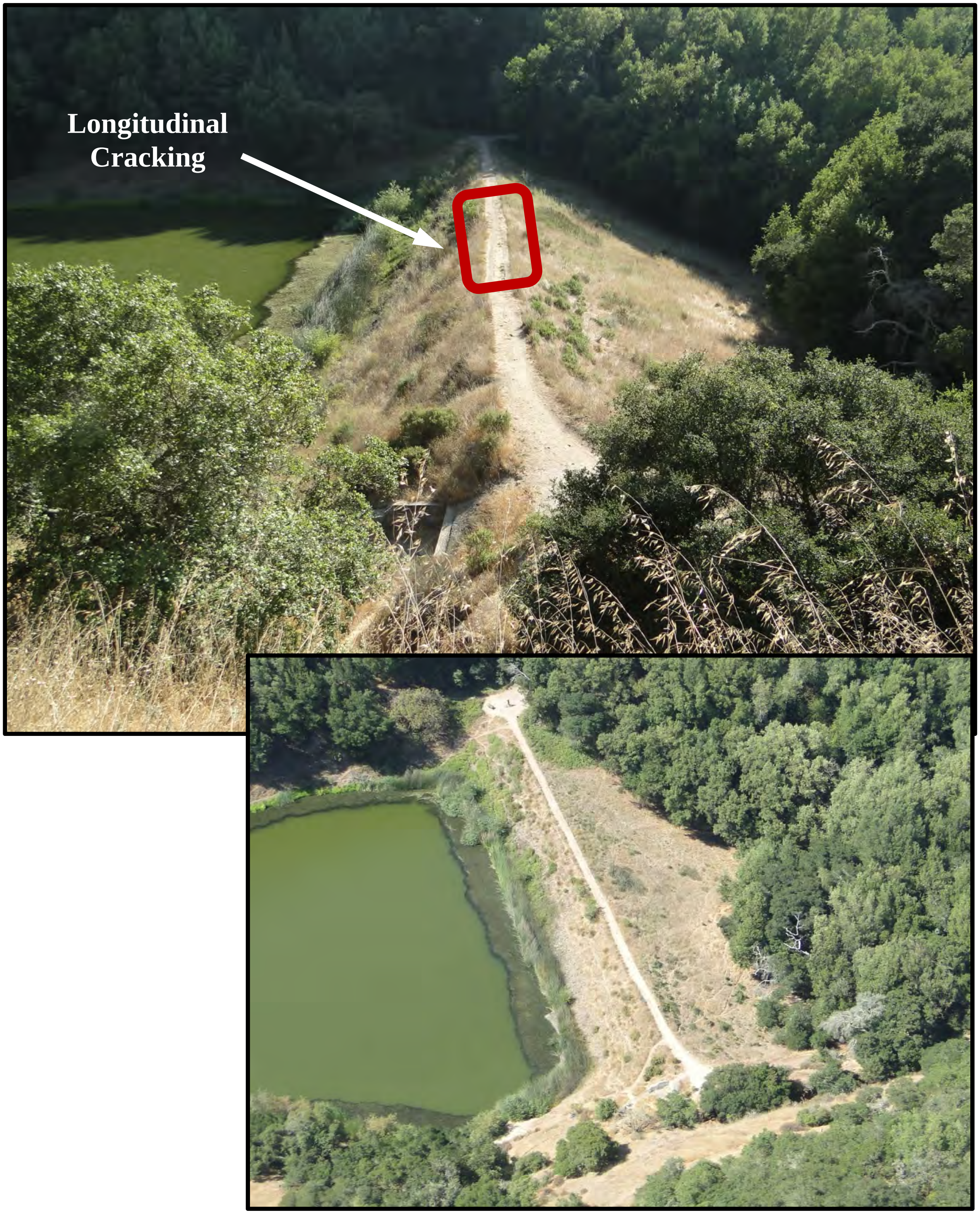

Figure 7-2: Ground and aerial photographs of Lake Marie Dam looking southeast
[NSF-GEER; Napa, CA; N38.260 W 122.230; Harder, L. F.; 09/01/14]

Figure 7-3: Photographs of longitudinal cracking on the upstream edge of the crest of Lake Marie Dam [Napa, CA; N38.260 W 122.230; from DSOD files; 08/24/14]

Figure 7-4: Photograph of longitudinal cracking on the upstream edge of the crest of Lake Marie Dam looking southeast [NSF-GEER; Napa, CA; N38.260 W 122.230; Harder, L. F.; 09/01/14]

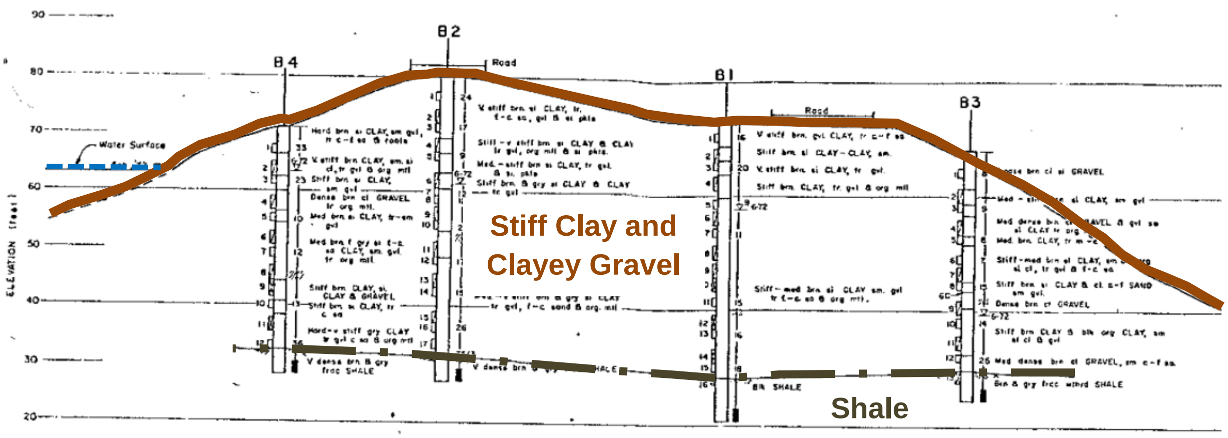

Figure 7-5: Cross section of Lake Chabot Dam
[Vallejo, CA; N38.141 W 122.241; from DSOD files]

Figure 7-6: Photograph of minor longitudinal cracking on the crest of Lake Chabot Dam looking southeast [NSF-GEER; Napa, CA; N38.141 W 122.241; Harder, L. F.; 08/27/14]

width on the dam crest (see Figures 7-6 and 7-7). Much of this cracking may have been associated with pre-existing longitudinally-dominated shrinkage cracks that simply opened up during the shaking. At the time of the August 27th inspection, the reservoir was approximately 4.3 meters below the dam crest. A relatively new reinforced concrete spillway on the right abutment of the dam appeared to be undamaged.

7.3.3 Summit Reservoir Dam

Summit Reservoir Dam was originally constructed in 1968 and currently has a maximum height of approximately 38 meters. Thus, it is one of the highest and most recently constructed dams shaken by the South Napa Earthquake. It is located in the hills above Vallejo and owned by the City of Vallejo. The dam appears to have had seepage issues in the past as there are several piezometers installed in the dam, and there is a plastic geomembrane lining placed within the reservoir to presumably reduce seepage through the dam and its foundation. There is also a 0.3-meter-high concrete parapet wall on the upstream edge of the 6-meter-wide asphalt-paved dam crest. The dam is shaped as an overall bowl and has a total length of about 274 meters. Figure 7-8 presents views of the dam.

Summit Reservoir Dam was approximately 10.4 kilometers away from the energy source associated with the South Napa Earthquake and is estimated to have sustained a peak ground acceleration of about 0.25g based on nearby strong motion instruments. A member of the GEER team inspected the dam on August 27th and found that the dam appeared to have little to no damage. The only distress noted was relatively minor longitudinal cracking, principally located near the downstream edge of the asphalt-paved crest of the main dam section. These cracks were generally only a few millimeters in width with a maximum opening on the order of a centimeter. However, it was clear that these were pre-existing cracks as weeds were growing in them and asphalt mastic had previously been poured over them in the past in an attempt to seal them up. Figure 7-9 illustrates some of the minor cracking noted. It is thought that at most, the effect of the earthquake was to perhaps slightly widen the pre-existing cracks.

Figure 7-7: Close-up photograph of minor longitudinal cracking on the crest of Lake Chabot Dam looking southeast [NSF-GEER; Napa, CA; N38.141 W 122.241; Harder, L. F.; 08/27/14]

Figure 7-8: Views of Summit Reservoir Dam looking southeast
[NSF-GEER; Napa, CA; N38.153 W 122.225; Harder, L. F.; 08/27/14]

Figure 7-9: Photographs of pre-existing longitudinal cracks on the crest of the maximum section of Summit Reservoir Dam
[NSF-GEER; Napa, CA; N38.153 W 122.225; Harder, L. F.; 08/27/14]

7.4 Overview of Levee System

The Napa River drainage basin is just north of San Pablo Bay and through the City of Napa almost all of the land adjacent to the river has been subject to flooding since 1862. By the mid-20th century, development had squeezed the river into a narrow channel as secondary channels were filled and the river was confined by small levees and floodwalls. Many of the levee systems on the Napa River, and on tributary channels upstream and downstream of the City of Napa, are privately owned. These levee systems are generally small, less than 2 meters in height, and intermittent.

To reduce the flood risk to the City of Napa, a federal flood control project led by the United States Army Corps of Engineers, with matching funds from state and local sources, has been underway for more than a decade. The project is being implemented in phases along approximately 12 kilometers along the river and is intended to provide protections for the 1 percent annual chance (100-year) flood within the city, approximately between Trancas Street and Imola Avenue (see Figure 7-10). Major features of the project include widening the channel of the Napa River and nearby Napa Creek, the construction of new flood walls, new pump stations, the replacement of bridges to accommodate the wider channel, the construction of a new bypass past the ox-bow in downtown Napa, and the removal of levees further downstream to allow the river to spread out into multiple channels and wetlands. The major portion of the downtown channel widening and floodwall construction along the Napa River was generally completed by 2006. The construction of the ox-bow bypass was in the early phases when the South Napa Earthquake occurred. Reconstruction and removal of low levees is on-going.

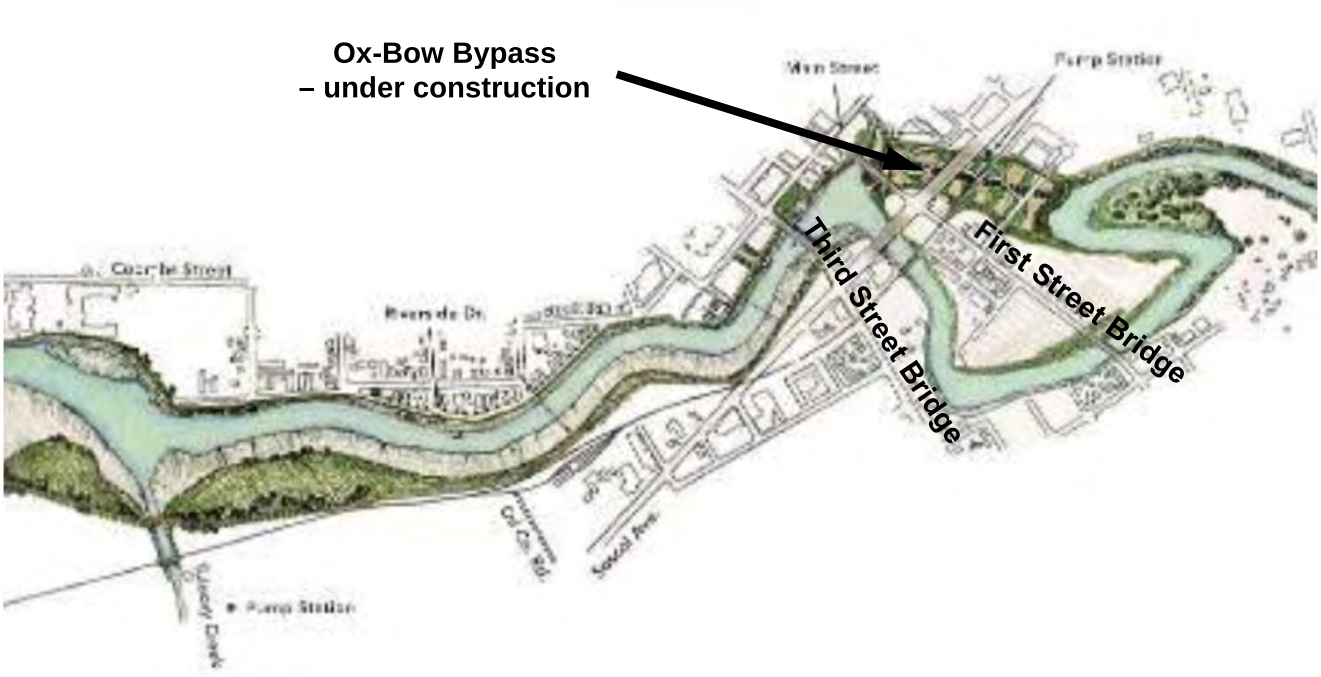

Figure 7-10: Views of improvement area of confined Napa River in downtown Napa [from County of Napa and USACE]

7.5 Performance of the Levee System

The Napa River levees and floodwalls that are part of the federal flood control project were reported by the Sacramento District of the United States Army Corps of Engineers to have little to no damage. Inspections by GEER team members found only minor cracking of the recently constructed levee/floodwall system in downtown Napa. This was despite very high accelerations reported in downtown Napa ranging up to 0.4 to 0.6g. Older floodwalls and foot-bridges nearby, however, experienced some damage. In addition, while a minor amount of liquefaction was observed in the form of cracking and sand boils in a sand bar in the Napa River near the Third Street Bridge, no signs of cracking or lateral spreading were observed on the riverbank above it.

Downstream of downtown Napa, GEER team members made several aerial surveys of the intermittent levee system along both sides of the Napa River, but no signs of damage were observed from the air. Follow-up inspections on the ground found only minor cracking of the levees themselves, with most of the damage on the levees observed on developed areas where homes and boat docks had been constructed onto the low 2-meter-high levees along Edgerley Island. Across from Edgerley Island, a small former salt pond dike developed longitudinal cracking along the downstream toe of the 2-meter-high embankment which might have been the result of foundation liquefaction. However, the damage was relatively minor.

Details and photographs for three of the levee/floodwall areas inspected by the GEER team are presented in the following sections:

- Downtown Napa Levees/Floodwalls
- Edgerley Island Levee
- Green Island Salt Pond Retaining Dike

7.5.1 Downtown Napa Levees/Floodwalls

In the area of the First and Third Street Bridges, the channel had been widened and new floodwalls and bridges were completed in 2006. Much of the new floodwall system is on the right (west) side of the river near the Third Street Bridge which allowed major new redevelopment in this area of downtown Napa. Figure 7-11 shows a Google Earth view of this area and Figure 7-12 presents an aerial photograph taken during the GEER team reconnaissance.

Downstream of the Third Street Bridge, remnant cracking and sand boils were observed in the sand/mud bar along the left (east) bank of the river and was suggestive that river sediments had liquefied during the earthquake (see Figures 7-12 and 7-13). The crack openings here were estimated to have a maximum width of approximately 2 centimeters. However, the adjacent riverbank appeared undamaged and there was no sign of cracking or lateral spreading on the concrete and gravel walkways above.

On the right (west) side of the river, the recently constructed large reinforced concrete floodwalls appeared to have performed well overall. However, the concrete deck slab behind the walls sustained minor cracking and had pulled away from the floodwalls by as much as 3 centimeters (see Figure 7-14). In addition, a lateral retaining wall supporting part of a restaurant had settled approximately 3 centimeters relative to the wall (see Figure 7-14).

Figure 7-11: Google Earth Plot of Downtown Napa
[NSF-GEER; Napa, CA; N38.308 W 122.281; Harder, L. F.; 09/11/14]

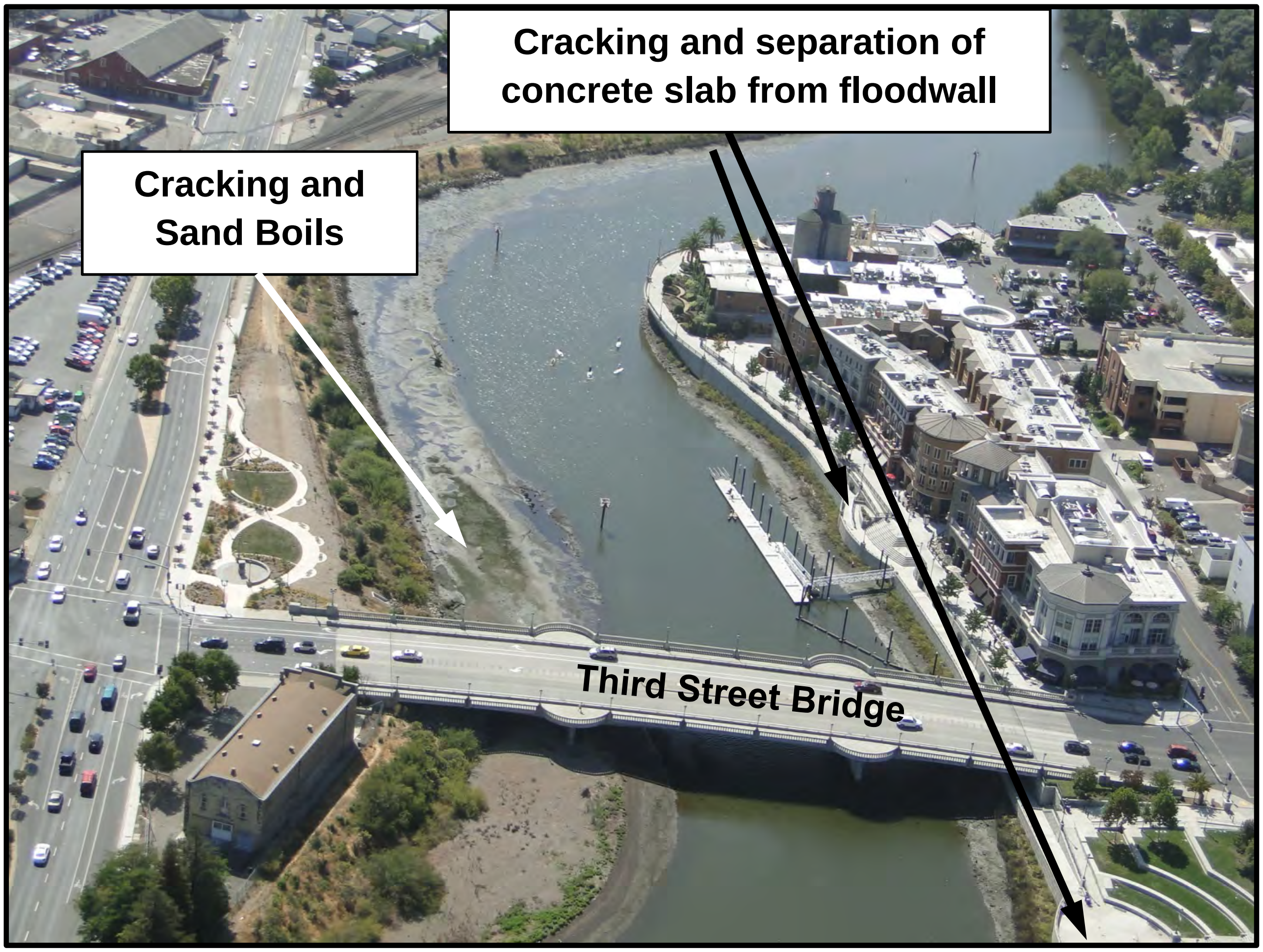

Figure 7-12: Aerial photograph of Napa River looking downstream near Third Street Bridge
[NSF-GEER; Napa, CA; N38.308 W 122.281; Harder, L. F.; 09/01/14]

Figure 7-13: Remnant cracking and sand boils in sand bar along left bank of Napa River looking downstream from Third Street Bridge
[NSF-GEER; Napa, CA; N38.298 W 122.283; Harder, L. F.; 09/04 and 09/07/14]

Figure 7-14: Separation of concrete slab and retaining wall from Napa River floodwall along right bank of Napa River looking upstream from Third Street Bridge
[NSF-GEER; Napa, CA; N38.299 W 122.285; Harder, L. F.; 09/04/14]

7.5.2 Edgerley Island Levee

Along the right (west) bank of the Napa River south of the epicenter the levees are commonly about 2 meters in height. On Edgerley Island, residences have been built on top of the levees along Milton Road and pilings and docks have been constructed on the relatively steep waterside slopes along the river. In many places, short floodwalls on the order of up to a meter in height have been constructed to provide wave protection and freeboard. Figure 7-15 presents a Google Earth plot and an aerial photograph illustrating the area.

In one location along Milton Road, ground cracking was observed across the asphalt pavement. This cracking continued to a fractured low cinderblock wall (see Figure 7-16). At the back of the residence on the waterside portion of the levee, the dock and floodwall had been damaged. It was not clear if the cracking and damage were associated with shaking or ground displacements associated with a continuation of the fault rupture south of the epicenter. The shaking must have been significant as a large water tank moved off its concrete pad and sheared its connection with the residence (see Figure 7-17). However, no damage was observed on the levee embankment itself.

7.5.3 Green Island Salt Pond Retaining Dike

Along the western edge of Green Island along mud flats east of the left (east) bank of the Napa River and south of the epicenter there are small retaining dikes that previously retained brine waters in salt ponds (see location in Figure 7-15). The area has largely been converted into an environmental restoration and recreation area, but many of the retaining ponds for the salt ponds remain in place. No significant damage was observed by the GEER team for the majority of the dikes visited on foot, and no damage was observed during the aerial reconnaissance. However, near the very western tip of the island, approximately 100 meters of longitudinal cracking was observed near the landside toe of the dike. The largest cracks were approximately 2½ centimeters in width, and, while longitudinal, appeared to have enlarged from shrinkage cracks. In addition, there appeared to be sandy ejecta along the cracks, but this was not definitive as the observations were made on September 4th, approximately 10 days after the earthquake (see Figure 7-18).

The retaining dike at this location was approximately 2 meters high and had crown widths on the order of 3 meters. In addition to the longitudinal cracking, four transverse cracks approximately 2 to 4 millimeters in width also crossed the levee in this 100-meter reach (see Figure 7-19). It is likely, but not definitive that the cracking was associated with a limited amount of liquefaction in the foundation in this area.

Contributing Sources:

Initial Observations: Keith Kelson (Sacramento District, USACE)

Computations of PGA estimates at dams using NGA-W2 GMPEs: Jorge Luis Macedo Escudero (University of California, Berkeley)

Background information on dams and DSOD inspections: Y-Nhi Enzler (DSOD); Mark Stanley (HDR Engineering); Brian Vanciel (City of Vallejo); Dan Hiteshew (City of Vallejo)

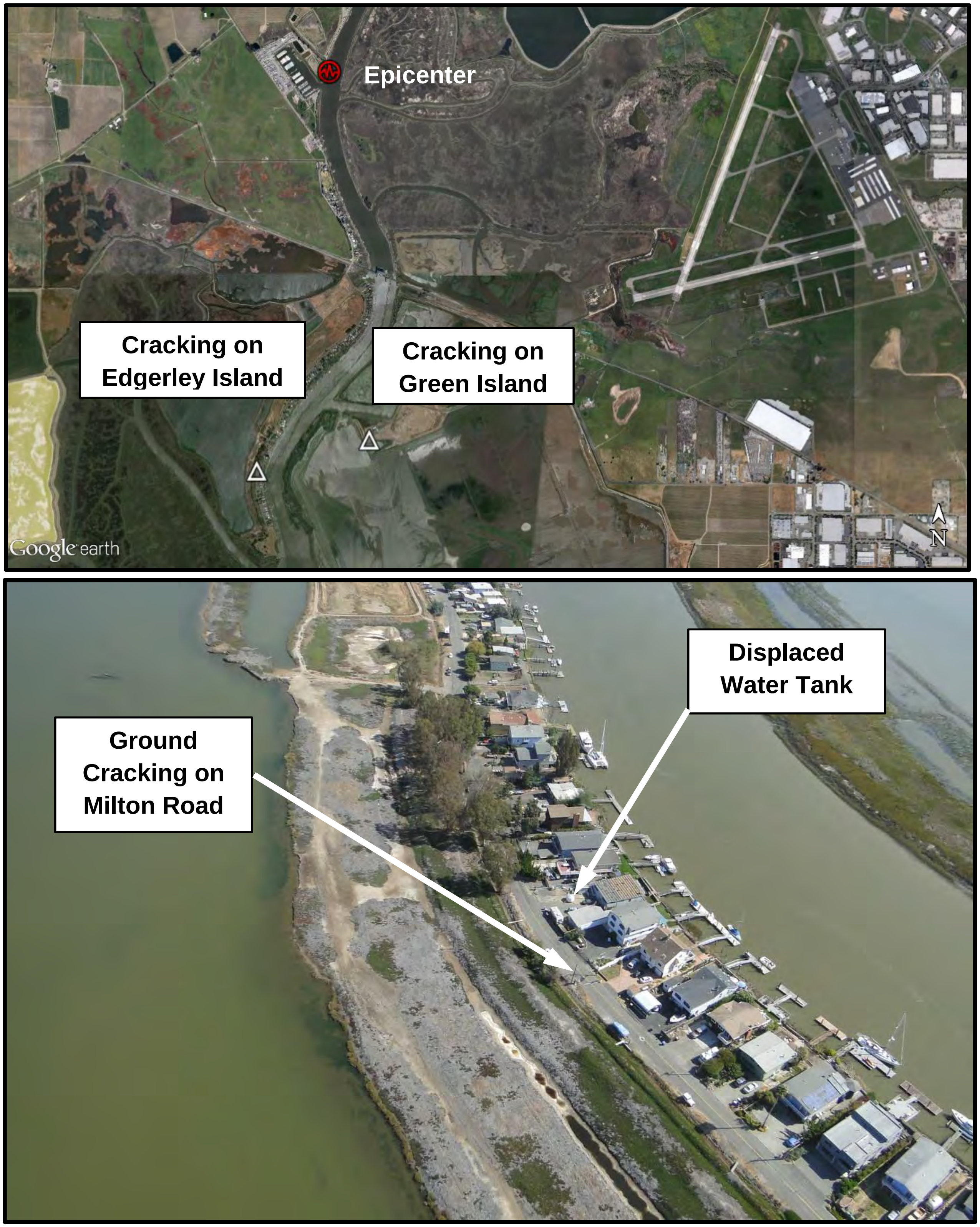

Figure 7-15: Google Earth plot and aerial photograph of Napa River along Edgerley Island south of the epicenter [NSF-GEER; Napa, CA; N38.198 W 122.316; Harder, L. F.; 09/01/14]

Figure 7-16: Photographs of cracked asphalt pavement on Milton Road, cracked cinderblock retaining wall, and damage to waterside floodwall/boat dock on Edgerley Island south of the epicenter [NSF-GEER; Napa, CA; N38.198 W 122.316; Harder, L. F.; 09/01/14]

Figure 7-17: Photographs of displaced water tank moved off its concrete pad and sheared pipe connection – note replacement tanks on pad in its place - on Edgerley Island south of the epicenter [NSF-GEER; Napa, CA; N38.198 W 122.316; Harder, L. F.; 09/01/14]

Figure 7-18: Photographs of longitudinal cracking and apparent ejecta along landside toe of salt pond retaining dike on western edge of Green Island south of the epicenter
[NSF-GEER; Napa, CA; N38.201 W 122.302; Harder, L. F.; 09/04/14]

Figure 7-19: Photographs of transverse cracking on crown of salt pond retaining dike on western edge of Green Island south of the epicenter
[NSF-GEER; Napa, CA; N38.201 W 122.302; Harder, L. F.; 09/04/14]

8 CONCLUSIONS

The August 24, 2014 M6.0 South Napa earthquake was the largest earthquake in the San Francisco Bay area since the October 17, 1989 M6.9 Loma Prieta earthquake. The rupture mechanism was primarily strike-slip and surface fault rupture was pervasively expressed along much of the ruptured fault plane trending NNW and extending for a distance of 12-14 km from the hypocenter. Surface faulting damaged homes, underground utilities, and other infrastructure when it traversed developed areas, such as the Browns Valley area in western Napa. The earthquake itself produced intense pulse-like motions that caused significant damage to older structures in parts of the City of Napa and immediately surrounding area. Noticeably, there was lack of liquefaction and liquefaction-induced ground failure resulting from this event, even in areas previously identified as being susceptible to the liquefaction hazard. Dam and levee performance was generally excellent, and only a few cases of minor cracking of dams and levees were observed. Similarly, underground storage caverns at local wineries performed well, with only minor cracking reported at some of the installations. The most unusual and distinct damage were compressional and extensional failures of relatively new, stiff concrete sidewalks and curbs in the Browns Valley area. The sidewalk failures appeared to be distinct from the surface fault rupture and appear to be a manifestation of localized zones of compression and extension, possibly induced by intense transient surface waves.

The observations and data presented in this report help document the geotechnical effects of the South Napa earthquake. There are several research opportunities presented by this event. Much can be learned by a comprehensive study of the ground motions produced by this earthquake, including near-fault velocity-pulse effects, the unusually intense high frequency spikes in the acceleration time series at the Carquinez bridge site, and the effects of the Napa basin and local site effects on ground motion characteristics. Most of the strong motion sites require shear wave velocity measurements to characterize the V_{s30} of the sites. The characteristics of surface fault rupture were well captured, and they offer the opportunity to better understand the characteristics of ground deformations in close proximity to the fault rupture. The effect of surface fault rupture on homes and other infrastructure is a particularly fruitful avenue of further study. Structures with different foundations can be investigated to better understand how each foundation system responds to and performs in areas of ground deformation from surface faulting. The alternating patterns of sidewalk compression zones and extension zones are relatively unique observations of ground performance that may provide insights regarding transient ground motions in the very near fault zone. Conversely, the ground deformation recorded in the sidewalks in the Browns Valley area may be a result of secondary ground deformation resulting from surface faulting, compacted earth fill, or slope movements. Thus, further study of these ground deformations is warranted. Sites that were previously mapped as being liquefiable, which did not exhibit surface manifestations of liquefaction, should be characterized better and added to the liquefaction triggering database. The cause of damage of buried utilities in areas that did not undergo permanent ground displacements should be investigated. Lastly, the documented performance of dams, levees, other earth structures, and natural slopes provides the opportunity to evaluate commonly employed analytical procedures. Thus, the South Napa earthquake presents several important opportunities to advance the profession’s understanding of the geotechnical effects of earthquakes. We hope that this report provides observations and data that support fruitful follow-on research activities.

APPENDIX A

Velocity Records Corresponding to the Component of Maximum Peak-to-Peak Velocity from the Hayden et al. (2014) Pulse Classification Scheme

Note that all records have a low-pass, three-pole, causal Butterworth
Filter applied to the record (see Hayden et al. (2014))

Table 1: Estimation of PGV and T_v using Bray et al. (2009) empirical relationship

Station Name	R_{rup}[1] (km)	PGV RotD50 (cm/s)	PGV[2] Median (cm/s)	PGV $-\sigma_{total}$ (cm/s)	PGV $+\sigma_{total}$ (cm/s)	T_v[3] Median (s)	T_v $-\sigma_{total}$ (s)	T_v $+\sigma_{total}$ (s)
Fire Station No. 3	1.8	80	62	40	96	1.2	0.7	2.0
Huichica Creek	4.2	43	53	34	82	1.2	0.7	2.0
Lovall Valley Loop Rd.	5.1	46	49	32	76	1.2	0.7	2.0
Main St. Napa	4.9	42	50	32	80	1.2	0.7	2.0
Napa College	4.5	56	51	33	80	1.2	0.7	2.0

1) R_{rup} is closest distance between station and rupture plane

2) PGV = Peak Ground Velocity

3) T_v = Pulse Period

Huichica Creek (RSN89)

Velocity Time History for Component with Max PPV (Hayden et al. (2014))

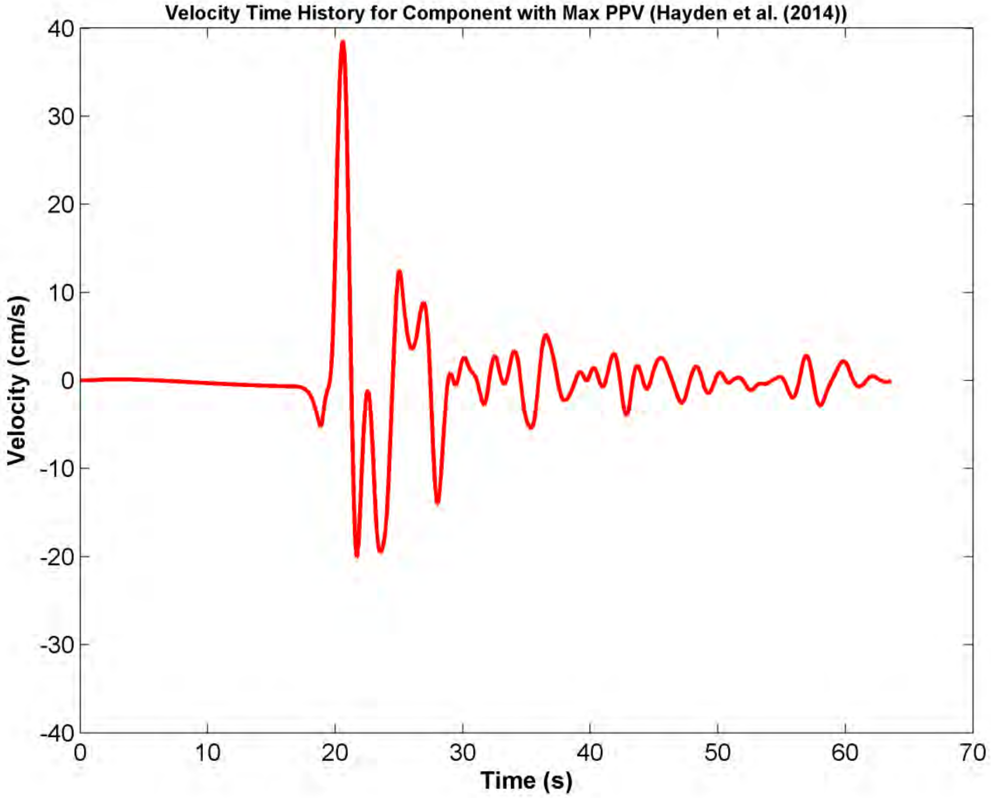

Lovall Valley Loop Rd (RSN212)

Velocity Time History for Component with Max PPV (Hayden et al. (2014))

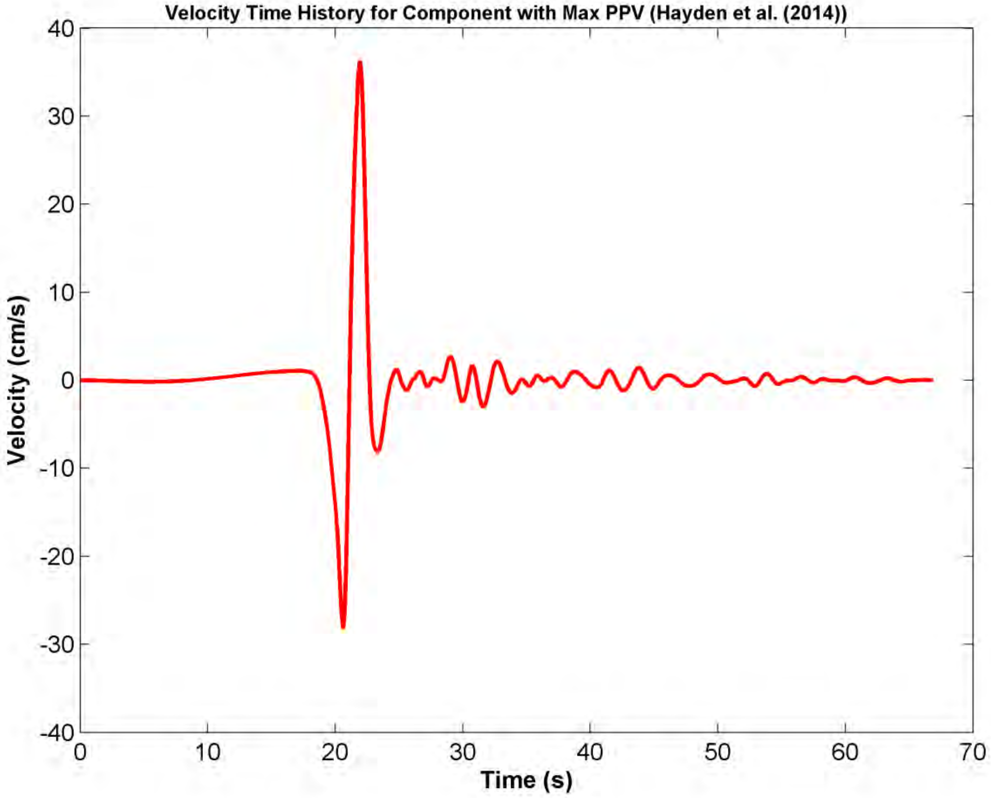

Main St Napa (RSN219)

Velocity Time History for Component with Max PPV (Hayden et al. (2014))

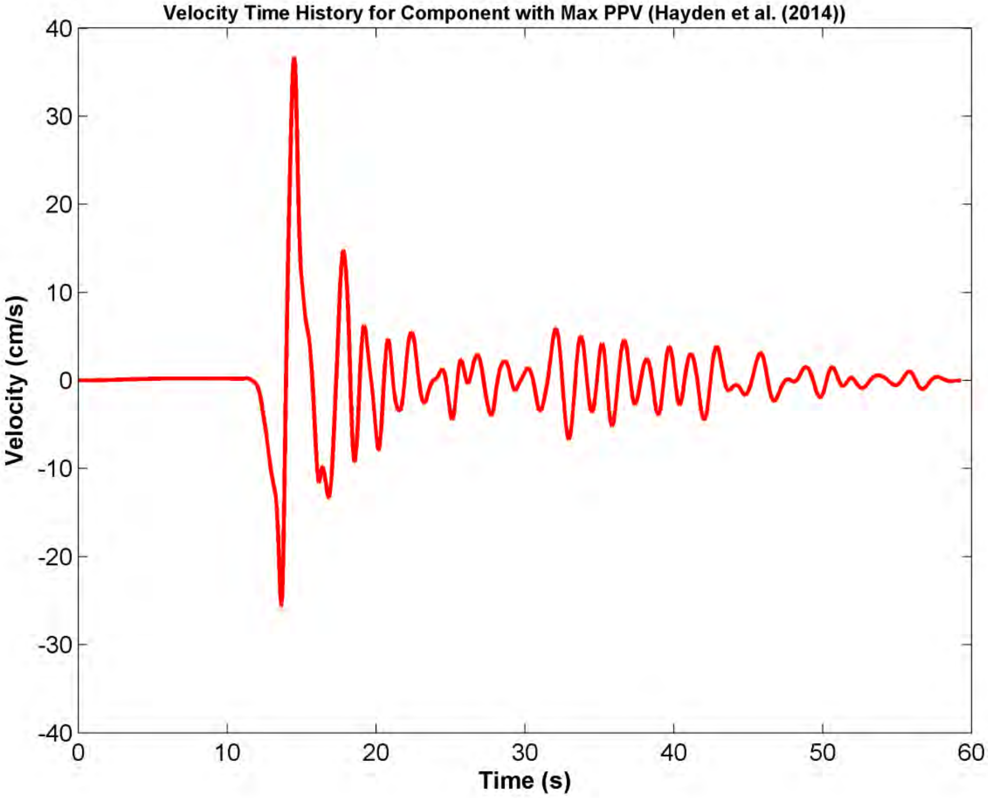

Napa College (RSN51)

Velocity Time History for Component with Max PPV (Hayden et al. (2014))

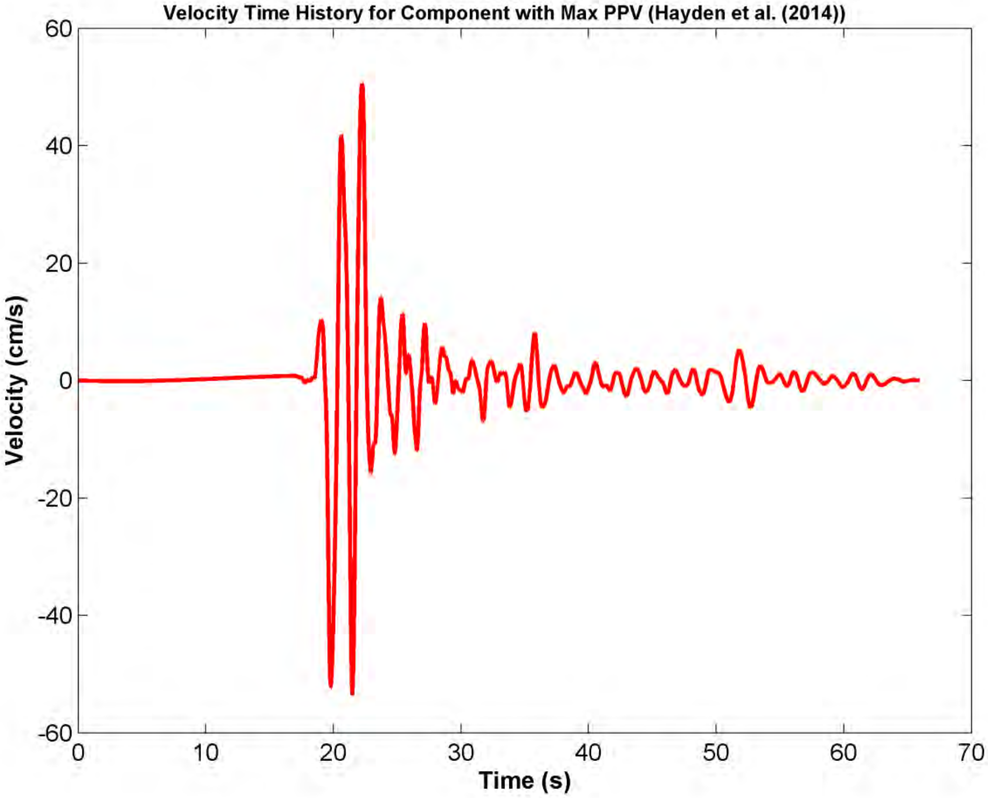

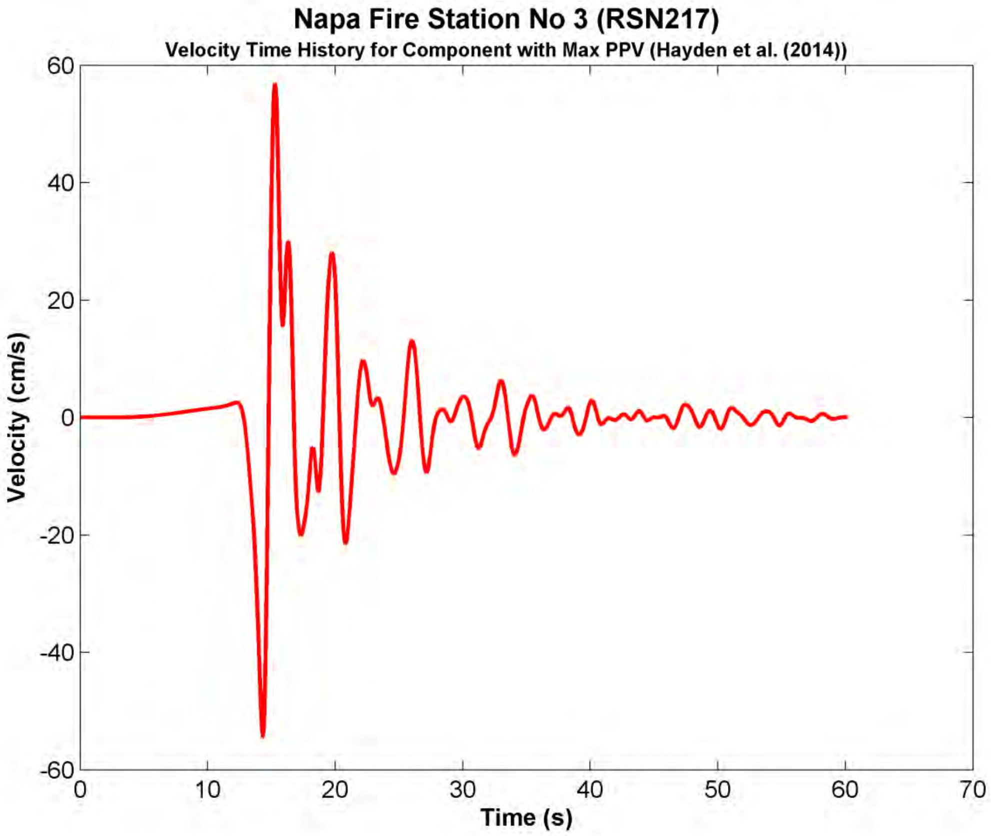
Napa Fire Station No 3 (RSN217)
Velocity Time History for Component with Max PPV (Hayden et al. (2014))
Velocity (cm/s)
60
40
20
0
-20
-40
-60
0
10
20
30
40
50
60
70
Time (s)

Velocity Records Corresponding to the Component with the Maximum Pulse Indicator for the Shahi (2013) Pulse Classification Scheme

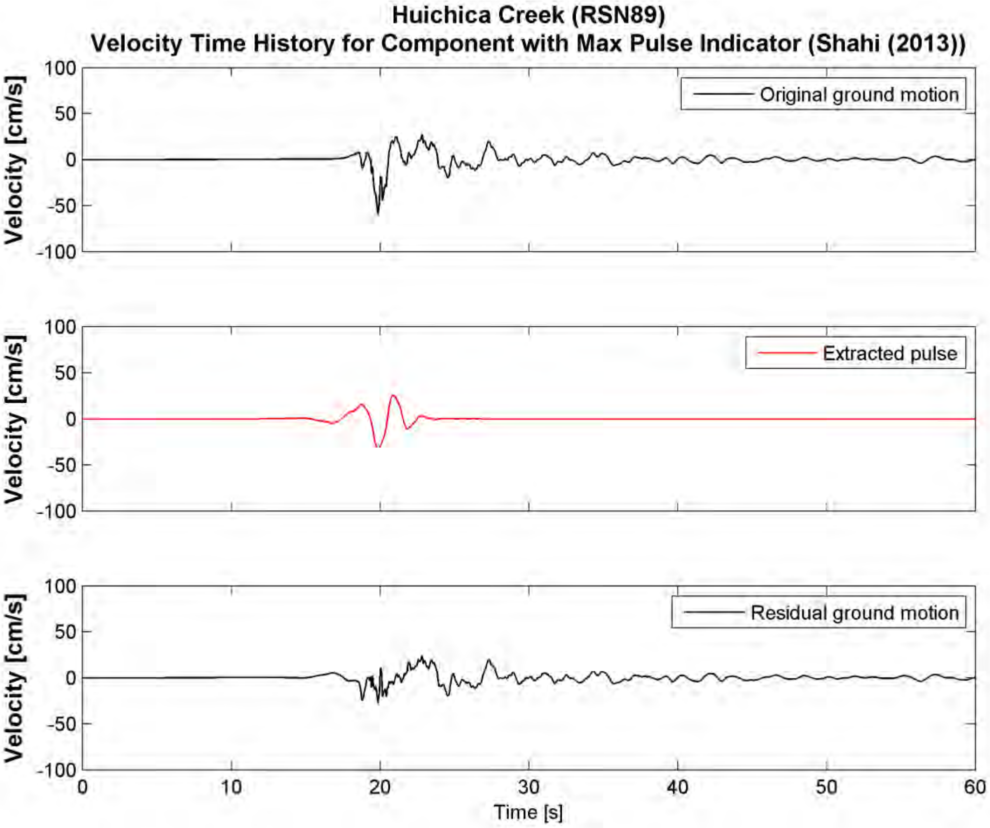
Huichica Creek (RSN89)
Velocity Time History for Component with Max Pulse Indicator (Shahi (2013))
Original ground motion
Extracted pulse
Residual ground motion
Velocity [cm/s]
100
50
0
-50
-100
Time [s]
0
10
20
30
40
50
60

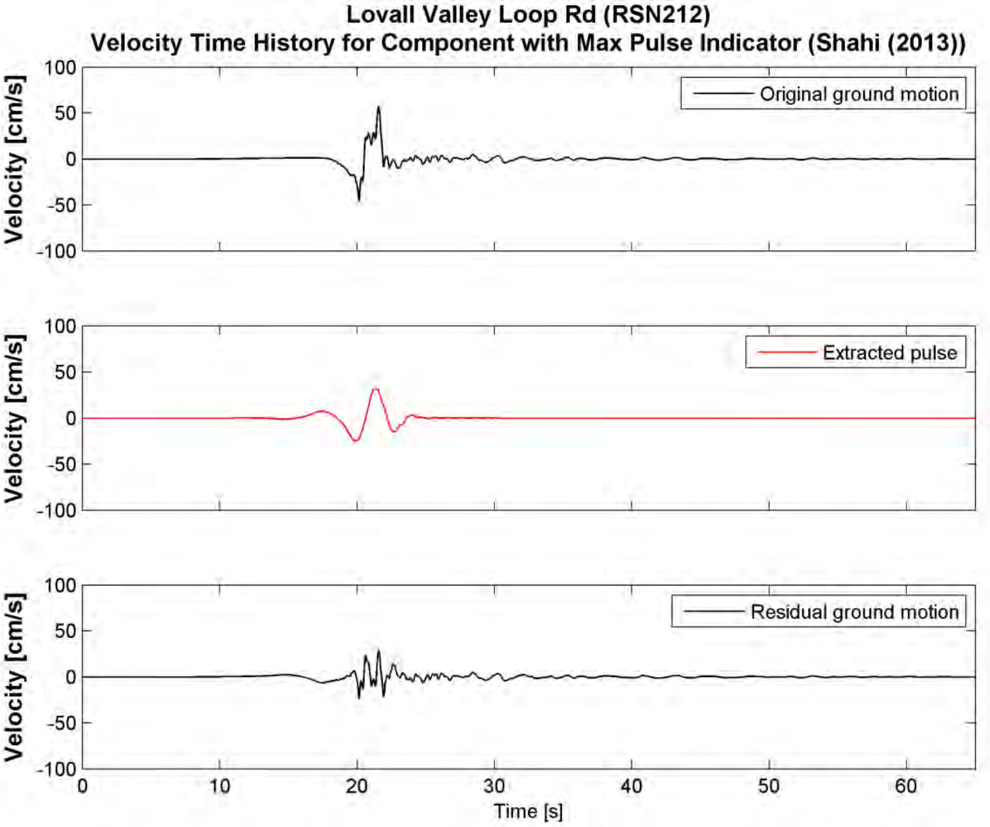
Lovall Valley Loop Rd (RSN212)
Velocity Time History for Component with Max Pulse Indicator (Shahi (2013))
Original ground motion
Extracted pulse
Residual ground motion
Velocity [cm/s]
100
50
0
-50
-100
Time [s]
0
10
20
30
40
50
60

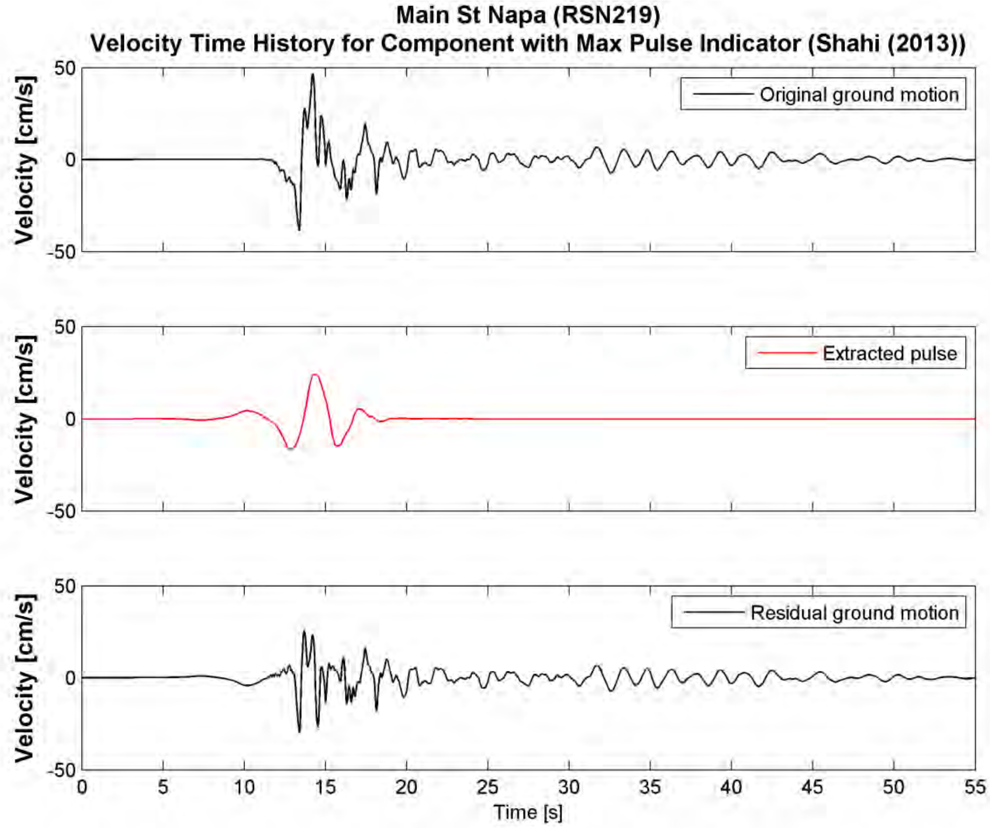

Main St Napa (RSN219)
Velocity Time History for Component with Max Pulse Indicator (Shahi (2013))

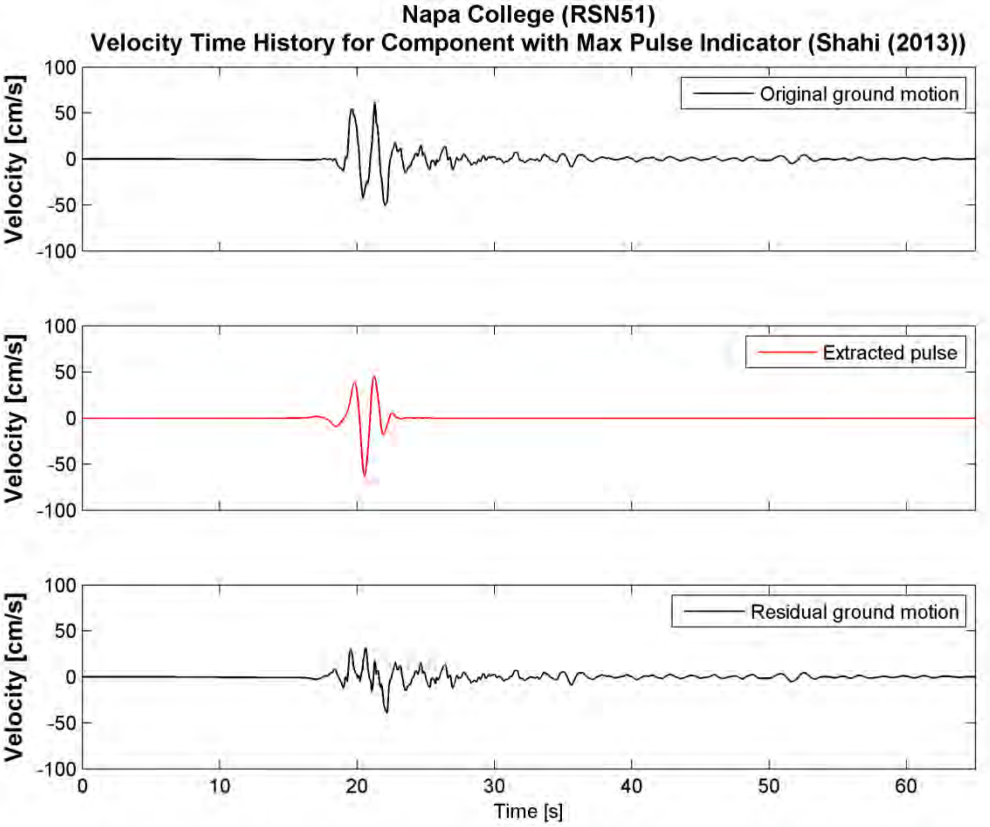

Napa College (RSN51)
Velocity Time History for Component with Max Pulse Indicator (Shahi (2013))

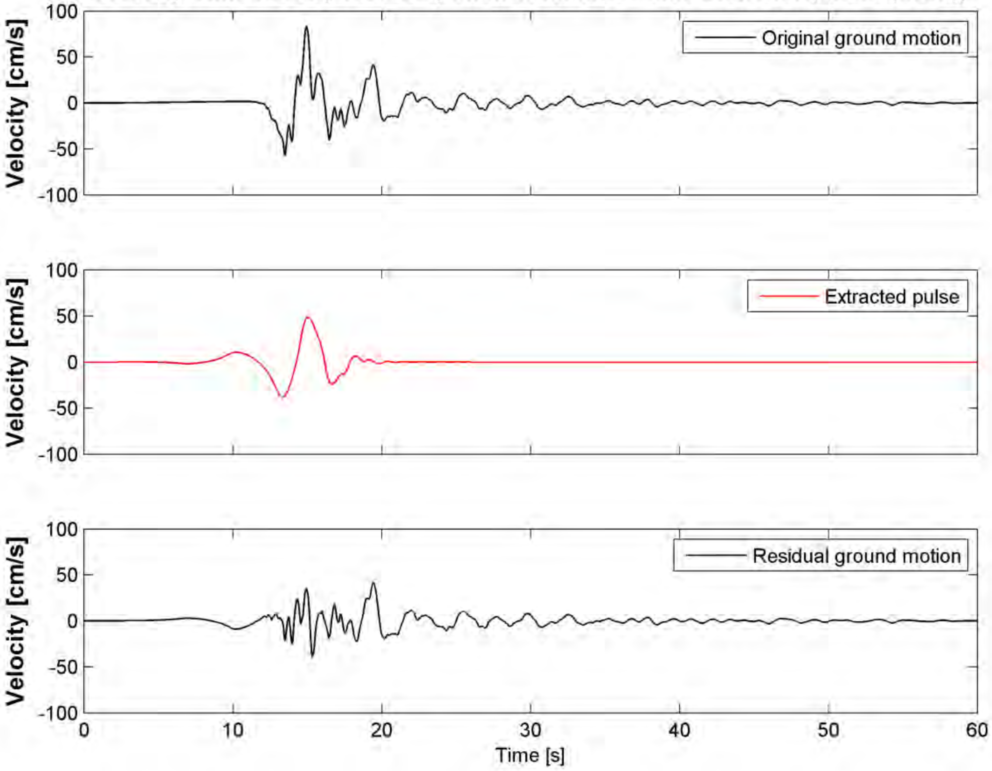

Napa Fire Sta No3 (RSN217)
Velocity Time History for Component with Max Pulse Indicator (Shahi (2013))

APPENDIX B

Acceleration, Velocity, Displacement Time Series, Pseudo-Spectral Acceleration, and Fourier Amplitude Spectra for Selected Recordings

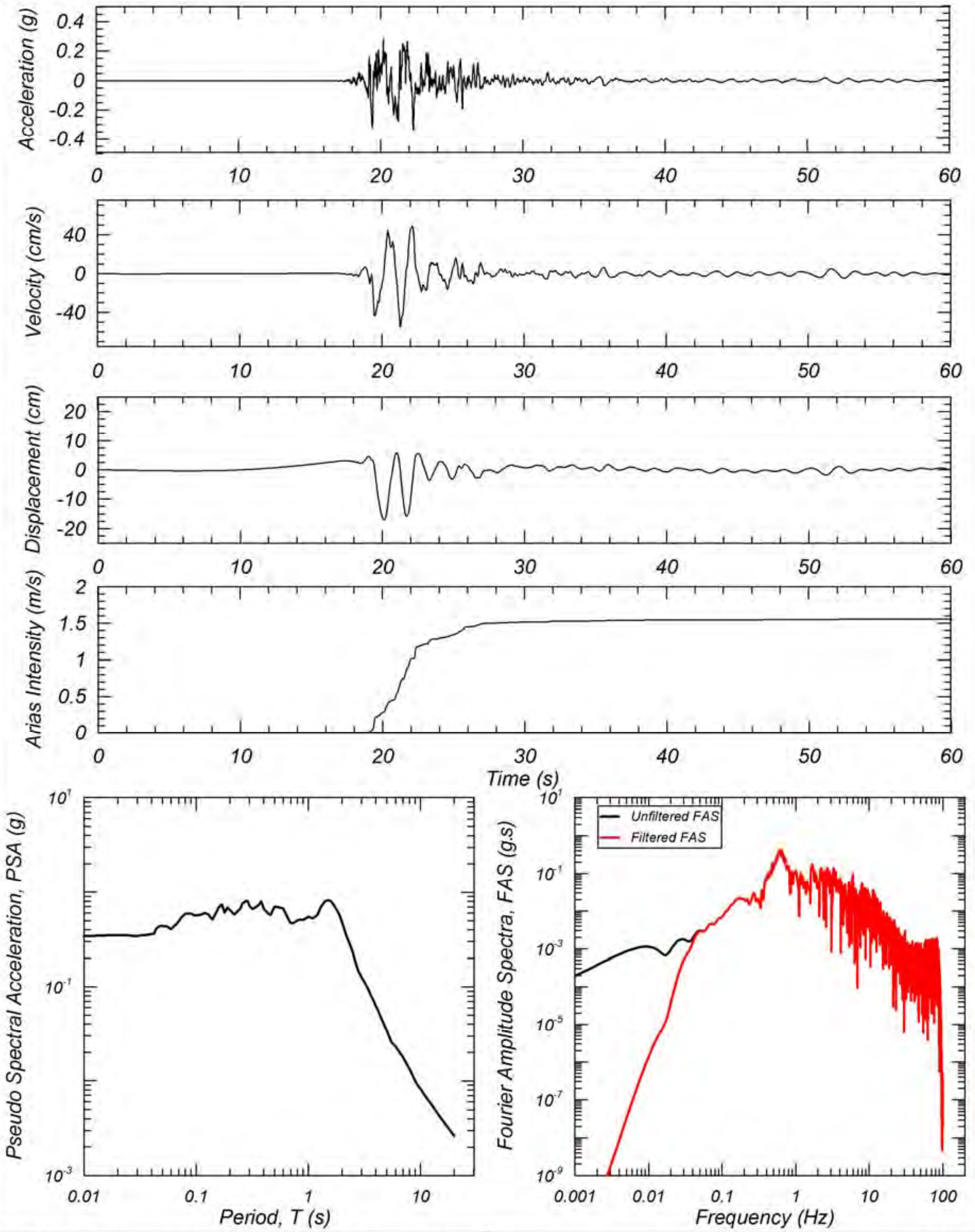

PEER Strong Motion Database Records | Station: Napa College, Component: 360

08/23/2014 South Napa Earthquake | Inferred V_{s30} = 339 m/s, R_{rup} = 4.1 km

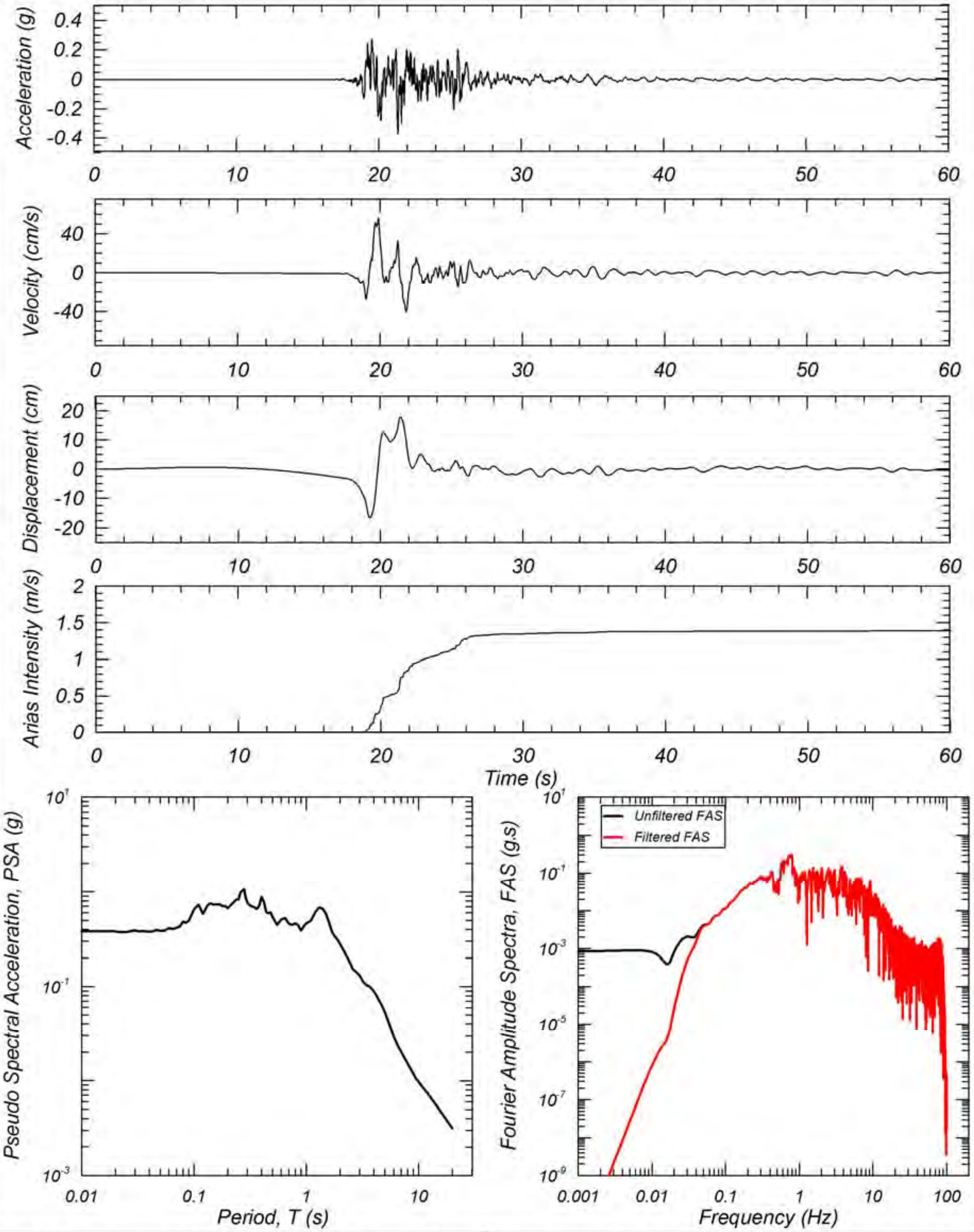

PEER Strong Motion Database Records	Station: Napa College, Component: 090
08/23/2014 South Napa Earthquake	Inferred V_{s30} = 339 m/s, R_{rup} = 4.1 km

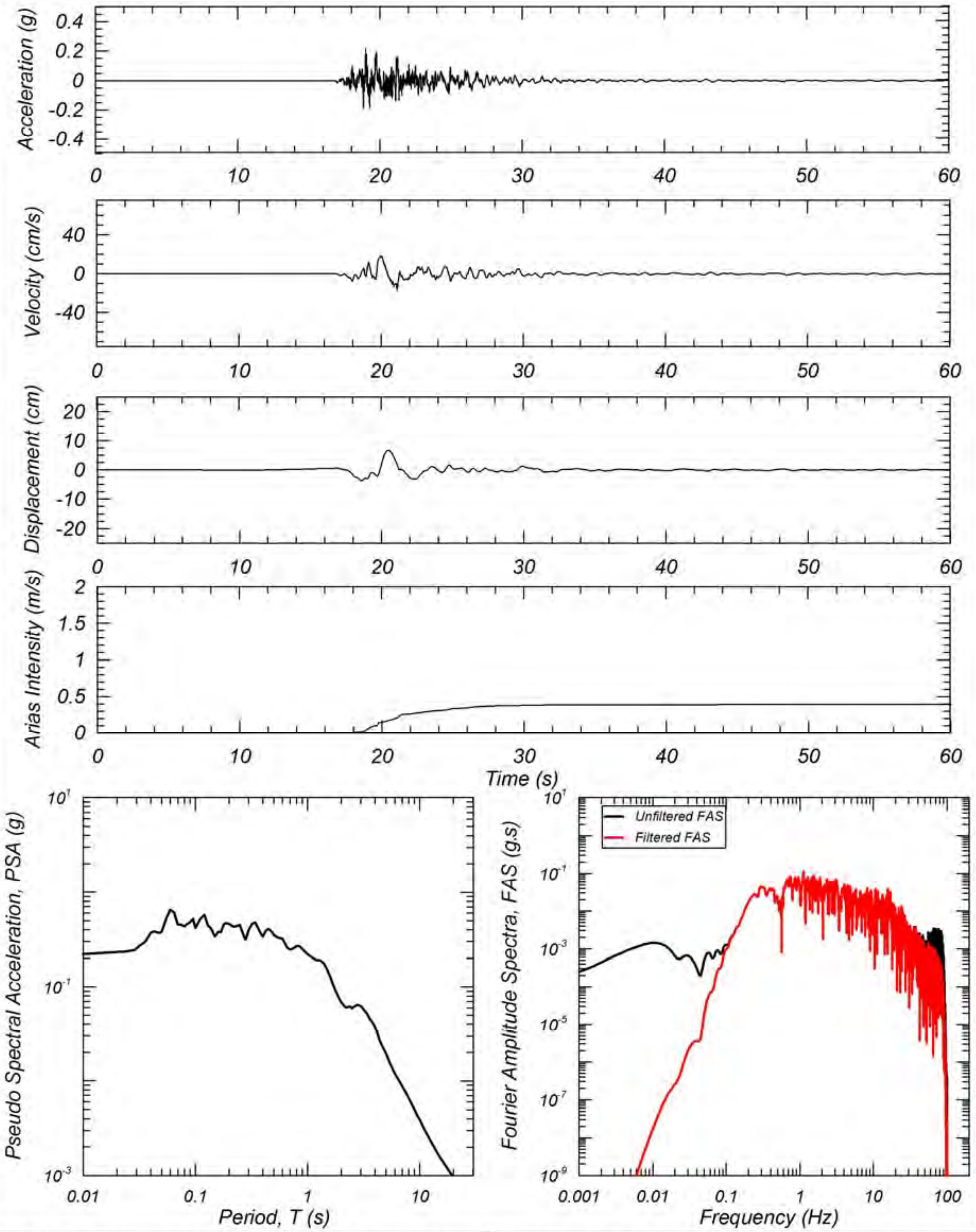

PEER Strong Motion Database Records	Station: Napa College, Component: UP
08/23/2014 South Napa Earthquake	Inferred V_{s30} = 339 m/s, R_{rup} = 4.1 km

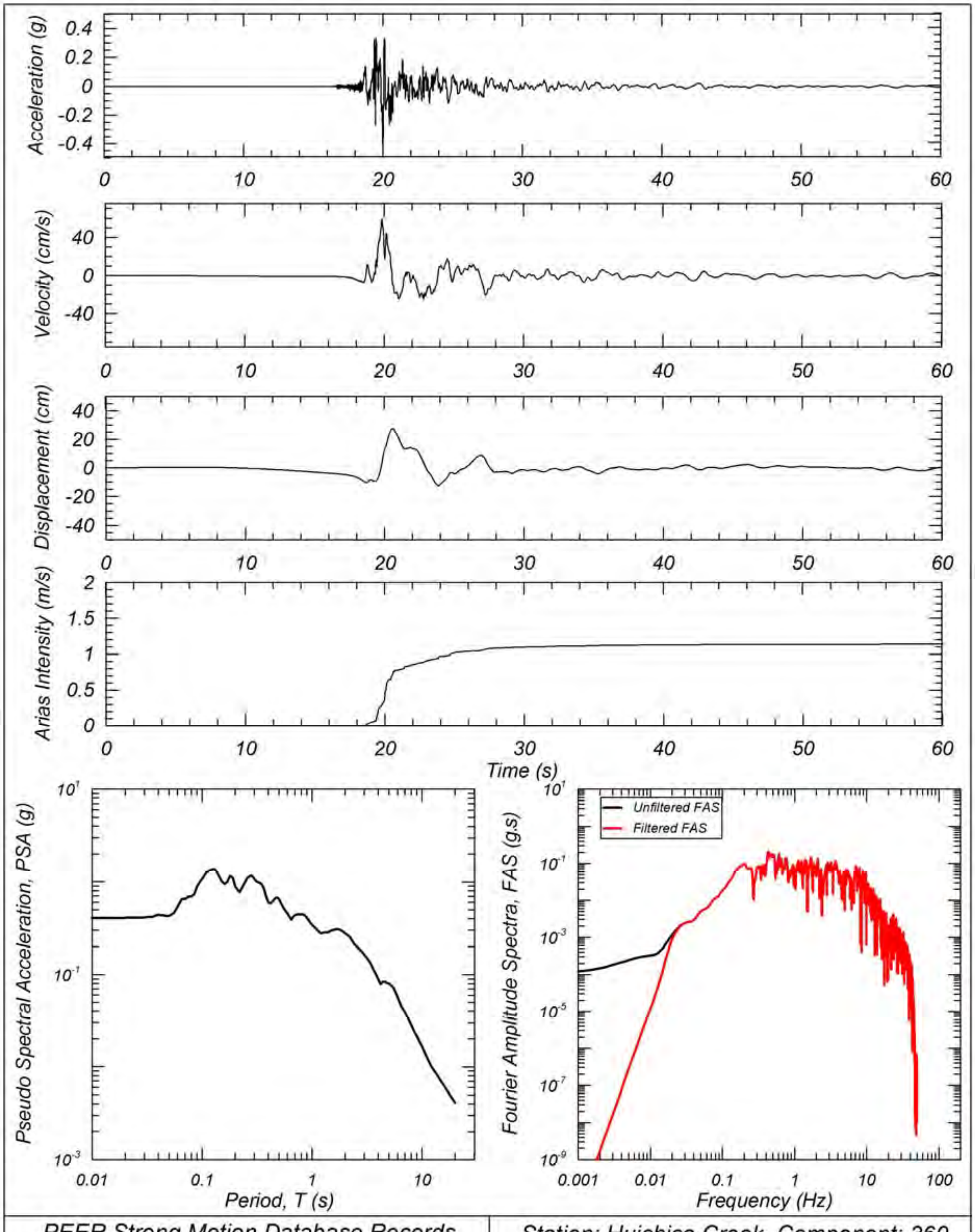

PEER Strong Motion Database Records	Station: Huichica Creek, Component: 360
08/23/2014 South Napa Earthquake	Inferred V_{s30} = 217 m/s, R_{rup} = 3.9 km

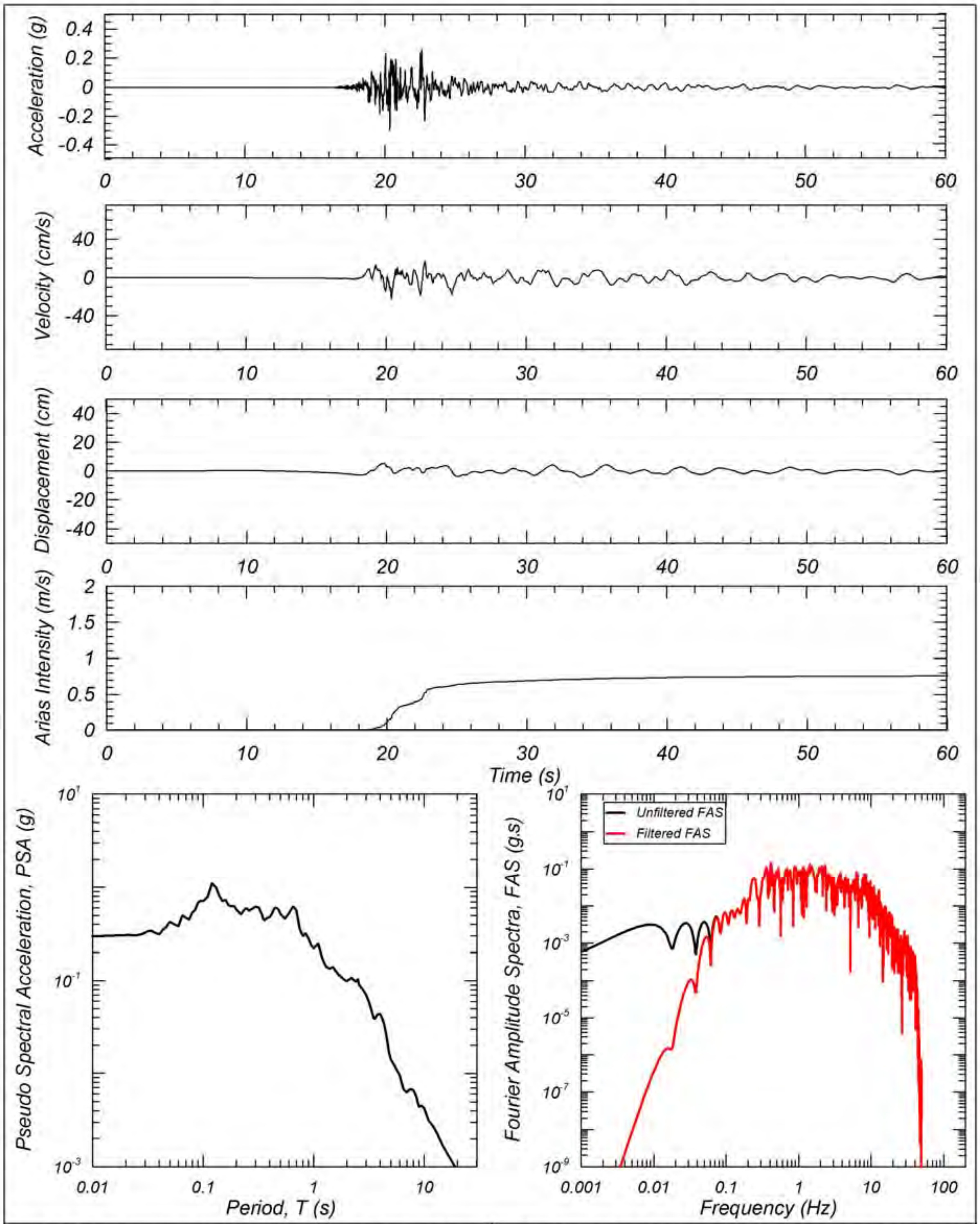

PEER Strong Motion Database Records	Station: Huichica Creek, Component: 090
08/23/2014 South Napa Earthquake	Inferred V_{s30} = 217 m/s, R_{rup} = 3.9 km

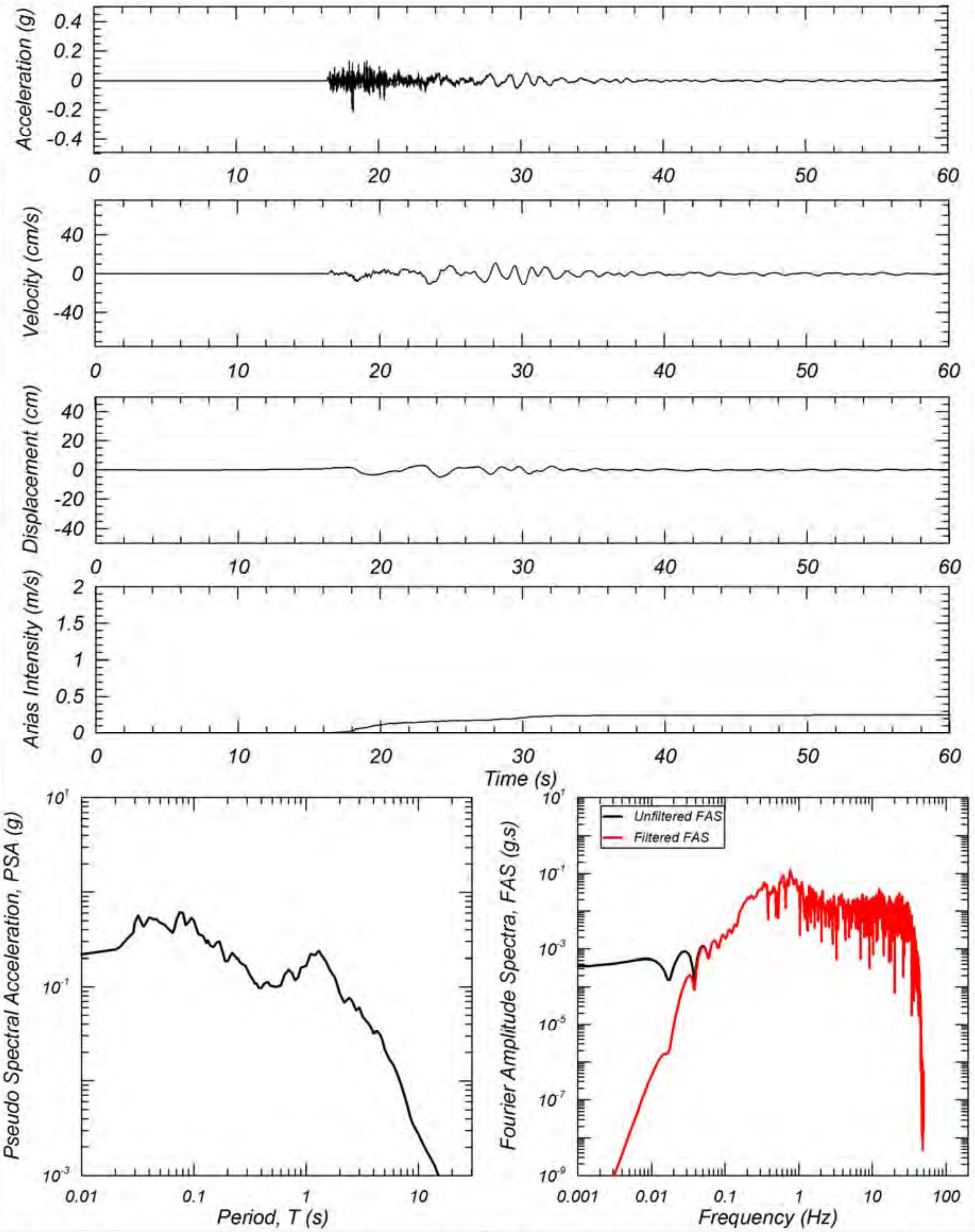

PEER Strong Motion Database Records

Station: Huichica Creek, Component: UP

08/23/2014 South Napa Earthquake

Inferred V_{s30} = 217 m/s, R_{rup} = 3.9 km

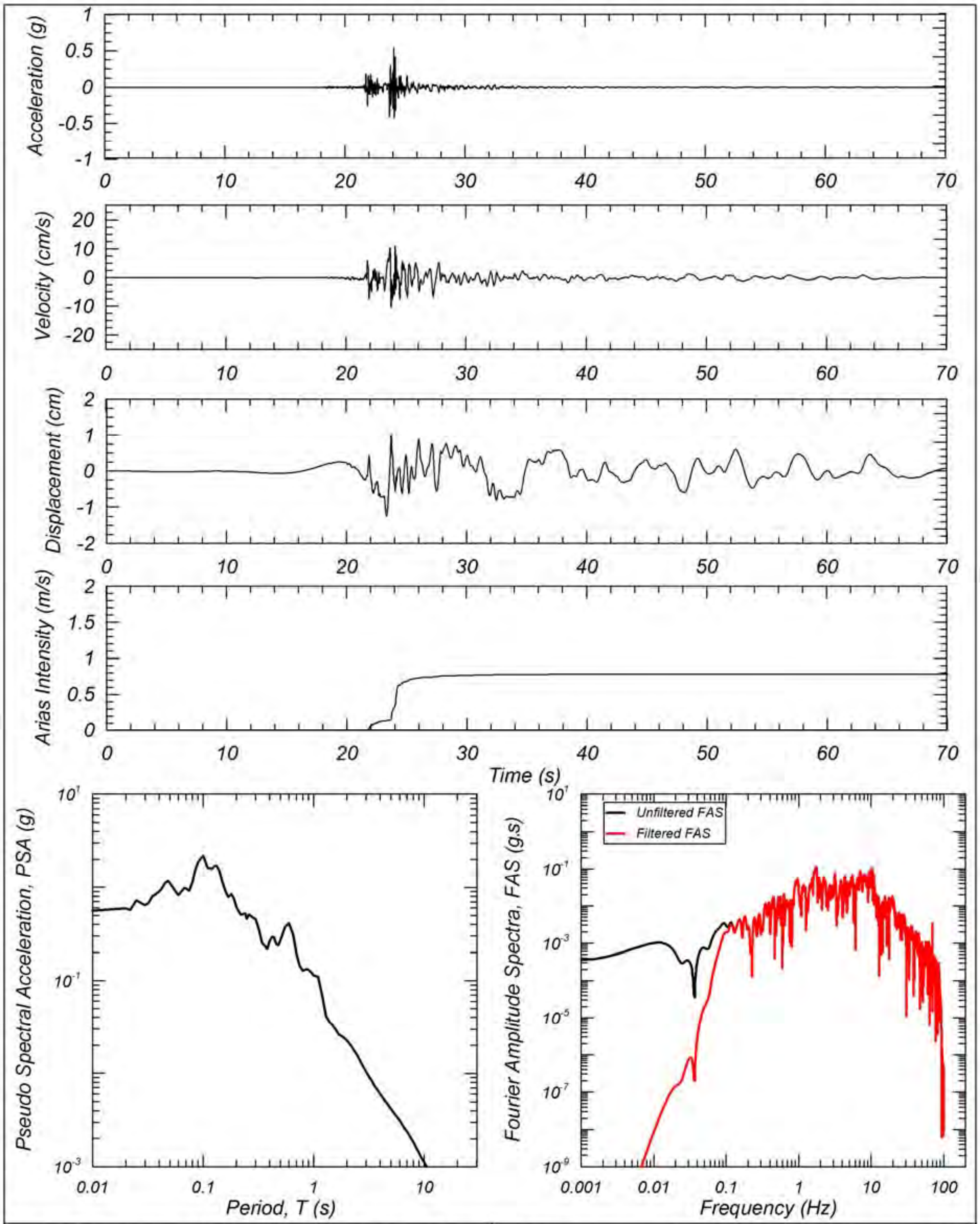

PEER Strong Motion Database Records	Station: Carquinez Br Geo Array #1 (0 m), Component: 090
08/23/2014 South Napa Earthquake	V_{s30} = 342 m/s, R_{rup} = 20 km

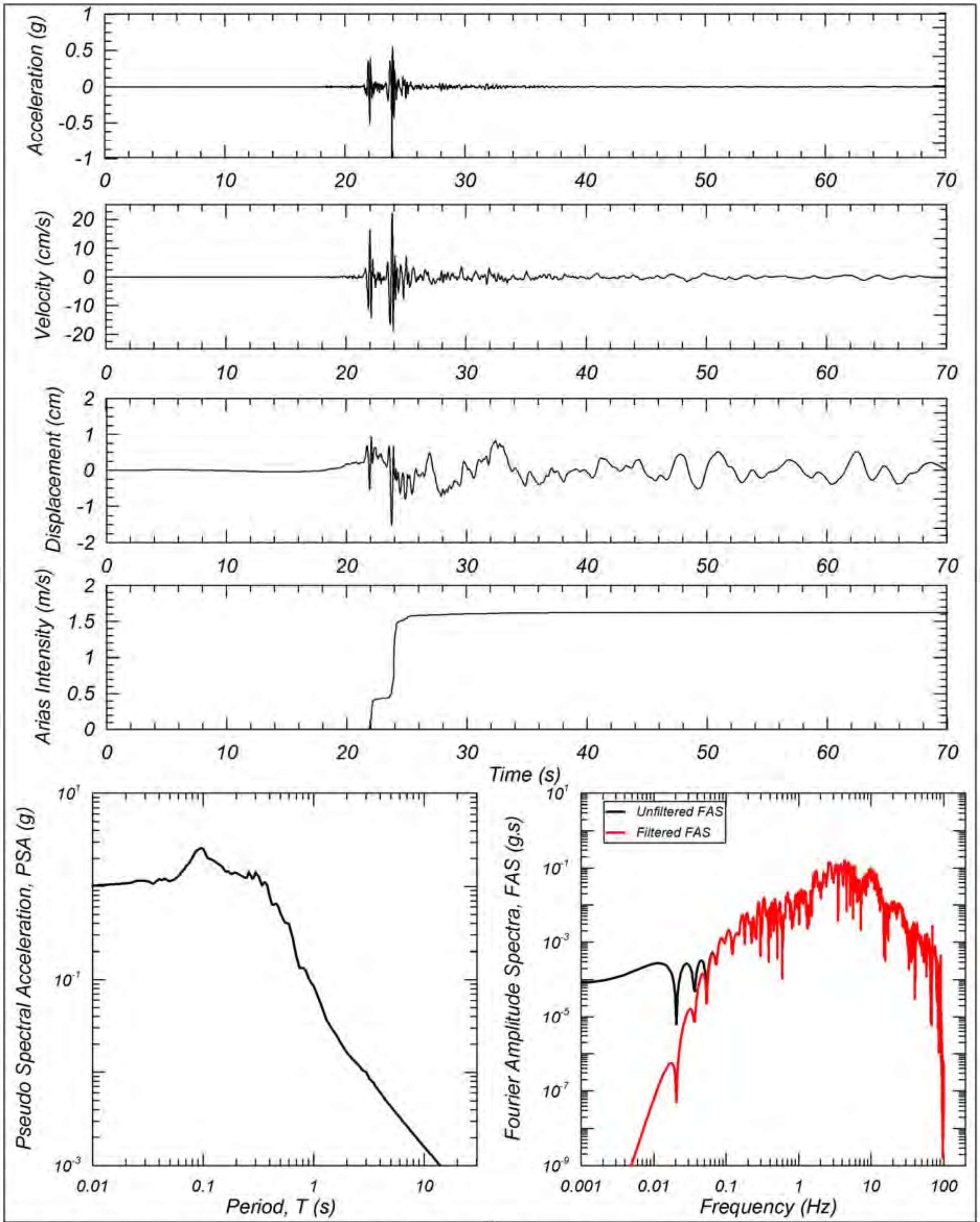

PEER Strong Motion Database Records	Station: Carquinez Br Geo Array #1 (0 m), Component: 180
08/23/2014 South Napa Earthquake	V_{s30} = 342 m/s, R_{rup} = 20 km

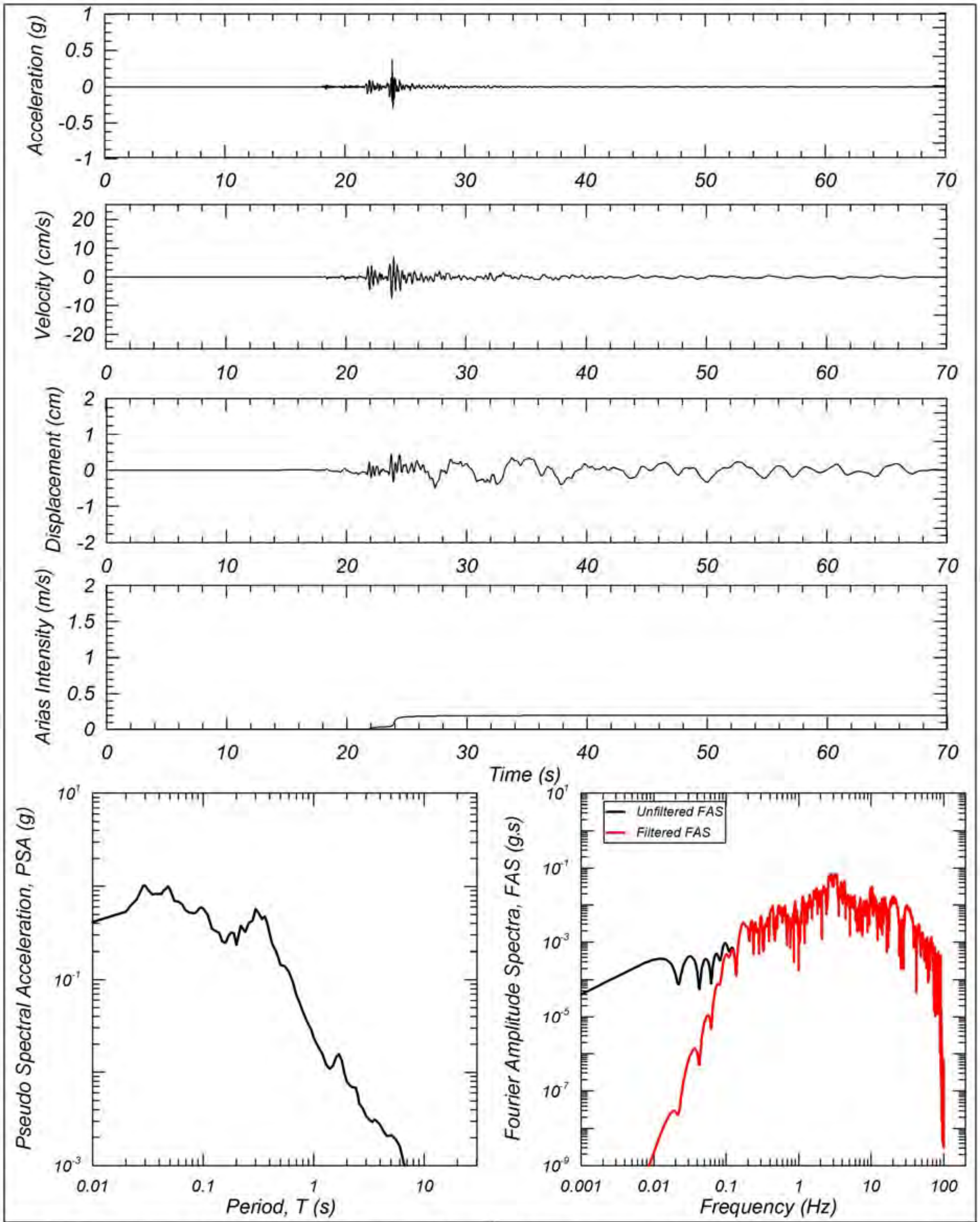

PEER Strong Motion Database Records

Station: Carquinez Br Geo Array #1 (0 m), Component: UP

08/23/2014 South Napa Earthquake

V_{s30} = 342 m/s, R_{rup} = 20 km

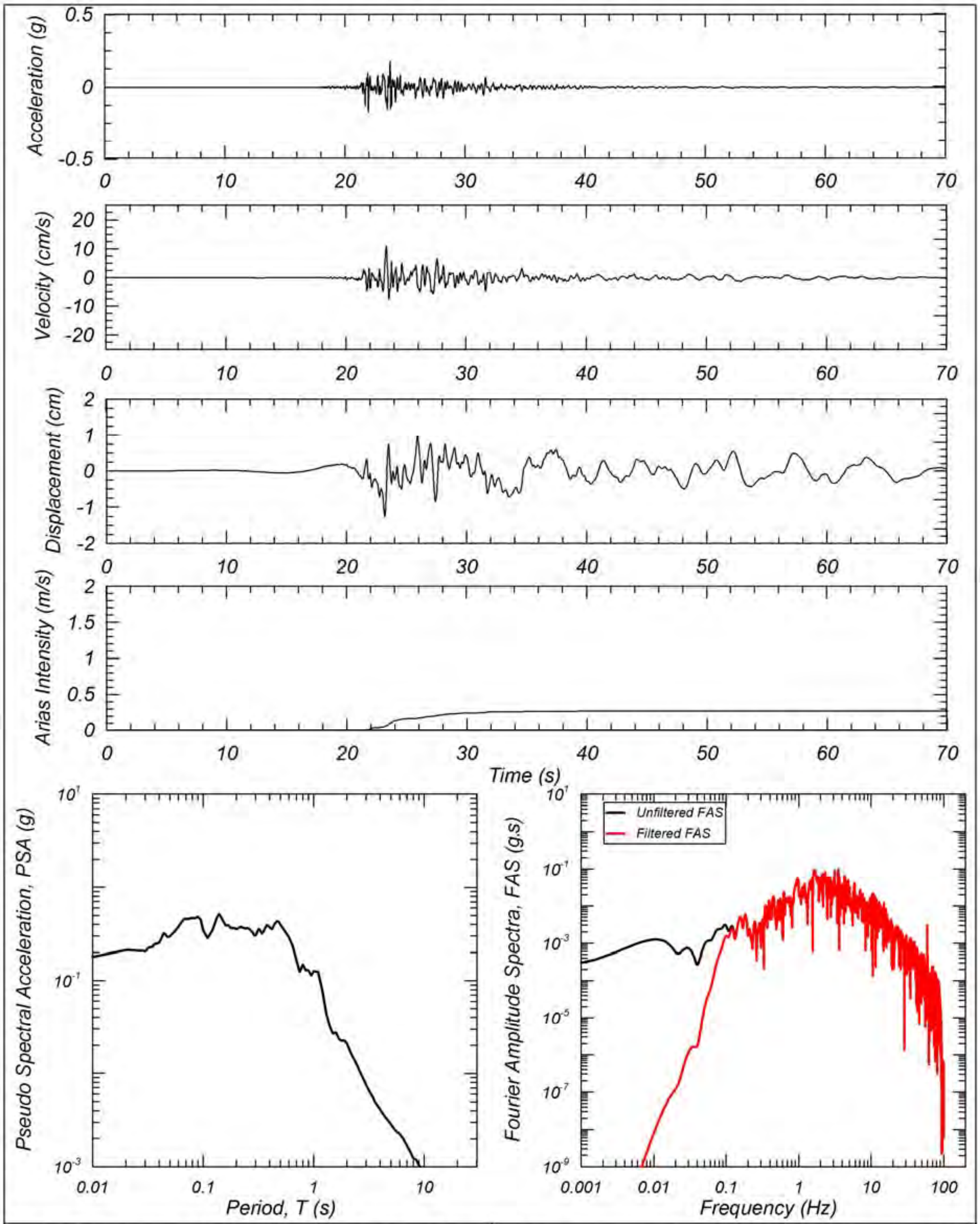

PEER Strong Motion Database Records	Station: Carquinez Br Geo Array #2 (0 m), Component: 090
08/23/2014 South Napa Earthquake	V_{s30} = 342 m/s, R_{rup} = 20 km

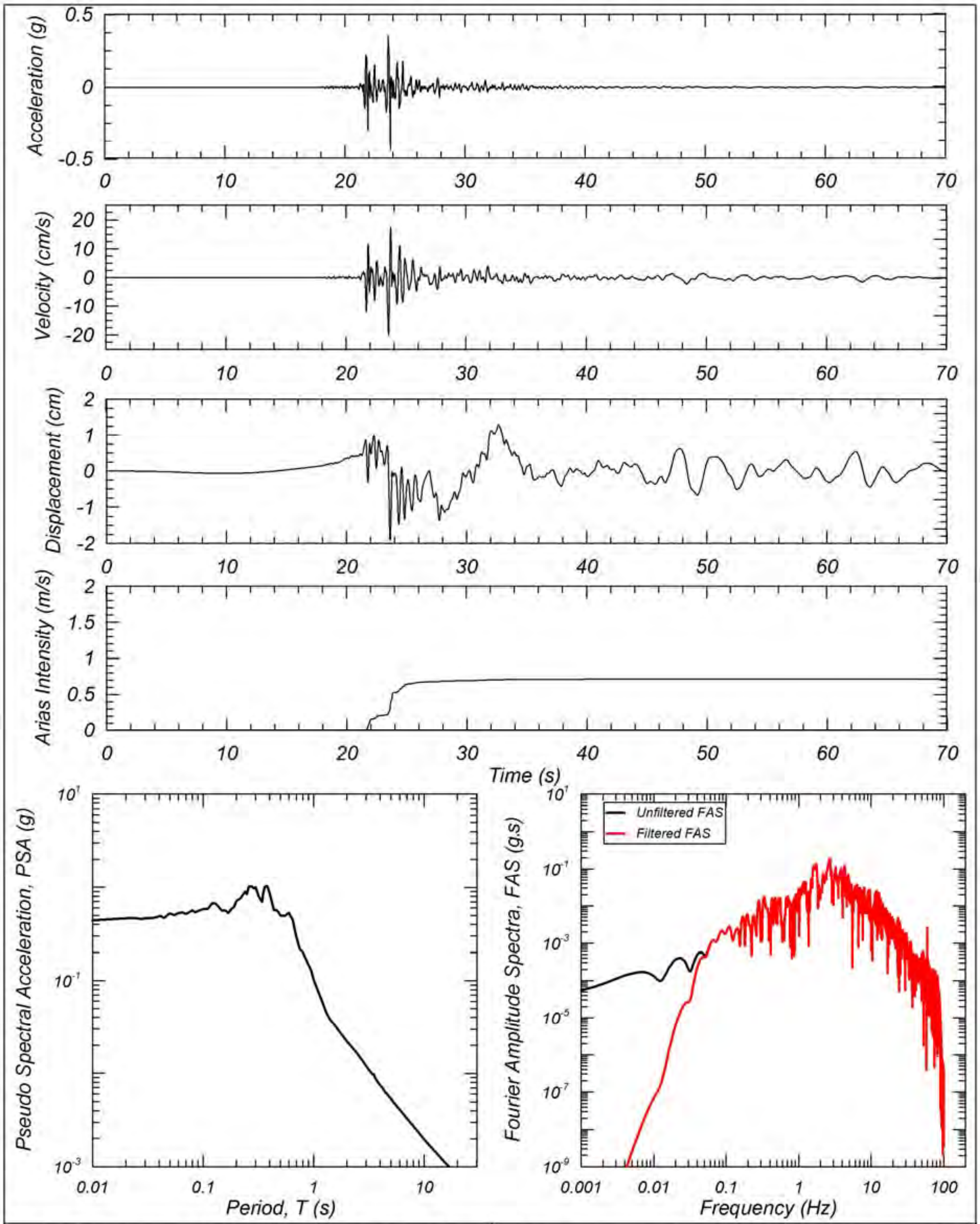

PEER Strong Motion Database Records	Station: Carquinez Br Geo Array #2 (0 m), Component: 180
08/23/2014 South Napa Earthquake	V_{s30} = 342 m/s, R_{rup} = 20 km

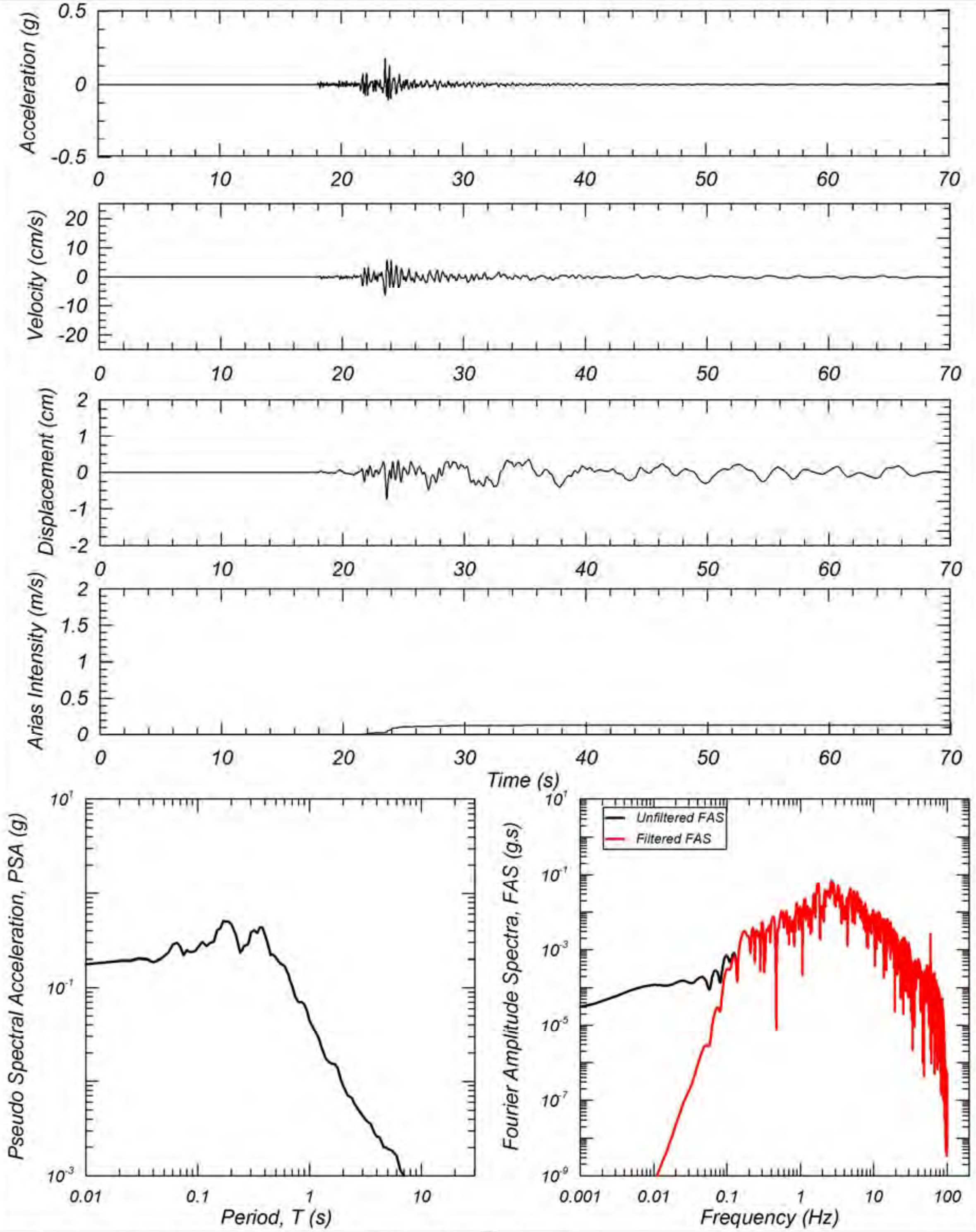

PEER Strong Motion Database Records	Station: Carquinez Br Geo Array #2 (0 m), Component: UP
08/23/2014 South Napa Earthquake	V_{s30} = 342 m/s, R_{rup} = 20 km

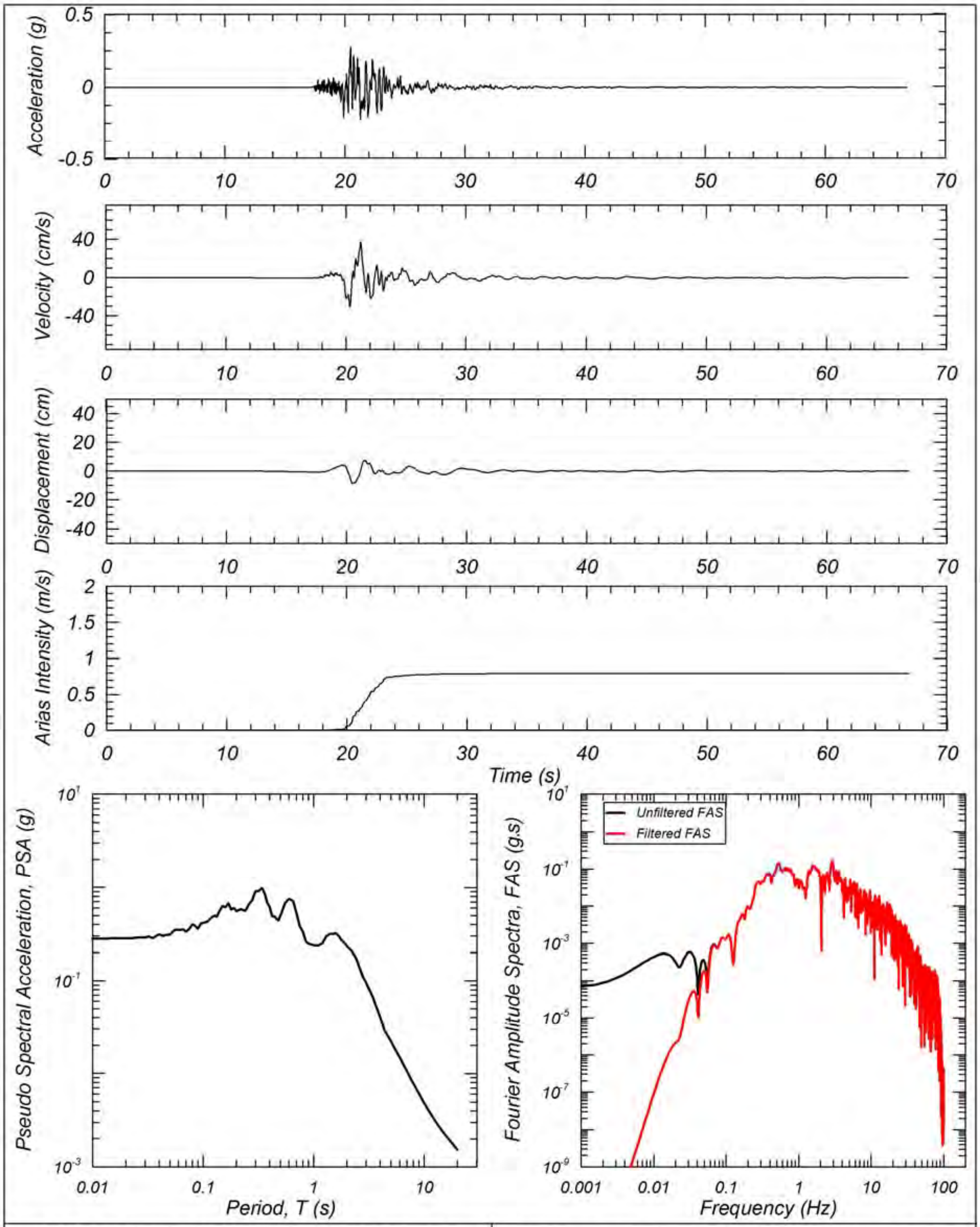

PEER Strong Motion Database Records	Station: Lovall Valley Loop Rd, Component: 360
08/23/2014 South Napa Earthquake	Inferred V_{s30} = 710 m/s, R_{rup} = 6.1 km

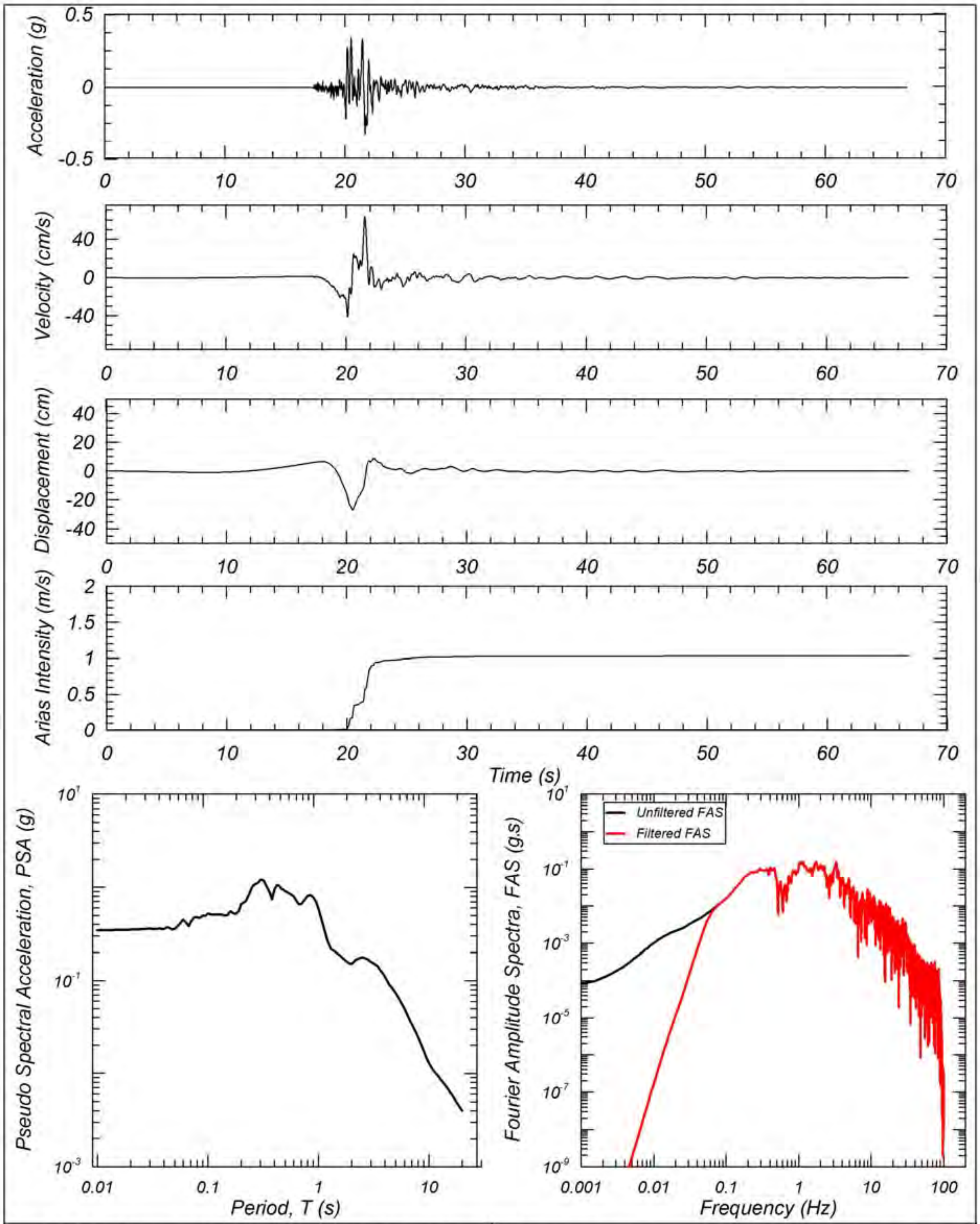

PEER Strong Motion Database Records	Station: Lovall Valley Loop Rd, Component: 090
08/23/2014 South Napa Earthquake	Inferred V_{s30} = 710 m/s, R_{rup} = 6.1 km

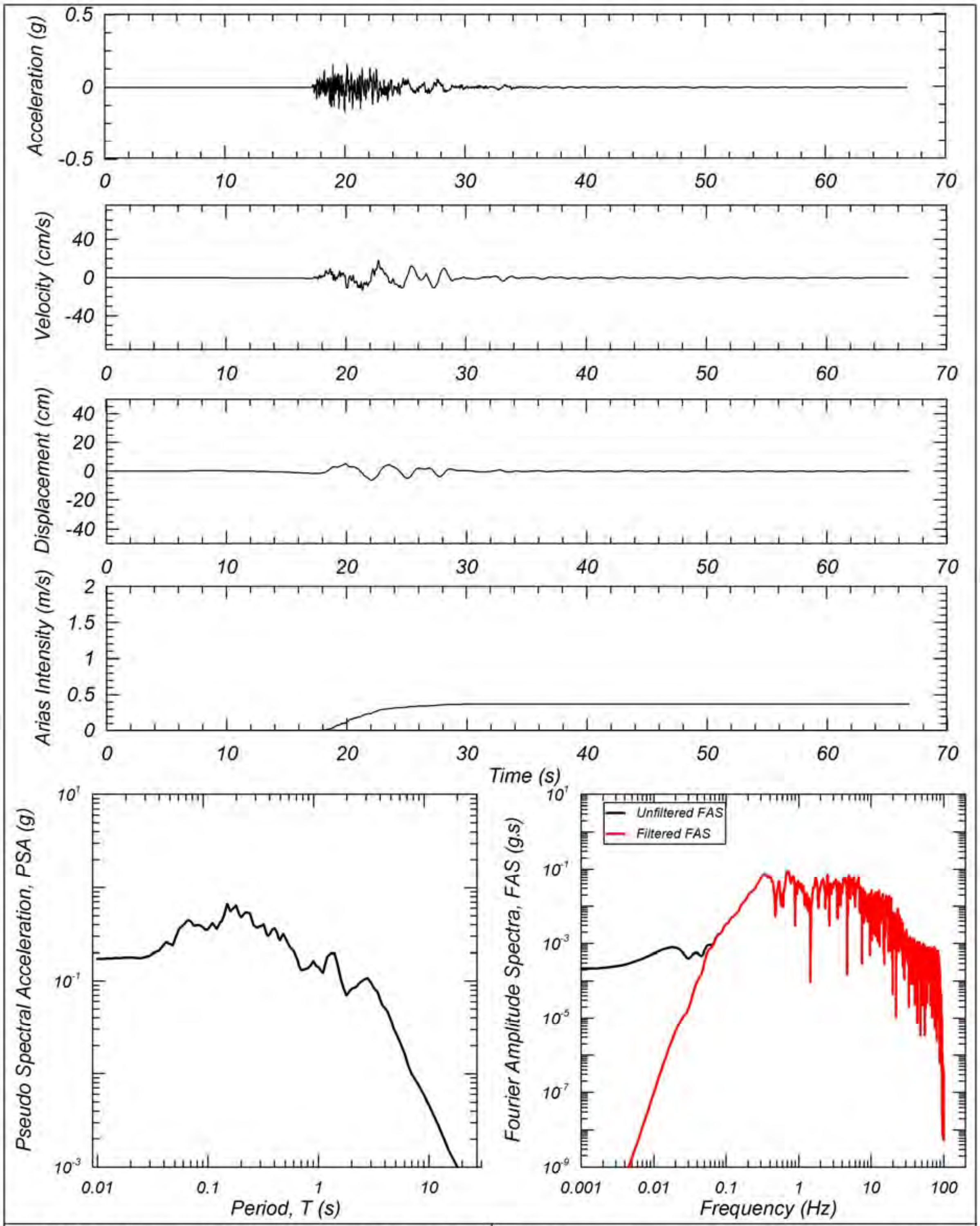

PEER Strong Motion Database Records	Station: Lovall Valley Loop Rd, Component: UP
08/23/2014 South Napa Earthquake	Inferred V_{s30} = 710 m/s, R_{rup} = 6.1 km

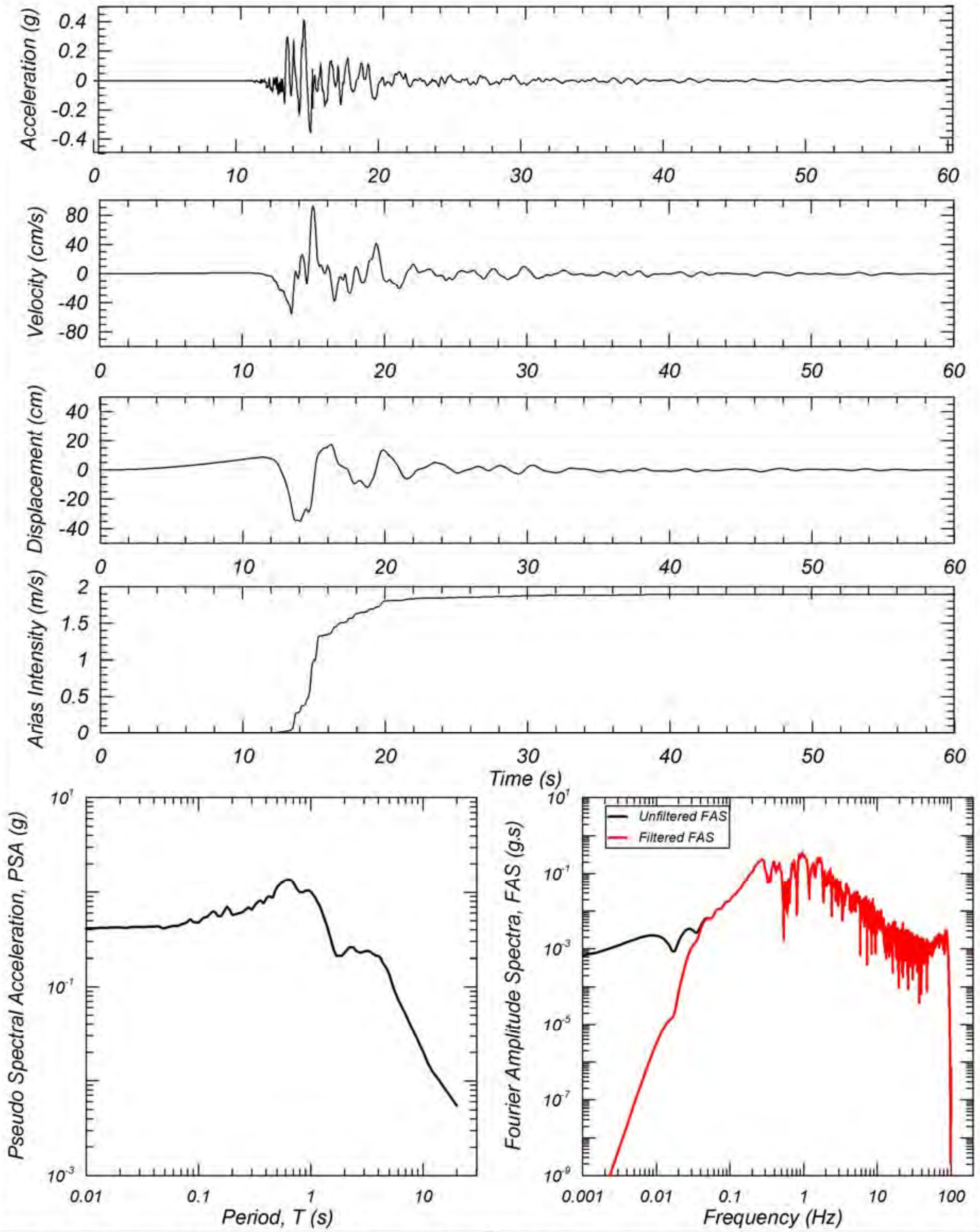

PEER Strong Motion Database Records	*Station: Napa; Fire Station No. 3, Component: 360*
08/23/2014 South Napa Earthquake	*Inferred V_{s30} = 332 m/s, R_{rup} = 2.6 km*

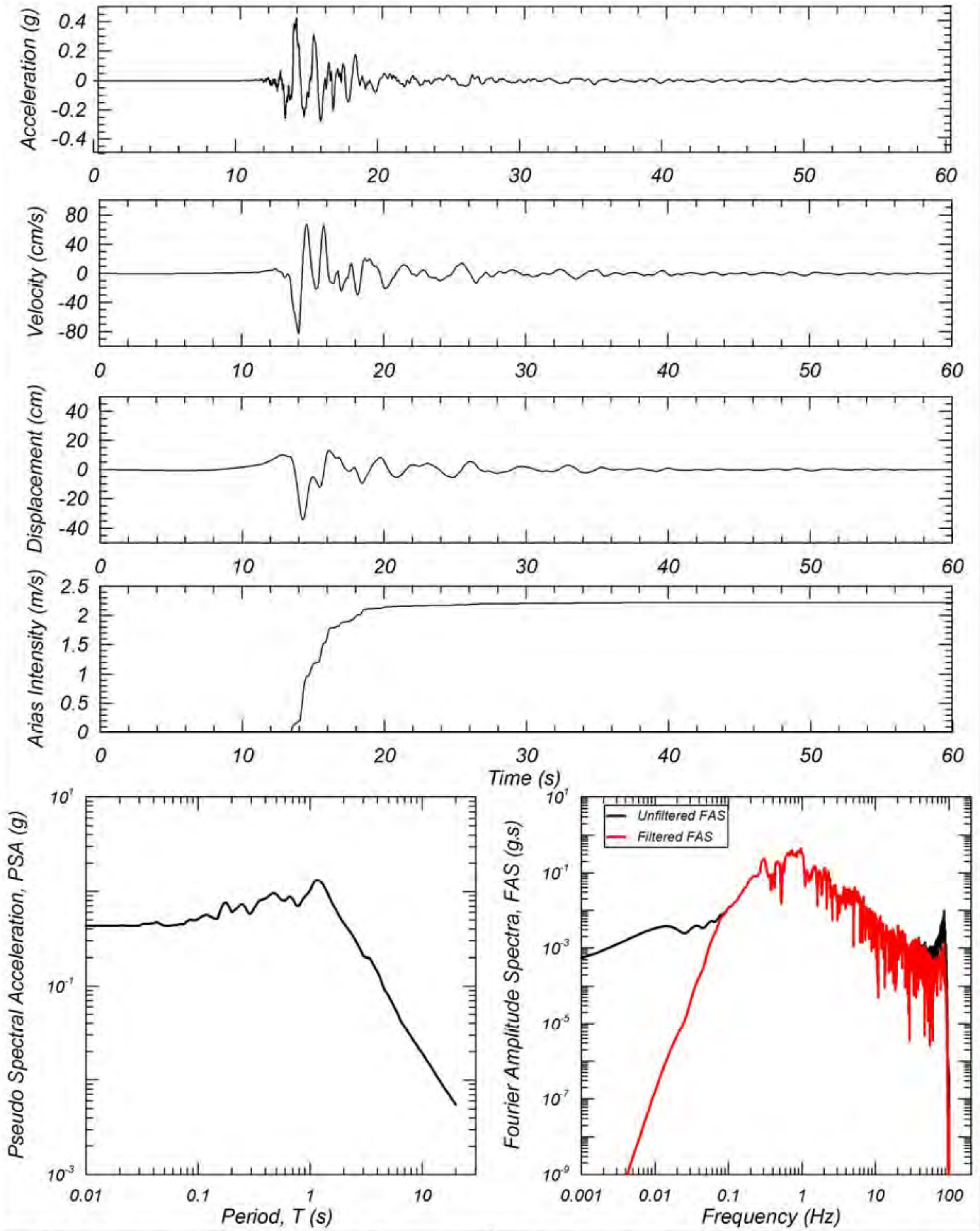

PEER Strong Motion Database Records	*Station: Napa; Fire Station No. 3, Component: 090*
08/23/2014 South Napa Earthquake	*Inferred V_{s30} = 332 m/s, R_{rup} = 2.6 km*

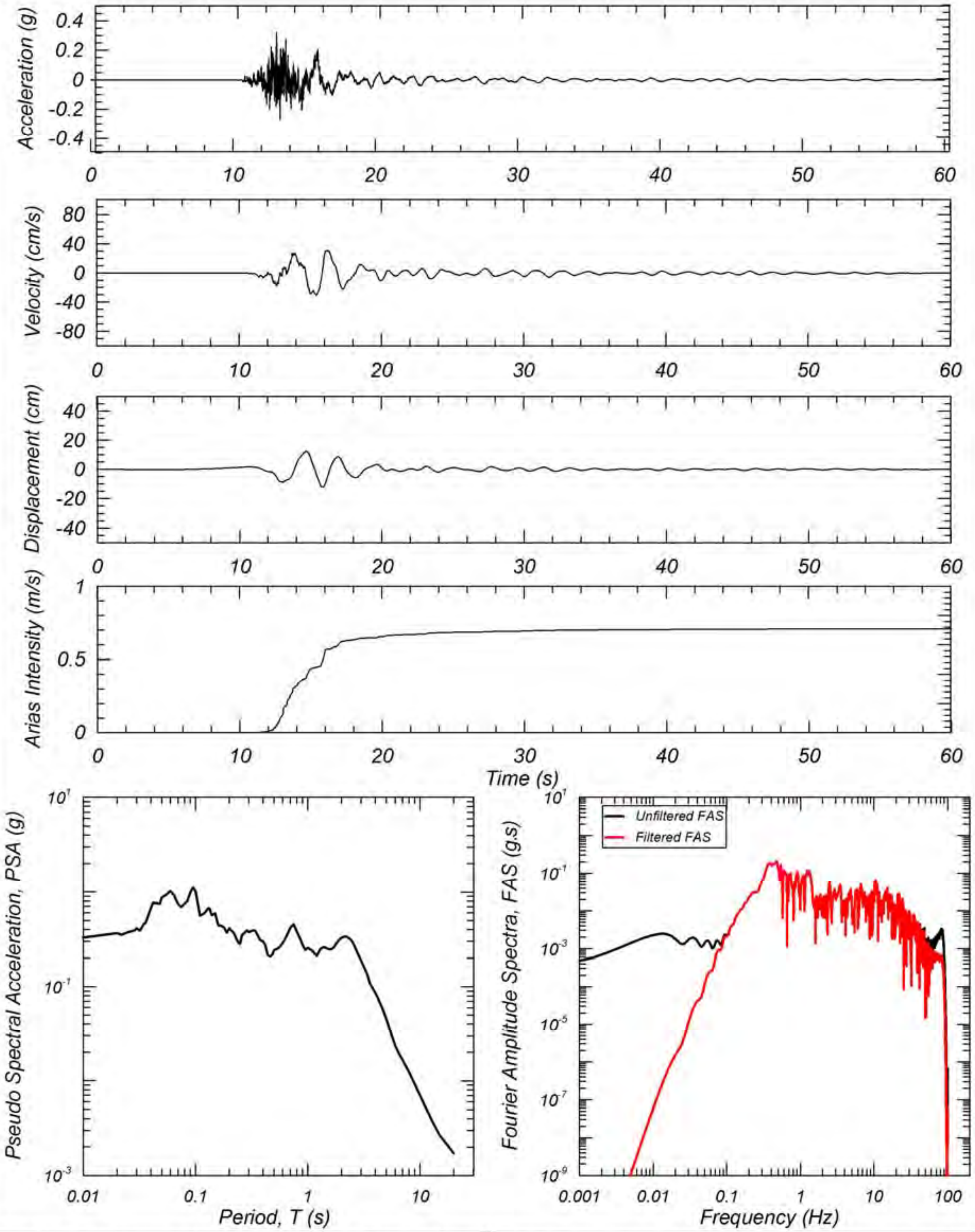

PEER Strong Motion Database Records	*Station: Napa; Fire Station No. 3, Component: UP*
08/23/2014 South Napa Earthquake	*Inferred V_{s30} = 332 m/s, R_{rup} = 2.6 km*

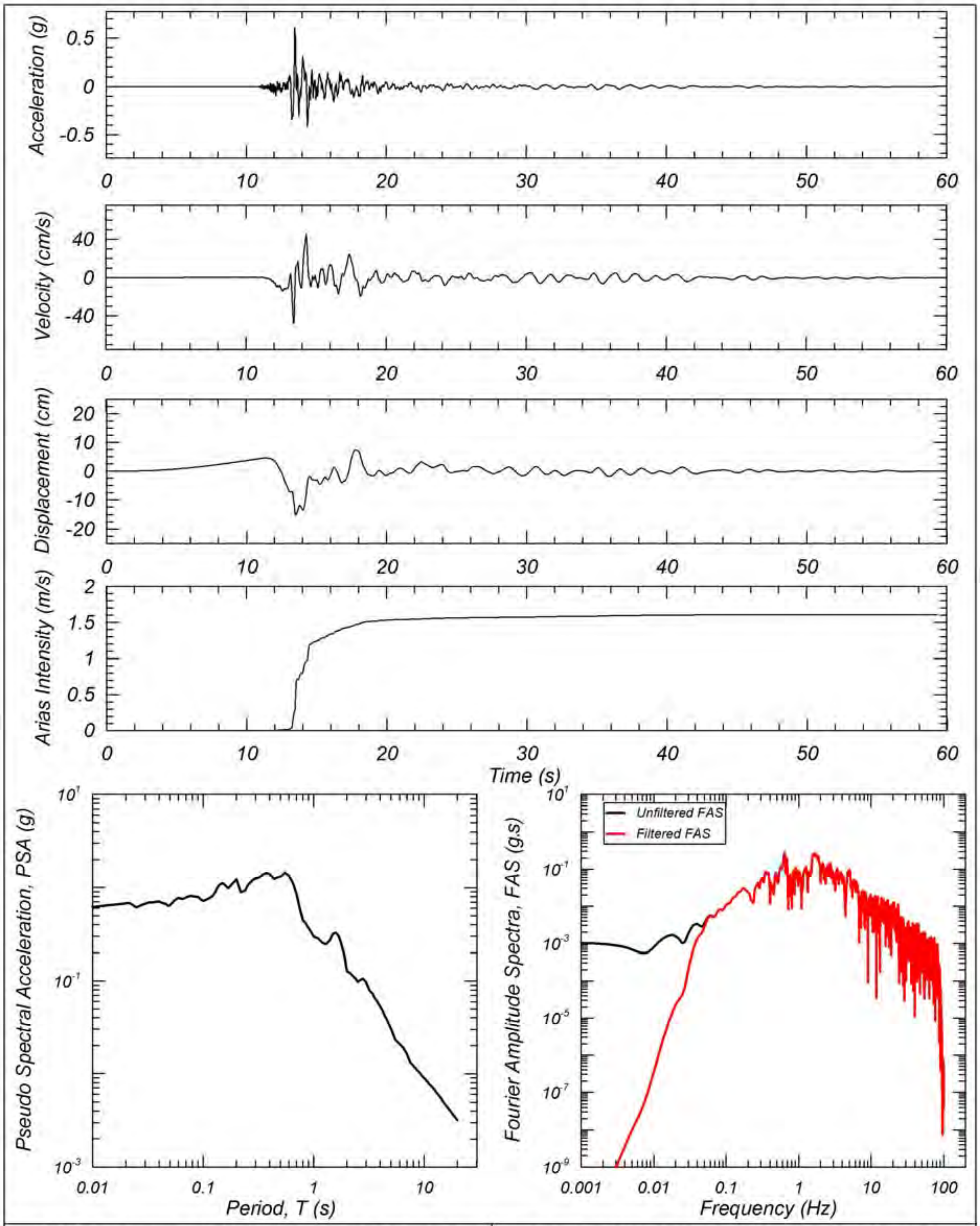

PEER Strong Motion Database Records	Station: Main St, Napa, CA, Component: 360
08/23/2014 South Napa Earthquake	Inferred V_{s30} = 285 m/s, R_{rup} = 3.9 km

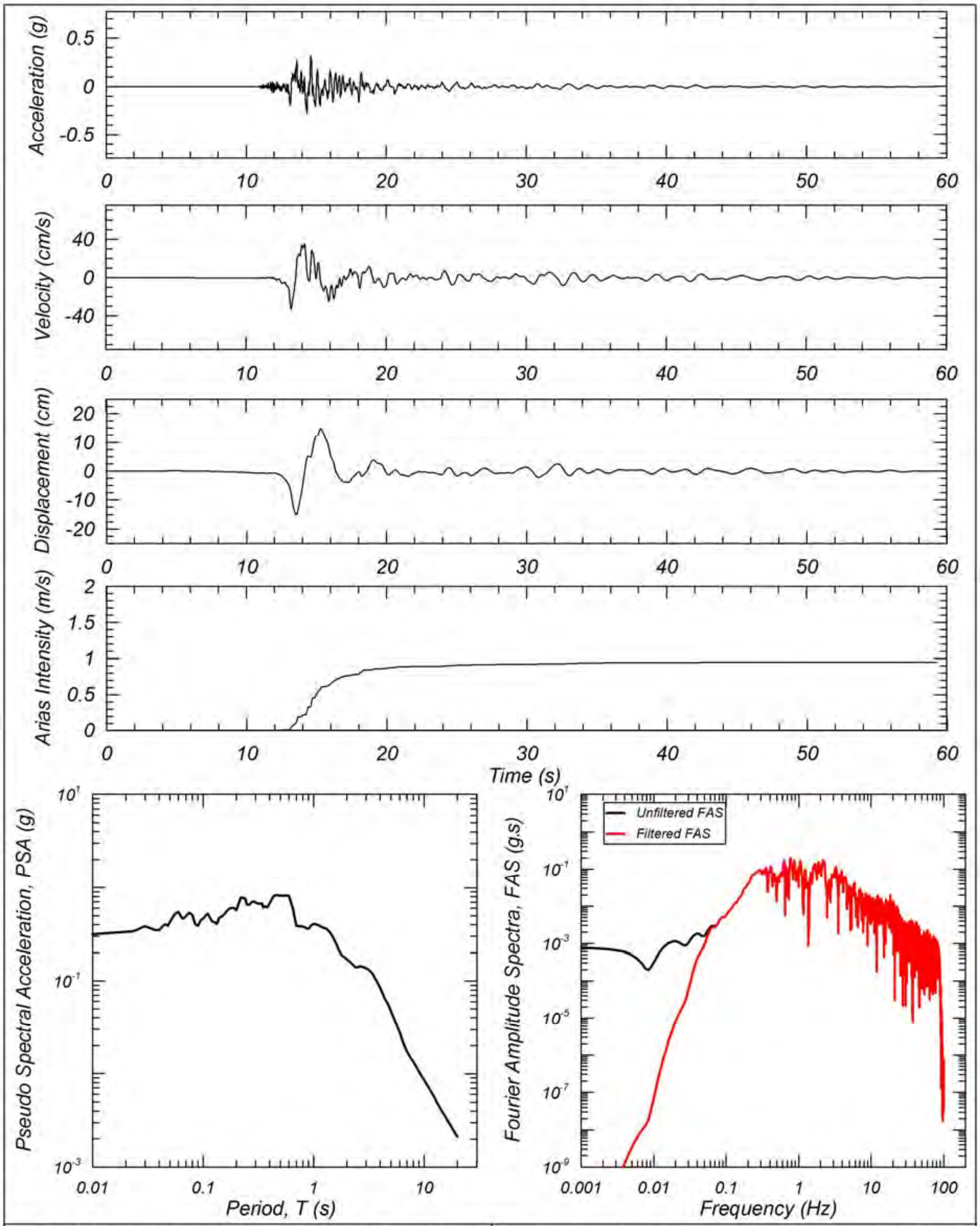

PEER Strong Motion Database Records	Station: Main St, Napa, CA, Component: 090
08/23/2014 South Napa Earthquake	Inferred V_{s30} = 285 m/s, R_{rup} = 3.9 km

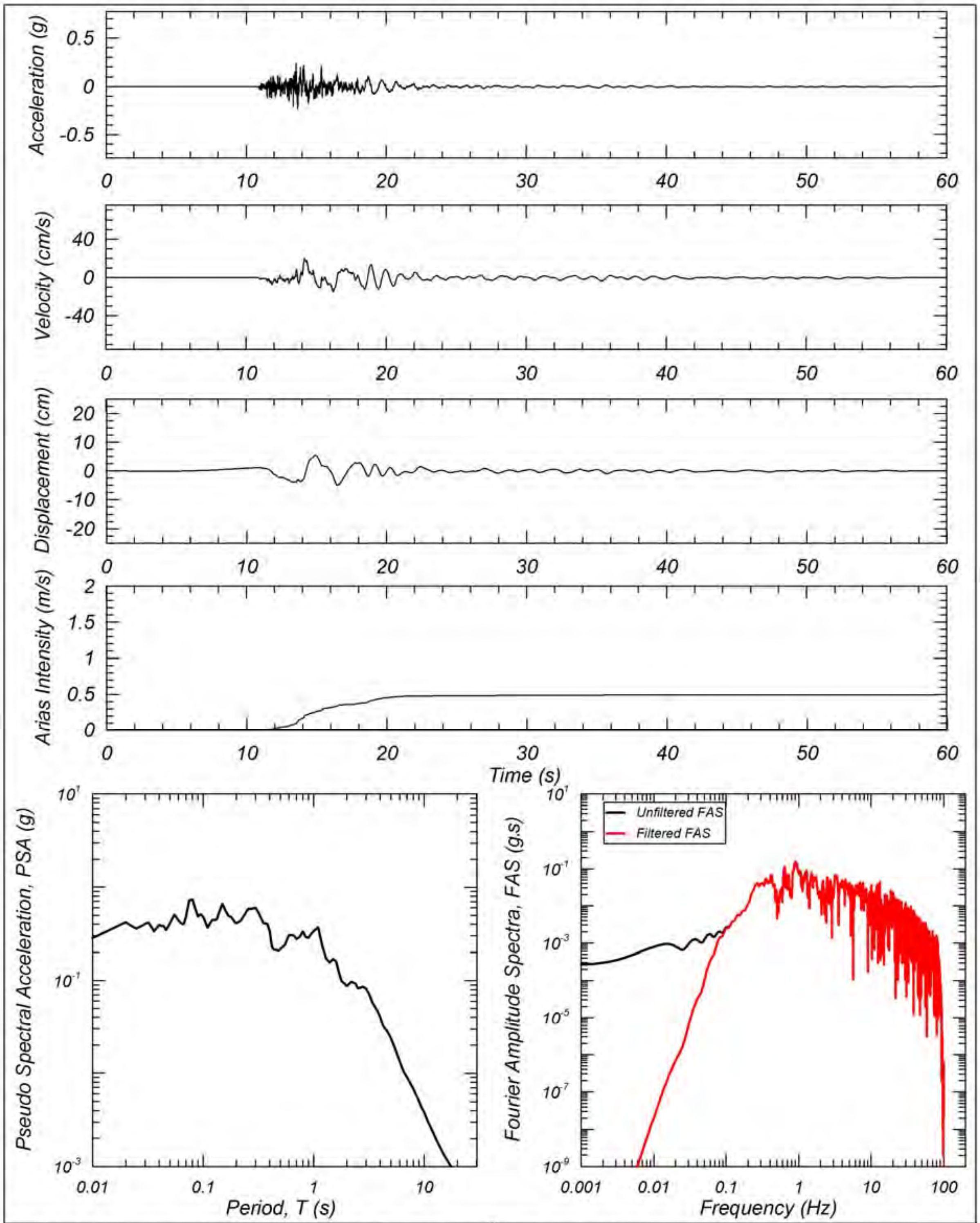

PEER Strong Motion Database Records	Station: Main St, Napa, CA, Component: UP
08/23/2014 South Napa Earthquake	Inferred V_{s30} = 285 m/s, R_{rup} = 3.9 km

APPENDIX C

Comparison of Recorded Response Spectra and Cod-Based Design Spectra

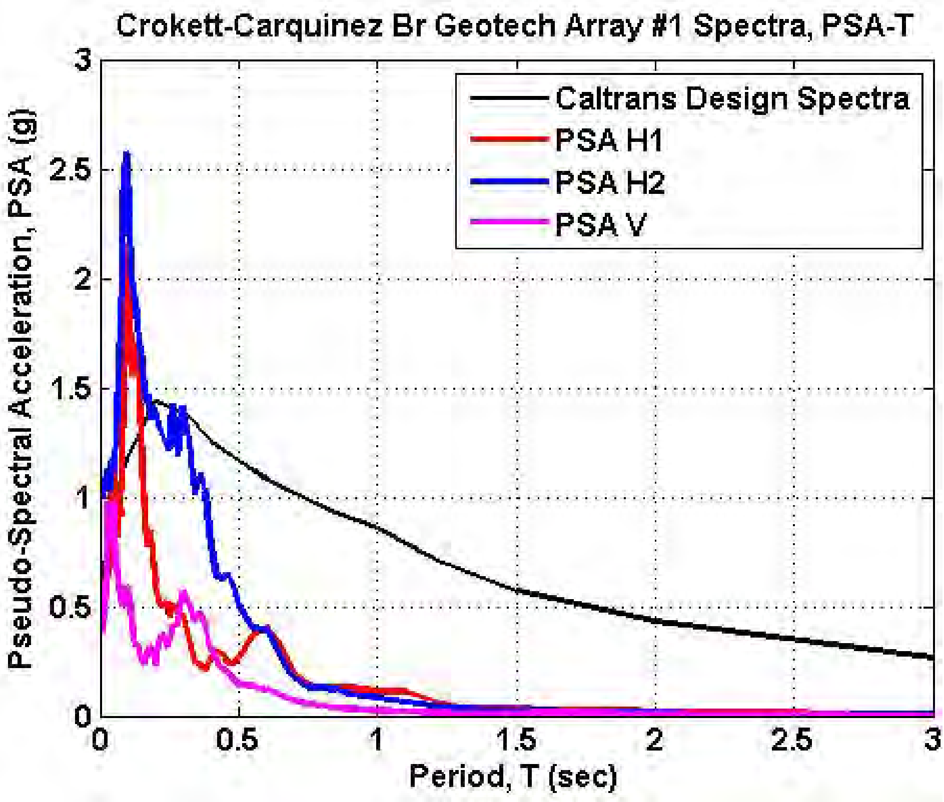
Crokett-Carquinez Br Geotech Array #1 Spectra, PSA-T
Caltrans Design Spectra
PSA H1
PSA H2
PSA V
Pseudo-Spectral Acceleration, PSA (g)
Period, T (sec)
0
0.5
1
1.5
2
2.5
3

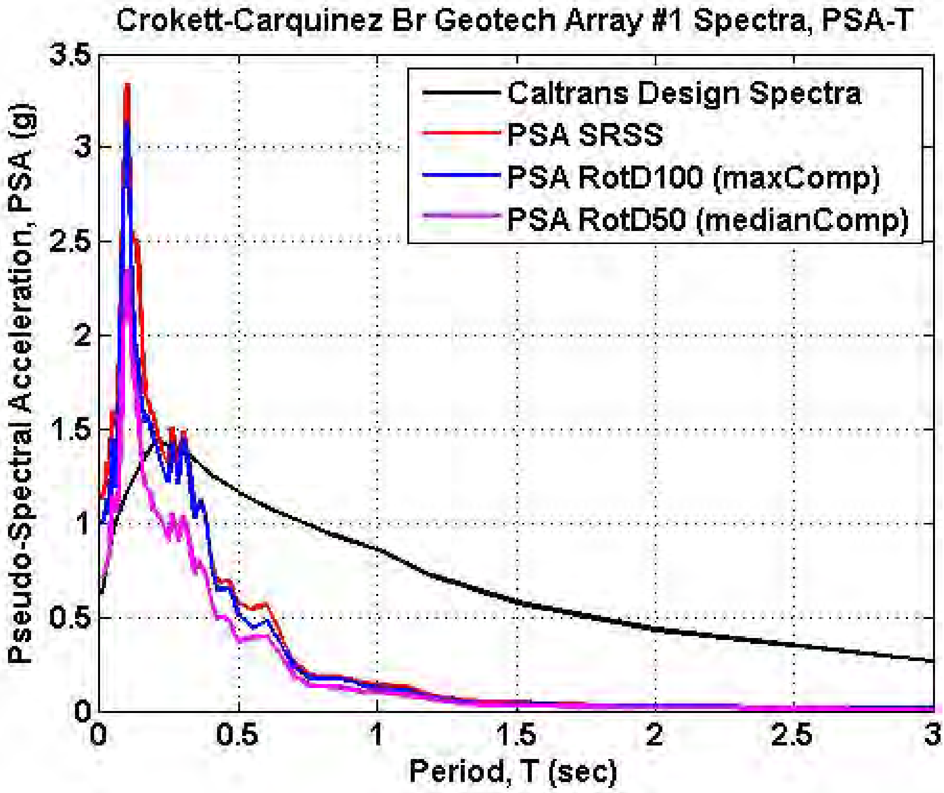
Crokett-Carquinez Br Geotech Array #1 Spectra, PSA-T
Caltrans Design Spectra
PSA SRSS
PSA RotD100 (maxComp)
PSA RotD50 (medianComp)
Pseudo-Spectral Acceleration, PSA (g)
Period, T (sec)
0
0.5
1
1.5
2
2.5
3
3.5

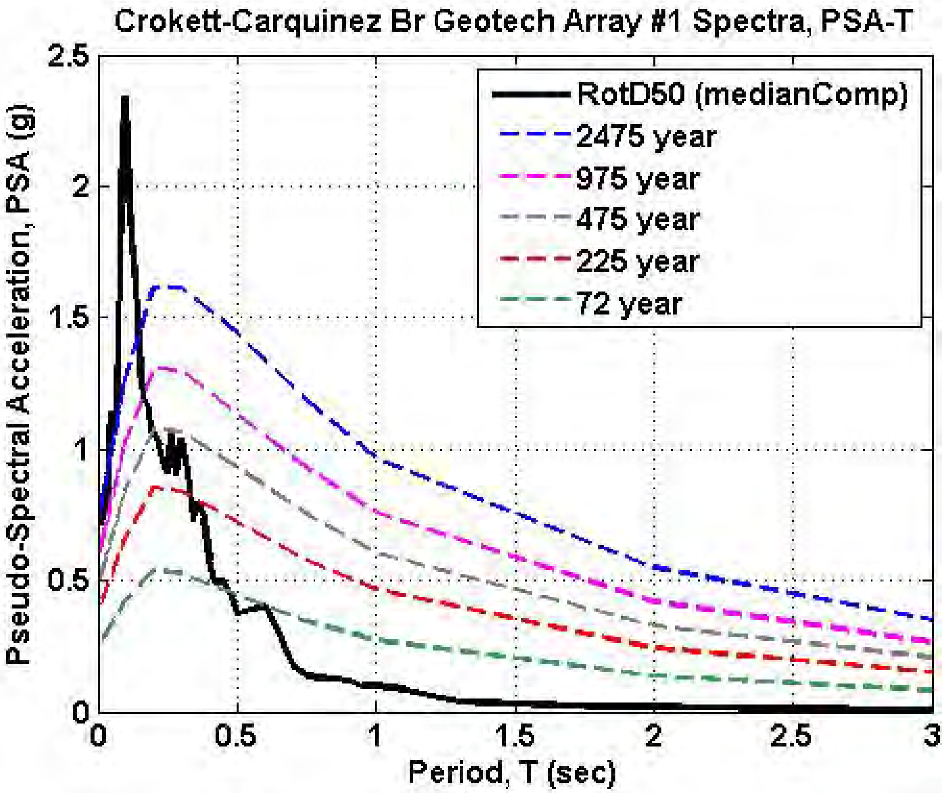
Crokett-Carquinez Br Geotech Array #1 Spectra, PSA-T
Pseudo-Spectral Acceleration, PSA (g)
Period, T (sec)
RotD50 (medianComp)
2475 year
975 year
475 year
225 year
72 year
0
0.5
1
1.5
2
2.5
0
0.5
1
1.5
2
2.5
3

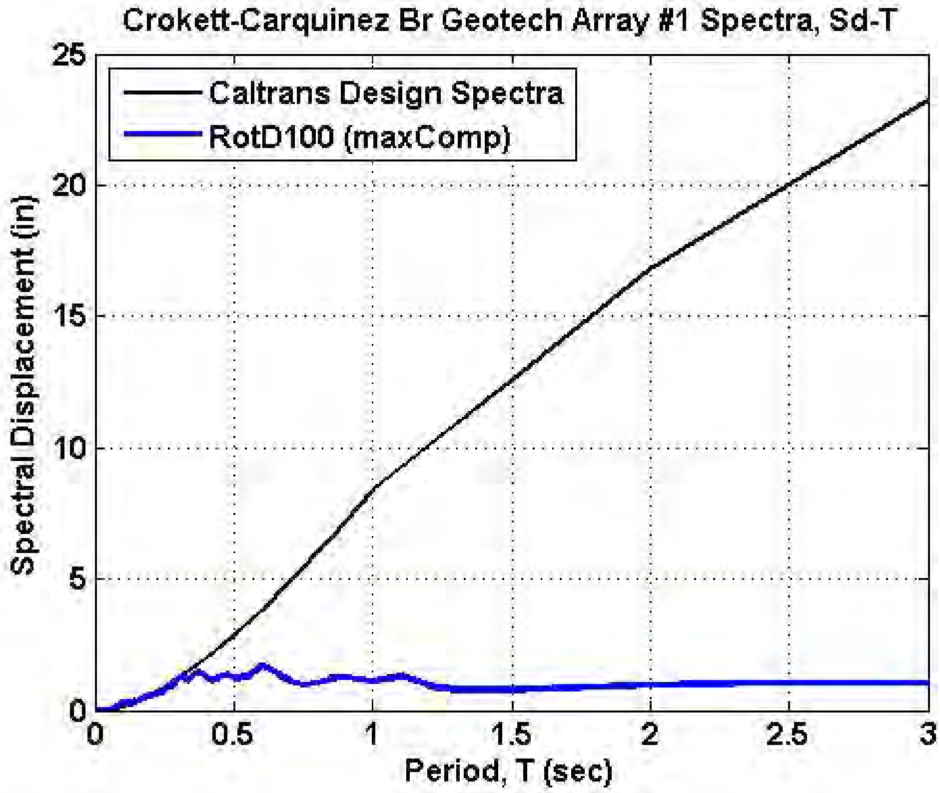
Crokett-Carquinez Br Geotech Array #1 Spectra, Sd-T
Spectral Displacement (in)
Period, T (sec)
Caltrans Design Spectra
RotD100 (maxComp)
0
5
10
15
20
25
0
0.5
1
1.5
2
2.5
3

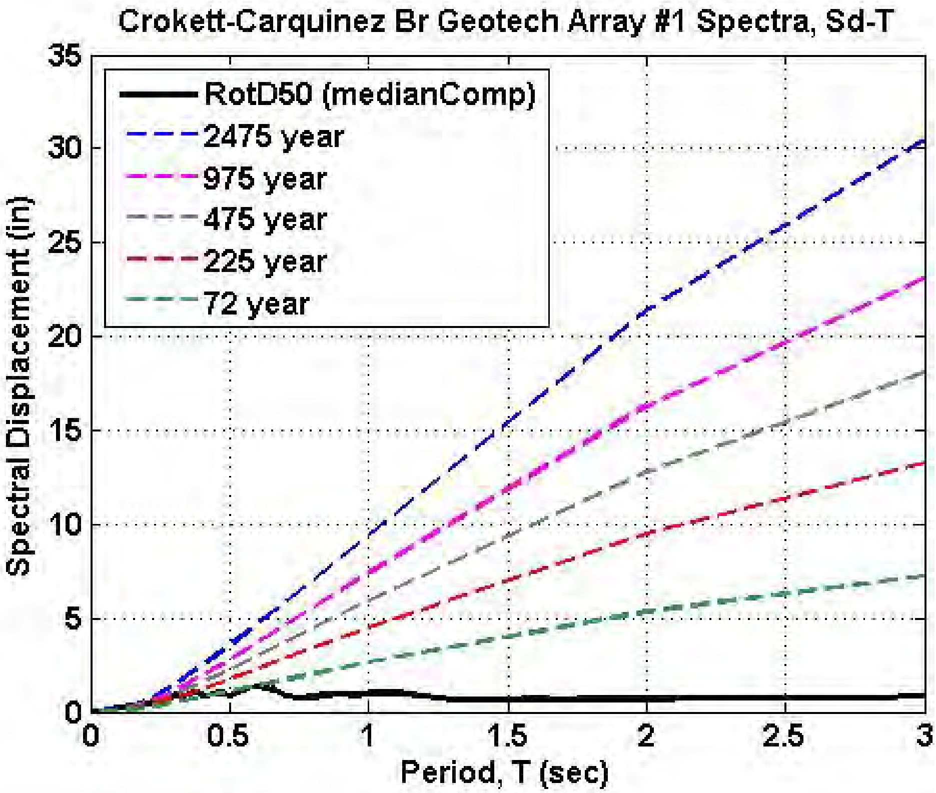
Crokett-Carquinez Br Geotech Array #1 Spectra, Sd-T
RotD50 (medianComp)
2475 year
975 year
475 year
225 year
72 year
Spectral Displacement (in)
Period, T (sec)
0
5
10
15
20
25
30
35
0
0.5
1
1.5
2
2.5
3

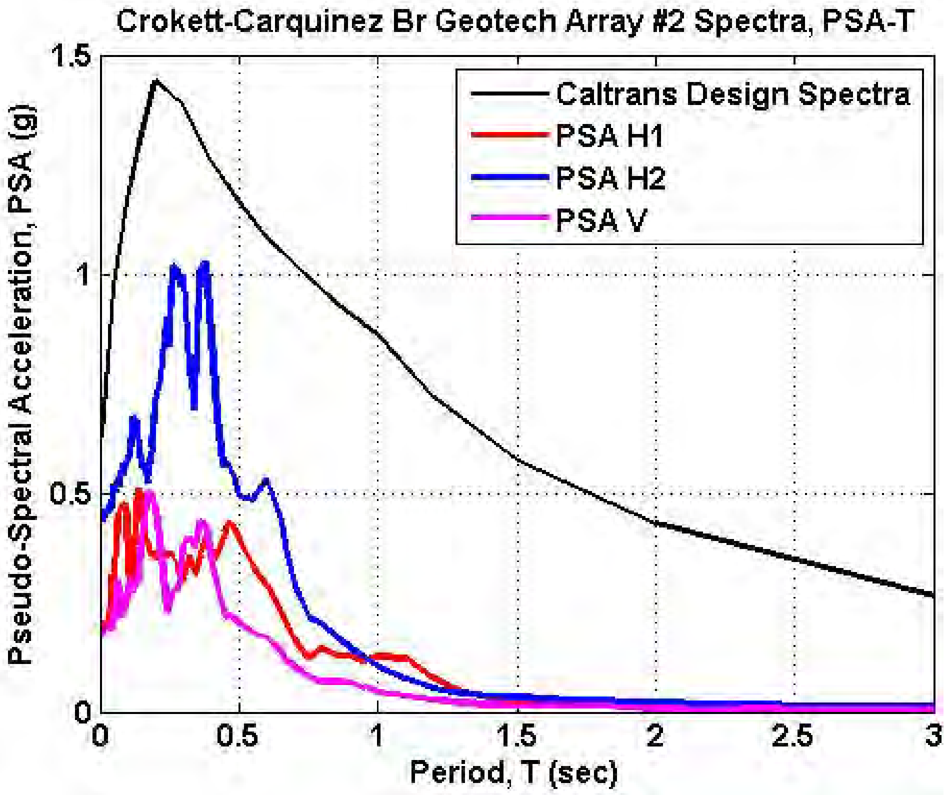
Crokett-Carquinez Br Geotech Array #2 Spectra, PSA-T

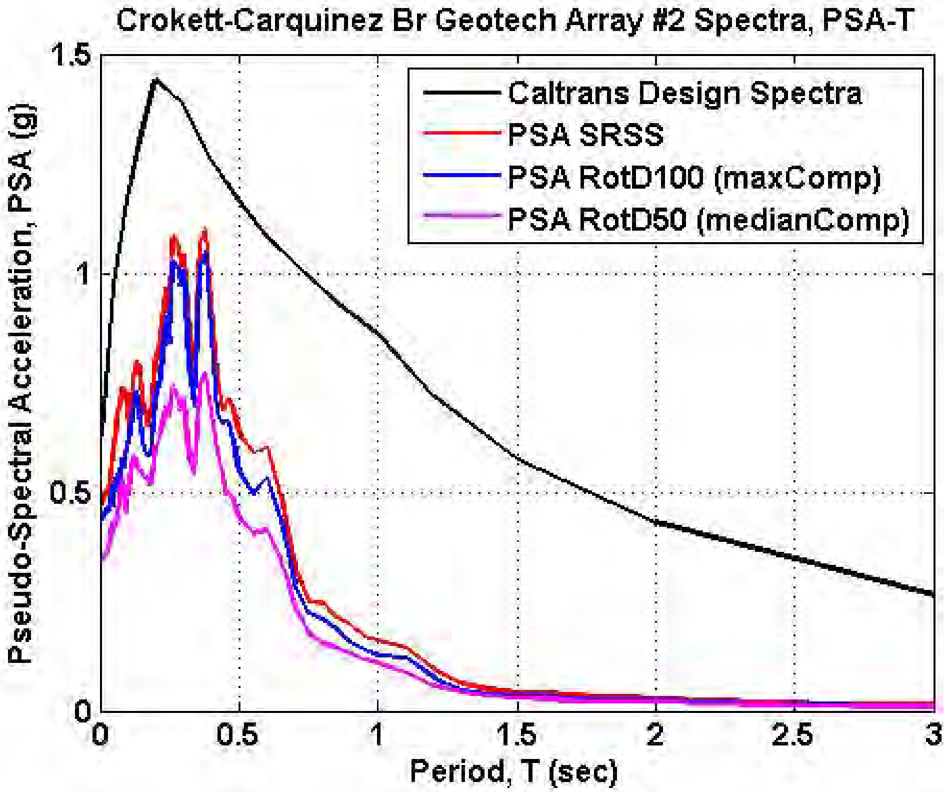
Crokett-Carquinez Br Geotech Array #2 Spectra, PSA-T

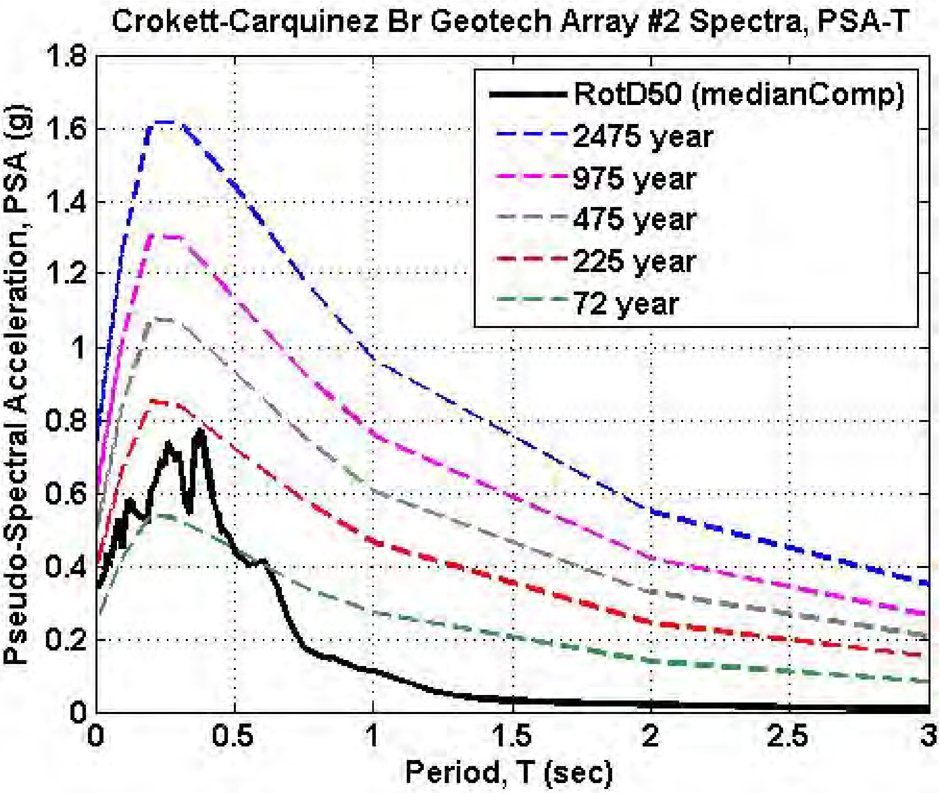
Crokett-Carquinez Br Geotech Array #2 Spectra, PSA-T

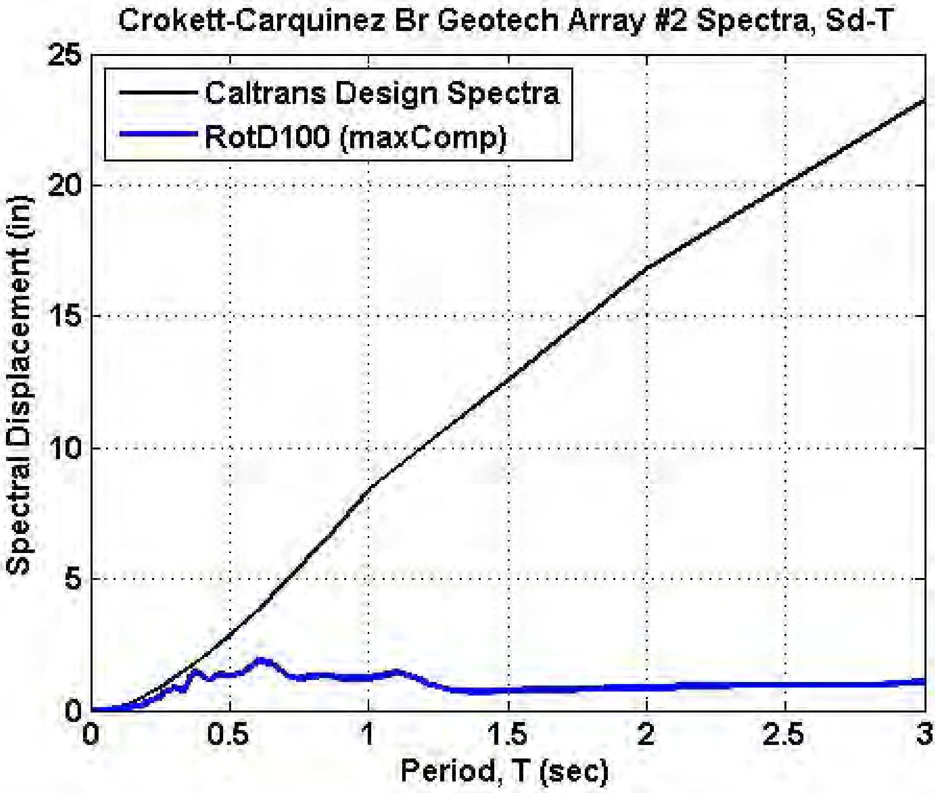
Crokett-Carquinez Br Geotech Array #2 Spectra, Sd-T

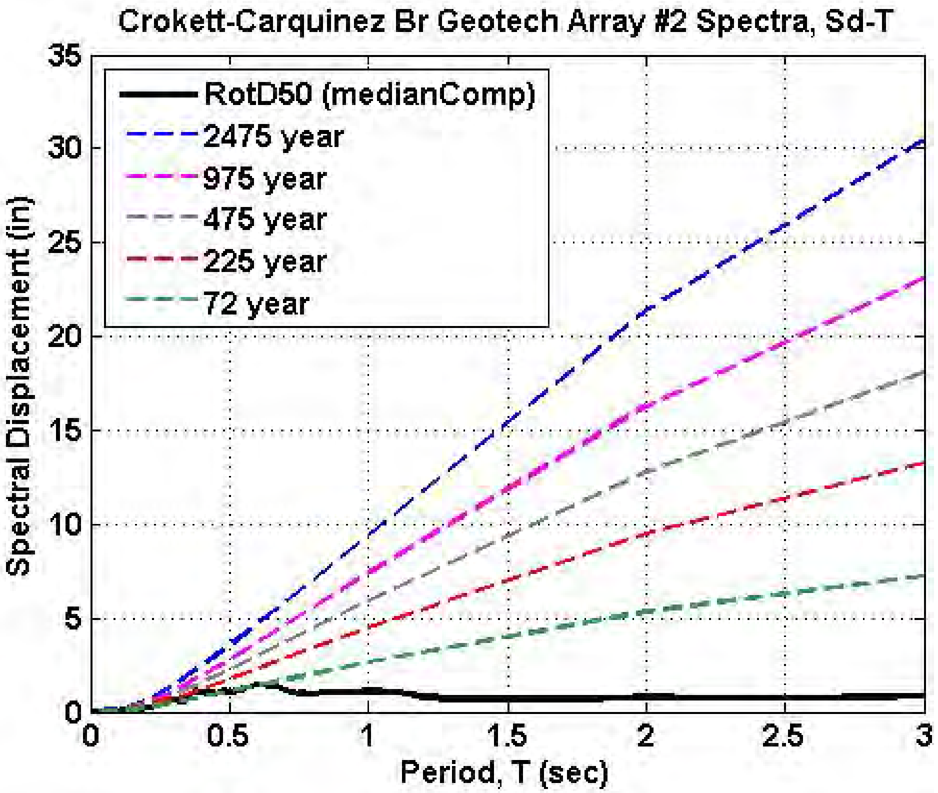
Crokett-Carquinez Br Geotech Array #2 Spectra, Sd-T
RotD50 (medianComp)
2475 year
975 year
475 year
225 year
72 year
Spectral Displacement (in)
Period, T (sec)
0
5
10
15
20
25
30
35
0
0.5
1
1.5
2
2.5
3

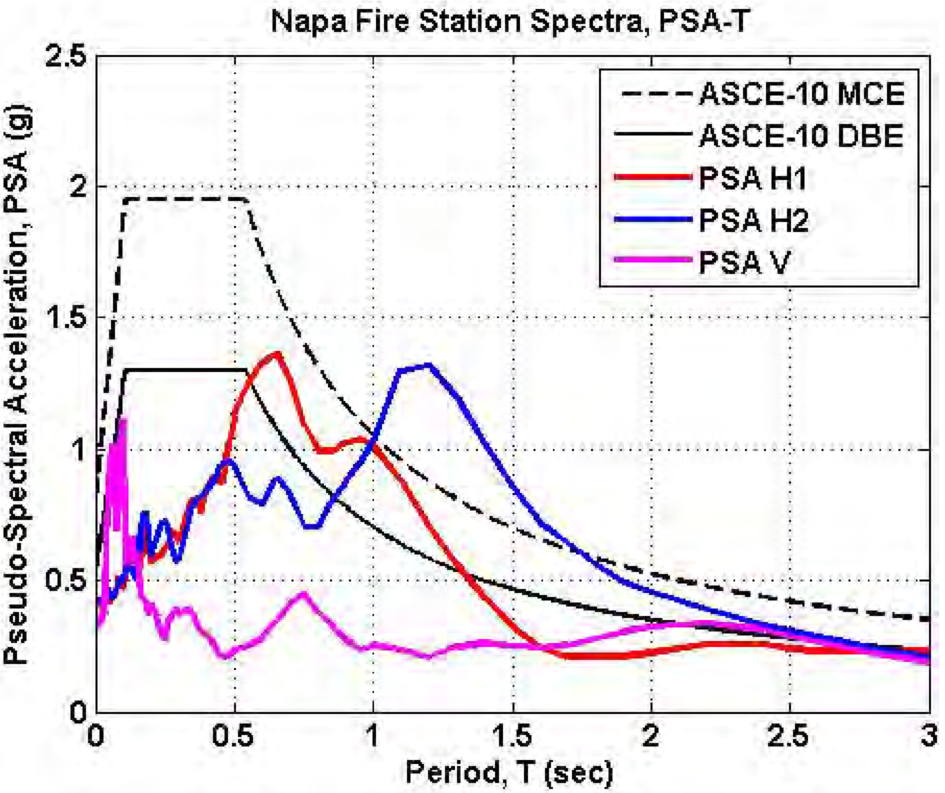
Napa Fire Station Spectra, PSA-T

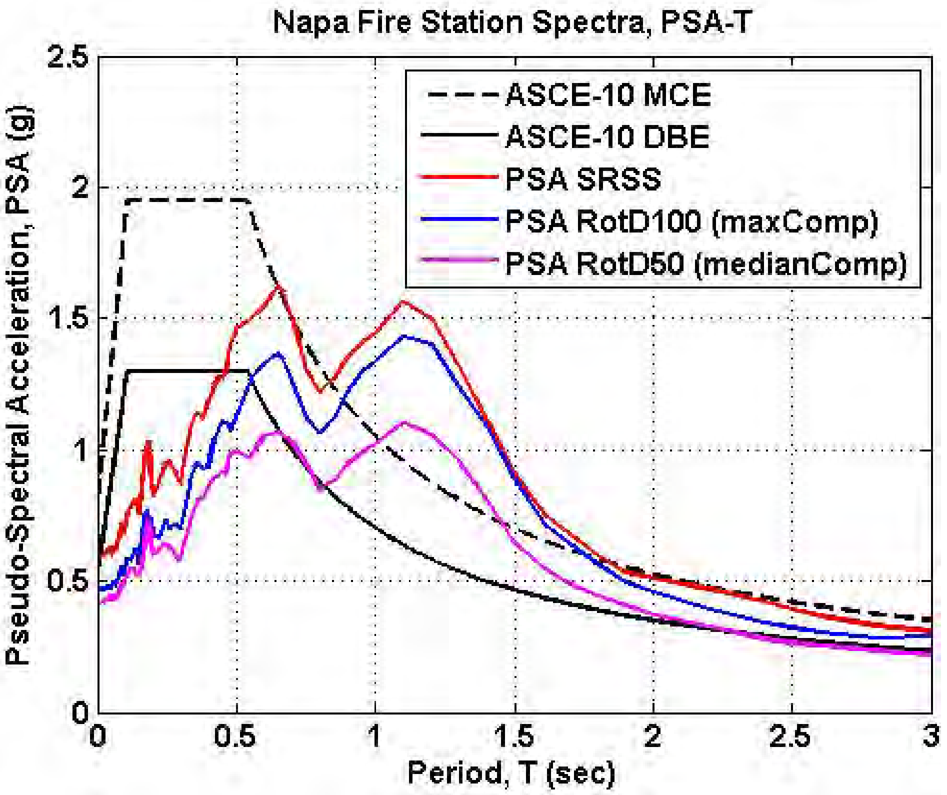
Napa Fire Station Spectra, PSA-T

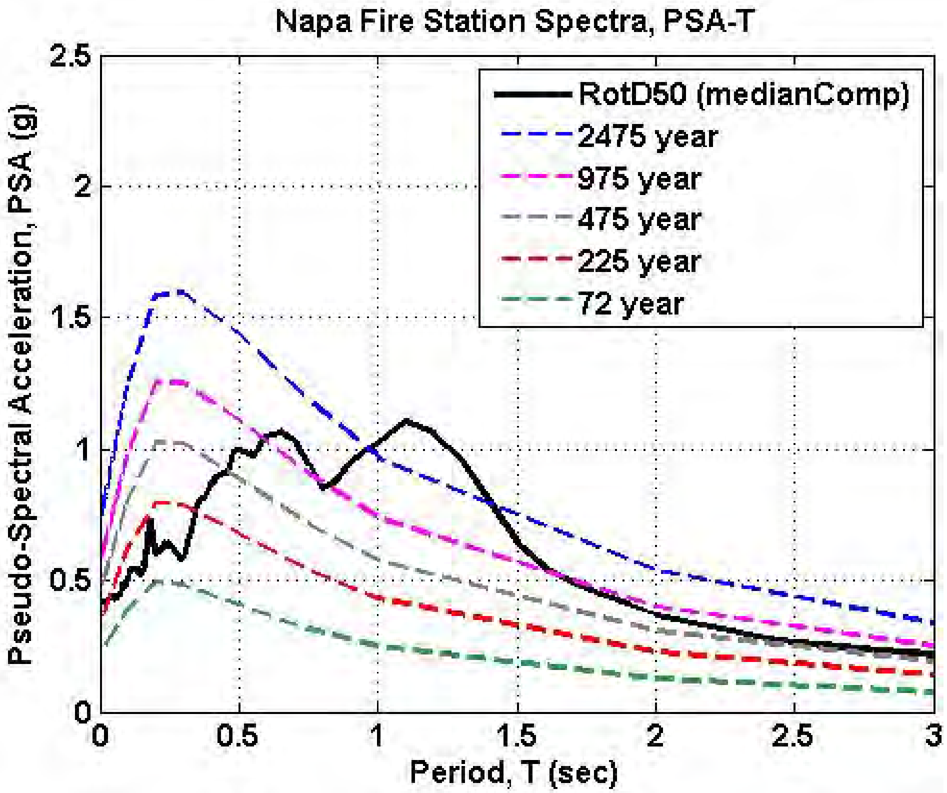

Napa Fire Station Spectra, PSA-T

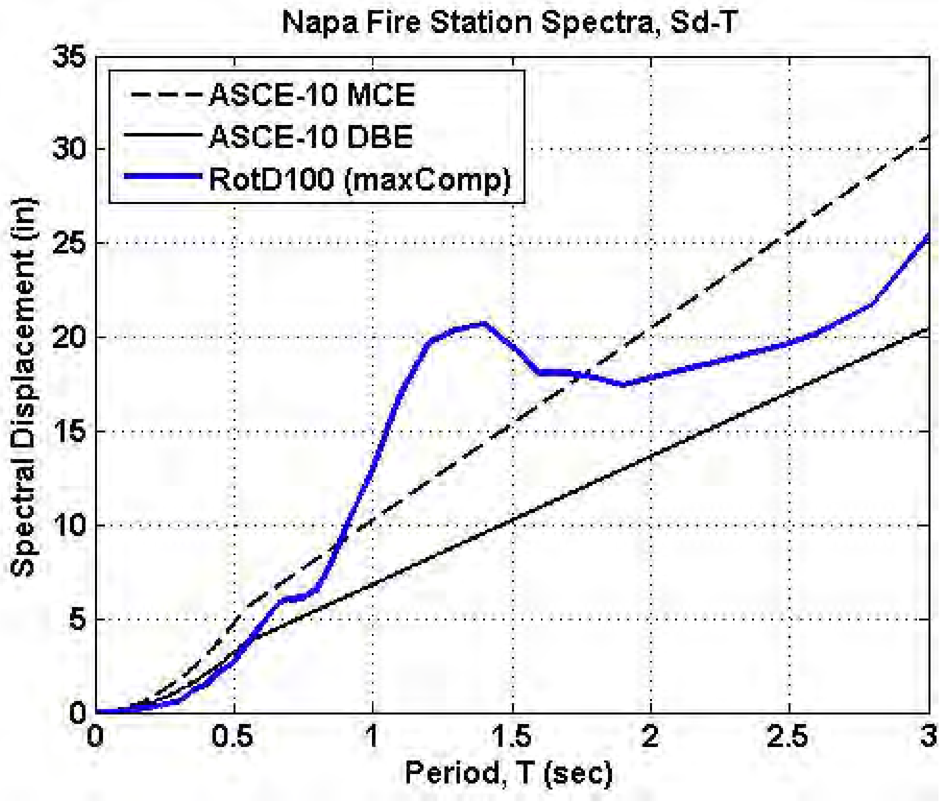

Napa Fire Station Spectra, Sd-T

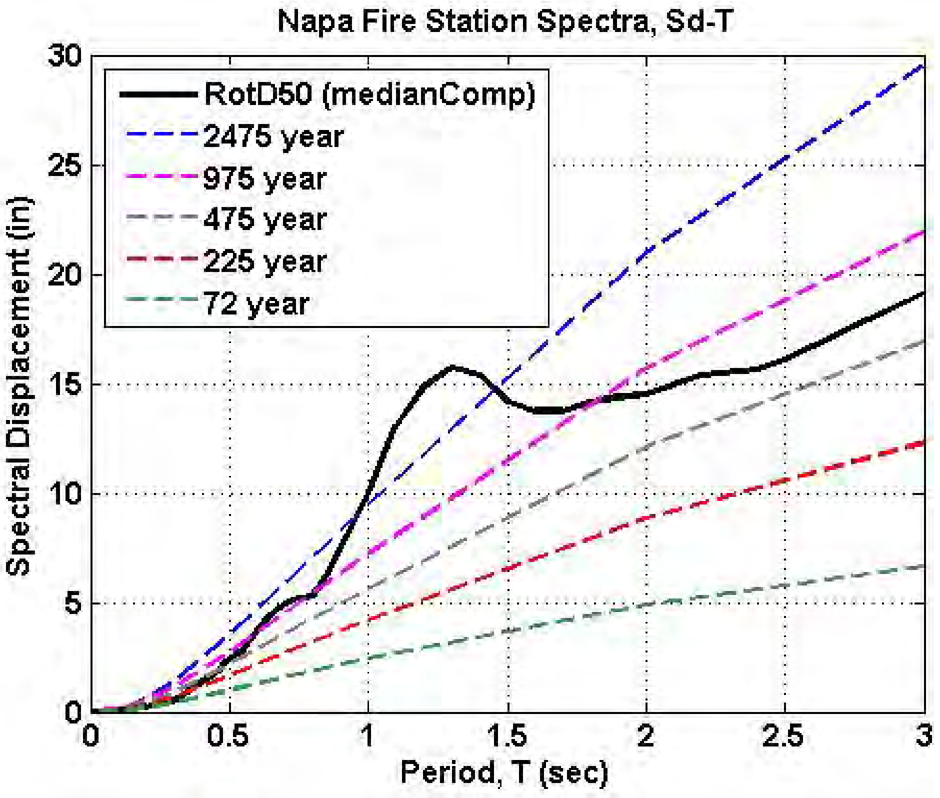
Napa Fire Station Spectra, Sd-T
Spectral Displacement (in)
Period, T (sec)
RotD50 (medianComp)
2475 year
975 year
475 year
225 year
72 year
0
5
10
15
20
25
30
0
0.5
1
1.5
2
2.5
3

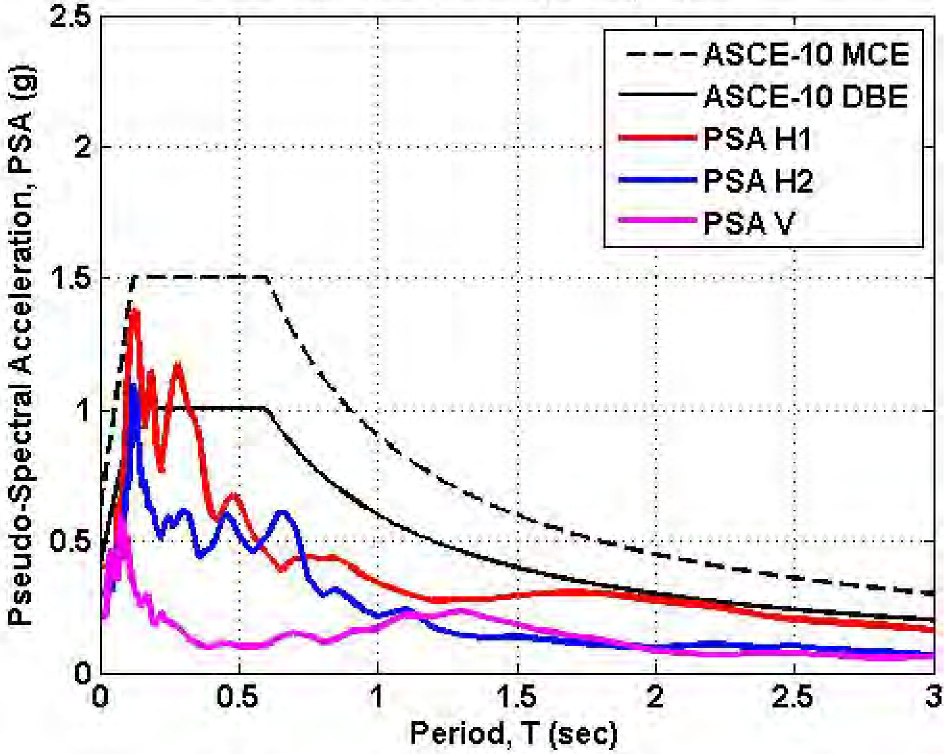

Huichica Creek Spectra, PSA-T

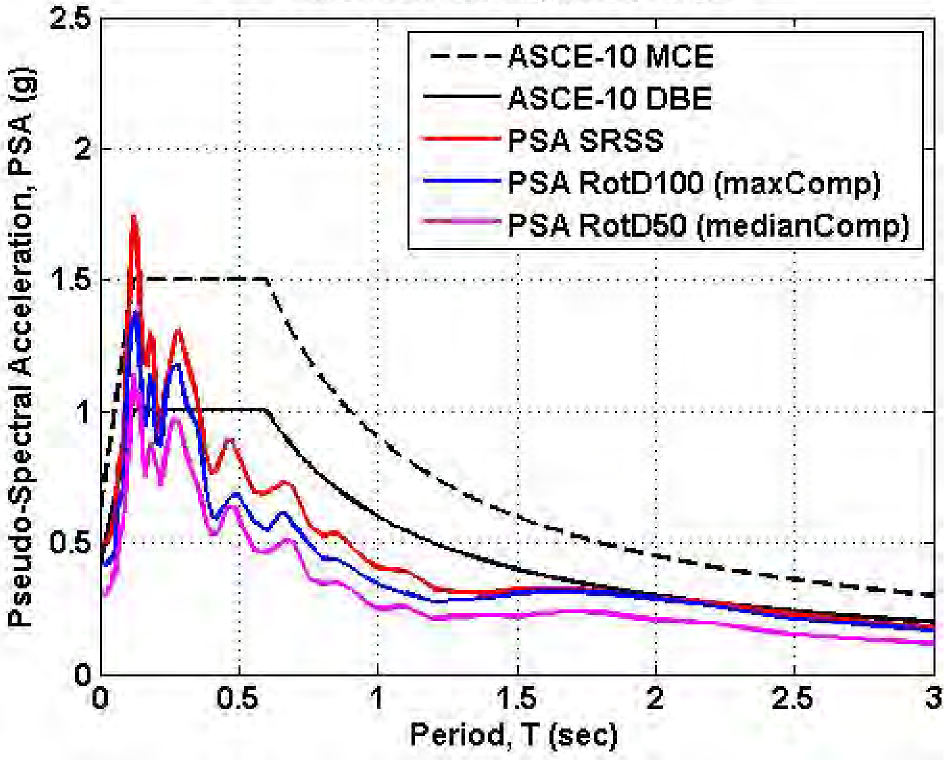

Huichica Creek Spectra, PSA-T

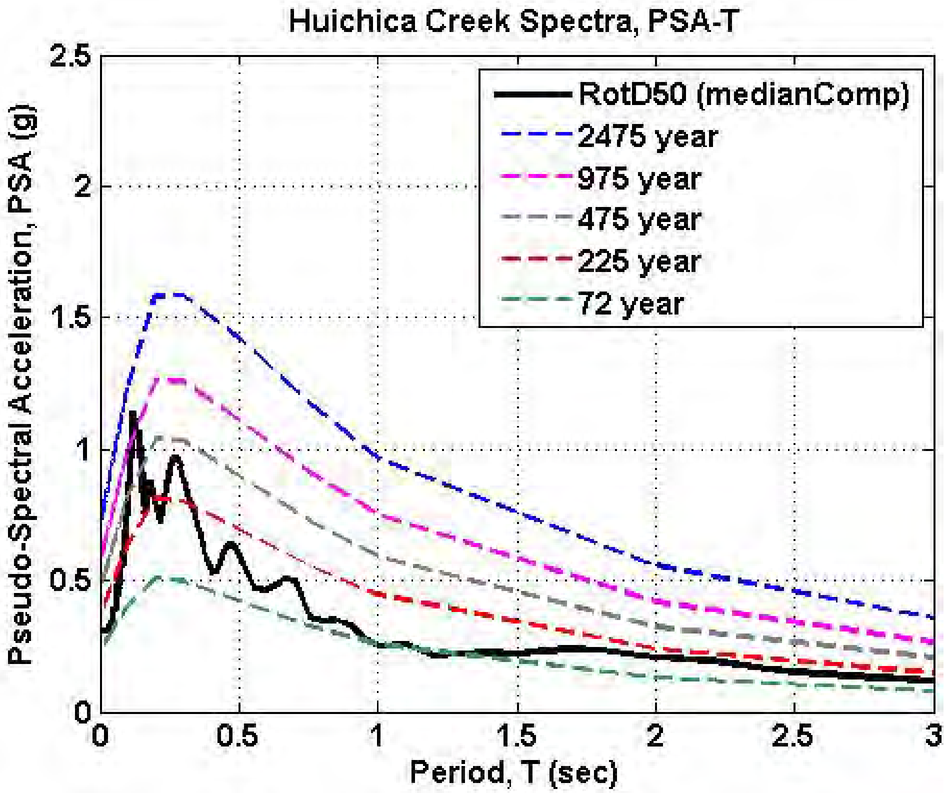
Huichica Creek Spectra, PSA-T
Pseudo-Spectral Acceleration, PSA (g)
Period, T (sec)
0
0.5
1
1.5
2
2.5
3
RotD50 (medianComp)
2475 year
975 year
475 year
225 year
72 year

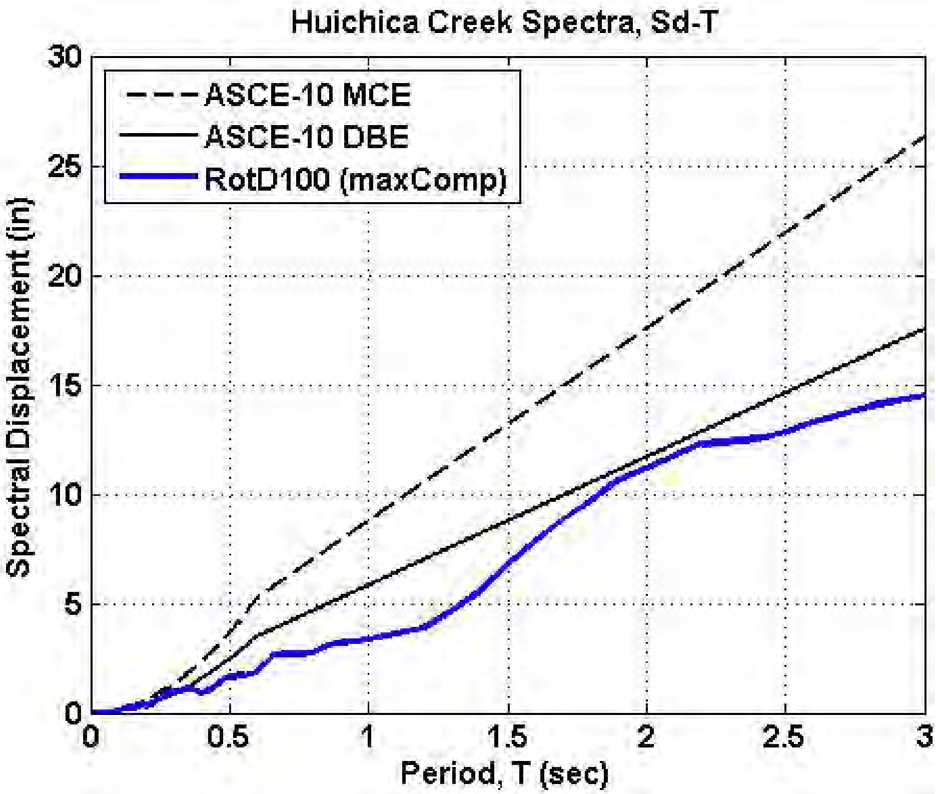
Huichica Creek Spectra, Sd-T
Spectral Displacement (in)
Period, T (sec)
0
5
10
15
20
25
30
0.5
1
1.5
2
2.5
3
ASCE-10 MCE
ASCE-10 DBE
RotD100 (maxComp)

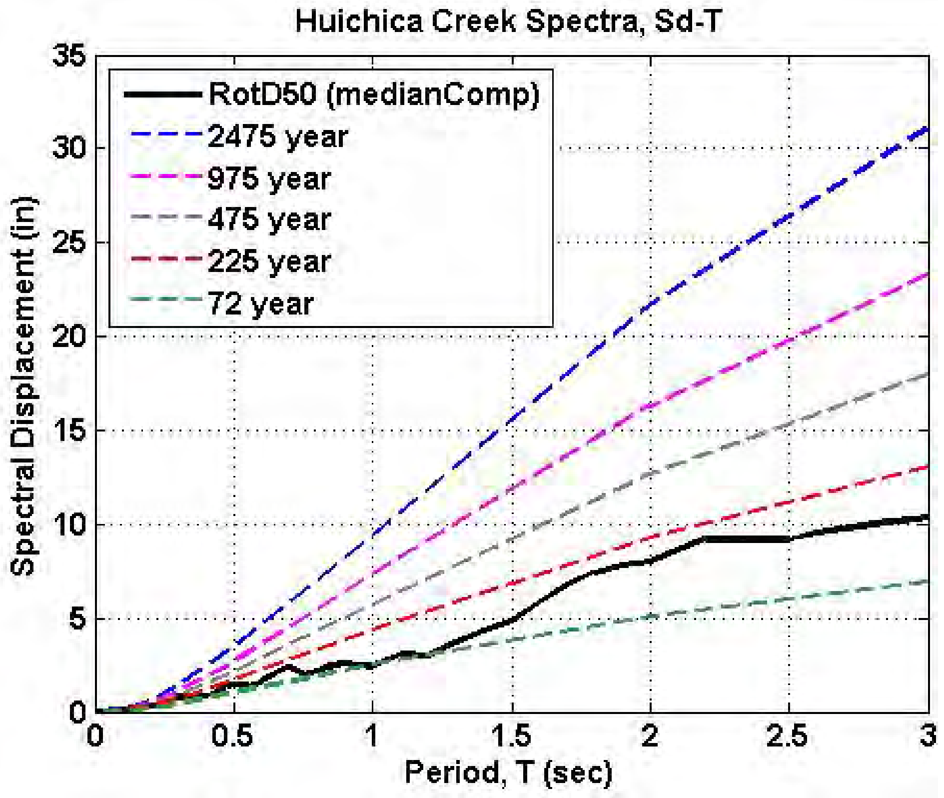

Huichica Creek Spectra, Sd-T
RotD50 (medianComp)
2475 year
975 year
475 year
225 year
72 year
Spectral Displacement (in)
Period, T (sec)
0
5
10
15
20
25
30
35
0
0.5
1
1.5
2
2.5
3

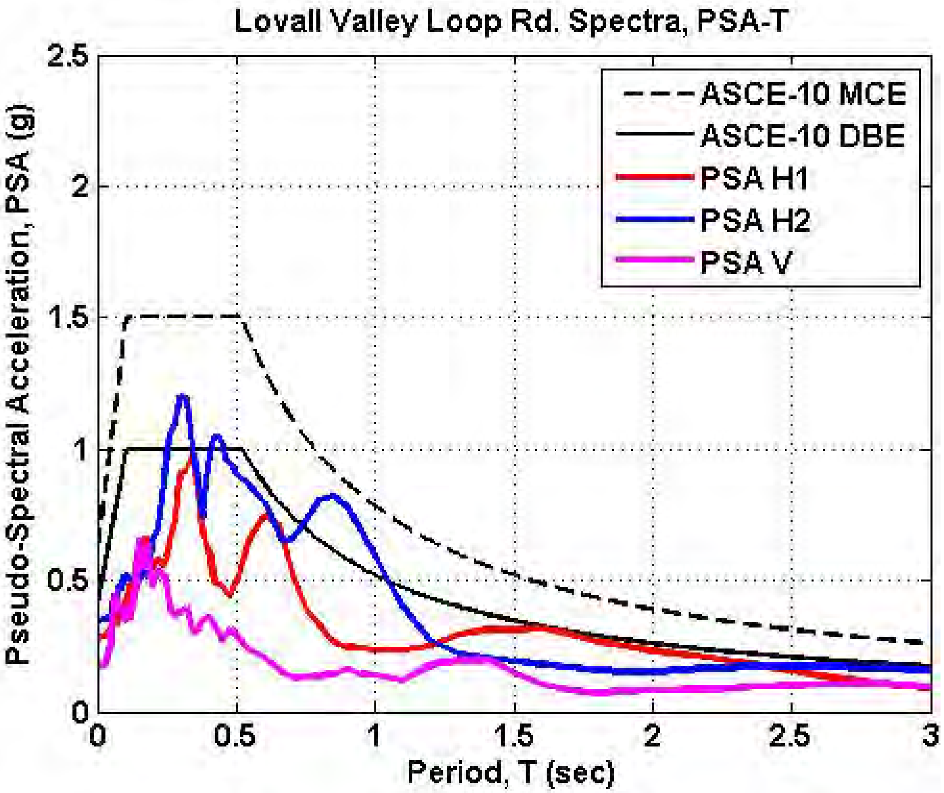
Lovall Valley Loop Rd. Spectra, PSA-T

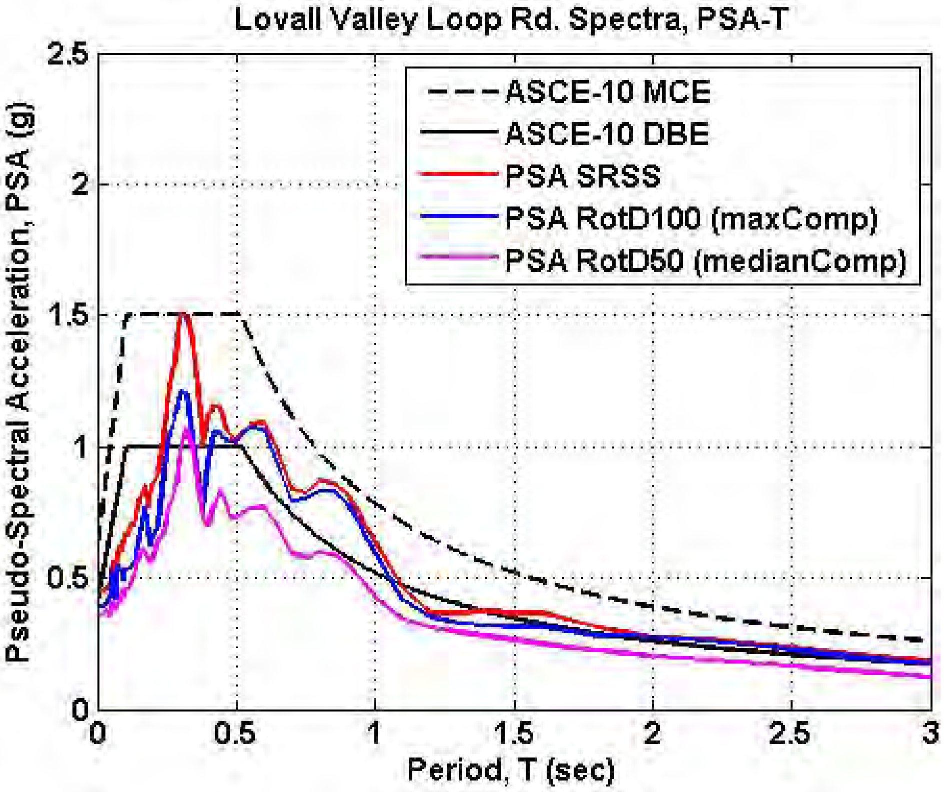
Lovall Valley Loop Rd. Spectra, PSA-T

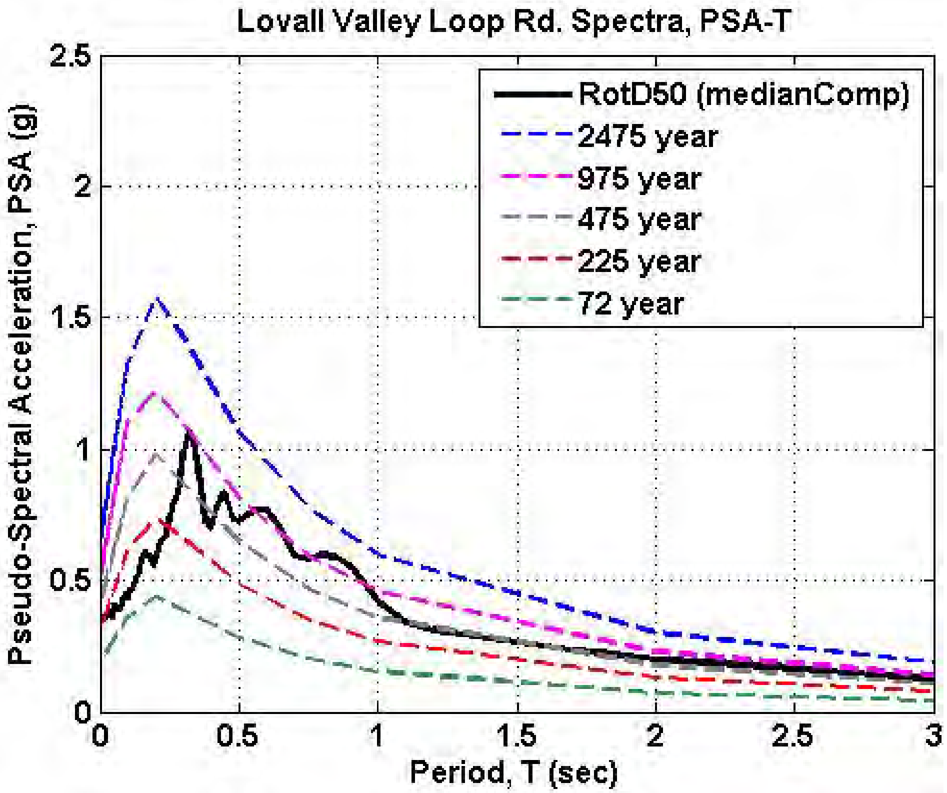
Lovall Valley Loop Rd. Spectra, PSA-T
Pseudo-Spectral Acceleration, PSA (g)
Period, T (sec)
0
0.5
1
1.5
2
2.5
3
RotD50 (medianComp)
2475 year
975 year
475 year
225 year
72 year

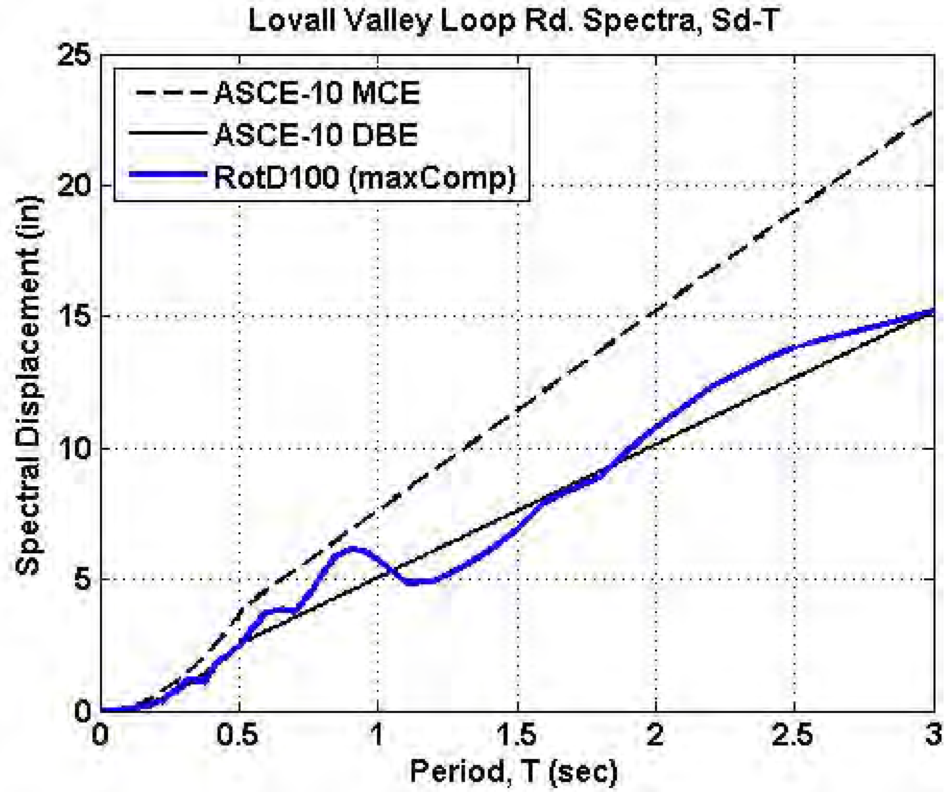
Lovall Valley Loop Rd. Spectra, Sd-T
Spectral Displacement (in)
Period, T (sec)
0
5
10
15
20
25
0.5
1
1.5
2
2.5
3
ASCE-10 MCE
ASCE-10 DBE
RotD100 (maxComp)

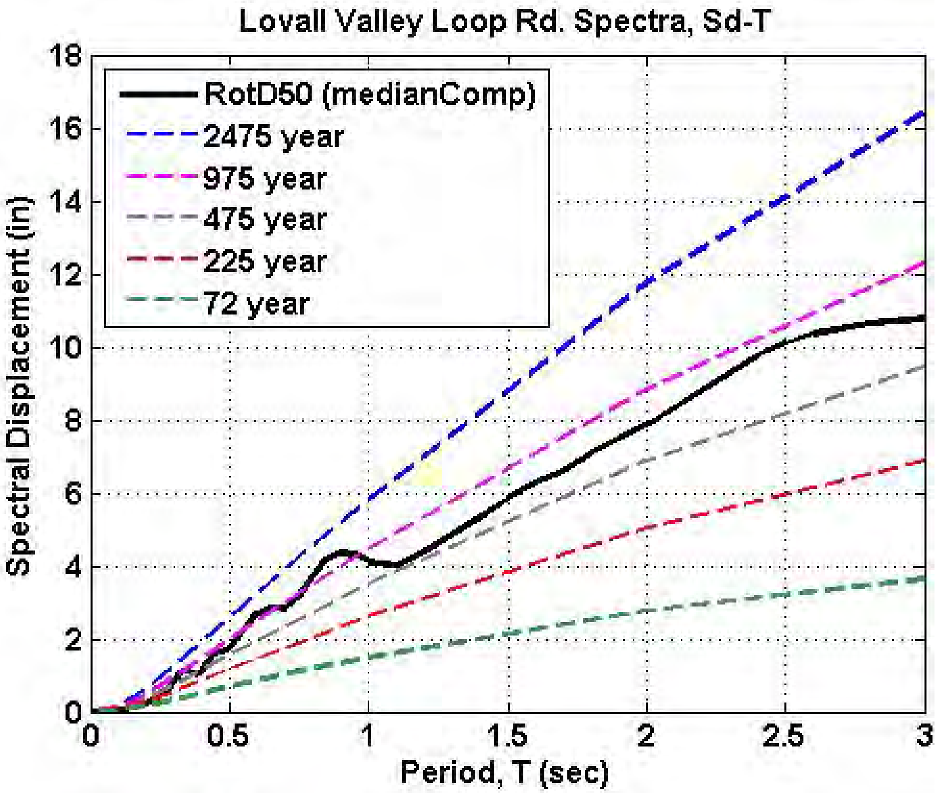
Lovall Valley Loop Rd. Spectra, Sd-T
RotD50 (medianComp)
2475 year
975 year
475 year
225 year
72 year
Spectral Displacement (in)
0
2
4
6
8
10
12
14
16
18
Period, T (sec)
0
0.5
1
1.5
2
2.5
3

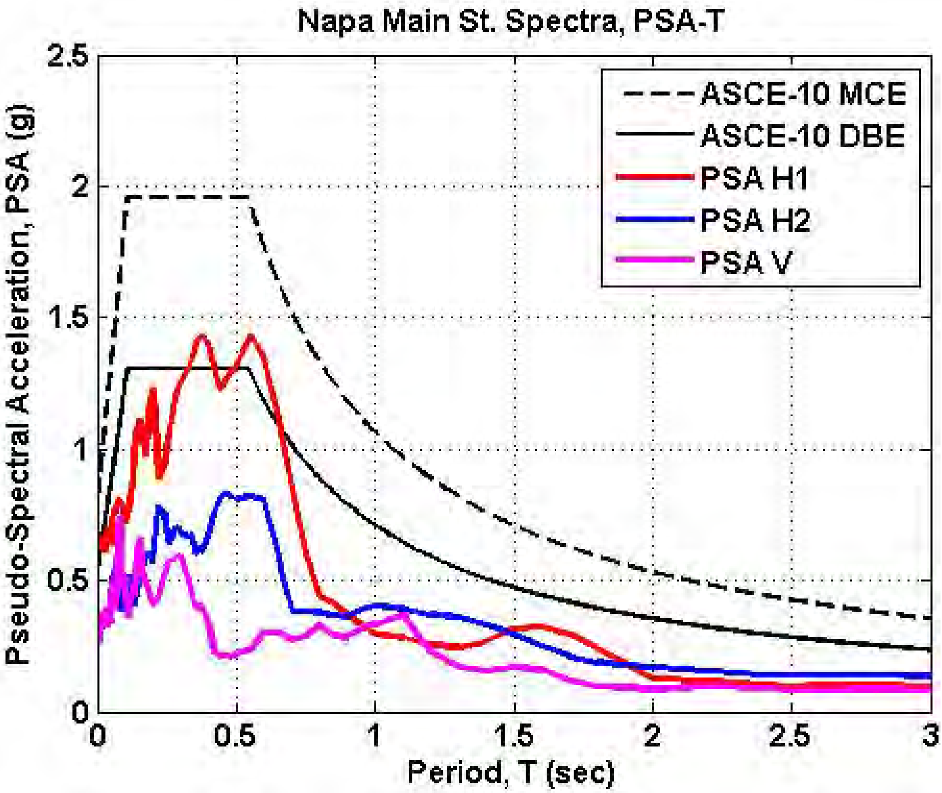
Napa Main St. Spectra, PSA-T
Pseudo-Spectral Acceleration, PSA (g)
Period, T (sec)
0
0.5
1
1.5
2
2.5
3
ASCE-10 MCE
ASCE-10 DBE
PSA H1
PSA H2
PSA V

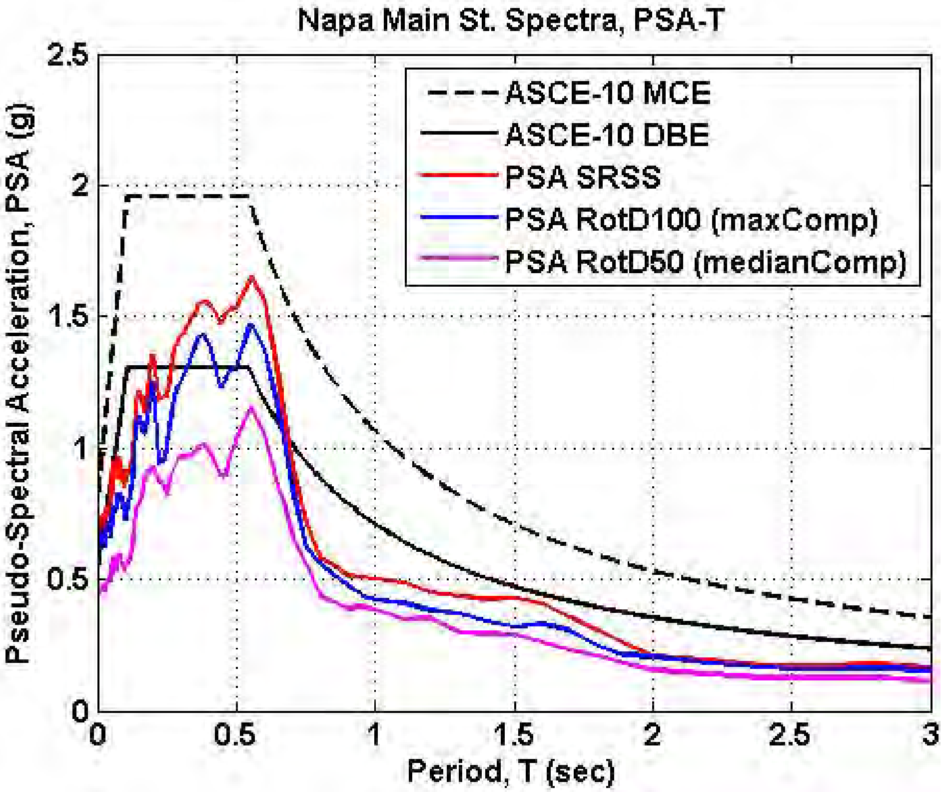
Napa Main St. Spectra, PSA-T
Pseudo-Spectral Acceleration, PSA (g)
Period, T (sec)
0
0.5
1
1.5
2
2.5
3
ASCE-10 MCE
ASCE-10 DBE
PSA SRSS
PSA RotD100 (maxComp)
PSA RotD50 (medianComp)

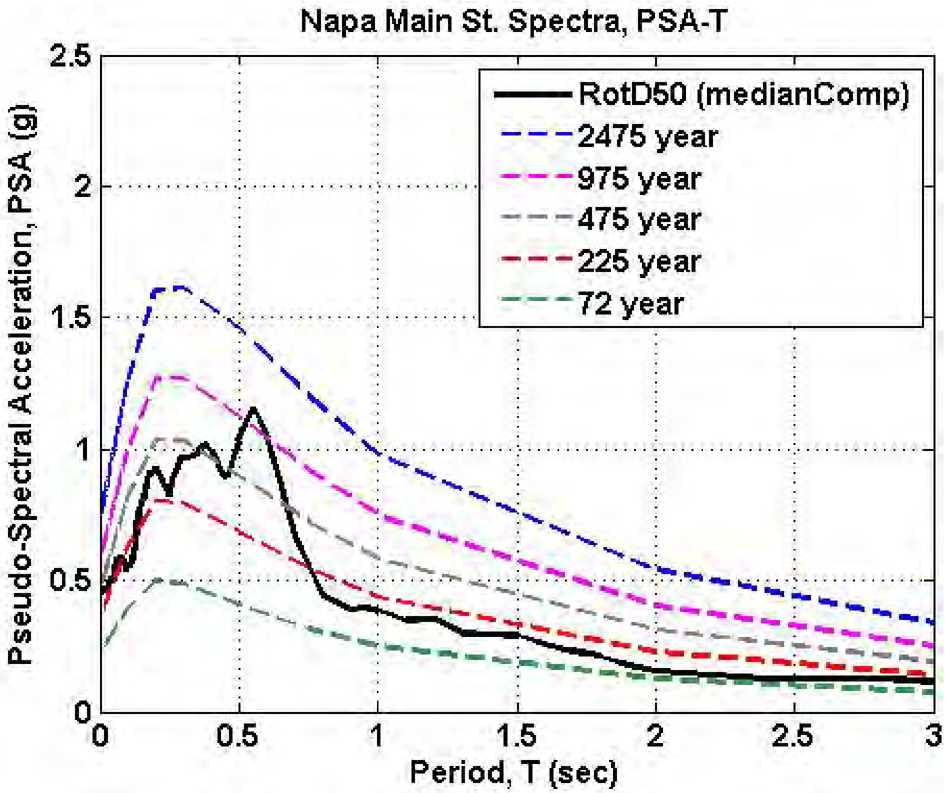
Napa Main St. Spectra, PSA-T
Pseudo-Spectral Acceleration, PSA (g)
Period, T (sec)
RotD50 (medianComp)
2475 year
975 year
475 year
225 year
72 year
0
0.5
1
1.5
2
2.5
3

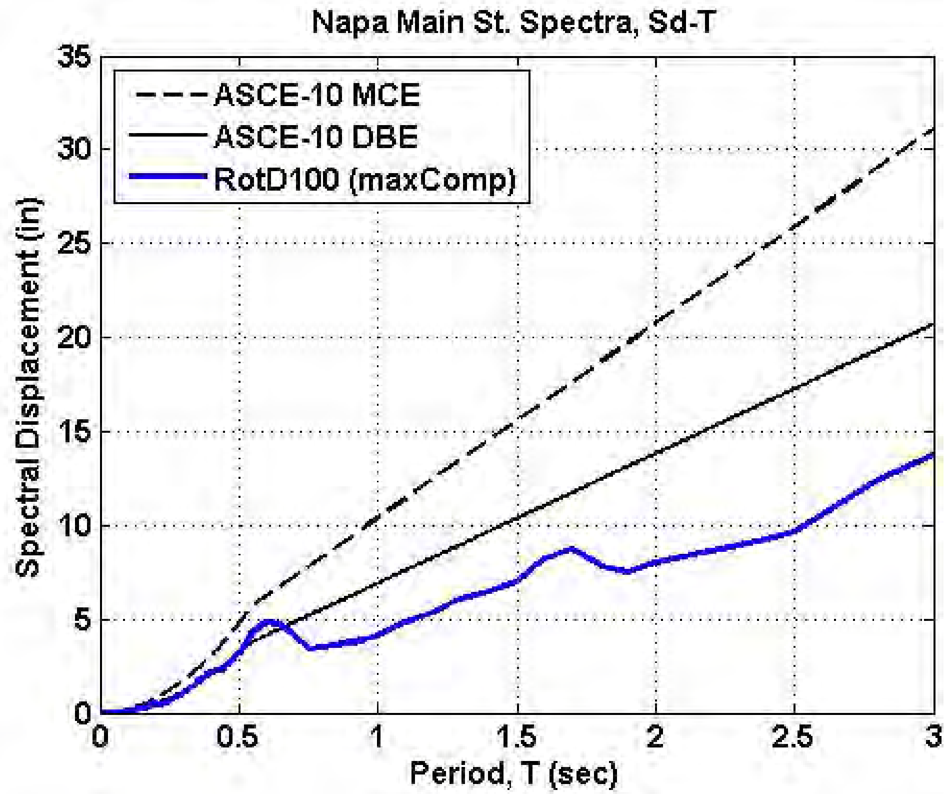
Napa Main St. Spectra, Sd-T
Spectral Displacement (in)
Period, T (sec)
ASCE-10 MCE
ASCE-10 DBE
RotD100 (maxComp)
0
5
10
15
20
25
30
35
0.5
1
1.5
2
2.5
3

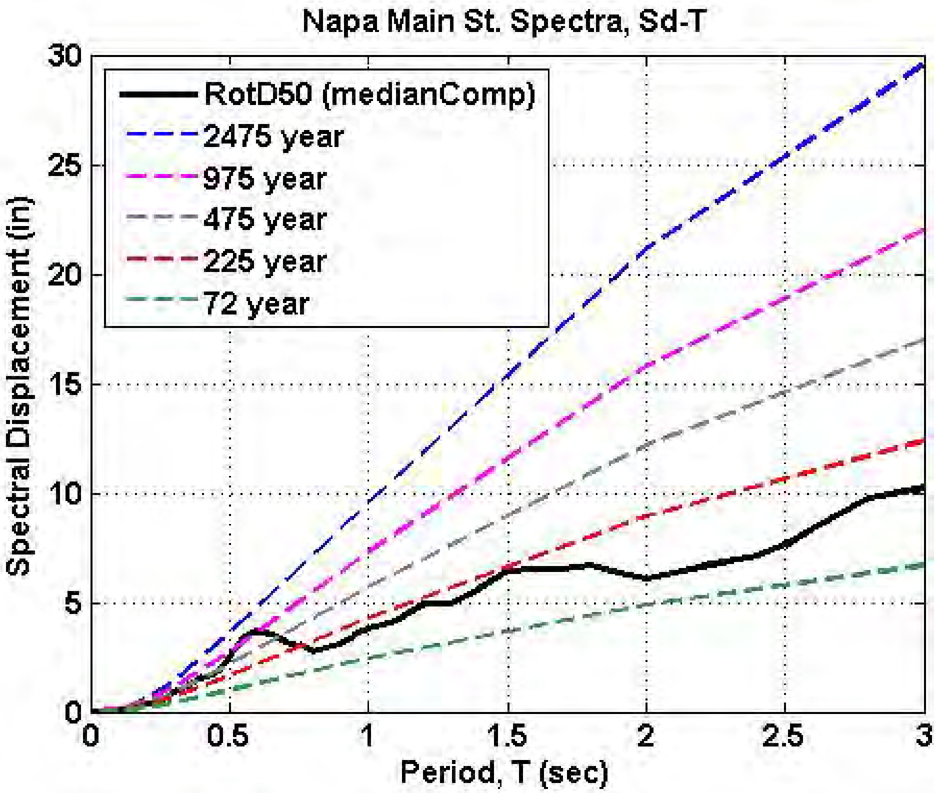
Napa Main St. Spectra, Sd-T
RotD50 (medianComp)
2475 year
975 year
475 year
225 year
72 year
Spectral Displacement (in)
Period, T (sec)
0
5
10
15
20
25
30
0
0.5
1
1.5
2
2.5
3

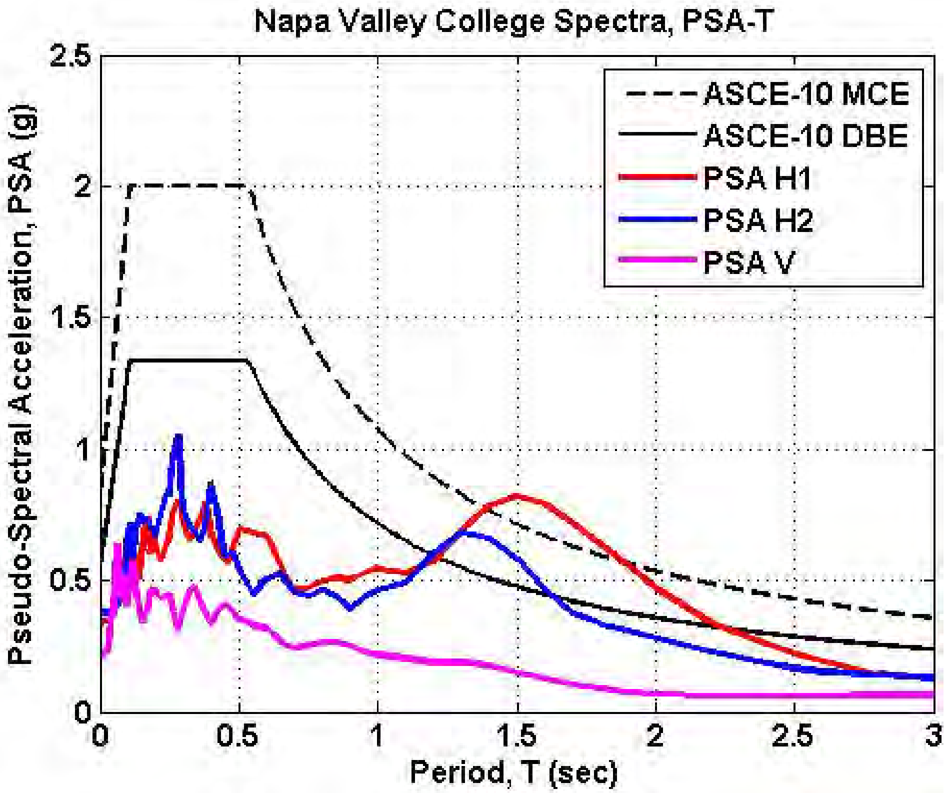
Napa Valley College Spectra, PSA-T
Pseudo-Spectral Acceleration, PSA (g)
Period, T (sec)
0
0.5
1
1.5
2
2.5
3
ASCE-10 MCE
ASCE-10 DBE
PSA H1
PSA H2
PSA V

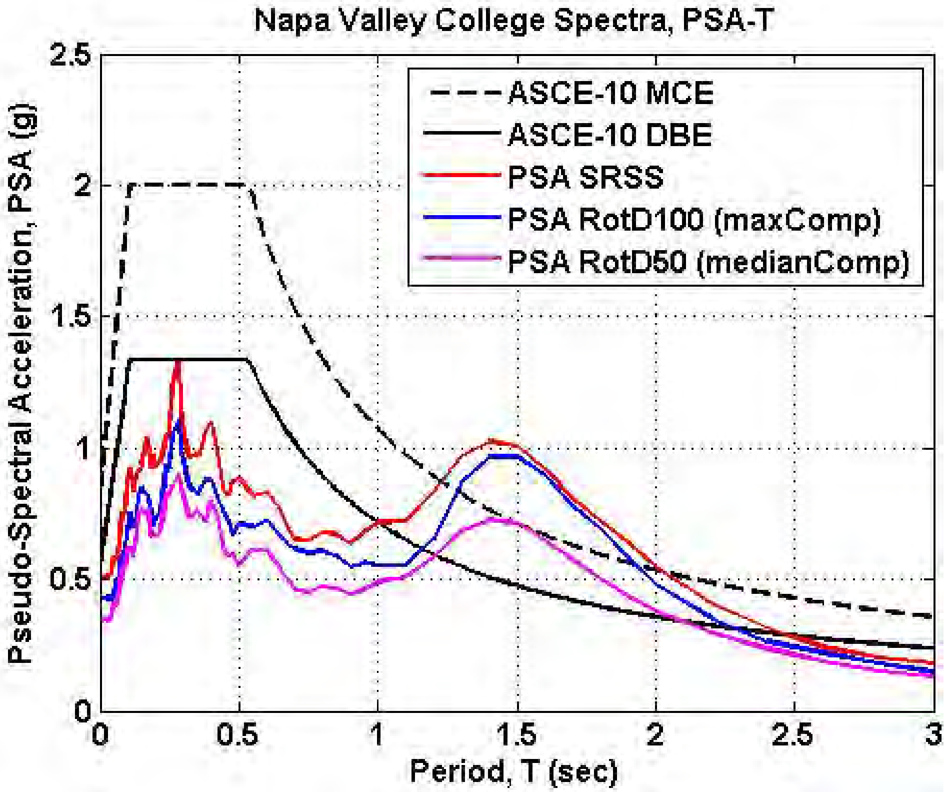
Napa Valley College Spectra, PSA-T
Pseudo-Spectral Acceleration, PSA (g)
Period, T (sec)
0
0.5
1
1.5
2
2.5
3
ASCE-10 MCE
ASCE-10 DBE
PSA SRSS
PSA RotD100 (maxComp)
PSA RotD50 (medianComp)

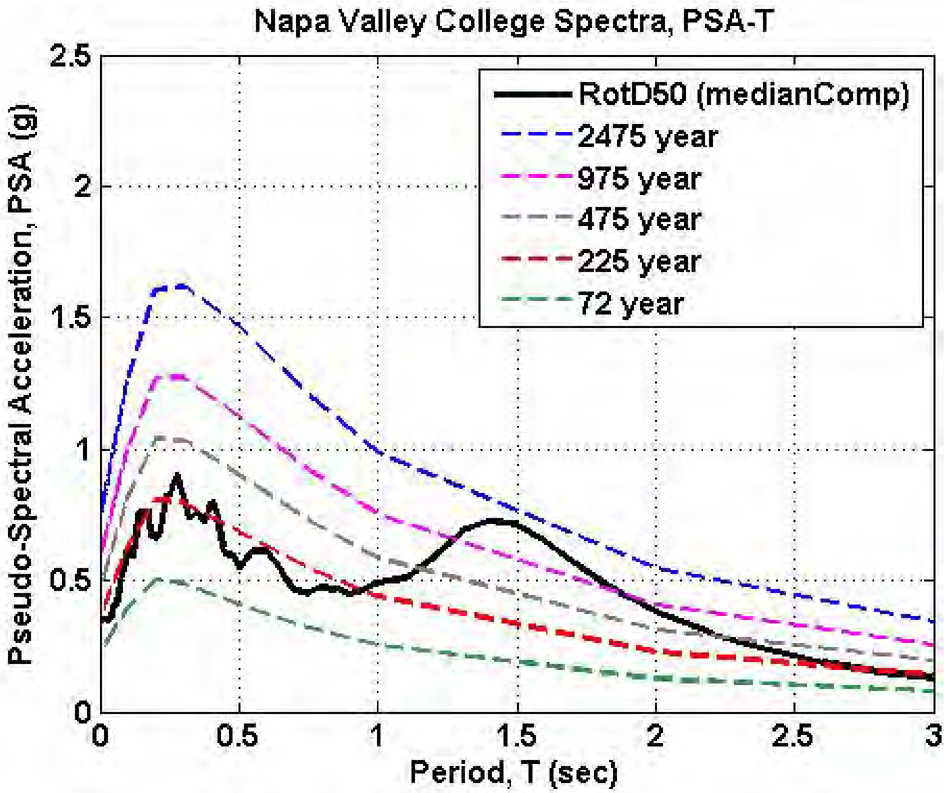
Napa Valley College Spectra, PSA-T
Pseudo-Spectral Acceleration, PSA (g)
Period, T (sec)
RotD50 (medianComp)
2475 year
975 year
475 year
225 year
72 year
0
0.5
1
1.5
2
2.5
0
0.5
1
1.5
2
2.5
3

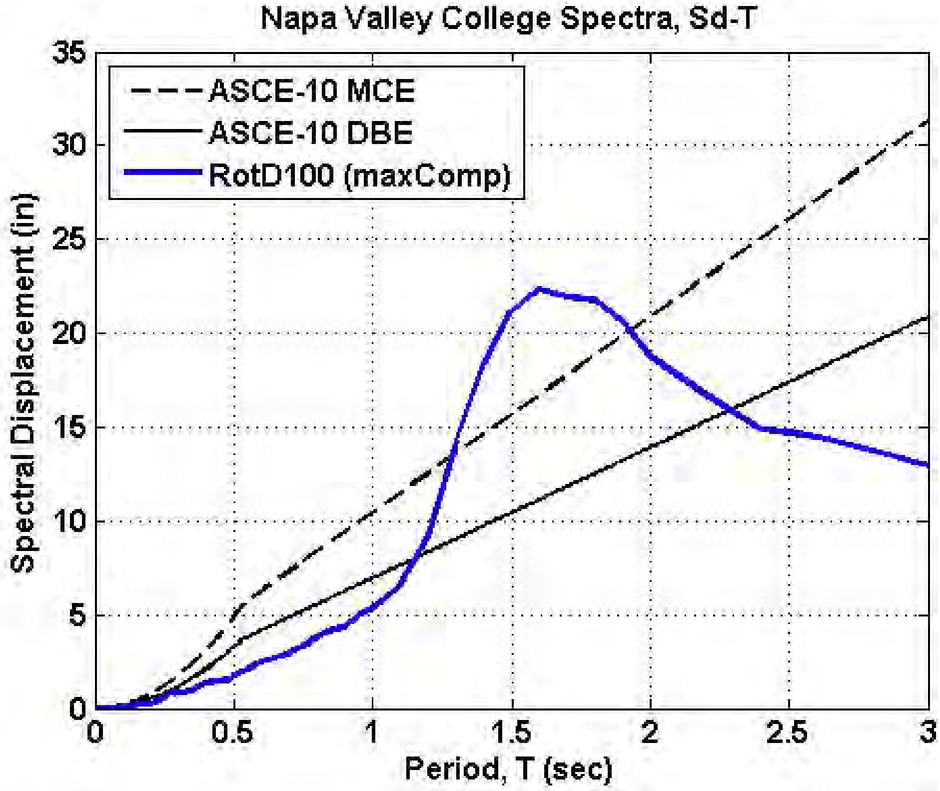
Napa Valley College Spectra, Sd-T
Spectral Displacement (in)
Period, T (sec)
ASCE-10 MCE
ASCE-10 DBE
RotD100 (maxComp)
0
5
10
15
20
25
30
35
0
0.5
1
1.5
2
2.5
3

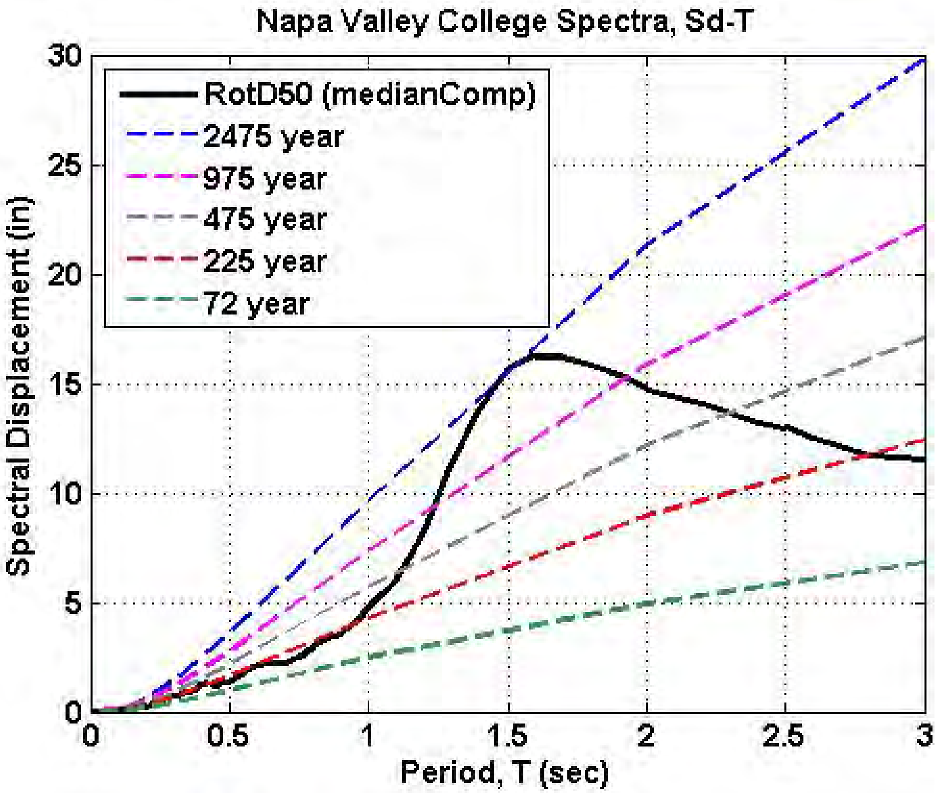
Napa Valley College Spectra, Sd-T
RotD50 (medianComp)
2475 year
975 year
475 year
225 year
72 year
Spectral Displacement (in)
0
5
10
15
20
25
30
Period, T (sec)
0
0.5
1
1.5
2
2.5
3

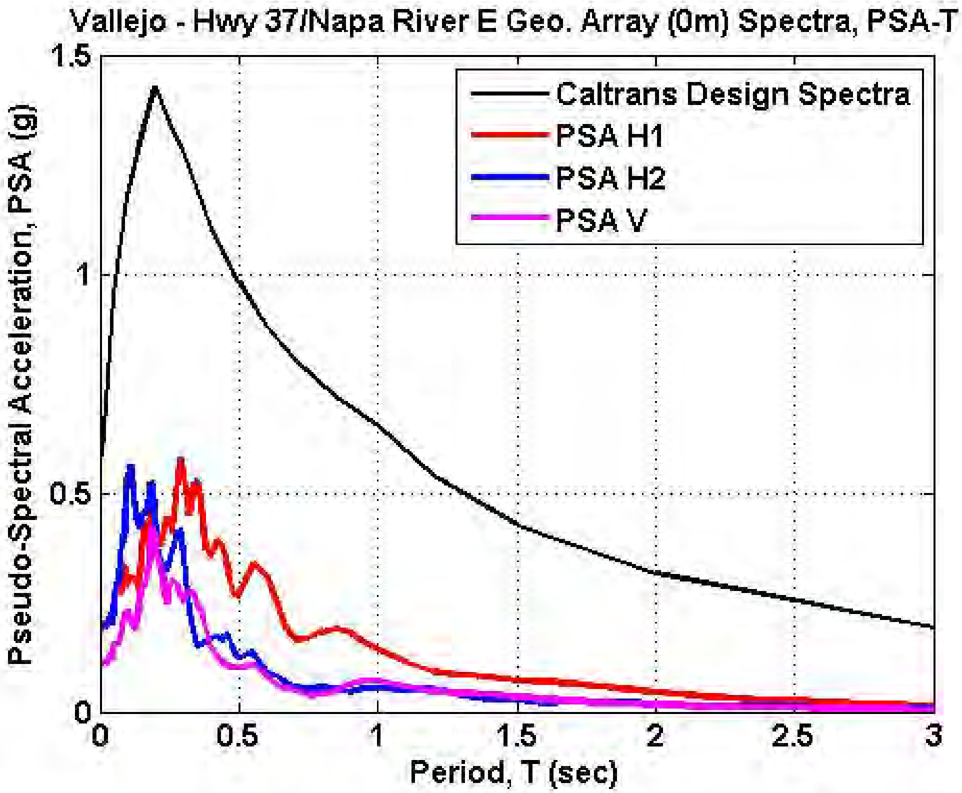
Vallejo - Hwy 37/Napa River E Geo. Array (0m) Spectra, PSA-T
Caltrans Design Spectra
PSA H1
PSA H2
PSA V
Pseudo-Spectral Acceleration, PSA (g)
Period, T (sec)
0
0.5
1
1.5
2
2.5
3
0
0.5
1
1.5

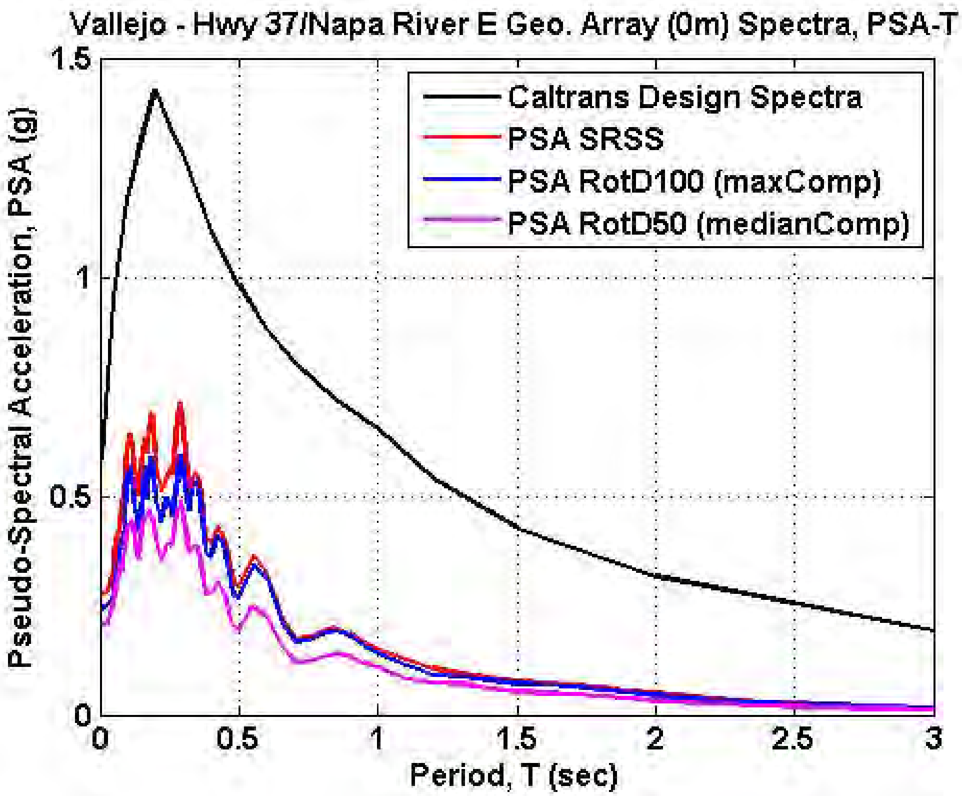
Vallejo - Hwy 37/Napa River E Geo. Array (0m) Spectra, PSA-T
Caltrans Design Spectra
PSA SRSS
PSA RotD100 (maxComp)
PSA RotD50 (medianComp)
Pseudo-Spectral Acceleration, PSA (g)
Period, T (sec)
0
0.5
1
1.5
2
2.5
3
0
0.5
1
1.5

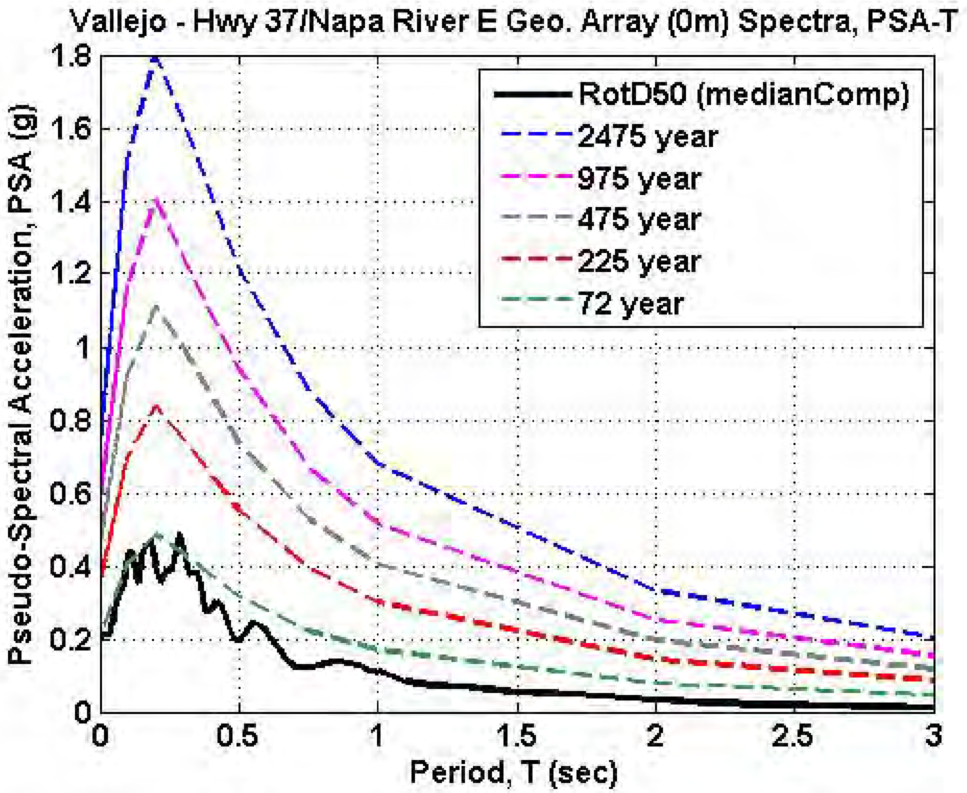
Vallejo - Hwy 37/Napa River E Geo. Array (0m) Spectra, PSA-T
Pseudo-Spectral Acceleration, PSA (g)
Period, T (sec)
RotD50 (medianComp)
2475 year
975 year
475 year
225 year
72 year
0
0.2
0.4
0.6
0.8
1
1.2
1.4
1.6
1.8
0
0.5
1
1.5
2
2.5
3

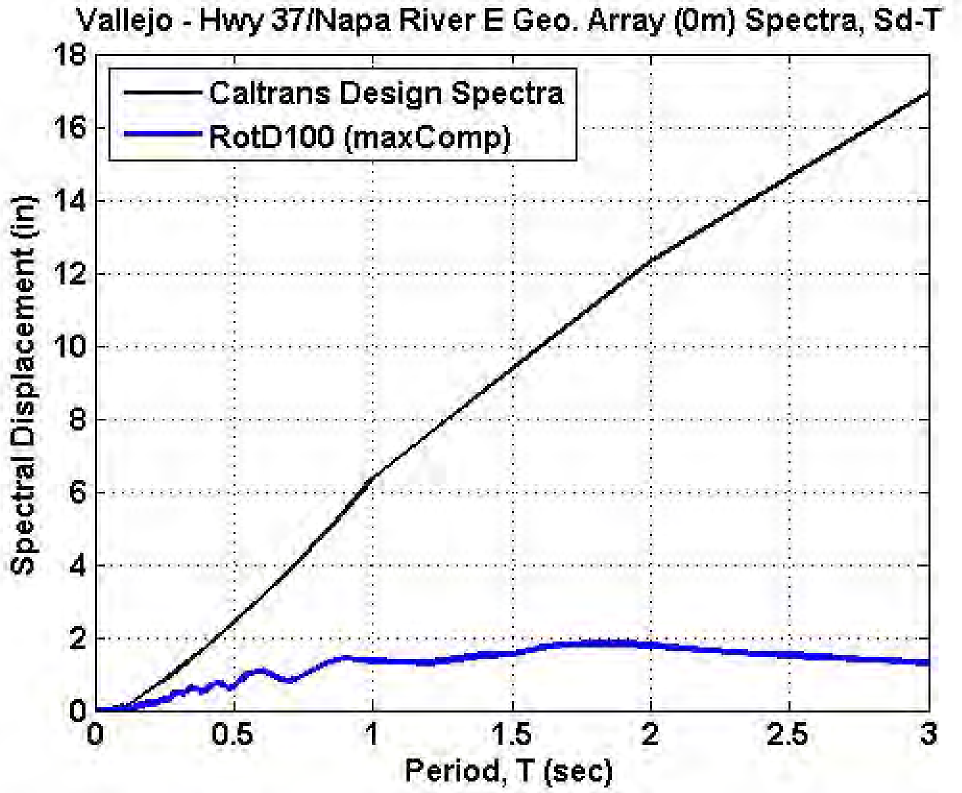
Vallejo - Hwy 37/Napa River E Geo. Array (0m) Spectra, Sd-T
Spectral Displacement (in)
Period, T (sec)
Caltrans Design Spectra
RotD100 (maxComp)
0
2
4
6
8
10
12
14
16
18
0
0.5
1
1.5
2
2.5
3

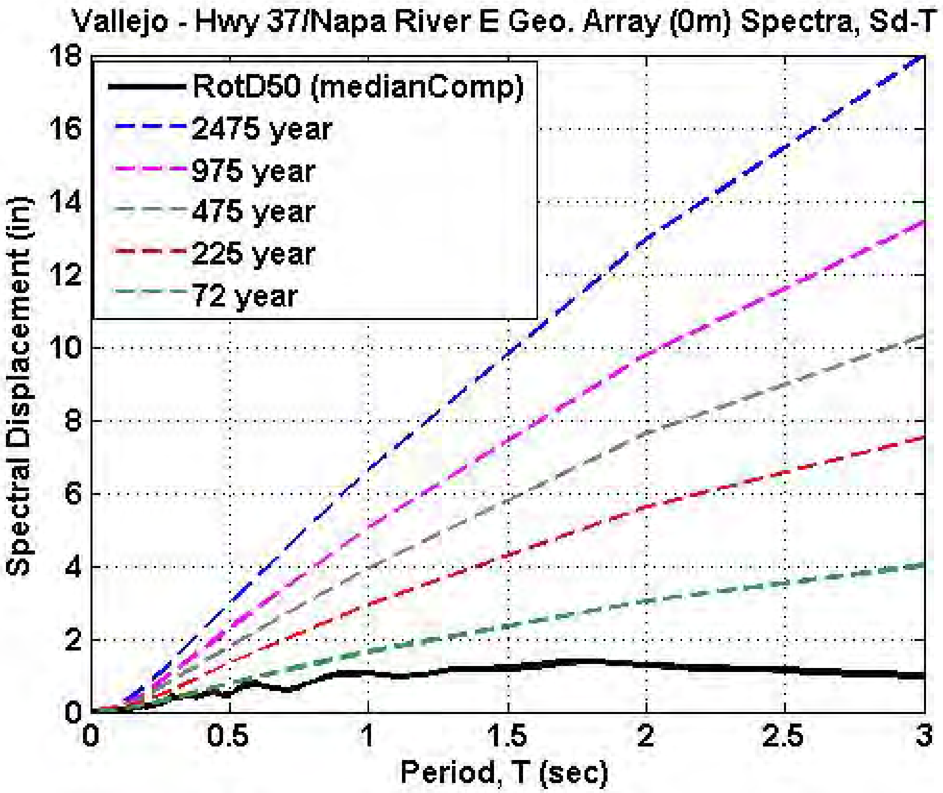
Vallejo - Hwy 37/Napa River E Geo. Array (0m) Spectra, Sd-T
Spectral Displacement (in)
Period, T (sec)
RotD50 (medianComp)
2475 year
975 year
475 year
225 year
72 year
0
2
4
6
8
10
12
14
16
18
0
0.5
1
1.5
2
2.5
3

APPENDIX D

Characterization of Near-fault Ground Motion Records by Lu and Panagiotou (2014)

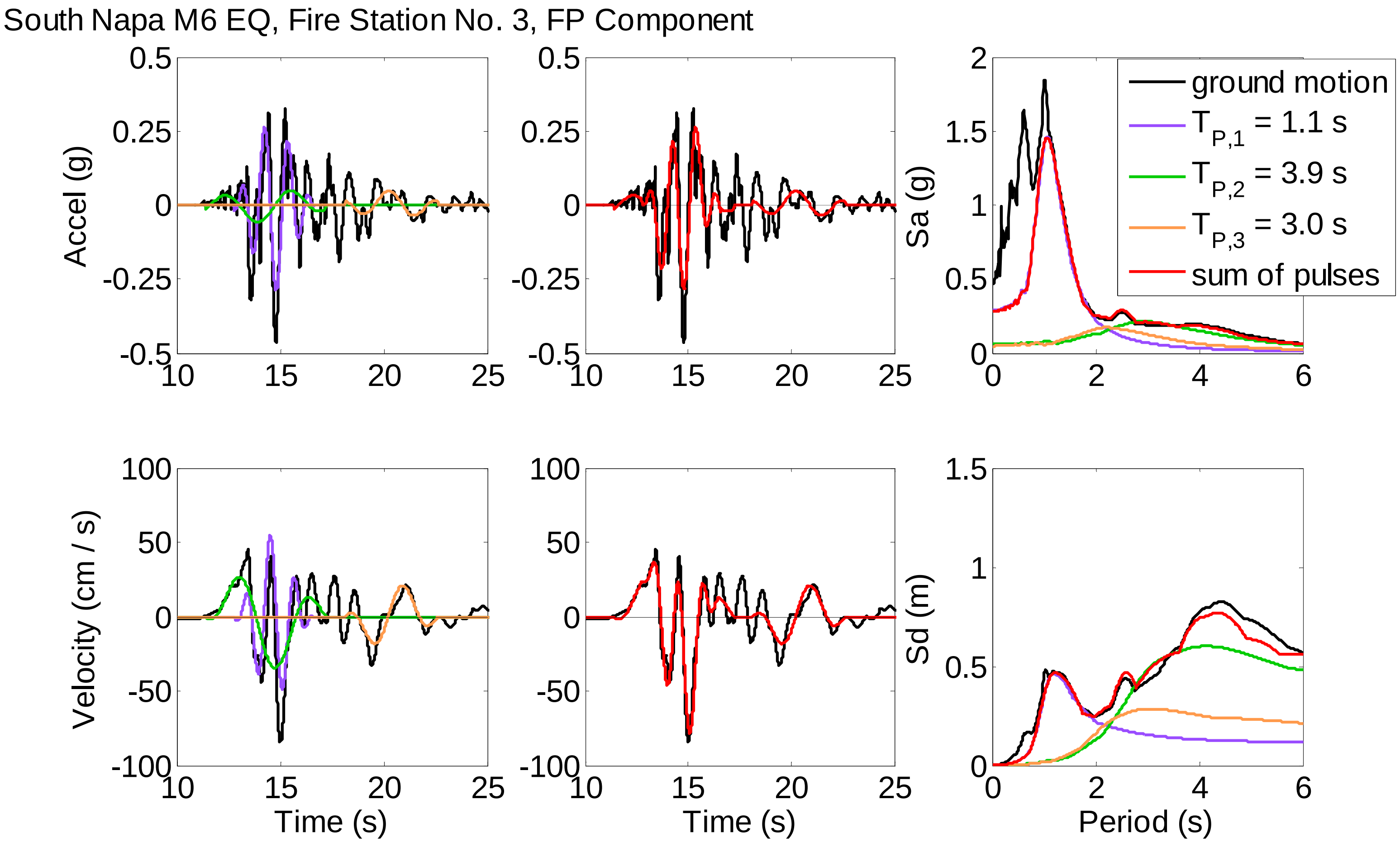

Figure 1. Fault-parallel component of ground acceleration and ground velocity histories recorded at the Fire Station No. 3; Extracted pulses using the $\text{CPE}_{\text{V,EN}}$ method; and Linear acceleration and displacement response spectra (2% damping) of the recorded histories, the extracted pulses, and the representation of the motion using the sum of the extracted pulses.

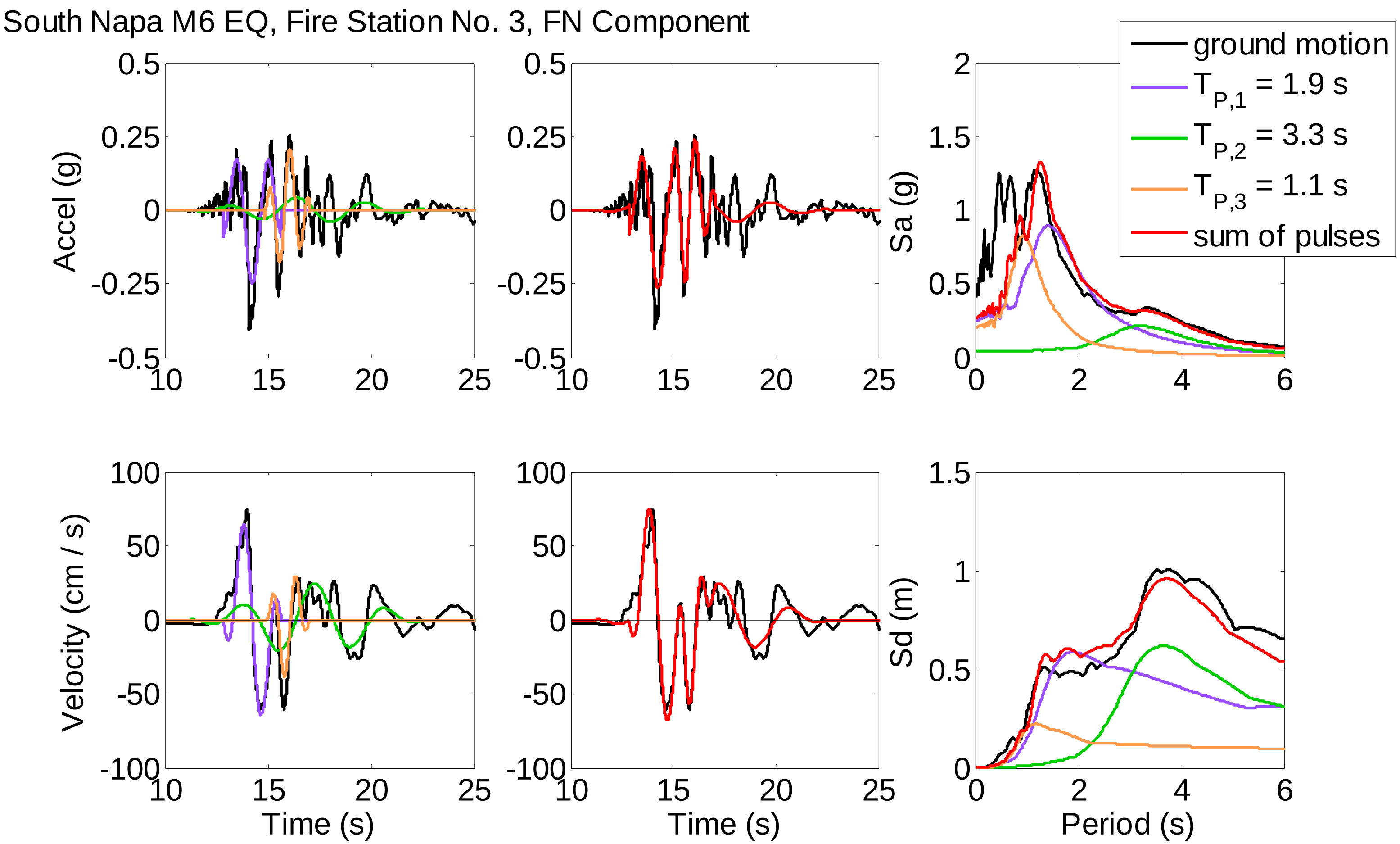

Figure 2. Fault-normal component of ground acceleration and ground velocity histories recorded at the Fire Station No. 3; Extracted pulses using the $CPE_{V,EN}$ method; and Linear acceleration and displacement response spectra (2% damping) of the recorded histories, the extracted pulses, and the representation of the motion using the sum of the extracted pulses.

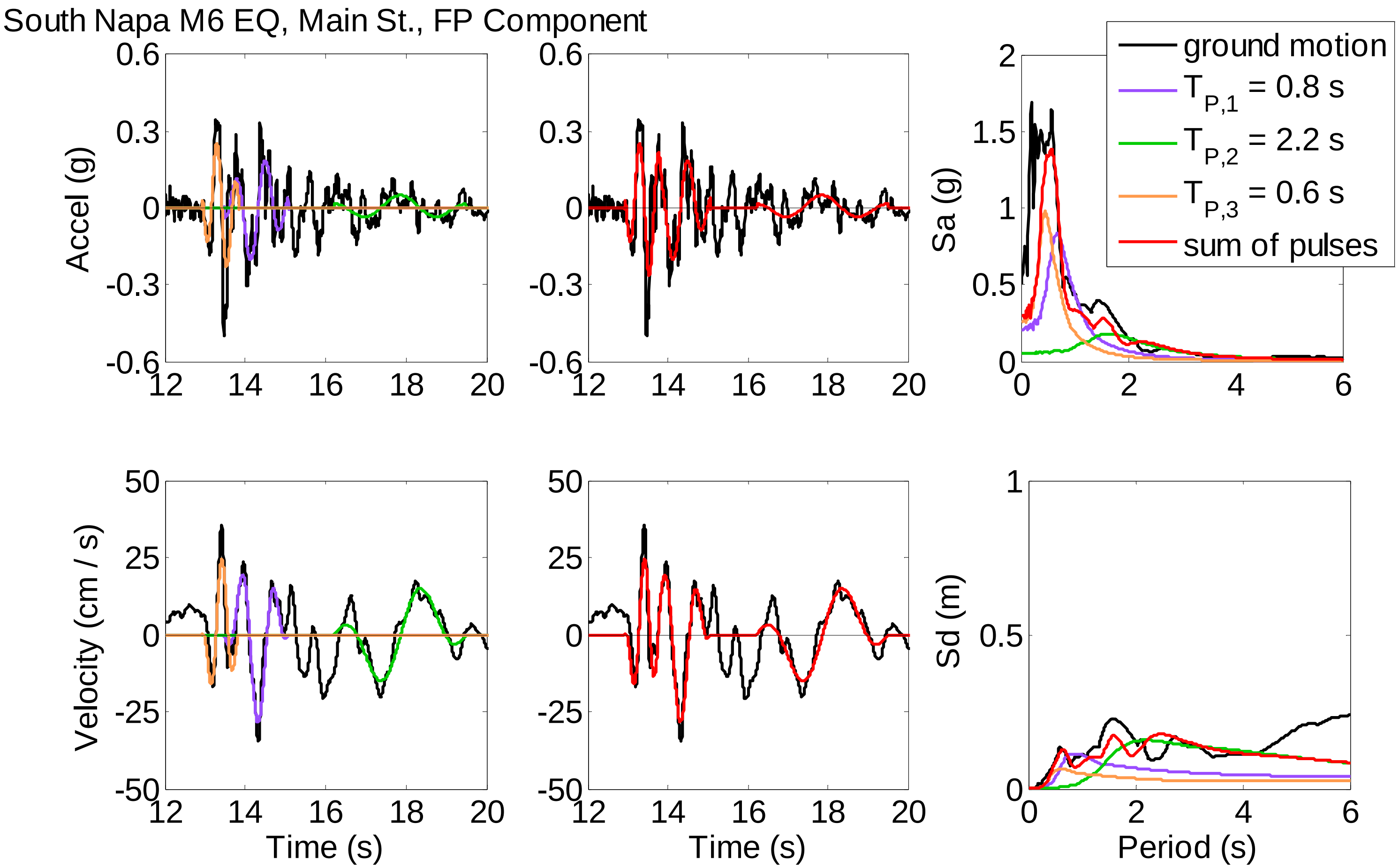

Figure 3. Fault-parallel component of ground acceleration and ground velocity histories recorded at Main St.; Extracted pulses using the $\mathrm{CPE}_{\mathrm{V,EN}}$ method; and Linear acceleration and displacement response spectra (2% damping) of the recorded histories, the extracted pulses, and the representation of the motion using the sum of the extracted pulses.

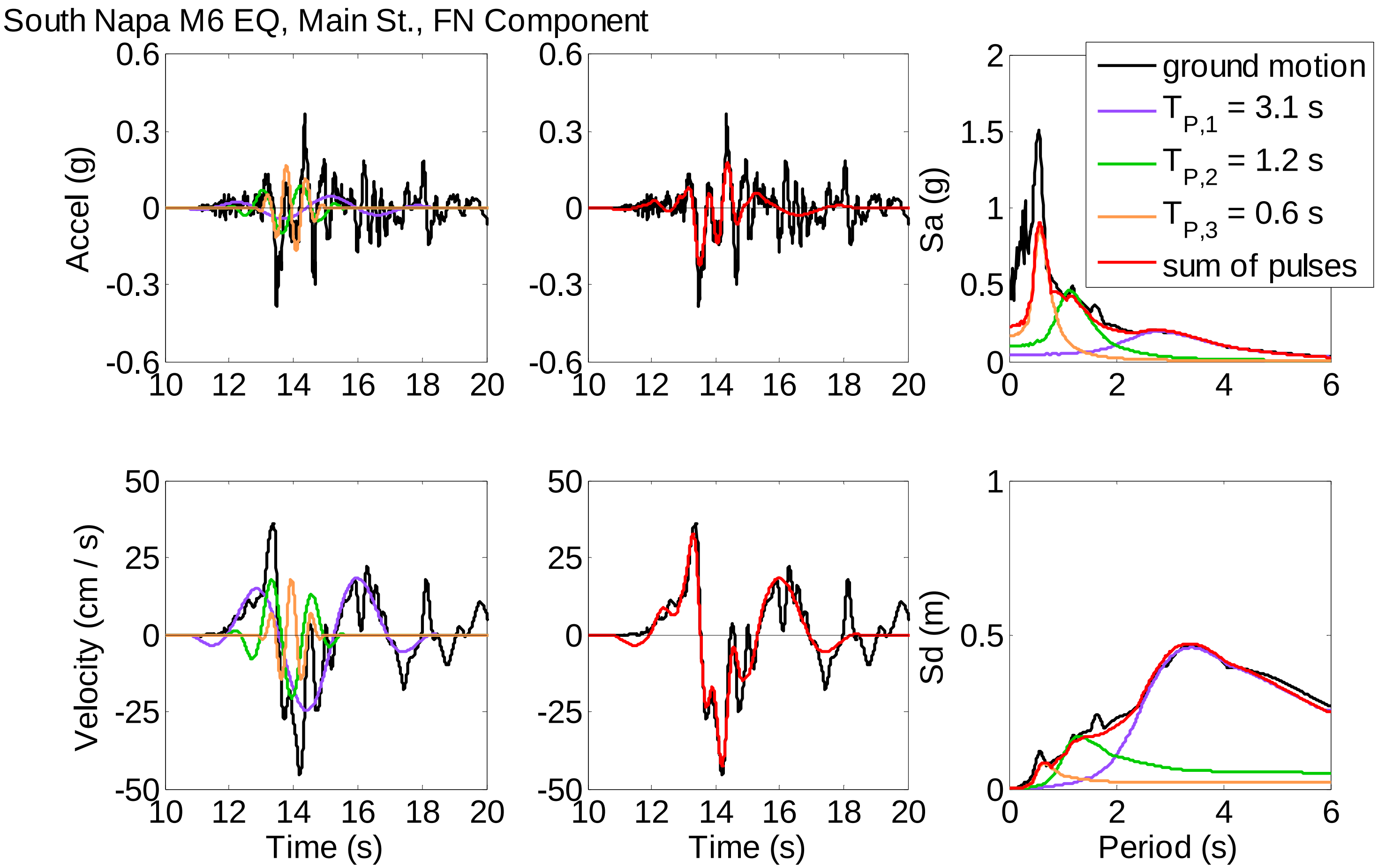

Figure 4. Fault-normal component of ground acceleration and ground velocity histories recorded at Main St.; Extracted pulses using the $\mathrm{CPE}_{\mathrm{V,EN}}$ method; and Linear acceleration and displacement response spectra (2% damping) of the recorded histories, the extracted pulses, and the representation of the motion using the sum of the extracted pulses.

APPENDIX B
SUPPLEMENTAL TO SURFACE FAULT RUPTURE ASSOCIATED WITH THE M6.0 SOUTH NAPA EARTHQUAKE OF AUGUST 24, 2014

National Science Foundation (NSF)
Geotechnical Extreme Events Reconnaissance (GEER)

The intent of this appendix is to provide a forum for the contributors to this report a place for additional figures, observations, and interpretations collected in the field not included in Section 3. The appendix sections are organized by field team and include additional figures and downloadable files. For further information regarding the individual subsections, please contact the field team lead.

Appendix B.1: Kelson and Wesling Detailed Observations
Appendix B.2: Leslie F. Harder, Preliminary Observations
Appendix B.3: Fugro observations
Appendix B.4: U.C. Davis observations, made available on SCEC Earthquake Response site via Dropbox: https://ucdavis.app.box.com/s/9zsz84638fp90grhikzx

B.1 Preliminary Observations of Surface Cracking Within the Epicentral Area of the M6.0 South Napa Earthquake of August 24, 2014

Prepared by Keith Kelson[1] C.E.G., and John Wesling[2] C.E.G.

B.1.1 Introduction / Overview

The South Napa M6.0 earthquake generated surface fault rupture over a length of approximately 12 to 15 km (Figure 1). This surface faulting extends from the northwestern bank of the Napa River at the Napa Sea Ranch (Cuttings Wharf area), northward through the Browns Valley residential area, and to Allston Park in the northwestern part of the City of Napa. In the epicentral area, rupture generally occurred along previously mapped traces of the West Napa fault. North of the epicentral area, rupture occurred along or between multiple strands of the West Napa fault and includes a complex pattern of north- to northeast-striking cracks and contractional deformation. South of the epicentral area, surface cracking coincided with mapped traces of the West Napa fault near the Napa County Municipal Airport, which may represent either surface rupture or triggered slip.

In the epicentral area, the rupture strikes about 340˚ to 345˚ (N20W to N15W) and is expressed as an *en echelon* pattern of left-stepping cracks that strike about 360 to 030 (N to N30E). At the time of this writing, a large percentage of the observed cracking occurred after the main earthquake energy release, as "afterslip" during a period at least 48 hours in duration.

---

[1] Engineering Geologist, U.S. Army Corps of Engineers, Sacramento, California
[2] Engineering Geologist, California Geological Survey, Sacramento, California

B.1.2 Fault Rupture in the Epicentral Area (Napa Sea Ranch to Congress Valley Rd)

This Appendix describes the primary characteristics of the surface fault rupture in the epicentral area, herein defined as the area from the epicentral location (Figure 1; 38.220˚, -122.313˚, http://earthquake.usgs.gov/earthquakes/eventpage/nc72282711#summary), north to Oak Rock Lane (38.296˚, -122.344˚). This section of the surface rupture is continuous, essentially straight along an azimuth of 340˚ to 345˚, and has distinct surface cracking along a length of about 9.3 km.

The southern end of this fault section is defined here as the western bank of the Napa River at the Napa Sea Ranch, where the rupture extends into an area affected by tidal-dominated river stages. The northern end of the epicentral section is defined here at Oak Rock Lane (38.296˚, -122.344˚), based on field observations of surface cracking to the south, a change in fault orientation from 340˚ to 360˚, and the northern extent of maximum slip distribution (USGS, 2014; (http://earthquake.usgs.gov/earthquakes/eventpage/nc72282711#scientific_finite-fault).

Much of the rupture is easily discernible where it extends through well-groomed vineyard crop rows and adjacent dirt farm roads; where the rupture extends into untilled, tall grassy fields, the cracking is difficult to identify and measure. As a result, rapid field-based offset measurements were easily obtained in vineyards and adjacent roadways, but were very difficult in untilled grassy areas. Also, the central part of the fault rupture includes several roadway crossings that allow for distinct identification of the fault trace and measurement of dextral fault offset.

Throughout this central section of the fault, the fault is expressed as a NW-striking zone of cracks arranged in an *en echelon* pattern (Figures 2 and 3). The zone of cracks generally ranges from about 2 to 10 m wide, measured orthogonal to fault strike, and includes cracks that range in length from about 5 to 10 m long (Figure 4). At the Stone Bridge School in the Carneros District of Napa County, the cracks developed in an asphalt parking lot project northward and in the adjacent dirt yard, cross a large-diameter gas transmission pipeline (Figure 5). The GEER team obtained anecdotal information suggesting little or no deformation of the pipeline, but was unable to collect specific offset information from the pipeline. In dirt areas, the cracks are well developed where not disturbed, and show a similar left-stepping pattern (Figure 6). The cracks almost exclusively show extension of the native ground, and are best expressed across relatively compacted dirt farm roads (Figure 7) or tilled vineyards (Figure 8). Where the rupture passes beneath road asphalt (Figure 9), the cracking tends to be narrower but more distinct, although the measurable amount of right-lateral offset appears to be lower than adjacent total offsets by about 10% to 50%.

At almost all locations, the pattern of surface deformation is consistent with right-lateral shearing, as observed in other lateral-slip earthquakes and summarized in structural geology textbooks. For example, the pattern of deformation across Los Carneros Road near the Stone Bridge School consists of left-stepping en echelon cracks at various scales, antithetic extensional cracks, and contractional features (Figure 10). Based on the originally horizontal plane of asphalt provided by Los Carneros Road, and the originally straight centerline striping, the pattern of deformation is similar to the textbook models of strike-slip deformation (Figure 11).

Field Measurements of Lateral Offset

Surface rupture involved both discrete right-lateral offset across individual cracks within the rupture zone, as well as ductile (folding) deformation over areas as much as 10 m wide. At many locations, reported offset measurements are minimum values because of the presence of multiple cracks within the rupture zone, and/or because of distributed deformation adjacent to the rupture zone. In addition, the observation of continued post-earthquake surface deformation ("afterslip", see below) indicates temporal variations in the amount of offset, so that the time of the offset measurement should also be noted. A summary of the limited field measurements is provided in Table 1.

The maximum offset measured during the initial, rapid-response GEER reconnaissance was obtained at a site approximately 6.7 km northwest of the M6.0 epicenter, in the northern part of the Clos du Val Vineyards. On August 25 (1430 hrs), members of the GEER team measured 40 to 45 cm right-lateral offset of a linear array of wooden vineyard posts (Figure 12). The measurement was made by extending a fiberglass tape along the southern edge of the wooden posts on the eastern side of the fault, and measuring the offset of posts on the western side of the fault (Figure 13). At this site, the fracture zone is essentially perpendicular to the vineyard rows, and is about 3 m wide. Warping adjacent to the fault extended about 5 to 7 m on both sides of the fault, and little or no measurable deformation was observed beyond the zones of brittle and warping deformations. Qualitative observations within the entire vineyard plot at this site suggests that the right-lateral offset decreased only slightly to the north and south, and probably was in the 30 to 40 cm through most of this plot. This site is on a low-gradient alluvial fan derived from rounded hills to the northwest; there is no topographic scarp associated with the fault rupture, and there is not a strong geomorphic expression of pre-existing fault-related topography.

Notably, this location coincides well with USGS slip distribution models (http://earthquake.usgs.gov/earthquakes/eventpage/nc72282711#scientific_finite-fault), which suggest that the maximum slip on the fault at depth occurred between Henry Road on the south, and Oak Rock Lane on the north. The offset measurement described here is located about 0.5 km north of Henry Road and above this zone of maximum slip. The site is about 7 km north of the epicenter, which corroborates seismological data indicative of a northerly-directed rupture at depth (Figure 14). The spatial relationship of this site to the cross-section slip distribution suggests that areas along the rupture directly to the north, to perhaps Oak Rock Lane, probably also have a comparable amount of right-lateral offset.

Other limited field measurements by the GEER reconnaissance team suggest that there was about 20 to 30 cm of right-lateral offset along most of the rupture in the epicentral area. Right-lateral offsets of 20 to 25 cm were measured on August 25 (1130 hrs and 1150 hrs) at two sites directly north of Old Sonoma Road (Figures 15 and 16, respectively). The fracture zone is about 3 m wide, and typically consisted of one or two primary open cracks with no vertical separation. These sites are about 5.5 km north of the epicenter and are within the southern part of the Clos du Val Vineyard parcel (Figure 16). Field discussion with the operation manager at these sites indicated that the metal posts in this vineyard were placed in a linear array and surveyed via GPS methods; the posts in adjacent rows were claimed to be exactly 7.5 ft apart, providing confidence that the posts were arranged in a straight line prior to the rupture. The rupture through this vineyard extended across an east-facing colluvial slope, and exhibited a subtle mid-slope depression. Aerial reconnaissance of this site on August 27 (1108 hrs) showed a distinct color-difference lineament in the vineyard that coincides with the observed surface rupture (Figure 17).

Right-lateral offset of 20 to 25 cm also was measured at a site located south of Las Amigas Road, about 1.2 km north of the epicenter (Poseidon Vineyard, Figure 18). This measurement was made on September 2 (1800 hrs); qualitatively, the amount of deformation was noticeably greater than that observed during a prior visit by the GEER team on August 25. Similar to the sites described above, the fault rupture included a 5-m-wide zone of extensional cracks, arranged in an *en echelon* pattern through the vineyard. The zone of fracturing coincides with a subtle topographic trough that traverses the vineyard, and is about 200 m east of a prominent linear escarpment bordering the floodplain of lower Carneros Creek. About 350 m south of the measurement site, the rupture zone intersects and coincides with an anomalously straight reach of lower Carneros Creek, and then continues southward to the surface features noted at Napa Sea Ranch (Figure 2).

Field Evidence of Afterslip

The amount and character of the surface deformation associated with the M6.0 South Napa earthquake evolved through the hours and days following the main shock at 3:20 am local time on August 24, 2014. There have been and will be many observations along the fault rupture by numerous workers, and these should be interpreted in context of the temporal changes in post-earthquake surface deformation ("afterslip"). This section presents a few field observations of the rupture during the few hours and days after the main shock, and may provide a basis for interpreting the temporal pattern of afterslip deformation.

Initial observations were made of the surface rupture at the Highway 12 fault crossing, near the intersection of Cuttings Wharf Road (4.2 km NW of the epicenter). Approximately 2.5 hrs after the main shock (at 5:45 local time), the northern edge of the highway asphalt was slightly buckled, and the centerline and sidelines exhibited little or no lateral offset (Figure 19). Minor cracking in the adjacent dirt embankments and vineyards was observed to consist of a series of left-stepping open cracks. Because of darkness and hazardous highway conditions, no measurements were made at that time. Approximately 2 hours later (local time 0745), observation of the highway fault crossing showed that the buckling on the northern part of the asphalt was substantially greater, and there was a few cm of lateral offset (Figure 20). As of September 2, subsequent observations have shown as much as about 20 to 25 cm of lateral offset across the zone at this location.

A similar temporal pattern of deformation occurred across the south-trending Cuttings Wharf Road directly south of Highway 12. At about 6:00 am local time on August 24 (about 3.5 hours after the main shock), there was no scarp or cracking across the asphalt. By about 10:00 am local time on August 25 (28 hours later) a 10-cm high scarp had developed (Figure 21). Subsequent to August 25, asphalt patches have been cracked and offset, which demonstrate continued surface deformation. Continued surface deformation is also demonstrated by cracking and offsets of road patches across Las Amigas Road, located about 2.0 km NW of the epicenter.

Post-earthquake surface deformation is also shown by observation of only minor deformation of Old Sonoma Road in the early hours of August 24 (Figure 22). At 0730 on August 24, a series of en echelon cracks had developed in the centerline striping of the road, with only minor offset and vertical uplift (Figure 23). Within 27 hours, this deformation was more distinct, and involved several centimeters of uplift across the road. The roadway was repaired soon thereafter, and there have been no subsequent notes on deformation at this fault crossing.

B.1.3 Summary and Conclusions

The South Napa M6.0 earthquake generated surface fault rupture over a length of approximately 12 to 15 km, from the northwestern bank of the Napa River near Cuttings Wharf, northward to the northwestern part of the City of Napa. In the epicentral area, rupture occurred along previously mapped traces of the West Napa fault, although additional offset occurred to the north and south of the previously mapped traces. In the epicentral area, the rupture strikes about 340˚ to 345˚ (N20W to N15W) and is expressed as an *en echelon* pattern of left-stepping cracks that strike about 360 to 030 (N to N30E). The largest measurement of right-lateral offset made by the authors was at a site about 7.3 km north of the epicenter, and showed an offset of vineyard rows of 40 to 45 cm. This measurement is consistent with existing slip distribution models produced by the USGS, as are measurements of lesser offsets in areas closer to the epicenter. These measurements also corroborate interpretations that the earthquake rupture at depth had a northward-directed pattern. Based on observations at multiple sites during the days following the earthquake, a large percentage of the observed cracking occurred after the main earthquake energy release, as “afterslip”. The pattern and duration of this afterslip will likely be defined more definitively through subsequent detailed analyses, but our observations suggest the much of the offset occurred during a period of at least 48 hours in duration.

Table 1. Offset measurements along the central surface fault rupture produced by the M6.0 South Napa earthquake [NSF-GEER: Kelson and Wesling; 08/25/14 and 9/2/14]

Date	Time	Site Number	Site Name	Latitude	Longitude	Fault zone strike	Measurement Azimuth	Apparent Offset (cm)	True Lateral Offset (cm)
25-Aug-14	1130	20140825-kik009	south Clos du Val-1	N38.2669	W122.3341 ,	005	148	20 to 25	25 to 31
25-Aug-14	1150	20140825-kik011	south Clos du Val-2	N38.2672	W122.3343 ,	005	148	20 to 25	25 to 31
25-Aug-14	1430	20140825-kik027	north Clos du Val	N38.2776	W122.3377	355	, 090	40 to 45	41 to 46
2-Sep-14	1915	20140902-kik027	Poseidon Vineyard	N38.2314	W122.3153	330	, 090	20 to 25	23 to 29

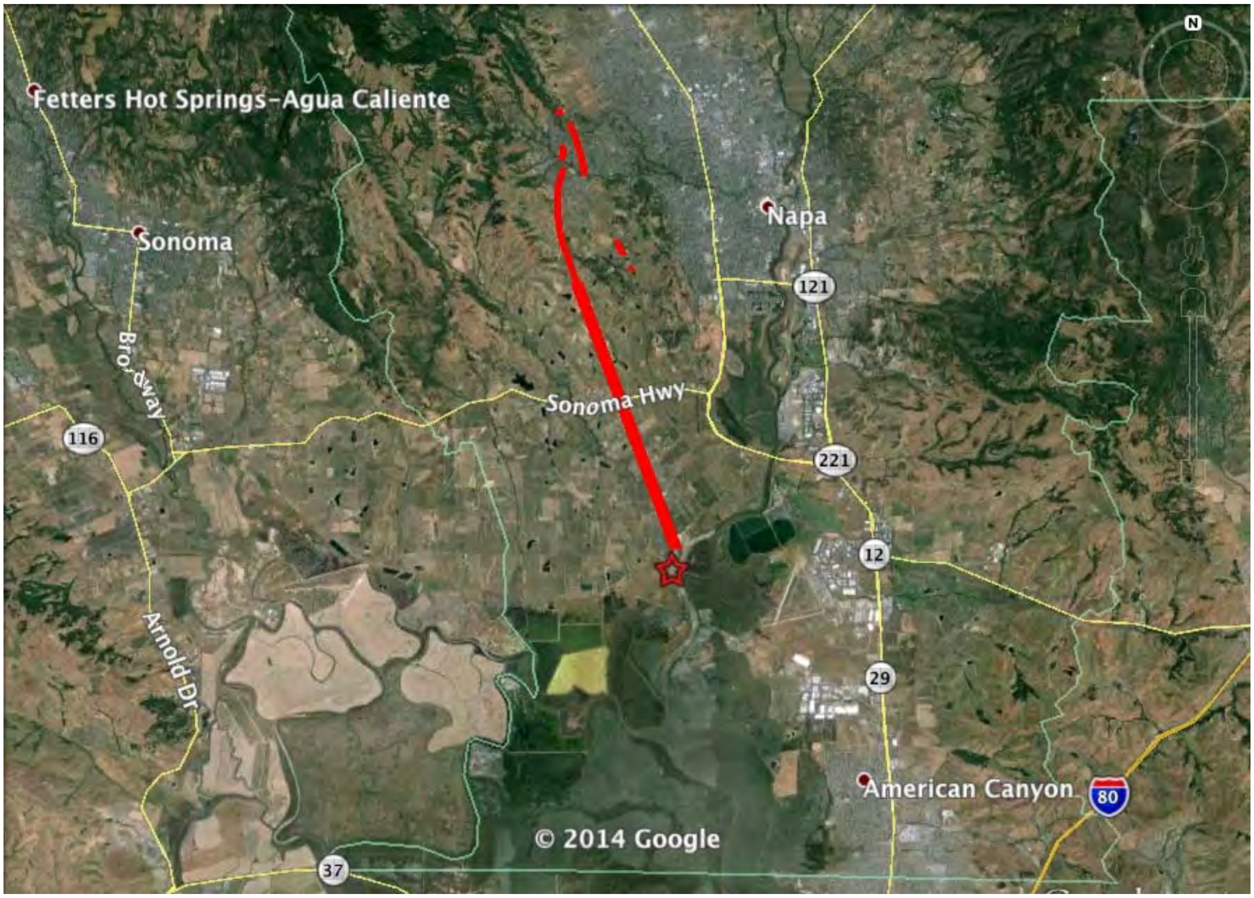

Figure 1. General map of surface fault rupture associated with the M6.0 South Napa earthquake of August 24, 2014.

Figure 2. Surface fault rupture at Napa Sea Ranch (0.5 km NW of epicenter), showing left-stepping pattern of transtensional cracking. Near-vertical view to the east. [NSF-GEER; GPS N38.225 W122.312; 08/25/14: 11:57 am]

Figure 3. Surface fault rupture at South Avenue (2.5 km NW of epicenter), showing left-stepping pattern of transtensional cracking within vineyard, across asphalt, and directly east of residence. Oblique view to the south. [NSF-GEER; GPS N38.242 W122.320; 08/27/14: 11:59 am]

Figure 4. Surface fault rupture at Stone Bridge School (2.7 km NW of epicenter), showing left-stepping pattern of transtensional cracking within asphalt parking lot. View to north-northwest. Overall fault zone strikes 340, cracks strike about 020 to 040. [NSF-GEER; GPS N38.2436 W122.3212; 08/25/14: 3:38 pm]

Figure 5. Oblique aerial photographs of the Stone Bridge School parking lot (Figure 4). Upper photo taken on August 27, 2014; 12:01 pm); view to northwest; cracks extend northwestward from parking lot into adjacent yard. Lower photo taken (by L. Harder, Sept 1; near-vertical) showing pipeline trench excavation along southern border of yard adjacent to school parking lot. [NSF-GEER; school lot: GPS N38.2436 W122.3212]

Figure 6. Surface fault rupture at horse corral west of Cuttings Wharf Road (3.9 km NW of epicenter), showing left-stepping pattern of transtensional cracking across compacted dirt slope. View to south-southeast. Individual cracks have as much as 5 cm lateral offset. [NSF-GEER; GPS N38.2536 W122.3262; 09/02/14: 6:07 pm]

Figure 7. Surface fault rupture at central part of Clos du Val Vineyard (5.9 km NW of epicenter), showing left-stepping pattern of transtensional cracking within compacted dirt farm road. View to south-southeast. [NSF-GEER; GPS N38.271 W122.335; 08/25/14: 12:10 pm]

Figure 8. Surface fault rupture at vineyard directly south of Highway 12 and east of Cuttings Wharf Road (4.1 km NW of epicenter), showing left-stepping pattern of transtensional cracking within vineyard. View to south. [NSF-GEER; GPS N38.2557 W122.3270; 08/25/14: 9:49 am]

Figure 9. Surface fault rupture at Henry Road (6.2 km NW of epicenter), showing left-stepping pattern of transtensional cracking across asphalt. View to southeast. Offset across most prominent crack within this zone is as much as 6 cm, but offset across entire zone measure in adjacent vineyard is about 40 cm [NSF-GEER; GPS N38.2732 W122.3366; 08/25/14: 1:45 pm]

Figure 10. Surface fault rupture at Los Carneros Road (2.5 km NW of epicenter), showing offset of centerline and complex, small-scale deformation in ductile asphalt. View to north. Compare with close up of centerline in Figure 11. [NSF-GEER; GPS N38.2432 W122.3209; 08/25/14: 3:31 pm]

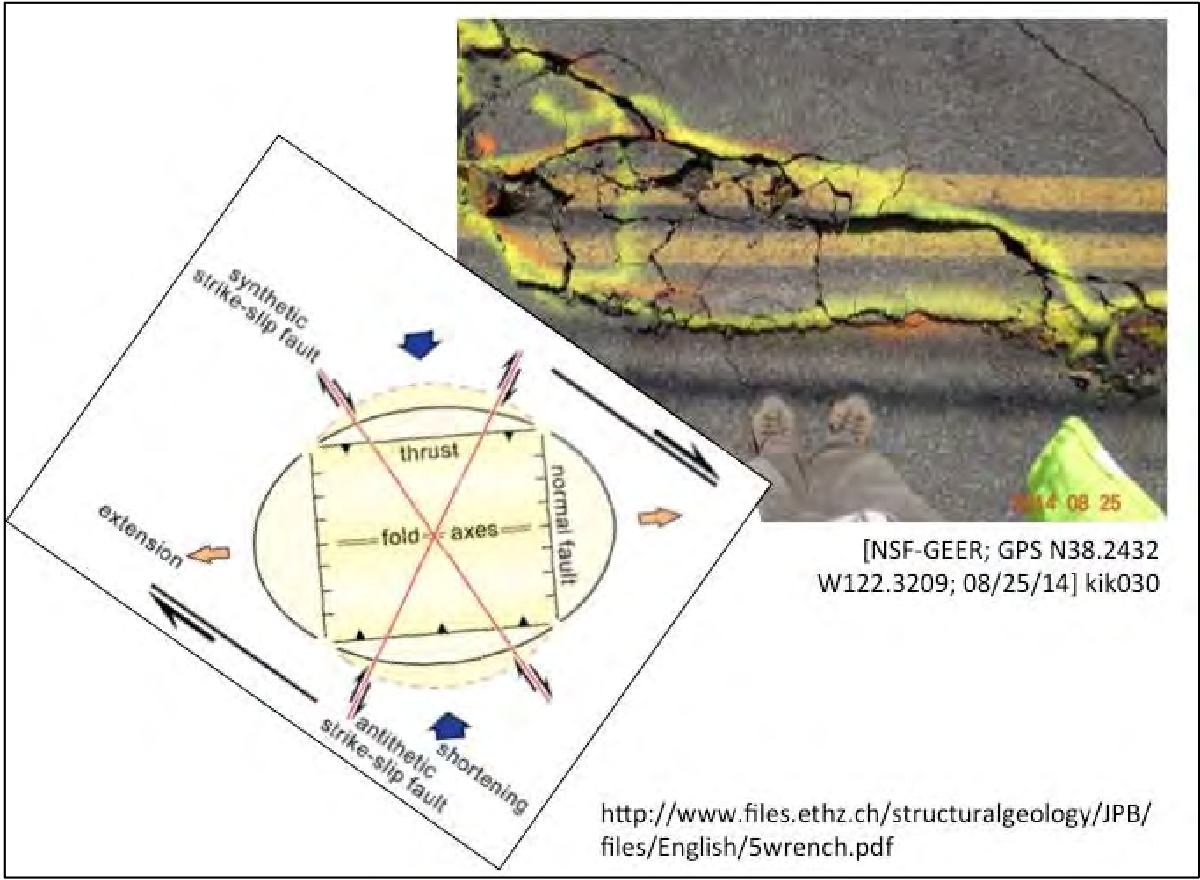

[NSF-GEER; GPS N38.2432 W122.3209; 08/25/14] kik030

http://www.files.ethz.ch/structuralgeology/JPB/files/English/5wrench.pdf

Figure 11. Surface deformation of the centerline of Los Carneros Road (2.5 km NW of epicenter), showing complex, small-scale deformation in ductile asphalt. View is vertical. Deformation is consistent with textbook models of pure shear. [NSF-GEER; GPS N38.2432 W122.3209; 08/25/14: 3:32 pm]

Figure 12. Surface fault rupture at northern part of Clos du Val Vineyard near 2121 Buhman Avenue (6.7 km NW of epicenter), showing measurement alignment along azimuth 090. Yellow engineer's scale is located west of fault zone; offset location is also discernible via offset of vine shadow within the vineyard row. [NSF-GEER; GPS N38.2776 W122.32377; 08/25/14: 2:23 pm]

Figure 13. Surface fault rupture at northern part of Clos du Val Vineyard near 2121 Buhman Avenue (6.7 km NW of epicenter), showing measurement alignment along azimuth 090. Yellow engineer's scale shows measurement of 40 to 45 cm from base of thick wooden post; tape placed along southern edge of wooden posts aligned on east side of fault zone. [NSF-GEER; GPS N38.2776 W122.3377; 08/25/14: 2:24pm]

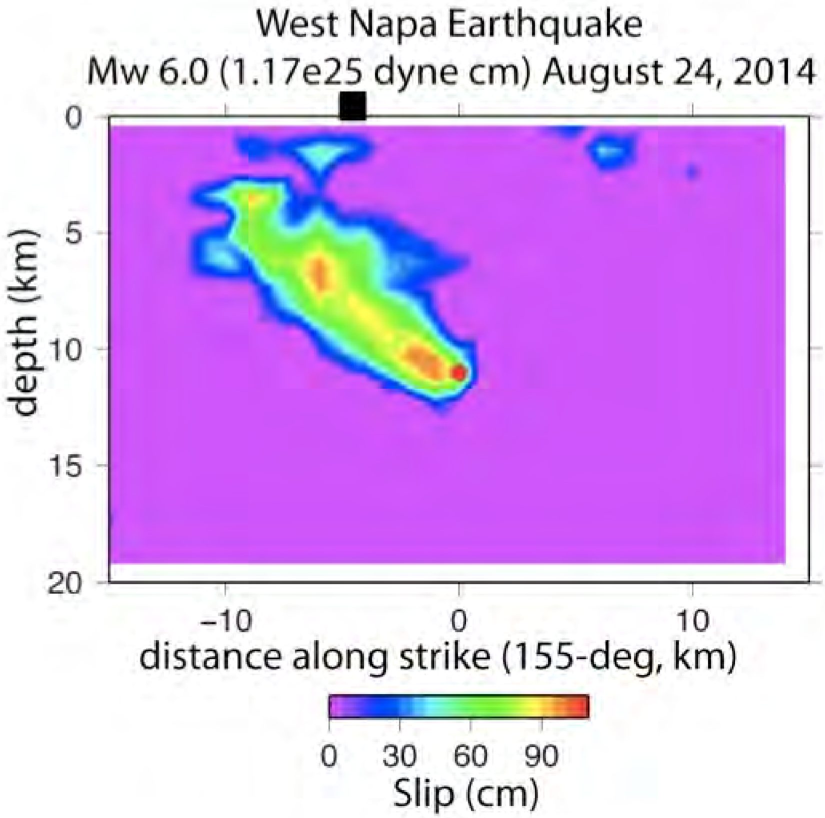

Figure 14. Cross section of slip distribution of the South Napa earthquake, from USGS (http://earthquake.usgs.gov/earthquakes/eventpage/nc72282711#scientific_finite-fault; accessed September 14, 2014; 1800), modified to show approximate location of largest field measurement of right-lateral offset at northern Clos du Val vineyard (black square at surface added by authors).

Figure 15. Surface fault rupture at southern part of Clos du Val Vineyard near Old Sonoma Road (5.6 km NW of epicenter), showing measurement alignment along azimuth 058. Yellow engineer's scale is located west of fault zone, showing 20 to 25 cm of apparent lateral offset. Tape was aligned at base of metal stakes east of fault zone. [NSF-GEER; GPS N38.2669 W122.3341; 08/25/14: 11:19 am].

Figure 16. Surface fault rupture at southern part of Clos du Val Vineyard near Old Sonoma Road (5.6 km NW of epicenter), showing measurement alignment along azimuth 058. This vineyard row is about 40 m northwest of similar row shown on Figure 12; also shows 20 to 25 cm of apparent lateral offset. Geologist Wesling standing on fault zone [NSF-GEER; GPS N38.2672 W122.3343; 08/25/14: 11:51 am]

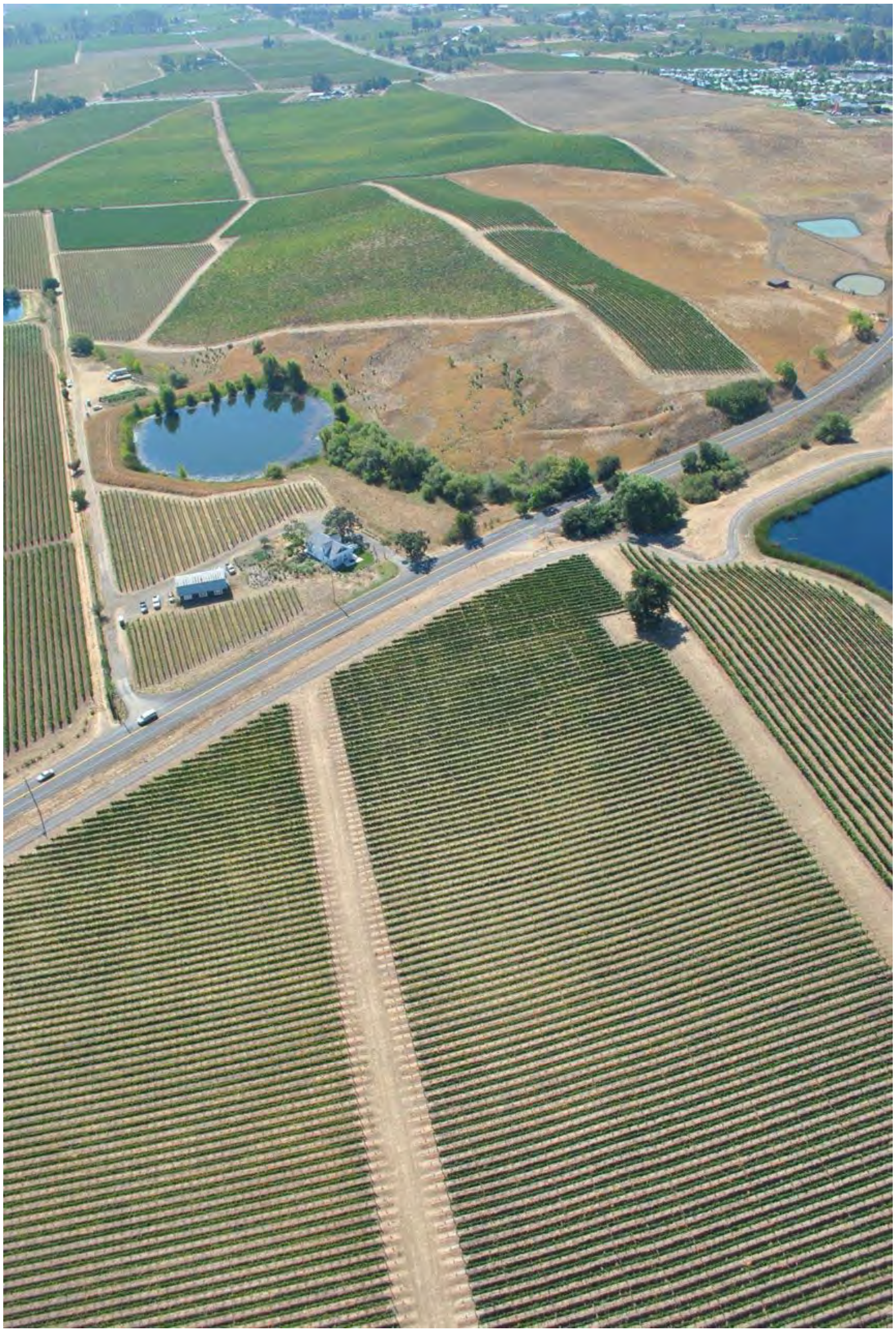

Figure 17. Oblique aerial view looking southeast along rupture toward the vineyard sites measured in Figures 11 and 12, in southern part of Clos du Val Vineyard near Old Sonoma Road (5.6 km NW of epicenter). Note prominent tonal lineament through vineyard north of Old Sonoma Road, which coincides with the 2014 surface rupture. [NSF-GEER; GPS N38.268 W122.334; 08/27/14: 12:07 pm]

Figure 18. Surface fault rupture at Poseidon Vineyard south of Las Amigas Road (1.2 km NW of epicenter), showing measurement alignment along azimuth 090. Yellow engineer's scale is located west of fault zone, showing 20 to 25 cm of apparent offset. [NSF-GEER; GPS N38.2314 W122.3153; 09/02/14: 7:17 pm]

Figure 19. Surface fault rupture at Highway 12 (4.2 km NW of epicenter), showing buckling of asphalt on northern margin and minor lateral offset. Taken at 0554 local time, this photograph precedes road repairs. [NSF-GEER; GPS N38.256 W122.327; 08/24/14: 5:54 am]

Figure 20. Surface fault rupture at Highway 12 (4.2 km NW of epicenter), showing increased buckling of asphalt on northern margin and lateral offset. Taken at 0746 local time, this photograph precedes road repairs. [NSF-GEER; GPS N38.256 W122.327; 08/24/14: 7:46 am]

Figure 21. Surface deformation at Cuttings Wharf Road (4.0 km NW of epicenter), showing recent development of scarp across asphalt (photograph taken at 1000). Field reconnaissance at 0600 on August 24, 2014 observed no deformation along the road at this site. [NSF-GEER; GPS N38.2544 W122.3265; 08/25/14: 9:57 am]

Figure 22. Surface deformation at Old Sonoma Road (5.4 km NW of epicenter, photograph taken at 0730, about 4 hours after main shock). Compare with photograph in Figure 23 [NSF-GEER; GPS N38.2659 W122.3338; 08/24/14: 7:34 am].

Figure 23. Surface deformation at Old Sonoma Road (5.4 km NW of epicenter, photograph taken onAugust 25 at 1036, about 29 hours after main shock). Compare with photograph in Figure 22 [NSF-GEER; GPS N38.2659 W122.3338; 08/25/14: 10:36 am].

B.2 Supplemental Preliminary Observations of Surface Cracking

B.2.1 Introduction

This document summarizes observations of surface cracking made within 5 to 14 days following the main shock of the August 24, 2014 Magnitude 6 Napa, California Earthquake (August 27 to September 7, 2014). The surface cracks were observed mainly on roadways in western Napa County and at least some of them are quite likely associated with surface rupture of the causative fault for the earthquake. Two main alignments of ground cracking potentially associated with fault rupture (A and B) were observed. The principal alignment of ground cracking (Alignment A) was observed from the epicentral area running semi-linearly north-northwest to a point on Redwood Road (Point A1) northwest of Brown's Valley (see green dashed line in Figure 1). No significant cracking was observed on Dry Creek Road north of Redwood Road (Point A1), thus potentially limiting the northern extent of potential surface rupture.

The total length of potential surface rupture between Points A1 and A14 (green dashed line) would thus be estimated to be approximately 12½ kilometers, running from Las Amigas Road (Pointe A14) to Redwood Road (Point A1). The length of rupture could potentially be greater given that the southern end of observed rupture ended in the marshy waters associated with the Napa River and thus could not be observed further south. Point A15 is located on Milton Road on the southern portion of Edgerley Island where ground cracking across the road was observed. However, it was not clear that this ground cracking represents the surface expression of the fault rupture as it was south of the epicenter and the pattern of cracking was not definitive. Nevertheless, the potential for surface fault rupture would have to be assumed to be somewhat greater than the 12½ kilometers observed across roadways.

A second semi-linear alignment of ground cracking, Alignment B (orange line in Figure 1), was also observed about 800 meters to east of Alignment A. Where observed, it had crack dimensions and offsets similar in magnitude to those associated with Alignment A.

B.2.2 Observation Approach

The general approach was to first estimate the general location where potential surface ground rupture might have occurred and to then drive to roadways where the rupture might cross and thus be observed. In many cases, the ground cracking was easily observed more or less where it was expected to be. By the time the observations were made, many of the areas of roadway cracking had already been repaired by City of Napa, Napa County, and Caltrans forces. However, several locations where ground cracking/rupture occurred had not been repaired at the time of this reconnaissance and were thus available for inspection.

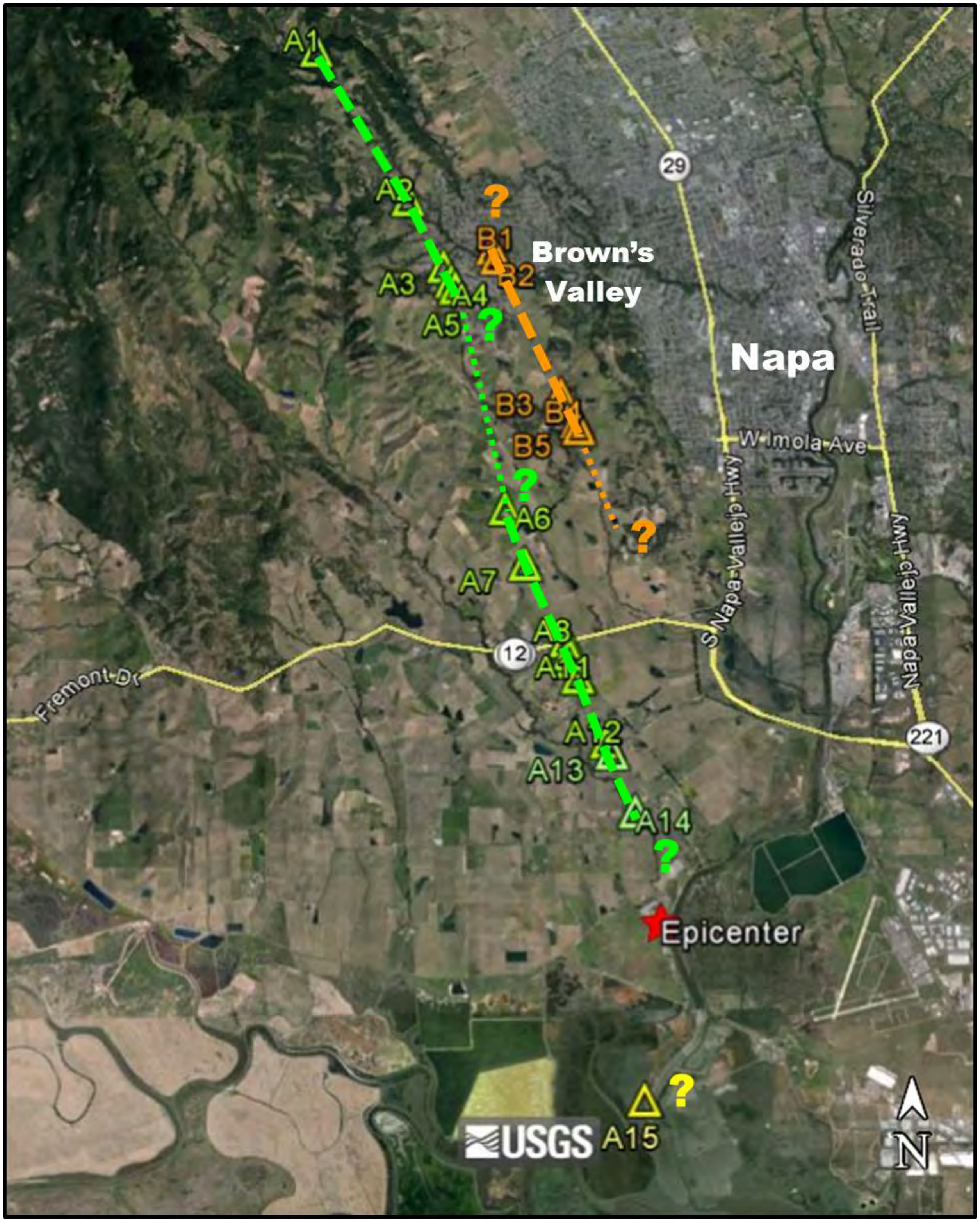

Figure 1: Alignment of surface cracking observed following August 24, 2014 Magnitude 6 Napa Earthquake (adapted from Google Earth [NSF-GEER; Napa, CA, processed 09/03/14]

B.2.3 Summary of Observations

The following represents a summary of the observed ground cracking:

- In all cases where unrepaired cracking was observed, the magnitude of ground cracking/rupture was relatively modest with displacements generally less than 13 centimeters. Nevertheless, many of these areas could be observed as linear features from the air riding in a helicopter.
- The principal displacement was often vertical, commonly on the order of 8 to 13 centimeters, with the western side of the crack/surface rupture higher than the eastern side.
- Horizontal displacements were generally a bit less than the vertical, commonly on the order of 5 centimeters, and generally right-lateral across the roadways. However, in at least one area to the north (Point A2, Partrick Road) and one area to the south (Point A10, Cuttings Wharf Road), the cracking across the roadway appeared to have left-lateral movements on the order of 4 to 5 centimeters – however, this may have been a function of how the pavement displaced over the deforming ground beneath it.
- Cracking was not always continuous, but often intermittent with cracking often disappearing beneath parking lots or roadways.
- The pattern of cracking varied – in some locations, there was one main crack while in other areas, the cracking became distributed over several sub-parallel cracks.
- Residents reported that the cracking had worsened in the days following the main shock on August 24th, perhaps as a result of aftershocks.
- The principal damage observed was pavement cracking, which frequently had been fitted with temporary emergency repairs to provide for interim use. Where the surface cracking ran through residential structures, homes commonly experienced damage, and in some cases were restricted for occupancy. In many developed areas where ground cracking extended, notably the Brown’s Valley area to the north, various utilities such as water mains were damaged and required emergency and/or interim repairs. South of State Highway 12/Highway 121 where the ground cracking crossed the alignment of a Pacific Gas and Electric natural gas pipeline, the pipeline was depressurized and, while no overt damage was reported after being inspected, a segment of the pipe was set to be replaced with a new pipe having a larger thickness.

Locations of Observed Surface Cracking

The following represents a summary of the observed ground cracking:

Alignment A:

1. Point A1: Redwood Road (N38° 19.967’, W122° 21.967’) – at the time of this observation (08-29-14), the roadway cracking had been repaired.
2. Point A2: Partrick Road (N38° 18.795’, W122° 21.087’) – ground cracking obliquely across Partrick Road and in front yards immediately west of the road. Three main cracks in road, each with about 1½ centimeters of left lateral movement for an overall horizontal displacement of about 4½ centimeters (08-29-14).

3. Point A3: Intersection of Meadowbrook Drive/Stonybrook Drive (N38^{o} 18.271’, W122^{o} 20.751’) – repaired pavement (08-29-14).
4. Point A4: Intersection of Twin Oaks Drive/Estates Drive (N38^{o} 18.153’, W122^{o} 20.676’) – repaired pavement (08-29-14)
5. Point A5: Northern end of Twin Oaks Court (N38^{o} 18.102’, W122^{o} 20.036’) – repaired pavement (08-29-14)
6. Point A6: Henry Road (N38^{o} 16.391’, W122^{o} 20.196’) – cracked roadway with approximately 1 to 1½ centimeters of right lateral horizontal displacement (09-01-14)
7. Point A7: Old Sonoma Road (N38^{o} 15.961’, 122.013’) – repaired roadway (09-01-14)
8. Point A8: State Highway 12/121 (N38^{o} 15.369’, W122^{o} 19.629’) – repaired highway near intersection with Cuttings Wharf Road, ground cracking leading south through vineyards towards Cuttings Wharf Road (08-29-14). Based on video footage from KTVU television, crack had vertical offset of about 10 centimeters (west side up) and right lateral displacement on the order of about 10 centimeters.
9. Point A9: Cuttings Wharf Road (N38^{o} 15.268’, W122^{o} 19.597’) – repaired roadway approximately 200 meters south of State Highway 12/121, vertical offset approximately 10 centimeters (west side up) with approximately 2½-centimeter left lateral displacement, ground cracking leading south towards horse pasture (08-30-14).
10. Point A10: Horse pasture adjacent and to the west of Cuttings Wharf Road (N38^{o} 15.208, W122^{o} 19.570’) – single, linear disruption of soil in horse pasture with right lateral displacement of electrical horse fence of about 4 centimeters (09-01-14).
11. Point A11: Withers Road (N38^{o} 15.089’, W122^{o} 19.519) – repaired roadway cracking, an extension of cracking from horse pasture immediately to the north (08-30-14).
12. Point A12: Los Carneros Road/Stone Bridge School (N38^{o} 14.591’, W122^{o} 19.254’) – ground cracking crossing obliquely across roadway and extending northerly across school parking lot (intermittent asphalt repairs) and across P.G. & E. natural gas pipeline (08-30-14 and 09-01-14).
13. Point A13: South Avenue (N38^{o} 14.506’, W122^{o} 19.203’) – repaired road, cracked driveway of adjacent property owner (08-30-14).
14. Point A14: Los Amigas Road (N38^{o} 14.056’, W122^{o} 19.986’) – immediately to the west of Carneros Creek, repaired road cracking.
15. Point A15: Milton Road (N38^{o} 11.879’, W122^{o} 18.974’) – This location is near the southern extent of Edgerley Island and approximately 2½ kilometers south of the epicenter. In this area, cracking of the road had been repaired with cracking extending eastward along cracked cinderblock wall separately residential properties. It is not clear if this cracking is an extension of the ground cracking/surface ruptures observed north of the epicenter.

Alignment B:

1. Point B1: Southeast intersection of Partrick Road and Rowena Lane (N38^{o} 18.410’, W122^{o} 20.257’) – repaired roadway (09-01-14).

2. Point B2: Browns Valley Road (N38^{o} 18.333', 122^{o} 20.222') - repaired cracked roadway, cracked driveways and residential property on both sides of street, approximately 30 meters east of Rowena Lane. A few centimeters of right lateral movement indicated (09-01-14).
3. Point B3: Thompson Road (N38^{o} 17.269', W122^{o} 19.620') – ground cracking in asphalt road with approximately 4 to 5 centimeters of right lateral displacements, cracks extending intermittently to the southeast, nearby house on alignment of cracking yellow-tagged for limited use (08-29-14).
4. Point B4: Congress Valley Road (N38^{o} 17.057', W122^{o} 19.471') – ground cracking of asphalt road extending into property and continuing to Old Sonoma Road. Displaced fence on Congress Valley Road property owner property adjacent to roadway indicates about 8 centimeters of vertical offset (west side up) and approximately 5 centimeters of right lateral displacement. Cracks in backyard between Congress Valley Road and Old Sonoma Road had up to 12 centimeters of vertical offset (08-29-14).
5. Point B5: Old Sonoma Road (N38^{o} 17.003', W122^{o} 19.453') – repaired section of roadway, location associated with cracking extending southeast from property and cracks in Congress Valley Road (08-29-14).

Ground Cracking Observed at Selected Locations

1) Point A4, Browns Valley

The Browns Valley area is northwest of downtown Napa and is an older residential area. Both of the alignments associated with surface rupture (Alignments A and B, see Figure 1) are believed to have extended into this area and caused damage to roadways, utilities, and residential structures. Presented in Figure 2 is an aerial photograph taken 8 days after the earthquake showing roadway repairs associated with ground cracking in the general vicinity of Alignment A. As may be seen, multiple roadway repairs (dark asphalt repairs) fall on a linear alignment between Twin Oaks Court and Sandybrook Lane. There were other linear alignments of ground cracking near this area, thus indicating multiple strands of surface rupture in this area.

Figure 2: Alignment of surface cracking observed along Alignment A in Browns Valley following August 24, 2014 Magnitude 6 Napa Earthquake - see dark asphalt patches [NSF-GEER; Napa, CA; N 38.304 W 122.344; Harder, L. F.; 09/01/14]

2) **Point B4, Congress Valley Road (N38° 17.057’, W122° 19.471’)** – In this area, ground cracking associated with Alignment B extended across Congress Valley Road, through the front fence of the property, through the property, and then across Old Sonoma Road. Selected photographs are as follows:

- Figure 3 presents a photograph of the cracked Congress Valley Road
- Figures 4 and 5 present photographs of the wooden front fence on the property indicating approximately 8 to 12 centimeters of vertical displacement (west side up) and about 5 to 8 centimeters of right lateral displacement as a result of ground cracking.
- Figures 6 and 7 present photographs of ground cracking between the Congress Valley Road property owner front fence and Old Sonoma Road (Point B5).

Figure 3: Photograph of cracking across Congress Valley Road in front of residence – looking southerly (Point B4)
[NSF-GEER; Napa, CA; N 38.284 W 122.325; Harder, L. F.; 08/29/14]

Figure 4: Photograph of wooden fence displaced by ground cracking in front of residence
(Congress Valley Road, Point B4) – looking easterly
– vertical fence displacements across ground cracking are approximately
8 to 12 centimeters with west side up
[NSF-GEER; Napa, CA; N 38.284 W 122.325; Harder, L. F.; 08/29/14]

Figure 5: Photograph of wooden fence displaced by ground cracking in front of residence (Congress Valley Road, Point B4) – looking easterly – right lateral fence displacement across ground cracking is approximately 5 to 8 centimeters [NSF-GEER; Napa, CA; N 38.284 W 122.325; Harder, L. F.; 08/29/14]

Figure 6: Photograph of ground cracking on property
(Congress Valley Road, Point B4) – looking southerly between front wooden fence
and towards damaged Old Sonoma Road (Point B5)
[NSF-GEER; Napa, CA; N 38.284 W 122.325; Harder, L. F.; 08/29/14]

Figure 7: Photograph of ground cracking on property
(Congress Valley Road, Point B4) – looking northerly from damaged Old Sonoma Road
(Point 5) - vertical offset up to 12 centimeters with west side up
[NSF-GEER; Napa, CA; N 38.284 W 122.325; Harder, L. F.; 08/29/14]

3) **Point A10: Horse pasture adjacent and to the west of Cuttings Wharf Road (N38° 15.208, W122° 19.570') –** single, linear disruption of soil in horse pasture with right lateral displacement of electrical horse fence of about 4 centimeters. Ground cracking extended from cracked pavements on State Highway 12/121 and Cuttings Wharf Road (Points A8 and A9) from the north, across the horse pasture, and continued southerly through vineyards to cracked pavement on Withers Road (Point A11). Figures 8 through 10 illustrate the cracking and displacements observed.

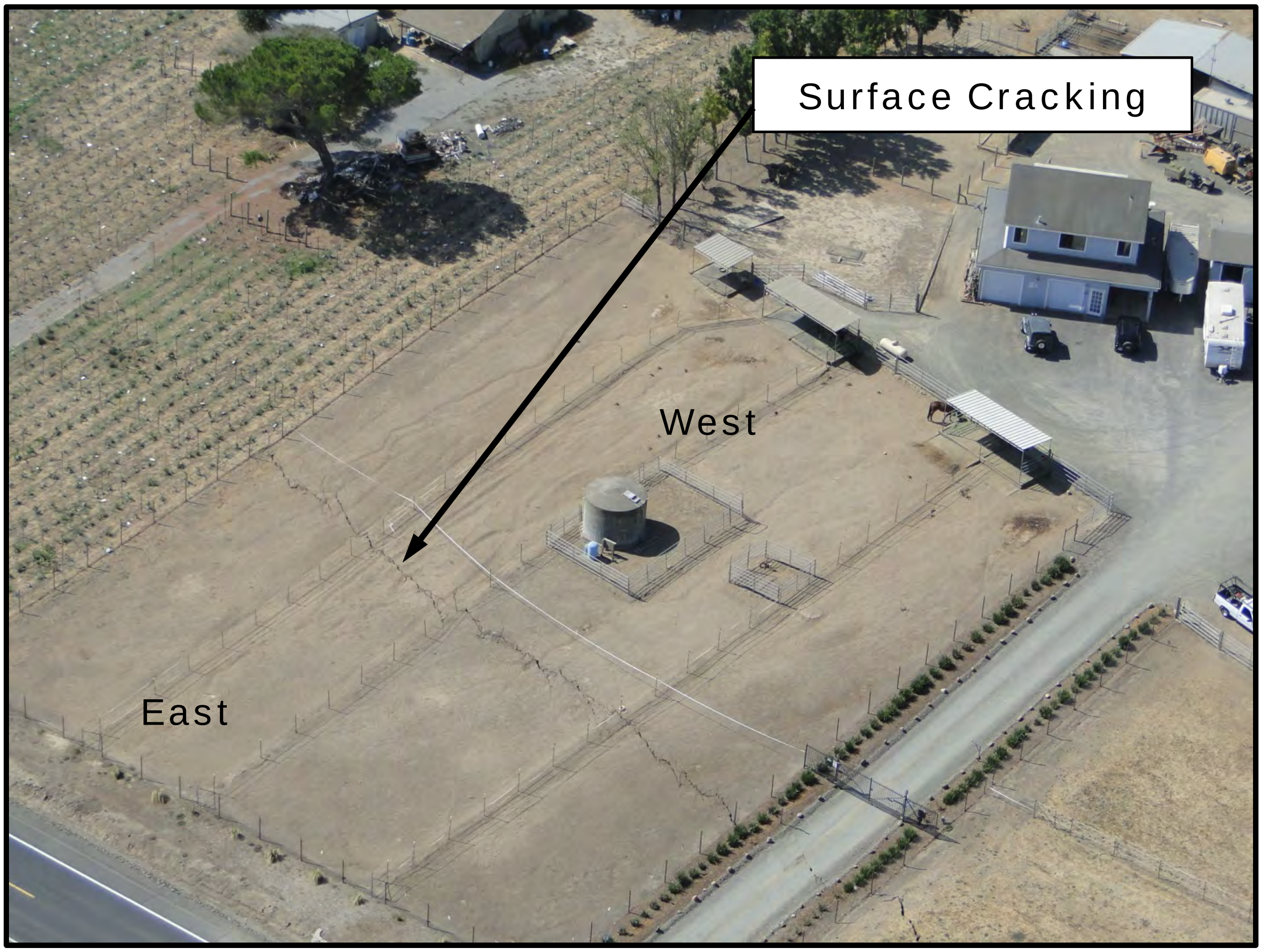

Figure 8: Aerial photograph of linear ground cracking in horse pasture along Cuttings Wharf Road south of Highway 12/121 (Point A10) – looking towards the southwest
[NSF-GEER; Napa, CA; N 38.253 W 122.326; Harder, L. F.; 09/01/14]

Figure 9: Photograph of linear ground cracking in horse pasture along Cuttings Wharf Road south of Highway 12/121 (Point A10) – view looking towards the southeast [NSF-GEER; Napa, CA; N 38.253 W 122.326; Harder, L. F.; 09/01/14]

Figure 10: Photograph of electrical fence in horse pasture along Cuttings Wharf Road south of Highway 12/121 (Point A10) with approximately 4 centimeters of right lateral offset induced by ground cracking – view towards the west
[NSF-GEER; Napa, CA; N 38.253 W 122.326; Harder, L. F.; 09/01/14]

4) **Point A12: Ground Cracking on Los Carneros Road near Stone Bridge School (N38° 14.591', W122° 19.254')** – At this location, ground cracking had displaced the Los Carneros Road and had also extended across the parking lot in front of the school. Damage to both the parking lot and roadway had been temporarily patched for interim use. A Pacific Gas and Electric (PG&E) natural gas pipeline exists immediately northward of the school and the ground cracking obliquely crossed its alignment. The pipeline is a steel pipeline approximately 66 centimeters in diameter and founded approximately 2 meters below the ground surface. The pipeline had been excavated with shoring to inspect the pipeline. According to PG&E personnel at the site on August 30th, preliminary inspections and testing reportedly indicated no damage to the steel pipeline, but the pipeline had been depressurized as a precaution and additional testing and evaluation was planned. During a September 7th visit to the site by a GEER team member, PG&E representatives stated that no damage had been detected as a result of further testing, but that it had been decided to replace the segment of the pipe near the surface cracking as a precaution. The new pipe has the same basic diameter, but has almost twice the thickness at 12.7 millimeters as the current pipeline has (~8 millimeters). Figures 11 through 14 present photographs illustrating the ground cracking observed at this location. Figures 15 and 16 show photographs of the unearthed PG&E pipeline after testing. Also shown in Figure 16 is a view of the new pipeline segments on site on September 7th and ready to be used to replace the segment across the fault.

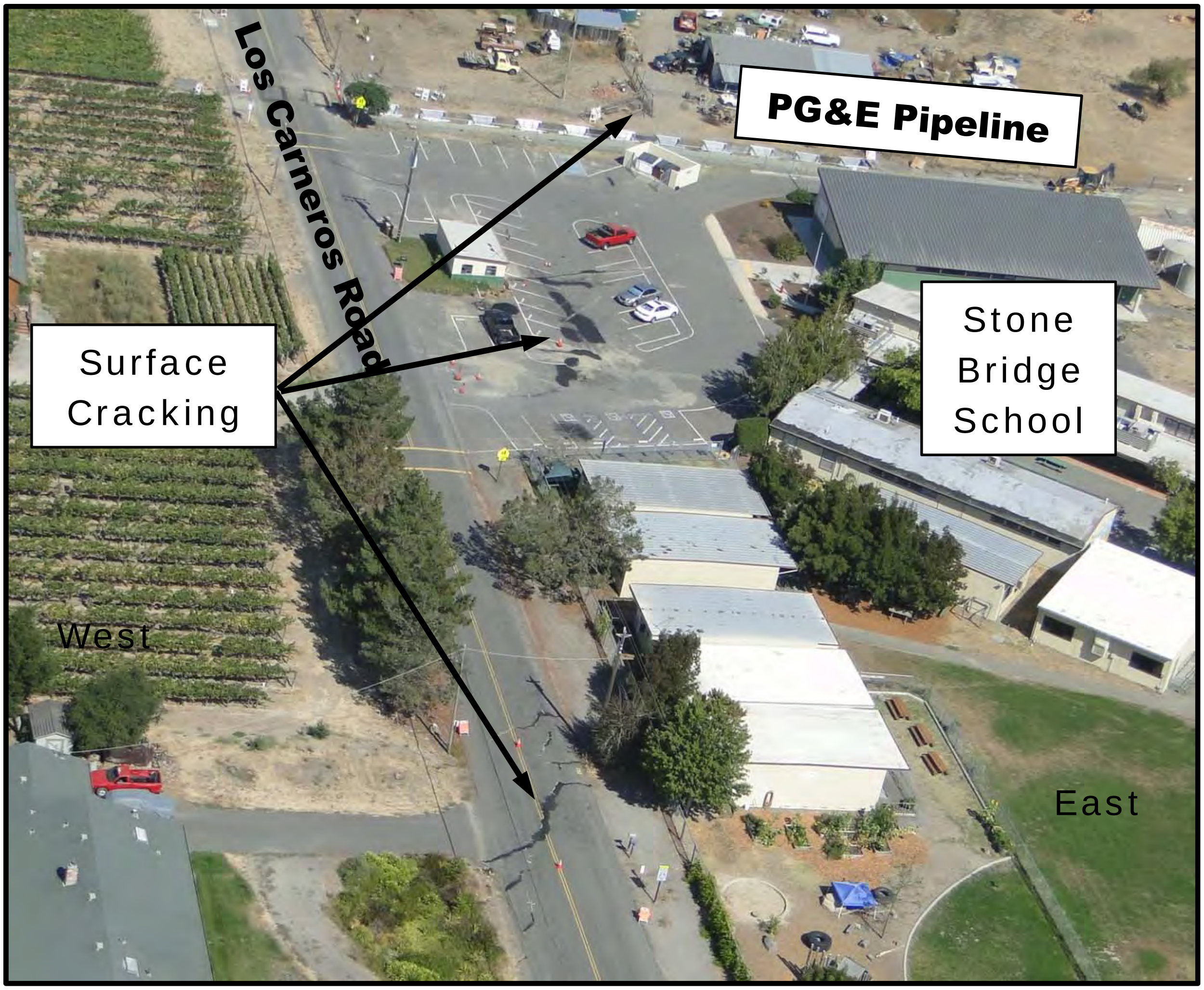

Figure 11: Aerial photograph of linear ground cracking across Los Carneros Road near Stone Bridge School (Point A12) – view looking towards the northeast
[NSF-GEER; Napa, CA; N 38.243 W 122.321; Harder, L. F.; 09/01/14]

Figure 12: Aerial photograph of ground cracking crossing PG&E natural gas pipeline on Los Carneros Road near Stone Bridge School (Point A12) – view looking towards the southeast [NSF-GEER; Napa, CA; N 38.243 W 122.321; Harder, L. F.; 09/01/14]

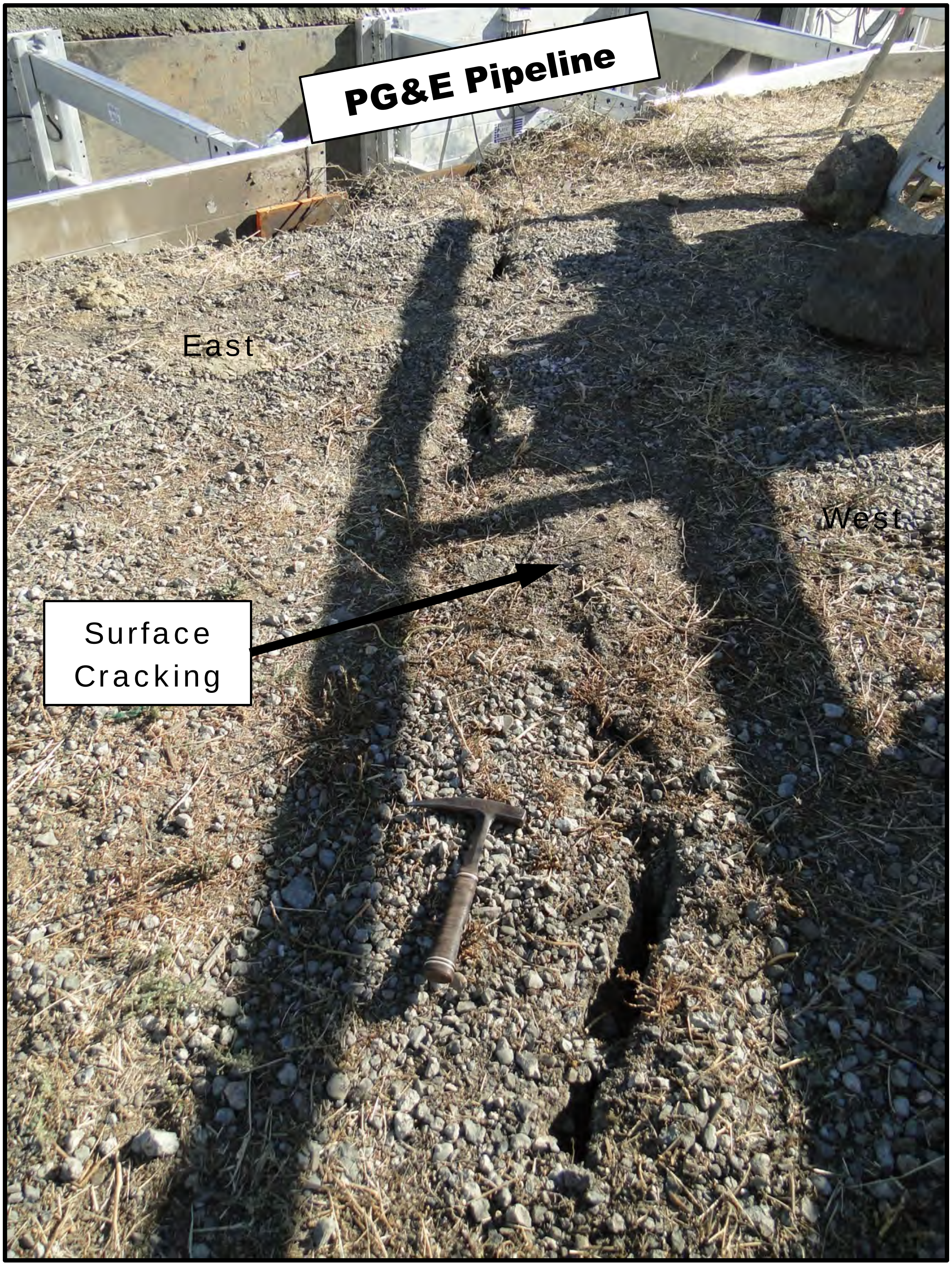

Figure 13: Photograph of linear ground cracking crossing PG&E natural gas pipeline near Los Carneros Road/Stone Bridge School (Point A12)
– view looking towards the southwest from northern side of pipeline
[NSF-GEER; Napa, CA; N 38.243 W 122.321; Harder, L. F.; 09/01/14]

Figure 14: Photograph of excavated and shored PG&E natural gas pipeline crossing
Los Carneros Road near Stone Bridge School (Point A12)
– view looking towards the east towards alignment of ground cracking
[NSF-GEER; Napa, CA; N 38.243 W 122.321; Harder, L. F.; 09/01/14]

Figure 15: Photograph of unwrapped/tested PG&E natural gas pipeline crossing Los Carneros Road near Stone Bridge School (Point A12) – view looking towards the west [NSF-GEER; Napa, CA; N 38.243 W 122.321; Harder, L. F.; 09/07/14]

Figure 16: Close-up view of unwrapped/tested PG&E natural gas pipeline crossing Los Carneros Road near Stone Bridge School (Point A12) – note also photograph of replacement pipe on site waiting to be installed [NSF-GEER; Napa, CA; N 38.243 W 122.321; Harder, L. F.; 09/07/14]

Contributing Sources:

Initial Observations: Keith Kelson (Sacramento District, USACE)

Information on ground cracking and access to property at Congress Valley Road: property owner at Congress Valley Road, Napa, CA.

B.3 Summary of South Napa Earthquake Field Reconnaissance on 8/25/14

Fugro Consultants, Inc. (David Trench, Michael Buga, Cooper Brossy)

The following series of observations and preliminary interpretations were collected by Fugro geologists on August 25, one day following the South Napa earthquake of August 24, 2014. At that time the locations of surface fault rupture verses locations of potential deformation from ground shaking were still being determined and the team's main goal was to differentiate between tectonic (surface fault) related and non-tectonic (i.e., ground shaking) features to aid in larger scale fault mapping efforts.

Location: Alston Park, CGS Trench site, 9:09 AM

Goal: Reconnaissance along mapped fault trace of West Napa fault to look for tectonic deformation

Completed brief recon of CGS trench site with John Wesling. No cracking or displacement of natural ground surfaces observed.

Location: Kingston Ave, 10:13 AM

Goal: Reconnaissance along mapped fault trace of West Napa fault near the previously mapped fault exposure on Napa Creek.

Kingston Ave. (38.306416 N, -122.319873 E;)

- Observed minor distributed ground cracking on freshly paved slope on Kingston Ave. In some cases, cracking radiates outward or projects toward manhole covers and utility boxes.
- Cracks up to 15 mm wide, orientations range from 015° - 310°; cracks vary in orientation adjacent to utility covers in the paved surface; population of cracks oriented appx.N-S.
- No apparent deformation in exposed hillslopes adjacent to deformed paved surfaces.
- No apparent lateral displacement of curbs and other linear markers that are oriented perpendicular to mapped fault traces

Interpretation: Distributed ground cracking with lack of clear evidence for tectonic deformation.

Kingston Ave., 10:57 AM (38.306277 N, -122.319082 E)

- Observed vertical displacements in paved surface appx.1.5 cm.
- Curb has apparent left-lateral separation, appx.2.5 cm
- Homeowner stated that vertical separation in paved surface had decreased since the event.

Interpretation: Observed deformation likely represent secondary deformation, not tectonic movement.

Location: Junction of Old Sonoma Rd. and Congress Valley Rd., 11:11 AM

Goal: Per recommendation from CGS assess deformation previously reported in the vicinity of Old Sonoma Rd. and Congress Valley Rd.; tectonic ground movement or secondary deformation?

Congress Valley Rd. (38.284287 N, -122.324500 E)

- Observed cracking in paved road surface perpendicular and parallel to NE-SW oriented Congress Valley Rd.; also evidence of buckling of paved road surface (Figure 1).
- Cracking observed in paved surface with up to appx.5 cm of separation.
- Measured appx.3.5 cm of right lateral separation of NW margin of yellow centerline on Congress Valley Rd. (Figure 2)
- Observed cracking of ground surface in the front yard of private residence on Congress Valley Rd directly adjacent to the south of deformation in paved surface; widths visually estimated at appx.3-5 cm; discontinuous lengths up to appx.2 m.
- No observed surface deformation in field and vineyard north of road; limited visual range due to roadside vegetation.

Backyard of private residence viewed from Old Sonoma Rd. (38.283517 N, -122.324225 E)

- Napa Public Works Dept. in the process of repairing damage to Old Sonoma Rd. upon arrival at 11:11 AM.
- Observed ground cracking north of Old Sonoma Rd. in the backyard of the private residence; linear alignment of left stepping en-echelon ground cracks up to appx.4 m long, with visually estimated vertical separation of appx.5 cm.
- Concrete lining in borrow ditch on south side of Old Sonoma Rd. cracked and deformed with apparent compression in the form of overlapped concrete sections. Apparent vertical movement of appx.8 cm (12:16 PM)

Interpretation: Continuity of deformation in natural ground surface and paved road surface suggest, observed deformation may represent surface fault rupture.

Location: Thompson Ave., 12:35 PM

Goal: Assess whether observed deformation in paved road surface along Thompson Ave. represents tectonic or secondary deformation.

Thompson Ave. (38.287868 N, -122.327012 E)

- Cracking in paved surface parallel and perpendicular to orientation of N-S oriented Thompson Rd. (Figure 3); also evidence of buckling of paved road surface; west side of road separated appx.11 cm from aggregate shoulder material. The zone of cracking ranges in orientation from 295°-305°. Measured appx.5 cm apparent right lateral separation of eastern margin of Thompson Ave. centerline (Figure 4); measured appx.4 cm apparent right lateral separation of western margin.

- Ground surface east of Thompson Ave. has apparent minor ground cracking; unclear if cracks represent tectonic deformation or existing desiccation cracking.

- Ground cracking propagated northwestward underneath private residence northwest of Thompson Ave and continued through the property to the northwest. Structural damage was observed within the house, and according to homeowner, apparent 2 inch movement off foundation. Deck pulled 6 cm from the house. Homeowner pointed to several ground cracks near the barn that appeared later in the day and others that had grown larger – suggesting after-slip.

- Individual ground cracks observed at private residence northwest of Thompson Ave were oriented in a left-stepping, en-echelon manner, oriented between 015° and 345° azimuth. Length of cracks varied between 3 – 12 m in length. The overall orientation of the zone of cracking was 345-350° azimuth. Measured right lateral offsets in natural ground surface ranging from 3-5 cm with a maximum vertical displacement of 7-8 cm.

Thompson Ave. ~1:05 PM (38.287536 N, -122.326769 E)

- Retaining wall on north side of house cracked and separated by appx.4mm in 4 locations; on coincident trend with cracks documented on Thompson Ave to the north. Discontinuous cracking observed in vineyard southeast of main house; cracks appx.6 m long; widths appx.3-5 cm. Homeowner noted that recently stacked wood pile was disrupted by event; additionally noted that landscaping feature with stacked rocks appx.30 m north of woodpile had no damage. A broken (in apparent tension) 1 inch PVC waterpipe at NW corner of residence was buried only 6” deep. A narrow concrete lawn edging on southeast side of yard was apparently right laterally separated by appx.4.5 cm (2:27 PM).

Thompson Ave. Area 2:34 PM

- Observed cracking in paved driveway surface perpendicular to NNE driveway orientation (38.286761 N, -122.325890 E). Four cracks in paved surface; widths range appx.2.5-3 cm; total width of deformation appx.53 ft (appx.16 m) (Figure 5); western-most crack coincident with CMP culvert beneath driveway.

- Apparent ground cracks south of driveway that are in-filled with overlying loose roto-tilled soil. Cracks no wider than appx.15 cm likely less than 10 cm appear to be oriented along strike with cracking documented in paved surface and at south end of vineyard of private residence southeast of Thompson Ave.

Interpretation: Apparent continuity of deformation along strike across paved road surface as well as adjacent natural ground surfaces suggests deformation represents tectonic surface fault rupture.

Location: Browns Valley neighborhood; NNW of Browns Valley Elementary School

Goal: Assess whether deformation previously observed in the Browns Valley neighborhood represents tectonic deformation or secondary deformation associated with ground shaking.

Glenbrook Ln. (38.305354 N, -122.342570 E), 3:27 PM

- Observed buckling of curb and gutter on south side of street in front of house; no apparent cracking in paved street surface north of deformed curb

- Measured deformed length of curb (22.3 ft) and compared to undeformed length (22.5 ft); 0.2 ft +/- 0.03 ft (appx.6-9 cm**) of contraction of curb. **This is only a near-field measurement over appx.22 ft within a 132 ft (appx.40 m) wide zone of deformed curbs and tented sidewalk panels.

- Another measurement of the same curb resulted in 0.3 ft (appx.9 cm) of contraction of curb. Measurements highly influenced by how well curb materials can be reconstructed.

Glenbrook Ln. (38.305288 N, -122.342878 E)

- Observed additional tenting of sidewalk panels on south side of street in front of private residence; no apparent cracking in adjacent paved street surface to north.
- Original length of panels 15.1 ft (appx.4.6 m); deformed length 14.1 ft (appx.4.3 m); 0.3 ft (appx.9-10) cm of shortening.

Total documented shortening based on measurements of buckled curbs appx. 15-19 cm along south side of street over distance of 132 ft (appx.40 m). Not clear if shortening at this site related to tectonic deformation or ground shaking.

Glenbrook Ln. (38.305408 N, -122.342963 E)

- Observed additional tenting of sidewalk panels on north side of Glenbrook Ln. No apparent cracking in adjacent paved street surface
- Original length of panels 10.35 ft (appx.3.15 m); deformed length 10.15 ft (3.09 m); 0.2 ft (appx.6 cm) of shortening.

Sandybrook Ln. (38.304649 N, -122.342822 E)

- Observed apparent right lateral offset of curb appx.11-12 cm.
- Paved road surface to south placed over (thrust) sidewalk and driveway in front of house.
- Buckling in paved road surface; unknown amount of shortening.

Sandybrook Ln. (38.304558 N, -122.342843 E)

- Observed ground cracking with apparent vertical displacement in side yard of private residence.
- Observed cracking but no apparent displacement of retaining wall at northern margin of yard adjacent to cracking in paved road surface and buckling of curb.
- Two sidewalk panels overturned in front of the retaining wall.
- Cracking projects towards private residence on north side of street.

Meadowbrook Rd. (38.303892 N, -122.343070 E)

- Observed buckling of paved road surface; unquantified amount of shortening.
- Observed ground cracking in yard of private residence north side of Meadowbrook Rd.; no address apparent.

Interpretation: Apparent alignment of cracking in paved surfaces and observed ground cracking in adjacent yards suggests surface deformation features through Browns Valley neighborhood may be due to surface fault rupture. However, it is likely that deformed curbs, paved surfaces, and houses may not represent true displacements and kinematics of potential tectonic deformation. The associated measurements should be qualified as such.

Location: Vicinity of Leaning Oak Rd., 5:15 PM

Goal: Assess whether deformation previously observed south of Browns Valley neighborhood represents tectonic deformation or secondary deformation associated with ground shaking.

Leaning Oak. Rd. (38.298249 N, -122.344272 E)

- Observed linear deformation of ground surface in natural ground surface / graded lot as linear mole track. Deformation apparently confined to zone appx.1-2 m wide and extends appx.50-60 m northward from paved road surface (Figure 5).
- Paved road surface to south buckled and cracked along strike with observed deformation in natural ground surface; width of deformation in paved surface appx.47 ft (appx.14 m).
- Plumbers on site repairing broken water pipe perpendicular to observed deformation in paved surface and natural ground surface; plumbers interpreted that the pipe had compressed and shattered during event.
- At appx.5:30 PM documented a maximum of 1.1ft (appx.33) cm of right lateral separation of aligned bricks at southern margin of crushed granite driveway (Figure 6). High confidence in this measurement because the only surface fault rupture observed in the natural ground surface was limited to a 1-2 meter wide zone that projected perpendicularly through the center of the driveway bricks such that the brick strain marker likely captured most of the deformation at that site.

Slope of private driveway north of Leaning Oak Rd. (38.299274 N, -122.344391 E)

- Observed linear mole track alluvial fan surface adjacent to unnamed creek. Visual estimate of deformation feature appx.20 m long, with apparent vertical displacement appx.3-4 cm (Figure 7); no apparent piercing lines to quantify lateral separation.

Interpretation: Continuity of deformation features in natural ground surface and paved road surfaces suggest tectonic movement and not secondary deformation associated with ground shaking. Deformation apparently confined in natural ground surfaces to narrow (i.e, 1-2 m-wide) zone.

Summary of interpretations:

Kingston Ave: Distributed ground cracking with lack of clear evidence for tectonic deformation. Observed deformation may represent secondary deformation, not tectonic movement.

Congress Valley Rd and Old Sonoma Rd: Continuity and alignment of linear deformation features in paved road surface and natural ground surface suggest observed deformation may represent surface fault rupture.

Thompson Ave: Continuity and alignment of linear deformation features in paved road surface and adjacent natural ground surface suggest observed deformation may represent surface fault rupture.

B.3 Summary of South Napa Earthquake Field Reconnaissance on 8/25/14

Fugro Consultants, Inc. (David Trench, Michael Buga, Cooper Brossy)

Measurements in the Congress Valley Rd-Old Sonoma Rd-Thompson Rd area suggest an approximate minimum of 3 to 5 cm right lateral displacement and with minor local vertical displacements of < 8 cm, depending on soil type and material response. These near-field measurements should be confirmed and supplemented with more far-field measurements.

Browns Valley subdivision: Apparent alignment of cracking in paved surfaces and observed ground cracking in adjacent yards suggests surface deformation features through Browns Valley neighborhood may be the result of surface fault rupture. However, unclear if deformed curbs, paved surfaces, and houses represent actual displacements and/or kinematics of tectonic deformation. The associated measurements should be qualified as such.

Leaning Oak Rd: Continuity and alignment of linear deformation features in paved road surface and natural ground surface suggest observed deformation may represent fault surface rupture. Deformation apparently confined in natural ground surfaces to narrow 1- to 2-m-wide zone and right lateral displacement of up to appx.33 cm observed.

B.3 Summary of South Napa Earthquake Field Reconnaissance on 8/25/14

Fugro Consultants, Inc. (David Trench, Michael Buga, Cooper Brossy)

Figure 1. Photograph showing cracking in paved road surface perpendicular and parallel to NE-SW oriented Congress Valley Rd. [NSF-GEER; N38.2842, W122.3245; 08/25/14; 11:49 AM]

Figure 2. Photograph showing approximately 3.5 cm of right lateral separation of NW margin of yellow centerline on Congress Valley Rd. [NSF-GEER; N38.2842, W122.3245; 08/25/14; 11:37 AM]

Figure 3. Photograph showing cracking in paved surface of N-S oriented Thompson Rd. [NSF-GEER; N38.2878, W122.3269; 08/25/14; 1:02 PM]

Figure 4. Photograph showing approximately 5 cm apparent right lateral separation of eastern margin of Thompson Ave. centerline. [NSF-GEER; N38.2878, W122.3269; 08/25/14; 1:02 PM]

B.3 Summary of South Napa Earthquake Field Reconnaissance on 8/25/14

Fugro Consultants, Inc. (David Trench, Michael Buga, Cooper Brossy)

Figure 5: Photograph showing linear deformation of ground surface in natural ground surface / graded lot as linear mole track. Deformation apparently confined to zone appx.1-2 m wide and extends appx.50-60 m. [NSF-GEER; N38.2983, W122.3442; 08/25/14; 4:13 PM]

Figure 6. Photograph showing right lateral displacement of aligned bricks at southern margin of crushed granite driveway on Leaning Oak Rd. Measured a maximum of 1.1ft (appx.33) cm of right-lateral displacement. [NSF-GEER; N38.2982, W122.3442; 08/25/14; 4:26 PM]

Figure 7. Photograph showing linear mole track in alluvial surface adjacent to unnamed creek. Location is along trend with deformation shown in Figures 5 and 6. Feature estimated at appx.20 m long, with apparent vertical displacement of appx.3-4 cm. [NSF-GEER; N38.2992, W122.3441; 08/25/14; 5:39 PM]

Appendix C: Effects of Surface Fault Rupture on Infrastructure

Numbering of the Appendix C contents for individually mapped houses are denoted with an "H##" that represents the house reference number. The first figure for each house includes a site map (Figure C-H##-1); subsequent figures numbers are photographs associated with the house. As an example, the second photo for house no. 7 would be: "Figure C-H07-3."

Pavement was mapped in 3 locations; the numbering for these maps are the same, except the letter "P" is used.

Table of Contents

Figure C-A - Overview of Mapping Area

Site Specific Maps & Photo Contents			
No.	Contents	House No.	Contents
H-01	Site map and 2 photos	H-25	Site map and 2 photos
H-02	Site map and 2 photos	H-27	Site map and 2 photos
H-03	Site map and 4 photos	H-28	Site map and 2 photos
H-04	Site map and 4 photos	H-29	Site map and 2 photos
H-05	Site map and 2 photos	H-30	Site map and 2 photos
H-06	Site map and 2 photos	H-31	Site map and 2 photos
H-07	Site map and 2 photos	H-32	Site map and 4 photos
H-14	Site map and 2 photos	H-33	Site map and 2 photos
H-15	Site map and 2 photos	H-34	Site map and 1 photo
H-16	Site map	H-35	Site map and 3 photos
H-17	Site map and 1 photos	H-36	Site map and 1 photos
H-20	Site map	H-37	Site map and 2photos
H-21	Site map and 2 photos	P-1	Site map and 3 photos
H-22	Site map and photos	P-2	Site map and 2 photos
H-23	Site map and 1 photo	P-3	Site map and 2 photos
H-24	Site map and 3 photos		

Total Figures in Appendix C: 105

Total Pages (including this one): 64

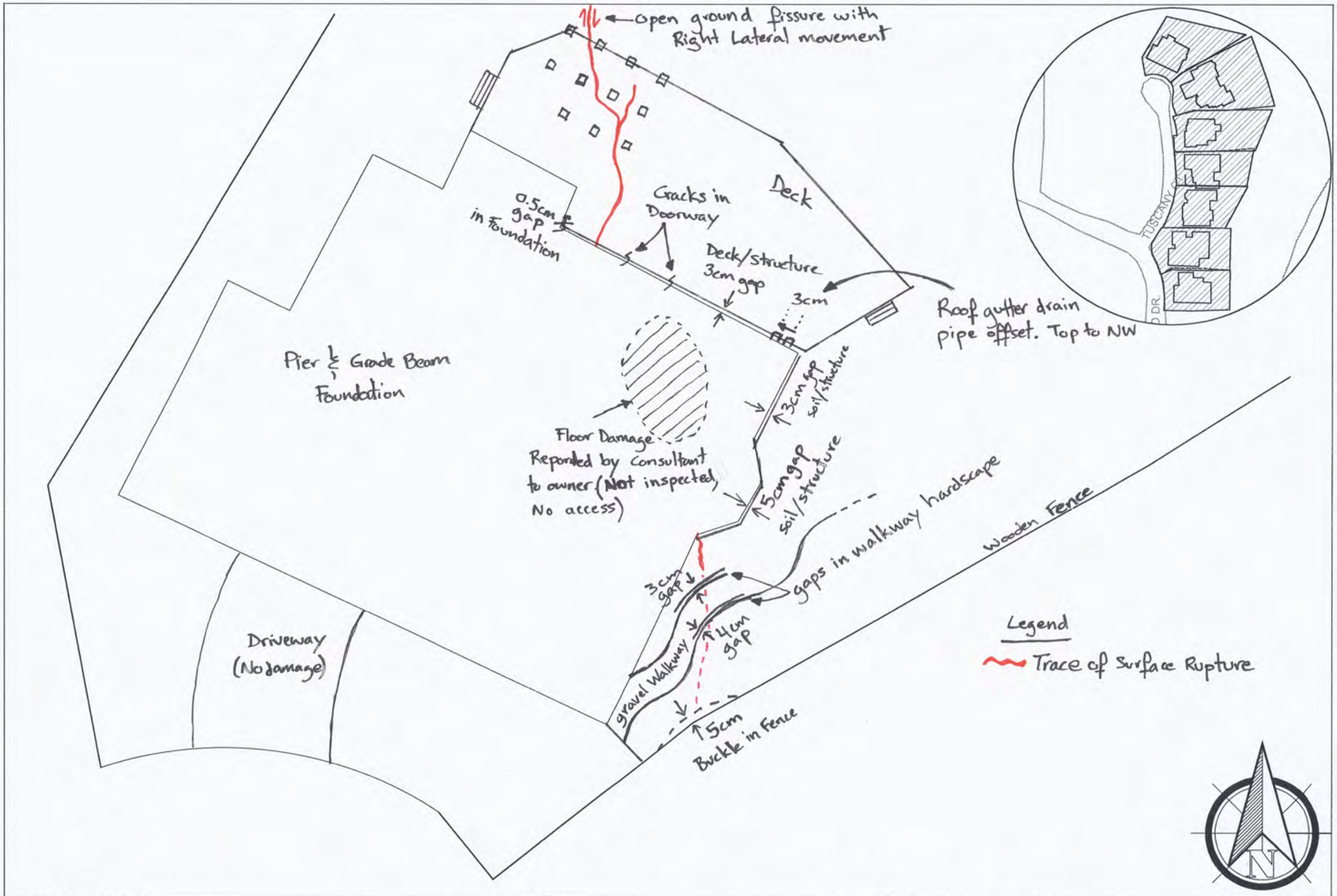

EVENT: AMERICAN CANYON EQ $M_W = 6.0$

ADDRESS: 38.3135 -122.3431 H01

DRAWING BY: J. Cohen-Waeber J. Weber , G. Harris

DESCRIPTION: Surface Fault Rupture through Private Residence

DATE OF INSPECTION: 08/28/2014

DATE OF DRAWING: 08/28/2014

SCALE: 1 cm : 2 m

5 m

Figure C-H01-2: Roof Beam separated from wall due to shearing. [NSF-GEER; N 38.3135 W 122.3431; 08/28/14 17:08]

Figure C-H01-3: South looking view of ground rupture under deck coming from under severely damaged house on pier foundations. [NSF-GEER; N 38.3135 W 122.3431; 08/28/14 17:15]

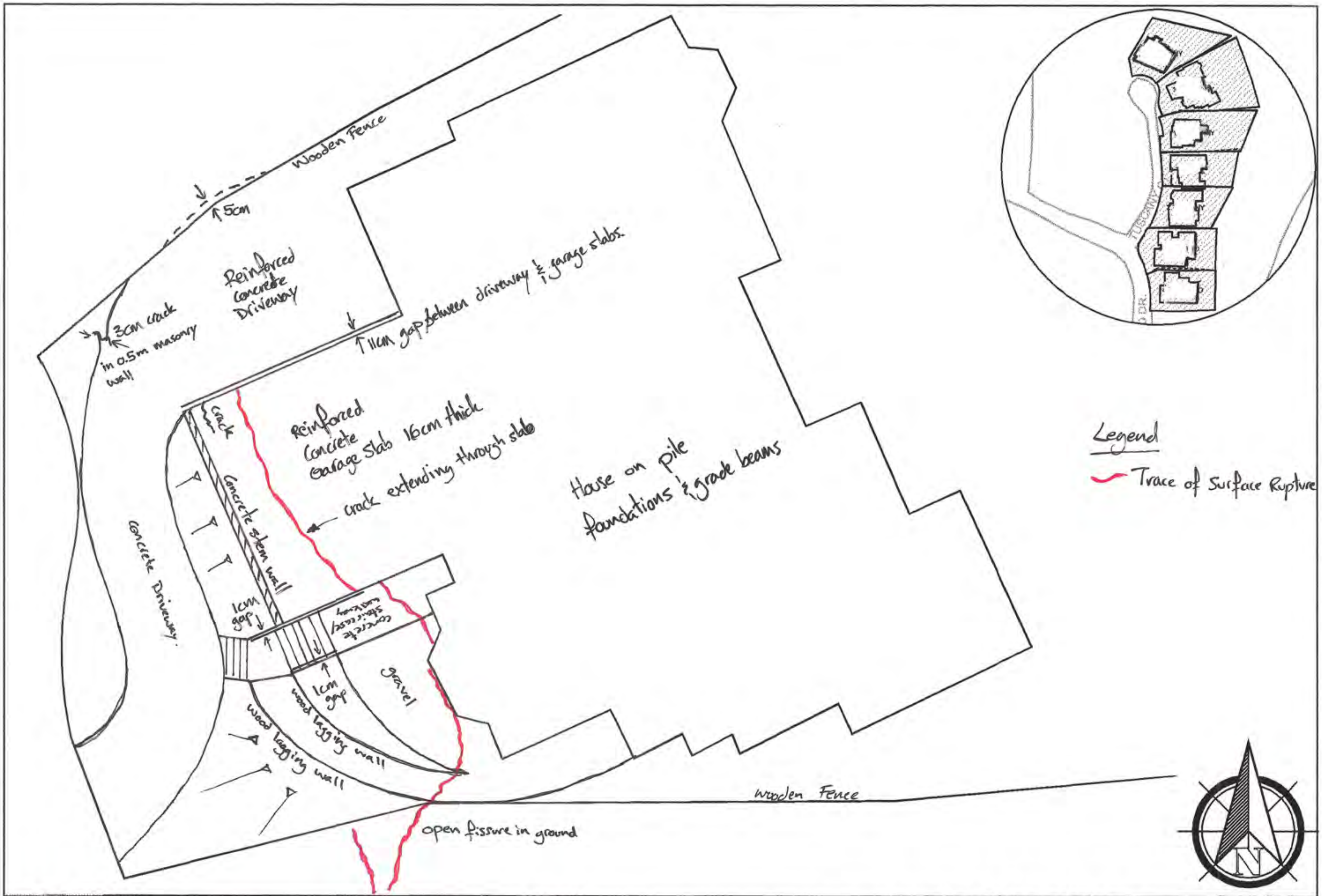

EVENT: AMERICAN CANYON EQ M_W = 6.0	ADDRESS: 38.3133 -122.3431 (H02)		DRAWING BY: J. Cohen-Waeber J. Weber, G. Harris, S. Foti
DESCRIPTION: Surface Fault Rupture through Private Residence-	DATE OF INSPECTION: 08/28/2014	DATE OF DRAWING: 08/28/2014	SCALE: 1 cm : 2 m 5 m

Figure C-H02-2: East looking view of crack extending through walkway and garage. [NSF-GEER; N 38.3133 W 122.3431; 08/28/14 12:46]

Figure C-H02-3: West looking view of driveway/garage slab separation and crack extending through 6 inch reinforced slab. [NSF-GEER; N 38.3133 W 122.3431; 08/28/14 12:44]

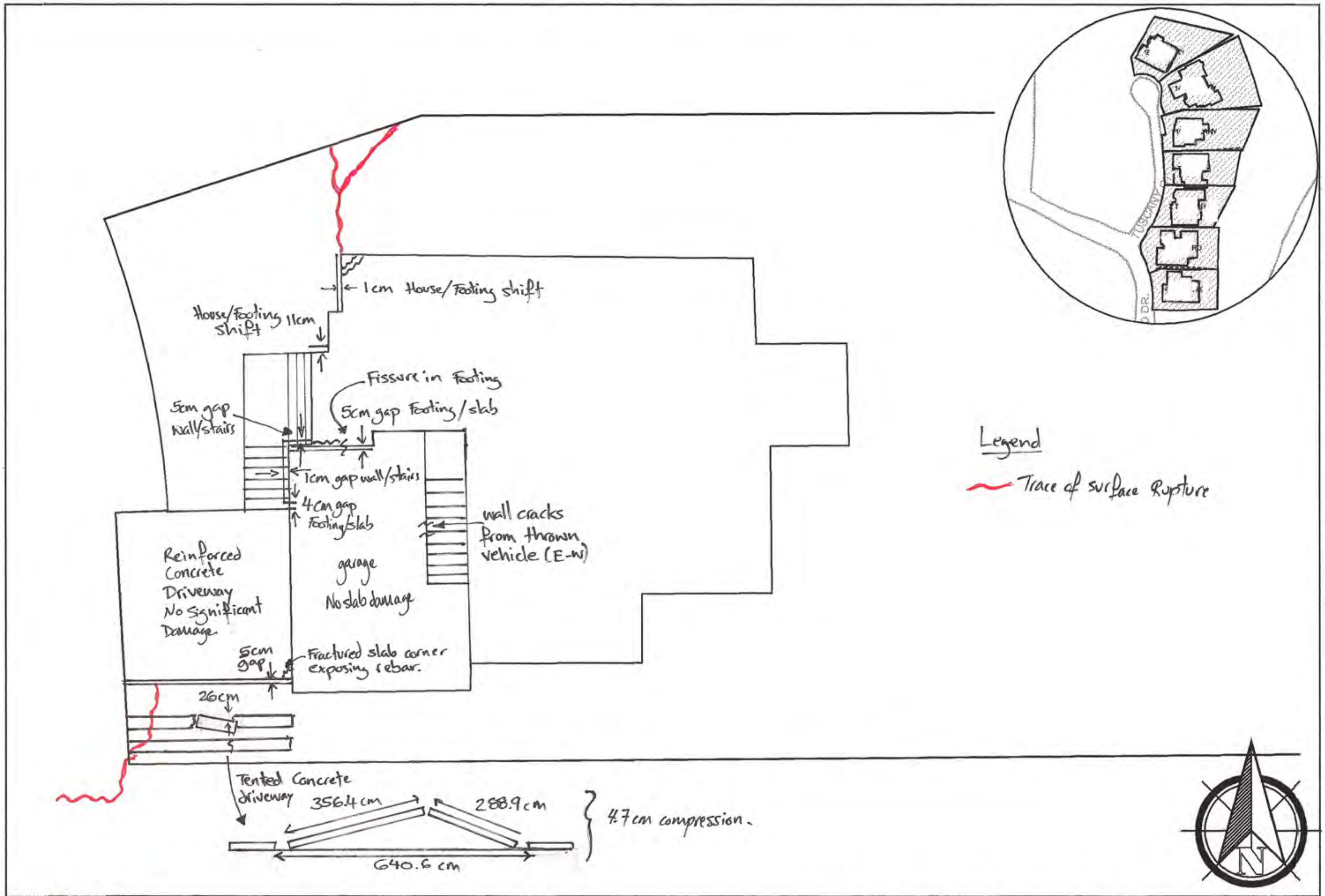

EVENT: AMERICAN CANYON EQ M_W = 6.0

ADDRESS: 38.3131 -122.3431 (H03)

DRAWING BY: J. Cohen-Waeber, J. Weber, G. Harris, S. Foti

DESCRIPTION: Surface Fault Rupture through Private Residence

DATE OF INSPECTION: 08/28/2014

DATE OF DRAWING: 08/28/2014

SCALE: 1 cm : 2 m

5 m

Figure C-H03-2: SE looking view of stair case/structure separation and cracks. [NSF-GEER; N 38.3131 W 122.3431; 08/28/14 11:52]

Figure C-H03-3: SE looking view of structure pushed off of foundation. [NSF-GEER; N 38.3131 W 122.3431; 08/28/14, 11:54]

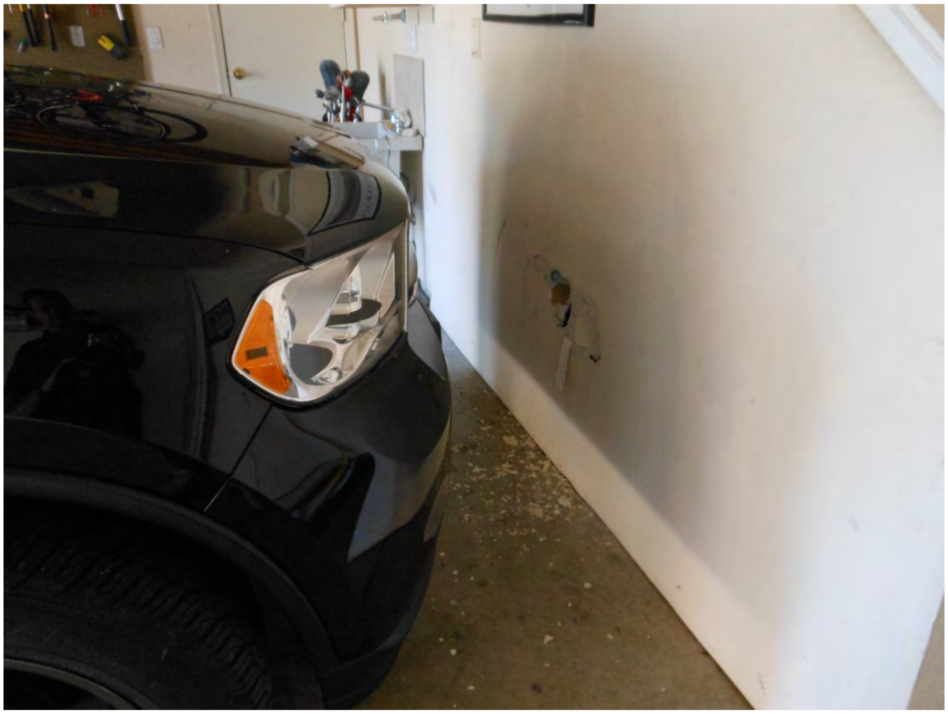

Figure C-H03-4: Vehicle thrown E-W into wall. [NSF-GEER; N 38.3131 W 122.3431; 08/28/14]

Figure C-H03-5: Fence buckled in compression. [NSF-GEER; N 38.3131 W 122.3431; 08/28/14]

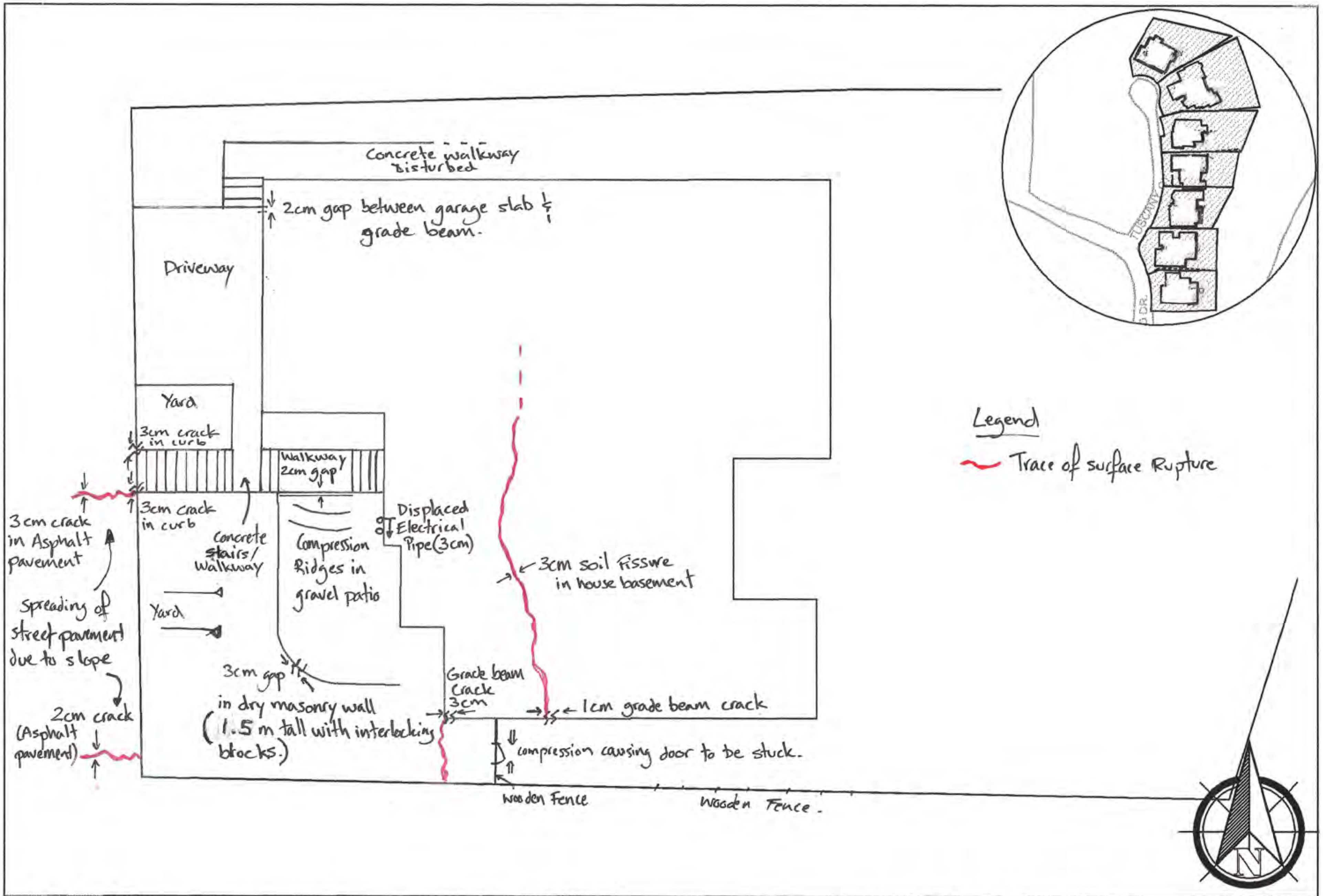

EVENT: AMERICAN CANYON EQ $M_W = 6.0$	ADDRESS: 38.3128 -122.3431 (404)		DRAWING BY: J. Cohen-Waeber J. Waeber, G. Harris, S. Fati
DESCRIPTION: Surface Fault Rupture through private property.	DATE OF INSPECTION: 08/28/2014	DATE OF DRAWING: 08/28/2014	SCALE: 1 cm : 2 m 5 m

Figure C-H04-2: Displaced masonry wall. [NSF-GEER; N 38.3128 W 122.3431; 08/28/14, 16:32]

Figure C-H04-3: Compression ridge in gravel above wall. [NSF-GEER; N 38.3128 W 122.3431; 08/28/14, 14:40]

Figure C-H04-4: Cracked foundation. [NSF-GEER; N 38.3128 W 122.3431; 08/28/14]

Figure C-H04-5: Soil fissure in basement. [NSF-GEER; N 38.3128 W 122.3431; 08/28/14, 12:08]

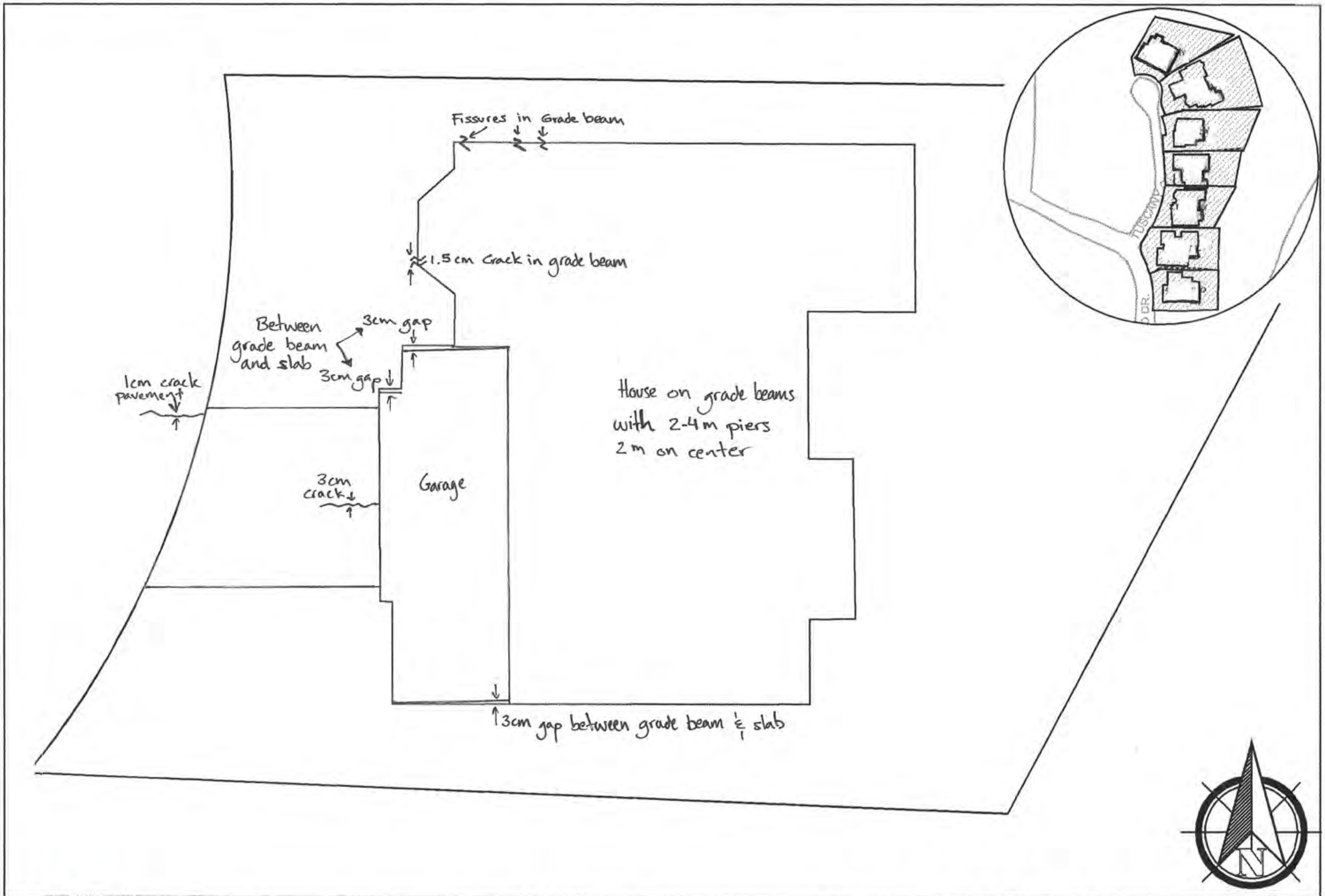

EVENT: AMERICAN CANYON EQ $M_W = 6.0$

ADDRESS: 38.3126 -122.3431 (405)

DRAWING BY: J. Cohen-Waeber
J.Waeber, G.Harris, S. Foti

DESCRIPTION: Surface Fault Rupture through Private property.

DATE OF INSPECTION: 08/28/2014

DATE OF DRAWING: 08/28/2014

SCALE: 1 cm : 2 m

5 m

Figure C-H05-2: Cracked slab foundation in garage. [NSF-GEER; N 38.3126 W 122.3431; 08/28/14, 15:20]

Figure C-H05-3: Cracked slab and separation from footing. [NSF-GEER; N 38.3126 W 122.3431; 08/28/14, 15:20]

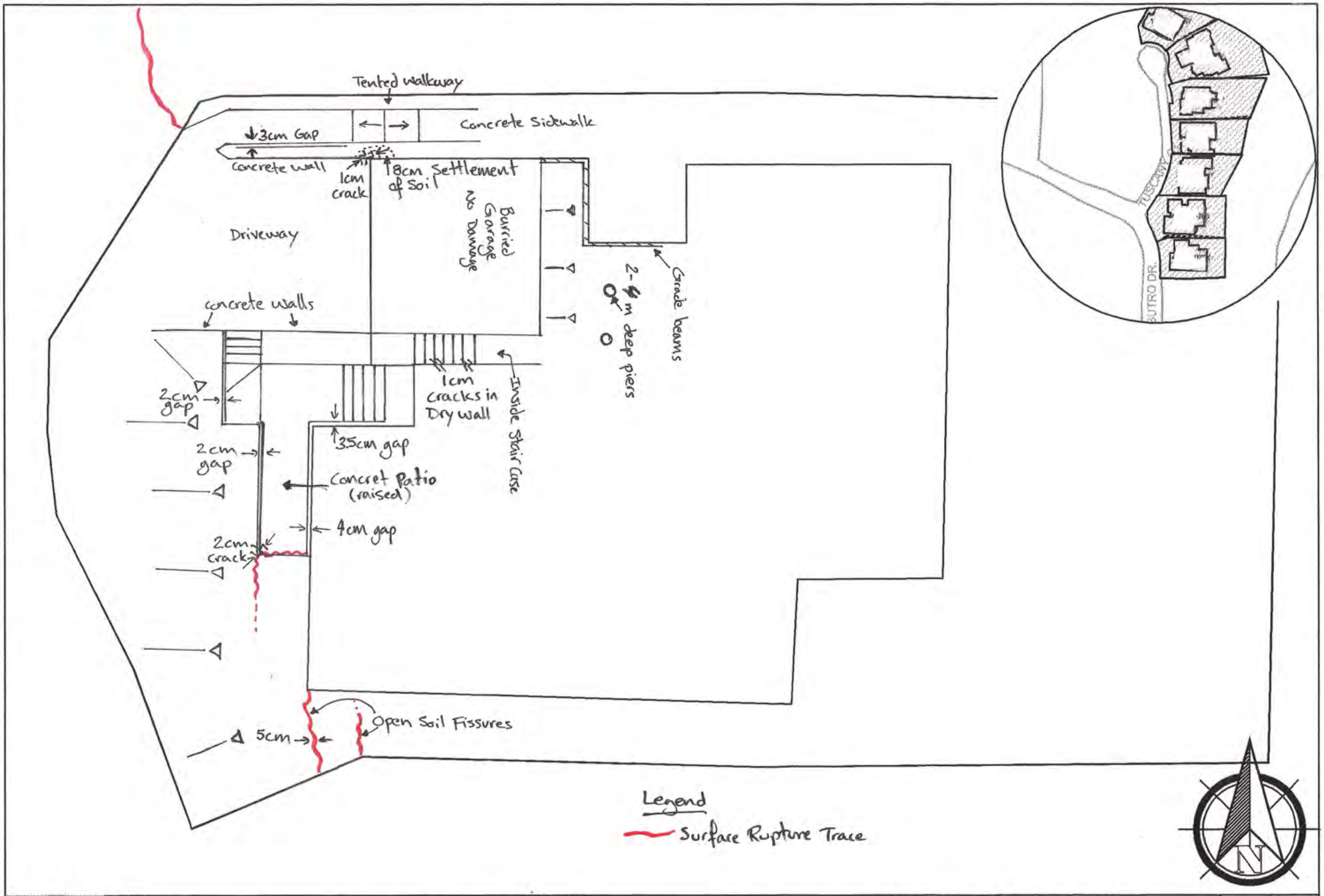

EVENT: AMERICAN CANYON EQ M_W = 6.0

ADDRESS: 38.3124 -122.3432 (406)

DRAWING BY: J. Cohen-Waeber
J. Weber, G. Harris, S. Foti

DESCRIPTION: Surface Fault Rupture through private property

DATE OF INSPECTION: 08/28/2014

DATE OF DRAWING: 08/28/2014

SCALE: 1 cm : 2 m

5 m

Figure C-H06-2: Soil fissure looking North. [NSF-GEER; N 38.3124 W 122.3431; 08/28/14, 17:31]

Figure C-H06-3: Staircase displaced from structure. [NSF-GEER; N 38.3124 W 122.3431; 08/28/14]

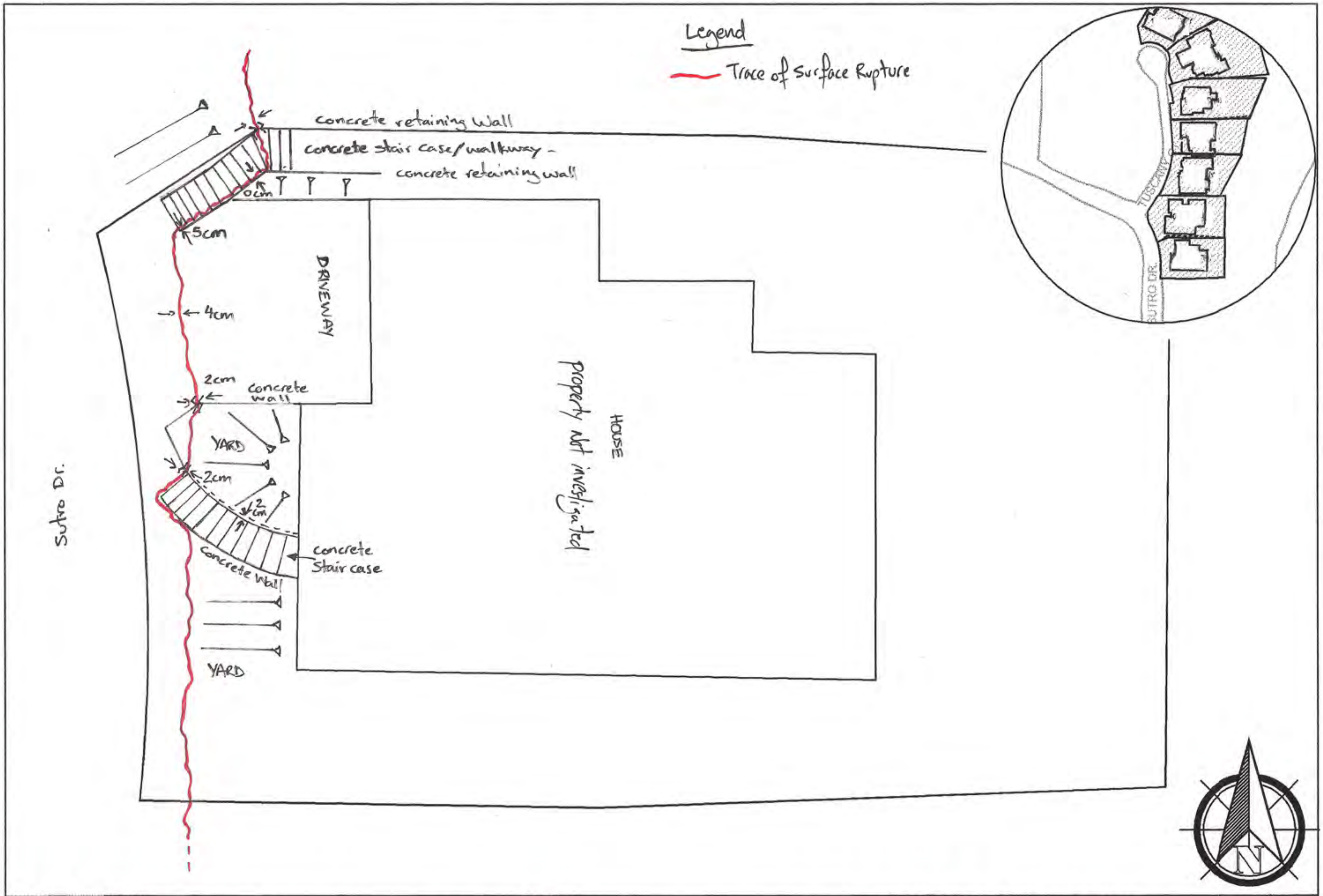

EVENT: AMERICAN CANYON EQ $M_W = 6.0$

ADDRESS: 38.3122 -122.3432 (H07)

DRAWING BY: J. Cohen-Waeber
J.Weber, G. Harris, S. Foti

DESCRIPTION: Surface Fault Rupture through Private Property.

DATE OF INSPECTION: 08/28/2014

DATE OF DRAWING: 08/28/2014

SCALE: 1 cm : 2 m

5 m

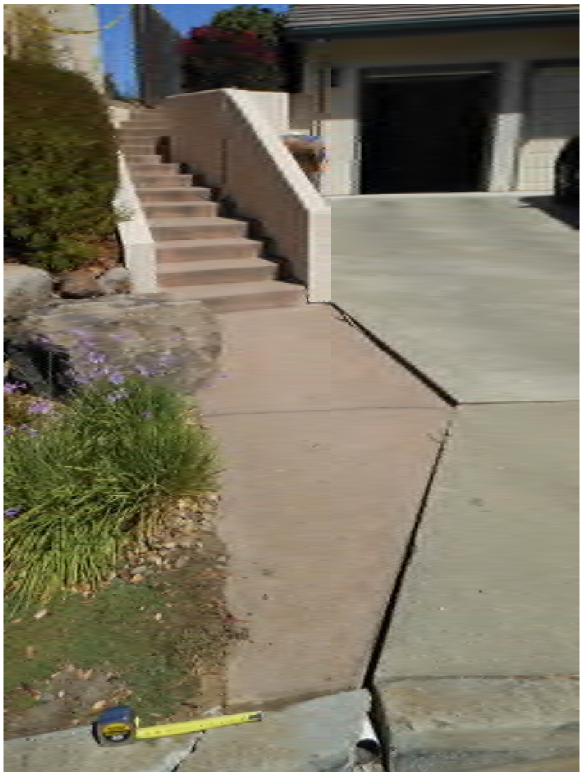

Figure C-H07-2: Crack extending along stair case and joint. [NSF-GEER; N 38.3122 W 122.3432; 08/28/14]

Figure C-H07-3: Crack extending along stair case and joint. [NSF-GEER; N 38.3122 W 122.3432; 08/28/14]

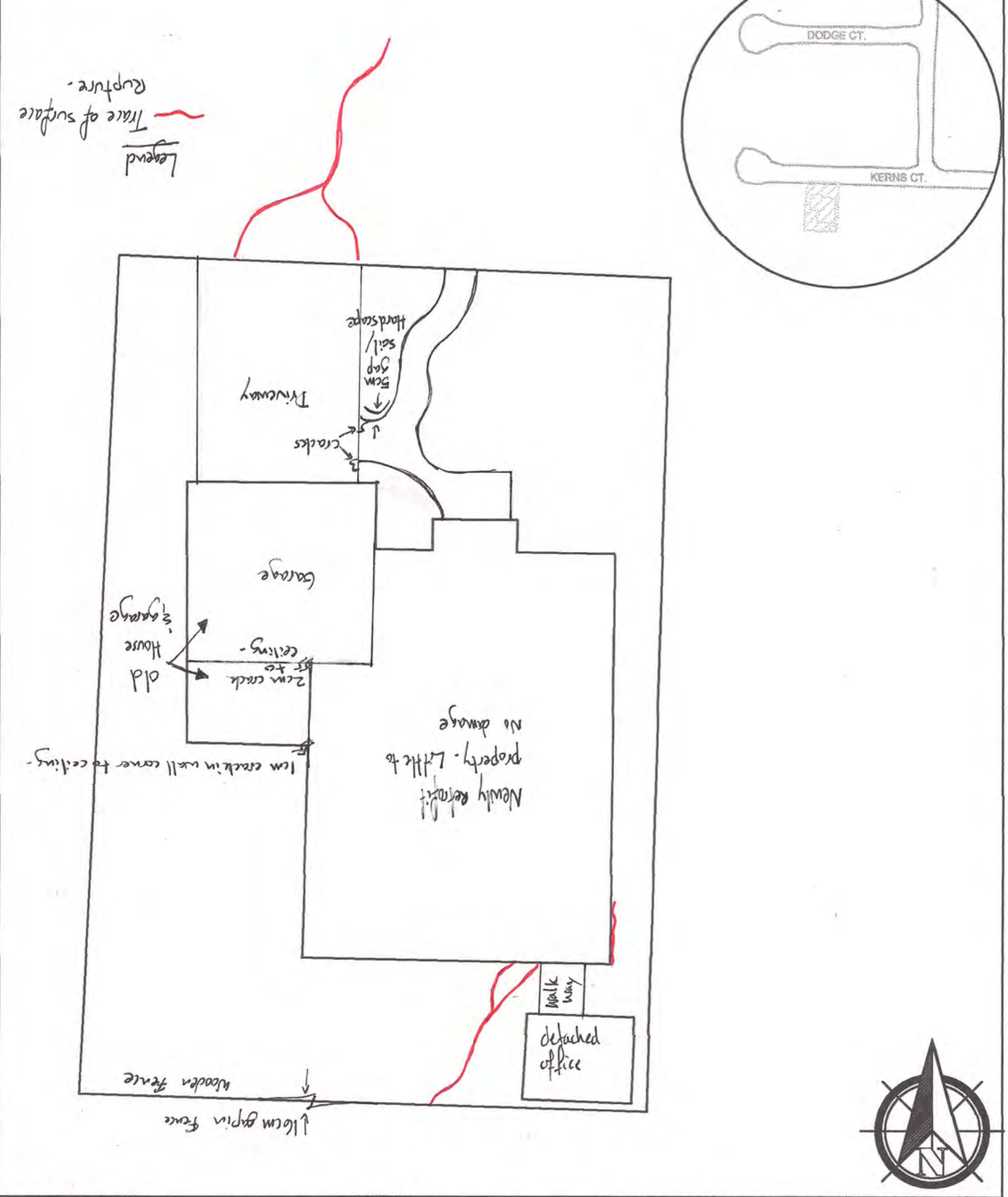

EVENT: AMERICAN CANYON EQ $M_W = 6.0$

ADDRESS: 38.3082 -122.3427 (H14)

DRAWING BY: J. Cohen-Waeber

DESCRIPTION: Surface Fault Rupture through Private Property.

DATE OF INSPECTION: 08/28/2014

DATE OF DRAWING: 08/28/2014

SCALE: 1 cm : 2 m

5 m

Figure C-H14-2: Crack along boundary with new construction. [NSF-GEER; N 38.3082 W 122.3427; 08/28/14, 18:26]

Figure C-H14-3: Street Crack. [NSF-GEER; N 38.3082 W 122.3427; 08/28/14, 18:27]

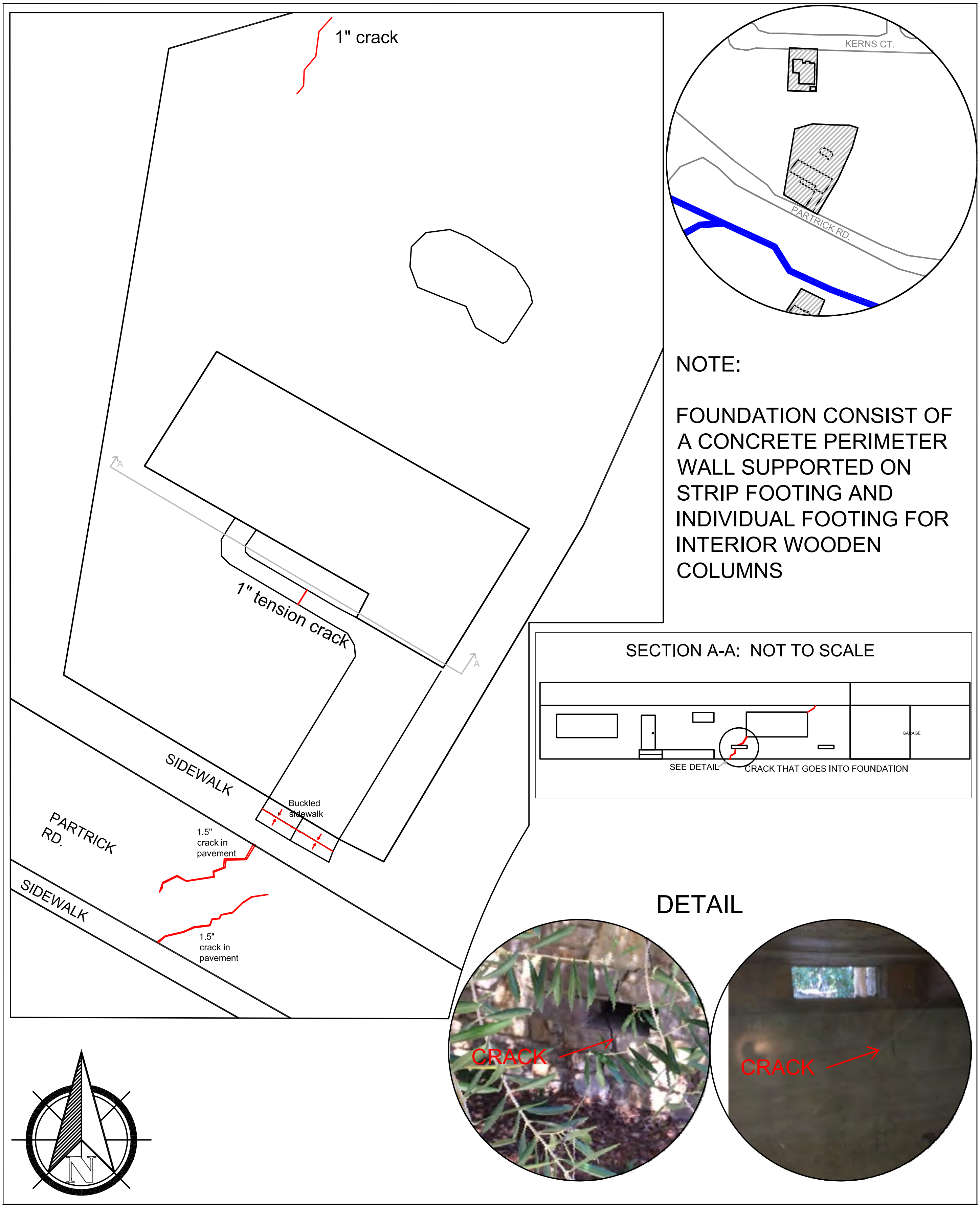

NOTE:

FOUNDATION CONSIST OF A CONCRETE PERIMETER WALL SUPPORTED ON STRIP FOOTING AND INDIVIDUAL FOOTING FOR INTERIOR WOODEN COLUMNS

EVENT:
AMERICAN CANYON EQ M_W = 6.0

LOCATION:
LAT 38.3075° LON -122.3426°

DRAWING BY:
ROBERTO LUQUE
JUSTIN HOLLENBACK

DESCRIPTION:
DAMAGE IN HOUSE

DATE OF INSPECTION:
08 / 29 / 2014

DATE OF DRAWING:
08 / 29 / 2014

SCALE:
1 cm : 4 m
10 m

Figure C-H15-2: Shifted wooden column. The column was shifted towards west. [NSF-GEER; N 38.3061 W 122.3427; 08/29/14 10:02]

Figure C-H15-3: Crack in the perimeter foundation wall [NSF-GEER; N 38.3066 W 122.3427; 08/31/14 10:02]

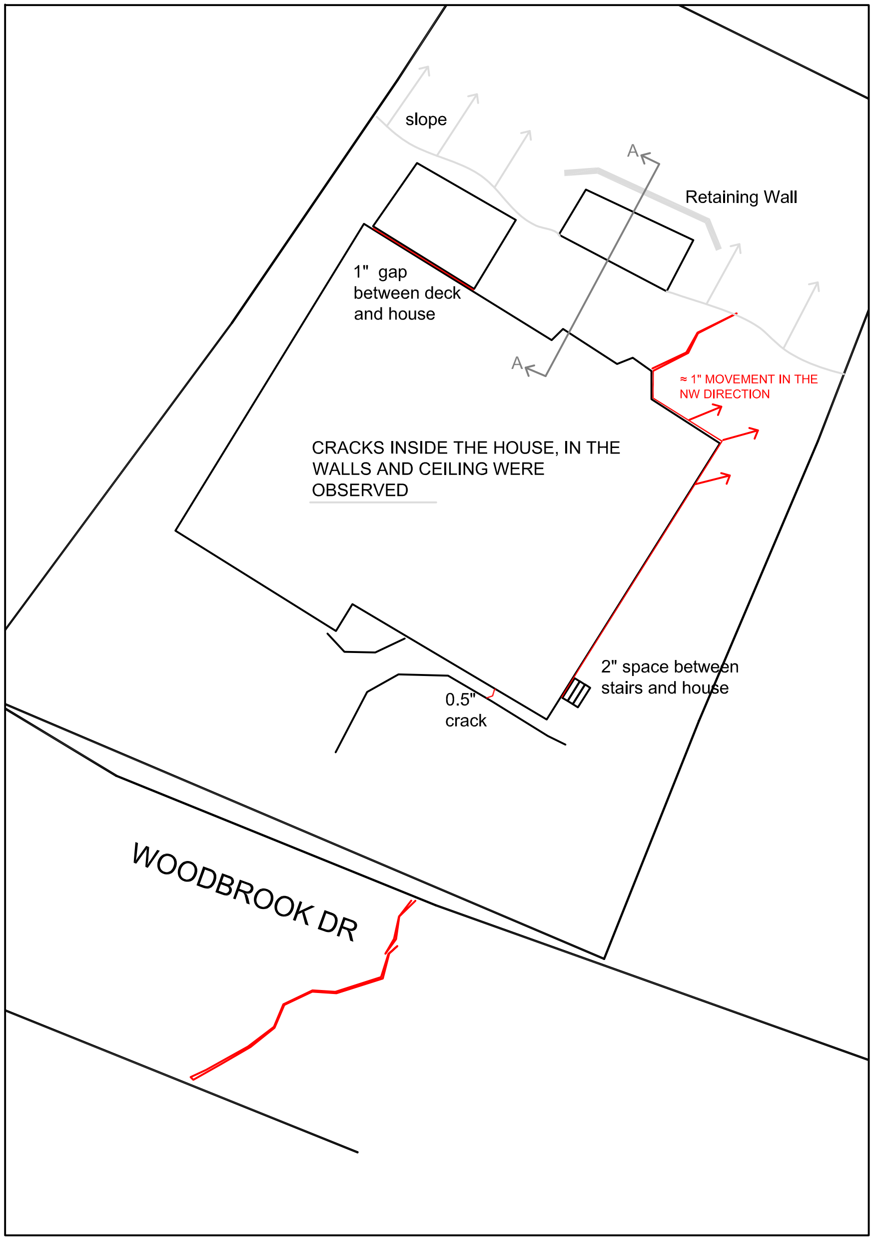

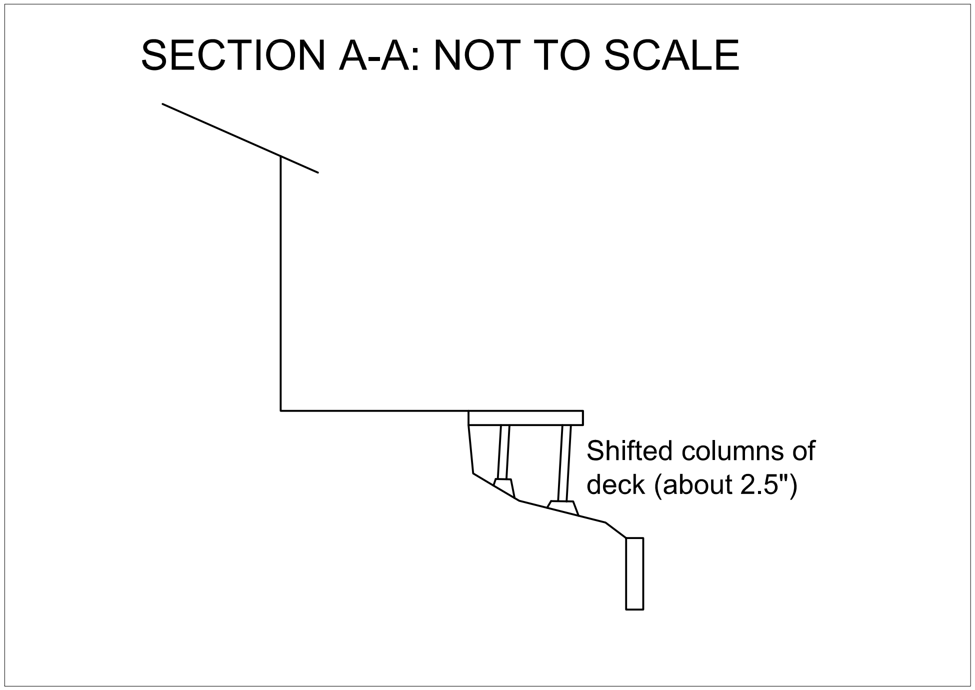

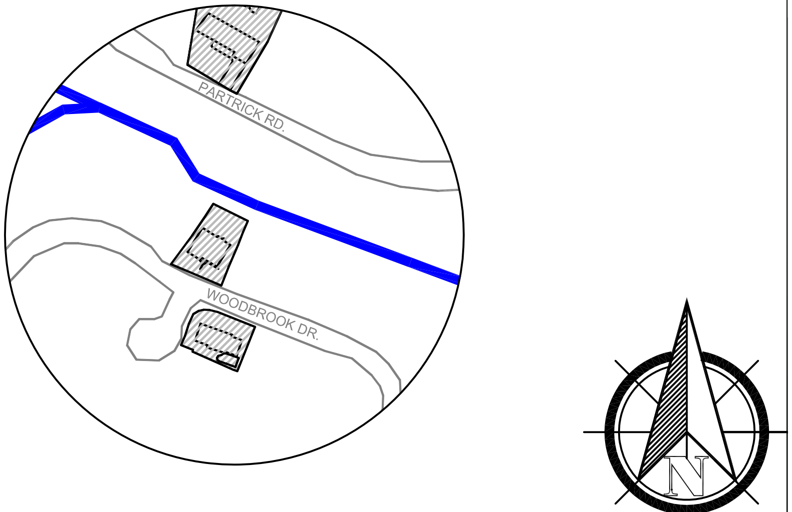

EVENT: AMERICAN CANYON EQ $M_W = 6.0$

LOCATION: LAT 38.3065° LON -122.3417°

DRAWING BY: ROBERTO LUQUE
JUSTIN HOLLENBACK

DESCRIPTION: DAMAGE IN HOUSE

DATE OF INSPECTION: 08 / 29 / 2014

DATE OF DRAWING: 08 / 29 / 2014

SCALE: 1 cm : 3 m

7.5 m

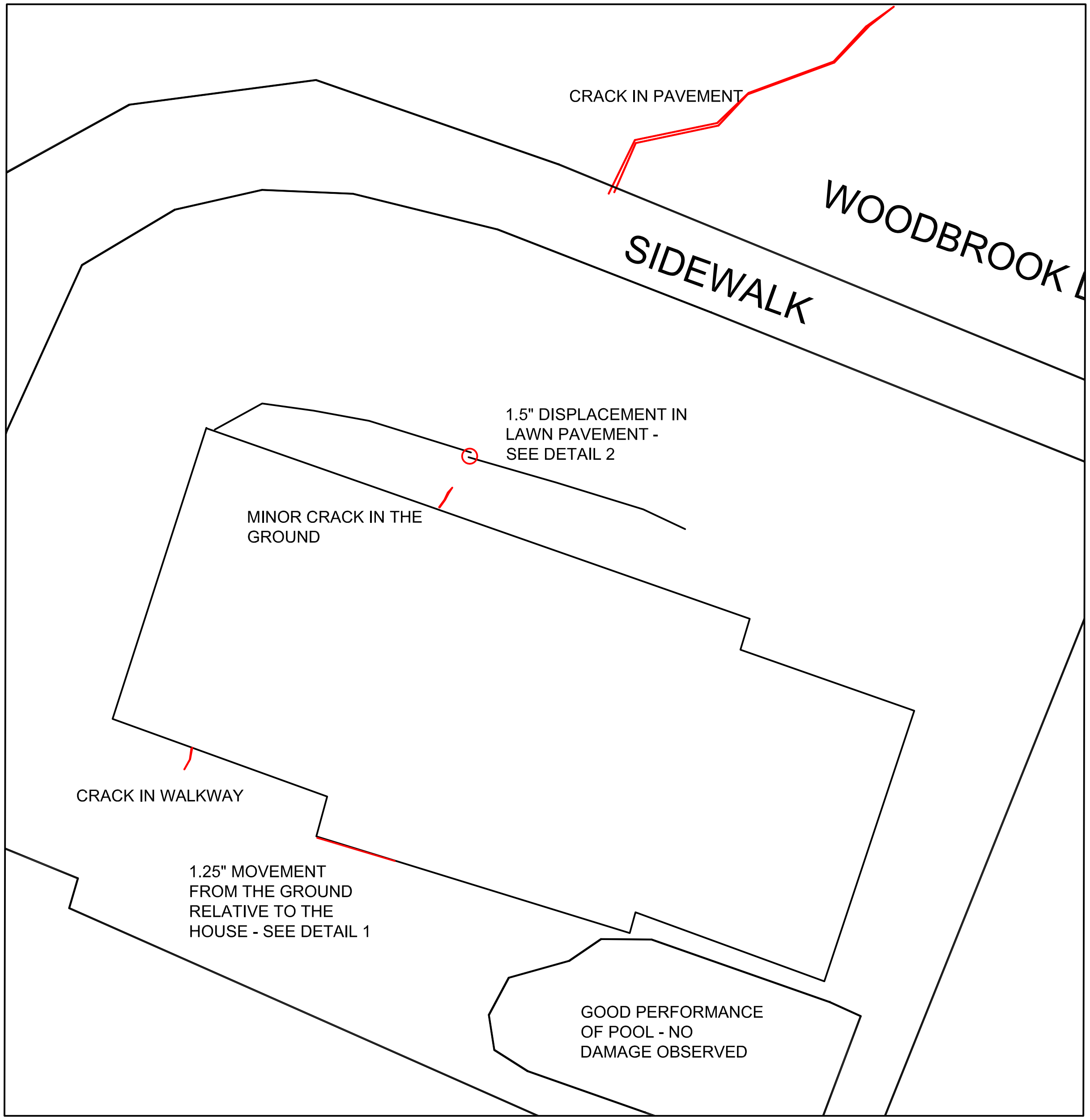

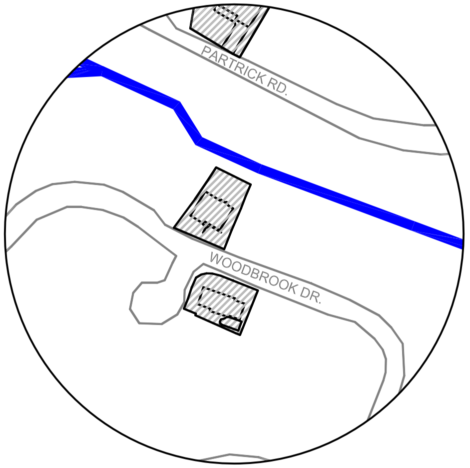

DETAIL 1

DETAIL 2

EVENT: AMERICAN CANYON EQ $M_W = 6.0$	LOCATION: LAT 38.3061° LON -122.3427°		DRAWING BY: ROBERTO LUQUE JUSTIN HOLLENBACK
DESCRIPTION: DAMAGE IN HOUSE	DATE OF INSPECTION: 08 / 29 / 2014	DATE OF DRAWING: 08 / 29 / 2014	SCALE: 1 cm : 2 m 5 m

Figure C-H17-2: Movement of the ground and foundation with respect to the wall [NSF-GEER; N 38.3066 W 122.3427; 09/05/14 16:01]

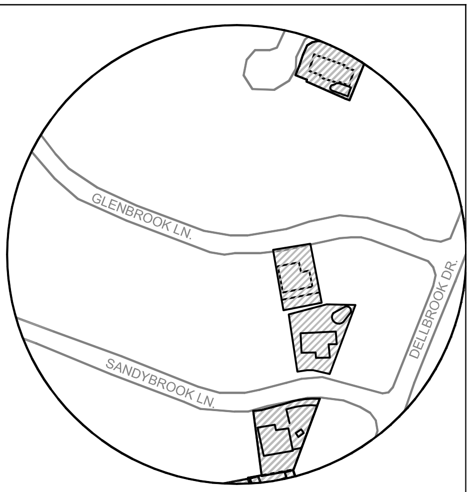

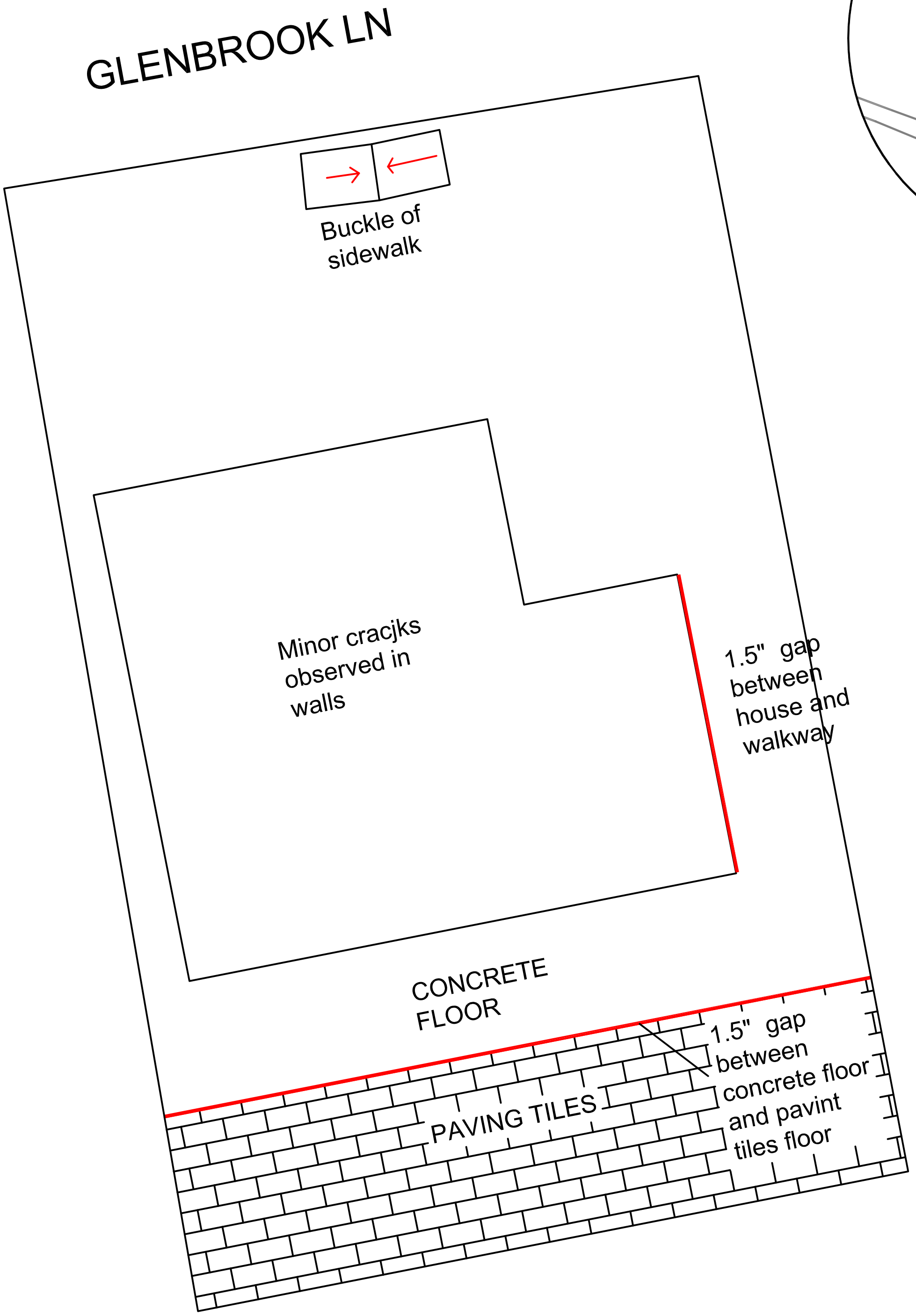

EVENT: AMERICAN CANYON EQ M_W = 6.0	ADDRESS: LAT 38.3051° LON -122.3429°		DRAWING BY: ROBERTO LUQUE JUSTIN HOLLENBACK
DESCRIPTION: DAMAGE IN HOUSE	DATE OF INSPECTION: 08 / 29 / 2014	DATE OF DRAWING: 08 / 29 / 2014	SCALE: 1 cm : 2 m 5 m

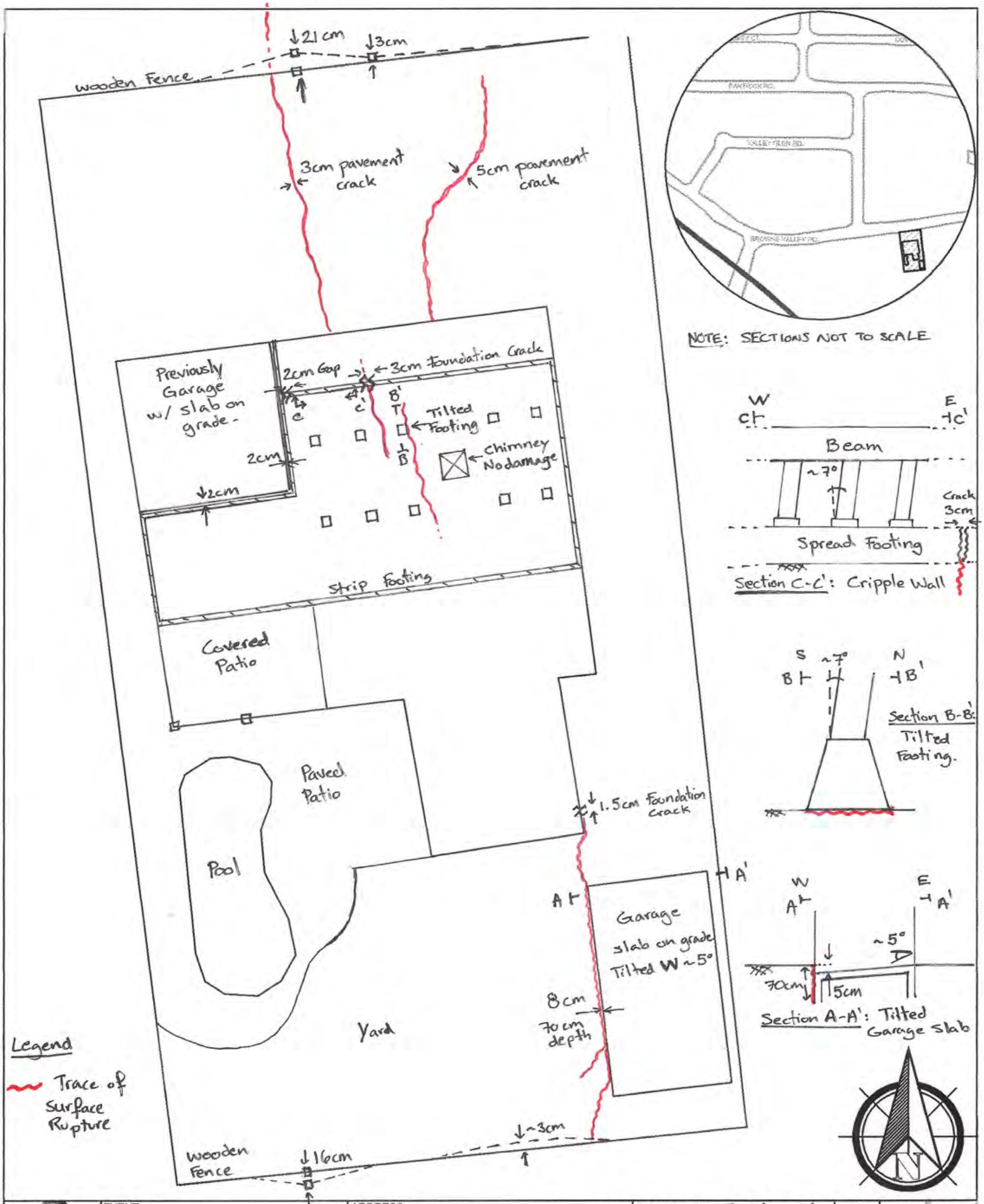

EVENT: AMERICAN CANYON EQ $M_W = 6.0$

ADDRESS: 38.3052 -122.3369 (H21)

DRAWING BY: J. Cohen-Waeber J. Weber, G. Harris, S. Foti

DESCRIPTION: Surface Fault rupture through private property.

DATE OF INSPECTION: 08/28/2014

DATE OF DRAWING: 08/28/2014

SCALE: 1 cm : 2 m

5 m

Figure C-H21-2: Open fissure along detached garage causing settlement to the right (West) [NSF-GEER; N 38.3052 W 122.3369; 08/28/14, 10:09]

Figure C-H21-3: Strip footing crack and tilted cripple wall (E-W) [NSF-GEER; N 38.3052 W 122.3369; 08/28/14, 10:15]

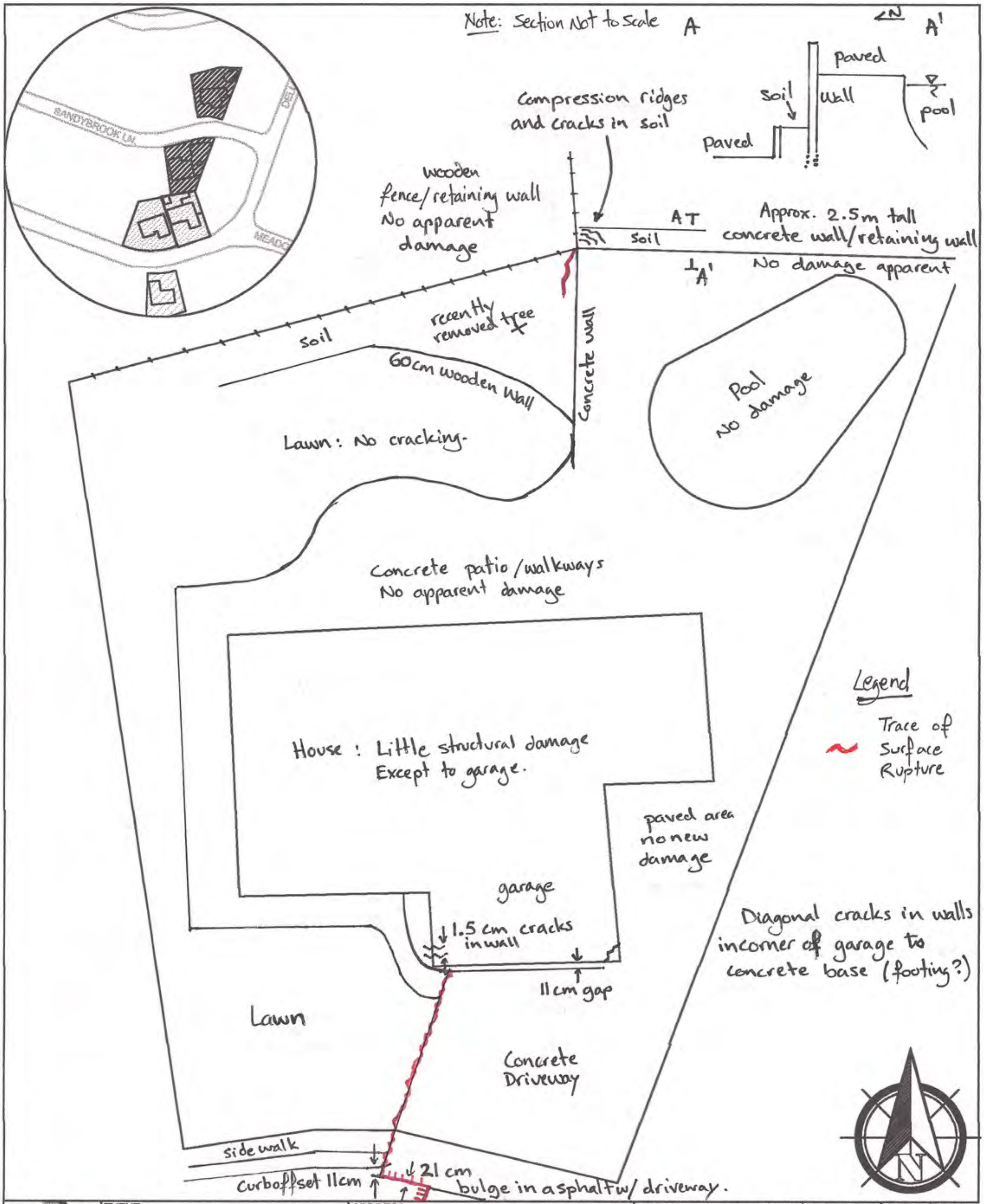

GEER

EVENT: AMERICAN CANYON EQ $M_W = 6.0$

ADDRESS: 38.3048 -122.3427 (H22)

DRAWING BY: C. Markham
Julien Cohen-Waeber

DESCRIPTION: Surface Fault Rupture through private property

DATE OF INSPECTION: 08/25/2014

DATE OF DRAWING: 08/25/2014

SCALE: 1 cm : 2 m

5 m

NSF

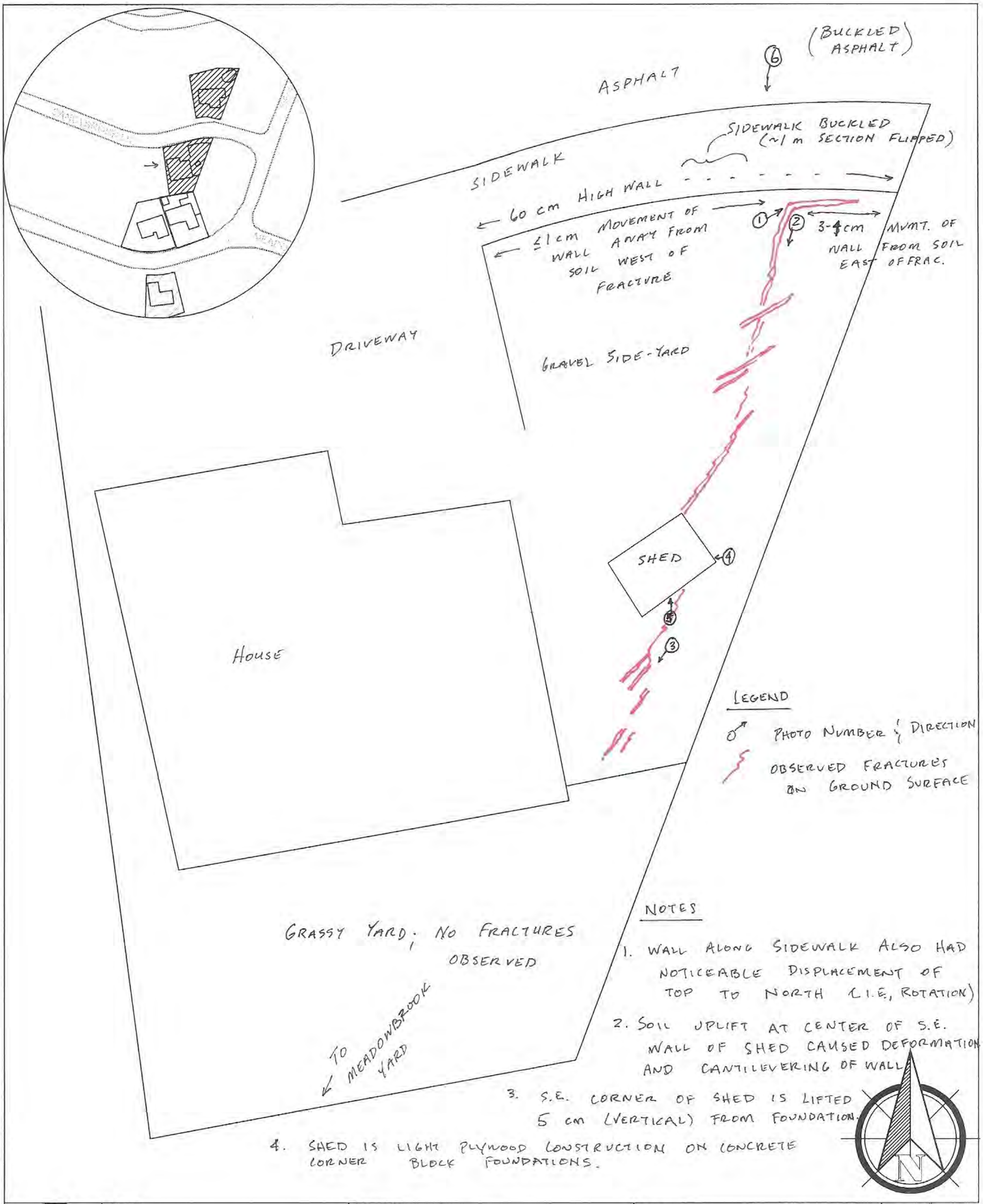

LEGEND

- PHOTO NUMBER & DIRECTION
- OBSERVED FRACTURES ON GROUND SURFACE

NOTES

1. WALL ALONG SIDEWALK ALSO HAD NOTICEABLE DISPLACEMENT OF TOP TO NORTH (I.E., ROTATION)
2. SOIL UPLIFT AT CENTER OF S.E. WALL OF SHED CAUSED DEFORMATION AND CANTILEVERING OF WALL
3. S.E. CORNER OF SHED IS LIFTED 5 cm (VERTICAL) FROM FOUNDATION.
4. SHED IS LIGHT PLYWOOD CONSTRUCTION ON CONCRETE CORNER BLOCK FOUNDATIONS.

EVENT: AMERICAN CANYON EQ $M_W = 6.0$	ADDRESS: N 38.3045° W 122.3429°		DRAWING BY: R. LANZAFAME N. WAGNER
DESCRIPTION: HOUSE MAPPING ㉓	DATE OF INSPECTION: 8/26/14	DATE OF DRAWING: 8/25/14	SCALE: 1 cm : 2 m 5 m

Figure C-H23-2: Ground surface rupture in side-yard
[NSF-GEER; N 38.3045 W 122.3427; 08/25/14 15:24]

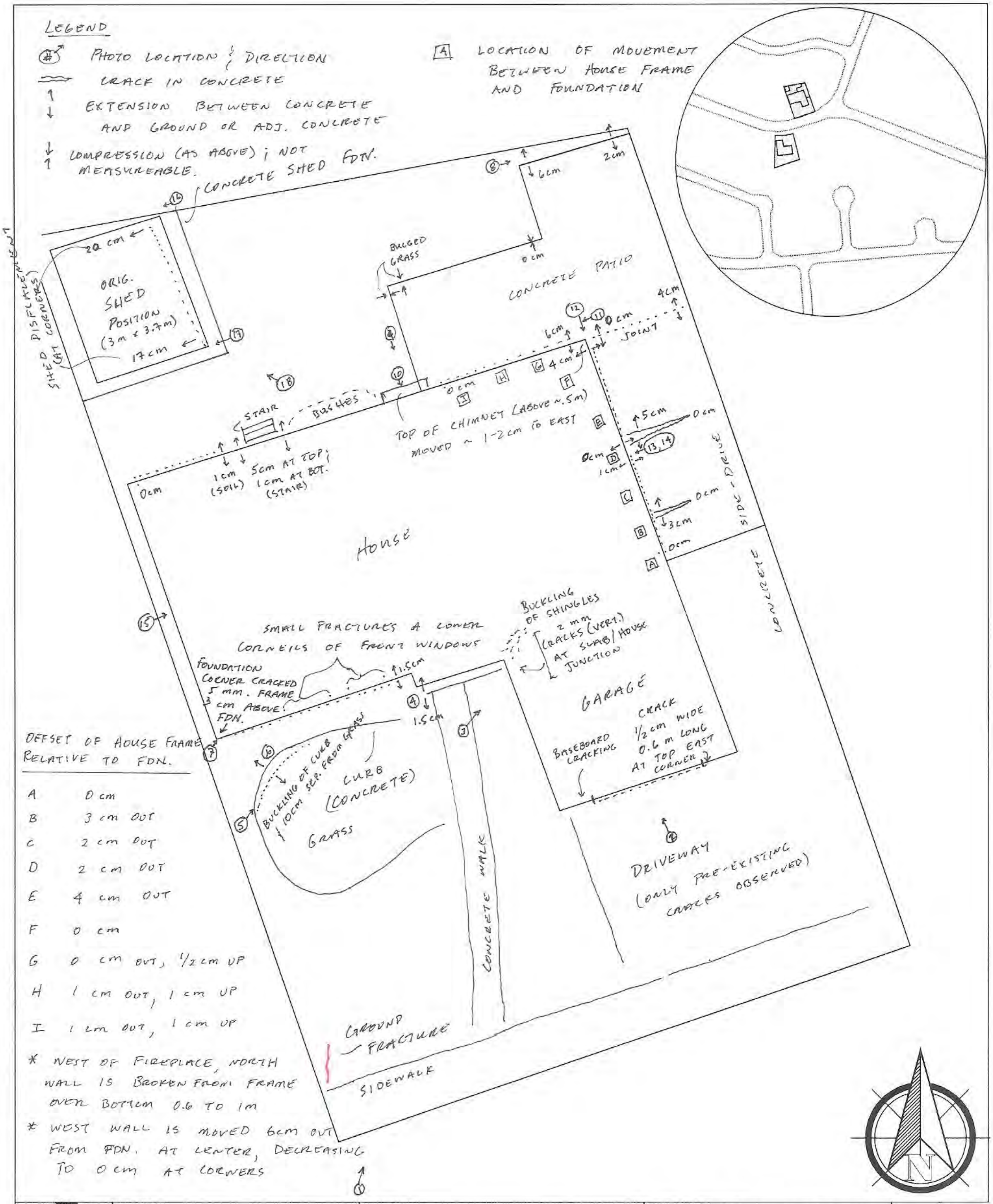

LEGEND

(#) PHOTO LOCATION ; DIRECTION

CRACK IN CONCRETE

↑↓ EXTENSION BETWEEN CONCRETE AND GROUND OR ADJ. CONCRETE

↓↑ COMPRESSION (AS ABOVE) ; NOT MEASUREABLE.

A LOCATION OF MOVEMENT BETWEEN HOUSE FRAME AND FOUNDATION

OFFSET OF HOUSE FRAME RELATIVE TO FDN.

A	0 cm
B	3 cm OUT
C	2 cm OUT
D	2 cm OUT
E	4 cm OUT
F	0 cm
G	0 cm OUT, 1/2 cm UP
H	1 cm OUT, 1 cm UP
I	1 cm OUT, 1 cm UP

* WEST OF FIREPLACE, NORTH WALL IS BROKEN FROM FRAME OVER BOTTOM 0.6 TO 1m

* WEST WALL IS MOVED 6cm OUT FROM FDN. AT CENTER, DECREASING TO 0 cm AT CORNERS

GEER

EVENT: AMERICAN CANYON EQ M_W = 6.0

ADDRESS: N 38.3041 W 122.3429°

DRAWING BY: R. LANZAFAME
N. WAGNER

DESCRIPTION: HOUSE MAPPING ㉔

DATE OF INSPECTION: 8/25/14

DATE OF DRAWING: 8/25/14

SCALE: 1 cm : 2 m

5 m

NSF

Figure C-H24-2: Displacement of patio slab relative to structure foundation; cracking of corner [NSF-GEER; N 38.3041 W 122.3429; 08/25/14 13:18]

Figure C-H24-3: Asphalt rupture and front of residence (building on right) [NSF-GEER; N 38.3038 W 122.3430; 08/25/14 14:02]

Figure C-H24-4: Offset of wall frame relative to foundation (view from top) [NSF-GEER; N 38.3040 W 122.3431; 08/25/14 14:15]

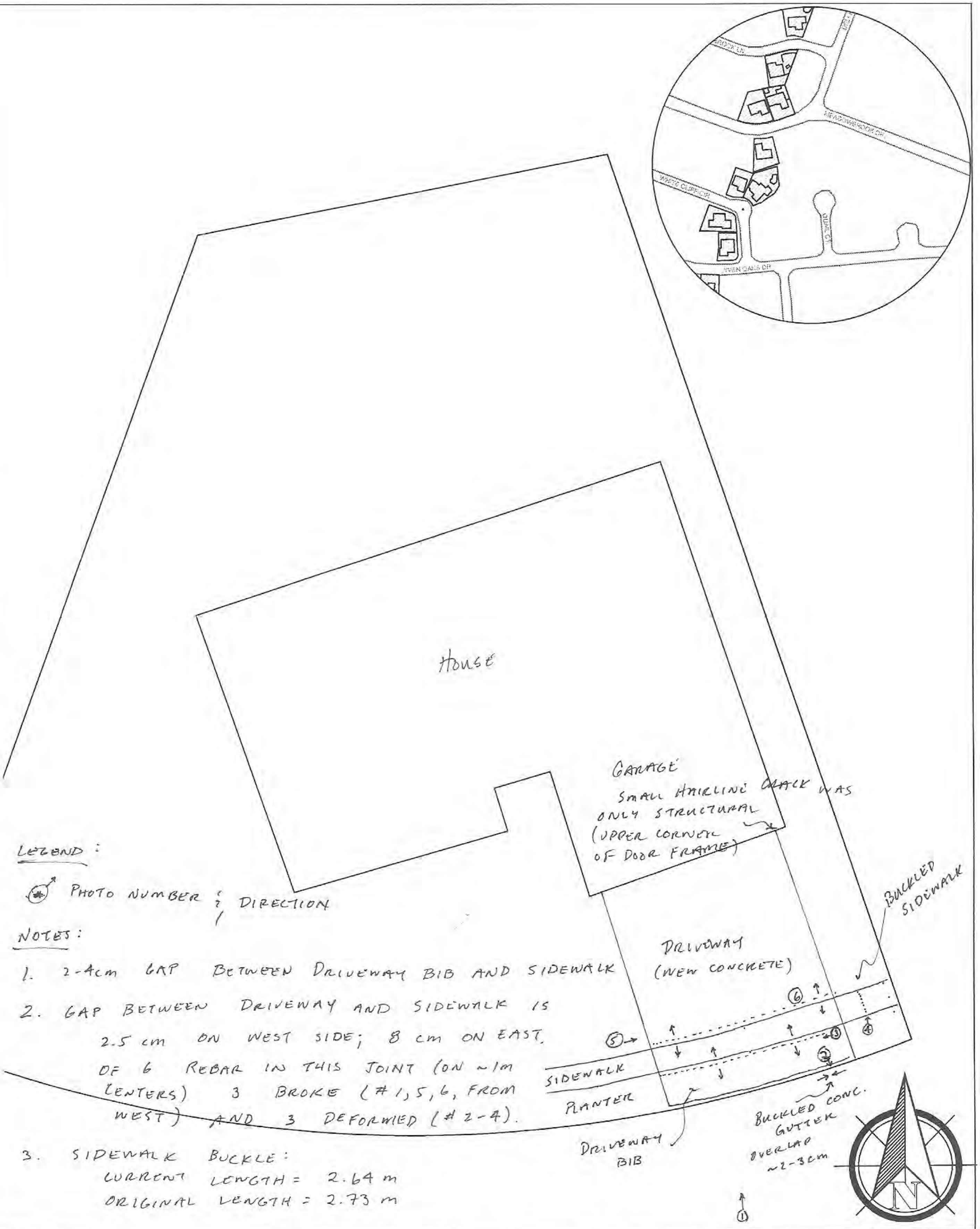

LEGEND:

⊛↗ PHOTO NUMBER & DIRECTION

NOTES:

1. 2-4cm GAP BETWEEN DRIVEWAY BIB AND SIDEWALK
2. GAP BETWEEN DRIVEWAY AND SIDEWALK IS 2.5 cm ON WEST SIDE; 8 cm ON EAST. OF 6 REBAR IN THIS JOINT (ON ~1m CENTERS) 3 BROKE (#1, 5, 6, FROM WEST) AND 3 DEFORMED (# 2-4).
3. SIDEWALK BUCKLE:
   CURRENT LENGTH = 2.64 m
   ORIGINAL LENGTH = 2.73 m

EVENT: AMERICAN CANYON EQ $M_W = 6.0$

N 38.3040° W122.3432°

DRAWING BY: R. LANZAFAME
N. WAGNER

DESCRIPTION: HOUSE MAPPING ㉕

DATE OF INSPECTION: 8/25/14

DATE OF DRAWING: 8/25/14

SCALE: 1 cm : 2 m

5 m

Figure C-H25-2: Offset of driveway, sidewalk and driveway bib [NSF-GEER; N 38.3038 W 122.3431; 08/25/14 13:29]

Figure C-H25-3: Deformation of rebar between driveway and sidewalk [NSF-GEER; N 38.3038 W 122.3430; 08/25/14 13:29]

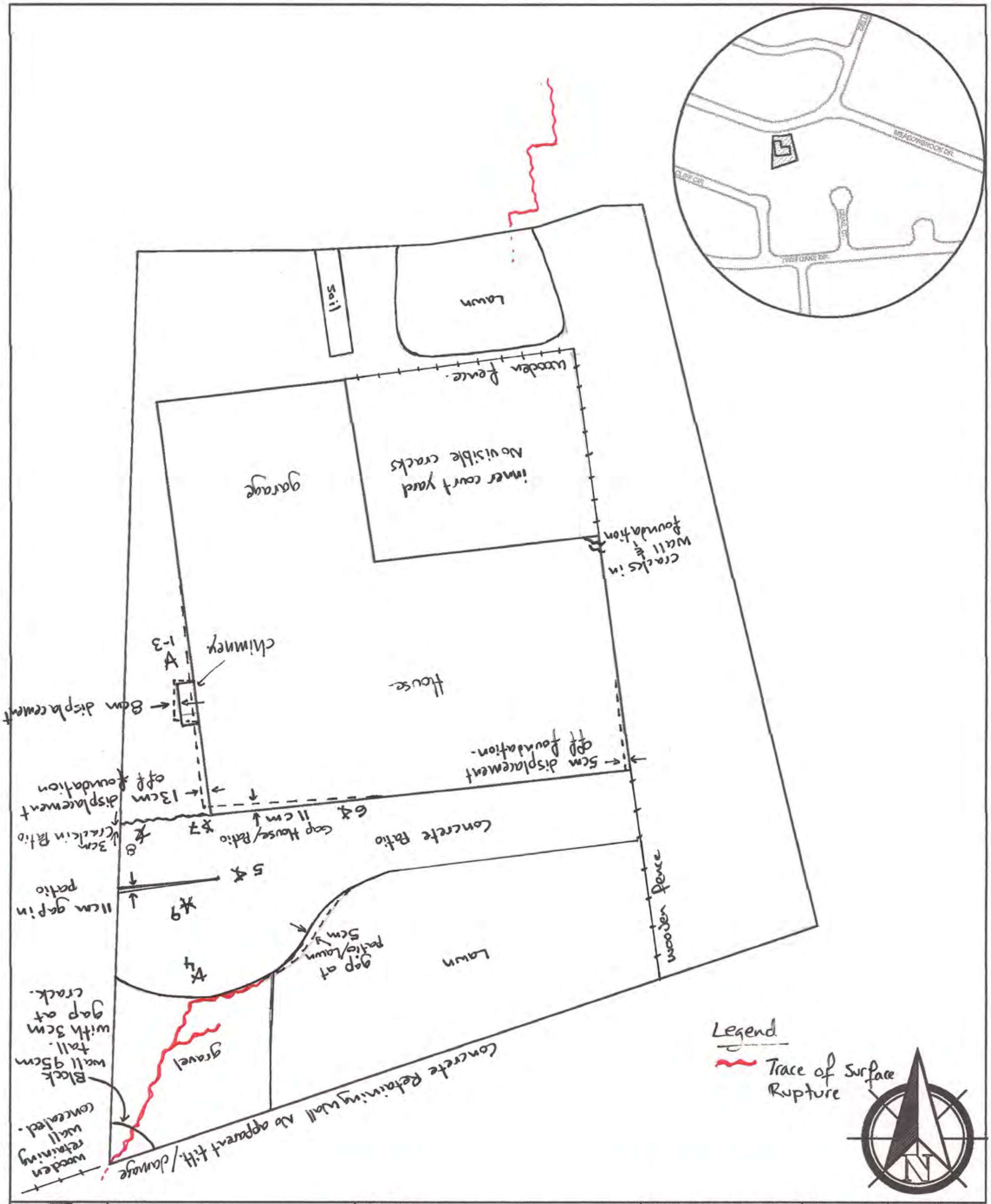

EVENT: AMERICAN CANYON EQ M_W = 6.0

ADDRESS: 38.3036 -122.3432 (H27)

DRAWING BY: C. Markham
Julien Cohen-Waeber

DESCRIPTION: Surface Fault Rupture through private property

DATE OF INSPECTION: 08/25/2014

DATE OF DRAWING: 08/25/2014

SCALE: 1 cm : 2 m
5 m

Figure C-H27-2: Structure shifted off of foundation. [NSF-GEER; N 38.3036 W 122.3432; 08/25/14 13:15]

Figure C-H27-3: Gap between structure and patio. [NSF-GEER; N 38.3036 W 122.3432; 08/25/14 13:28]

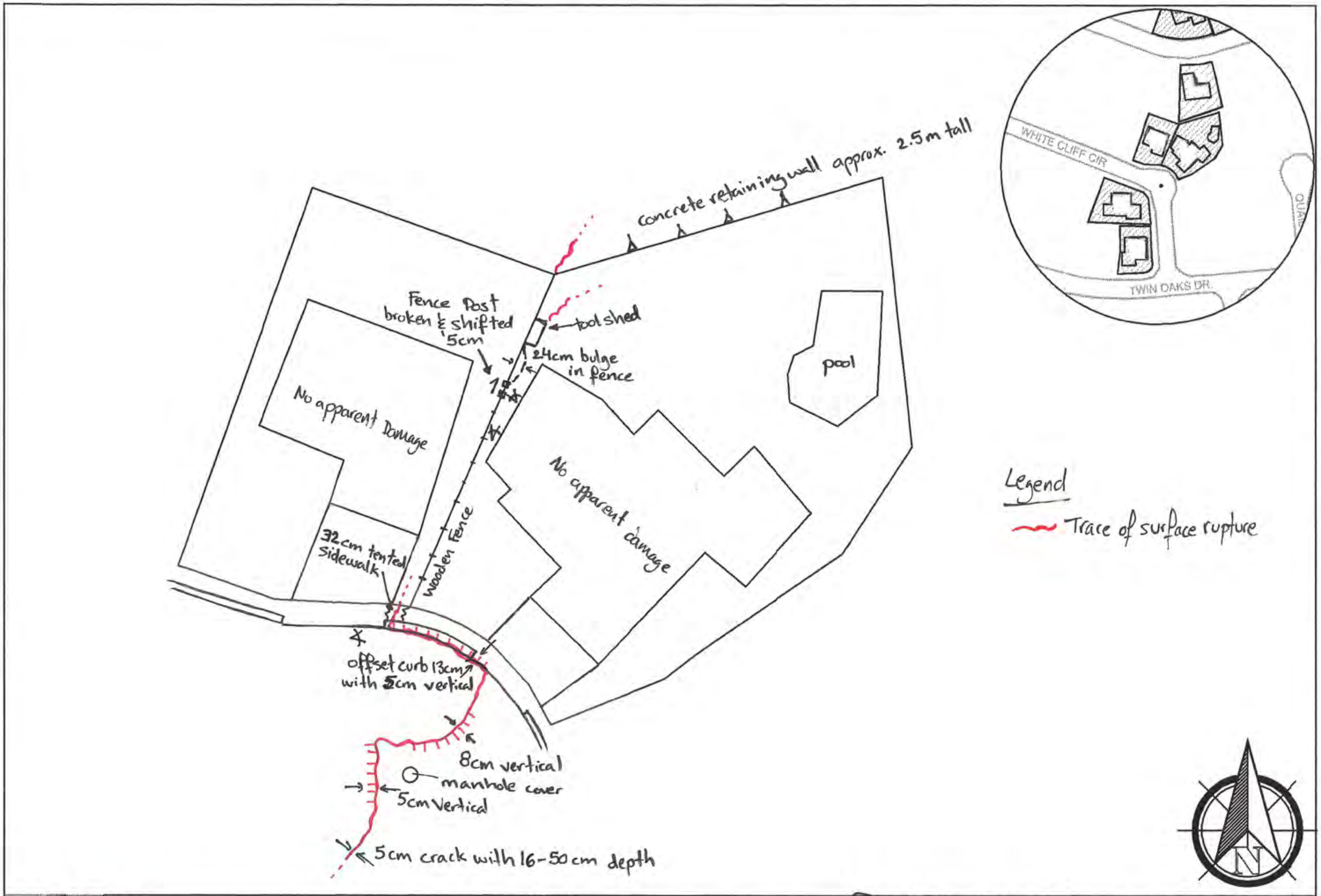

EVENT: AMERICAN CANYON EQ $M_W = 6.0$	ADDRESS: 38.3033 −122.3434	⑷28 ⑷29	DRAWING BY: C. Markham, J. Bray Julien Cohen-Waeber
DESCRIPTION: Surface Fault Rupture through private property	DATE OF INSPECTION: 08/25/2014	DATE OF DRAWING: 08/25/2014	SCALE: 1 cm : 4 m 10 m

Figure C-H28-H29-2: Compression between asphalt and curb showing right lateral movement. [NSF-GEER; N 38.3033 W 122.3434; 08/25/14 09:29]

Figure C-H28-H29-3: Buckling of wooden fence showing post displacement [NSF-GEER; N 38.3033 W 122.3434; 08/25/14 09:52]

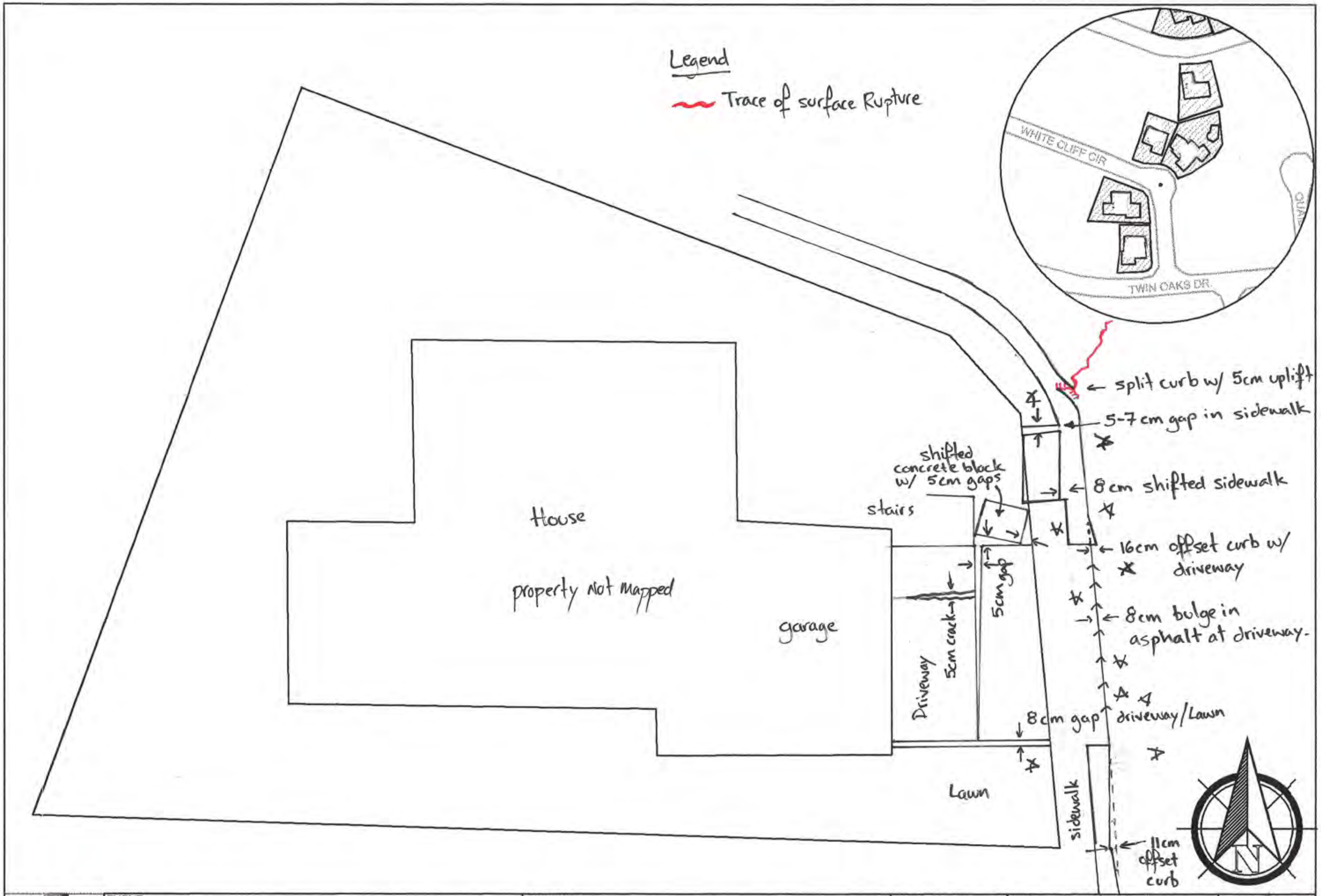

EVENT: AMERICAN CANYON EQ M_W = 6.0

DESCRIPTION: Surface fault rupture through private property

ADDRESS: 38.3029 -122.3435 (H30)

DATE OF INSPECTION: 08/25/2014

DATE OF DRAWING: 08/25/2014

DRAWING BY: Chris Markham
Julien Cohen-Waeber

SCALE: 1 cm : 2 m

5 m

Figure C-H30-2: Compression between asphalt and curb showing. [NSF-GEER; N 38.3029 W 122.3435; 08/25/14 09:15]

Figure C-H30-3: Severe cracking across White Cliff Circ. [NSF-GEER; N 38.3029 W 122.3435; 08/25/14 09:17]

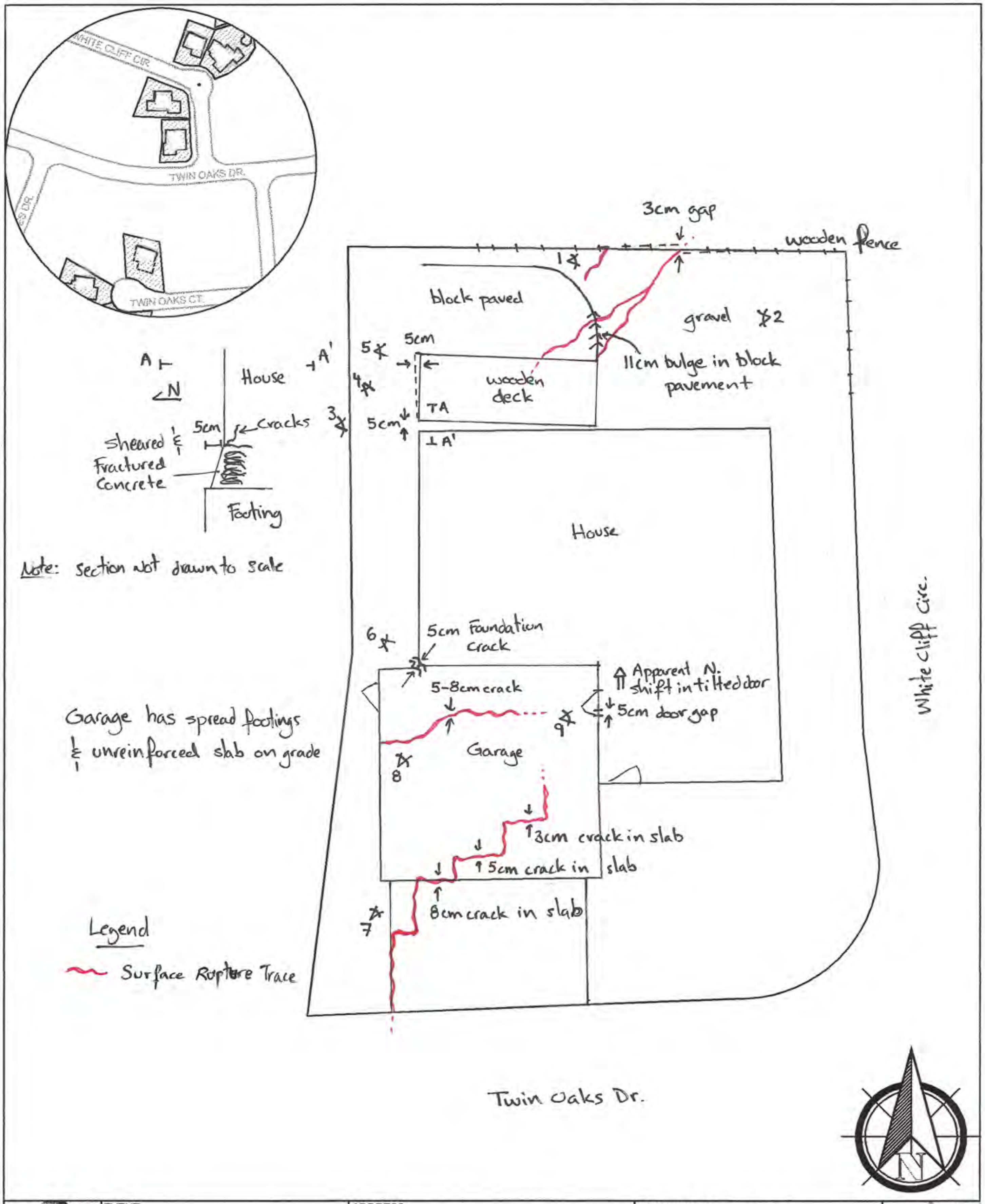

EVENT: AMERICAN CANYON EQ M_W = 6.0

ADDRESS: 38.3027 -122.3436 (#30)

DRAWING BY: C. Markham
J. Cohen-Waeber

DESCRIPTION: Surface Fault Rupture through Private Property.

DATE OF INSPECTION: 08/25/2014

DATE OF DRAWING: 08/25/2014

SCALE: 1 cm : 2 m

5 m

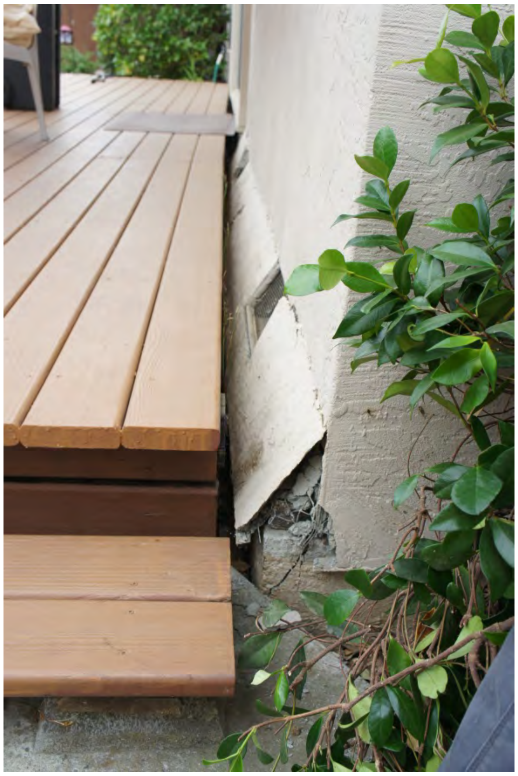

Figure C-H31-2: Structure shifted on foundation. [NSF-GEER; N 38.3027 W 122.3436; 08/25/14 10:11]

Figure C-H31-3: Structure shifted on foundation and foundation crack [NSF-GEER; N 38.3027 W 122.3436; 08/25/14 10:22]

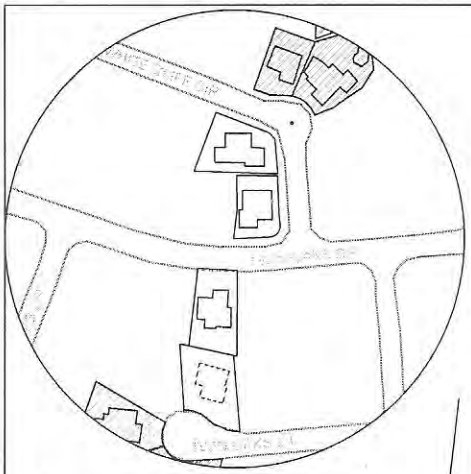

LEGEND

FRACTURES IN CONCRETE

NOTES:

1. GARAGE WALLS SUPP. ON GRADE BEAMS SEPARATE FROM GARAGE SLAB.
2. BEAM UNDER N.E. GARAGE WALL CORNER ROTATE OUT TO STREET AT TOP ~7°
3. FRACTURED GARAGE SLAB SLOPES DOWN TO NORTHWEST
4. NO DAMAGE ON SECOND FLOOR
5. GAP BETWEEN CROWN MOLDING & WALL UP TO 2mm THROUGHOUT HOUSE (1st FLOOR)
6. APPROX. 5-15 cm OFFSET OF 1st STORY SHINGLE FLASHING AND 2nd FLOOR OUTER WALL.
7. OWNER DESCRIBED FOUNDATION AS A T-FOOTING ON "A FEW" PIERS.

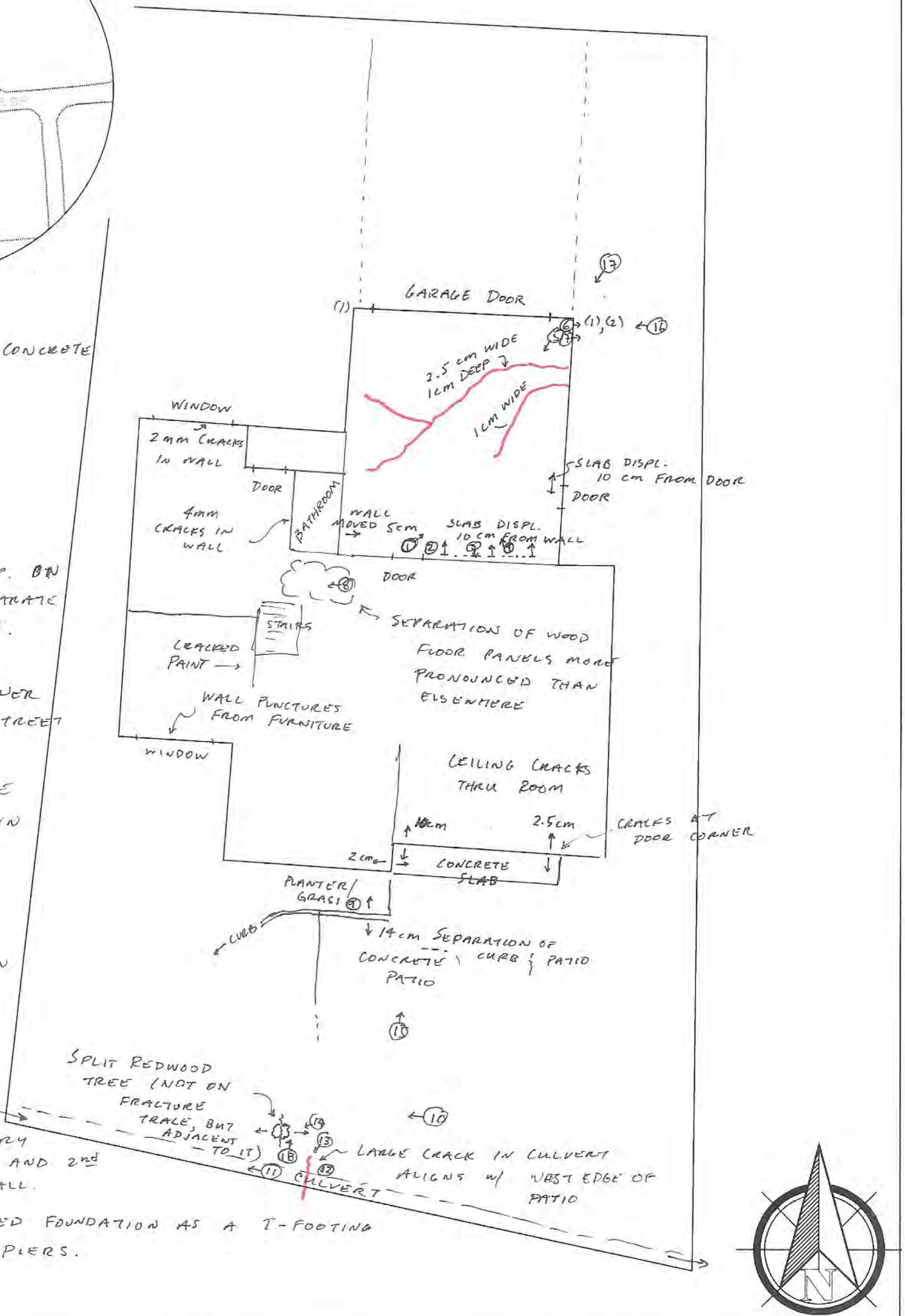

EVENT: AMERICAN CANYON EQ M_W = 6.0

LOCATION: N 38.3022° W 122.3438°

DRAWING BY: R. LANZAFAME M. GARDNER N. WAGNER

DESCRIPTION: HOUSE MAPPING (32)

DATE OF INSPECTION: 8/27/14

DATE OF DRAWING: 8/27/14

SCALE: 1 cm : 2 m

5 m

Figure C-H32-2: Garage slab cracking [NSF-GEER; N 38.3024 W 122.3436; 08/27/14 11:33]

Figure C-H32-3: Separation of garage slab and wall [NSF-GEER; N 38.3022 W 122.3438; 08/27/14 11:33]

Figure C-H32-4: Damage to strip footing at garage corner [NSF-GEER; N 38.3023 W 122.3438; 08/27/14 11:47]

Figure C-H32-5: Split tree trunk adjacent to rupture alignment [NSF-GEER; N 38.3021 W 122.3439; 08/27/14 15:13]

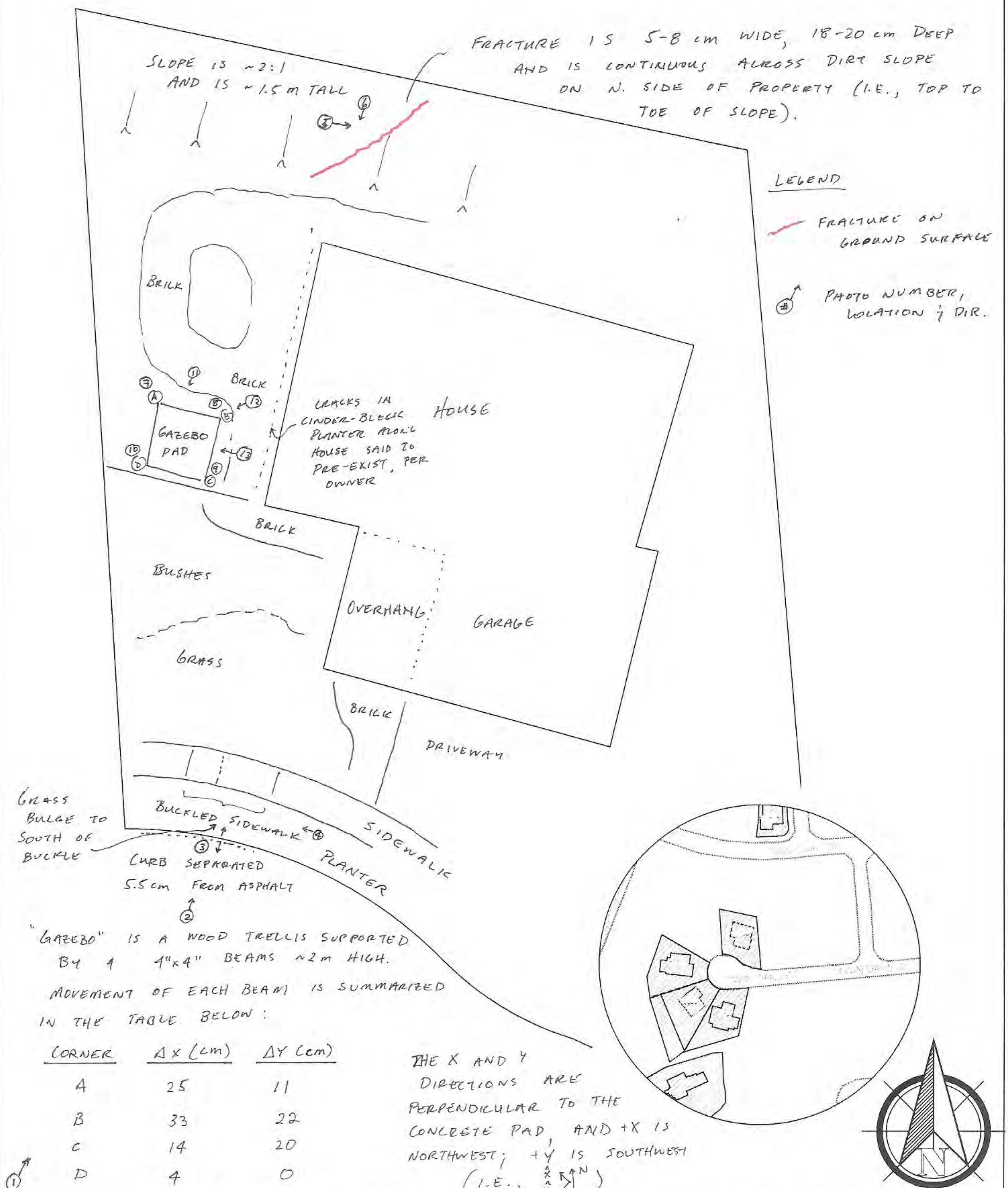

FRACTURE IS 5-8 cm WIDE, 18-20 cm DEEP AND IS CONTINUOUS ACROSS DIRT SLOPE ON N. SIDE OF PROPERTY (I.E., TOP TO TOE OF SLOPE).

CRACKS IN CINDER-BLOCK PLANTER ALONG HOUSE SAID TO PRE-EXIST, PER OWNER

GRASS BULGE TO SOUTH OF BUCKLE

CURB SEPARATED 5.5 cm FROM ASPHALT

"GAZEBO" IS A WOOD TRELLIS SUPPORTED BY 4 4"x4" BEAMS ~2 m HIGH.
MOVEMENT OF EACH BEAM IS SUMMARIZED IN THE TABLE BELOW:

CORNER	Δx (cm)	ΔY (cm)
A	25	11
B	33	22
C	14	20
D	4	0

THE X AND Y DIRECTIONS ARE PERPENDICULAR TO THE CONCRETE PAD, AND +X IS NORTHWEST; +Y IS SOUTHWEST (I.E., $\overset{x}{\underset{y}{\updownarrow}}$ ↖↗N)

EVENT: AMERICAN CANYON EQ $M_W = 6.0$
ADDRESS: N 38.3019° W 122.3439°
DRAWING BY: R. LANZAFAME
N. WAGNER
DESCRIPTION: HOUSE MAPPING (33)
DATE OF INSPECTION: 8/25/14
DATE OF DRAWING: 8/25/14
SCALE: 1 cm : 2 m
5 m

Figure C-H33-2: View across court to residence [NSF-GEER; N 38.3015 W 122.3443; 08/25/14 10:23]

Figure C-H33-3: Fracture along backyard slope [NSF-GEER; N 38.3020 W 122.3439; 08/25/14 11:22]

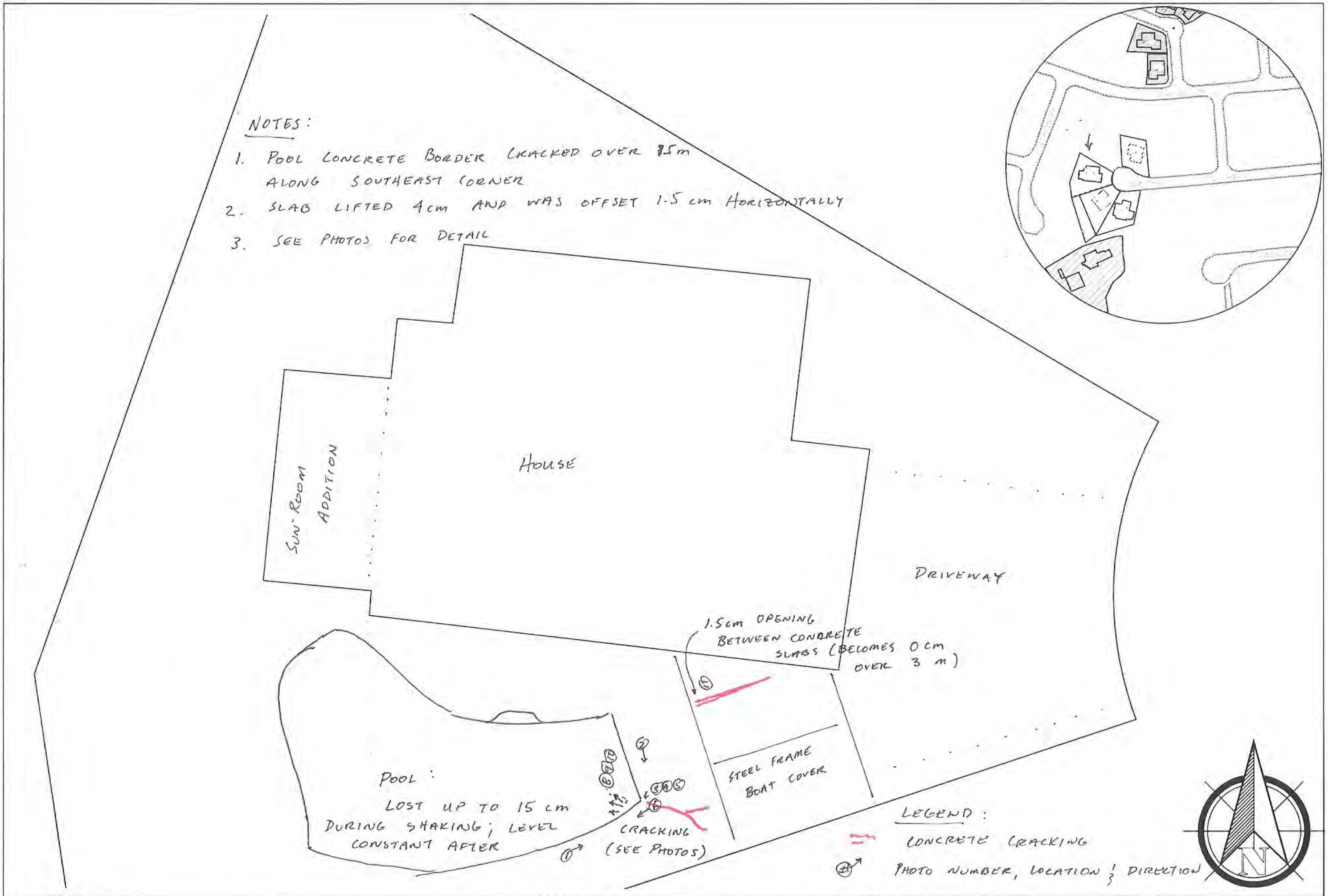

NOTES :

1. POOL CONCRETE BORDER CRACKED OVER 35m ALONG SOUTHEAST CORNER
2. SLAB LIFTED 4cm AND WAS OFFSET 1.5 cm HORIZONTALLY
3. SEE PHOTOS FOR DETAIL

EVENT: AMERICAN CANYON EQ $M_W = 6.0$

ADDRESS: N 38.3017° W 122.3443°

DRAWING BY: R. LANZAFAME N. WAGNER

DESCRIPTION: HOUSE MAPPING ㉞

DATE OF INSPECTION: 8/25/14

DATE OF DRAWING: 8/25/14

SCALE: 1 cm : 2 m

5 m

Figure C-H34-2: Concrete cracking at edge of pool

[NSF-GEER; N 38.3016 W 122.3443; 08/25/14 11:05]

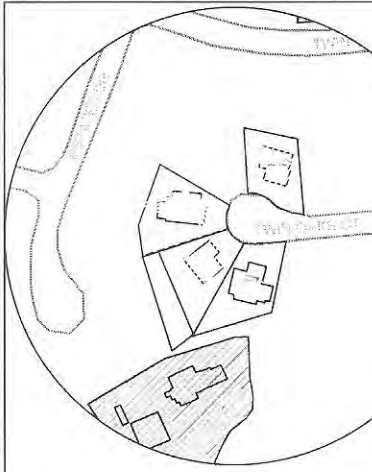

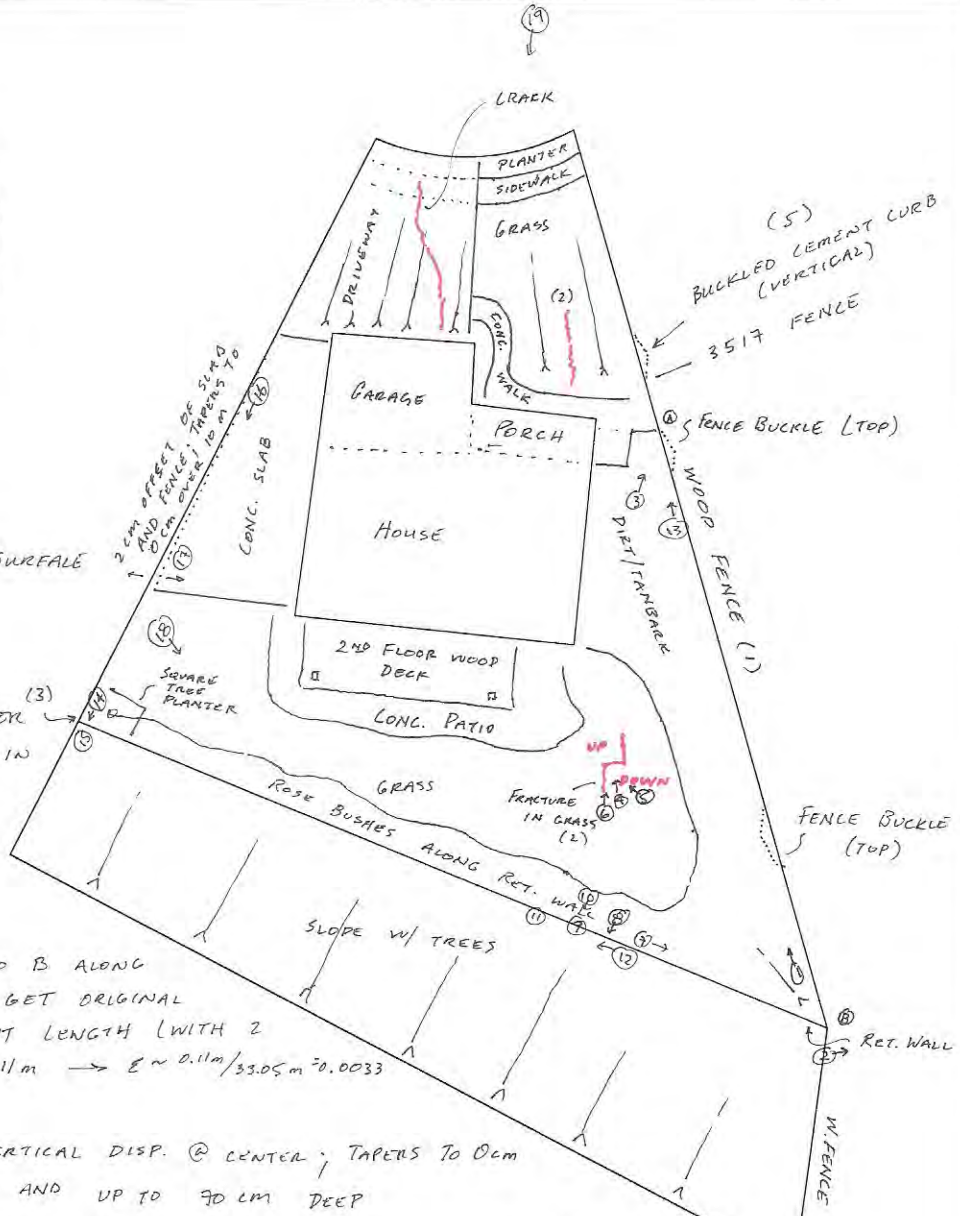

LEGEND:

🟥 FRACTURES IN GROUND SURFACE

⋯ BUCKLED FEATURES

(#) NOTE ANNOTATION

Ⓗ DIRECTION & REF. NUMBER OF PHOTO (NUMBERED IN ORDER OF TIME STAMP)

NOTES:

1. FENCE MEASURED FROM A TO B ALONG HORIZONTAL 2"x4" AT TOP TO GET ORIGINAL LENGTH OF 33.05 m. CURRENT LENGTH (WITH 2 BUCKLES) IS 32.94 m. $\Delta = 0.11 m \rightarrow \varepsilon \sim 0.11m/33.05m = 0.0033$

2. FRACTURES IN GRASS:
   - BACKYARD – 5-6 cm VERTICAL DISP. @ CENTER; TAPERS TO 0 cm
   - FRONT YARD – ~3 m LONG AND UP TO 70 cm DEEP

3. OWNER NOTES APPROX. DOUBLING OF GAP BETWEEN RET. WALL & WEST FENCE; AT TIME OF MEASUREMENT, GAP WAS 8 cm AT BOTTOM, 10 cm AT TOP; WALL IS ~80 cm HIGH

4. RETAINING WALL IS 20 cm THICK UNREINFORCED CINDERBLOCK COATED WITH GUNNITE AND CONTAINS 2 BREAKS FOR STAIRS AT ~1/3 & ~2/3 THROUGH IT'S 41.8 m LENGTH. THERE IS A 1 cm GAP BETWEEN WALL TOP AND RETAINED SOIL FOR THE ENTIRE SOUTHEASTERN HALF. CRACKS (VERTICAL) ARE SUMMARIZED IN THE FOLLOWING TABLE:

LENGTH (FROM S.E. END)	MAX. CRACK THICKNESS	WALL HEIGHT
4.01 m	8 mm	40 cm
6.10 m	10 mm	70 cm
8.84 m	5 mm	79 cm
11.1 m	8 mm	80 cm
15.1 m	5 mm	80 cm
20.2 m	4 mm	80 cm
20.2 m to ~30m	6 HAIRLINE CRACKS; 80 cm HIGH TO END	

5. BUCKLED CURB MEASURED 210 cm ORIGINAL LENGTH (128 cm & 82 cm PIECES) AND 203 cm CURRENT LENGTH.

EVENT: AMERICAN CANYON EQ $M_W = 6.0$

ADDRESS: N 38.3015° W 122.3442°

DRAWING BY: R. LANZAFAME, N. WAGNER

DESCRIPTION: HOUSE MAPPING ㉟

DATE OF INSPECTION: 8/25/14

DATE OF DRAWING: 8/25/14

SCALE: 1 cm : 4 m, 10 m

Figure C-H35-2: Fracture in grass [NSF-GEER; N 38.3015 W 122.3440; 08/25/14 10:49]

Figure C-H35-3: Buckled wood fence [NSF-GEER; N 38.3015 W 122.3440; 08/25/14 10:55]

Figure C-H35-4: Retaining wall crack [NSF-GEER; N 38.3015 W 122.3440; 08/25/14 10:58]

NOTES :

1. BULGE IN UNREINFORCED, UNCEMENTED MASONRY WALL IS 20 cm TO E. OVER 1.47 m LENGTH.

2. FRACTURE IN DESSICATED SANDY CL MEASURES ~43 TO 76 cm DEEP 8 TO 13 cm WIDE AND 6 m LONG

3. 6 STATUES 0.3 m TO 1m TALL AND 1 TREE FELL ON W. SIDE OF YARD:
   - 4 STATUES, 1 TREE FELL IN N.-S. DIRECTION
   - 2 STATUES FELL IN E.-W. DIRECTION

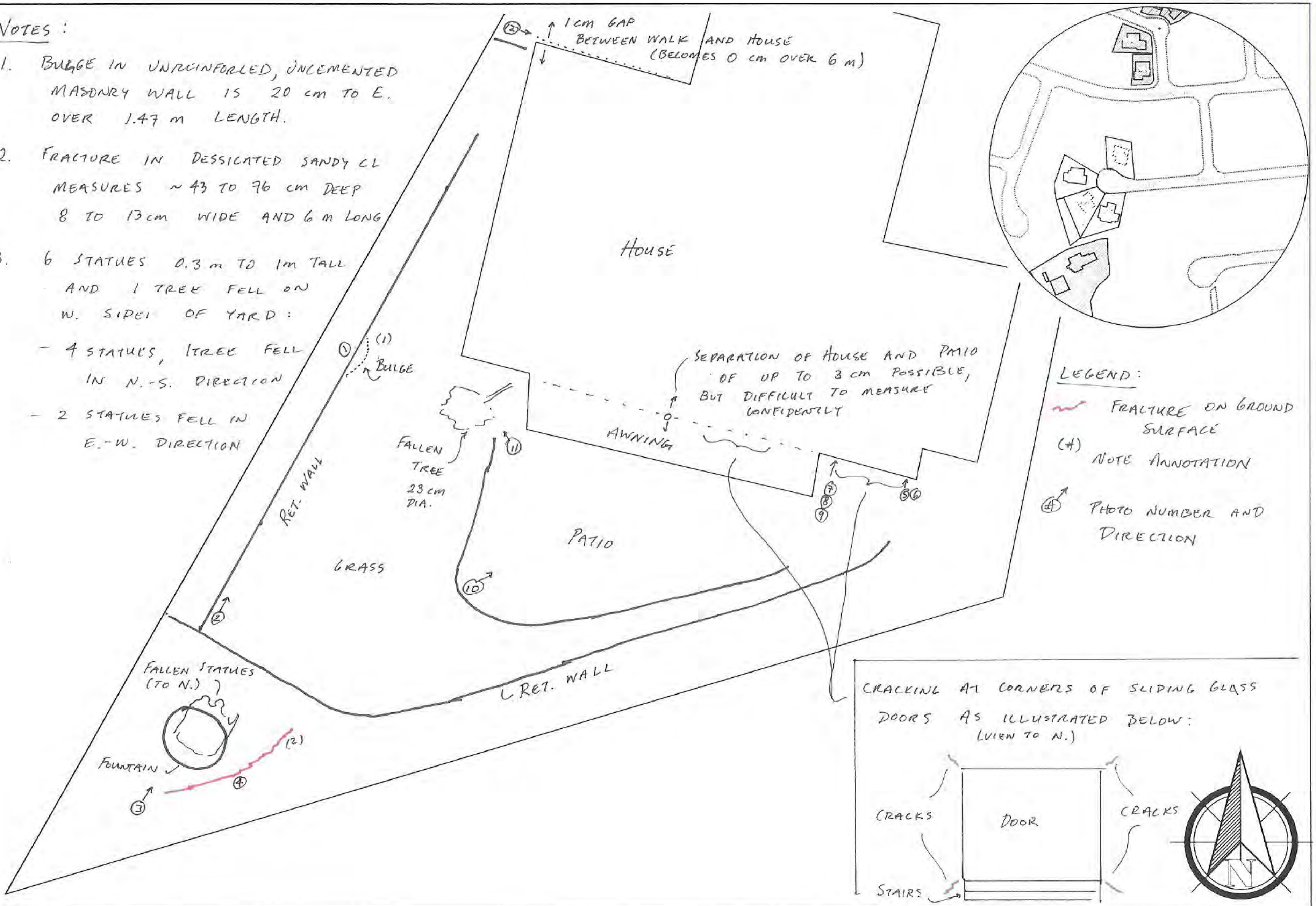

1 cm GAP BETWEEN WALK AND HOUSE (BECOMES 0 cm OVER 6 m)

SEPARATION OF HOUSE AND PATIO OF UP TO 3 cm POSSIBLE, BUT DIFFICULT TO MEASURE CONFIDENTLY

LEGEND:

- 〰 FRACTURE ON GROUND SURFACE
- (#) NOTE ANNOTATION
- #↗ PHOTO NUMBER AND DIRECTION

CRACKING AT CORNERS OF SLIDING GLASS DOORS AS ILLUSTRATED BELOW: (VIEW TO N.)

EVENT: AMERICAN CANYON EQ $M_W = 6.0$

ADDRESS: N 38.3015° W 122.3440°

DRAWING BY: R. LANZAFAME
N. WAGNER

DESCRIPTION: HOUSE MAPPING ㊱

DATE OF INSPECTION: 8/25/14

DATE OF DRAWING: 8/25/14

SCALE: 1 cm : 2 m

5 m

Figure C-H36-2: Buckled retaining wall [NSF-GEER; N 38.3013 W 122.3441; 08/25/14 11:57]

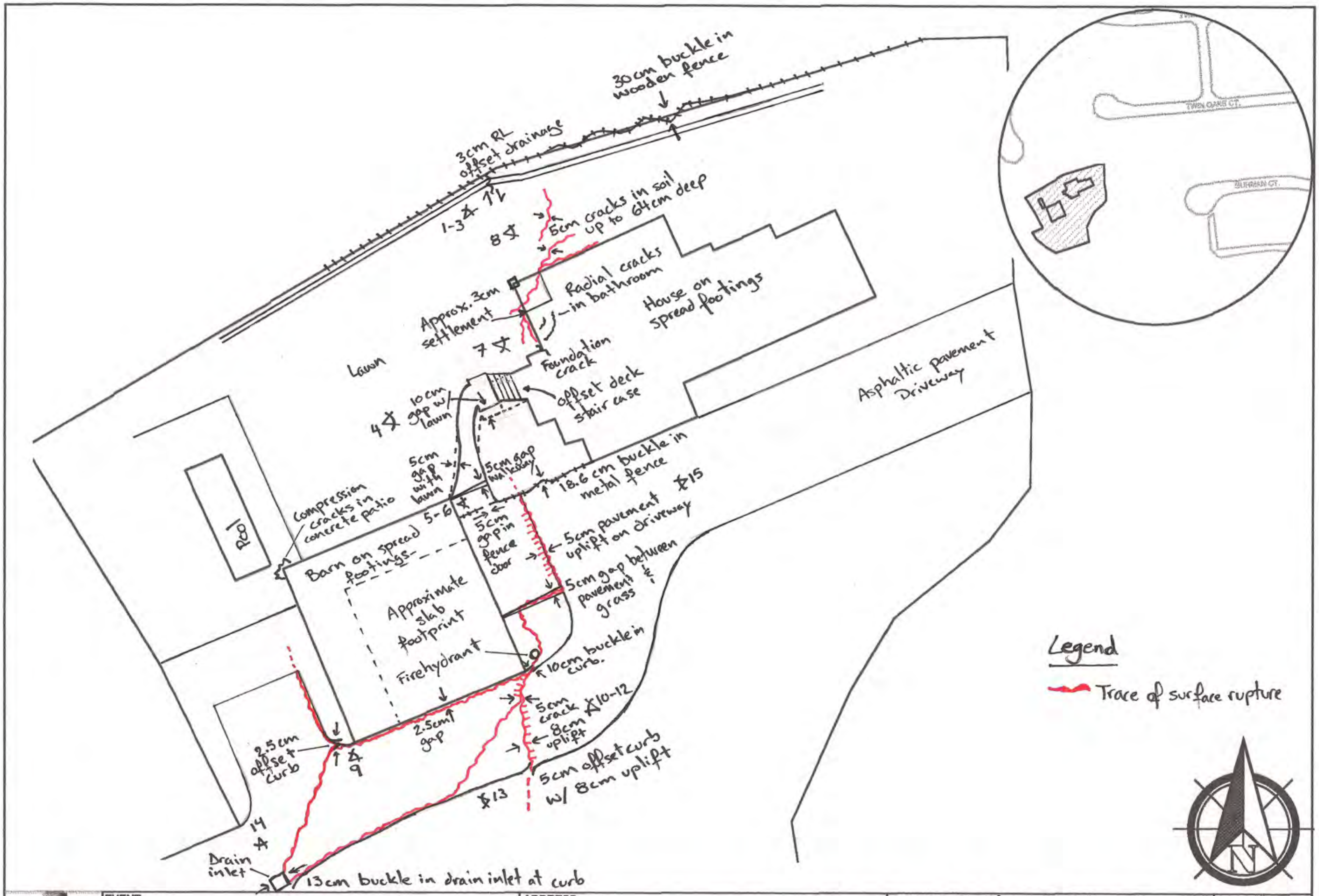

EVENT: AMERICAN CANYON EQ M_W = 6.0	ADDRESS: 38.3011 -122.3442 (H37)		DRAWING BY: Chris Markham Julien Cohen-Waeber	
DESCRIPTION: Surface faultrupture through private property	DATE OF INSPECTION: 08/25/2014	DATE OF DRAWING: 08/25/2014	SCALE: 1 cm : 4 m	10 m

Figure C-H37-2: Cracked and settling strip footing [NSF-GEER; N 38.3011 W 122.3442; 08/25/14 11:41]

Figure C-H37-3: Open cracks in pavement [NSF-GEER; N 38.3011 W 122.3442; 08/25/14 11:36]

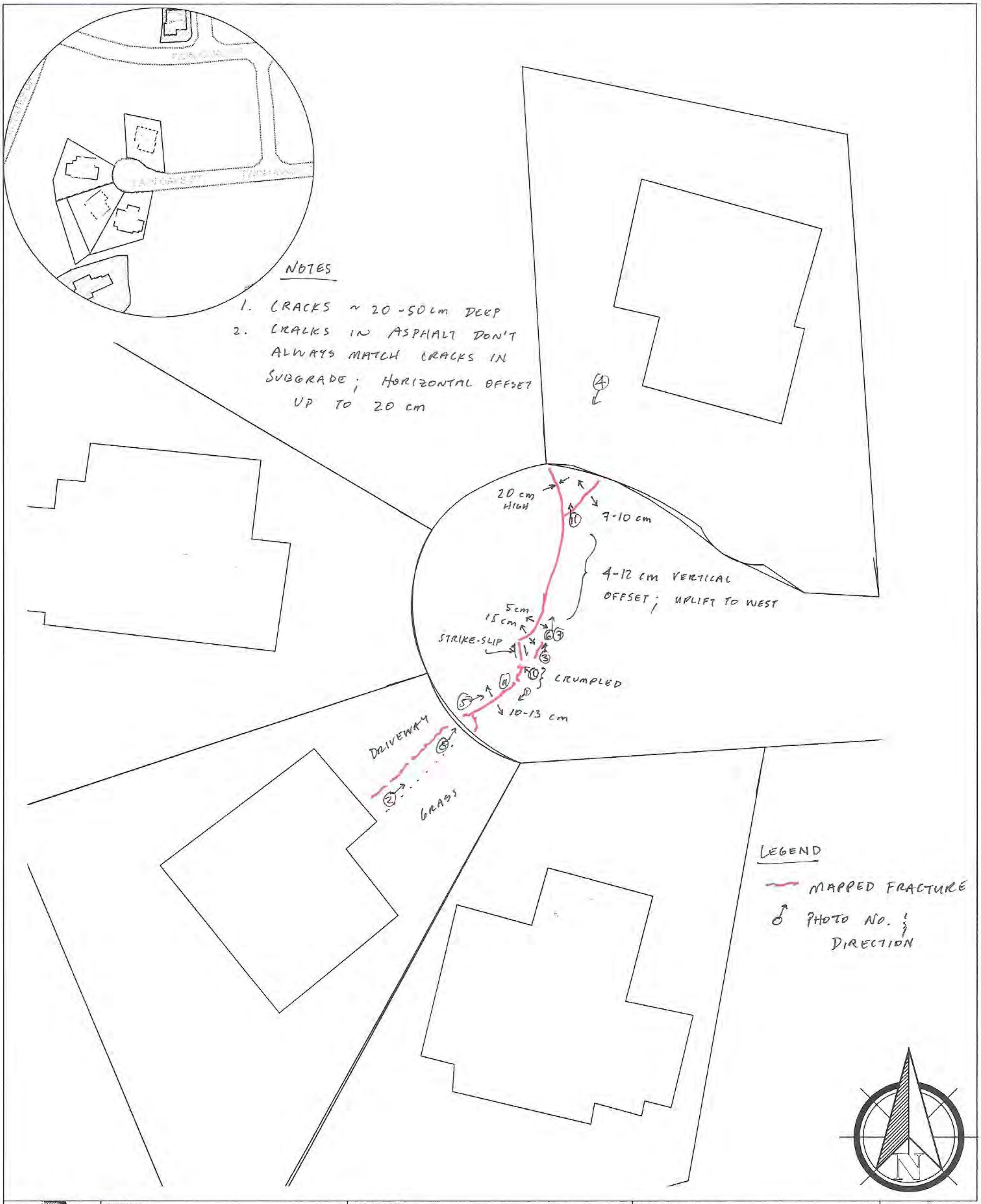

NOTES

1. CRACKS ~ 20-50 cm DEEP
2. CRACKS IN ASPHALT DON'T ALWAYS MATCH CRACKS IN SUBGRADE ; HORIZONTAL OFFSET UP TO 20 cm

EVENT: AMERICAN CANYON EQ $M_W = 6.0$

ADDRESS: PAVEMENT IN TWIN OAKS CT.

DRAWING BY: N. WAGNER
R. LANZAFAME

DESCRIPTION: HOUSE MAPPING (P1)

DATE OF INSPECTION: 8/25/14

DATE OF DRAWING: 8/25/14

SCALE: 1 cm : 4 m

10 m

Figure C-P1-2: General view of fracturing [NSF-GEER; N 38.3016 W 122.3441; 08/25/14 10:24]

Figure C-P1-3: General view of fracturing [NSF-GEER; N 38.3018 W 122.3437; 08/25/14 10:42]

Figure C-P1-4: Asphalt fracture [NSF-GEER; N 38.3017 W 122.3440; 08/25/14 11:33]

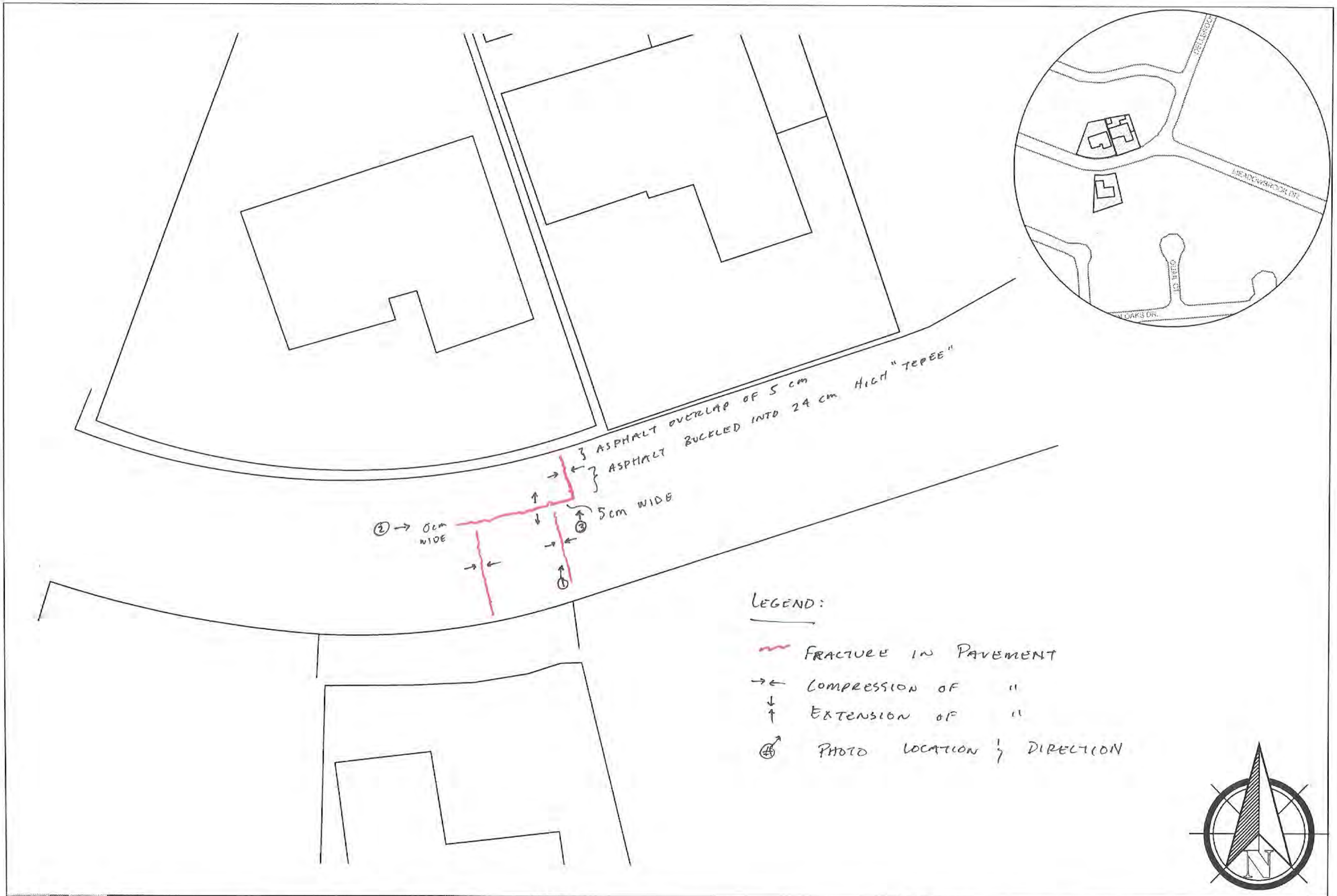

EVENT: AMERICAN CANYON EQ $M_W = 6.0$	ADDRESS: PAVEMENTI IN MEADOWBROOK DR		DRAWING BY: R. LANZAFAME N. WAGNER
DESCRIPTION: HOUSE MAPPING (P2)	DATE OF INSPECTION: 8/25/14	DATE OF DRAWING: 8/25/14	SCALE: 1 cm : 4 m 10 m

Figure C-P2-2: General view of fracturing [NSF-GEER; N 38.3038 W 122.3441; 08/25/14 13:18]

Figure C-P2-3: Asphalt buckling from end [NSF-GEER; N 38.3038 W 122.3430; 08/25/14 13:20]

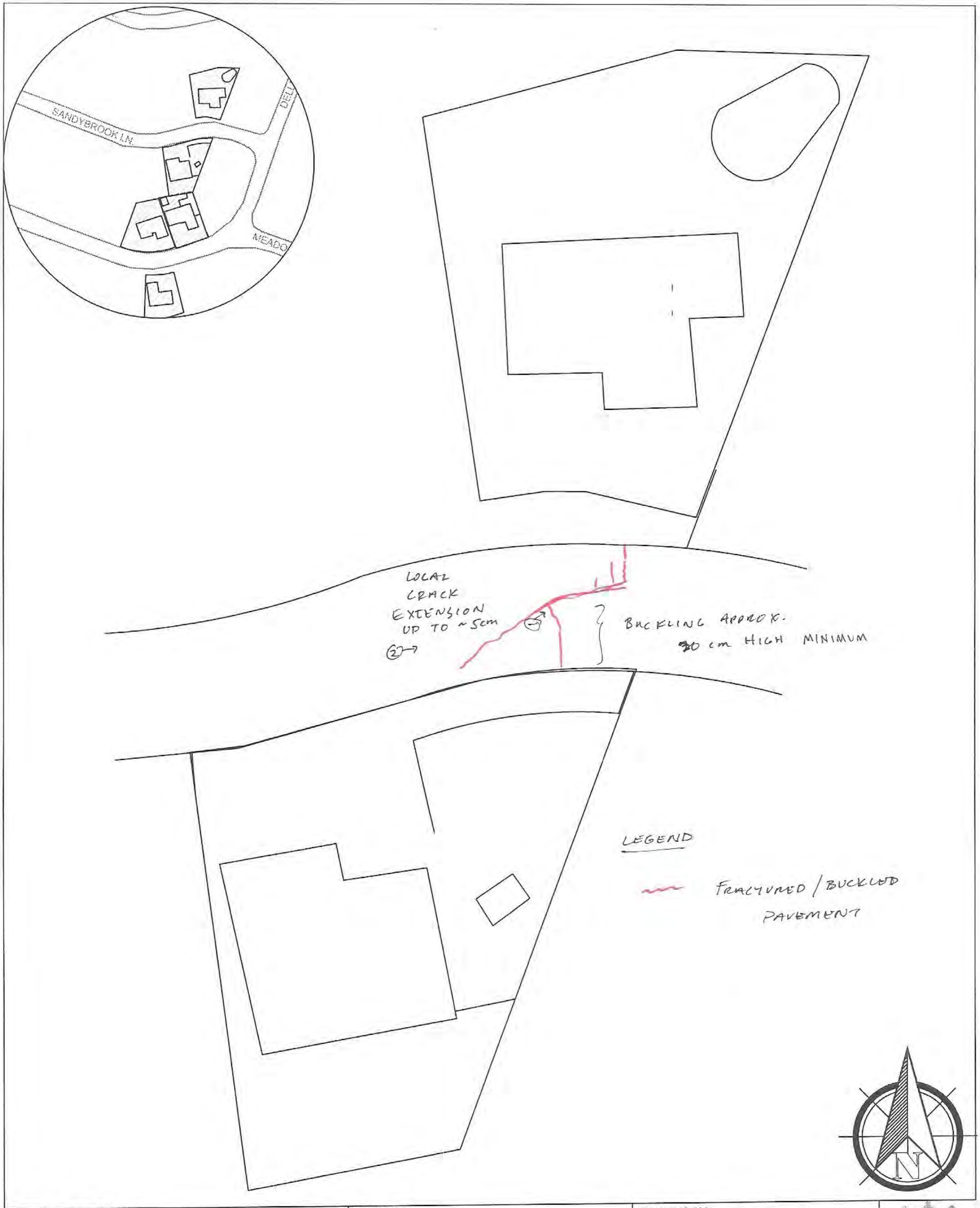

EVENT:
AMERICAN CANYON EQ $M_W = 6.0$

ADDRESS:
PAVEMENT IN SANDYBROOK DR.

DRAWING BY:
R. LANZAFAME
N. WAGNER

DESCRIPTION:
House Mapping ⓟ3

DATE OF INSPECTION:
8/25/14

DATE OF DRAWING:
8/25/14

SCALE:
1 cm : 4 m
10 m

Figure C-P3-2: [NSF-GEER; N 38.3046 W 122.3428; 08/25/14 15:26]

Figure C-P3-3: [NSF-GEER; N 38.3046 W 122.3428; 08/25/14 15:28]

Appendix D: Ground Deformation in the Very Near Fault Region

Figure D-1: Observation and measurement segments of ground strain (red lines) & approximate observed fault trace (yellow line); produced in Google Earth; [NSF-GEER; Napa, CA; N 38.3040 W 122.3443; 8/26/14 - 8/28/14]

Figure D-2: Observed and measured tension (orange) and compression (green) locations; produced in AutoCAD; [NSF-GEER; Luque, R.; Wagner, N.; processed 9/5/14]

Figure D-3: Typical buckled compression zone in pavement perpendicular to fault, near observed fault trace [NSF-GEER; N 38.3039 W 122.3430; 8/26/2014 15:24]

Figure D-4: Overlapping compression zone in pavement parallel to fault, near road crossing [NSF-GEER; N 38.3054 W 122.3455; 8/26/2014 17:20]

Figure D-5: Buckled and crushed compression zone in pavement parallel to fault [NSF-GEER; N 38.3048 W 122.3460; 8/26/2014 18:52]

Figure D-6: Overlapping compression zone in pavement perpendicular and adjacent to fault [NSF-GEER; N 38.3025 W 122.3436; 8/27/2014 12:01]

Figure D-7: Lateral offset of overlapping compression zone in pavement perpendicular and adjacent to fault; offset is parallel to fault [NSF-GEER; N 38.3026 W 122.3437; 8/27/2014 12:02]

Figure D-8: Slight uplift in compressed zone of pavement perpendicular and near fault [NSF-GEER; N 38.3037 W 122.3430; 8/26/2014 15:48]

Figure D-9: Typical extension cracks in thermal joints of sidewalk pavement parallel to fault; ~13mm gap (left), ~7mm gap (right) [NSF-GEER; N 38.3067 W 122.3464; 8/28/2014 15:18]

Figure D-10: Extension crack in sidewalk pavement parallel to fault; ~3mm gap [NSF-GEER; N 38.3055 W 122.3454; 8/26/2014 18:30]

Figure D-11: Example of extension crack not considered due to shaved concrete [[NSF-GEER; N 38.3021 W 122.3430; 8/28/2014 09:17]

Figure D-12: Crushed section in pavement parallel to fault with compression features in curb strip perpendicular to fault, across from creek [NSF-GEER; N 38.3055 W 122.3467; 8/28/2014 14:30]

Figure D-13: Buckled section in pavement perpendicular to fault with compression features in curb strip and lawn parallel to fault, near observed fault trace [NSF-GEER; N 38.3018 W 122.3439; 8/25/2014 10:38]

Figure D-14: Compression feature in curb strip perpendicular to fault, across from creek [NSF-GEER; N 38.3065 W 122.3455; 8/28/2014 13:52]

Figure D-15: Cracks in asphalt perpendicular to fault trace near manhole covers [NSF-GEER; N 38.3063 W 122.3458; 8/28/2014 14:15 (left); N 38.3068 W 122.3465; 8/28/2014 15:19 (right)]

Figure D-16: Crushed curb perpendicular to fault trace [NSF-GEER; N 38.3035 W 122.3411; 8/25/2014 14:47]

Figure D-17: Extension crack in curb parallel to fault trace [NSF-GEER; N 38.3066 W 122.3465; 8/28/2014 15:08]

Figure D-18: Buckled curb parallel to fault trace [NSF-GEER; N 38.3073 W 122.3443; 8/28/2014 13:41]

Figure D-19: Buckled curb adjacent to pavement perpendicular to fault trace; visible cracking in soil aligns with cracks in curb [NSF-GEER; N 38.3027 W 122.3407; 8/28/2014 10:25]

Figure D-20: Buckled section of fence for strain measurements [NSF-GEER; N 38.3015 W 122.3442; 8/25/2014 09:57]

Table D-1: Summary of strain measurements in parallel trending roads [NSF-GEER; Wagner, N.; processed 9/3/2014]

N-S (PARALLEL) TRENDING ROADS				
	East Side		West Side	
	Total Length (m)	Average Strain (%)	Total Length (m)	Average Strain (%)
West of Fault				
Estates Dr	90.0	-0.01	77.5	-0.07
White Cliff Cir (West)	71.4	0.05	71	-0.02
Stonybrook Dr	459.2	-0.04	508.0	-0.03
Tall Grass Dr	N/A	N/A	199.0	-0.05
Casper Way	203.9	0.01	220.2	-0.01
Weighted Average Strain		**-0.01**		**-0.03**
East of Fault				
Twin Oaks Ct	69.8	0.00	69.8	0.00
Dellbrook Dr	75	0.00	44.15	0.00
Weighted Average Strain		**0.00**		**0.00**
Crossing Fault				
White Cliff Cir (East)	50.7	**0.01**	50.7	**0.36**

Table D-2: Summary of strain measurements in perpendicular trending roads [NSF-GEER; Wagner, N.; processed 9/3/2014]

E-W (PERPENDICULAR) TRENDING ROADS				
	North Side		South Side	
	Total Length (m)	Average Strain	Total Length (m)	Average Strain
West of Fault				
Twin Oaks Dr	297.3	-0.02	274.1	0.01
White Cliff Cir	163.0	-0.05	164.5	0.04
Meadowbrook Dr	221.7	0.00	221.7	0.00
Weighted Average Strain		**-0.02**		**0.01**
East of Fault				
Twin Oaks Dr	212.1	0.00	208.9	0.00
Meadowbrook Dr	209.4	0.00	N/A	N/A
Weighted Average Strain		**0.00**		**0.00**
Crossing Fault				
Meadowbrook Dr	40	**-0.24**	30	**-0.17**

Table D-3: Strain measurements for Estates Drive [NSF-GEER; Cohen-Waeber, J.; Gardner, M.; Lanzafame, R.; Wagner, N.; measured 8/26/2014]

Location:	Estates Drive
Approximate orientation relative to fault trace:	Parallel & West

EAST SIDE MEASUREMENTS:

Bounding Streets	Gage Number	Heading (deg)	Length (m)	Orig. Length (m)	Total Ext (in)	Total Comp (in)	Strain (%)
Lowry Ct & Twin Oaks Dr	1	21.5	25.0	25.0	0	0.25	-0.03
	2	21.5	25.0	25.0	0	0	0.00
	3	21.0	25.0	25.0	0	0	0.00
	4	21.5	15.0	15.01	0	0.25	-0.04
		Total	90.00	90.01		**Average Strain**	**-0.01**
						Average Disp. (m)	**-0.01**

WEST SIDE MEASUREMENTS:

Bounding Streets	Gage Number	Heading (deg)	Length (m)	Orig. Length (m)	Total Ext (in)	Total Comp (in)	Strain (%)
Twin Oaks Dr & Lowry Ct	1	201.5	25.00	25.05	0	2	-0.20
	2	201.0	25.00	25.00	0	0	0.00
	3	200.5	25.00	25.00	0	0	0.00
	4	201.0	2.45	2.45	0	0	0.00
		Total	77.45	77.50		**Average Strain**	**-0.07**
						Average Disp. (m)	**-0.05**

Table D-4: Strain measurements for White Cliff Circle (continued on next page) [NSF-GEER; Carlosama, H.; Gardner, M.; Wagner, N.; measured 8/27/2014]

Location: White Cliffs Cir

WESTERN NORTH-SOUTH LEG

EAST SIDE MEASUREMENTS:

Approximate orientation relative to fault trace: Parallel & West

Bounding Streets	Gage Number	Heading (deg)	Length (m)	Orig. Length (m)	Total Ext (in)	Total Comp (in)	Strain (%)
Twin Oaks Dr & White Cliffs Cir	1	226.0	71.4	71.4	1.5	0	0.05
		Total	71.4	71.4		**Average Strain**	**0.05**
						Average Disp. (m)	**0.04**

WEST SIDE MEASUREMENTS:

Approximate orientation relative to fault trace: Parallel & West

Bounding Streets	Gage Number	Heading (deg)	Length (m)	Orig. Length (m)	Total Ext (in)	Total Comp (in)	Strain (%)
Twin Oaks Dr & White Cliffs Cir	1	28.0	25	25.0	0	0	0.00
	2	40.5	25	25.0	12.25	13	-0.08
	3	40.5	21	21.0	0.24	0	0.03
		Total	71	71.01		**Average Strain**	**-0.02**
						Average Disp. (m)	**-0.01**

EASTERN NORTH-SOUTH LEG

EAST SIDE MEASUREMENTS:

Approximate orientation relative to fault trace: Parallel & East

Bounding Streets	Gage Number	Heading (deg)	Length (m)	Orig. Length (m)	Total Ext (in)	Total Comp (in)	Strain (%)
Twin Oaks Dr & White Cliffs Cir	1	355.5	25.7	25.7	0.125	0	0.01
	2	357.0	25	25.0	0.125	0	0.01
		Total	50.7	50.7		**Average Strain**	**0.01**
						Average Disp. (m)	**0.01**

WEST SIDE MEASUREMENTS:

Approximate orientation relative to fault trace: Parallel & West (gage#1) and East(rest)

Bounding Streets	Gage Number	Heading (deg)	Length (m)	Orig. Length (m)	Total Ext (in)	Total Comp (in)	Strain (%)
Twin Oaks Dr & White Cliffs Cir	1	176.0	25	24.8	7	0	0.72
	2	177.0	25.7	25.7	0.125	0	0.01
		Total	50.7	50.5		**Average Strain**	**0.36**
						Average Disp. (m)	**0.18**

NOTE: *Fault trace runs through portion of gage #1, sidewalk very distorted*

EAST-WEST LEG

NORTH SIDE MEASUREMENTS:

Approximate orientation relative to fault trace: Perpendicular & West

Bounding Streets	Gage Number	Heading (deg)	Length (m)	Orig. Length (m)	Total Ext (in)	Total Comp (in)	Strain (%)
White Cliffs Cir & White Cliffs Cir	1	275.5	13	13.0	0	1.75	-0.34
	2	291.5	25	25.0	0	0	0.00
	3	290.5	25	25.0	0	0	0.00
	4	291.0	25	25.0	0.125	0	0.01
	5	291.0	25	25.0	0.25	2	-0.18
	6	291.0	25	25.0	0.125	0	0.01
	7	291.5	25	25.0	0.20	0	0.02
		Total	163	163.08		**Average Strain**	**-0.05**
						Average Disp. (m)	**-0.08**

SOUTH SIDE MEASUREMENTS:

Approximate orientation relative to fault trace: Perpendicular & West

Bounding Streets	Gage Number	Heading (deg)	Length (m)	Orig. Length (m)	Total Ext (in)	Total Comp (in)	Strain (%)
White Cliffs Cir & White Cliffs Cir	1	111.0	25	25.0	0.625	0	0.06
	2	112.0	25	25.0	0.29	0.5	-0.02
	3	111.5	25	25.0	0.125	0	0.01
	4	111.0	25	25.0	0	0	0.00
	5	111.5	25	25.0	0.25	0	0.03
	6	110.5	25	25.0	0.41	0	0.04
	7	111.0	14.5	14.5	1.125	0	0.20
		Total	164.5	164.44		**Average Strain**	**0.04**
						Average Disp. (m)	**0.05**

Table D-5: Strain measurements for Stonybrook Drive (continued on next page) [NSF-GEER; Cohen-Waeber, J.; Gardner, M.; Lanzafame, R.; Wagner, N.; measured 8/26/2014]

Location:	Stonybrook Drive
Approximate orientation relative to fault trace:	Parallel & West

EAST SIDE MEASUREMENTS:

Bounding Streets	Gage Number	Heading (deg)	Length (m)	Orig. Length (m)	Total Ext (in)	Total Comp (in)	Strain (%)
Timberhill Ln & Twin Oaks Dr	1	60.5	25	25.0	0	0	0.00
	2	60.0	25	25.0	0	0	0.00
	3	65.5	25	25.0	0	0	0.00
	4	59.0	17.9	17.92	0	0.625	-0.09
Twin Oaks Dr & Meadowbrook Dr	5	46.0	15.8	15.8	0	1	-0.16
	6	42.5	25	25.0	0	0	0.00
	7	32.5	25	25.1	0	5.5	-0.56
	8	25.5	25	25.0	0	0.25	-0.03
	9	20.0	25	25.0	0	0.75	-0.08
	10	21.0	2.05	2.1	0	0	0.00
Meadowbrook Dr & Sandybrook Ln	11	23.5	6	6.0	0	0	0.00
	12	20.5	25	25.0	0.25	1.75	-0.15
	13	23.0	25	25.0	0.25	0.25	0.00
	14	21.0	25	25.0	0	0	0.00
	15	50.5	15	14.9	0	-4.5	0.77
Sandybrook Ln & Glenbrook Ln	16	52.5	17.45	17.5	0	0	0.00
	17	53.0	25	24.0	0	1.5	-0.15
	18	52.5	25	25.0	0	0.25	-0.03
	19	52.5	6.8	6.8	0	0	0.00
Glenbrook Ln & Woodbrook Dr	20	46.5	3.2	3.2	0	0	0.00
	21	44.0	25	25.0	0	0	0.00
	22	42.5	25	25.0	0	0	0.00
	23	42.0	25	25.0	0	0	0.00
		Total	459.20	459.37		**Average Strain**	**-0.04**
						Average Disp. (m)	**-0.17**

NOTE: *Twin Oaks Dr intesection width 16.3m*
Meadowbrook Dr intesection width 16.95m
Sandybrook Ln intesection width 17.55m
Glenbrook Ln intesection width 15.0m

WEST SIDE MEASUREMENTS:

Bounding Streets	Gage Number	Heading (deg)	Length (m)	Orig. Length (m)	Total Ext (in)	Total Comp (in)	Strain (%)
Woodbrook Dr & Meadowbrook Dr	1	221.5	25	25.0	0	0	0.00
	2	223.0	25	25.0	0	0	0.00
	3	223.5	25	25.0	0.25	0	0.03
	4	229.5	25	25.0	0.375	0.75	-0.04
	5	233.0	25	25.0	0.125	0	0.01
	6	233.5	25	25.1	0.75	6	-0.53
	7	233.5	25	25.0	1.5	0	0.15
	8	228.0	25	25.0	0.75	0	0.08
	9	204.5	25	25.0	0	1.75	-0.18
	10	200.5	25	25.0	0	0	0.00
	11	200.5	25	25.0	0	1.125	-0.11
	12	204.0	6.35	6.4	0	0	0.00
MeadowbrookDr & Timberhill Ln	13	205.0	1.6	1.6	0	0	0.00
	14	200.5	25	25.0	0	-1	0.10
	15	204.0	25	25.0	0	0	0.00
	16	212.0	25	25.0	0.25	0.75	-0.05
	17	221.5	25	25.0	0	0	0.00
	18	230.0	25	25.0	0	0	0.00
	19	239.5	25	25.0	0	0	0.00
	20	248.5	25	25.0	0	0.75	-0.08
	21	248.0	25	25.0	0	0	0.00
	22	237.5	25	25.0	0	0	0.00
		Total	507.95	508.10		**Average Strain**	**-0.03**
						Average Disp. (m)	**-0.15**

NOTE: *Meadowbrook Dr intesection width 17.05m*

Table D-6: Strain measurements for Tall Grass Drive [NSF-GEER; Carlosama, H.; Lanzafame, R.; Luque, R.; Wagner, N.; measured 8/28/2014]

Location:	Tall Grass Dr
Approximate orientation relative to fault trace:	Parallel & West

WEST SIDE MEASUREMENTS:

Positive strain is extension, negative is compression

Bounding Streets	Gage Number	Heading (deg)	Length (m)	Orig. Length (m)	Total Ext (in)	Total Comp (in)	Strain (%)
North Bridge & Skylark Way	1	221.5	25	25.0	0	1.25	-0.13
	2	221.0	25	25.0	0	0	0.00
	3	229.5	25	25.0	0	0	0.00
	4	241.0	25	25.0	0	0	0.00
	5	245.5	23.95	24.0	0	0	0.00
Skylark Way & Beartooth Lane	6	217.5	25	25.1	0	5.25	-0.53
	7	218.5	25	25.0	1.625	0.25	0.14
	8	235.0	25	25.0	1.375	0	0.14
	9	235.0	25	25.0	1	0	0.10
	10	226.5	25	25.0	0.25	0	0.03
	11	216.5	25	25.0	0.125	0	0.01
	12	209.0	25	25.0	0.375	0	0.04
	13	219.5	17	17.0	0.5	0	0.07
		Total	198.95	199.04		**Average Strain**	**-0.05**
						Average Disp. (m)	**-0.04**

NOTE:
- *Crushed curb in Section 2*
- *Asphalt crack in Section 7*
- *Crushed curb / displacement toward creek and asphalt crack in Section 8*
- *Most of deformation toward creek (transverse to pavement) in Section 13*
- *Skylark Way Intersection width 14.80m*

Table D-7: Strain measurements for Casper Way [NSF-GEER; Carlosama, H.; Lanzafame, R.; Luque, R.; Wagner, N.; measured 8/28/2014]

Location:	Casper Way
Approximate orientation relative to fault trace:	Parallel & West

EAST SIDE MEASUREMENTS:

Bounding Streets	Gage Number	Heading (deg)	Length (m)	Orig. Length (m)	Total Ext (in)	Total Comp (in)	Strain (%)
Beartooth Lane & Skylark Way	1	29.0	22.50	22.5	0.0625	0	0.01
	2	40.0	24.75	24.8	0	0	0.00
	3	40.0	25.00	25.0	0	0.5	-0.05
	4	38.0	25.70	25.7	1	0	0.06
	5	39.0	24.15	24.1	0.625	0.5	0.01
	6	44.0	24.15	24.1	0.4375	0	0.05
	7	52.5	23.60	23.6	0.0625	0	0.01
	8	60.0	34.00	34.0	0.125	0	0.01
		Total	203.85	203.83		**Average Strain**	**0.012**
						Average Disp. (m)	**0.008**

WEST SIDE MEASUREMENTS:

Bounding Streets	Gage Number	Heading (deg)	Length (m)	Orig. Length (m)	Total Ext (in)	Total Comp (in)	Strain (%)
Beartooth Lane & Skylark Way	1	29.0	27.25	27.3	0	0	0.00
	2	40.5	25.8	25.8	0	1	-0.10
	3	40.5	29.8	29.8	0.06	0	0.01
	4	38.5	24.25	24.2	0.06	0	0.01
	5	38.5	26	26.0	0.4375	0	0.04
	6	45.0	25.8	25.8	0.1875	0	0.02
	7	51.5	26	26.0	0.0625	0.25	-0.02
	8	59.0	35.25	35.3	0	0	0.00
		Total	220.15	220.16		**Average Strain**	**-0.005**
						Average Disp. (m)	**-0.004**

Table D-8: Strain measurements for Twin Oaks Court [NSF-GEER; Carlosama, H.; Lanzafame, R.; Luque, R.; Wagner, N.; measured 8/28/2014]

Location:	Twin Oaks Court
Approximate orientation relative to fault trace:	Parallel & East

EAST SIDE MEASUREMENTS:

Bounding Streets	Gage Number	Heading (deg)	Length (m)	Orig. Length (m)	Total Ext (in)	Total Comp (in)	Strain (%)
Twin Oaks Ct & Twin Oaks Dr	1	175.5	25	25.0	0	0	0.00
	2	175.5	25	25.0	0	0	0.00
	3	175.5	19.8	19.8	0	0	0.00
		Total	69.8	69.80		**Average Strain**	**0.000**
						Average Disp. (m)	**0.00**

NOTE: *- Symmetric to west side measurements; no cracks*

WEST SIDE MEASUREMENTS:

Bounding Streets	Gage Number	Heading (deg)	Length (m)	Orig. Length (m)	Total Ext (in)	Total Comp (in)	Strain (%)
Twin Oaks Ct & Twin Oaks Dr	1	357.0	25	25.0	0.125	0	0.01
	2	355.5	25	25.0	0	0	0.00
	3	356.5	19.8	19.8	0	0	0.00
		Total	69.8	69.80		**Average Strain**	**0.005**
						Average Disp. (m)	**0.003**

NOTE: *- Gage 3 has ~1/8" gaps in sidewalk corresponding to expansion joints every 3.7m; not included since debris inside crack suggested they existed prior to earthquake*

Table D-9: Strain measurements for Dellbrook Drive [NSF-GEER; Carlosama, H.; Lanzafame, R.; Luque, R.; Wagner, N.; measured 8/28/2014]

Location: Dellbrook Dr

Approximate orientation relative to fault trace: Parallel & East

EAST SIDE MEASUREMENTS:

Bounding Streets	Gage Number	Heading (deg)	Length (m)	Orig. Length (m)	Total Ext (in)	Total Comp (in)	Strain (%)
Meadowbrook Dr & Woodbrook Dr	1	21.5	25	25.0	0	0	0.00
	2	21.0	25	25.0	0	0	0.00
	3	21.0	25	25.0	0	0	0.00
	4	21.0	25	25.0	0	0	0.00
	5	21.0	25	25.0	0	0.125	-0.01
	6	20.5	25	25.0	0	0	0.00
	7	21.0	25	25.0	0	0	0.00
	8	21.5	30	30.0	0	0	0.00
		Total	75	75.00		**Average Strain**	**0.000**
						Average Disp. (m)	**0.000**

NOTE: *- West side of street not measured, no cracks or pavement buckles observed*

- On west side, Glenbrook crossing is 15.35m and Sandybrook crossing is 15.50m

Table D-10: Strain measurements for Twin Oaks Drive west of fault (continued on next page) [NSF-GEER; Carlosama, H.; Gardner, M.; Wagner, N.; measured 8/27/2014]

Location:	Twin Oaks Drive
Approximate orientation relative to fault trace:	Perpendicular & West

NORTH SIDE MEASUREMENTS:

Bounding Streets	Gage Number	Heading (deg)	Length (m)	Orig. Length (m)	Total Ext (in)	Total Comp (in)	Strain (%)
~8.4m east of fault trace & White Cliffs Cir	1	269.0	25	25.1	1.75	5	-0.33
	2	276.0	25	25.0	0.16	0	0.02
	3	282.0	25	25.0	0	0	0.00
	4	290.5	25	25.0	0.25	0.5	-0.03
	5	291.5	25	25.0	0	0	0.00
	6	290.5	25	25.0	0.04	0	0.00
	7	291.5	25	25.0	0	0	0.00
	8	290.5	25	25.0	0.125	0	0.01
	9	291.0	15.82	15.8	0.125	0	0.02
White Cliffs Cir & Stonybrook Dr	10	301.0	25	25.0	0	0	0.00
	11	309.0	25	25.0	0.125	0	0.01
	12	321.0	31.5	31.5	0.04	0	0.00
		Total	297.32	297.39		**Average Strain**	**-0.02**
						Average Disp. (m)	**-0.07**

NOTE: *- Gage 1 starts east of fault rupture and continues west. Fault trace intesects gauge length at ~ 8.4m. 2 inches of north-south offset noted 18.0m along gage length*

- White Cliffs Cir intesection width 10.80m

SOUTH SIDE MEASUREMENTS:

Bounding Streets	Gage Number	Heading (deg)	Length (m)	Orig. Length (m)	Total Ext (in)	Total Comp (in)	Strain (%)
Stonybrook Dr & Estates Dr	1	141.0	25	25.0	0.75	0.375	0.04
	2	133.0	25	25.0	0.5	0	0.05
	3	124.0	25	25.0	0	0	0.00
	4	115.0	25	25.0	0	0	0.00
	5	111.0	25	25.0	0	0	0.00
	6	111.0	25	25.0	0	0	0.00
	7	111.5	25	25.0	0	0	0.00
	8	112.0	28.1	28.1	0	0	0.00
Estates Dr & ~fault trace	9	110.0	25	25.0	0	0	0.00
	10	103.0	25	25.0	0.25	0	0.03
	11	96.0	21	21.0	0.25	0	0.03
		Total	274.1	274.07		**Average Strain**	**0.01**
						Average Disp. (m)	**0.03**

NOTE: *- Gage 11 ends ~3m west of estimated fault trace*

- Repairs to road & sidewalk on Twin Oaks Drive in vicinity of fault trace made it impossible to take strain reading of the sidewalk

- Compression perpendicular to Gage #3 in driveway of 3587 Twin Oaks Drive

- Estates Dr intesection width 15.77m

Table D-11: Strain measurements for Meadowbrook Drive west of fault [NSF-GEER; Carlosama, H.; Lanzafame, R.; Luque, R.; Wagner, N.; measured 8/28/2014]

Location:	Meadowbrook Dr
Approximate orientation relative to fault trace:	Perpendicular & West

NORTH SIDE MEASUREMENTS:

Bounding Streets	Gage Number	Heading (deg)	Length (m)	Orig. Length (m)	Total Ext (in)	Total Comp (in)	Strain (%)
~37.5m west of fault trace & Stonybrook Dr	1	291.0	25	25.0	0	0	0.00
	2	291.0	25	25.0	0	0	0.00
	3	291.5	25	25.0	0	0	0.00
	4	291.0	25	25.0	0.13	0	0.01
	5	291.5	25	25.0	0	0.5	-0.05
	6	291.5	25	25.0	0	0	0.00
	7	290.5	25	25.0	0	0	0.00
	8	290.0	25	25.0	0	0	0.00
	9	291.0	21.7	21.7	0	0	0.00
		Total	221.7	221.71	**Average Strain**		**-0.004**
					Average Disp. (m)		**-0.003**

SOUTH SIDE MEASUREMENTS:

Bounding Streets	Gage Number	Heading (deg)	Length (m)	Orig. Length (m)	Total Ext (in)	Total Comp (in)	Strain (%)
~37.5m west of fault trace & Stonybrook Dr	1	291.0	25	25.0	0	0	0.00
	2	291.0	25	25.0	0	0	0.00
	3	291.0	25	25.0	0	0.125	-0.01
	4	292.5	25	25.0	0.563	0.5	0.01
	5	291.5	25	25.0	0	0	0.00
	6	290.5	25	25.0	0	0	0.00
	7	291.0	25	25.0	0	0	0.00
	8	291.5	25	25.0	0	0	0.00
	9	291.5	21.7	21.7	0	0	0.00
		Total	221.7	221.70	**Average Strain**		**-0.001**
					Average Disp. (m)		**-0.001**

Table D-12: Strain measurements for Twin Oaks Drive east of fault [NSF-GEER; Carlosama, H.; Lanzafame, R.; Luque, R.; Wagner, N.; measured 8/28/2014]

Location:	Twin Oaks Drive
Approximate orientation relative to fault trace:	Perpendicular & East

NORTH SIDE MEASUREMENTS:

Bounding Streets	Gage Number	Heading (deg)	Length (m)	Orig. Length (m)	Total Ext (in)	Total Comp (in)	Strain (%)
White Cliff Cir & Quail Ct	1	85.0	25	25.0	0	0	0.00
	2	85.0	25	25.0	0	0	0.00
	3	87.0	21.3	21.3	0	0	0.00
Quail Ct & Sunburst Ct	4	85.5	25	25.0	0.125	0	0.01
	5	85.5	25	25.0	0	0	0.00
	6	84.5	17.1	17.1	0	0	0.00
Sunburst Ct & Buhman Ave	7	88.0	25	25.0	0	0	0.00
	8	96.5	25	25.0	0	0	0.00
	9	108.0	23.7	23.7	0	0	0.00
		Total	212.10	212.10		**Average Strain**	**0.001**
						Average Disp. (m)	**0.003**

SOUTH SIDE MEASUREMENTS:

Bounding Streets	Gage Number	Heading (deg)	Length (m)	Orig. Length (m)	Total Ext (in)	Total Comp (in)	Strain (%)
Twin Oaks Ct & Buhman Ave	1	287.5	23.7	23.7	0	0	0.00
	2	275.5	25	25.0	0	0	0.00
	3	266.0	25	25.0	0	0	0.00
	4	266.0	25	25.0	0	0	0.00
	5	265.5	25	25.0	0	0.25	-0.03
	6	265.5	25	25.0	0	0	0.00
	7	265.0	25	25.0	0	0	0.00
	8	266.5	25	25.0	0	0	0.00
	9	266.5	10.2	10.2	0	0	0.00
		Total	208.9	208.9		**Average Strain**	**-0.003**
						Average Disp. (m)	**-0.01**

NOTE:

- *Lengths on south side inferred from gage numbers and lengths on north side*
- *South side is 38.8m shorter at western end, but does not include the gaps due to street crossings at Quail Ct (16.4m) and Sunburst Ct (26.50m)*
- *No noticeable cracks except for single compression zone*

Table D-13: Strain measurements for Meadowbrook Drive east of fault [NSF-GEER; Cohen-Waeber, J.; Gardner, M.; Lanzafame, R.; Wagner, N.; measured 8/26/2014]

Location: Meadowbrook Dr

Approximate orientation relative to fault trace: Perpendicular & East

NORTH SIDE MEASUREMENTS:

Bounding Streets	Gage Number	Heading (deg)	Length (m)	Orig. Length (m)	Total Ext (in)	Total Comp (in)	Strain (%)
Twin Oaks Ct & Twin Oaks Dr	1	291.5	100	100.0	0.75	0.75	0.00
	2	291.5	100	100.0	0.25	0.5	-0.01
	3	291.5	9.35	9.4	0	0	0.00
		Total	209.35	209.36		**Average Strain**	**-0.003**
						Average Disp. (m)	**-0.006**

NOTE: *- First segment measured, so the gage lengths are very long before we realized that a shorter gage would be better suited for this task*

Table D-14: Strain measurements for Meadowbrook Drive across the fault [NSF-GEER; Cohen-Waeber, J.; Gardner, M.; Lanzafame, R.; Wagner, N.; measured 8/26/2014]

Location:	Meadowbrook Dr
Approximate orientation relative to fault trace:	Perpendicular & Across

NORTH SIDE MEASUREMENTS:

Bounding Streets	Gage Number	Heading (deg)	Length (m)	Orig. Length (m)	Total Ext (in)	Total Comp (in)	Strain (%)
Across fault	1	73.5	10.6	10.7	0	3.75	-0.89
	2	74.0	29.4	29.4	0	0	0.00
		Total	40	40.09		**Average Strain**	**-0.235**
						Average Disp. (m)	**-0.09**

SOUTH SIDE MEASUREMENTS:

Bounding Streets	Gage Number	Heading (deg)	Length (m)	Orig. Length (m)	Total Ext (in)	Total Comp (in)	Strain (%)
Across fault	1	88.0	18	18.0	0.25	1.5	-0.18
	2	75.0	12	12.0	0	0.75	-0.16
		Total	30	30.05		**Average Strain**	**-0.169**
						Average Disp. (m)	**-0.051**

Table D-15: Strain measurements for fence adjacent to fault trace [NSF-GEER; Lanzafame, R; Wagner, N.; measured 8/25/2014]

Section Number (Top)	Length (m)	Section Number (Bottom)	Length (m)
1	1.5	1	11.9
2	4.8		
3	2.4		
4	2.4		
5	4.9	2	9.8
6	4.9		
7	2.4		
8	2.4		
9	2.4	3	11.2
10	2.4		
11	2.4		
Total	33.0		32.9
		Average Strain	**-0.36**
		Average Disp. (m)	**-0.12**

APPENDIX E: Non-Near-Fault Ground Performance Observations

List of Figures

List of Tables

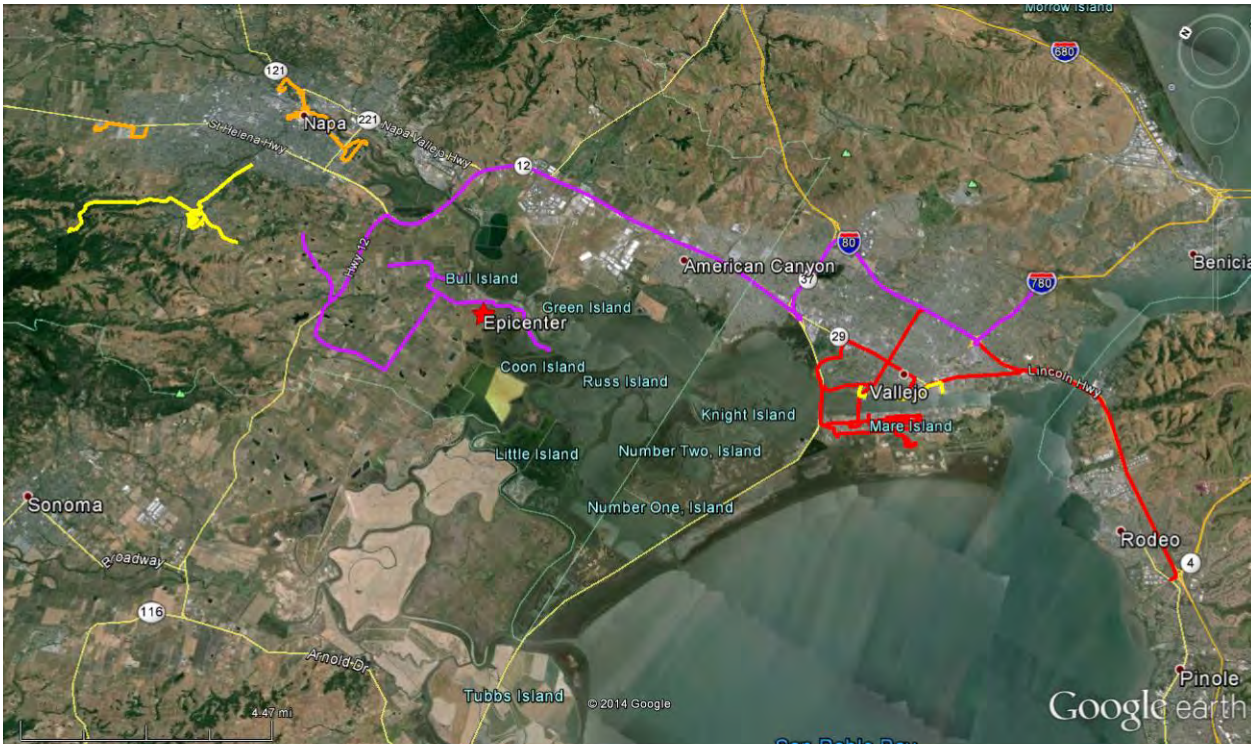

Figure E.1: GPS Track for all GEER teams outside near-fault region [NSF-GEER; 08/24/14]

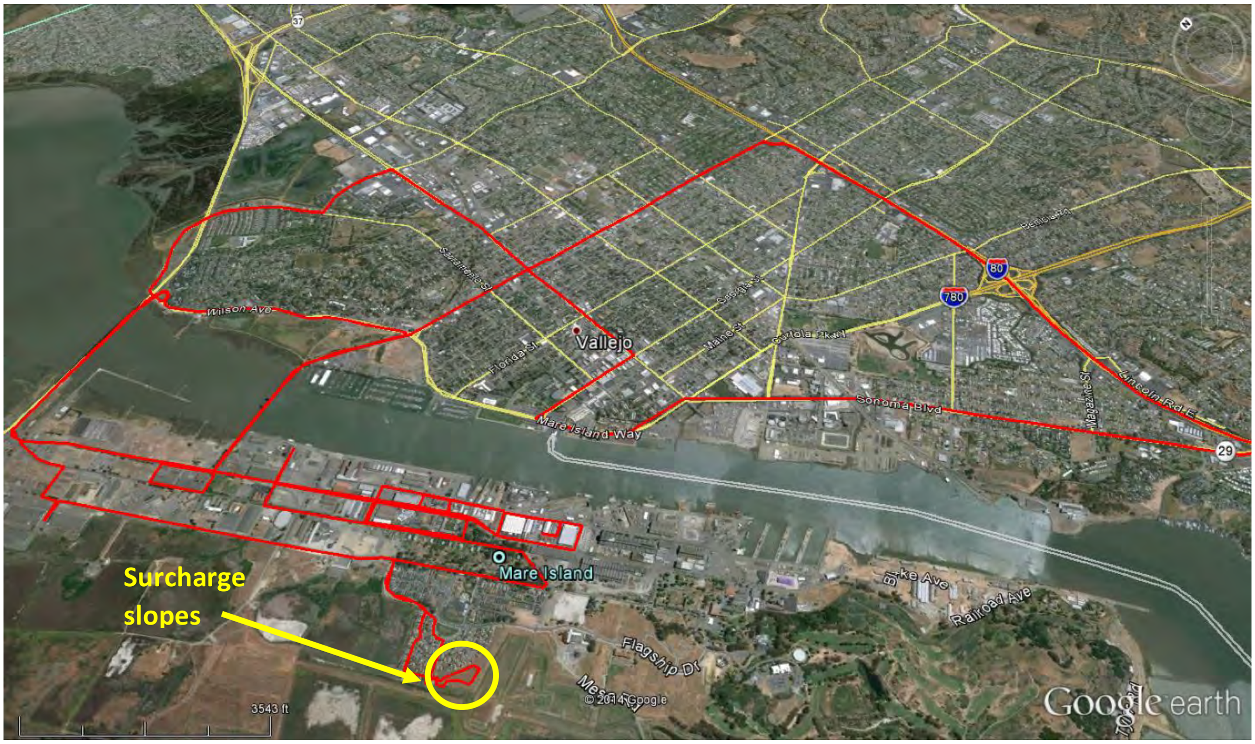

Figure E.2: GPS Track for C. Beyzaei and M. Shriro, Mare Island & Vallejo [NSF-GEER; 08/24/14]

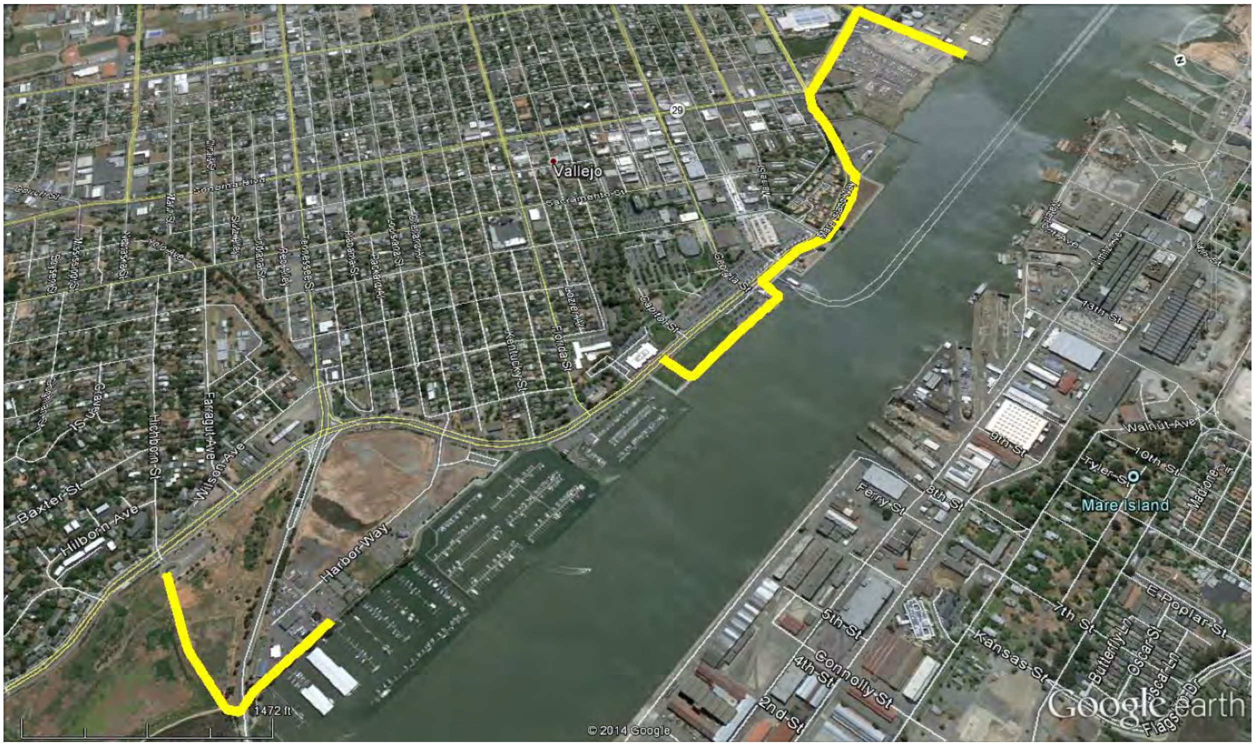

Figure E.3: GPS Track for Gardner and Markham, Vallejo [NSF-GEER; 08/24/14]

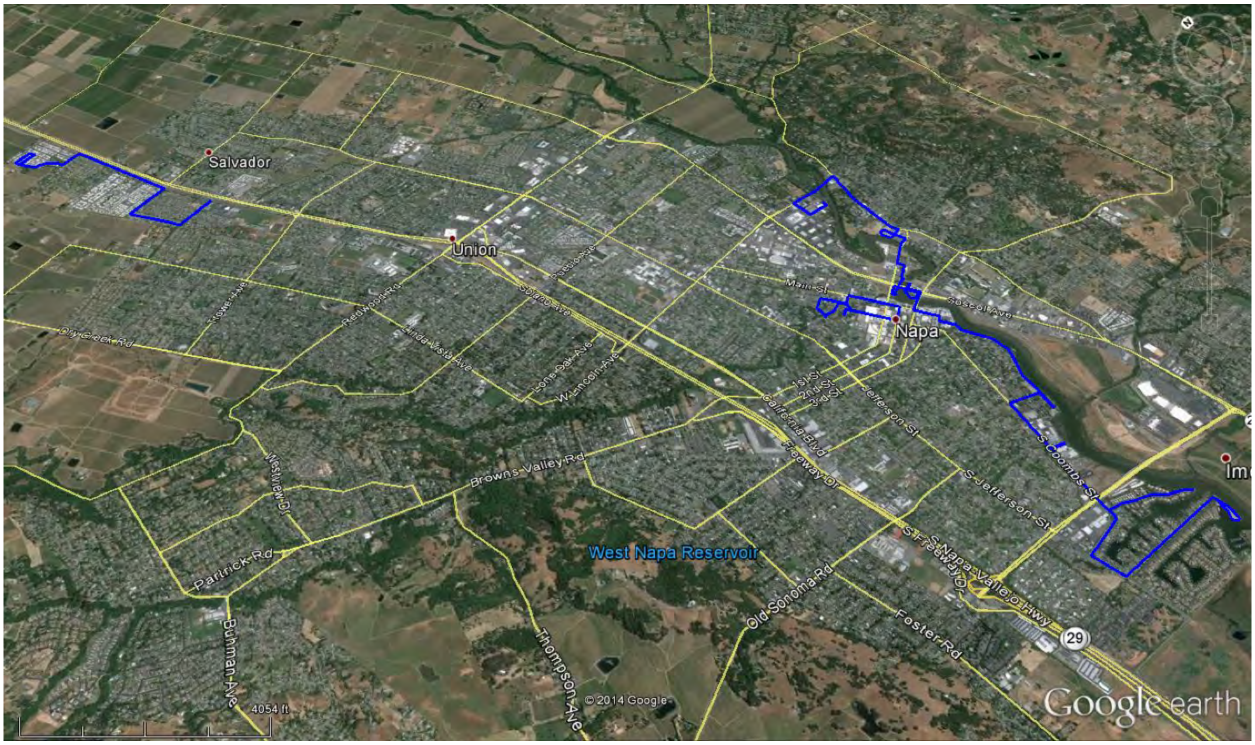

Figure E.4: GPS Track for J. Cohen-Waeber and R. Luque, Napa [NSF-GEER; 08/24/14]

Table E.1: Mare Island Observations – Officers' Quarters on Walnut Avenue [NSF-GEER: Beyzaei and Shriro; 08/24/14]

Location (listed from north to south)	Damage	Post-Earthquake Classification
Quarters 21	Brick chimney - damaged	Yellow tag
Quarters 29	Brick chimney - damaged	Yellow tag
Quarters 19	Metal chimney - no visible damage	No tag
Quarters 17	Metal chimney - no visible damage	No tag
Quarter F (Island Energy)	Brick chimney - no visible damage	No tag
Quarters P	Brick chimney - no visible damage	No tag
Quarters O	Brick chimney - damaged	No visible tag; caution tape in place across access
Quarters N	Brick chimney - damaged	Yellow tag
Quarters M	Brick chimney - damaged but not lost	Yellow tag
Quarters L	Brick chimney - damaged	Yellow tag
Quarters K	Brick chimney - damaged chimney fell onto and sheared adjacent tree at trunk	Yellow tag
Quarters J	Brick chimney - damage to building concealed by vegetation, but bricks on ground indicated likely loss of chimney	Yellow tag
Quarters A	Brick chimneys - one is damaged	Yellow tag
Quarters B	Metal chimney – no visible damage	Green tag
Quarters C	Metal chimney – no visible damage	Green tag
Quarters D	Metal chimney – no visible damage	Green tag
Quarters E	Brick chimney – damaged	Yellow tag
Quarters G	No visible damage	No tag; access appears unrestricted
Quarters H	Brick chimney – partially damaged	Yellow tag
Saint Peter's Chapel	No visible damage from outside; Tiffany windows not inspected up close for hairline cracks but no obvious broken windows observed	Access unrestricted; no tag
Walnut Ave.	Paving stones loose in areas of the sidewalk	Possibly earthquake related

Table E.2: Mare Island Observations – Historic Core [NSF-GEER: Beyzaei and Shriro; 08/24/14]

Location	**Observation**
Building 87	Looks OK (west side, on Nimitz Ave)
Building 71	Looks OK (maybe some minor cracks reopened)
Building 69 (?)	Looks OK
Building 273	Broken glass windows, likely not earthquake related
Building 571	Green and white building, corrugated sheet metal siding was deformed with some damage to roll-up door on opposite side of siding damage; white building next to 571 appeared undamaged
Building 47	Looks OK
Building 65	Looks OK (minor cracks might be earthquake related)
Building 52	Some bricks have fallen from the large circular window, otherwise undamaged; similar façade to Building 106 but it didn't fail

Building 126	@ Nimitz & Rickover intersection; most pronounced surface effects seen on Mare Island are the uplifted asphalt at the hydrant and possible surface cracking; water flowing out of pipe from building – had significantly decreased flow about an hour later (water line breaks within the building); roll-up door damaged
Building 106	Major masonry (brick) damage
Building 113	Looks OK, including hydrant in front of the building
Building 116	Looks OK (some broken glass on the ground)
Building 118	Major masonry (brick) damage on all sides but top façade appears undamaged; red-tagged; concrete façade on columns has buckled off
Building 114	Major masonry (brick) damage, including top façade
Building 112	Corrugated roll-up doors damaged, sprinkler system/water line breaks inside the building
Building 165	Looks OK (under construction, vertical cracks in wood columns might be earthquake related or due to construction, no bricks on the ground)
Dry dock	Undamaged according to security guard at Shipyard Gate 1 (he noted that there had been major shaking but no noticeable damage)

Table E.3: Vallejo Waterfront Observations [NSF-GEER: Gardner and Markham; 08/24/14]

Location	**Observation**
N38.111°,W122.271°	No indicators of any lateral spreading or EQ induced displacement (Vallejo Marina, up to Ferry Terminal)
N38.097°, W122.258°	Broken waterline along Mare Island Way
N38.093°, W122.254°	Broken waterline in Kiewit Vallejo yard

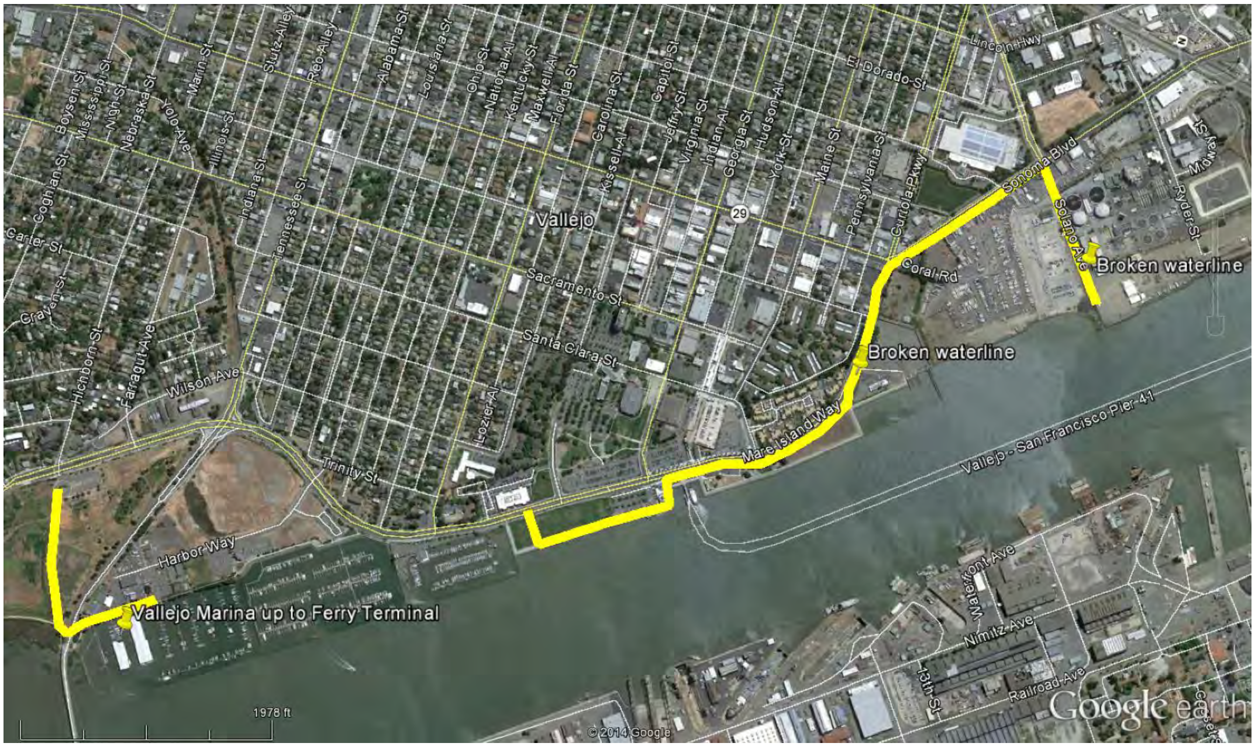

Figure E.5: Vallejo Waterfront Observation Locations [NSF-GEER: Gardner and Markham; 08/24/14]

Figure E.6: Corrugated siding damage [NSF-GEER; GPS N38.111 W122.282; 08/24/14; 13:53]

Figure E.7: Corrugated siding, no damage [NSF-GEER; GPS N38.110 W122.283; 08/24/14; 13:54]

Figure E.8: Brick chimney damage [NSF-GEER; GPS N38.100 W122.274; 08/24/14; 14:13]

Figure E.9: Brick chimney damage [NSF-GEER; GPS N38.099 W122.273; 08/24/14; 14:19]

Figure E.10: Metal chimney, no damage [NSF-GEER; GPS N38.097 W122.272; 08/24/14; 17:06]

Figure E.11: Brick facade damage [NSF-GEER; GPS N38.097 W122.268; 08/24/14; 14:43]

Figure E.12: Brick facade damage [NSF-GEER; GPS N38.095 W122.268; 08/24/14; 15:38]

Figure E.13: Possible earthquake damage [NSF-GEER; GPS N38.098 W122.269; 08/24/14; 14:37]

Figure E.14: Pavement damage at hydrant [NSF-GEER; GPS N38.098 W122.269; 08/24/14; 14:39]

Figure E.15: Pavement damage at hydrant [NSF-GEER; GPS N38.098 W122.269; 08/24/14; 14:37]

Figure E.16: Pavement damage along concrete [NSF-GEER; GPS N38.098 W122.269; 08/24/14; 14:38]

Figure E.17: Pavement damage at concrete corner [NSF-GEER; GPS N38.098 W122.269; 08/24/14; 14:38]

Figure E.18: Hydrant, no damage [NSF-GEER; GPS N38.097 W122.268; 08/24/14; 14:51]

Figure E.19: Soundwall alignment, no deformation [NSF-GEER; GPS N38.096, W122.276; 08/24/14; 17:31]

Figure E.20: Soundwall, minor crack [NSF-GEER; GPS N38.096 W122.276; 08/24/14; 17:31]

Figure E.21: Surcharge slope, no damage [NSF-GEER; GPS N38.092, W122.277; 08/24/14; 17:49]

Figure E.22: Slope, no damage [NSF-GEER; GPS N38.092 W122.277; 08/24/14; 17:50]

Figure E.23: Slopes, no damage [NSF-GEER; GPS N38.092 W122.277; 08/24/14; 17:53]

Figure E.24: Surcharge slope, no damage [NSF-GEER; GPS N38.092 W122.277; 08/24/14; 17:51]

Figure E.25: Highway 37 Bridge pier, no damage [NSF-GEER; GPS N38.122 W122.276; 08/24/14; 18:24]

Figure E.26: Water main break at Napa Valley Mobile Home Park [NSF-GEER; N 38.3465 W -122.330; 08/24/14 10:39]

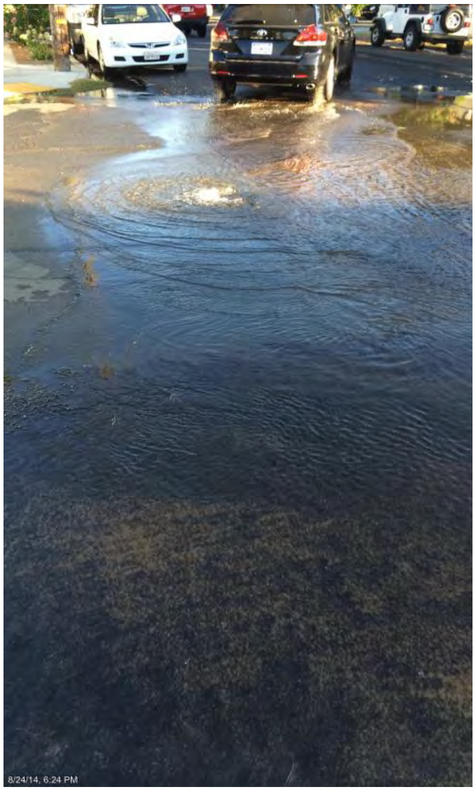

Figure E.27: Water main break at Brown St. (Downtown Napa) [NSF-GEER; N 38.3016 W -122.288; 08/24/14 18:24]

Figure E.28: Water break at Arroyo Dr. (Downtown Napa). Soil below asphalt ejected by water. [NSF-GEER; N 38.3008 W -122.289; 08/25/14 18:34]

Figure E.29: Lincoln Bridge. No damage was observed. [NSF-GEER; N 38.311 W -122.278; 08/25/14 12:02]

Figure E.30: 1st St. Bridge. No damage observed. [NSF-GEER; N 38.3023 W -122.2794; 08/25/14 12:26]

Figure E.31: Railroad Bridge. Crack observed in the interface between the North abutment foundation and the soil. [NSF-GEER; N 38.3002 W -122.282; 08/25/14 12:41]

Figure E.32: Railroad Bridge. Crack observed in the interface between the South abutment foundation and the soil. [NSF-GEER; N 38.2995 W -122.2821; 08/25/14 13:28]

Figure E.33: Railroad Bridge. Crack observed in the interface between the South abutment foundation and the soil. [NSF-GEER; N 38.2995 W -122.2821; 08/25/14 13:28]

Figure E.34: Failure of the stone retaining wall in South abutment of Soscol Bridge [NSF-GEER; N 38.2994 W -122.282; 08/24/14 13:44]

Figure E.35: Crack parallel to the River in North abutment of Soscol Bridge [NSF-GEER; N 38.2997 W -122.283; 08/24/14 13:09]

Figure E.36: Movement of the deck in 3rd St. Bridge East abutment [NSF-GEER; N 38.2981 W -122.284; 08/24/14 14:44]

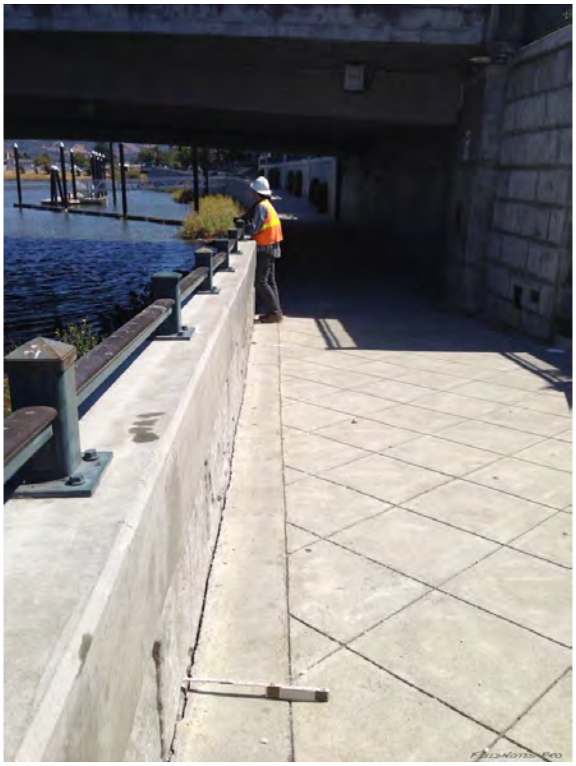

Figure E.37: Crack parallel to the River in West abutment of 3rd St. Bridge [NSF-GEER; N 38.2980 W -122.2840; 08/24/14 14:44]

Figure E.38: of the deck in 3rd St. Bridge East abutment [NSF-GEER; N 38.2981 W -122.284; 08/24/14 14:44]

Figure E.39: Ground cracking due to liquefaction in Napa River point bar below 3rd St. Bridge, between the two columns of the eastern pier. [NSF-GEER; N 38.2980 W -122.2840; 08/24/14 14:44]

Figure E.40: Ground cracking and settlement due to liquefaction in Napa River point bar below 3rd St. Bridge [NSF-GEER; N 38.2980 W -122.2840; 08/24/14 14:44]

Figure E.41: Settlement of backfill near the retaining wall in the Pedestrian Bridge [NSF-GEER; N 38.3003 W -122.2881; 08/24/14 17:58]

Figure E.42: Crack in pavement beind the retaining wall in the Pedestrian Bridge [NSF-GEER; N 38.3003 W -122.2881; 08/24/14 17:58]

Figure E.43: Crack along sheet pile wall behind the retaining wall in the Pedestrian Bridge [NSF-GEER; N 38.3003 W -122.2881; 08/24/14 17:58]

Figure E.44: Step between bridge's deck and access ramp in North abutment. [NSF-GEER; N 38.3003 W -122.2881; 08/24/14 17:58]

Table E.4: Description of damage observed in bridges

Bridge	**Damage Observed**
Lincoln Bridge	No damage observed
1st St. Bridge	No damage observed
Railroad bridge	North and south abutment: Cracks in the interface between foundation of abutment and soil oriented in both directions; perpendicular and parallel to the river.
Soscol Bridge	South abutment: Failure of masonry retaining. Fissure of the soil was observed in the EW direction, parallel to the river. Settlement of the street was observed relative to the deck of the bridge. North abutment: Crack parallel to the river bank was observed.
3rd St. Bridge	West abutment: About 0.75" displacement between walkway and retaining wall. Bridge deck was displaced about 2" in the E-W direction. The expansion joint connecting the deck to the road shows a widened gap by about 2 inches. East abutment: About 2" of displacement of the bridge deck was observed. Point River sand deposit below bridge: In the natural soil bank formed in the east side of the bridge are localized two larga columns that support the bridge's deck. Around these columns, ground cracks due to liquefaction were observed. It was also apparent that the soil had settled respect to the pier. The settlement measured was between 5 and 25 cm. No sand boil was observed but cracks with very fine silty sand was observed. The cracks were spaced every 25 to 30 cm in a radial pattern around the bridge piers. Ground cracking was also observed south and north of the bridge and the cracks were always oriented parallel to the shore.
Pedestrian Bridge (Coombs St)	This bridge crosses the Napa creek, not the Napa River. South abutment: The south abutment of the pedestrian bridge is founded on the backfill of a large retaining wall (H ≈ 3m). About 1.5 meters away from the retaining wall it was found a sheet pile wall. Along this sheet pile wall cracks were observed. To the north, on Coombs St, a large radial crack was observed 4 meters away from the retaining wall, suggesting a backfill failure. Adjacent to the wall 30 cm settlement was measured. North abutment: The bridge deck is raised approximately 15 cm above the north abutment and ramp. Cracks parallel to the creek were observed in the parking lot pavement and around the North abutment.

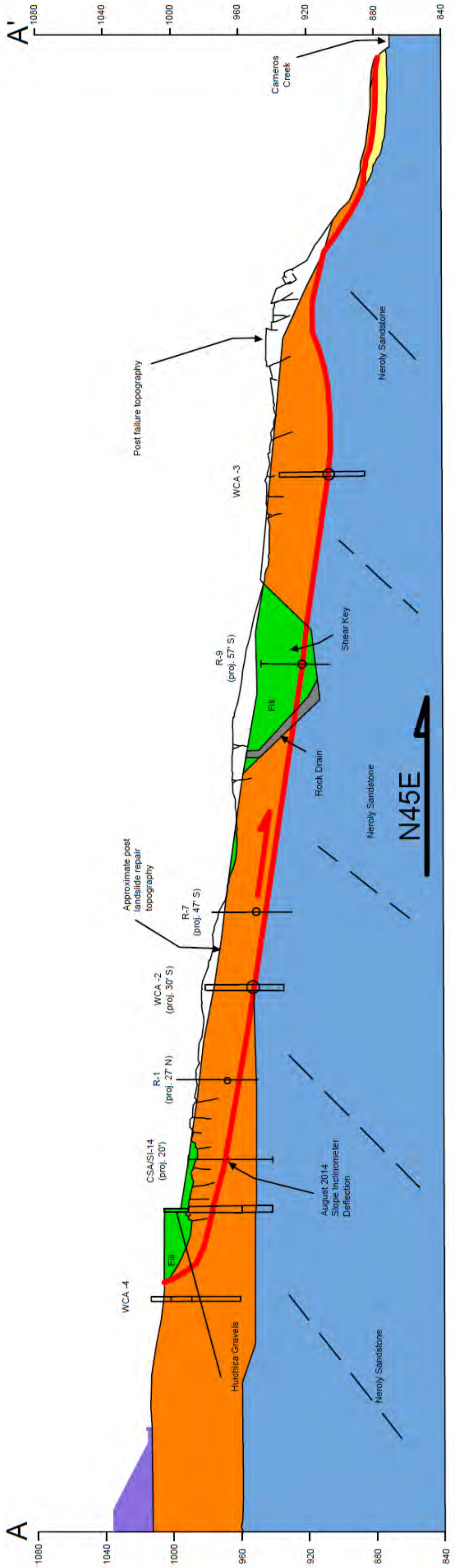

Figure E.45: Napa winery cross-section

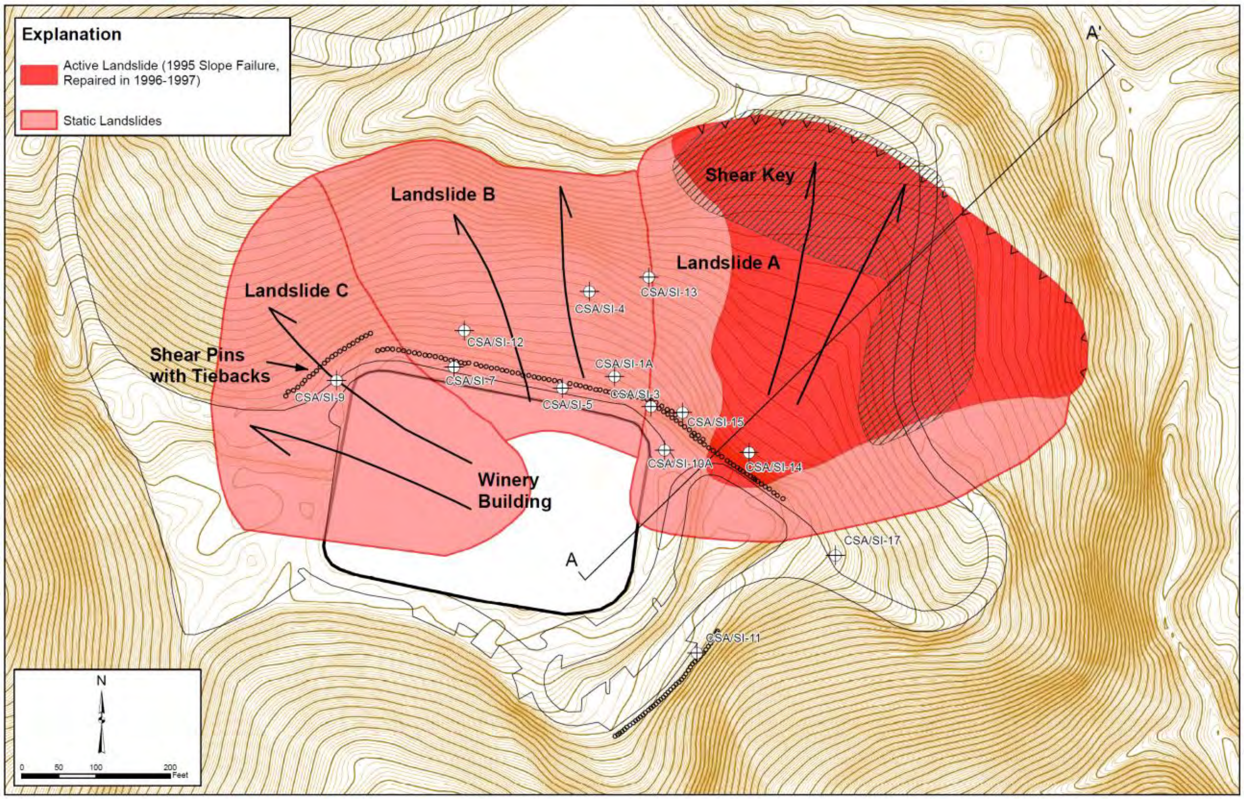

Figure E.46: Napa winery overview map

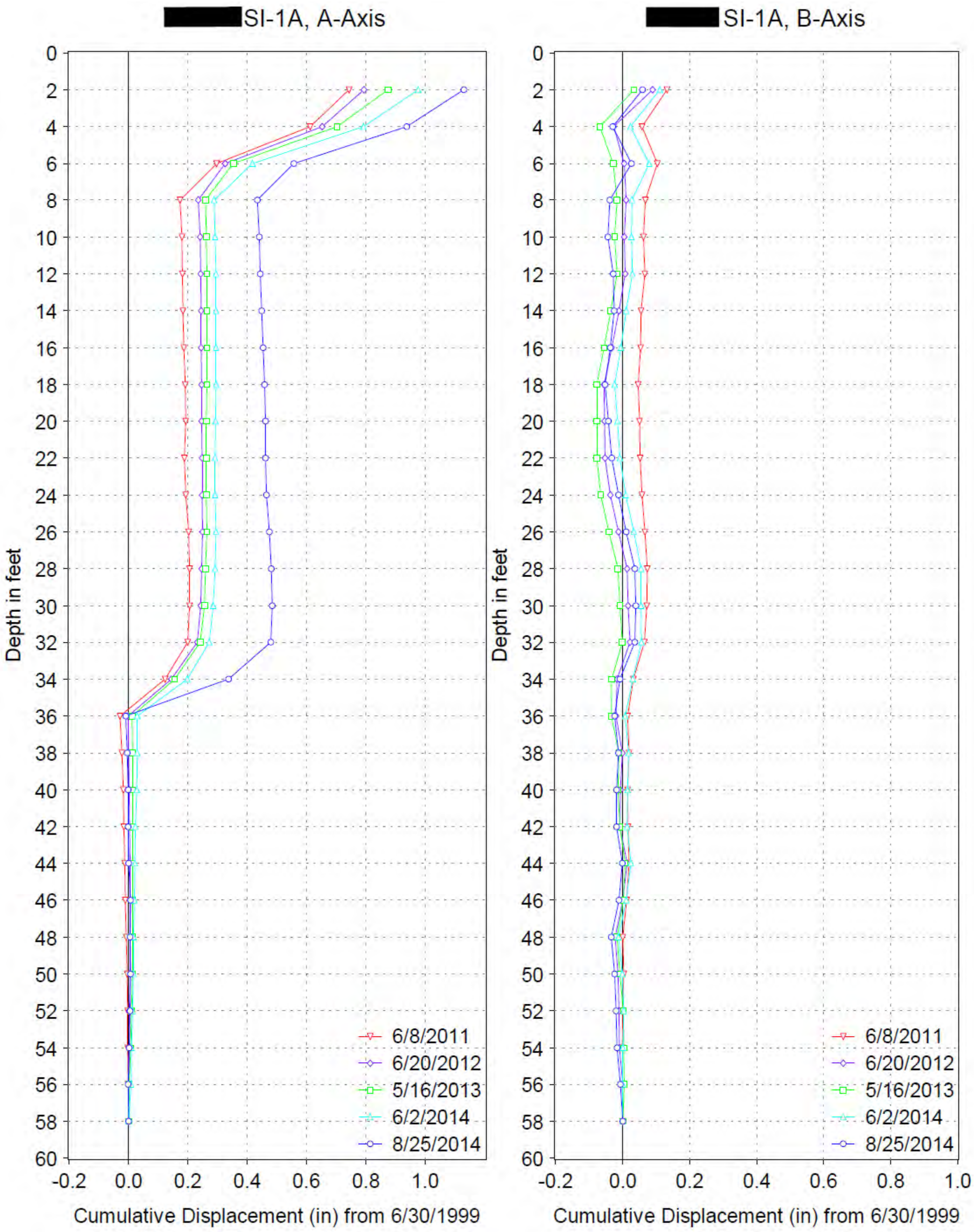

[redacted] SI-1A, A-Axis

[redacted] SI-1A, B-Axis

Figure E.47: Napa winery slope inclinometer data, SI-1A

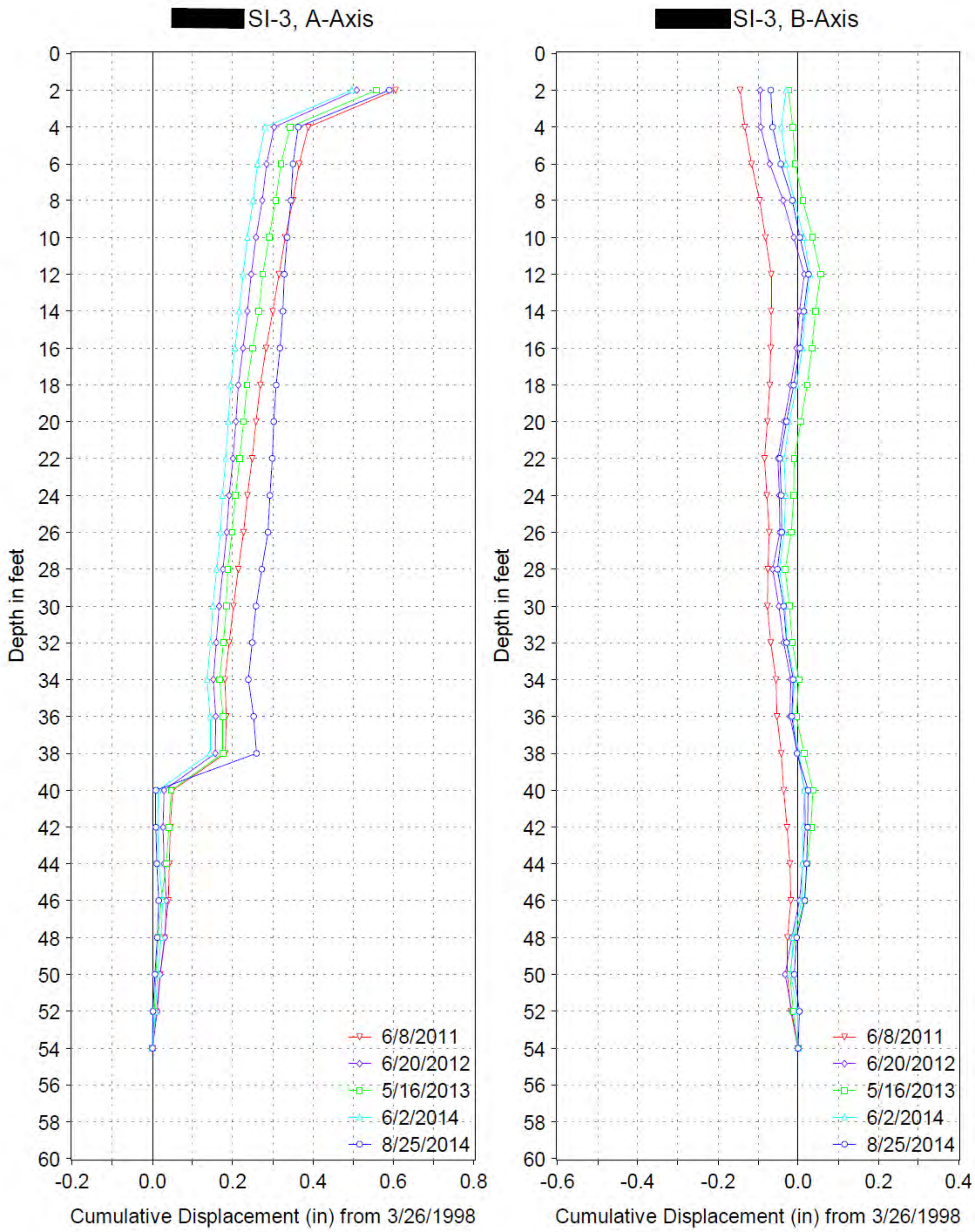
[redacted] SI-3, A-Axis

[redacted] SI-3, B-Axis

Figure E.48: Napa winery slope inclinometer data, SI-3

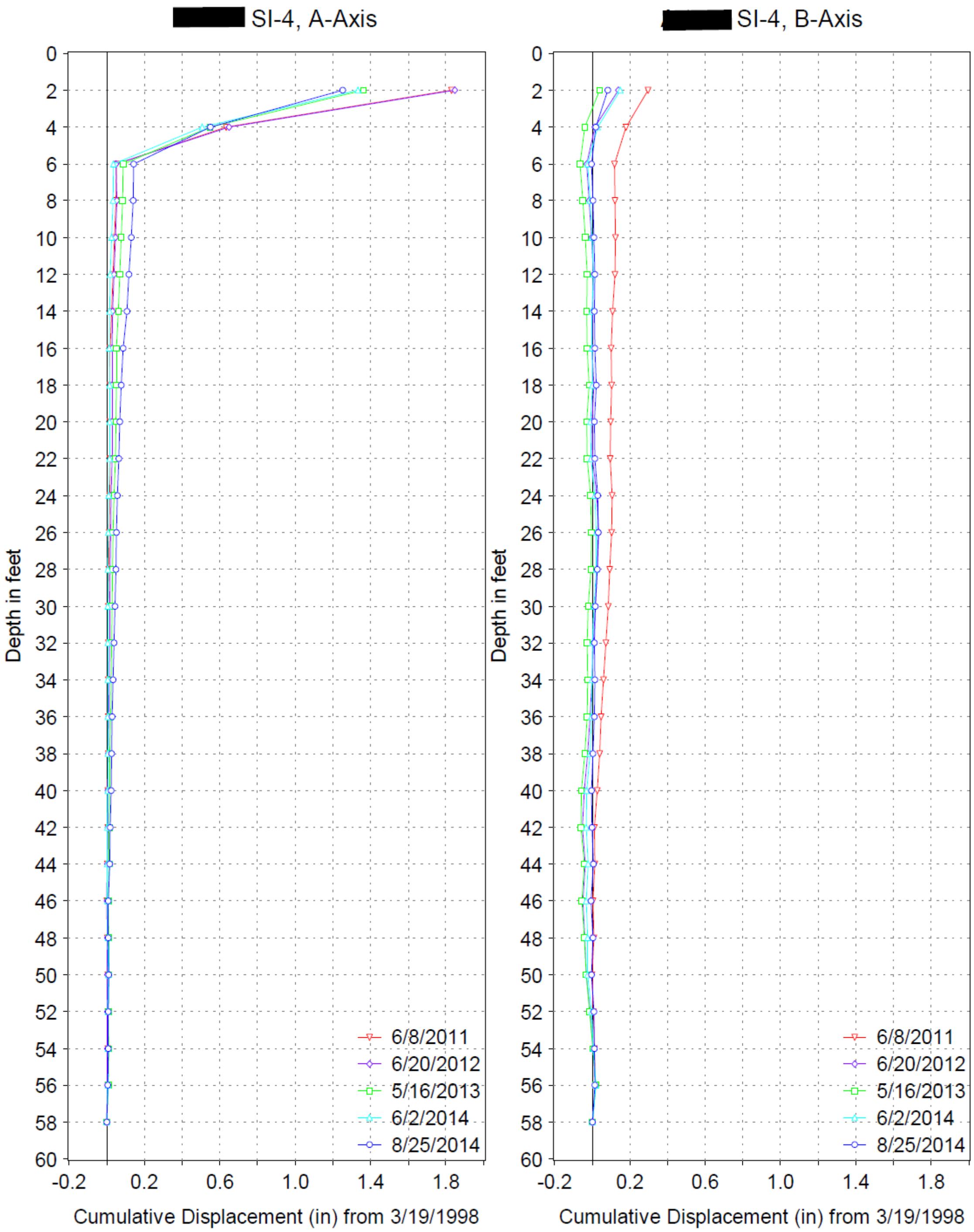

Figure E.49: Napa winery slope inclinometer data, SI-4

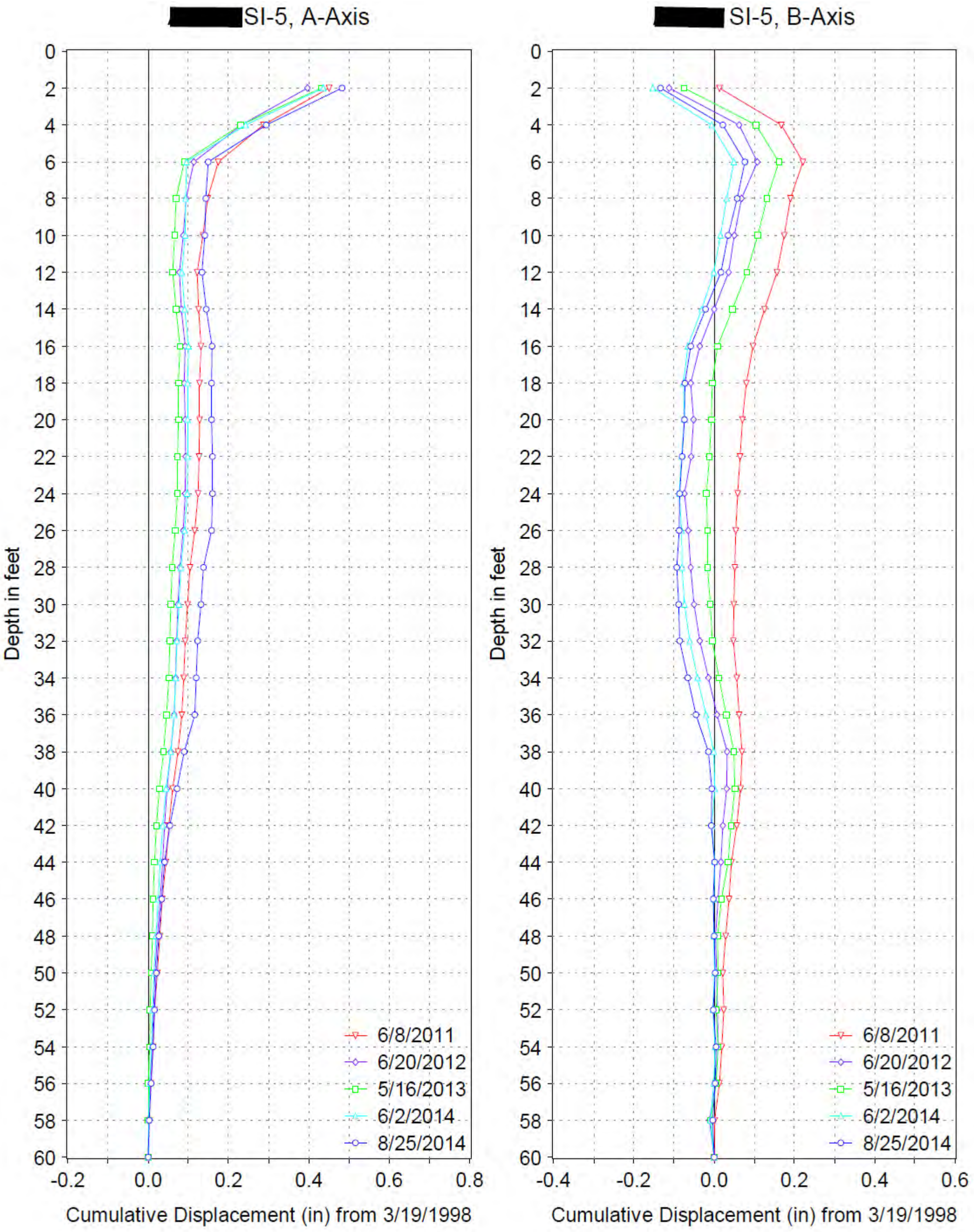

Figure E.50: Napa winery slope inclinometer data, SI-5

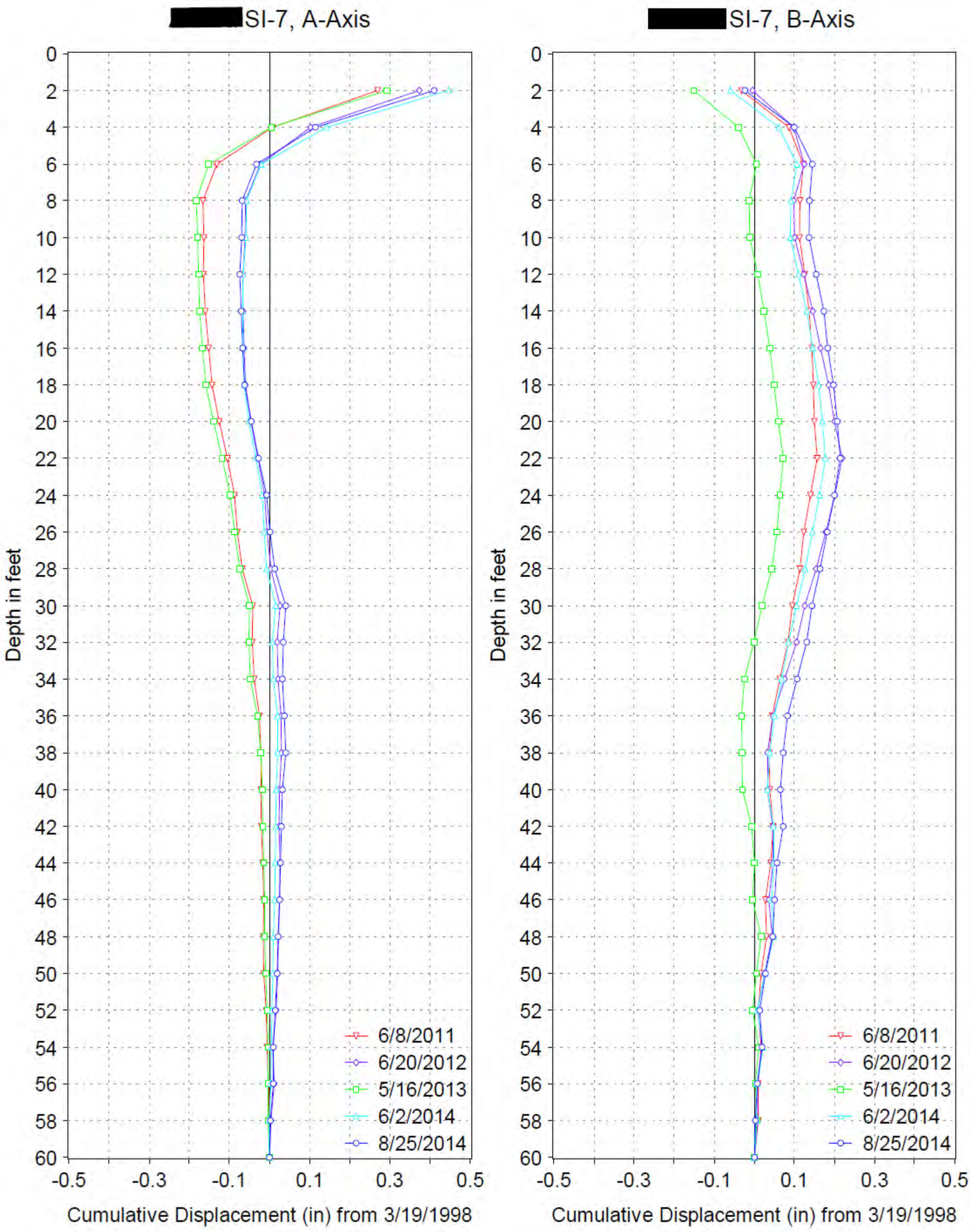

Figure E.51: Napa winery slope inclinometer data, SI-7

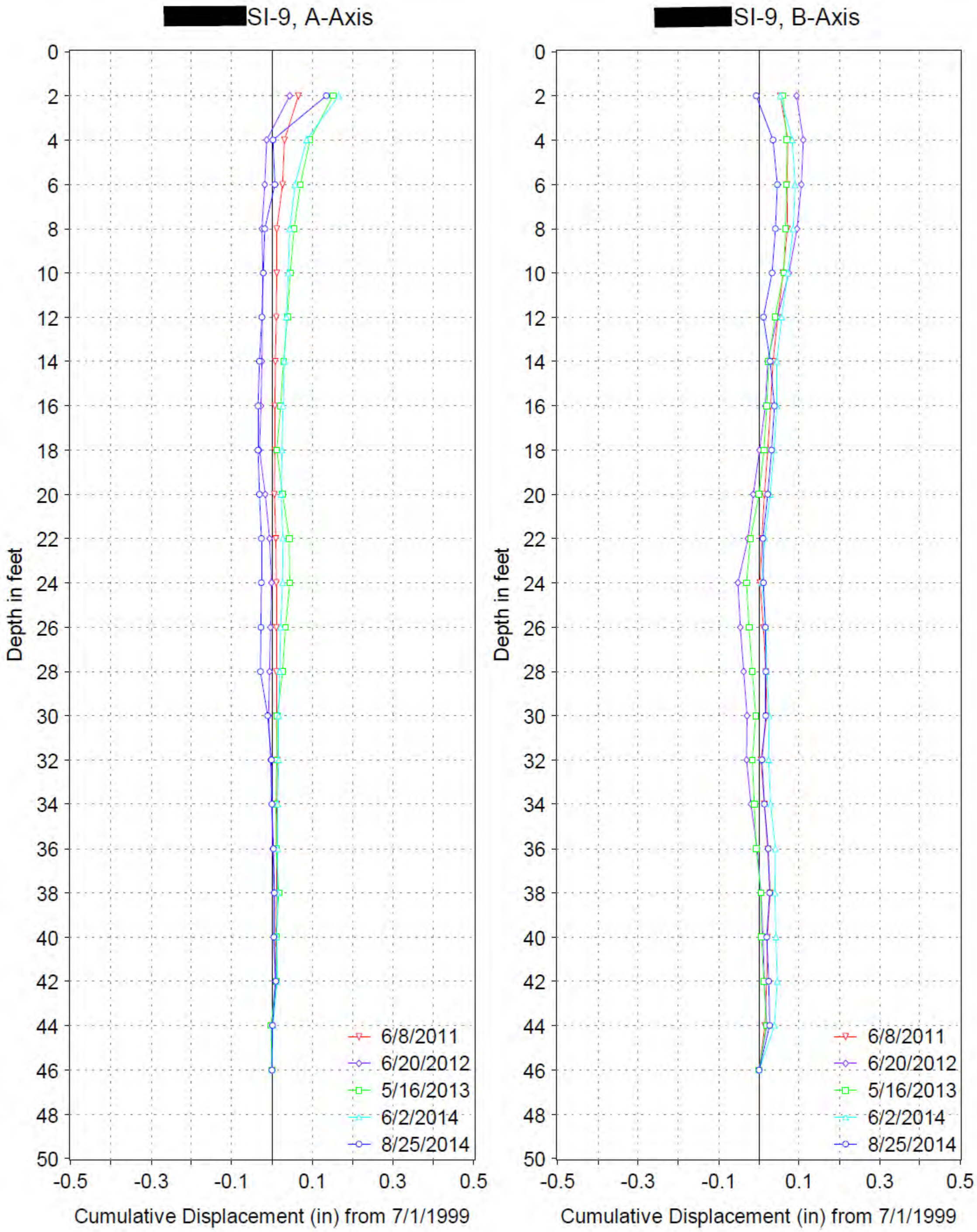

Figure E.52: Napa winery slope inclinometer data, SI-9

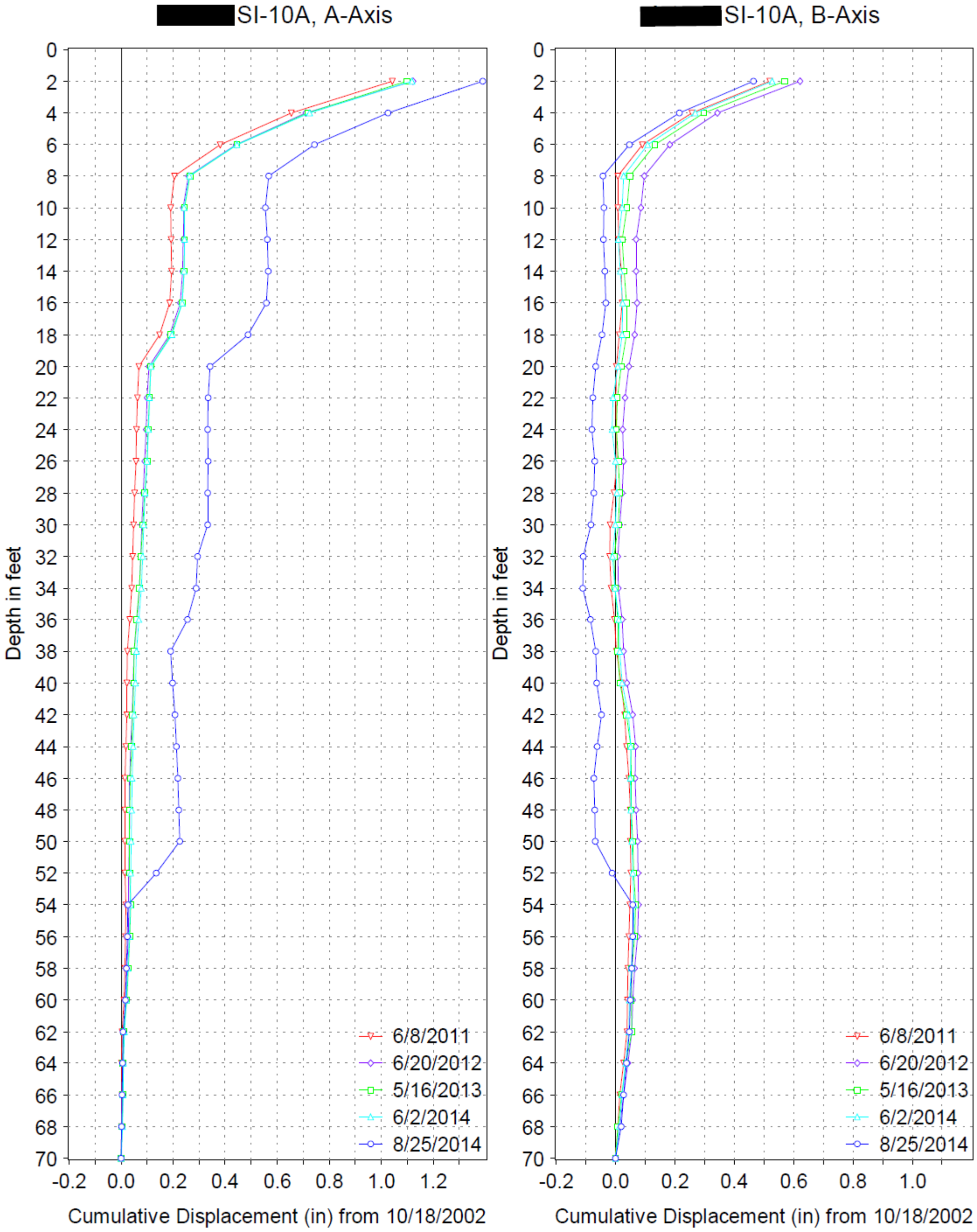

Figure E.53: Napa winery slope inclinometer data, SI-10A

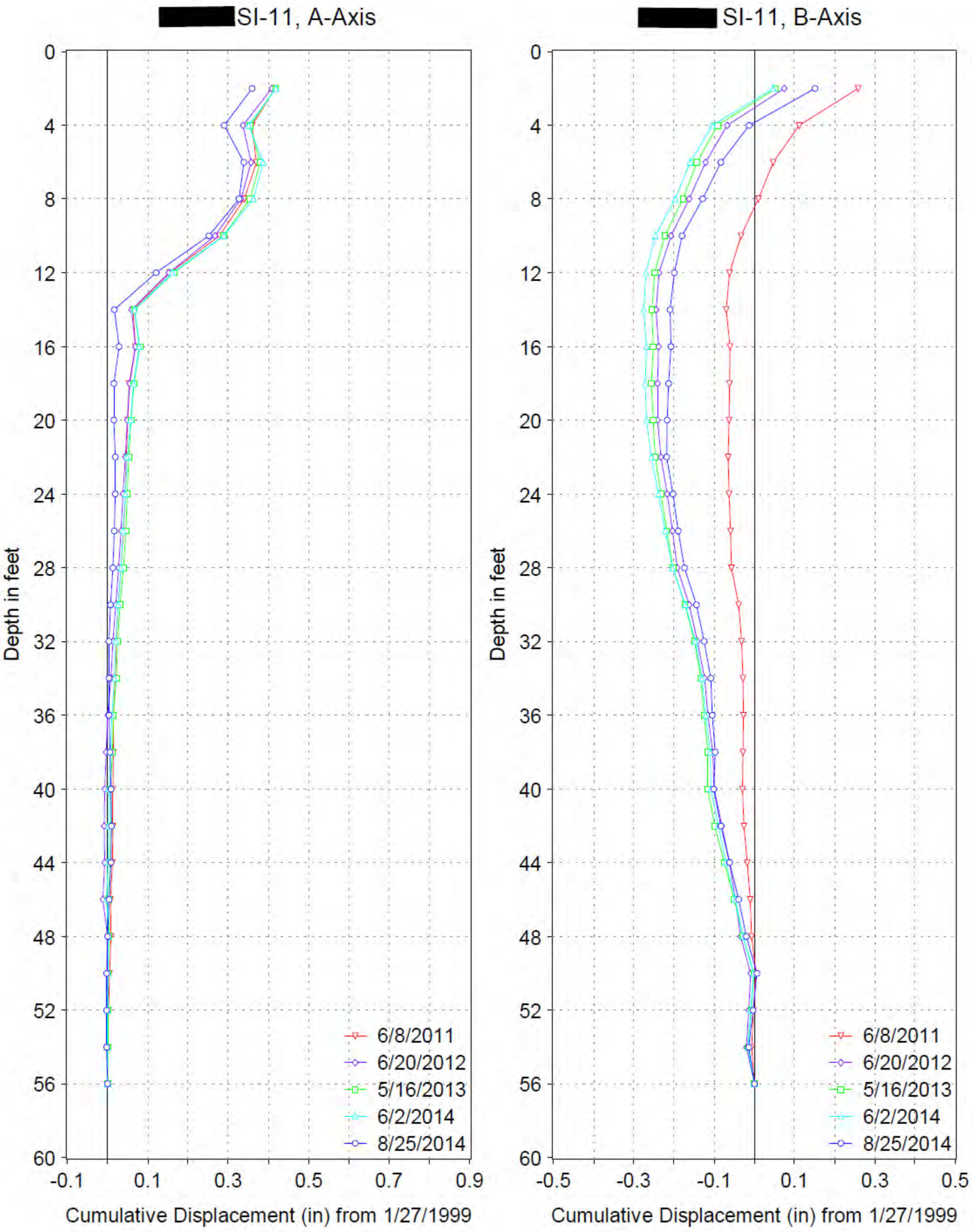

Figure E.54: Napa winery slope inclinometer data, SI-11

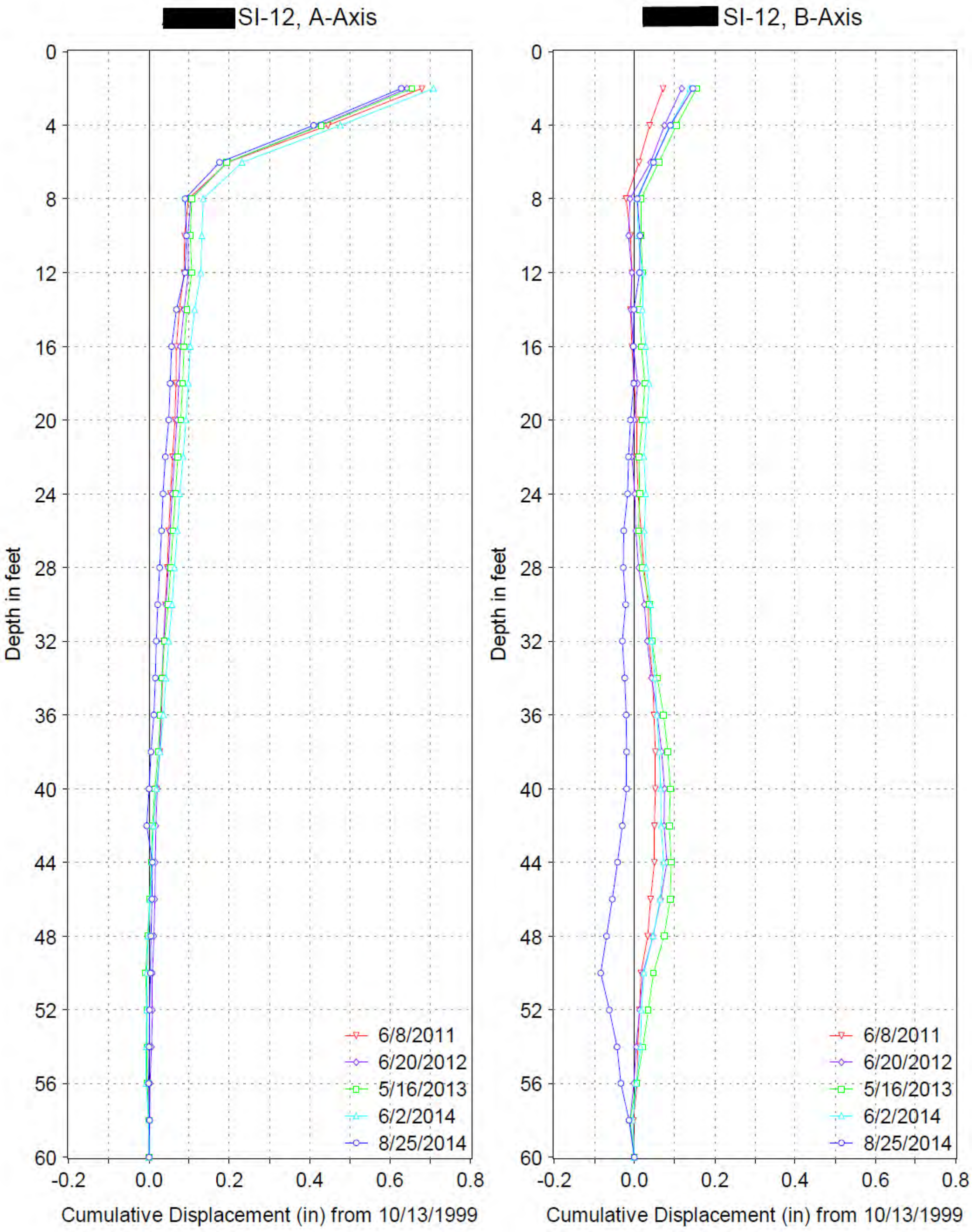

Figure E.55: Napa winery slope inclinometer data, SI-12

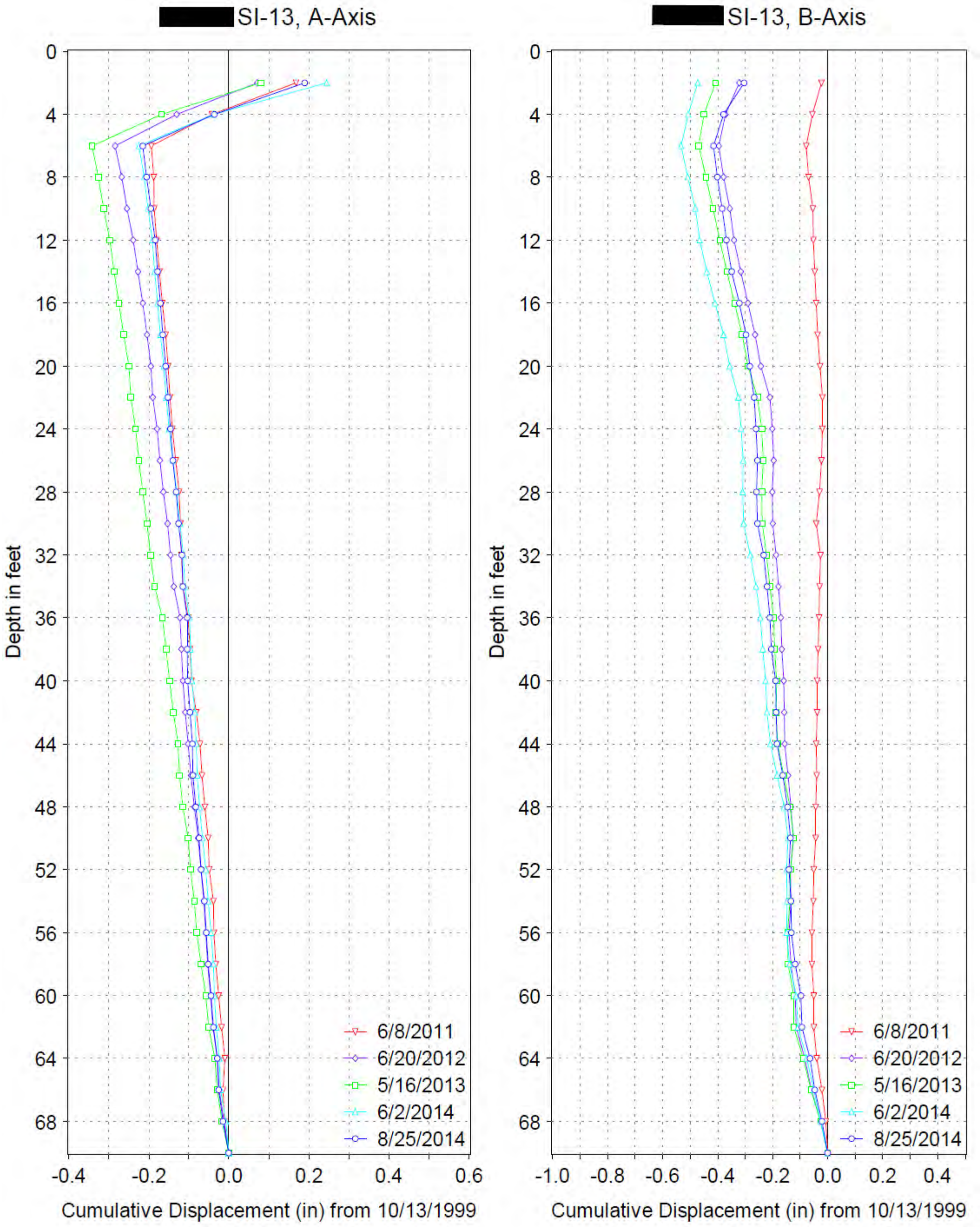

Figure E.56: Napa winery slope inclinometer data, SI-13

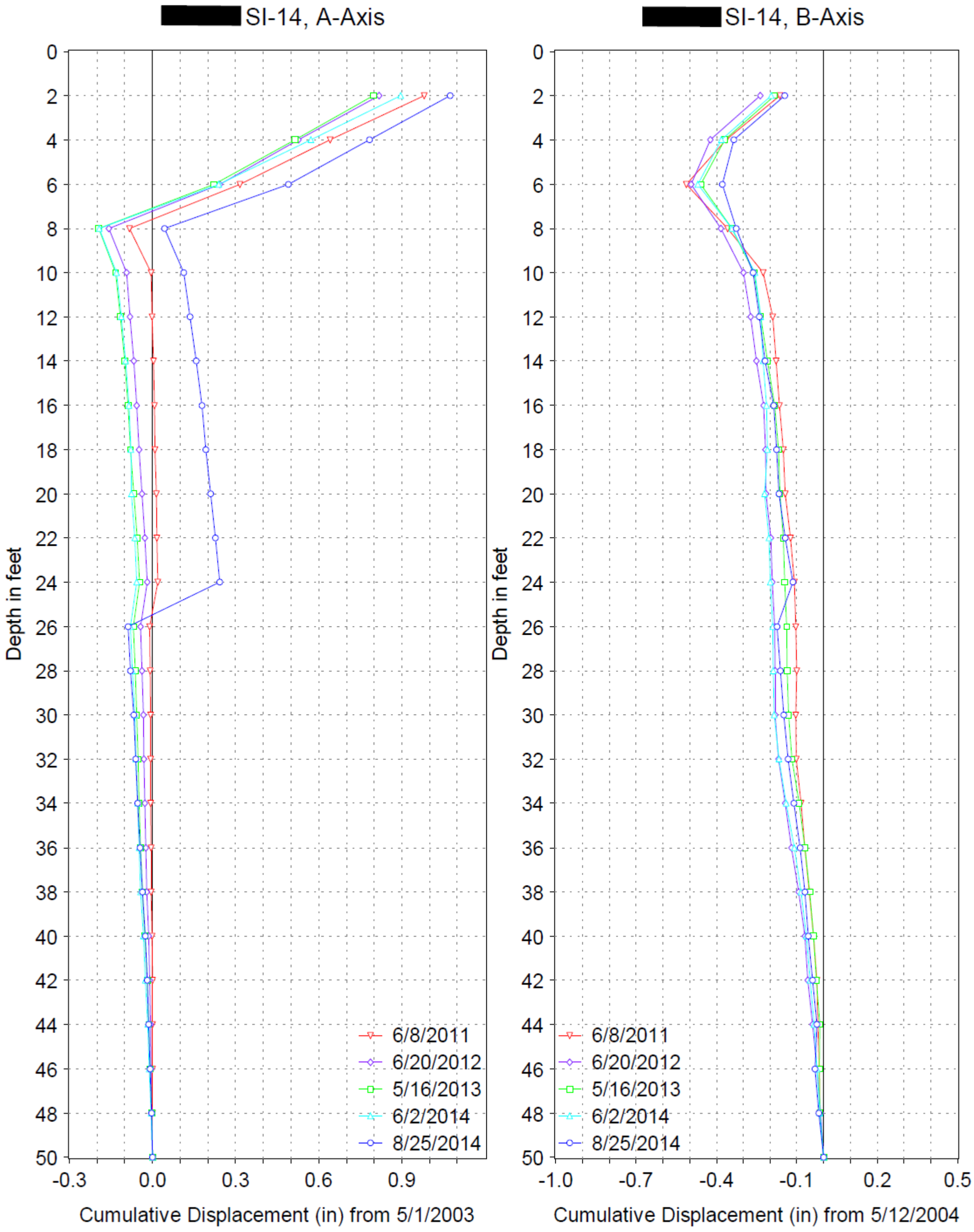

[redacted] SI-14, A-Axis

[redacted] SI-14, B-Axis

Figure E.57: Napa winery slope inclinometer data, SI-14

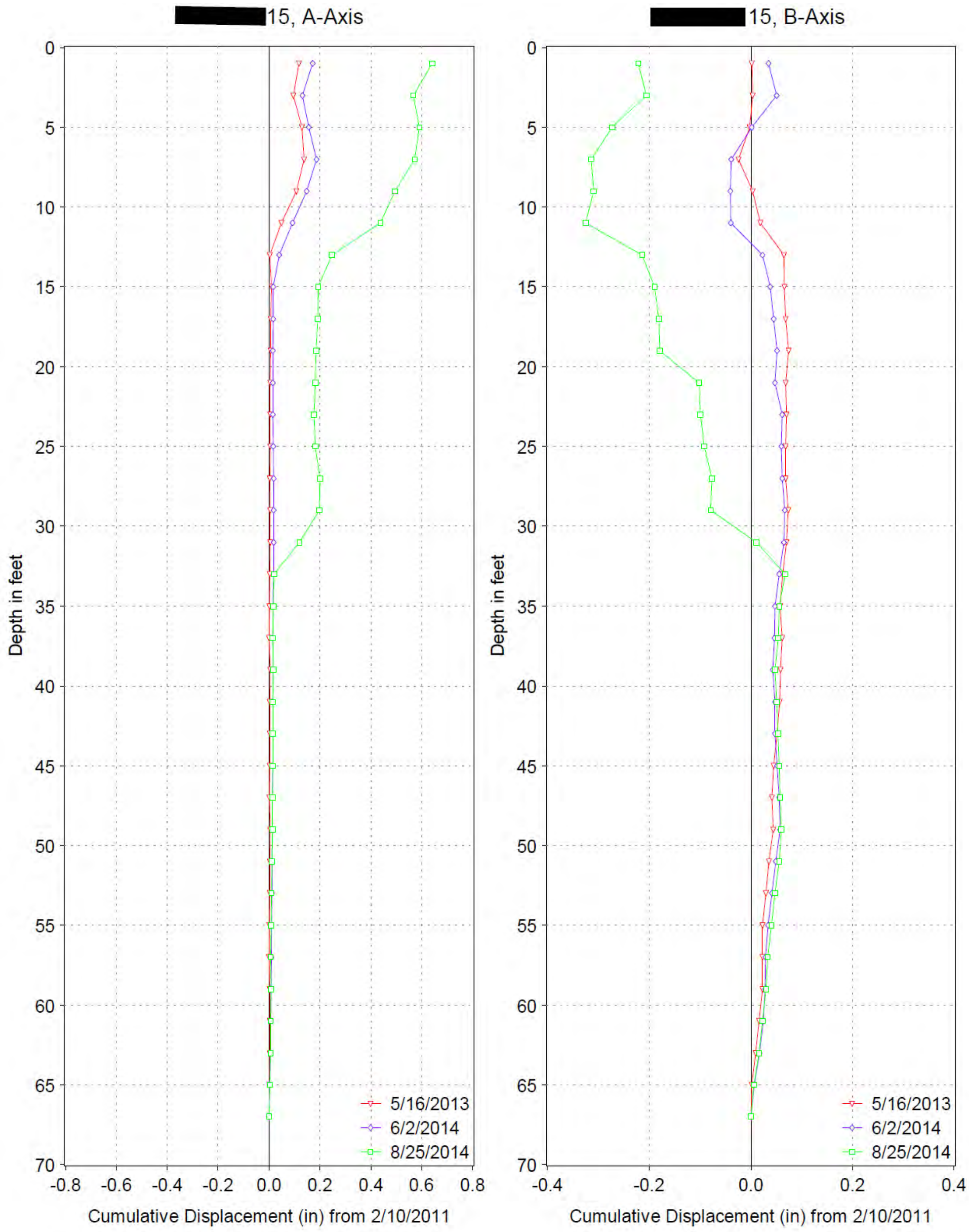

Figure E.58: Napa winery slope inclinometer data, SI-15

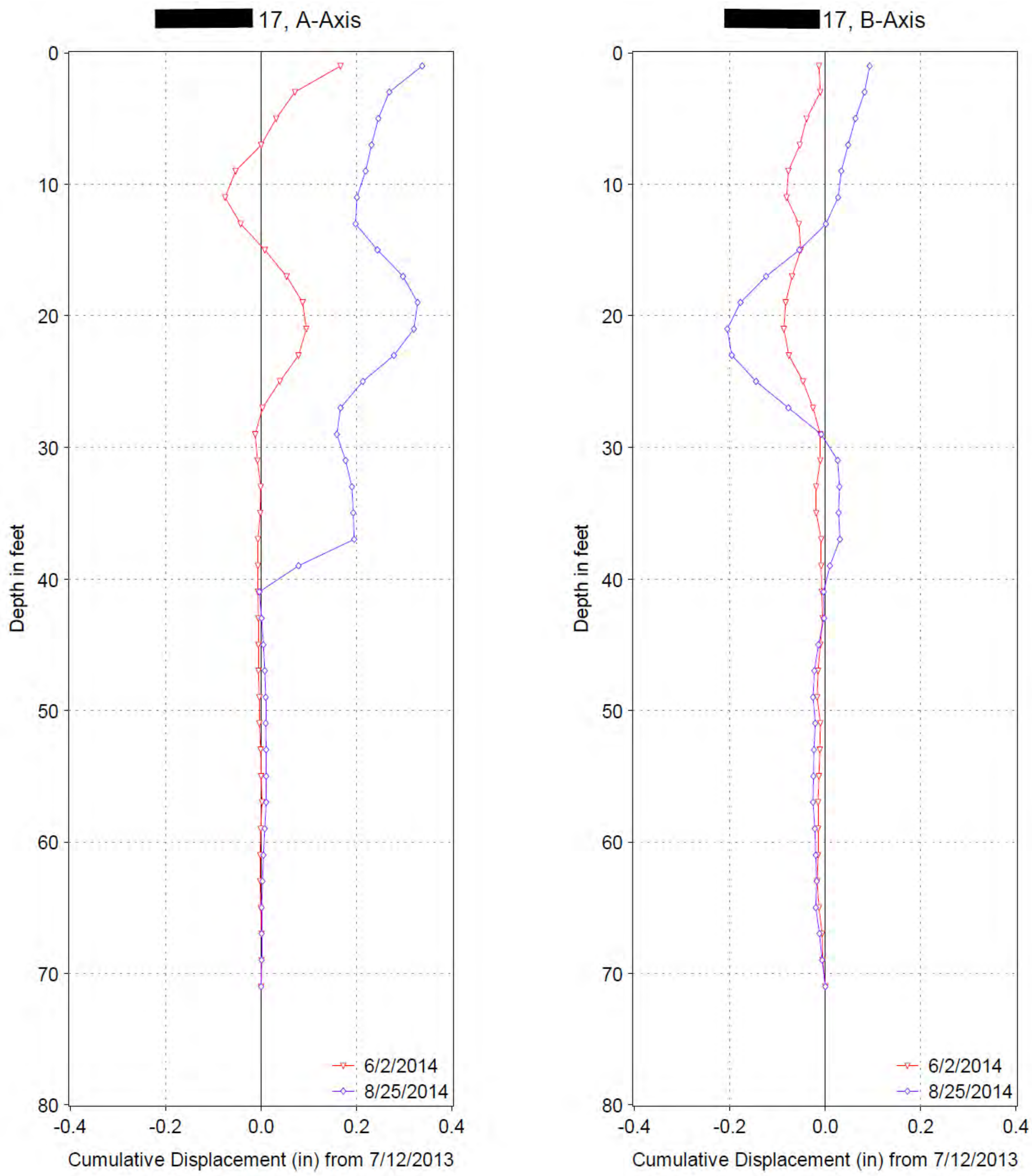

Figure E.59: Napa winery slope inclinometer data, SI-17

Appendix F: Performance of Dams and Levees

1. Introduction

Preliminary reconnaissance efforts of dams and levees were made by GEER team members between August 24 and September 7, 2014 following the main shock. Reconnaissance efforts included several flights in a California Highway Patrol (CHP) helicopter over several dams and levee reaches to look for any major damage from the air. No significant damage was observed at any of the areas viewed from the air. These efforts were then followed up by ground investigations in areas where higher accelerations were thought to have been sustained, notably in the central Napa area and in Vallejo. Again, no major damage was observed at any of the dams or levee reaches visited by GEER team members. The majority of damage observed on either dams or levees consisted of relatively small longitudinal cracks either on the dam/levee crest, or in one location along the landside toe of a small dike on Green Island. New cracking associated with the earthquake, or any other damage, was often not observed at all. Where present, the cracking was commonly less than a few millimeters in width. The largest crack observed was on the crest of Lake Marie Dam and was only about 2½ centimeters in width. Overall, the performance of the small to medium-sized dams and the relatively small levees in the area was very good. The good performance of the dams was confirmed in discussions with several dam owners and with the California Division of Safety of Dams (DSOD).

2. Overview of Dams in Earthquake Area

The DSOD regulates non-federal dams in the State of California. According to DSOD's listings of jurisdictional dams (dams that are typically over 2 meters in height and with a minimum reservoir size) there were 34 dams within 20 kilometers of the energy source associated with the 2014 South Napa Earthquake. The locations of these dams are shown in the Google Earth plot presented in Figure F-1. Tables F-1 and F-2 list the names, locations, and basic dimensions for each dam. Tables F-1 and F-2 also present estimated peak ground accelerations sustained by the dams during the main shock. The peak accelerations were estimated using two approaches. The first approach estimated peak ground accelerations at the dams by interpolating or extrapolating from the nearest peak accelerations recorded from any nearby strong motion instruments (from ShakeMap, United States Geological Survey). The second approach was to use the geometric mean of the four NGA-W2 GMPEs currently available (ASK14, BSSA14, CB14, and CY14). As shown in the two tables, the two different approaches result in generally similar estimates, although there are some differences in some locations. Table F-3 presents the numbers of dams shaken to various levels of peak ground acceleration.

The majority of the dams are relatively small, older earth dams. Two of the dams are concrete dams: Milliken Dam is a concrete arch dam that appears to have sustained only about 0.1g peak ground acceleration, whereas the Old Waterworks Dam in Napa is a concrete gravity dam, but its reservoir has not been in use for some time and was empty at the time of the earthquake. As summarized in Table F-4, the dam heights range from 6 to 50 meters in height, but 20 of the 34 dams are between only 6 and 15 meters in height. Only two dams with heights greater than 20 meters are believed to have sustained peak accelerations greater than about 0.1g: Summit Reservoir Dam (Height = 38 meters, PGA ~0.25g) and Swanzy Lake Dam (Height = 26 meters, PGA ~0.30g), both in the Vallejo area (see Table F-5).

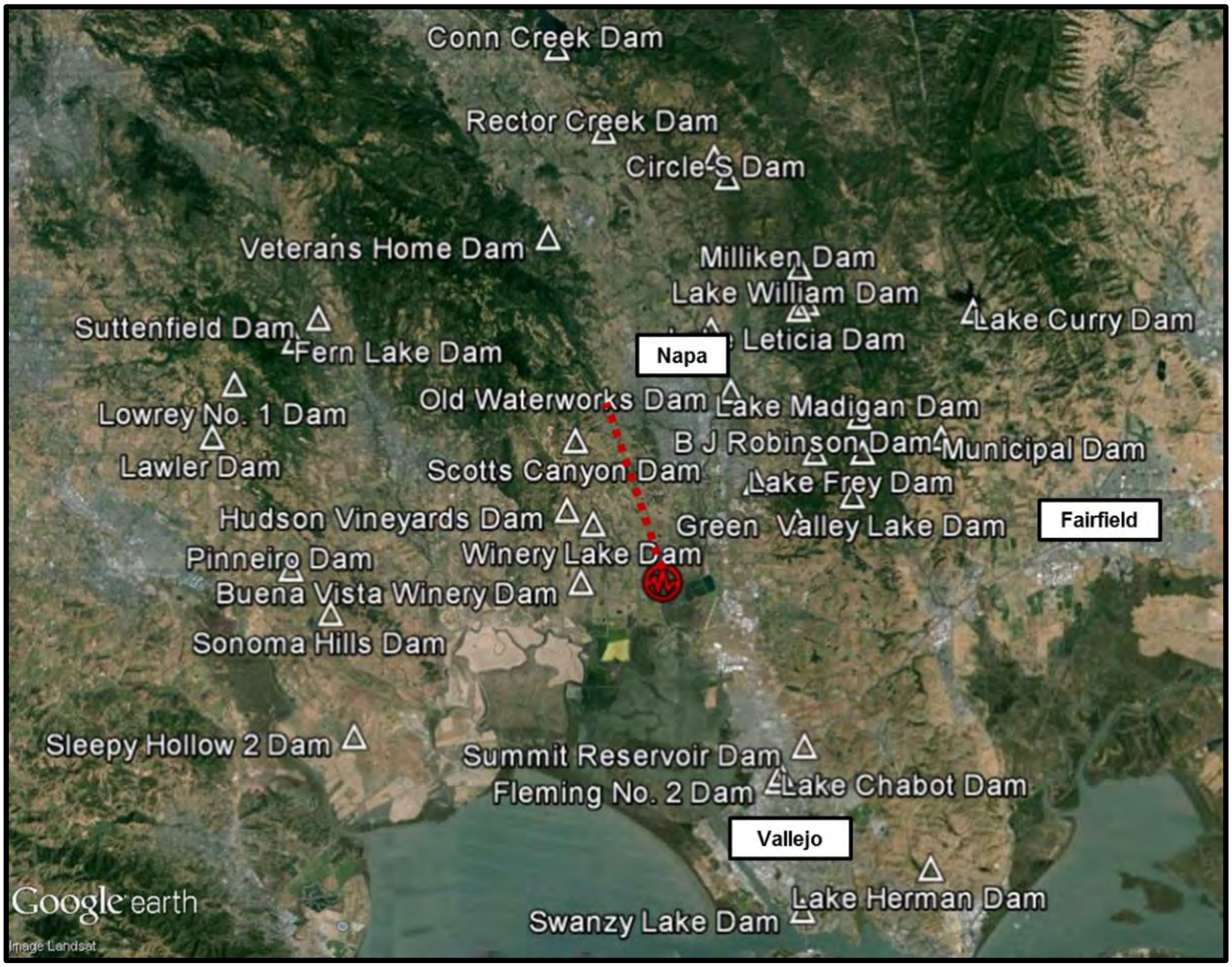

Figure F-1: Locations of Jurisdictional Dams within 20 kilometers of the energy source associated with the 2014 South Napa Earthquake [NSF-GEER; Harder, L. F.; 09/11/14]

Table F-6 shows that the majority of the dams within 20 kilometers of the energy source of the earthquake are also quite old, with several dams having been originally constructed back in the 19th century. Only six of the dams have been constructed since 1960. Of course, several of the dams have had dam safety modifications and improvements since their original construction.

In addition to the jurisdictional dams, there are dozens of small agricultural ponds in the area that are used principally to support the wine industry. These are small ponds with retaining embankments generally less than 3 to 6 meters in height. Many of these ponds were created by borrowing from the pond area for materials to construct the retaining embankments; thus, the upstream slopes are often higher than the downstream slopes. Some of the ponds also have synthetic geomembrane liners.

Due to the ongoing California Drought, many of the reservoirs and ponds were at less than their maximum operating level at the time of the earthquake, and some were very low.

Table F-1: Summary of Dams in Napa County within 20 kilometer of the energy source of the 2014 South Napa Earthquake [NSF-GEER; Harder, L. F.; Escudero, J. L. M.; 09/11/14)]

Dam	Height (m)	Crest Length (m)	Crest Width (m)	Year Completed	Approx. Distance (km)	Latitude/ Longitude	Prel. PGA[1] (g)
B J Robinson	14	213	5	1957	9.1	N 38° 17.4’ W 122° 13.2’	0.11[a]/0.20[b]
Circle S	9	126	4	1979	13.7	N 38° 25.2’ W 122° 16.3’	0.10/0.15
Conn Creek	38	213	6	1946	18.7	N 38° 28.9’ W 122° 22.4’	0.10/0.10
Foss Valley	17	762	6	1988	14.2	N 38° 25.7’ W 122° 16.7’	0.10/0.15
Hudson Vineyards	8	122	4	1983	2.8	N 38° 15.9’ W 122° 22.0’	0.41/0.37
Lake Camille	9	183	7	1880	6.8	N 38° 16.6’ W 122° 15.3’	0.27/0.29
Lake Curry	33	174	5	1926	19.1	N 38° 21.4’ W 122° 7.5’	0.05/0.13
Lake Cynthia	7	229	3	1955	6.9	N 38° 20.9’ W 122° 16.9’	0.35/0.30
Lake Leticia	15	119	5	1960	11.2	N 38° 21.5’ W 122° 13.7’	0.11/0.20
Lake Marie	18	138	2	1908	8.0	N 38° 15.6’ W 122° 13.8’	0.19/0.22
Lake William	20	175	6	1960	11.8	N 38° 21.6’ W 122° 13.4’	0.11/0.18
Milliken Dam*	34	197	8	1924	12.3	N 38° 22.7’ W 122° 13.6’	0.10/0.17
Old Waterworks**	13	66	2	1883	6.1	N 38° 19.2’ W 122° 16.1’	0.35/0.31
Rector Creek	50	271	9	1946	14.3	N 38° 26.5’ W 122° 20.7’	0.10/0.13
Scotts Canyon	12	98	6	1948	1.6	N 38° 17.8’ W 122° 21.7’	0.45/0.47
Veterans Home	14	98	2	1908	13.6	N 38° 23.5’ W 122° 22.7’	0.10/0.18
Winery Lake	9	189	4	1953	2.1	N 38° 15.5’ W 122° 21.1’	0.41/0.41

Notes: [1] PGA estimates are based on: a) nearest recorded motions and b) NGA-W2 GMPEs

* Denotes concrete arch dam

** Denotes concrete gravity dam, reservoir empty and out of service

▨ Denotes dam inspected or viewed by GEER team

Table F-2: Summary of Dams in Solano and Sonoma Counties within 20 kilometers of the energy source of the 2014 South Napa Earthquake
[NSF-GEER; Harder, L. F.; Escudero, J. L. M., 09/11/14)]

Dam	Height (meters)	Crest Length (meters)	Crest Width (meters)	Year Completed	Approx. Distance (km)	Latitude/ Longitude	Prel. PGA (g)
Buena Vista Winery	12	169	4	1971	3.6	N 38° 13.8’ W 122° 21.5’	0.41[a]/0.38[b]
Fern Lake	12	91	5	1921	14.7	N 38° 20.6’ W 122° 31.8’	0.09/0.11
Fleming Hill No. 2	12	174	12	1912	11.1	N 38° 8.2’ W 122° 14.5’	0.30/0.20
Green Valley	12	101	4	1956	11.2	N 38° 16.3’ W 122° 11.8’	0.10/0.19
Lake Chabot	13	113	5	1870	10.9	N 38° 8.4’ W 122° 14.4’	0.30/0.21
Lake Frey	25	175	5	1894	11.7	N 38° 17.5’ W 122° 11.5’	0.10/0.19
Lake Herman	16	213	4	1905	11.6	N 38° 5.8’ W 122° 9.0’	0.09/0.12
Lake Madigan	27	203	5	1908	11.6	N 38° 18.5’ W 122° 11.6’	0.10/0.19
Lawler	12	351	7	1910	19.1	N 38° 17.9’ W 122° 34.7’	0.08/0.09
Lowrey No. 1	6	64	3	1954	17.9	N 38° 19.4’ W 122° 33.8’	0.08/0.10
Municipal	17	131	5	1934	15.6	N 38° 17.9’ W 122° 8.6’	0.07/0.11
Pinneiro	8	220	4	1967	17.5	N 38° 14.2’ W 122° 34.7’	0.04/0.10
Sleepy Hollow 2	12	183	4	1949	17.7	N 38° 9.5’ W 122° 29.7’	0.03/0.10
Sonoma Hills	12	98	5	1991	17.1	N 38° 12.9’ W 122° 30.5’	0.04/0.13
Summit Reservoir	38	274	6	1968	10.4	N 38° 9.2’ W 122° 13.5’	0.25/0.19
Suttenfield	23	294	3	1938	13.6	N 38° 21.3’ W 122° 31.0’	0.10/0.14
Swanzy Lake	26	114	5	1931	17.4	N 38° 4.6’ W 122° 13.6’	0.30/0.13

Notes: [1] PGA estimates are based on: a) nearest recorded motions and b) NGA-W2 GMPEs

▨ Denotes dam inspected or viewed by GEER team

Table F-3: Estimated Peak Ground Accelerations at dams within 20 kilometers of the energy source of the 2014 South Napa Earthquake [NSF-GEER; Harder, L. F.; processed 09/11/14)

Range in estimated Peak Ground Acceleration (g)	Number of Dams
< 0.10	9
0.10 – 0.19	14
0.20 – 0.29	2
0.30 – 0.39	5
> 0.40	4
Total	34

Table F-4: Heights of dams within 20 kilometers of the energy source of the 2014 South Napa Earthquake [NSF-GEER; Harder, L. F.; processed 09/11/14)

Range in Dam Height (meters)	Number of Dams
0 – 5	0
6 – 10	7
10 – 15	13
16 – 20	5
21 – 25	2
26 – 30	2
31 – 35	2
36 – 40	2
> 40	1
Total	34

Table F-5: Dams with the highest estimated peak ground accelerations associated with the 2014 South Napa Earthquake [NSF-GEER; Harder, L. F.; processed 09/11/14)

Dam	Height (meters)	Year Completed	Estimated PGA (g)
Scotts Canyon	12	1948	0.45
Winery Lake	9	1953	0.41
Buena Vista Winey	12	1971	0.41
Hudson Vineyards	8	1983	0.41
Lake Cynthia	7	1955	0.35
Old Waterworks*	13	1883	0.35
Lake Chabot	13	1870	0.30
Fleming Hill No. 2	12	1912	0.30
Swanzy Lake	26	1931	0.30
Lake Camille	9	1880	0.27
Summit Reservoir	38	1968	0.25

* Denotes concrete gravity dam, reservoir empty and out of service

Table F-6: Original construction dates for dams within 20 kilometers of the energy source of the 2014 South Napa Earthquake [NSF-GEER; Harder, L. F.; processed 09/11/14)

Year of Original Dam Construction	Number of Dams
1870 - 1900	4
1901 - 1920	6
1921 - 1940	7
1941 - 1960	11
1961 - 1980	3
1980 -2014	3
Total	34

3. Performance of Dams

Immediately following the main shock of the 2014 South Napa Earthquake, personnel in DSOD received information from ShakeCast (USGS) regarding the level of shaking in the area and began putting together a list of dams that received different levels of shaking. For dams that were within areas having a Damage Intensity of V or more, DSOD staff contacted the owners within a day and asked them to inspect their dams. Dams in areas associated with a Damage Intensity of VII or greater were contacted within a few hours. The DSOD then put together a priority list of dams for their own inspections with priorities based on the estimated level of shaking and the history of the dam. Dams with the highest priorities were inspected later the same day as the earthquake. Dams with lower priorities were inspected within a few days after the earthquake. As a result of these inspections, DSOD found little to no damage to the dams and appurtenances. As mentioned previously, the main type of damage noted, where any damage at all was observed, reportedly consisted of relatively minor longitudinal cracks on the crest of the dam. The largest such cracking was found on Lake Marie Dam and was approximately 2½ centimeters wide at its widest location.

The GEER team inspected on the ground or viewed from the air 11 of the 34 dams within 20 kilometers of the energy source associated with the earthquake (see brown shaded areas in Tables F-1 and F-2). The GEER team inspections that were done supported the results from the dam owners and DSOD inspections in that little to no damage was observed at the dams in the area. The reasons for this low level of damage likely include:

- The level and duration of shaking for most of the dams was relatively small
- Many of the dams are relatively small
- Many of the dams and their foundations are made out of clayey materials and the depths in the foundation to bedrock are small
- Some of the reservoirs were relatively low either due to the ongoing California Drought or due to restrictions imposed for dam safety
- Some of the dams have had various retrofits made to increase their static and seismic stability

Details and photographs for eight of the dams inspected by the GEER team are presented in the following sections:

- ➢ Lake Marie Dam
- ➢ Lake Chabot Dam
- ➢ Summit Reservoir Dam
- ➢ Municipal Dam
- ➢ Lake Frey Dam
- ➢ Lake Madigan Dam
- ➢ Swanzy Lake Dam
- ➢ Lake Herman Dam

3.1 Lake Marie Dam

Lake Marie Dam was originally constructed in 1908 and currently has a maximum height of approximately 18 meters. It is owned by the Napa State Hospital, but is operated as part of a recreation area. According to DSOD's files, Lake Marie Dam is reportedly a clayey earthfill dam (not hydraulic fill) with a concrete core wall. In 1931, the dam crest was reportedly raised 0.6 meters using vertical rock walls on both edges of the crest with soil fill placed in between to improve freeboard. While the records indicate that the dam crest is about 3 meters in width, the inspection by the GEER team on September 1st indicated that the crest width is only about 2 meters. The crest length of the dam is approximately 138 meters. The upstream slope is relatively steep with a slope of approximately 1.5:1, while the downstream slope is significantly flatter at about a 2.5:1 slope. A 1947 inspection report indicated that the freeboard at that time between the dam crest and the uncontrolled spillway was about 3.2 meters. However, following a seismic evaluation in the 1980's, a 30-centimeter diameter steel riser pipe was installed downstream of the upstream valve of the outlet pipeline. This riser pipe limits the maximum reservoir storage to about 7.5 meters below the dam crest. At the time of the September 1st GEER inspection, the reservoir was more than 10 meters below the crest of the dam, leaving less than 8 meters of water on the 18-meter-high dam itself.

Lake Marie Dam was approximately 8.0 kilometers away from the energy source associated with the South Napa Earthquake and is estimated to have sustained a peak ground acceleration of about 0.19g based on nearby strong motion instruments. DSOD personnel inspected the dam during the same day as the earthquake and noted only a longitudinal crack in the upstream portion of the dam crest. The crack ran approximately 17 meters in length along the left central portion of the dam (see Figure F-2 for general location) and had a maximum width of about 2½ centimeters (see Figure F-3). Figures F-3 and F-4 present photographs taken by DSOD and by the GEER team of the cracking. The cracking may be related to movement of the upstream rock wall reportedly placed on the upstream edge of the dam crest in 1931. The cracking is considered minor, but DSOD staff report that they may require the cracking to be remediated.

3.2 Lake Chabot Dam

Lake Chabot Dam was originally constructed in 1870 and currently has a maximum height of approximately 13 meters. It is owned by the City of Vallejo and retains the lake used by the Six Flags Discovery Kingdom in Vallejo. According to DSOD's files, Lake Chabot Dam is a clayey earthfill dam generally composed of stiff clay and clayey gravel. The depth to shale bedrock is less than 3 meters below the foundation. The crest of the dam is approximately 5 meters wide and approximately113 meters in length. Due to stability concerns, a wide berm was added to the downstream side of the dam several years ago. Figure F-5 presents a cross section of the dam obtained from DSOD files illustrating the general geometry of the dam and downstream berm. Figure F-6 presents a photograph of the dam taken by the GEER team also illustrating the dam and berm geometry.

Lake Chabot Dam was approximately 11 kilometers away from the energy source associated with the South Napa Earthquake and is estimated to have sustained a peak ground acceleration of about 0.30g based on nearby strong motion instruments. A member of the GEER team inspected the dam on August 27th and found only minor longitudinal cracking less than 2 centimeters in

Figure F-2: Ground and aerial photographs of Lake Marie Dam looking southeast
[NSF-GEER; Napa, CA; N38.260 W 122.230; Harder, L. F.; 09/01/14]

Figure F-3: Photographs of longitudinal cracking on the upstream edge of the crest of Lake Marie Dam [Napa, CA; N38.260 W 122.230; from DSOD files; 08/24/14]

Figure F-4: Photograph of cracking on the upstream edge of the crest of Lake Marie Dam looking southeast [NSF-GEER; Napa, CA; N38.260 W 122.230; Harder, L. F.; 09/01/14]

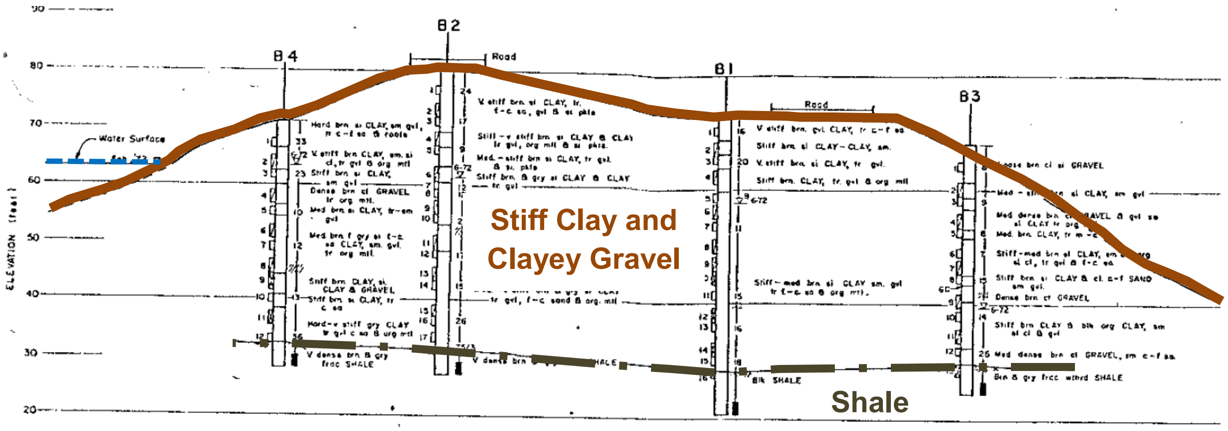

Figure F-5: Cross section of Lake Chabot Dam
[Vallejo, CA; N38.141 W 122.241; from DSOD files]

Figure F-6: Photograph of minor longitudinal cracking on the crest of Lake Chabot Dam looking southeast [NSF-GEER; Napa, CA; N38.141 W 122.241; Harder, L. F.; 08/27/14] width on the dam crest (see Figures F-6 and F-7). Much of this cracking may have been associated with pre-existing longitudinally-dominated shrinkage cracks that simply opened up during the shaking. At the time of the August 27th inspection, the reservoir was approximately 4½ meters below the dam crest. A relatively new reinforced concrete spillway on the right abutment of the dam appeared to be undamaged.

3.3 Summit Reservoir Dam

Summit Reservoir Dam was originally constructed in 1968 and currently has a maximum height of approximately 38 meters. Thus, it is one of the highest and most recently constructed dams shaken by the South Napa Earthquake. It is located in the hills above Vallejo and owned by the City of Vallejo. The dam appears to have had seepage issues in the past as there are several piezometers installed in the dam, and there is a plastic geomembrane lining placed within the reservoir to presumably reduce seepage through the dam and its foundation. There is also a 0.3-meter-high concrete parapet wall on the upstream edge of the 6-meter-wide asphalt-paved dam crest. The dam is shaped as an overall bowl and has a total length of about 274 meters. Figure F-8 presents views of the dam.

Summit Reservoir Dam was approximately 10.4 kilometers away from the energy source associated with the South Napa Earthquake and is estimated to have sustained a peak ground acceleration of about 0.25g based on nearby strong motion instruments. A member of the GEER team inspected the dam on August 27th and found that the dam appeared to have little to no damage. The only distress noted was relatively minor longitudinal cracking, principally located near the downstream edge of the asphalt-paved crest of the main dam section. These cracks were generally only a few millimeters in width with a maximum opening on the order of a centimeter. However, it was clear that these were pre-existing cracks as weeds were growing in them and asphalt mastic had previously been poured over them in the past in an attempt to seal them up. Figure F-9 illustrates some of the minor cracking noted. It is thought that at most, the effect of the earthquake was to perhaps slightly widen the pre-existing cracks.

Figure F-7: Close-up photograph of minor longitudinal cracking on the crest of Lake Chabot Dam looking southeast [NSF-GEER; Napa, CA; N38.141 W 122.241; Harder, L. F.; 08/27/14]

Figure F-8: Views of Summit Reservoir Dam looking southeast
[NSF-GEER; Napa, CA; N38.153 W 122.225; Harder, L. F.; 08/27/14]

Figure F-9: Photographs of pre-existing longitudinal cracks on the crest of the maximum section of Summit Reservoir Dam
[NSF-GEER; Napa, CA; N38.153 W 122.225; Harder, L. F.; 08/27/14]

3.4 Municipal Dam

Municipal Dam was originally constructed in 1939 and currently has a maximum height of approximately 17 meters. It is located in the hills north of Fairfield and owned by the City of Benicia. The dam has a crest width of approximately 3 meters and a crest length of length of approximately 131 meters. The dam has a relatively steep downstream slope at about 1½:1.

Municipal Dam was approximately 15.6 kilometers away from the energy source associated with the South Napa Earthquake and is estimated to have sustained a peak ground acceleration of only about 0.07g based on nearby strong motion instruments. A member of the GEER team inspected the dam on August 27th and found that the dam appeared to have little to no damage. The only distress noted was relatively minor, intermittent longitudinal cracking, principally located near the downstream edge of the dam's crest. These cracks were generally only a few millimeters in width with a maximum opening on the order of a centimeter. Most of these cracks appeared to be pre-existing shrinkage cracks that had simply opened up following the earthquake. On the left abutment near the downstream toe of the dam, seepage was flowing in the groin area to the creek below. However, the seepage obviously pre-existed the earthquake as there were numerous green grasses and brush growing in the seepage area. Figure F-10 presents views of the dam and the small cracking observed.

3.5 Lake Frey Dam

Lake Frey Dam was originally constructed in 1894 and currently has a maximum height of approximately 25 meters. It is located in the hills east of Napa and owned by the City of Vallejo. The dam has a crest width of approximately 5 meters and a crest length of approximately 175 meters. In addition to the main dam, there is a much smaller auxiliary dam that helps retain the reservoir.

Lake Frey Dam was approximately 11.7 kilometers away from the energy source associated with the South Napa Earthquake and is estimated to have sustained a peak ground acceleration of only about 0.10g based on nearby strong motion instruments. A member of the GEER team viewed the dam by helicopter on September 1st and did not observe any damage. Staff from the City of Vallejo reported that there was no damage to the dam. During the September 1st helicopter survey, the reservoir appeared to be approximately 5 meters feet below the crest of the dam. Figure F-11 presents aerial photographs of the main and auxiliary dams taken on September 1st.

3.6 Lake Madigan Dam

Lake Madigan Dam was originally constructed in 1908 and currently has a maximum height of approximately 27 meters. It is located in the hills east of Napa and owned by the City of Vallejo. The dam has a crest width of approximately 5 meters and a crest length of length of approximately 203 meters.

Lake Madigan Dam was approximately 11.6 kilometers away from the energy source associated with the South Napa Earthquake and is estimated to have sustained a peak ground acceleration of only about 0.10g based on nearby strong motion instruments. A member of the GEER team viewed the dam by helicopter on September 1st and did not observe any damage. Staff from the

Figure F-10: Photographs of Municipal Dam and longitudinal cracks observed along the downstream edge of the crest of Municipal Dam
[NSF-GEER; Napa, CA; N38.298 W 122.144; Harder, L. F.; 08/27/14]

Figure F-11: Aerial Photographs of Lake Frey Dam – main dam and auxiliary dam
[NSF-GEER; Napa, CA; N38.292 W 122.192; Harder, L. F.; 09/01/14]

City of Vallejo reported that there was no damage to the dam. Based on the September 1st helicopter survey, the reservoir appeared to be approximately 6 meters feet below the crest of the dam. Figure F-12 presents aerial photographs of the dam taken on September 1st.

3.7 Swanzy Lake Dam

Swanzy Lake Dam was originally constructed in 1931 and currently has a maximum height of approximately 26 meters. It is located in the hills in the southern portion of Vallejo and owned by the City of Vallejo. Over time, the upstream slope of the dam became a covered reservoir with supporting columns and footings founded on the upstream slope. The dam has a crest width of approximately 5 meters and a crest length of length of approximately 114 meters.

Swanzy Lake Dam was approximately 17.4 kilometers away from the energy source associated with the South Napa Earthquake and is estimated to have sustained a peak ground acceleration of about 0.30g based on nearby strong motion instruments. A member of the GEER team inspected the dam on August 27th and found that the dam appeared to have little to no damage. At the time of the August 27th inspection, the reservoir appeared to be approximately 3½ meters below the asphalt crest of the dam. The only distress noted was relatively minor longitudinal cracking, principally located near the downstream edge of the asphalt-paved crest of the main dam section. These cracks were generally only a few millimeters in width with a maximum opening on the order of a centimeter. However, it was clear that these were pre-existing cracks as weeds were growing in them and asphalt mastic had previously been poured over them in the past in an attempt to seal them up. Figure F-13 illustrates a view of the dam and some of the minor cracking noted. It is thought that at most, the effect of the earthquake was to perhaps slightly widen the pre-existing cracks.

3.8 Lake Herman Dam

Lake Herman Dam was originally constructed in 1905 and currently has a maximum height of approximately 16 meters. It is located in the hills between Benicia and Fairfield to the south of the epicenter and is owned by the City of Benicia. The dam has a crest width of approximately 4 meters and a crest length of length of approximately 213 meters.

Lake Herman Dam was approximately 11.6 kilometers away from the energy source associated with the South Napa Earthquake and a strong motion instrument at the site recorded a peak ground acceleration of 0.09g. A member of the GEER team inspected the dam on August 27th and found no observable dam to the dam. Figure F-14 presents photographs of the dam.

Figure F-12: Aerial Photographs of Lake Madigan Dam
[NSF-GEER; Napa, CA; N38.308 W 122.193; Harder, L. F.; 09/01/14]

Figure F-13: Photographs of Swanzy Dam and minor longitudinal cracking
[NSF-GEER; Napa, CA; N38.077 W 122.227; Harder, L. F.; 08/27/14]

Figure F-14: Photographs of Lake Herman Dam
[NSF-GEER; Napa, CA; N38.097 W 122.150; Harder, L. F.; 08/27/14]

4. Overview of Levee System

The Napa River drainage basin is just north of San Pablo Bay and through the City of Napa almost all of the land adjacent to the river has been subject to flooding since 1862. By the mid-20th century, development had squeezed the river into a narrow channel as secondary channels were filled and the river was confined by small levees and floodwalls. Many of the levee systems on the Napa River, and on tributary channels upstream and downstream of the City of Napa, are privately owned. These levee systems are generally small, less than 2 meters in height, and intermittent.

To reduce the flood risk to the City of Napa, a federal flood control project led by the United States Army Corps of Engineers, with matching funds from state and local sources, has been underway for more than a decade. The project is being implemented in phases along approximately 12 kilometers along the river and is intended to provide protections for the 1 percent annual chance (100-year) flood within the city, approximately between Trancas Street and Imola Avenue (see Figure F-15). Major features of the project include widening the channel of the Napa River and nearby Napa Creek, the construction of new flood walls, new pump stations, the replacement of bridges to accommodate the wider channel, the construction of a new bypass past the ox-bow in downtown Napa, and the removal of levees further downstream to allow the river to spread out into multiple channels and wetlands. The major portion of the downtown channel widening and floodwall construction along the Napa River was generally completed by 2006. The construction of the ox-bow bypass was in the early phases when the South Napa Earthquake occurred. Reconstruction and removal of low levees is on-going.

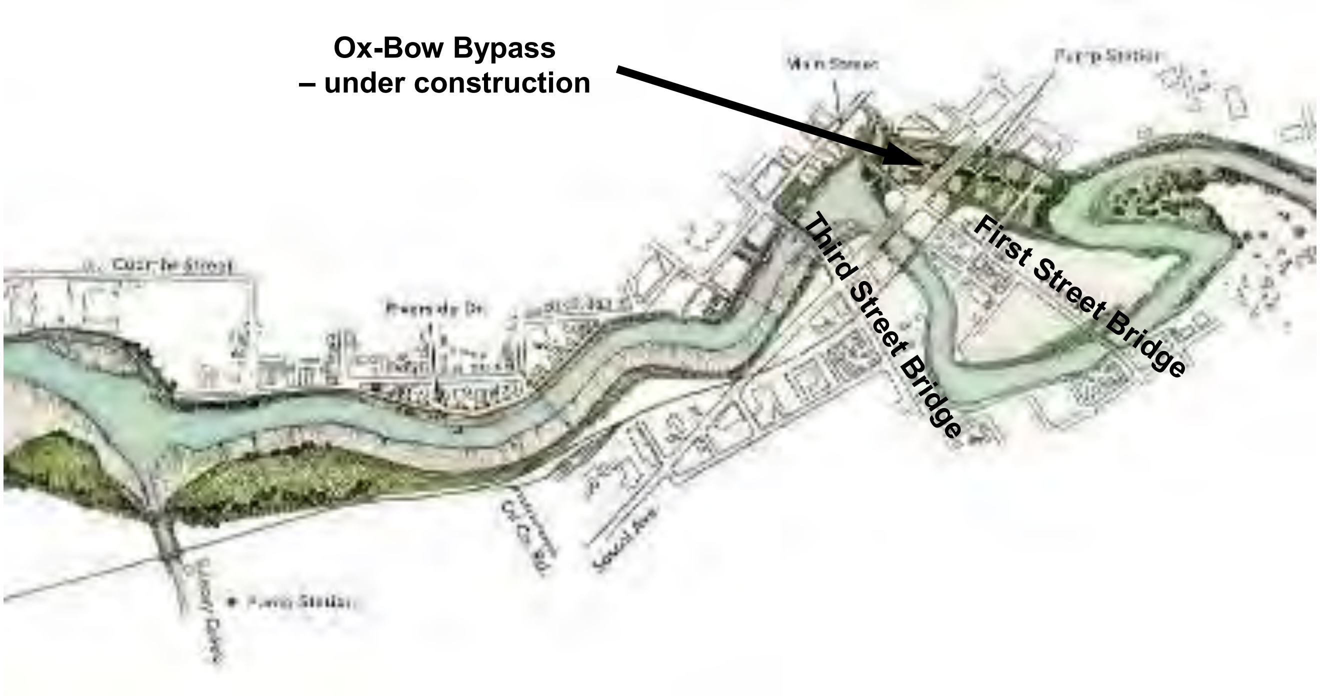

Figure F-15: Views of improvement area of confined Napa River in downtown Napa [from County of Napa and USACE]

5. Overview of Levee System Performance of the Levee System

The Napa River levees and floodwalls that are part of the federal flood control project were reported by the Sacramento District of the United States Army Corps of Engineers to have little to no damage. Inspections by GEER team members found only minor cracking of the recently constructed levee/floodwall system in downtown Napa. This was despite very high accelerations reported in downtown Napa ranging up to 0.4 to 0.6g. Older floodwalls and foot-bridges nearby, however, experienced some damage. In addition, while a minor amount of liquefaction was observed in the form of cracking and sand boils in a sand bar in the Napa River near the Third Street Bridge, no signs of cracking or lateral spreading were observed on the riverbank above it.

Downstream of downtown Napa, GEER team members made several aerial surveys of the intermittent levee system along both sides of the Napa River, but no signs of damage were observed from the air. Follow-up inspections on the ground found only minor cracking of the levees themselves, with most of the damage on the levees observed on developed areas where homes and boat docks had been constructed onto the low 2-meter-high levees along Edgerley Island. Across from Edgerley Island, a small former salt pond dike developed longitudinal cracking along the downstream toe of the 2-meter-high embankment which might have been the result of foundation liquefaction. However, the damage was relatively minor.

Details and photographs for three of the levee/floodwall areas inspected by the GEER team are presented in the following sections:

- Downtown Napa Levees/Floodwalls
- Edgerley Island Levee
- Green Island Salt Pond Retaining Dike

5.1 Downtown Napa Levees/Floodwalls

In the area of the First and Third Street Bridges, the channel had been widened and new floodwalls and bridges were completed in 2006. Much of the new floodwall system is on the right (west) side of the river near the Third Street Bridge which allowed major new redevelopment in this area of downtown Napa. Figure F-16 shows a Google Earth view of this area and Figure F-17 presents an aerial photograph taken during the GEER team reconnaissance.

Downstream of the Third Street Bridge, remnant cracking and sand boils were observed in the sand/mud bar along the left (east) bank of the river and was suggestive that river sediments had liquefied during the earthquake (see Figures F-17 and F-18). The crack openings here were estimated to have a maximum width of approximately 2 centimeters. However, the adjacent riverbank appeared undamaged and there was no sign of cracking or lateral spreading on the concrete and gravel walkways above.

On the right (west) side of the river, the recently constructed large reinforced concrete floodwalls appeared to have performed well overall. However, the concrete deck slab behind the walls sustained minor cracking and had pulled away from the floodwalls by as much as 3 centimeters (see Figure F-19). In addition, a lateral retaining wall supporting part of a restaurant had settled approximately 3 centimeters relative to the wall (see Figure F-19).

Figure F-16: Google Earth Plot of Downtown Napa
[NSF-GEER; Napa, CA; N38.308 W 122.281; Harder, L. F.; 09/11/14]

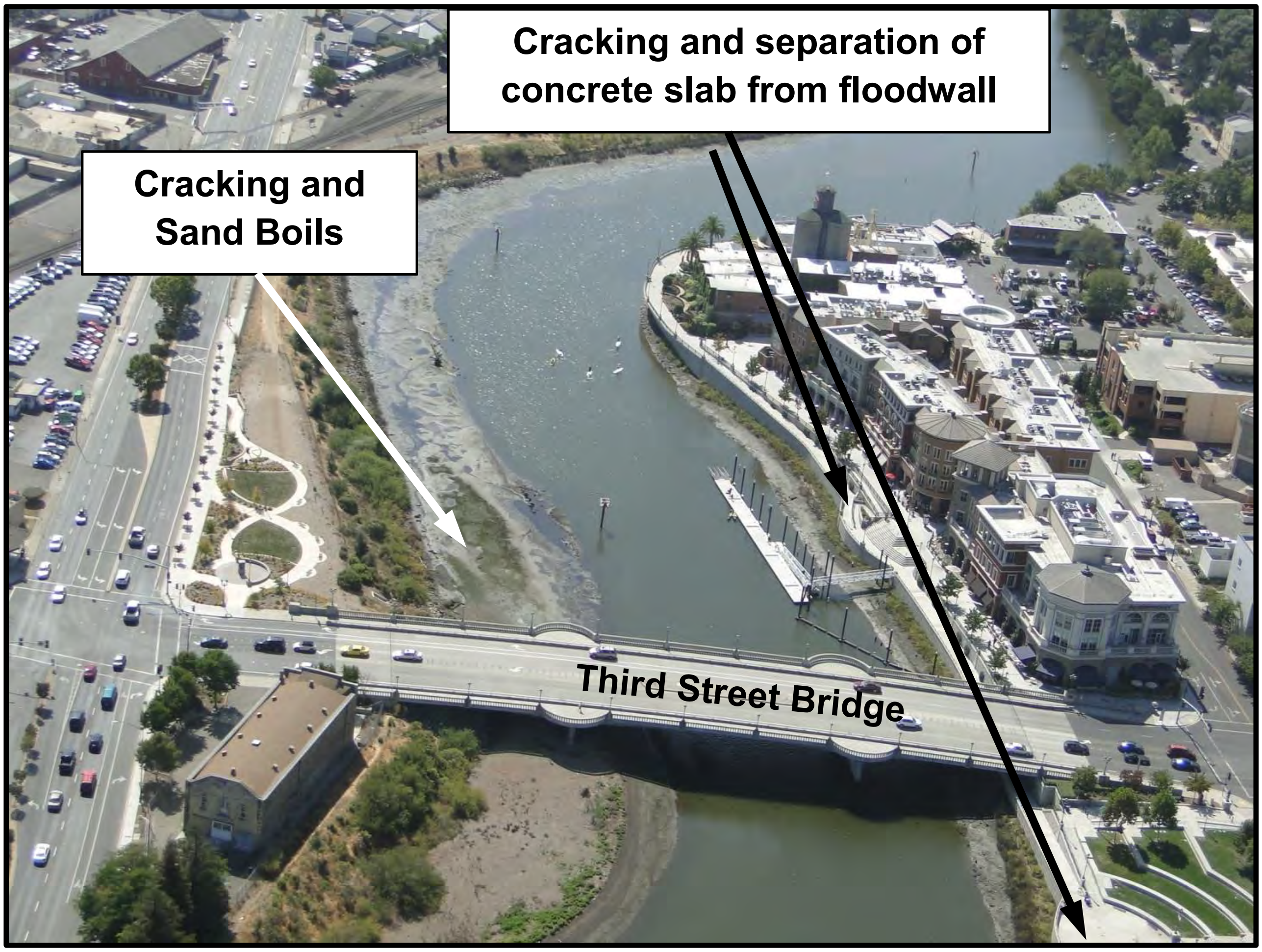

Figure F-17: Aerial photograph of Napa River looking downstream near Third Street Bridge
[NSF-GEER; Napa, CA; N38.308 W 122.281; Harder, L. F.; 09/01/14]

Figure F-18: Remnant cracking and sand boils in sand bar along left bank of Napa River looking downstream from Third Street Bridge
[NSF-GEER; Napa, CA; N38.298 W 122.283; Harder, L. F.; 09/04 and 09/07/14]

Figure F-19: Separation of concrete slab and retaining wall from Napa River floodwall along right bank of Napa River looking upstream from Third Street Bridge
[NSF-GEER; Napa, CA; N38.299 W 122.285; Harder, L. F.; 09/04/14]

5.2 Edgerley Island Levee

Along the right (west) bank of the Napa River south of the epicenter the levees are commonly about 2 meters in height. On Edgerley Island, residences have been built on top of the levees along Milton Road and pilings and docks have been constructed on the relatively steep waterside slopes along the river. In many places, short floodwalls on the order of up to a meter in height have been constructed to provide wave protection and freeboard. Figure F-20 presents a Google Earth plot and an aerial photograph illustrating the area.

In one location along Milton Road, ground cracking was observed across the asphalt pavement. This cracking continued to a fractured low cinderblock wall (see Figure F-21). At the back of the residence on the waterside portion of the levee, the dock and floodwall had been damaged. It was not clear if the cracking and damage were associated with shaking or ground displacements associated with a continuation of the fault rupture south of the epicenter. The shaking must have been significant as a large water tank moved off its concrete pad and sheared its connection with the residence (see Figure F-22). However, no damage was observed on the levee embankment itself.

5.3 Green Island Salt Pond Retaining Dike

Along the western edge of Green Island along mud flats east of the left (east) bank of the Napa River and south of the epicenter there are small retaining dikes that previously retained brine waters in salt ponds (see location in Figure F-20). The area has largely been converted into an environmental restoration and recreation area, but many of the retaining ponds for the salt ponds remain in place. No significant damage was observed by the GEER team for the majority of the dikes visited on foot, and no damage was observed during the aerial reconnaissance. However, near the very western tip of the island, approximately 100 meters of longitudinal cracking was observed near the landside toe of the dike. The largest cracks were approximately 2½ centimeters in width, and, while longitudinal, appeared to have enlarged from shrinkage cracks. In addition, there appeared to be sandy ejecta along the cracks, but this was not definitive as the observations were made on September 4th, approximately 10 days after the earthquake (see Figure F-23).

The retaining dike at this location was approximately 2 meters high and had crown widths on the order of 3 meters. In addition to the longitudinal cracking, four transverse cracks approximately 2 to 4 millimeters in width also crossed the levee in this 100-meter reach (see Figure F-24). It is likely, but not definitive that the cracking was associated with a limited amount of liquefaction in the foundation in this area.

Contributing Sources:

Initial Observations: Keith Kelson (Sacramento District, USACE)

Computations of PGA estimates at dams using NGA-W2 GMPEs: Jorge Luis Macedo Escudero (University of California, Berkeley)

Background information on dams and DSOD inspections: Y-Nhi Enzler (DSOD); Mark Stanley (HDR Engineering); Brian Vanciel (City of Vallejo); Dan Hiteshew (City of Vallejo)

Figure F-20: Google Earth plot and aerial photograph of Napa River along Edgerley Island south of the epicenter [NSF-GEER; Napa, CA; N38.198 W 122.316; Harder, L. F.; 09/01/14]

Figure F-21: Photographs of cracked asphalt pavement on Milton Road, cracked cinderblock retaining wall, and damage to waterside floodwall/boat dock on Edgerley Island south of the epicenter [NSF-GEER; Napa, CA; N38.198 W 122.316; Harder, L. F.; 09/01/14]

Figure F-22: Photographs of displaced water tank moved off its concrete pad and sheared pipe connection – note replacement tanks on pad in its place - on Edgerley Island south of the epicenter [NSF-GEER; Napa, CA; N38.198 W 122.316; Harder, L. F.; 09/01/14]

Figure F-23: Photographs of longitudinal cracking and apparent ejecta along landside toe of salt pond retaining dike on western edge of Green Island south of the epicenter
[NSF-GEER; Napa, CA; N38.201 W 122.302; Harder, L. F.; 09/04/14]

Figure F-24: Photographs of transverse cracking on crown of salt pond retaining dike on western edge of Green Island south of the epicenter
[NSF-GEER; Napa, CA; N38.201 W 122.302; Harder, L. F.; 09/04/14]